Declassified in Part - Sanitized Copy Approved for Release 2013/01/23 : CIA-RDP81-01043R001600090003-8

STAT

Page Denied

Declassified in Part - Sanitized Copy Approved for Release 2013/01/23 : CIA-RDP81-01043R001600090003-8

Declassified in Part - Sanitized Copy Approved for Release 2013/01/23 : CIA-RDP81-01043R001600090003-8

STAT

TERRESTRIAL MAGNETISM

Zemnoy Magnetizm /Torrestrial Magnetism/, 1953, Moscow,
Pages 3-591

B. M. Yanovskiy

TABLE OF CONTENTS

Foreword	1
Introduction	4
Section 1. Brief historical information	4
Section 2. Basic laws of a stationary magnetic field	20
Section 3. Magnetic field of a closed linear circuit	24
Section 4. Magnetic potential of elemental circuit	26
Section 5. Magnetic field of a linear circular circuit	28
Section 6. The effect of finite dimensions of the cross section of the circuit	33
Section 7. Magnetic field of Helmholtz rings	36
Section 8. Magnetic field of a cylindrical solenoid	41
Section 9. Magnetic field of a multilayer solenoid (coil)	45
Section 10. Magnetization of rocks	47
Section 11. Magnetic potential of a magnetized body	51
Section 12. Magnetic potential of a uniformly magnetized sphere	53
Section 13. Potential of a uniformly magnetized cylinder	55
Section 14. Magnetic potential of an ellipsoid	55
Section 15. Magnetization of rocks in a uniform magnetic field	58
Section 16. Determination of demagnetization coefficients	64
Section 17. Effect of the shape of the sample on the magnitude of magnetic moment and magnetization	67
Section 18. The permanent magnet and its properties	70
Section 19. Magnetic materials and alloys	82

Declassified in Part - Sanitized Copy Approved for Release 2013/01/23 : CIA-RDP81-01043R001600090003-8

Declassified in Part - Sanitized Copy Approved for Release 2013/01/23 : CIA-RDP81-01043R001600090003-8

Part One

The Permanent Magnetic Field of the Earth 90

Chapter I. Description of the Magnetic Field of the Earth 90

Section 1. The elements of terrestrial magnetism 90

Section 2. Graphic representation of the earth's magnetic field. Magnetic maps 93

Section 3. Methods of Investigating the magnetic field of the earth. Magnetic surveys, magnetic observatories 99

Chapter II. Analytic Representation of the Earth's Magnetic Field 106

Section 1. The earth's magnetic field as the field of a uniformly magnetized sphere 106

Section 2. Expansion of earth's magnetic potential to a series. The theory of Gauss 116

Section 3. Physical meaning of the terms of Gaussian series 124

Section 4. Separation of the earth's magnetic field into "internal" and "external" 131

Section 5. Vortical magnetic field 136

Chapter III. Structure and Physical Theories of the Origin of the Earth's Magnetic Field 138

Section 1. Structure of the earth's magnetic field 138

Section 2. Continental or residual field and its theory 140

Section 3. Magnetic anomalies 152

Section 4. Hypotheses of the origin of earth's magnetic field 159

Chapter IV. Secular Variations 174

Section 1. Phenomena associated with secular variations 174

Section 2. Theory of secular variations 181

Part Two

Variable Magnetic Field of the Earth 187

Declassified in Part - Sanitized Copy Approved for Release 2013/01/23 : CIA-RDP81-01043R001600090003-8

Declassified in Part - Sanitized Copy Approved for Release 2013/01/23 : CIA-RDP81-01043R001600090003-8

Chapter V. Classification of Variations of the Earth's Magnetic Field and Methods for their Investigation 187

Section 1. General information and classification of magnetic variations 187

Section 2. Methods for differentiation of daily magnetic variations (statistical processing) 189

Section 3. The method of spheric and harmonic analysis of variations 193

Section 4. Magnetic activity 200

Chapter VI. Magnetic Variations and Aurora Polaris 210

Section 1. Solar diurnal variations 210

Section 2. Lunar diurnal variations 224

Section 3. Magnetic disturbances 227

Section 4. Variations of high latitudes 236

Section 5. The aurora 242

1. Forms of aurora polaris 242

2. Direction of rays of aurora polaris 244

3. Height of aurora polaris 245

4. Geographical distribution of aurora polaris 248

5. Diurnal distribution of aurora polaris 249

6. Spectrum of aurora polaris 250

7. Connection between aurora polaris and magnetic and solar activities 251

Chatper VII. Theory of Magnetic Variations and Aurora Polaris 253

Section 1. The ionosphere and its properties 253

1. Propagation of radio waves within the ionosphere 253

2. Methods of investigation of the ionosphere 258

3. Measurement of the altitude of the reflecting layer 260

Declassified in Part - Sanitized Copy Approved for Release 2013/01/23 : CIA-RDP81-01043R001600090003-8

Declassified in Part - Sanitized Copy Approved for Release 2013/01/23 : CIA-RDP81-01043R001600090003-8

4. Composition of the ionosphere and formation of ionized layers 264
5. Conductivity of the ionosphere 270
6. Sporadic layer 272
7. Tidal phenomena in the ionosphere 272
Section 2. Theory of daily variations 274
1. Theory of atmospheric dynamo 275
2. Theory of drifting current 278
Section 3. Fundamental propositions of the theory of aurora polaris and magnetic disturbances 285
Section 4. Movement of charges within the magnetic field of a dipole 287
Section 5. The theory of Chapman and Ferraro 298
Section 6. The theory of Al'fven [transliterated] 303

Part Three

Practical Utilization of the Phenomena of Terrestrial Magnetism 308
Chapter VIII. Magnetic Prospecting 308
Section 1. The magnetometric prospecting method and its development 308
Section 2. Magnetic properties of rocks and minerals 313
Section 3. Residual magnetization of rock formations and the causes of its occurrence 329
Section 4. Effect of variations on the state of magnetization of rocks 334
Section 5. Methods of investigation of the magnetic properties of rocks 337
1. Ballistic method 340
2. The magnetometric method 342
3. The magnetometer of B. M. Yanovskiy and Ye. T. Chernyshev 352

Declassified in Part - Sanitized Copy Approved for Release 2013/01/23 : CIA-RDP81-01043R001600090003-8

Declassified in Part - Sanitized Copy Approved for Release 2013/01/23 : CIA-RDP81-01043R001600090003-8

4. The method of attraction and repulsion in a non-uniform magnetic field 355
5. Cylinder method 360
6. Astatic magnetometer of S. Sh. Dolginov 362
7. The method of T. N. Roze 365
8. Constant magnetometer for measuring the magnetic properties of rocks and materials of small volume 367
Section 6. Procedure of conducting magnetometric operations 368
Section 7. Aerial magnetic surveying 371
Section 8. The main problem of magnetometry. Magnetic fields of regularly shaped bodies 375
1. Sphere 377
2. Cylinder with small diameter-to-length ratio, magnetized in the direction of its geometric axis 380
3. Ellipsoid 384
4. Infinitely long circular cylinder magnetized perpendicularly to the axis 386
5. Elliptical cylinder of infinite length magnetized along the major axis of the ellipse 389
6. A thin and infinitely long plate, magnetized in width 390
7. Infinitely long rectangular prism magnetized vertically. Vertical stratum 393
8. A thin, infinitely long plate. Thin horizontal stratum 395
9. Horizontal, semi-infinite stratum 397
10. Vertically magnetized sloping stratum of infinite length 398
11. The method of cards for solving the main problem of magnetometry 400

Declassified in Part - Sanitized Copy Approved for Release 2013/01/23 : CIA-RDP81-01043R001600090003-8

Declassified in Part - Sanitized Copy Approved for Release 2013/01/23 : CIA-RDP81-01043R001600090003-8

12. Experimental method of solving the main problem 405

Section 9. The possibility of utilizing the plane problem 407

Section 10. The inverse problem of magnetometry 411

1. Determination of the shape of a rock formation 411

2. Multiple-valued nature of the inverse problem of magnetometry 415

3. Analytical methods of solving the inverse problem 417

Section 11. Procedures of interpreting magnetic anomalies 437

Chapter IX. Ship's Magnetic Compass Deviation 445

Section 1. The basic equations of a ship's magnetic field 445

Section 2. Transformation of Poisson's equations 447

Section 3. Determination of deviation 449

Section 4. Elimination of deviation 450

Section 5. Deflector magnetometer of Dekolong 453

Part Four

Methods and Apparatus for the Measurement of the Elements of Terrestrial Magnetism 457

Chapter X. Measurement of the Elements of Terrestrial Magnetism 457

Section 1. Classification of measurement methods and of measuring apparatus 457

Section 2. The principle of measuring declination 460

Section 3. Astronomical observations during magnetic surveys 467

Section 4. Measurement of dip with a needle inclinator 480

Section 5. Measurement of dip by means of an induction inclinator 486

Section 6. Measurement of dip by the method of induction in soft iron 498

Declassified in Part - Sanitized Copy Approved for Release 2013/01/23 : CIA-RDP81-01043R001600090003-8

Declassified in Part - Sanitized Copy Approved for Release 2013/01/23 : CIA-RDP81-01043R001600090003-8

Section 7. Measurement of the horizontal component. The absolute method of Gauss 503

Section 8. Sequence of observations of the absolute method 516

Section 9. Determination of the constant coefficients 525

Section 10. Errors in determination of H caused by incidental errors of direct observations 532

Section 11. Systemic errors caused by imperfections of instruments 536

Section 12. Absolute electric method of determining the horizontal component 544

Section 13. Absolute magnetic theodolite of VNIIM 547

Section 14. The relative method of Gauss for determination of the horizontal component 550

Section 15. Measurement of the horizontal component by the method of deflections (abridged method of Gauss) 552

Section 16. The relative electric method of measurement of H 554

Section 17. The "combined" magnetic theodolite 557

Section 18. Measurement of the horizontal component by means of the quartz magnetometer 558

Section 19. Double compass for measuring H 562

Section 20. Measurement of vertical component by the electric method 566

Chapter XI. Methods of Measurement used during Investigation of Magnetic Anomalies 567

Section 1. Introduction 567

Section 2. M-1 field magnetometer 568

Section 3. M-2 magnetic balance 575

Section 4. The aeromagnetometer of A. A. Logachev 585

Section 5. Magnetically saturated sondes 588

Declassified in Part - Sanitized Copy Approved for Release 2013/01/23 : CIA-RDP81-01043R001600090003-8

Declassified in Part - Sanitized Copy Approved for Release 2013/01/23 : CIA-RDP81-01043R001600090003-8

Chapter XII. Variation Instruments 601

Section 1. General theory of variation instruments 601

Section 2. Variometers of horizontal component and declination (unifilar) 605

Section 3. The influence of temperature on the unifilar readings. Methods of compensation 610

Section 4. Unifilar as a northward and eastward component variometer 617

Section 5. Vertical component variometer based on magnetic balance 619

Section 6. Effect of temperature on the readings of the magnetic balance 623

Section 7. Methods of determining scale division of variometers 627

Section 8. Variometer of the vertical component designed by B. M. Yanovskiy 630

Section 9. Construction of variation instruments 633

Section 10. Magnetographs of B. Ye. Bryunelli 638

Section 11. High speed magnetographs of La Kur [transliterated] 640

Section 12. Station of A. G. Kalashnikov 641

Declassified in Part - Sanitized Copy Approved for Release 2013/01/23 : CIA-RDP81-01043R001600090003-8

Declassified in Part - Sanitized Copy Approved for Release 2013/01/23 : CIA-RDP81-01043R001600090003-8

TERRESTRIAL MAGNETISM

Foreword

The present edition of the Textbook of Terrestrial Magnetism differs substantially from the first edition which was published more than 10 years ago. Those differences are due on one hand to advances in our knowledge of terrestrial magnetism and on the other hand to the intended purpose of the new edition. While the first edition was designed to be a textbook for use at hydrographic institutes and faculties and had as its principal aim familiarization of students with magnetic measurement procedures as applied in conjunction with determination of the spatial distribution of the earth's magnetic field. The new edition is a text for university students of the departments of physics and geology who are specializing in geophysics. Hence the scope and contents of the book are entirely different from the first edition since it includes all the basic problems of theoretical as well as of practical nature relating to terrestrial magnetism phenomena.

The text is arranged in accordance with the schedule of lectures given at the department of physics of the Leningrad Order of Lenin, State University imeni A. A Zhdanov, for students specializing in geophysics. However, some problems are treated in a somewhat wider scope, in order that those who study terrestrial magnetism may be in a position to understand more thoroughly and clearly phenomena which due to a lack of time cannot be dealt with in detail in the lectures.

The course is divided into 4 parts, each of which includes a definite range of problems of an individual nature. Presentation of the material as a whole is preceded by an introduction of considerable

Declassified in Part - Sanitized Copy Approved for Release 2013/01/23 : CIA-RDP81-01043R001600090003-8

Declassified in Part - Sanitized Copy Approved for Release 2013/01/23 : CIA-RDP81-01043R001600090003-8

length describing some specific problems of magnetism not usually included in general texts of physics, but which are of great importance to the mastery of many aspects of a course in terrestrial magnetism. These problems include: calculation of the magnetic fields of various coils, magnetization of ferromagnetic bodies, magnetic materials and several others.

The first part constitutes a study of the permanent portion of the earth's magnetic field and its secular variations. Attention is focused primarily on the physical aspects of the phenomena and on analytical investigation methods which enable ascertainment of the structure of the magnetic field, while questions of a theoretical nature are considered only to the extent necessary to form a general conception of the situation that prevails in this field. This is due to the fact that as yet there is no fully evolved theory, nor even an adequate outline of the theory of terrestrial magnetism. There are only a number of hypotheses none of which can claim any degree of reliability.

The second part of the course relates to the variable portion of the earth's magnetic field, magnetic variations and the phenomena associated therewith, such as the aurora polaris and ionospheric phenomena. Although the theories of these phenomena cannot be considered as being fully developed at the present time, their foundations, in contrast with the theory of the permanent magnetic field, are more or less clear and can be accepted as objective facts. Therefore, more space is allocated to presentation of the existing theories of magnetic variations and aurora polaris.

The third part describes the practical applications of terrestrial magnetism phenomena, namely magnetic prospecting for

Declassified in Part - Sanitized Copy Approved for Release 2013/01/23 : CIA-RDP81-01043R001600090003-8

Declassified in Part - Sanitized Copy Approved for Release 2013/01/23 : CIA-RDP81-01043R001600090003-8

useful minerals, and compass deviation. These are independent problems and are treated in separate courses. However, their inclusion in a general text of terrestrial magnetism is necessary to the extent that they follow directly from the study of terrestrial magnetism phenomena and are integrally associated with the latter. At the present time it is impossible to visualize the study of terrestrial magnetism divorced from its practical applications. Since the present text is one of a purely physical nature wherein phenomena are considered from the standpoint of physical laws, the chapter on magnetic prospecting also is physical and thus no consideration is given to problems of a geological nature connected with the interpretation of any given deposits.

The fourth part describes problems of procedure, including the theory and practice of geomagnetic determinations in the course of field work as well as of observatory observations. Many of the problems in their part are considered on a somewhat wider scope than is required by the curricula, but we believe such an elaboration is fully justified because until the present there has been no manual or monograph in which these problems would be presented in an orderly and systematic fashion, although the need of such a manual is very apparent.

I consider it my duty to express profound gratitude to the associates of the Institute of Terrestrial Magnetism N. V. Pushkov, Professor Yu. D. Kalinin, N. P. Ben'kova, V. P. Orlov, S. I. Isayev, S. M. Manourov, and others who contributed to the editing of the manuscript and have made many, very valuable suggestions.

Declassified in Part - Sanitized Copy Approved for Release 2013/01/23 : CIA-RDP81-01043R001600090003-8

Declassified in Part - Sanitized Copy Approved for Release 2013/01/23 : CIA-RDP81-01043R001600090003-8

INTRODUCTION

Section 1. Brief Historical Review

Together with astronomy and geodesy, the science of terrestrial magnetism has one of the oldest histories in the development of science. The Chinese were the first in discovering the phenomenon of magnetism and the possibility of its practical utilization. They have the priority in the discovery of the basic magnetic properties and in the invention of the compass. According to Chinese chronicles the phenomenon of magnetic polarity and the use of the compass were known in China more than 1,000 years prior to the beginning of the new era.

Thus the Chinese historian Su-Ma-Tzyan, who lived in the first century B. C., in relating the event of the reception in the year 1100 B. C. of Vietnamese envoys by the Chinese emperor Chey-Kun, writes: "Chey-Kun presented them with 5 travel chariots so designed that they always indicated the direction of south. The envoys of Yue-Chen (the ruler of Vietnam) departed in these chariots, reached the seacoast, passed Fu Nan and Lin-I, and one year later arrived in their homeland. The chariots which indicated the south were always in the lead in order to guide those that followed and to show the direction of the 4 cardinal points."

The first written record of the property of magnetic polarity is found in a Chinese dictionary compiled about 121 A. D. while a report of the use of the compass also is found in a later work entitled "Treatise on Vehicles and Clothing" which, according to Chinese chronicles was written in the fifth century A. D.

In this source it is stated that after the secret of making chariots which indicate the south had been lost in the first century B. C., the scholar Ma-Nuin again invented such chariots in 226 A. D.

Declassified in Part - Sanitized Copy Approved for Release 2013/01/23 : CIA-RDP81-01043R001600090003-8

Declassified in Part - Sanitized Copy Approved for Release 2013/01/23 : CIA-RDP81-01043R001600090003-8

"On these chariots was a wooden figurine, the outstretched arm of which pointed to the south. No matter how the chariot was turned or its direction reversed, this figurine continued to indicate the south" (Figure 1).

Furthermore, at that time the Chinese already knew that a needle which had been rubbed with a lodestone points not exactly to the south, but is deflected slightly to the west, which is stated in a number of instances in various works of Chinese authors which were written in the tenth and eleventh century A. D.

In Europe the first information concerning magnetism came to light several centuries B. C. References to a "mysterious stone" which possesses the remarkable property of attracting iron are found in the writings of several Greek authors. At first it was referred to as "Hercules stone" "Lydian stone," "Siderite" and also simply as "stone." Later these terms were replaced by "magnet."

The basic properties of magnetic attraction were well-known to the Greeks back in the VII century B. C. Thus, references to this fact are found in the writings of Thales, who lived about 640-546 B. C. However, the phenomenon of polarity became known in Europe only in the twelfth century. The use of a compass by Europeans is first mentioned in the work of the English monk Alexander Neckham written in the twelfth century: "Seafarers while sailing, when they cannot orient themselves by the sun because of cloudy weather or when the world is plunged into the darkness of night and when they do not know in which direction to sail, make use of a freely turning magnetic needle one end of which points to the north."

All this convinces us that at the beginning of our era the Chinese had knowledge of the properties of magnets and of the magnetic

Declassified in Part - Sanitized Copy Approved for Release 2013/01/23 : CIA-RDP81-01043R001600090003-8

Declassified in Part - Sanitized Copy Approved for Release 2013/01/23 : CIA-RDP81-01043R001600090003-8

field of the earth which far exceeded that of the Europeans of the same period.

Yet, the present day bourgeois scientists of Europe and America in writings on the history of magnetism make every effort to minimize the role and priority of the Chinese in the discovery of terrestrial magnetism, by arguing, for example, that the Chinese could not possibly have invented the compass before the Europeans since they were not at that time a maritime nation and had no ships. Such reasoning is found, for example, in the "Encyclopedia Britannica."

The earliest European treatise concerning the magnet and its properties is the letter of Peter Peregrine to a certain Siger, dated 12 August 1269. In this writing Peregrine describes all the properties of magnet known in his days and names for the first time the poles of the magnet. The end of the needle pointing to the north Peregrine proposed to name the north pole, and the opposite end the south pole, But the principal achievement of Peregrine is the improvement of the compass, which at that time was a fairly primitive instrument in the form of a magnet floating in a vessel filled with water and having neither a pointer for taking readings nor a card. Peregrine combined the compass with a marine astrolobe, providing it with a graduated scale and a base line which enabled sailors not only to direct the ship, but also to determine the azimuth of heavenly bodies. At first Peregrine made use of a floating compass, but later on he adopted a compass turning on a vertical pivot. Figure 2 shows the 2 types of compasses used by Peregrine.

The contents of Peregrine's letter did not become widely known until the sixteenth century and therefore his discoveries were not put to extensive use.

Declassified in Part - Sanitized Copy Approved for Release 2013/01/23 : CIA-RDP81-01043R001600090003-8

Declassified in Part - Sanitized Copy Approved for Release 2013/01/23 : CIA-RDP81-01043R001600090003-8

Invention of the mariner's compass (1302-1318) in its present form has been attributed to the Italian Flavio Gioia who lived in the early nineteenth century. Gioia set the compass needle on a pointed pivot as is done in modern compasses and provided it with a paper disc (card) divided in 32 sections known as the Rose of Winds or compass points.

The next step forward in the development of the science of terrestrial magnetism was the discovery of magnetic declinations by Columbus during his journey from Europe to America. Strictly speaking, it is the starting point of the science of terrestrial magnetism. Before the discovery of Columbus, i.e., up to the fifteenth century, it was believed that the magnetic needle pointed exactly to the north and this was thought to be due to the attraction exercised by the north star on the magnetic needle. Only after the first voyage of Columbus to the New World was it known that the magnetic needle changes its direction on passing from one locale to another.

Several days after Columbus had sailed from Europe, on the 13 September 1492, it was noted to the utter amazement of the mariners, that the magnetic needle had changed its direction having become deflected to the NW. On the following morning the change occurred again in the same direction and to the same extent. On 17 September the navigator, having determined the azimuth of the sun, found that during the 4 days the needle had undergone a change in direction amounting to an entire division of the compass and scale. To reassure his crew Columbus had to resort to deceit and altered the compass scale, explaining that it was not the needle that had changed its direction, but the north star which had altered its position.

Declassified in Part - Sanitized Copy Approved for Release 2013/01/23 : CIA-RDP81-01043R001600090003-8

Declassified in Part - Sanitized Copy Approved for Release 2013/01/23 : CIA-RDP81-01043R001600090003-8

Readings taken after the arrival in the New World, showed that the needle was again pointing exactly to the north.

Thus by the end of the fifteenth century the Europeans had knowledge of 2 facts, namely: (1) the needle is deflected from the true meridian, and (2) that the magnitude of the deflection changes from one locale to another. These facts prompted the undertaking of measurement of the elements of terrestrial magnetism, and consequently constituted the beginning of the science of terrestrial magnetism.

The discovery of magnetic declination and inclination apparently was made by George Hartmann of Nuerenberg, a master craftsman who made compasses and sun dials. He was the first to determine the declination at Rome about 1510, but did not report this discovery until 1544, when he mentioned it in a letter to Count Albert of Prussia.

In the same letter he also stated that "the magnet is not only deflected to the east by about 9°, as I have already reported, but also dips downward. This can be shown in the following manner. I made a needle about as long as a finger, which was mounted exactly horizontally on a pointed pivot, but as soon as I touched one of its ends with a magnet the needle could no longer remain horizontal but was deflected downward by an angle of 90°."

The first extensive series of carefully conducted observations of declination at sea was carried out by Jean de Castro in 1538 during his journey from Europe to the East Indies.

The first work on magnetic declination was published by Burroughs in England in 1585. By the end of the sixteenth century

Declassified in Part - Sanitized Copy Approved for Release 2013/01/23 : CIA-RDP81-01043R001600090003-8

Declassified in Part - Sanitized Copy Approved for Release 2013/01/23 : CIA-RDP81-01043R001600090003-8

declination measurements had been taken at almost a hundred different locations at various parts of the globe, including Russia. Thus, in 1556-1557 declination readings were taken at the estuary of the Pechora river, on Novaya Zemlya, Vaygach Island and at the town of Kholmogorsk, and in 1580 at the towns of Astrakhan and Derbent.

Hartmann's letter had not been published and possibly was not known to his contemporaries. In 1581 the English navigator-hydrographer Norman published the results of his measurements and was the first to express the idea that the cause of the needle's assuming a certain direction is located within the earth. Norman also showed experimentally that within the terrestrial field the magnet undergoes only a rotary movement. He did this by placing the magnetic needle in a vessel containing water and balanced it so that it could move freely over the surface or within the water.

The next noteworthy step in the development of the science of terrestrial magnetism was the publication in 1600 of Gilbert's book in Latin "Magnets, Magnetic bodies, and the Great Magnet -- the Earth."

In this work is stated for the first time a theoretical idea of the causes of terrestrial magnetism, which has retained its significance up to present time. Gilbert expressed the opinion that the earth is a magnet, the poles of which coincide with the geographical poles, and he substantiated his assertion by experiments with a magnetized sphere. As the principal argument in support of his theory Gilbert cited the fact that the dip of the magnetic needle was found to be about the same when using a small model of the terrestrial globe made from a natural magnet, as in the case of the earth.

Declassified in Part - Sanitized Copy Approved for Release 2013/01/23 : CIA-RDP81-01043R001600090003-8

Declassified in Part - Sanitized Copy Approved for Release 2013/01/23 : CIA-RDP81-01043R001600090003-8

To explain the phenomenon of "declination" which is in conflict with his theory Gilbert postulated that the continents had magnetic properties which deflect the needle. The significance of Gilbert's theory was the fact that he had definitely established the relationship between the magnetic field of the earth and terrestrial globe, by pointing out that the cause of terrestrial magnetism must be sought not outside but within the earth.

Up to the end of the eighteenth century all the observations of terrestrial magnetism were limited to measurements of declination and dip, since no methods were available enabling determination of the magnitude of magnetic force. Only in 1785, when Coulomb found a method for measuring torque, was it possible to work out a method for measuring the intensity of a magnetic field. The first such method was proposed by Coulomb himself and it found immediate extensive application during various expeditions in taking magnetic measurements.

The method of Coulomb consisted of determination of the period of oscillation of a pendulum and therefore gave only relative values of the field intensity. Moreover, it involved the flaw that the period of oscillation depended not only on intensity but also on magnetic moment, which could vary and thus alter the period of oscillation.

In 1839 the classical works of Gauss; written in Latin and entitled "Intensity of Terrestrial Magnetic Force Reduced to an Absolute Sclae" appeared. In it Gauss provided a theoretical foundation for the method of measuring the horizontal component on an absolute scale, a method which has remained up to now unique for this purpose, and at the same time he also provided an experimental

Declassified in Part - Sanitized Copy Approved for Release 2013/01/23 : CIA-RDP81-01043R001600090003-8

Declassified in Part - Sanitized Copy Approved for Release 2013/01/23 : CIA-RDP81-01043R001600090003-8

technique which increased the accuracy of the measurements. Almost simultaneously with the latter Gauss published another work entitled "General Theory of Terrestrial Magnetism" in which without relying on any hypotheses he formulated the problem of interpretation of the terrestrial magnetic field in an entirely different manner. On the bases of the single assumption that the cause of terrestrial magnetism is within the earth, Gauss was able to formulate the magnetic potential at any point on the surface of the terrestrial globe as a function of the coordinates of latitude and longitude, expanded to an infinite series of spherical functions. By using a finite number of terms of this series it is possible to determine the coefficients of this series from observational data and thus calculate theoretically the potential at any point of the earth's surface.

Prior to 1634 all investigators assumed that magnetic declination varies only from one locale to another and that at a definite point it remains constant. In 1634 Henry Hellibrand found the declination at London to be $+4^{\circ}6'$, whereas Burrough and Norman in 1580 had obtained the value $+11^{\circ}15'$. This fact showed that over 34 years the magnetic declination had undergone such substantial hanges that they could not be attributed to observational errors and therefore the fact of a gradual change of this element with time had to be recognized, and which subsequently was designated as "secular variation."

This was the manner in which the secular variations of declination were discovered. Diurnal variations were first discovered in 1682 by Guy Tachard, who on observing the declination of the town of Luvo in Siam during 3 consecutive days found that it varies in a

Declassified in Part - Sanitized Copy Approved for Release 2013/01/23 : CIA-RDP81-01043R001600090003-8

Declassified in Part - Sanitized Copy Approved for Release 2013/01/23 : CIA-RDP81-01043R001600090003-8

different manner from day to day. Since the observations were probably made at different times of the day, the changes observed were unquestionably diurnal variations.

A more thorough proof of this phenomenon was provided by the London clockmaker Graham, who in 1722 made hundreds of observations of the magnetic needle during a single day and also found the occurrence of these same variations. The observations of Graham were confirmed during the same year by Professor Celsius at Upsala (Sweden), after which the diurnal variations became a recognized fact.

Later observations revealed the existence of variations in dip and at the end of the eighteenth century, after methods had been worked out for measuring the horizontal component, variations in this element also were found to occur. This gave rise to an investigation of these variations by means of regular, continuous observations at special magnetic observatories which were established in Russia and in Western Europe in the second decade of the nineteenth century.

The first Russian to devote serious attention to terrestrial magnetism phenomena was the brilliant scientist M V. Lomonosov, who as early as 1759 provided the solution for a number of problems relating to terrestrial magnetism in his work "Discourse on the Great Accuracy of Maritime Navigation."

In this work Lomonosov gave very valuable suggestions concerning compass design, ensuring more accurate readings. Like a true scientist Lomonosov also considered the causes which bring about the definite orientation of a magnetized needle in space. Prior to

Declassified in Part - Sanitized Copy Approved for Release 2013/01/23 : CIA-RDP81-01043R001600090003-8

Declassified in Part - Sanitized Copy Approved for Release 2013/01/23 : CIA-RDP81-01043R001600090003-8

Lomonosov the prevailing notion of the magnetic field of the earth was that it was similar to the field of a single magnet having 2 poles. Lomonosov was the first to consider the structure of the terrestrial globe as a body consisting of minute, differently magnetized particles which in combination form a non-uniformly magnetized sphere, and which in turn causes unequal declination at different parts of the globe. Thus he anticipated Gauss' idea of a random magnetization of the terrestrial globe.

On the basis of such an assumption Lomonosov considered it unfeasible to base any mathematical theory of terrestrial magnetism upon a small number of observations and indicated the following as the manner in which its true theory should be evolved: "the best method for determining the truth is to derive a theory from observations, and to correct observations by means of the theory." This proposition of Lomonosov applies not only to the theory of terrestrial magnetism but is a prerequisite in the development of the theory of any natural and social phenomenon.

To meet these requirements he recommended the establishment of permanent observation points (observatories) on land and systematic observations aboard ships at sea. As stated above, however, this idea of Lomonosov was put into effect only some 60 years later.

Lomonosov also was the first to suggest that variations in declination with time are due to an external magnetic field not associated with the magnetic field of the earth, although he gave an incorrect interpretation of its origin.

Lomonosov's ideas, which were many years ahead of the contemporary knowledge of terrestrial magnetism, unfortunately were not

Declassified in Part - Sanitized Copy Approved for Release 2013/01/23 : CIA-RDP81-01043R001600090003-8

Declassified in Part - Sanitized Copy Approved for Release 2013/01/23 : CIA-RDP81-01043R001600090003-8

enlarged upon due to the attitude concerning science which prevailed in Russia at that time. The work of Lomonosov was forgotten and remained unknown for more than a century.

During the first half of the nineteenth century Professor I. M. Simonov (1794-1855) and Academician A. Ya. Kupfer (1799-1865) made classical contributions to science which revived the basic ideas of Lomonosov although the authors themselves did not suspect that these ideas already had been expressed by Lomonosov.

Even before the publication of Gauss' treatise I. M. Simonov, a professor at the Kazan University, published in 1935 in the "Uchenyye Zapiski" [Scientific Records] of the University a paper entitled "Experiments on Mathematical Theory of Terrestrial Magnetism."

In this paper I. M. Simonov showed that the magnetic field of the earth induced by the cumulative action of its magnetic particles is equal to that of a dipole field, assuming that the particles are uniformly distributed. The dipole potential as a function of latitude and longitude was found to be identical with the first term of the expansion of the potential as derived by Gauss.

The contributions of I. M Simonov and Gauss are the foundation of modern concepts of the magnetic field of the earth and their publication may be regarded as the beginning of the current phase of development of the science of terrestrial magnetism. This phase consists of rapid gathering and organization of materials on the distribution of elements of terrestrial magnetism over the surface of the earth, the evolution of number of hypotheses concerning the origin of the magnetic field of the earth, and finally in recent times widespread practical utilization is being made of magnetic observations.

Declassified in Part - Sanitized Copy Approved for Release 2013/01/23 : CIA-RDP81-01043R001600090003-8

Declassified in Part - Sanitized Copy Approved for Release 2013/01/23 : CIA-RDP81-01043R001600090003-8

In addition to this work I. M. Simonov discovered the periodic nature of variations in declination. In his "Notes and Recollections Concerning a Journey to England, France, Belgium and German in 1842," published at Kazan in 1844, Simonov states that he was able to ascertain the following 3 periods of declination: "the first period lasts one year and depends upon the movement of the earth around the sun; the second, which is due to the sun's rotation about its axis, lasts for about 27 days; the third period is diurnal, and is determined by the position of the sun in relation to the horizon. All these periods are confirmed by observations."

In 1825 the work of Academician A. Ya. Kupfer was published in which a fact entirely novel at that time, namely the simultaneous occurrence of magnetic storms at Paris and Kazan, separated by a distance of 43° of longitude, was established. This work was the result of observations of variations in declination carried out by Kupfer and Simonov at Kazan, and provided the stimulus for the organization of systematic observations of variations in declination at different points of the terrestrial globe.

The work of Simonov and Kupfer constituted the beginning of detailed studies of magnetic variations and determination of their causes.

It is of interest to note that as early as the eighteenth century Russian inhabitants of the Kola peninsula had independently discovered, another fact relating to variations in declination, namely the occurrence of magnetic storms during aurora borealis. A. Ya. Kupfer is credited with organizing systematic observation of variations at a number of observatories which were established through his efforts.

Declassified in Part - Sanitized Copy Approved for Release 2013/01/23 : CIA-RDP81-01043R001600090003-8

Declassified in Part - Sanitized Copy Approved for Release 2013/01/23 : CIA-RDP81-01043R001600090003-8

In 1829 he organized a magnetic observatory at Petersburg, where beginning on October 1829, observations of declination were made every hour. Due to the efforts of A. Ya. Kupfer observatories were built in 1832 at the Siberian Mining Works of Nerchinsk, Barnaul and Kolyvan, with funds supplied by the Department of Mines and in 1836 an observatory was established at Yekaterinburg (Sverdlovsk) at the center of the Ural mining district.

It should be mentioned that of all the observatories organized by Kupfer only the one at Sverdlovsk has been in continuous operation up to the present time.

The observatories at Nerchinsk, Barnaul and Kolyvan were discontinued in the early sixtites when the mining industry of Siberia and the Urals, which had been based on forced labor, declined due to the abolition of serfdom. "But the same system of serfdom which helped the Urals to rise to such a high level during the epoch of incipient development of European capitalism also was the cause of its downfall during the height of the capitalistic era." (Lenin, complete works, Volume 3, 4th edition, page 424.)

The Petersburg observatory was not in operation between 1852 and 1870.

A. Ya. Kupfer was the first to note changes in the moment of magnetic needles with changes in temperature and to determine the law governing these changes, inabling temperature corrections in determinination of the horizontal component by the Gauss method and thus increasing the accuracy of these determinations.

In a historical article published by the Main Geophysical Observatory, Academician M. A. Rykachev wrote, concerning the work

Declassified in Part - Sanitized Copy Approved for Release 2013/01/23 : CIA-RDP81-01043R001600090003-8

Declassified in Part - Sanitized Copy Approved for Release 2013/01/23 : CIA-RDP81-01043R001600090003-8

conducted during the thirties and forties of the past century in the field of terrestrial magnetism: "In no country did the discoveries of Gauss produce a greater effect than in Russia, where at that time Kupfer was undertaking the establishment of a system of magnetic and meteorological observations."

During the seventies of the past century I. N. Smirnov, a docent at the University of Kazan, conducted an important magnetic survey, and work was resumed at the Petersburg magnetic observatory, which was later transferred to the town of Pavlovsk.

From 1871 to 1878 I. N. Smirnov, on his own initiative, carried out a magnetic survey of almost the entire territory of European Russia, which included determinations at 281 points, and it was only due to his untimely death that he was prevented from extending this survey over all of Russia. This survey revealed the existence of a large magnetic anomaly in the region of Kursk and supplied valuable information concerning the magnetic field of the territory of Russia. Its results provided the basic data for the first magnetic maps of European Russia, which were drawn up by A. Tillo in 1881 and 1885.

The work started by I. N. Smirnov was continued in the late nineties by P. T. Passal'skiy, a docent at the Odessa University, who in 1898 and 1900 made a detailed survey of the Crimean peninsula and the adjoining areas, including observations at more than 200 points.

At the initiative of Academician G. I. Vil'd, observations of variations were resumed in 1870 at Petersburg, and in 1878, they were continued at Pavlovsk, where a first rate magnetic observatory

Declassified in Part - Sanitized Copy Approved for Release 2013/01/23 : CIA-RDP81-01043R001600090003-8

Declassified in Part - Sanitized Copy Approved for Release 2013/01/23 : CIA-RDP81-01043R001600090003-8

had been established and which has served as a model for all such observatories throughout the world. Vil'd is accredited with having developed and built a series of new instruments for observatory recordings. He built 3 types of absolute magnetic theodolites, a declinator and induction inclinator and designed a series of variational instruments. All this equipment was in use at the Pavlovsk observatory up to the time of its evacuation on 1941. The same instruments also were used at the Sverdlovsk, Irkutsk and Tbilisi observatories.

Until the end of the nineteenth century all investigations of the magnetic field of the earth were conducted by independent institutions and by individual scientists, with no consolidating or coordinating agency. At the beginning of the present century it became evident that there exists a correlation between the magnetic field of the earth and its geological structure, and the undertaking of a magnetic survey throughout Russia in accordance with a single plan and under the general direction of the Academy, was proposed by the St. Petersburg Academy of Sciences, the costs being defrayed from a special fund allocated by the State Treasury. The imitiator of this undertaking was Academician M. A. Rykachev, director of the Main Geophysical Observatory, who in advocating the survey in an address delivered on 31 December 1901 at the Twelfth Congress of Russian Naturalists and Doctors stated: "The general distribution of magnetism over the surface of the terrestrial globe is such that the entire globe can be regarded as a magnet, the magnetic axis of which forms an angle with the axis of rotation of the earth. However, over extensive regions and at small individual areas there are sizeable deviations from this symmetrical distribution. The study of these deviations shows that such local anomalies are correlated

Declassified in Part - Sanitized Copy Approved for Release 2013/01/23 : CIA-RDP81-01043R001600090003-8

Declassified in Part - Sanitized Copy Approved for Release 2013/01/23 : CIA-RDP81-01043R001600090003-8

with the geological structure of the given area. From this it is apparent that a study of the magnetic characteristics of the earth is of great importance to the advancement of science."

The magnetic survey undertaken by the St. Petersburg Academy of Sciences was initiated in 1910 and continued until 1914 when it was discontinued due to the wartime conditions, and was resumed only after the October Revolution.

The extensive theoretical contributions of the earth twentieth century include the work of the reknowned Russian physicist N. A. Umov, professor at the Moscow University entitled: "Geometric Expression of Gaussian Potential as a Means of Determining the Laws of Terrestrial Magnetism," which contained the first interpretation of the constant terms of the Gauss analysis, the physical meaning of which until that time had remained unknown.

Following the Great October Revolution, when extensive possibilities were provided for rapid and effective utilization of all natural phenomena, a vigorous development took place in the study of terrestrial magnetism.

At the initiative of V. I. Lenin, a thorough investigation of the Kursk magnetic anomalies was started during the first years of the Soviet regime, which led to the discovery of extensive iron ore deposits.

In 1930 a general magnetic survey was initiated, which over a period of 10 years covered 26,000 magnetic points throughout the USSR, and which has enabled the construction of magnetic maps of the USSR with an accuracy not thought to be possible prior to that time.

Declassified in Part - Sanitized Copy Approved for Release 2013/01/23 : CIA-RDP81-01043R001600090003-8

Declassified in Part - Sanitized Copy Approved for Release 2013/01/23 : CIA-RDP81-01043R001600090003-8

In 1924 the first polar observatory in the world was established at Matochkin Shar strait on Novaya Zemlya. During the following years similar observatories were established at a number of points extending from Franz Joseph Land to Bearing Strait.

In 1932 the Institute of Terrestrial Magnetism was founded which has grown to a large scientific establishment of the USSR. The number of magnetic observatories directed by this institute increased several fold after the revolution.

Under the Soviet regime, Soviet scientists have worked out new investigation methods, gathered and consolidated vast amounts of data concerning the distribution and variations of the magnetic field over the surface of the earth and finally, a new branch of terrestrial magnetism of an applied nature has been developed, namely, magnetic prospecting, which through the work of Soviet scientists has received both theoretical basis and widespread practical application.

Section 2. Basic Laws of a Stationary Magnetic Field

The magnetic field of the earth can be regarded as stationary since its changes with time constitute only a small portion of the total field. It is sufficient to note that the amplitude of static daily variations does not exceed several tens of gammas. Moreover the frequency of variations ranges between 10^{-4} and 10^{-1} hertz, so that they have very little effect on the magnitude of an inductive electric field in a study of many phenomena of terrestrial magnetism. Therefore in most studies of terrestrial magnetism the laws of a stationary field must be used, which are particular instances of the general laws of an electromagnetic field expressed by Maxwell's equations.

Declassified in Part - Sanitized Copy Approved for Release 2013/01/23 : CIA-RDP81-01043R001600090003-8

Declassified in Part - Sanitized Copy Approved for Release 2013/01/23 : CIA-RDP81-01043R001600090003-8

Maxwell's equations of a stationary magnetic field are of the form:

$$\text{rot } H = 4\pi j, \tag{0.1a}$$

$$\text{div } H = 0, \tag{0.1b}$$

where H is the intensity of the magnetic field and j the current density.

The first equation provides a correlation between the intensity of magnetic field and current density at a given point, while the second expresses the continuity characteristic of the magnetic field. Since the vector H has no origins, it can be made equal to the rotor of another vector A, i.e.,

$$H = \text{rot } A. \tag{0.2}$$

Thus equation (0.1a) assumes the form:

$$\text{rot rot } A = 4\pi j$$

or, replacing rot rot A by its equivalent expression we obtain:

$$\text{grad div } A - \Delta A = 4\pi j,$$

where Δ is a Laplace operator.

If vector A is made to conform to the condition

$$\text{div } A = 0$$

we obtain the equation which vector A must satisfy:

$$\Delta A = -4\pi j. \tag{0.3}$$

Vector A is designated as the vector-potential, and if it is known the vector H may be determined. The necessity of introducing the new function of vector-potential is due to the fact that equation (0.1a), which correlates H and j, cannot be resolved directly, whereas equation (0.3) of the vector-potential can be solved by mathematical physics equations.

Declassified in Part - Sanitized Copy Approved for Release 2013/01/23 : CIA-RDP81-01043R001600090003-8

Declassified in Part - Sanitized Copy Approved for Release 2013/01/23 : CIA-RDP81-01043R001600090003-8

The solution of equation (0.3) is of the form:

$$A = \int \frac{j}{r}\, dv,$$

where r is the distance of the volume element dv through which current of density j flows from the point at which the vector-potential is considered.

From this equation by means of rotor operations (differentiation) for the coordinates of point P at which the vector A is being considered, we obtain:

$$H = \mathrm{rot}_p A = \int \mathrm{rot}_p \frac{j}{r}\, dv = \int \frac{1}{r} \mathrm{rot}_p j dv - \int [j\ \mathrm{grad}_p \frac{1}{r}]dv.$$

Since the value of vector j does not depend on the point P, it follows that

$$\mathrm{rot}\ pj = 0.$$

Moreover

$$\mathrm{grad}_p \frac{1}{r} = -\frac{\vec{r}}{r^3},$$

and thus

$$H = \int \frac{[j, r]}{r^3}\, dv. \qquad (0.4)$$

This expression represents the law of Biot-Savar in its integral form.

From equation (0.1a) integration of both parts over a surface S we yield

$$\int_S (\mathrm{rot}\ H dS) = 4\pi \int (j dS),$$

or, on applying the theorem of Stokes:

$$\oint (Hdl) = 4\pi I, \qquad (0.5)$$

where I is the intensity of the current flowing across the surface, and the integration must be carried out according to the contour of the surface.

Declassified in Part - Sanitized Copy Approved for Release 2013/01/23 : CIA-RDP81-01043R001600090003-8

Declassified in Part - Sanitized Copy Approved for Release 2013/01/23 : CIA-RDP81-01043R001600090003-8

Equations (0.4) and (0.5) show that a constant magnetic field within a medium of permeability equal to unity, may exist only if electric conductivity currents, or equivalent convection currents are present in the latter, with current density

$$j = evn,$$

where e is the charge of a particle (electron, ion), v the velocity of its movement and n the number of particles per unit volume.

The magnetic field within the portion of the medium containing no current must satisfy the equations:

$$\text{rot } H = 0, \tag{0.6a}$$

$$\text{div } H = 0. \tag{0.6b}$$

In this case vector H may be represented by the gradient of a scalar function φ, since rot grad $\varphi = 0$, and the first equation is satisfied. Taking

$$H = -\text{grad } \varphi (x, y, z) \tag{0.7}$$

and taking into account equation (0.6b) we obtain:

$$\text{div grad } \varphi = \Delta \varphi = 0, \tag{0.8}$$

i.e., the function φ which is termed the magnetic potential, satisfies the Laplace equation, and plotting of the function requires solution of this equation. This solution is possible if the boundary conditions are known, i.e., the distribution of φ or of its derivative over the normal to a surface.

In an investigation of phenomena connected with the movement of charges within a magnetic field the following equation, the equation of Lorenz, must be added to the above equations, which fully define the status of a magnetic field:

$$F = eE + \frac{e}{c}[v, H], \tag{0.9}$$

Declassified in Part - Sanitized Copy Approved for Release 2013/01/23 : CIA-RDP81-01043R001600090003-8

Declassified in Part - Sanitized Copy Approved for Release 2013/01/23 : CIA-RDP81-01043R001600090003-8

where F is the force acting on a charge e, moving at a velocity v within the electric and magnetic fields, c is the velocity of light; and e and E are exposed in absolute electrostatic units and H in absolute electromagnetic units.

Section 3. Magnetic Field of a Closed Linear Circuit

In considering many problems of the theory of terrestrial magnetic field the magnetic field of an elemental magnet (dipole) or of its equivalent elemental circuit current are encountered. Therefore, it is most important to know the laws which govern the magnetic field of such models and how they are derived from the general equations of a magnetic field.

Let us consider first the magnetic field of a linear circuit current of any shape. A linear circuit is taken to mean a closed conductor the cross sectional area of which is infinitely small, and the intensity of the current flowing through this closed circuit has a finite value I. The field of such a circuit is determined by the law of Biot-Savar (0.4) which in this instance has the form:

$$H = I \oint \frac{[dl, r]}{r^3},$$

because jdv = Idl, where dl is the element of the length of the circuit. The component of vector H on the x-axis is:

$$H_x = I \oint \left(\frac{r_z}{r^3}\, dy - \frac{r_y}{r^3}\, dz\right). \qquad (0.10)$$

Denoting the coordinates of point P, at which the vector is applied, by x_1, y_1, z_1, and the coordinates of element dl by x, y, z, then

$$r_y = y_1 - y, \quad r_z = z_1 - z. \qquad (0.11)$$

We introduce the auxiliary vector L, the components of which are:

$$L_x = 0, \quad L_y = \frac{r_z}{r^3}, \quad L = -\frac{r_y}{r^3}. \qquad (0.12)$$

Declassified in Part - Sanitized Copy Approved for Release 2013/01/23 : CIA-RDP81-01043R001600090003-8

Declassified in Part - Sanitized Copy Approved for Release 2013/01/23 : CIA-RDP81-01043R001600090003-8

From the above correlations it is apparent that the direction of vector L is fully determined by the coordinates of point P and by element dl.

Here, formula (0.10) may be written in the form:

$$H_x = I \int (L, dl),$$

or, on applying the theorem of Stokes on the conversion of a contour integral to a surface integral:

$$H_x = I \int (\text{rot } L dS), \qquad (0.13)$$

wherein the integration must be extended over the entire surface involved in circuit; the shape and dimensions of the surface being irrelevant. On the other hand, the direction of the normal to the surface element dS depends upon the direction of circuit element dl, which coincides with the direction of the current.

According to the formula we have for the scalar product:

$$(\text{rot } LdS) = \text{rot}_x\, LdS_x + \text{rot}_y\, LdS_y + \text{rot}_z\, LdS_z.$$

Substituting the rotor components according to vector analysis formulas, and the components of the surface element by the corresponding cosines between the normal and the coordinate axes we obtain:

$$(\text{rot } LdS) = [(\frac{\partial L_z}{\partial y} - \frac{\partial L_y}{\partial z}) \cos(n, x) + (\frac{\partial L_x}{\partial z} - \frac{\partial L_z}{\partial x}) \cos(n, y) + (\frac{\partial L_y}{\partial x} - \frac{\partial L_x}{\partial y}) \cos(n, z)]dS. \qquad (0.14)$$

Further, using the correlations (0.11) and (0.12) to determine the derivatives $\frac{\partial L_x}{\partial y}$ and $\frac{\partial L_y}{\partial z}$ and substituting them in equation (0.14) we obtain:

$$(\text{rot } L\ S) = -[\frac{\partial^2(\frac{1}{r})}{\partial x_1 \partial x} \cos(n, x) + \frac{\partial^2(\frac{1}{r})}{\partial x_1 \partial y} \cos(n, y) + \frac{\partial^2(\frac{1}{r})}{\partial x_1 \partial z} \cos(n, z)]dS.$$

Declassified in Part - Sanitized Copy Approved for Release 2013/01/23 : CIA-RDP81-01043R001600090003-8

Declassified in Part - Sanitized Copy Approved for Release 2013/01/23 : CIA-RDP81-01043R001600090003-8

The cosines of the angles between the normal n to the surface element dS and the coordinate axes are derivatives of the corresponding coordinates of the normal, and the above expression assumes the form:

$$(\mathrm{rot}\, A\, dS) = -\frac{\partial}{\partial x_1}\left[\frac{\partial\left(\frac{1}{r}\right)}{\partial x}\cdot\frac{dx}{dn} + \frac{\partial\left(\frac{1}{r}\right)}{\partial y}\cdot\frac{dy}{dn} + \frac{\partial\left(\frac{1}{r}\right)}{\partial z}\cdot\frac{dz}{dn}\right] dS,$$

or

$$(\mathrm{rot}\, A\, dS) = -\frac{\partial}{\partial x_1}\left[\frac{d\left(\frac{1}{r}\right)}{dn}\right].$$

Substituting derivatives for the product of the rotor and the surface element dS in equation (0.13), we have:

$$H_x = -I\frac{\partial}{\partial x_1}\int\frac{d\left(\frac{1}{r}\right)}{dn}\,dS,$$

The components Hy and Hz are determined analogously:

$$H_y = -I\frac{\partial}{\partial y_1}\int\frac{d\left(\frac{1}{r}\right)}{dn}\,dS,$$

whence,

$$H = -I\,\mathrm{grad}\int\frac{d\left(\frac{1}{r}\right)}{dn}\,dS = -I\,\mathrm{grad}\int\frac{dS}{r^2}\cos(r, n).$$

The expression $-\frac{dS}{r^2}\cos(n, r)$ is in fact an element of the solid angle $d\Omega$, at which the element dS is seen from point P, thus we have

$$H = \mathrm{grad}\, I\Omega \qquad (0.15)$$

where Ω is the solid angle at which the circuit is seen from point P, and therefore the quantity $-I\Omega$ may be designated as the magnetic potential of the closed circuit, taking

$$U = -I\Omega. \qquad (0.16)$$

Section 4. Magnetic Potential of an Elemental Circuit

If the closed linear circuit constitutes an elemental circuit the area of which is infinitely small, then in accordance with formula (0.16) its potential dU is given by the equation

$$dU = \frac{I\,dS}{r^2}\cos(r, n)$$

or, in a vectorial form:

$$dU = \frac{I\,(dS, r)}{r^3} \qquad (0.17)$$

Declassified in Part - Sanitized Copy Approved for Release 2013/01/23 : CIA-RDP81-01043R001600090003-8

Declassified in Part - Sanitized Copy Approved for Release 2013/01/23 : CIA-RDP81-01043R001600090003-8

The potential produced by a magnetic dipole is of exactly the same form, i.e., that of 2 point magnetic charges of different sign located very close to each other, because by denoting the magnitude of the magnetic charge by m and the distance between the charges by dl, we readily find by applying Coulomb's law, that

$$dV = \frac{m\,dl}{r^2}\cos(dl, r) = \frac{m(dl, r)}{r^3} \qquad (0.18)$$

The product mdl is termed the magnetic moment u, which is a vector coinciding in direction with dl and equal in magnitude to the product of mass m by the distance between the charges, i.e.,

$$mdl = \mu.$$

Comparison of expressions (0.17) and (0.18) shows that they are equated at:

$$IdS = mdl, \qquad (0.19)$$

i.e., on substituting the elemental current with a magnetic dipole the magnetic moment of which is equal to the product IdS. Therefore, by analogy, the quantity IdS acquires the designation of magnetic moment of elemental current. Thus it may be stated that the designation of magnetic moment of elemental current is given to a vector which in magnitude is proportional to the product of current intensity and area of circuit current, and coincides in direction with the normal to the circuit area dS, i.e.,

$$\mu = IdS.$$

The orientation of the direction remains arbitrary. It has been agreed to consider as positive that direction of the normal which coincides with the direction of advance of a corkscrew which is turned in the direction of the current.

Thus the potential of a magnetic field created by an elemental circuit, and consequently also the magnitude of field strength, are proportional to the magnitude of the magnetic moment of the circuit, i.e.,

Declassified in Part - Sanitized Copy Approved for Release 2013/01/23 : CIA-RDP81-01043R001600090003-8

Declassified in Part - Sanitized Copy Approved for Release 2013/01/23 : CIA-RDP81-01043R001600090003-8

$$U = \frac{(\mu n)}{r^3} \qquad \mu = (A, -),$$

$$F = \mu \nabla \frac{(\mu n)}{r^3} = \mu \left[\frac{3(r n) r}{r^5} - \frac{n}{r^3} \right], \qquad (0.20)$$

where n is a unit vector coinciding in direction with the direction of the magnetic moment.

Therefore the motion of a magnetic moment plays the same part in the treatment of the magnetic field of an electric current, as is played by the motion of the magnetic charge in the treatment of the field of permanent magnets. Applying this motion to a circuit of finite dimensions, it can be shown that the intensity of the magnetic field of a linear circuit also is proportional to the product of current intensity and circuit area which is known as the magnetic moment of the circuit.

In calculating the magnetic potentials of current circuits formulas (0.17) and (0.18) make it possible to replace elemental currents with magnetic dipoles.

Section 5. Magnetic Field of a Circular Linear Current

To find the magnetic potential of a circular linear current of radius R it is necessary to calculate the solid angle Ω as a function of the coordinates of point P. Taking the axis of the circular circuit OX as the basic axis of polar coordinates, then because of the symmetry of the magnetic field in relation to this axis the magnetic potential will depend only on the latitude θ and the polar distance r of point P from the origin of the coordinates 0 (Figure 3), i.e,

$$\Omega = f(r, \theta)$$

From the theory of spherical functions it is known that any function of r and θ which satisfies the Laplace equation can be expanded to a series in powers of r according to one of the following formulas:

$$\Omega = \sum_{n=0}^{\infty} A_n r^n P_n(\cos\theta), \quad \Omega = \sum_{n=0}^{\infty} \frac{B_n P_n(\cos\theta)}{r^{n+1}} \qquad (0.21)$$

Declassified in Part - Sanitized Copy Approved for Release 2013/01/23 : CIA-RDP81-01043R001600090003-8

Declassified in Part - Sanitized Copy Approved for Release 2013/01/23 : CIA-RDP81-01043R001600090003-8

where $P_n(\cos\theta)$ are Legendre polynomials, and A_n and B_n are constant coefficients which are independent of the coordinates of point P.

The Legendre polynomials are algebraic functions of cos θ of powor n and are the coefficients of α in the expansion to a series of the expression

$$\varphi(\alpha) = [1 + \alpha^2 - 2\alpha\cos\theta]^{-\frac{1}{2}},$$

i.e.,

$$\varphi(\alpha) = 1 + \alpha\cos\theta + \alpha^2\left(\frac{3}{2}\cos^2\theta - \frac{1}{2}\right) + \alpha^3\left(\frac{5}{2}\cos^3\theta - \frac{3}{2}\cos\theta\right) + \ldots \sum_{n=0}^{\infty} \alpha^n P_n(\cos\theta),$$

consequently,

$$\left.\begin{aligned} P_0(\cos\theta) &= 1, \quad P_1(\cos\theta) = \cos\theta, \\ P_2(\cos\theta) &= \frac{3}{2}\cos^2\theta - \frac{1}{2}, \\ P_3(\cos\theta) &= \frac{5}{2}\cos^3\theta - \frac{3}{2}\cos\theta \end{aligned}\right\} \qquad (0,22)$$

Of all the properties of Legendre polynomials the following, which are necessary for subsequent deviations, are mentioned:

(1) If the argument of the polynomial cos θ changes its sign the polynomials of even power remain unchanged, and the polynomials of odd power change their sign;

(2) The cos θ derivative of the Legendre polynomial is expressed by the formula:

$$\frac{dP_n(\cos\theta)}{d(\cos\theta)} = \frac{n}{\sin^2\theta}\left[P_{n-1}(\cos\theta) - \cos\theta P_n(\cos\theta)\right], \qquad (0,23)$$

which may be obtained directly by differentiating expression (0.22);

(3) At cos θ = 1 all the polynomials are converted to unity, i.e., $P_n(1) = 1$;

(4) At cos θ = 0 the odd polynomials become zero, and the even:

$$P_{2n}(0) = (-1)^n \frac{1 \cdot 3 \cdot 5 \ldots (2n-1)}{2 \cdot 4 \ldots 2n} \qquad (0,24)$$

Declassified in Part - Sanitized Copy Approved for Release 2013/01/23 : CIA-RDP81-01043R001600090003-8

Declassified in Part - Sanitized Copy Approved for Release 2013/01/23 : CIA-RDP81-01043R001600090003-8

Following these remarks we turn to the derivation of the expression for the solid angle Ω, i.e., to the determination of coefficients A_n and B_n of equation (0.21).

Expansion of Ω for some particular instance and comparison of the coefficients of this expansion with the coefficients A_n and B_n of the same powers, r^n or $\frac{1}{r^{n+1}}$, are sufficient for determination of the coefficients A_n and B_n. Taking the point P_1 on the axis of coordinates, the solid angle Ω to its circular circuit can be readily determined.

Indeed, on circumscribing a spherical surface of radius $P_1C = P$ from point P_1 we obtain

$$\Omega_{P_1} = -\int_S \frac{ds}{\rho^2}\cos(n,\rho) = -2\pi\int_{\zeta=0}^{\alpha}\cos(n,\rho)\sin\zeta\,d\zeta = -2\pi\cos(n,\rho)(1-\cos\alpha),$$

where α is the angle OP, C, and cos (n, p) has a value of either plus one, or minus one, depending upon the direction of the current in the circuit. Assuming that the current is directed clockwise, on looking at it from the origin of the coordinates, then

$$\cos(n,p) = +1,$$

and

$$\cos\alpha = \frac{\rho_1\cos\psi + r_0}{\sqrt{\rho_1^2 + r_0^2 - 2\rho_1 r_0\cos(\pi-\psi)}},$$

where $\psi = \angle OP_1C$ (Figure 3).

Assuming $r_0 < \rho_1$ and removing ρ_0 outside the radical sign, we have:

$$\cos\alpha = \left(\cos\psi + \frac{r_0}{\rho_1}\right)\left[1 + \left(\frac{r_0}{\rho_1}\right)^2 - 2\frac{r_0}{\rho_1}\cos(\pi-\psi)\right]^{-\frac{1}{2}}.$$

The expression within the second pair of parentheses may be written in the form of a Legendre polynomial series, so that:

$$\cos\alpha = \cos\psi\sum_{n=0}^{\infty}\left(\frac{r_0}{\rho_1}\right)^n P_n[\cos(\pi-\psi)] + \frac{r_0}{\rho_0}\sum_{n=0}^{\infty}\left(\frac{\rho}{r_0}\right)^n P_n[\cos(\pi-\psi)],$$

Declassified in Part - Sanitized Copy Approved for Release 2013/01/23 : CIA-RDP81-01043R001600090003-8

Declassified in Part - Sanitized Copy Approved for Release 2013/01/23 : CIA-RDP81-01043R001600090003-8

Substituting this value of $\cos\psi$ in the expression P_1, and after simple transpositions, we obtain

$$\Omega_{P_1} = -2\pi\left\{1-\cos\psi-\cos\theta+\sum_{n=0}^{\infty}\left(\frac{r}{r_0}\right)^n P_n[\cos(\pi-\psi)]+\right.$$

$$\left.\sum_{n=0}^{\infty}\left(\frac{r}{r_0}\right)^n P_n[\cos(\pi-\theta)]\right\}=$$

$$-2\pi\left\{1-\cos\psi-\sum_{n=1}^{\infty}\left(\frac{r}{r_0}\right)^n[P_{n-1}(\cos(\pi-\psi))-P_n(\cos(\pi-\psi))]\right\}$$

The expression within the summation sign in brackets may be substituted by the derivative of the polynomial according to formula (0.23) because of the properties of Legendre polynomials.

$$\Omega_P = -2\pi\left\{1-\cos\psi-2\sum_{n=1}\frac{1}{n}\left(\frac{r}{r_0}\right)^n\frac{dP_n[\cos(\pi-\psi)]}{d\cos(\pi-\psi)}\right\} \quad (0.25)$$

For points located on the axis of the circuit $\theta = 0$, and therefore the expression for the solid angle (0.21) becomes one of the following:

$$\Omega = -\sum A_n r^n, \qquad r < r_0,$$

or

$$\Omega = -\sum\frac{C_n}{r^{n+1}}, \qquad r > r_0,$$

where P_0 is the distance from the origin of the coordinates to the circuit.

Equating the first of the above equations with the expression (0.25) we obtain:

$$A_0 = 1-\cos\psi, \quad A_n = \sin^2\psi\,\frac{1}{n}\cdot\frac{dP_n[\cos(\pi-\psi)]}{d\cos(\pi-\psi)}\cdot\frac{1}{r_0^n}.$$

Consequently, the potential of a circular circuit at any point of its extent, under the conditions $r < P_0$ and $\theta < \frac{\pi}{2}$, has the form:

$$U = -\Omega I =$$

$$I\left\{1-\cos\psi-\sin^2\psi\sum_{n=1}\frac{1}{n}\left(\frac{r}{r_0}\right)^n P_n(\cos\theta)\frac{dP_n[\cos(\pi-\psi)]}{d\cos(\pi-\psi)}\right\} \quad (0.26)$$

For points located to the left of the origin of coordinates, for which $\theta > \frac{\pi}{2}$, the expression for the potential is:

Declassified in Part - Sanitized Copy Approved for Release 2013/01/23 : CIA-RDP81-01043R001600090003-8

Declassified in Part - Sanitized Copy Approved for Release 2013/01/23 : CIA-RDP81-01043R001600090003-8

$$U = -2\pi I\left(1 - \cos\psi - \cos^2\psi \sum_{n=1}^{\infty} \frac{n}{n+1}\left(\frac{r}{r_0}\right)^n P_n(\cos\theta)\frac{P'_n(\cos\psi)}{\sin\psi}\right)$$

The components of the intensity of the magnetic field along axis x and the axis y are determined by the relationships

$$H_x = -\frac{1}{x} = -\frac{1}{r_0} \sum_{n=1}^{\infty} \left(\frac{r}{r_0}\right)^{n-1} P'_n(\cos\psi)$$

$$[\cos\theta P_n(\cos\theta) + \frac{\sin^2\theta}{n} P'_n(\cos\theta)] \quad (0.27)$$

$$H_y = -\frac{\partial U}{\partial y} = -2I \frac{\sin\psi}{r_0^2} \sum_{n=1}^{\infty} (n+1)\left(\frac{r}{r_0}\right)^{n-1} P_n(\cos\theta)[P_n(\cos\psi) - \frac{\cos\psi}{n} P'_n(\cos\psi)]. \quad (0.28)$$

where $P'_n(\cos\theta)$ and $P'_n(\cos\psi)$ denote the derivatives of $\cos\theta$ and $\cos\psi$.

Furthermore, on substituting the expression in brackets according to formula (0.23) we obtain the following expression for H_x:

$$H_x = \frac{-2\pi I \sin\psi}{r_0} \sum_{n=1}^{\infty} \left(\frac{r}{r_0}\right)^{n-1} P_{n-1}(\cos\psi).$$

Taking into account the formulas for Legendre polynomials and substituting $\sin\psi$ and $\cos\psi$ with their values at $x_0 = 00\frac{1}{2}$ and p_0, we have:

$$H_x = \frac{-2\pi I K^2}{r_0^3}\left[1 + \frac{3}{2}\left(-x_0^2 - K^2\right)\cos\theta + \frac{1}{4}\left(\frac{r_0}{r}\right)^2\left(3\cos^2\theta - 1\right) + \frac{3}{4}\left(\frac{r_0}{r}\right)^3\left(5\cos^3\theta - 3\cos\theta\right) + \frac{15}{4}\left(\frac{r_0}{r}\right)^4\left(21\cos^4\theta - 14\cos^2\theta + 1\right)\right], \quad (0.29)$$

$$H_y = \frac{2\pi I K^2 y}{r_0^5}\left[1 + \frac{5}{2}\left(-x_0^2 - 2K^2\right)\cos\theta - \frac{5}{2}\left(\frac{r_0}{r}\right)^2\left(7\cos^2\theta - 1\right)\right]. \quad (0.30)$$

For points located on the y axis, where $\theta = 90^\circ$ and $r = y$, the formulas for H_x and H_y, which are accurate up to terms of fourth order, assume the form:

Declassified in Part - Sanitized Copy Approved for Release 2013/01/23 : CIA-RDP81-01043R001600090003-8

Declassified in Part - Sanitized Copy Approved for Release 2013/01/23 : CIA-RDP81-01043R001600090003-8

$$H_y = \frac{2\pi I}{\rho_0}\left[1 + \frac{3}{4}\frac{r^2}{\rho_0^2}\left(1 - 4k^2 + 4k^2\frac{x^2}{\rho_0^2}\right) + \frac{15}{64}\frac{r^4}{\rho_0^4}\left(1 - 12k^2 + 24k^2\frac{x^2}{\rho_0^2} - 8k^2\frac{y^2}{\rho_0^2}\right)\right], \qquad (0.29a)$$

$$H_x = \frac{2\pi I}{\rho_0}\frac{x}{\rho_0}\left[1 - \frac{3}{8}\frac{r^2}{\rho_0^2}\left(3k^2 - 4\frac{y^2}{\rho_0^2}\right) - \frac{35}{64}\frac{r^4}{\rho_0^4}\left(5k^4 - 20k^2\frac{y^2}{\rho_0^2} + 8\frac{y^4}{\rho_0^4}\right)\right] \qquad (0.30a)$$

At the origin of coordinates, the point 0:

$$H_x = \frac{2\pi I k^2}{\rho_0}; \qquad H_y = 0$$

which result is known from elementary physics.

Since the magnitude of the field intensity does not depend upon the selsction of the coordinates, for practical purposes the most convenient formulas are (0.29a) and (0.30a) in which the origin of the coordinates coincides with a projection of the point under consideration on the axis of the circular circuit.

Section 6. The Effect of Finite Dimensions of the Circuit Cross-Section

In the formulas for magnetic potential and field intensity derived in the presiding section it was assumed that the current flows over an infinitely thin (linear) wire. Actually the cross section of the wire always has finite dimensions and therefore it is necessary to ascertain the extent of the effect of these dimensions and the degree to which formulas (0.29a) and (0.30a) must be altered in order that field intensity values calculated with their aid coincide with the observed values.

Assuming that the cross section of the circular circuit has the shape of a rectangle with sides 2a and 2b, and that a current of uniform density j (Figure 4) flows through this circuit.

Declassified in Part - Sanitized Copy Approved for Release 2013/01/23 : CIA-RDP81-01043R001600090003-8

Declassified in Part - Sanitized Copy Approved for Release 2013/01/23 : CIA-RDP81-01043R001600090003-8

Dividing the area of rectangle S into an infinite number of elemental areas dS, which may be regarded as cross sections of linear circuits, and the circuit itself as regarded as a combination of an infinitely large number of linear circuits, then the magnetic potential U produced by the entire circuit at point P is the sum of the magnetic potentials produced by an infinitely large number of linear circuits; or in the integral form:

$$U = \int dU.$$

where dU is the potential produced by the linear circuit and equals:

$$dU = -\Omega\, dI.$$

where Ω is the solid angle at which one of the linear circuits Q is seen from point P, and $dI = jdS = Iw/S\ dS$. Thus

$$U = -\,w/S \int I\,\Omega\, dS,$$

where w is the number of windings in one of the circuits, and the integration is taken over the entire area of cross section S.

The product $-I\Omega$ may be regarded as the magnetic potential U' produced by a linear circuit with current of intensity I, and therefore we may state:

$$U = w/S \int U'dS. \qquad (0.31)$$

But as we have seen, U' is a function of the radius of the linear circuit R and of its distance x from the origin of the coordinates. Taking one of the circuits with coordinates R_o and x_o as being the initial, circuit, and taking the cross section of this circuit at the center of the rectangle O_1, if the transverse dimensions za and zb of the circuit are small in comparison with the coordinates Ro and Xo, the potential can be expanded to a series according to the formula of Taylor:

$$U' = Uo + \partial Uo/\partial x\ (x-xo) + \partial Uo/\partial R\,(R-Ro) + 1/2\,\partial^2 uo/\partial x^2\,(x-xo)^2 + \partial^2 Uo/\partial x\,\partial R\,(x-xo)\,(R-Ro) + \ldots$$

Declassified in Part - Sanitized Copy Approved for Release 2013/01/23 : CIA-RDP81-01043R001600090003-8

Declassified in Part - Sanitized Copy Approved for Release 2013/01/23 : CIA-RDP81-01043R001600090003-8

wherein Uo is the potential produced by the initial circuit which has a current I.

Substituting this value in formula (0.31), substituting dS = dxdR, and taking into account that all the derivatives will be constant upon integration, we obtain:

$$U = Uo + w/S \cdot \partial Uo/\partial x \int_{-a}^{+a}\int_{-b}^{+b}(x-xo)dxdR + w/S \cdot \partial Uo/\partial R \int_{-a}^{+a}\int_{-b}^{+b}$$

$$(R-Ro)dxdR + \ldots$$

The potential of the initial circuit Uo is expressed in the form of a series (0.26) which may be written as follows:

$$Uo = U1 + U2 + U3 + \ldots$$

Therefore

$$U = U_1 + w/S \cdot \partial U1/\partial x \int_{-a}^{+a}\int_{-b}^{+b}(x-xo)dxdR + w/S \cdot \partial U1/\partial R \int_{-a}^{+a}\int_{-b}^{+b}$$

$$(R-Ro)dxdR + \ldots + U2 + w/S \cdot \partial U2/\partial x \int_{-a}^{+a}\int_{-b}^{+b}(x-xo)dxdR +$$

$$w/S \cdot \partial U2/\partial R \int_{-a}^{+a}\int_{-b}^{+b}(R-Ro)dxdR + \ldots$$

It is readily apparent that the integrals in which the differences $x-x_o$ and $R-R_o$ appear at odd powers become zero, while those of even powers assume the values:

$$\int_{-a}^{+a}\int_{-b}^{+b}(x-x_o)^2\,dx\,dR = \frac{2a^3}{3}\cdot 2b, \qquad \int_{-a}^{+a}\int_{-b}^{+b}(R-R_o)^2\,dx\,dR = \frac{2a}{3}\cdot 2b^3$$

In such a case

$$U = U_1 + \frac{a^2}{2}\cdot\frac{\partial^2 U_1}{\partial x^2} + \frac{b^2}{2}\cdot\frac{\partial^2 U_1}{\partial R^2} + \frac{1}{2!}\cdot\frac{1}{1\cdot 2}\cdot\frac{\partial^4 U_1}{\partial x^2\,\partial R^2} + \frac{2a^2}{5!}\cdot\frac{\partial^4 U_1}{\partial x^4} + \ldots$$

$$\frac{1}{5!}\cdot\frac{\partial^4 U_1}{\partial R^4} + \ldots + U_2 + \frac{a^2}{2}\cdot\frac{\partial^2 U_2}{\partial x^2} + \ldots \qquad (0.32)$$

Analogous expressions are obtained for components of the magnetic field intensity, in which U_2 is derived for the corresponding coordinates, instead of U_1.

Declassified in Part - Sanitized Copy Approved for Release 2013/01/23 : CIA-RDP81-01043R001600090003-8

Declassified in Part - Sanitized Copy Approved for Release 2013/01/23 : CIA-RDP81-01043R001600090003-8

Applying this result to formula (0.29) for the component of field intensity produced on the x axis by a circular circuit having a rectangular cross section, and limiting the corrections made in the first 2 terms, which are of the form

$$\frac{\partial U_1}{\partial x} = \frac{\pi I k^2 \omega}{\rho_0^3}; \quad \frac{\partial U_2}{\partial x} = \frac{3}{2}\frac{\pi I_y^2 k^2 \omega}{\rho_0^5}(k^2 - 4x_0^2).$$

we obtain:

$$H_x = \frac{2\pi I k^2 \omega}{\rho_0^3}\left[1 + \frac{3}{4}(4y_0^2 - k^2) + \frac{3}{16}(8x_0^4 - 1x_0^2(k^2 + r^2))\right] + \frac{3\pi I_y^2 k^2 \omega}{2\rho_0^7}\left[\frac{k^4}{8} - \frac{5}{4}x_0^2 k^2 + \frac{35}{16}x_0^4 - \frac{15}{16}y_0^2 k^2 + \frac{105}{16}x_0^2 y_0^2 + \frac{3}{16}k^4\right] \quad (0.33)$$

Section 7. Magnetic Field of Helmholtz Rings

Two circular circuits of equal diameter placed parallel to each other at a distance equal to their radius R, with their centers on a common axis cc', are called Helmholtz rings.

The peculiarity of these rings is the uniformity of the magnetic field at the center between the rings, and because of this as a source of a uniform magnetic field.

To determine the intensity of the magnetic field of these rings formulas (0.27) and (0.28) will be used, taking the origin of the coordinates at the center of the rings, and arbitrarily taking the distance between the rings as equal to 2d (Figure 5).

Since r, θ and ρ_0 are the same for both circuits, angle ψ differs by 180°, it follows that

$$H_x = \frac{2\pi I \omega \sin^2\psi}{\rho_0^3}\sum_{n=1}^{\infty}\left(\frac{r}{\rho_0}\right)^{n-1} P_{n-1}(\cos\theta)\left\{P_n'(\cos\psi) + P_n'[\cos(\pi - \psi)]\right\}.$$

Because of the properties of Legendre polynomials:

$$P_{2n}(\cos\psi) = -P_{2n}[\cos(\pi - \psi)],$$

$$P_{2n-1}'(\cos\psi) = P_{2n-1}'[\cos(\pi - \psi)].$$

Declassified in Part - Sanitized Copy Approved for Release 2013/01/23 : CIA-RDP81-01043R001600090003-8

Declassified in Part - Sanitized Copy Approved for Release 2013/01/23 : CIA-RDP81-01043R001600090003-8

Because of this all terms containing even powers of the Legendre polynomial derivatives are cancelled and the odd powers are doubled, consequently

$$H_x = 4\pi Iw \sin^2\psi / p_o \sum_{n=1}^{\infty} \left(\frac{r}{p_o}\right)^{2n-1} P_{2n-2}(\cos\theta) P'_{2n-1}(\cos\psi).$$

Retaining only the terms of the fourth order we obtain

$$H_x = \frac{4\pi Iw \sin^2\psi}{p_o}\left[1 + \frac{r^2}{p_o^2} P'_3(\cos\psi) P_2(\cos\theta) + \frac{r^4}{p_o^4} P'_5(\cos\psi) P_4(\cos\theta)\right] \quad (0.34)$$

In an analogous manner we obtain

$$H_y = \frac{4\pi Iw \sin^2\psi}{p_o^2}\left\{\frac{r}{p_o} P_3(\cos\psi)\left[P_3(\cos\theta) - \frac{\cos\psi}{3} P'_3(\cos\theta)\right] + \frac{r^3}{p_o^3} P_5(\cos\psi)\left[P_5(\cos\theta) - \frac{\cos\psi}{5} P'_5(\cos\theta)\right] + \ldots\right.$$

(0.35)

Selecting angle ψ in a manner so that the second order term in equation (0.34) becomes zero, this requires that $P'_3(\cos\psi) = 0$, or $5/2 \cos^2\psi - 1/2 = 0$, hence

$$\cos^2\psi = 1/5.$$

since

$$\cos^2 = d^2/d^2 + R^2, \text{ it follows that } d = R/2.$$

Consequently, when the circuits are separated by a distance equal to their radius, the term of the second order, on expansion of H to a series, becomes equal to zero. Therefore for points located at a distance r from the center, which is small in comparison with half the distance between the circuits, the field intensity component on the axis CC' will be almost the same, i.e., the magnetic field in the central portion of the circuits may be considered as uniform and accurate up to the terms of the fourth order.

Declassified in Part - Sanitized Copy Approved for Release 2013/01/23 : CIA-RDP81-01043R001600090003-8

Declassified in Part - Sanitized Copy Approved for Release 2013/01/23 : CIA-RDP81-01043R001600090003-8

The advantage of this system over a solenoid, in the center of which the field also is uniform, is the accessibility of this field to the observer. The space within which the uniform field is formed is entirely free of any apparatus and makes it possible to place any specimens of materials or instruments inside the field, provided their overall dimensions do not exceed those of the coil.

The disadvantage of Helmholtz rings with respect to a solenoid is the fact that strong fields cannot be produced.

The intensity of the magnetic field produced by Helmholtz rings usually does not exceed several tens of oersteds, whereas a solenoid may produce a uniform field of the order of 1,000 Oe.

Substituting the values of p, sin θ and cos θ, expressed by means of R, for H_x and H_y in formulas (0.34) and (0.35) we obtain:

$$H_x = \frac{3 2\pi i w}{\sqrt{\quad}} \left[1 + \frac{\quad}{\quad} \frac{r^2}{R^2} P_2'(\cos\theta) - \ldots \right] \qquad (0.36)$$

$$H_\theta = \frac{\quad}{\sqrt{\quad}} \frac{r}{R} \left[P_1'(\cos\theta) - \frac{r^2}{R^2} P_3'(\cos\theta) + \ldots \right] \qquad (0.37)$$

Since,

$$P_2'(\cos\theta) = \frac{1}{2}\left(3\cos^2\theta - 1\right) = \frac{1}{2}\left(3\cos 2\theta + 3\right)$$

and

$$P_4'(\cos\theta) = \frac{1}{8}\left(35\cos^3\theta - 30\cos\theta + 3\right),$$

at $\cos\theta = x/r$ and $r^2 = x^2 + y^2$, upon substituting these values in the above expressions and bearing in mind that Ia is equal to 0.1 of the absolute electromagnetic unit, we obtain

$$H_x = 0.9918 \frac{I w}{R} \left[1 - 0.114 \frac{r^2}{R^2} (8x^2 - 24x^2y^2 + 3y^4) + \ldots \right] \qquad (0.38)$$

$$H_y = 0.35792 \frac{I w}{R^3} \left[x(4x^2 - 3y^2) + \ldots \right]. \qquad (0.39)$$

where x and y are the coordinates of point P, taken from the center of the rings.

Declassified in Part - Sanitized Copy Approved for Release 2013/01/23 : CIA-RDP81-01043R001600090003-8

Declassified in Part - Sanitized Copy Approved for Release 2013/01/23 : CIA-RDP81-01043R001600090003-8

To give an idea of the degree of uniformity of the magnetic field of Helmholtz rings, tables 1 and 2 are included, showing relative values of both components at different points in the space within the rings, i.e., for different values of the coordinates x and y. The value at the center of the field is taken as the unit of field intensity and x and y are expressed as the length of the radius of the rings.

TABLE 1

VALUES OF H_x

x \ y	0	0.05	0.10	0.15	0.20
0	1.00000	0.999997	0.999957	0.999781	0.999309
0.05	0.999993	1.000012	1.000036	0.999969	0.999847
0.10	0.999885	0.999968	1.000187	1.000444	1.000576
0.20	0.998157	0.998500	0.999496	1.001049	1.002995

TABLE 2

VALUES OF H_y

x \ y	0	0.05	0.10	0.15	0.20
0	0	0	0	0	0
0.05	0	$+ 0.4 \cdot 10^{-6}$	$- 5.8 \cdot 10^{-6}$	$- 24.8 \cdot 10^{-6}$	$-63.3 \cdot 10^{-6}$
0.10	0	$+ 9.3 \cdot 10^{-6}$	$+ 5.8 \cdot 10^{-6}$	$- 2.4 \cdot 10^{-6}$	$-92.2 \cdot 10^{-6}$
0.15	0	$+35.6 \cdot 10^{-6}$	$+ 51.8 \cdot 10^{-6}$	$+ 29.2 \cdot 10^{-6}$	$-51.8 \cdot 10^{-6}$
0.20	0	$+87.8 \cdot 10^{-6}$	$+149.8 \cdot 10^{-6}$	$+160 \cdot 10^{-6}$	$+92.2 \cdot 10^{-6}$

These results refer to Helmholtz rings consisting of 2 linear circular currents. In practice they usually consist of 2 coils of rectangular cross section placed so that the central windings form Helmholtz rings. The formulas derived in the preceding sections for a circular circuit having a cross section with finite dimensions may be used for making corrections for the finite dimensions of the cross section of the coil.

Declassified in Part - Sanitized Copy Approved for Release 2013/01/23 : CIA-RDP81-01043R001600090003-8

Declassified in Part - Sanitized Copy Approved for Release 2013/01/23 : CIA-RDP81-01043R001600090003-8

Since in the Helmholtz rings the origin of the coordinates is taken at their center, in making corrections it is necessary to use formulas of the general form (0.29), (0.30) and to determine the appropriate correction for each of the terms.

For the first and third terms the corrections were given in equation (0.33). The correction for the second term contains the factor X_0, and since the Helmholtz rings comprise 2 circuits, located at the same distance X_0 from the origin of the coordinates, it follows that for one circuit this correction has the factor $+X_0$ and for the other $-X_0$, and as a sum they are cancelled.

In applying the expression (0.33) to the Helmholtz rings the condition $X_0 = R/2$ must be assumed. Under the condition equation (0.33) becomes:

$$H_x = 32\pi Iw/5\sqrt{5}R\ [1-b^2/15R^2-16/375\ (36a^6-31b^2)r^2/R^4\ (3\cos^2\theta-1)],$$

or, on substituting x and y for r and θ, accurate to terms of the second order:

$$H_x=32\pi Iw/5\ 5R[1-b^2/15R^2-16/375R^4(2x^2-y^2)(36a^2-31b2)].$$

If the dimensions of the cross section are selected so that

$36a^2-31b^2=0$, that is $a/b=\sqrt{31/36}$,

the corrections for the third term also become zero. Corrections of the subsequent terms may be disregarded since they contain R^6 and R^8 in the denominator.

Thus the component of field intensity on the x axis, accurate to terms of the fourth order, assumes the form:

$$H_x = \ldots \frac{Iw}{R}\left[1-\frac{b^2}{15R^2}-\ldots\frac{a^4}{R^4}(4x^2-y^2)\right.$$
$$\left.\ldots\right)-\ldots\frac{a^4}{R^4}(4x^4-12x^2y^2+3y^4)\Big].$$

(0.40)

Declassified in Part - Sanitized Copy Approved for Release 2013/01/23 : CIA-RDP81-01043R001600090003-8

Declassified in Part - Sanitized Copy Approved for Release 2013/01/23 : CIA-RDP81-01043R001600090003-8

Corrections of the y axis component may be disregarded because they contain R at a power higher than 5 in the denominator.

Section 8. Magnetic Field of a Cylindrical Solenoid

A single-layer solenoid may be considered as a cylinder over the surface of which a circular current flows porpendicularly to the turns of wire which form the cylinder, assuming that the surface density of the current remains constant. Taking the length L of the solenoid and the number of turns w, the density of this current will be:

$$j = Iw/L,$$

where I is the intensity of the current in the winding.

The field of this solenoid is equivalent to the field of an infinite number of linear circular currents each of which has a current intensity

$$dI = jdl = Iwdl/L,$$

where dl is the solenoid length.

Therefore the potential U of such current is equal to the sum of potentials produced by each of them and is defined by the expression (0.26), in which it is necessary only to substitute the former for current intensity, i.e.,

$$U = -Iw/L \int \Omega \, dl.$$

Taking theorigin of coordinates at some point 0 on the axis of the solenoid (Figure 6), the point P, at which the potential is being considered, is at distance r from the origin of the coordinates, r being less than the radius of the cylinder, and Q as one of the linear circuits of the solenoid, defined by the coordinates P_o and ψ, then

$$U = \frac{2\pi Iw}{L} \int [1 - \cos\psi - \cos^2\psi \sum_{n=1}^{\infty} A_n \left(\frac{r}{r_0}\right)^n P_n(\cos\theta) P'_n (\cos\psi)] \, dR.$$

Declassified in Part - Sanitized Copy Approved for Release 2013/01/23 : CIA-RDP81-01043R001600090003-8

Declassified in Part - Sanitized Copy Approved for Release 2013/01/23 : CIA-RDP81-01043R001600090003-8

wherein the integration must be carried out for the entire length L of the solenoid.

In the integration r and θ remain constant. Moreover, the first term of the series $\int(1-\cos\psi)$ also is constant and is of no significance in determination of the components of field intensity. Eliminating the latter and transposing the constant factors outside the sign of integration we obtain:

$$U = \frac{2\pi I w}{L} \sum_{n=1} \frac{1}{n} F(\cos\psi) \int \frac{\sin\psi}{r} P'_n(\cos\psi)\, d\psi$$

where the derivative of $P_n(\cos\psi)$ with respect to $\cos\psi$ is designated by $P'_n(\cos\psi)$. The triangle OCB, in which OC is denoted by l, yields:

$$r_1 = \frac{a}{\sin\psi} \qquad \cos\psi = \frac{l}{r_1}$$

whence

$$d\psi = \frac{a}{l^2 + a^2}\, dl$$

Substituting the derived values for P_o and dl in the function within the integration sign, we obtain:

$$U = -\frac{2\pi I w}{L} \sum_{n=1} \frac{1}{n} F(\cos\psi) \int_{l_1}^{l_2} P'_n(\cos\psi)\, dl \qquad (0.41)$$

where ψ_1 and ψ_2 are the angles at which the radii of the ends of the solenoid are seen from point O. From the statement:

$$A_n = \frac{1}{n-1} \int_{\psi_1}^{\psi_2} P'_{n-1}(\cos\psi)\, d\psi \qquad (0.42)$$

we have

$$U = -\frac{2\pi I}{L} \sum_{n=1}^{\infty} A_n \cdot P_n(\cos\theta) \qquad (0.43)$$

The coefficients A_n are constant at the given dimensions of the solenoid and vary changes in the origin of coordinates. The series (0.43) is absolutely converging only if $r < a$.

The components H_x and H_y of the intensity of the magnetic field

Declassified in Part - Sanitized Copy Approved for Release 2013/01/23 : CIA-RDP81-01043R001600090003-8

Declassified in Part - Sanitized Copy Approved for Release 2013/01/23 : CIA-RDP81-01043R001600090003-8

of the solenoid are determined by the formulas:

$$H_x = -\frac{\partial U}{\partial x} \quad H_y = -\frac{\partial U}{\partial y} \quad H_\theta = -\frac{\partial U}{r\partial\theta}$$

Substituting the values of U from the expression (0.41) we obtain:

$$H_x = \frac{2\pi I\omega}{L} \sum_{n=1}^{\infty} n \left[\ldots \right],$$

$$H_y = \frac{2\pi I\omega}{L} \sum_{n=1}^{\infty} A_n \left[\ldots \right].$$

Replacing $P'_n(\cos\theta)\sin^2\theta$ with value from equation (0.23), we obtain for H_x the expression:

$$H_x = \frac{2\pi I\omega}{L} \sum_{n=1}^{\infty} A_{n-1} P_{n-1}(\cos\theta)$$

Since the origin of coordinates can be taken at any point provided r is less than the radius of the solenoid a, it is most convenient to place it at the intersection of the axis of the solenoid with a perpendicular from point P (Figure 9).

In this case $\theta = 90$, $\cos\theta = 0$ and $r = y$. But at $\cos\theta = 0$ all the polynomials P_n having odd powers become zero, while the even powers become constant numbers. The derivatives of $P'_n(\theta)$ polynomials will be zero at even powers and constants at odd powers, hence

$$H_x = \frac{2\pi I\omega}{L} \sum_{n=0}^{\infty} A_{2n+1} P_{2n+1}(\cos\theta), \quad \cos\theta = 0,$$

$$H_y = \frac{2\pi I\omega}{L} \sum_{n=1}^{\infty} n A_{n-1} P_{n-1}(\cos\theta)$$

Substituting the value of $P_{2n}(0)$ obtained from equation (0.24), we have:

$$H_x = \frac{2\pi I\omega}{L} \sum_{n=0}^{\infty} (-1)^n \frac{1\cdot3\cdot5\cdots(2n+1)}{2\cdot4\cdot6\cdots 2n} A_{2n+1} y^{2n}, \qquad (0.44)$$

$$H_y = \frac{2\pi I\omega}{L} \sum_{n=0}^{\infty} (-1)^n \frac{1\cdot3\cdot5\cdots(2n-1)}{2\cdot4\cdot6\cdots(2n-2)} A_{2n} y^{2n-1} \qquad (0.45)$$

These formulas hold for every point within the radius of the solenoid. Thus the coefficients A_{2n} and A_{2n+1} are functions of the distance of the origin of coordinates from the center of the solenoid.

Declassified in Part - Sanitized Copy Approved for Release 2013/01/23 : CIA-RDP81-01043R001600090003-8

Declassified in Part - Sanitized Copy Approved for Release 2013/01/23 : CIA-RDP81-01043R001600090003-8

For points located on the solenoid axis for which y = 0, the formulas assume the form:

$$H_x = 2\pi Iw/L \quad A_1; \qquad H_y = 0.$$

To determine the A_n coefficients it is necessary only to insert the values of the Legendre polynomial derivatives in expression (0.42) and to integrate, which gives:

$$A_1 = \cos\psi_1 + \cos\psi_2, \quad A_2 = \frac{1}{2a}(\cos^2\psi_1 - \cos^2\psi_2),$$

$$A_3 = -\frac{1}{2a^2}\left[\left(\cos^3\psi_1 + \cos^3\psi_2\right) - 3\left(\cos\psi_1 + \cos\psi_2\right)\right],$$

$$A_4 = \frac{1}{8a^3}\left[\left(\cos^4\psi_1 - \cos^4\psi_2\right) - \frac{3}{2}\left(\cos^2\psi_1 - \cos^2\psi_2\right)\right],$$

$$A_5 = -\frac{1}{8a^4}\left[\frac{3}{2}\left(\cos^5\psi_1 + \cos^5\psi_2\right) - 5\left(\cos^3\psi_1 + \cos^3\psi_2\right) + \frac{15}{4}\left(\cos^2\psi_1 + \cos^2\psi_2\right) - \left(\cos\psi_1 + \cos\psi_2\right) + \frac{1}{2}\left(\cos\psi_1 + \cos\psi_2\right)\right].$$

It is seen from Figure 6 that the cosines and sines of the angles are defined by the formulas:

$$\cos\psi_1 = \frac{l-x}{\sqrt{(l-x)^2 + r^2}}; \quad \sin\psi_1 = \frac{r}{\sqrt{(l-x)^2 + r^2}};$$

$$\cos\psi_2 = \frac{l+x}{\sqrt{(l+x)^2 + r^2}}; \quad \sin\psi_2 = \frac{r}{\sqrt{(l+x)^2 + r^2}}, \qquad (0.46)$$

where l is half the length of the solenoid, and x the distance from the center of the solenoid to point P.

Consequently, for points located on the solenoid axis:

$$H = \frac{2\pi Iw}{L}\left[\frac{l+x}{\sqrt{r^2 + (l+x)^2}} + \frac{l-x}{\sqrt{r^2 + (l-x)^2}}\right] \qquad (0.47)$$

Declassified in Part - Sanitized Copy Approved for Release 2013/01/23 : CIA-RDP81-01043R001600090003-8

Declassified in Part - Sanitized Copy Approved for Release 2013/01/23 : CIA-RDP81-01043R001600090003-8

For the central point, where x = 0,

$$H_o = 4\pi Iw/L \cdot 1/\sqrt{a^2 + 1^2}, \qquad (0.48)$$

and at 1, much greater than a:

$$H_o = 4\pi Iw/L \left[1-1/2(a/1)^2+3/8(a/1)^4+ \ldots\right].$$

For the point located at the end of the solenoid, where x=1:

$$H_1 = 2\pi Iw/L \cdot 21/\sqrt{a^2 + 41^2},$$

or

$$H_1 = 2\pi Iw/L \left[1-1/2(2/21)^2 + 3/8(a/21)^4 - \ldots\right],$$

i.e., the intensity of the field at the end of the solenoid is almost one-half the intensity at the center.

The nature of variations of field intensity inside the solenoid, along its axis, is indicated in Table 3.

TABLE 3

Distance from center in parts of the solenoid length	0	0.01	0.02	0.05	0.1	0.5
Intensity of the field	1	0.99995	0.99981	0.99875	0.99503	0.98058

Section 9. Magnetic Field of a Multilayer Solenoid (Coil)

The magnetic field of a multilayer solenoid, consisting of w_2 layers with w_1 turns in each layer, of total length L, and having a depth of layers D, is determined analogously to the case of a single-layer solenoid, by integration of the potential of an infinitely thin wire, the current intensity in which is

$$dI = Iw_1w_2/LD \; dLdD,$$

i.e.,

$$U = \frac{2\pi I w_1}{L} \sum_{n=1} \frac{1}{n} \cdot P_n(\cos\vartheta) \iint \frac{r^2}{\rho_0} P_n'(\cos\psi) dD \; L.$$

Declassified in Part - Sanitized Copy Approved for Release 2013/01/23 : CIA-RDP81-01043R001600090003-8

Declassified in Part - Sanitized Copy Approved for Release 2013/01/23 : CIA-RDP81-01043R001600090003-8

Taking $O_1M = a$ and $OO_1 = x$, (Figure 7) we have:

Substituting P_o, dD and dL with their values, we obtain:

where a is the internal radius of the solenoid and b the external radius.

It must be remembered that the series converge on the condition that point P. for which potential is sought, is located at a distance from the solenoid axis, less than the internal radius of the solenoid a. Inserting the former conditional values (0.42), we obtain as the first integral:

Since the integral $\int_a^b A_n da$ does not depend on the coordinates of point P, on denoting this integral by B_n we obtain the following expressions for the components of the intensity of the magnetic field, which are analogous to the expression (0.44) for a single-layer solenoid:

(0.49)

(0.50)

The coefficients B_n may be found by simple integration of expressions (0.42) in which sin φ and cos are replaced by their values determined from the equation (0.46), i.e.,

It is apparent the determination of the integrals reduces itself to an integration of irrational functions of the form:

Declassified in Part - Sanitized Copy Approved for Release 2013/01/23 : CIA-RDP81-01043R001600090003-8

Declassified in Part - Sanitized Copy Approved for Release 2013/01/23 : CIA-RDP81-01043R001600090003-8

$$\Sigma_n = \int f(a, \sqrt{a^2 + c^2})\, da,$$

where f(x, y) is a rational function of the variables x and y. Such functions are integrated by substitution of $\sqrt{a^2 + c^2} = z - a$, where z is a new variable.

The rational functions which remain after the substitution are easily integrated.

Thus for example, for B_1 the substitution yields:

$$\Sigma = (I + x) \int \frac{\quad}{\quad} + (I - x) \int \frac{\quad}{\quad},$$

whence

$$\Sigma_1 = (I + x) \frac{\quad}{\quad} + (I - x) \frac{\quad}{\quad} \qquad (0.51)$$

In accordance with expression (0.49) the field intensity of the axis of the solenoid, where y = 0 is:

$$H = \frac{\quad}{DL},$$

where I is the current intensity in amperes and B_1 is the function defined by equation (0.51).

The formulas derived above establish the correlation between the intensity of the magnetic field and the dimension of the coils, their shape and the current intensity, and consequently enable determination of the intensity of the magnetic field from measurement of the geometric dimensions of the coil and current intensity.

Section 10. Magnetization of Geological Rock

All rocks possess magnetic properties by which they may be classified according to 3 types: diamagnetic, paramagnetic and ferromagnetic.

Among the elements of the periodic table of D. I. Mendeleyev the ferromagnetic elements include iron, nickel, cobalt and gadolinium. The other elements are either diamagnetic or paramagnetic.

Declassified in Part - Sanitized Copy Approved for Release 2013/01/23 : CIA-RDP81-01043R001600090003-8

Declassified in Part - Sanitized Copy Approved for Release 2013/01/23 : CIA-RDP81-01043R001600090003-8

The ferromagnetic rocks of greatest interest and importance since the local characteristics of the magnetic field of the earth are associated with the presence of ferromagnetic rocks within the earth's crust.

Ferromagnetism, according to the current concepts developed by the Soviet physicists Ya. G. Dorfman, Ya. I. Frenkel, N. S. Akulov, S. V. Vonsovskiy, Ye. I. Kondorskiy and others, is brought about by orientation of the natural magnetic moments u (spins) of electrons in a single direction. However, such an orientation does not occur throughout the entire volume of a given body but only in a small portion of the order of 10^{-9} cm^3, called the region of spontaneous magnetization, or domain. Each domain is oriented in such a manner that in combination the total magnetization is equal to zero and in its natural state the rock is "neutral", i.e., is not magnetized.

Under the influence of a magnetic field a redistribution of the dimensions of the individual domains and also in the direction of their magnetization occurs and the rock becomes magnetized in a single direction parallel to the field.

Without considering the process of this redistribution, which explains the phenomenon of magnetization of ferromagnetic materials, only the formal aspects of this problem which enable determination of the quantitative correlations between the magnetizing field and the magnetization of the rock will be discussed.

As previously stated, the theory of ferromagnetism is based on the experimental fact of the presence in the electron of a natural magnetic moment u which, as does the charge of the electron, constitutes elemental magnetic moment.

Declassified in Part - Sanitized Copy Approved for Release 2013/01/23 : CIA-RDP81-01043R001600090003-8

Declassified in Part - Sanitized Copy Approved for Release 2013/01/23 : CIA-RDP81-01043R001600090003-8

The geometric sum of all the elemental moments within a given rock is called the magnetic moment M of the rock and characterizes the degree of magnetization of the rock. Considerably separate small portions of the rock volume, in every such part dv the geometric sum of elemental magnetic moments, with an equal value dv, can differ in magnitude as well as in direction. Indicating the magnetic moment of this volume by dM, the ratio of the latter to the volume dv is called the intensity of magnetization or simply the magnetization of the rock, and is denoted by the letter J, i.e.,

$$J = dM/dv. \tag{0.52}$$

As is apparent, magnetization is a vector which coincides in direction with the vector dM and characterizes the magnetic state of the rock at all of its points.

In accordance with equation (0.52) the magnetic moment M of a rock is expressed:

$$M = \int J dv,$$

where the integration extends to the entire volume of the rock.

Magnetization may be distributed within a rock according to any law, provided the condition that the flow of vector J through its entire surface is equal to zero is satisfied, i.e.,

$$\int (J, ds) = 0. \tag{0.53}$$

If the magnetization J is identical in magnitude and direction at all points of a rock, the magnetization of the rock is termed uniform. It is clear that in the case of a uniformly magnitized rock its magnetic moment is equal to the produce of the magnetization and the volume, i.e.,

$$M = Jv.$$

Declassified in Part - Sanitized Copy Approved for Release 2013/01/23 : CIA-RDP81-01043R001600090003-8

Declassified in Part - Sanitized Copy Approved for Release 2013/01/23 : CIA-RDP81-01043R001600090003-8

In the CGS system the unit of magnetization is the magnetization of a body of 1 cm^3 volume having a magnetic moment equal to unity. The unit of magnetization has no specific name.

As stated above, under the influence of a magnetic field the rock acquires a magnetic moment, i.e., its magnetization J becomes different from zero. With increasing intensity of the field H the magnitude of J also increases, but only to a certain magnitude which is called saturation and is denoted by the symbol J_s. Consequently, each value of H at any point of the rock has a corresponding value J.

The ratio of the quantity J to the quantity H is called magnetic susceptibility and is denoted by the letter N, i.e.,

$$N = J/H.$$

In paramagnetic and diamagnetic rocks the quantity N does not depend upon J and is constant. It characterizes the magnetic properties of these rocks and is called the parameter of the rock.

In the case of ferromagnetic substances the susceptibility N is a complex function not only of J but also of the previous history of the magnetic state of the ferromagnetic substance, therefore its magnetic properties of ferromagnetic substances only on the condition that the magnitude of J to which it relates and its magnetic state prior to magnetization is specified.

The magnitude of specific susceptibility X, i.e., of the susceptibility relating to a unit of density, ordinarily is used in measuring N for the characterization of para- and diamagnetic substances.

$$X = x/d,$$

where d is the density of the substance.

Declassified in Part - Sanitized Copy Approved for Release 2013/01/23 : CIA-RDP81-01043R001600090003-8

Declassified in Part - Sanitized Copy Approved for Release 2013/01/23 : CIA-RDP81-01043R001600090003-8

Section 11. Magnetic Potential of a Magnetized Body

Since every ferromagnetic substance consists of domains of small dimensions the volumes of which may be considered infinitely small and may be regarded as elemental magnets, i.e., as dipoles, the magnetic potential dU of each of which is expressed as:

$$dU = (d\mu, r)/r^3$$

where $d\mu$ is the magnetic moment of the domain.

Since $d\mu = J\,dv$ where dv is the volume, it follows that

$$DU = (J, r)/r^3\,dv,$$

or

$$dU = -(J \text{ grad } 1/r)\,dv.$$

Consequently, the potential U of the entire body at point P (Figure 8) is:

$$U = -\int (J \text{ grad } 1/r)\,dv \qquad (0.54)$$

the integration being carried out for the entire volume of the given body, and the gradient taken for coordinates of point P.

If the gradient of function 1/r is formulated in coordinates of a point Q, it is known that

$$\text{grad}_P\, 1/r = -\text{grad}_Q\, 1/r,$$

and the preceding expression becomes:

$$U = \int (J \text{ grad}_Q\, 1/r)\,dv.$$

Applying the familiar vector analysis formula for the divergence of the vector-scalar product to the expression within the integration, we obtain:

$$U = \int \text{div}(J/r)\,dv - \int \text{div } J/r\,dv.$$

The first integral is converted to a surface integral according to the formula of Ostrogradskiy-Gauss, and therefore:

Declassified in Part - Sanitized Copy Approved for Release 2013/01/23 : CIA-RDP81-01043R001600090003-8

Declassified in Part - Sanitized Copy Approved for Release 2013/01/23 : CIA-RDP81-01043R001600090003-8

$$U = \int_S Jds/r - \int_V \text{div } J/r \, dv. \qquad (0.55)$$

The first integral applies to the entire surface of the magnetized body, and the second to its entire volume.

The derived expression is entirely analogous to the expression of the potential of electric charges distributed on the surface with a density σ and within the body with a density p, assuming that fictitious magnetic charges are distributed on the surface of the body with a density

$$\sigma = Jn \qquad (0.56)$$

and within the body, with a volume density

$$p = -\text{div } J \qquad (0.57)$$

Expression (0.55) holds for any point of space, both within and outside the body.

Assuming vector J is constant in equation (0.54), i.e., assuming the body is uniformly magnetized, this equation is converted as follows:

$$U = -(J \int \text{grad}_p \ 1/r \, dv).$$

Since the gradient operation is carried out with respect to the coordinates of point P, and integration is carried out with respect to the coordinates of point Q, the sequence of the gradient and integration operations may be reversed, and we have:

$$U = -(J \text{ grad} \int dv/r). \qquad (0.58)$$

Introducing the expression

$$V = \int dv/r,$$

we obtain a simple expression for the magnetic potential:

$$U = -(J \text{ grad } V), \qquad (0.59)$$

where the quantity V is proportional to the gravitational potential by the magnetized body on the assumption that the density throughout the body is equal to unity.

Declassified in Part - Sanitized Copy Approved for Release 2013/01/23 : CIA-RDP81-01043R001600090003-8

Declassified in Part - Sanitized Copy Approved for Release 2013/01/23 : CIA-RDP81-01043R001600090003-8

Thus, with the opposite sign, the magnetic potential of a uniformly magnetized body constitutes the scalar product of magnetization J and the gradient of the potential of the gravitational mass of the magnetized body, assuming its density is equal to unity. The equation (0.58) is called the theorem of Poisson, and it enables determination of the magnetic potential of uniformly magnetized bodies having a constant density, provided the gravitational potential of a body of the same shape and dimensions is known.

Another expression for a uniformly magnetized body is derived from equation (0.55).

Since div J = 0, we have:

$$U = \int J_n/r \quad dS. \tag{0.60}$$

To determine the magnetic potential by means of this formula it is necessary to know the surface distribution of the normal component of the vector of magnetization. The shape of the magnetic body determines which of the 2 formulas (0.59) and (0.60) should be used in calculating the magnetic potential. For certain shapes, such as spheres and ellipsoids, it is more convenient to use formula (0.59). Because for other shapes such as prisms or cylinders the gravitational potentials are known, equation (0.60) is indicated.

In the following section the field of a uniformly magnetized sphere, cylinder and ellipsoid, will be considered as examples of great importance in terrestrial magnetism using the formulas derived above.

Section 12. Magnetic Potential of a Uniformly Magnetized Sphere

The gravitational potential of a sphere V at an external point located at distance R from the center of the sphere, is:

$$V = v/R.$$

Declassified in Part - Sanitized Copy Approved for Release 2013/01/23 : CIA-RDP81-01043R001600090003-8

Declassified in Part - Sanitized Copy Approved for Release 2013/01/23 : CIA-RDP81-01043R001600090003-8

Therefore the magnetic potential at the same point will be:

$$U = v\ (JR)/R^3 \qquad \text{or} \qquad U = (MR)/R^3$$

i.e., the magnetic potential of a uniformly magnetized sphere within its external space is equivalent to the potential of a dipole.

The potential inside the sphere at a distance R_1 from its center is determined by dividing the sphere into 2 hemispherical surfaces of radius R_1.

The magnetic potential U at a point located on this spherical surface will be the sum of potential U_1 produced by a sphere of radius R_1, and the potential U_2 of the spherical layer.

In view of the above the first mentioned potential is expressed by the equation

$$U_1 = r/3\ \pi\ R_1^3/R_1^3(JR_1) = 4/3\ \pi\ (JR_1)$$

Gravitational potential within the spherical layer is a constant quantity and its gradient is equal to zero, hence:

$$U_2 = 0$$

Consequently the potential inside the sphere is:

$$U = U_1 = 4/3\ \pi\ (JR_1),$$

and the intensity of the magnetic field inside the sphere is:

$$H = -\text{grad}\ U = -4/3\ \pi\ J \qquad (0.61)$$

Thus, H is proportional to the magnetization J and has a direction opposite to that of J.

The proportionality coefficient

$$N = 4/3\ \pi$$

is called the coefficient of demagnetization.

Declassified in Part - Sanitized Copy Approved for Release 2013/01/23 : CIA-RDP81-01043R001600090003-8

Declassified in Part - Sanitized Copy Approved for Release 2013/01/23 : CIA-RDP81-01043R001600090003-8

Section 13. Potential of a Uniformly Magnetized Cylinder

Assuming that a cylinder can be uniformly magnetized along its axis, then the normal component J_n of the vector of magnetization J must be the same at both end surfaces and equal to the vector J. Therefore to determine the magnetic potential it is more convenient to use equation (0.60) which for the external point P is:

$$U = J \int dS/r_1 - J\, dS/r_2,$$

where the first integral extends to one end of the surface, the second to the other.

In the general case, i.e., for any point in the space, the integrals cannot be resolved in the simplest functions and therefore discussion will be limited to the points located on the axis of the cylinder. Indicating the radius of the cylinder by a, its length by ℓ, the distance of point P from the nearest surface S_1 by R, and the distance of the surface element dS from its center 0 by P, the potential of the first end surface is:

$$U_1 = J \int_0^{2\Theta} \int_0^{a} p\,d\Theta\,dp / \sqrt{R^2 + p^2} = 2\pi J(\sqrt{R^2 + a^2} - R).$$

The potential of the second end surface is indicated by a similar expression in which $R + \ell$ appears in lieu of R, Hence the external potential is:

$$U = 2\pi J \left[\sqrt{R^2 + a^2} - \sqrt{(R + \ell)^2 + a^2} + \ell \right]. \qquad (0.62)$$

For the point P (internal point) the potential is:

$$U = 2\pi J \left[\sqrt{R^2 + a^2} + \sqrt{(\ell + R)^2 + a^2} - 2R \right]. \qquad (0.63)$$

Section 14. Magnetic Potential of an Ellipsoid

The magnetic potential of an ellipsoid is determined in accordance with the theorem of Poisson. Since its gravitational

Declassified in Part - Sanitized Copy Approved for Release 2013/01/23 : CIA-RDP81-01043R001600090003-8

Declassified in Part - Sanitized Copy Approved for Release 2013/01/23 : CIA-RDP81-01043R001600090003-8

potential is known and is expressed for a point P located outside of the ellipsoid having coordinates x, y, z by the formula

where a, b, c are the half-axes of the ellipsoid, $\varphi(\theta) = (a^2+\theta)(b^2+\theta)(c^2+\theta)$, and n is the root of the equation:

$$x^2/a^2+n + y^2/b^2+n + z^2/c^2+n = 1. \qquad (0.64)$$

First, the magnetic potential on the surface of the ellipsoid is determined. In this case the root of equation (0.64) is n = 0 and therefore the gravitation potential is

$$V = -\pi abc \int_0^{\infty} \left(\frac{x^2}{a^2+\theta} + \frac{y^2}{b^2+\theta} + \frac{z^2}{c^2+\theta} \right) \frac{d\theta}{\sqrt{\varphi(\theta)}} + \Phi.$$

This expression may be written in the form:

$$V = -\frac{1}{2}\left[Lx^2 + My^2 + Nz^2 \right] + \Phi$$

where L, M, N and Φ are constants and are expressed by definite elliptic integrals

$$L = 2\pi abc \int_0^{\infty} \frac{d\theta}{(a^2+\theta)\sqrt{\varphi(\theta)}}, \quad M = 2\pi abc \int_0^{\infty} \frac{d\theta}{(b^2+\theta)\sqrt{\varphi(\theta)}}, \qquad (0.65)$$

$$N = 2\pi abc \int_0^{\infty} \frac{d\theta}{(c^2+\theta)\sqrt{\varphi(\theta)}}, \quad \Phi = \pi abc \int_0^{\infty} \frac{d\theta}{\sqrt{\varphi(\theta)}}$$

Consequently the magnetic potential on the surface of the ellipsoid is of the form:

$$U = J_x Lx + J_y My + J_z Nz, \qquad (0.66)$$

and the products L_x, M_y and N_z represent the components of the gravitational attraction force of the ellipsoid.

The magnetic potential of the ellipsoid at an external point is, according to the theorem of Poisson,

$$U = J_x f_x + J_y f_y + J_z f_z,$$

Declassified in Part - Sanitized Copy Approved for Release 2013/01/23 : CIA-RDP81-01043R001600090003-8

Declassified in Part - Sanitized Copy Approved for Release 2013/01/23 : CIA-RDP81-01043R001600090003-8

where f_x, f_y, f_z also are the components of the gravitational potential at the external point P. To determine these forces an ellipsoid co-focal with the given ellipsoid is constructed through point P so that their axes coincide. Then acending to the theorem of Maclaurin, assuming both ellipsoids are of the same density the attraction of such an ellipsoid is greater by as many times, as its volume is greater than that of the given ellipsoid, i.e.,

$$f'x/fx = f'y/fy = f'z/fz = a_1b_1c_1/abc$$

where a_1 b_1 c_1 are the half axes and f'x, f'y, f'z the component forces of attraction of the co-focal ellipsoid.

Since point P is located on the surface of the co-focal ellipsoid, it follows that according to formula (0.66):

$$f'x = L_1 x;\ f'y = M_1 y \text{ and } f'z = N_1 z.$$

where L_1, M_1 and N_1 are constant quantities defined by formulas (0.65), in which the half axes a, b, c are replaced by half axes a_1, b_1, c_1.

Consequently,

$$fx = abc/a_1b_1c_1\ L_1x, \quad fy = abc/a_1b_1c_1\ M_1y, \quad fz = abc/a_1b_1c_1\ N_1z.$$

whence

$$U_e = abc/a_1b_1c_1[J_xL_1x + J_yM_1y + J_zN_1z] \qquad (0.67)$$

The half axes a_1, b_1, c_1 are determined on the assumption that the 2 ellipsoids are co-focal and that the point P is located on the surface of the ellipsoid having the axes a_1, b_1, c_1. The first condition gives:

$$a_1^2 - b_1^2 = a^2 - b^2 = q_1^2; \quad a_1^2 - c_1^2 = a^2 - c^2 = q_2^2 \qquad (0.68)$$

and the second:

$$\frac{x^2}{a_1^2} + \frac{y^2}{b_1^2} + \frac{z^2}{c_1^2} = 1. \qquad (0.69)$$

These 3 equations enable the desired determination of the half axes.

Declassified in Part - Sanitized Copy Approved for Release 2013/01/23 : CIA-RDP81-01043R001600090003-8

Declassified in Part - Sanitized Copy Approved for Release 2013/01/23 : CIA-RDP81-01043R001600090003-8

Section 15. Magnetization of Rocks in a Uniform Magnetic Field

Magnetization of para- and ferromagnetic bodies in a uniform field is of great importance in the theory of magnetic prospecting since magnetic anomalies are caused by rocks occurring at relatively shallow depth in the form of individual masses of different shapes and possessing the property of being magnetized under the influence of the magnetic field of the earth, which because of the relatively small volume of these rocks may be regarded as uniform. Therefore, the magnetization of a rock of susceptibility N and located within the uniform magnetic field of the earth will be discussed below.

The magnetic potential U at a point P within the rock is equal to the sum of the potential of the external field U_e, and the potential U_i, produced by the rock itself, i.e.,

$$U = U_i + U_3.$$

Hence the field intensity H at point P is:

$$H = \text{grad}\ (U_e + U_i) = H_e + H_i.$$

where H_e is the intensity of the external magnetizing field, and H_i the intensity of the internal field.

On the other hand, the magnetization J is expressed by the equation:

$$J = xH_e + xH_i. \qquad (0.70)$$

Consequently, magnetization due to the action of the external uniform field depends not only on the intensity of this field but also upon the field produced by the magnified body itself. The quantity H_i is the intensity of this field and, as is shown by theory and experiment involving uniform magnetization, this quantity always

Declassified in Part - Sanitized Copy Approved for Release 2013/01/23 : CIA-RDP81-01043R001600090003-8

Declassified in Part - Sanitized Copy Approved for Release 2013/01/23 : CIA-RDP81-01043R001600090003-8

negative, i.e., H_i has a direction opposite to the external field, and therefore is designated the intensity of the internal demagnitizing field.

The internal demagnetizing field is nothing but the field in which the magnet is located and which is produced by the magnet itself. Indeed from Figure 9, which shows the lines of force around the magnet, it is clearly apparent that near the surface of the sample the direction of the lines of force is opposite to their direction inside the magnet, and their density is inversely proportional to the length of a magnet of constant diameter. The picture is exactly the same as if this flux of the lines of force represented a magnetic field produced by external sources and the magnet were places in this field. It is clear that such a field will produce a demagnetizing action, i.e., will reduce the magnetization.

In the general case, at different points within the rock H_i may have different directions in relation to the magnetizing field H_e, with the result that the magnetization J' itself may have different directions, which correspond to nonuniform magnetization.

Since H_i is a function of magnetization J, determination of J requires the expression of H_i in equation (0.70) in terms of J, and this equation is solved for J.

The expression for H_i is given in Section 11, however it cannot be utilized to determine J in the general case. Therefore, several particular cases are discussed below.

Assuming that the rock is magnetized uniformly; then in view of equation (0.59) we have:

Declassified in Part - Sanitized Copy Approved for Release 2013/01/23 : CIA-RDP81-01043R001600090003-8

Declassified in Part - Sanitized Copy Approved for Release 2013/01/23 : CIA-RDP81-01043R001600090003-8

$$J = \varkappa[H_e + \operatorname{grad}(J \operatorname{grad} V)]. \tag{0.71}$$

The components of magnetization vector J are determined from the equation

$$J_k = \varkappa \left[H_{ek} + \sum_{i=1}^{3} N_{ki} J_i\right], \tag{0.72}$$

where the indices k and i denote one of the coordinates x, y, z, and N_{ki} denotes the partial derivatives of V of second order on the corresponding corrdinates. The values of N_{ki} are the components of a certain tensor N, which is called the demagnetization tensor. Since $N_{xy} = N_{yx}$, $N_{xz} = N_{zx}$ and $N_{yz} = N_{zy}$ the tensor N is symmetrical.

In order that J = const, the components of tensor N must be constant, and not dependent upon the position of point P. The equations show that at uniform magnetization of rocks of arbitrary shape the magnetization vector does not coicide with the vector of the magnetizing field H_e, but forms a certain angle with the latter, which depends upon the shape of the rock stratum.

In the case of a sphere the magnetization is determined in accordance with equations (0.61) and (0.70) by the following relationship:

$$J = \varkappa H_e - 4/3\pi\varkappa J,$$

which gives

$$J = \varkappa/1 + 4/3\pi\varkappa \; H_e, \tag{0.73}$$

i.e., in a sphere magnetization coincides with the direction of the magnetizing field. From the same equations it follows that in a uniform field the sphere is magnetized uniformly, since the assumption of uniform magnetization of a sphere, made in the derivation of its potential is not contrary to equation (0.73), and from which it also follows that J = const.

Declassified in Part - Sanitized Copy Approved for Release 2013/01/23 : CIA-RDP81-01043R001600090003-8

Declassified in Part - Sanitized Copy Approved for Release 2013/01/23 : CIA-RDP81-01043R001600090003-8

In addition to the sphere, ellipsoids having any ratio of axes, which also possess the property of uniform magnetization, is readily shown below.

In accordance with the derivations of the preceding section the magnetic potential inside an ellipsoid is of the form:

$$U = J_x N_{xx} x - J_y N_{yy} y + J_z N_{zz} z.$$

Denoting by K a constant vector of components $J_x N_{xx}, J_y N_{yy}, J_z N_{zz}$, the magnetization of an ellipsoid by the action of a uniform field H_e is expressed by the equation

$$J = \chi H_e - \chi \operatorname{grad}(K, r),$$

or, since K = const,

$$J = \chi H_e - \chi K.$$

Since H_e and K are constant quantities, the vector J also is a constant quantity, i.e., the ellipsoid actually is uniformly magnetized by the action of a uniform field, but the vector J does not coincide with vector H_e. Its components on the coordinate axes are:

$$J_x = \chi/1 + \chi N_{xx} H_x, \quad J_y = \chi/1 + \chi N_{yy} H_y, \quad J_z = \chi/1 + \chi N_{zz} H_z.$$

The coefficients N_{xx}, N_{yy}, N_{zz} are components of the ellipsoid demagnetization tensor, which are expressed by formula (0.65) where

$$L = N_{xx}, \; M = N_{yy} \text{ and } N = N_{zz}.$$

If any 2 axes are equal, i.e., the ellipsoid is an ellipsoid of revolution, the coefficients of demagnetization may be expressed in the simplest functions. Thus for example, for an elongated ellipsoid in which a = b < c:

$$N_{xx} = N_{yy} = \pi\left(\frac{1}{c^2} - \frac{1}{2}\ln\frac{1+\varepsilon}{1-\varepsilon}\right),$$

$$N_{zz} = 4\pi\left(\frac{1}{\varepsilon^2} - 1\right)\left(\frac{1}{2\varepsilon}\ln\frac{1+\varepsilon}{1-\varepsilon} - 1\right), \qquad (0.74)$$

Declassified in Part - Sanitized Copy Approved for Release 2013/01/23 : CIA-RDP81-01043R001600090003-8

Declassified in Part - Sanitized Copy Approved for Release 2013/01/23 : CIA-RDP81-01043R001600090003-8

where e is the ellipsoid eccentricity.

For a compressed ellipsoid in which a = b > c:

$$N_{zz} = 4\pi\left(\frac{\sqrt{1-e^2}}{e^3}\arccos e - \frac{1-e^2}{e^2}\right),$$

$$N_{xx} = N_{yy} = 2\pi\left(\frac{\sqrt{1-e^2}}{e^3}\arccos e - \frac{1-e^2}{e^2}\right). \qquad (0.75)$$

An example of the fact that bodies of different shapes cannot be uniformly magnetized is the case of a circular cylinder placed within a uniform field, with the cylinder axis parallel to the direction of the field. Assuming that the cylinder becomes uniformly magnetized, the following expression for the potential on the cylinder axis is obtained through expression (0.63) and equation (0.71):

$$J = \chi H_e + \chi 2\pi J\frac{a}{l}\left[\sqrt{R^2+a^2} - \sqrt{(l-R)^2+a^2} - 2R\right].$$

Differentiating for R, we obtain:

$$J = \chi H_e - 4\pi\chi J\left[1 - \frac{l}{2\sqrt{R^2+a^2}} - \frac{l-R}{2\sqrt{(l-R)^2+a^2}}\right].$$

This equation shows that J cannot be a constant quantity, since the right half of the equation varies with R, i.e., varies with the position of the point inside the cylinder.

Thus at the center of the cylinder, where $R = l/2$,

$$J = \chi H_e - 4\pi\chi J\left(1 - \frac{l}{\sqrt{\frac{l^2}{4}+a^2}}\right) = \chi H_e - 4\pi\chi J\left(1 - \frac{1}{\sqrt{1+\beta^2}}\right),$$

and at one end of the cylinder, where $l = R$

$$J = \chi H_e - 4\pi\chi J\left(1 - \frac{l}{2\sqrt{l^2+a^2}}\right) = \chi H_e - 4\pi\chi J\left(1 - \frac{1}{\sqrt{4+\beta^2}}\right),$$

where β denotes the ratio of the diameter of the cylinder to its length.

Thus in the central portion of the cylinder the magnitude of J reaches a maximum, and at the ends reaches a minimum. With an increase in the diameter of the cylinder or a decrease in its length the difference between maximum and minimum values decreases and at $\beta = 0$ it is equal to zero, while the magnitude the magnetization has the value:

$$J = \chi/1 + 4\pi\chi \ H_e.$$

Declassified in Part - Sanitized Copy Approved for Release 2013/01/23 : CIA-RDP81-01043R001600090003-8

Declassified in Part - Sanitized Copy Approved for Release 2013/01/23 : CIA-RDP81-01043R001600090003-8

In this case the coefficient of demagnetization N of such a cylinder is $N = 4\pi$.

Therefore, a cylinder with a very large ratio of diameter to length is magnetized practically uniformly. For example, at $p = 6$ magnetization at the center and at the ends of the cylinder differs only by 6%, and at $p = 10$, differs only 1%.

It is not difficult to see that a thin plate placed perpendicularly to the field is equivalent to a cylinder with a large ratio of diameter to length, and therefore may be considered as being uniformly magnetized and having a demagnetization coefficient equal to 4π.

With non-uniform magnetization the components of vector J may be expressed by equations (0.72) only if the variations of vector J inside the magnetized body are the same at different values of the magnetizing field.

Experiments show that this is true in fields in which the degree of magnetization in the central portion of the body is less than one-half of saturation. However, in this case the components of the demagnetization vector no longer are constant but vary from one point to another within the body.

In the case of a cylinder of prism the direction of vector J coincides with the direction of the axis at points on the axis, and therefore:

$$J = x(H_e - NJ), \qquad (0.76)$$

hence

$$J = x/1 + xN \; H_e = x'H_e.$$

Declassified in Part - Sanitized Copy Approved for Release 2013/01/23 : CIA-RDP81-01043R001600090003-8

Declassified in Part - Sanitized Copy Approved for Release 2013/01/23 : CIA-RDP81-01043R001600090003-8

The quantity x' is called the apparent susceptibility or shape susceptibility, in contrast to x, which is called true susceptibility or susceptibility of the material. It is evident that

$$x' = x/1 + xN, \qquad (0.77)$$

where N is a scalar quantity which is different at different points. The value of N is lowest at the central portion of the cylinder where the value of J is maximum.

This equation is applicable not only to a cylinder, but to any shape of rock, provided magnetization is considered in the neutral portion of the rock, where the value of J is maximum.

Equation (0.76) shows that the magnetization J of a rock cannot be greater than xH_e and approximates this value only at small values of the coefficient N.

Section 16. Determination of Demagnetization Coefficients

Numerical values of the demagnetization coefficients of bodies of any shape except spheres and illipsoids must be determined by experiment. This requires measurement of the magnetization J of a sample under the action of a field H_e of a solenoid. The field intensity of the solenoid, provided its length is sufficiently large in comparison to the length of the sample, is determined by the formula $H_e = 0.4\pi wI$, where w is the number of turns for centimeter length of the solenoid, and I is the current intensity in amperes.

If J and H_e are known, we have in view of equation (0.76):

$$H = x H_e/J - 1,$$

Determination of x requires additional determination of J under the action of the same field H_e, by placing the sample in a

Declassified in Part - Sanitized Copy Approved for Release 2013/01/23 : CIA-RDP81-01043R001600090003-8

Declassified in Part - Sanitized Copy Approved for Release 2013/01/23 : CIA-RDP81-01043R001600090003-8

permeameter wherein the phenomenon of "self-demagnetization" does not occur and therefore N = 0. Denoting the magnetization in a closed circuit by J_o, we have

$$x = J_o/H_e,$$

whence

$$N = J_o - J/J \qquad (0.77a)$$

The value of J may be measured either by the ballistic or the magnetometric methods, the results of which produce coefficients of different values. Therefore, a differentiation is made between the ballistic coefficient of demagnetization N_e and the magnetometric coefficient of demagnetization N_m. The magnetimetric coefficient always is larger than the ballistic coefficient since the quantity J measured magnitometrically always is smaller than that measured by the ballistic method.

Indeed, the ballistic method measures the magnitude of induction B_1 and consequently also the magnetization J of the sample at its central portion where the former is maximum. The magnitometric method, on the other hand, determines the mean value of magnetization J which always is smaller than the maximum magnitude, and thus in view of (0.77a) $N_m \geqslant N_b$, The relationship between the 2 values is expressed by the correlation:

$$N_m = \int N_b dv/v,$$

where v is the volume of the sample, dv the volume element, and the integration includes the entire volume of the sample.

For ellipsoids and spheres, it is evident that

$$N_m = N_b,$$

Declassified in Part - Sanitized Copy Approved for Release 2013/01/23 : CIA-RDP81-01043R001600090003-8

Declassified in Part - Sanitized Copy Approved for Release 2013/01/23 : CIA-RDP81-01043R001600090003-8

Table 4 shows the values of the demagnetization coefficients of cylindrical samples having different ratios β of diameter to length, and for comparison the demagnetization coefficients of ellipsoids having the same values of β also are included.

TABLE 4

VALUES OF DEMAGNETIZATION COEFFICIENTS

β	N_m	N_b	N ellipsoid	β	N_m	N_b	N ellipsoid
1/2	1.75	-	2.18	1/60	0.0131	0.0104	0.0132
1/5	0.680	-	0.7015	1/70	0.0099	0.00795	0.0101
1/10	0.255	0.204	0.2549	1/80	0.0078	0.00625	0.0080
1/15	0.140	0.106	0.1350	1/90	0.0063	0.00507	0.0065
1/20	0.0898	0.0642	0.0348	1/100	0.0052	0.00430	0.0054
1/25	0.0628	0.0467	0.0587	1/150	0.0025	0.00204	0.0026
1/30	0.0160	0.0344	0.0432	1/200	0.0015	0.00120	0.0016
1/40	0.0274	0.0211	0.0266	1/300	0.0008	0.0008	0.0008
1/50	0.0183	0.0144	0.0181				

From this table it is apparent that an increase in the length of a magnet of constant diameter results in a decrease in the coefficient of demagnetization and it becomes equal to the coefficient of demagnetization of an ellipsoid of the same dimensions.

Many authors have attempted to derive a formula for the coefficient of demagnetization for magnets of different shapes, but all such attempts are only rough approximations since the law of distribution of magnetization throughout the volume of a magnet remains unknown. For example, in the case of a broken ring magnet (Figure 10) the value of N may be expressed by the formula

$$N = k\, S/ld, \qquad (0.78)$$

Declassified in Part - Sanitized Copy Approved for Release 2013/01/23 : CIA-RDP81-01043R001600090003-8

Declassified in Part - Sanitized Copy Approved for Release 2013/01/23 : CIA-RDP81-01043R001600090003-8

where S is the area of cross-section of the ring, l is mean length of the ring magnet, d the distance between the ends of the ring magnet, and k is a constant.

Section 17. Effect of the Shape of the Sample on the Magnitude of Magnetic Moment and Magnetization

Formula (0.76) indicates that on one hand J is a function of the demagnetization coefficient N with the magnetization J decreasing with an increase in N, and on the other hand N is a function of the dimensions of the sample with the volume remaining the same, as is apparent from Table 4 and formula (0.78).

Therefore, the magnitude of magnetic moment M, expressed by the formula:

$$M = J_m v$$

where J is mean magnetization and v the volume, is a function of the shape of the sample when the volume remaining constant. Thus, for a cylinder in which $v = \pi/4\, d^2 l$,

$$M = \pi/4\, J_m \beta^2 l^2 \quad (\beta = d/l).$$

If the length of the sample remains constant and only the diameter is changed, with increasing d, β increases, and consequently the coefficient of demagnetization N also increases. The latter causes a decrease in magnetization, as a result of which the magnetic moment M must reach maximum value at certain values of d, i.e., for a definite length of the sample there is always one diameter, or cross sectional area, for which the magnetic moment will be maximum.

All the formulas derived in the previous sections, which establish the correlations between magnetization J and the magnetizing field H_e are valid for the entire range of J values with a constant

Declassified in Part - Sanitized Copy Approved for Release 2013/01/23 : CIA-RDP81-01043R001600090003-8

Declassified in Part - Sanitized Copy Approved for Release 2013/01/23 : CIA-RDP81-01043R001600090003-8

value of magnetic susceptibility x, which is exhibited by paramagnetic substances.

These formulas may be applied to ferromagnetic substances in which x is a function of J and H_e at the values of J and H at which x is a known quantity.

In the general case, when x is a function of magnetization, in equation (0.76) x must be expressed as a function of J, and the equation must be solved for J.

Since the analytical correlation between x and J is not known, the solution of equation (0.76) in the general case does not appear possible. Therefore the quantity J is determined from experimental magnetization curves which establish the correlation between J and H_e.

Since J depends not only on H_e but also on the shape of the sample, the magnetization curves are determined for samples in which the coefficient of demagnetization is zero. This is done by joining the sample NS (Figure 11) by means of a soft iron yoke A, by making a sample in the shape of a closed ring, or by direct measurement of the intensity of the magnetic field on the surface of the sample, which is equal to the difference $H_e - NJ$.

If the sample was first demagnetized, i.e., J = 0, its magnetization under an external field will vary according to curve I (Figure 12) called the basic curve of magnetization of a closed magnetic circuit. In the opposite direction, i.e., on decrease of the field to zero, because of the hysteresis of ferromagnetic substances magnetization varies according to curve II, called the hysteresis curve, and at $H_e = 0$ it has a certain definite value J_r,

Declassified in Part - Sanitized Copy Approved for Release 2013/01/23 : CIA-RDP81-01043R001600090003-8

Declassified in Part - Sanitized Copy Approved for Release 2013/01/23 : CIA-RDP81-01043R001600090003-8

called the residual magnetization of the substance. In a field of opposite direction magnetization decreases and at a certain value $H_e = H_c$ becomes zero. The quantity H_c is called the coercive force of the substance.

To determine the curve of magnetization of a sample with free ends, having a coefficient of demagnetization N, and given a magnetization curve I for a closed magnetic circuit (Figure 13), a straight line OC is drawn from the origin of coordinates forming angle α with the axis of ordinates, the tangent of which is equal to $1/\beta N$, where β is the ratio of J to H. A number of straight lines then are drawn parallel to the abscissa axis and the segments a_1b_1, a_2b_2, ..., are plotted between the ordinate and the straight line OC, to the right of the basic magnetization curve.

The points b_1, b_2, ... of curve II indicate the magnetization which takes place in an open circuit, because for each point b the equation:

$$J = x(H_e - NJ)$$

must be true. Indeed for any point, for example point b_2:

$$J = b_2P_1 = a_2P_2 = \beta x H_1,$$

where

$$H_1 = OP_2,\ H_3 = OP_1 = OP_2 + a_2b_2 = H_1 + C_2d_2.$$

However,

$$c_2d_2 = c_2 O\,tg\,\alpha = 1/\beta JN,$$

and therefore,

$$H = H_1 + 1/\beta JN \qquad \text{and } J = x(H_e - NJ).$$

Declassified in Part - Sanitized Copy Approved for Release 2013/01/23 : CIA-RDP81-01043R001600090003-8

Declassified in Part - Sanitized Copy Approved for Release 2013/01/23 : CIA-RDP81-01043R001600090003-8

The same plotting procedure also applies to the hysteresis curve. Taking a portion of the hysteresis curve J_rH_c (Figure 14) between the positive ordinate axis and the negative abscissa axes, if the demagnetizing field did not exist in the sample the residual magnetization at any point of the sample is determined by the ordinate OJ_r.

In the presence of a demagnetizing field the intensity of magnetization NJ is less and is determined by plotting a straight line from the origin of coordinates at an angle α = arc tg N/β to intersect with the hysteresis curve at the point M. The ordinate $\overline{OJ}$ represents the magnitude of residual magnetization, and the abscissa $\overline{OH}$ represents the intensity of the demagnetizing field because

$$\overline{OH} = \overline{MH} \text{ tg } \alpha = 1/\beta \text{ JM}.$$

Thus the coefficient of demagnetization enables determination of the magnitude of residual magnetization and thereby the magnetic moment, provided the hysteresis curve for the material of the given magnet is made known.

Section 18. The Permanent Magnet and Its Properties

Because most contemporary measurement methods are based on the interaction between a permanent magnet and the magnetic field of the earth the permanent magnet is an important component of the apparatus for measurement of the elements of terrestrial magnetism. The results of measurements using these methods depend on the quality and properties of the permanent magnet.

Reliable measurement of the elements of terrestrial magnetism requires magnets of mineral dimensions, a determined magnitude of field and high constancy of magnetic moment. Moreover, the properties

Declassified in Part - Sanitized Copy Approved for Release 2013/01/23 : CIA-RDP81-01043R001600090003-8

Declassified in Part - Sanitized Copy Approved for Release 2013/01/23 : CIA-RDP81-01043R001600090003-8

of the magnet must be known, so that changes of the magnetic moment which may occur during the measurements may be taken into account.

The magnetic properties of a permanent magnet depend on the material from which it is made, the shape and dimensions of the magnet, methods of thermal treatment, magnetization, stabilization procedures, i.e., the attaining of a stable state, and finally the maintenance and protection of the magnet from extraneous influences.

1. Dependence of Magnitude of Magnetic Moment on the Material and Shape of the Magnet. The permanent magnet is magnetized by exposure to an external magnetic field. As we have seen, the process of magnetization takes place in accordance with the basic curve of magnetization and the upper portion of the hysteresis curve. On total disappearance of the external field magnetization of a certain magnitude is retained which is called the residual magnetization of the magnet; given the coefficient of demagnetization of the magnet the magnitude of residual magnetization may be determined from the hysteresis curve by the method described in the preceding section (Figure 14). Therefore the coefficient of demagnetization is one of the quantities which characterize a given magnet.

The other principal quantities which characterize a magnet are the residual magnetization, magnetic moment and maximum intensity of the demagnetizing field at which the magnetic moment varies not more than 0.1% of its value.

All these quantities, in turn depend upon the shape and dimensions of the portion of the hysteresis curve between the positive ordinates and the negative abscissa axes. This portion, which will be called the demagnetization portion, is the characteristic of the

Declassified in Part - Sanitized Copy Approved for Release 2013/01/23 : CIA-RDP81-01043R001600090003-8

Declassified in Part - Sanitized Copy Approved for Release 2013/01/23 : CIA-RDP81-01043R001600090003-8

material from which the magnet is made. The terminal points of the portion, or the residual magnetization (induction) in a closed circuit and the coercive force, may be taken as rough approximations of the characteristics of the material.

To show the influence of the composition of a variety of steel or alloy on the magnitude of the magnetic moment of a magnet Figure 15 is included, showing the demagnetization curves of 4 varieties of steel: magnico (NiAlCo), alni (APNi), cobalt (Co) and tungsten (W) steel. The same drawing also shows a number of straight lines OA, OB extending from the origin of coordinates, and corresponding to the different values of the demagnetization coefficients.

From this illustration it is apparent that for a given variety of steel the residual magnetization J is greatest when the demagnetization coefficient is least, i.e., at a high ratio of length to diameter of the sample. To produce magnets of equal magnetization the length must be decreased by using steel having greater coercive force.

Thus to attain magnetization equal to 300 CGS μ, a magnet made of tungsten steel must have a coefficient of demagnetization N = 0.17; one made of cobalt steel must have a coefficient N = 0.65; nickel-aluminum steel, N = 0.94; and for magnico, N = 1.35, which corresponds approximately to magnets of length 10, 5, 4 and 2.8 cm, respectively, with diameter d = 1 cm.

Example: Determine the magnetic moments of cylindrical magnets with length l = 5 cm and diameter d = 1cm, made of tungsten steel and magnico-aluminum steel, respectively.

From the tabulated data we find that the coefficient of demagnetization N corresponding to a ratio l/d = 5 is N = 0.68.

Declassified in Part - Sanitized Copy Approved for Release 2013/01/23 : CIA-RDP81-01043R001600090003-8

Declassified in Part - Sanitized Copy Approved for Release 2013/01/23 : CIA-RDP81-01043R001600090003-8

A line OP is drawn from the origin of coordinates (Figure 15) forming an angle α with the ordinate axis the tangent of which is equal to the demagnetization coefficient multiplied by the ratio b of the dimensions. In the present case this ratio is equal to 2 and therefore $tg\alpha = 1.36$, which corresponds to an angle $\alpha = 53^{\circ}$.

The points of intersection of this straight line with the curves W and NiAPCo give the ordinates $J_1 = 95$ and $J_2 = 530$ CGSμ. Hence the magnetic moment of the tungsten magnet is

$$M_1 = J_1 v = J_1 \pi d^2 l/4 = 370 \text{ CGS}\mu$$

and that of the magnico magnet is

$$M_2 = 2010 \text{ CGS}\mu.$$

2. Effect of an External Magnetic Field. On placing a permanent magnet into a magnetic field its magnetic moment M is altered depending on the magnitude of the intensity of this field, because the material from which the magnet is made possesses magnetic susceptibility. Consequently M is a function of the intensity of the external magnetic field, i.e.,

$$M = f(H).$$

For small values of H, by expanding this function to a series and retaining only the first 2 terms, we have

$$M = M_0 + \partial M_0/\partial H \, \Delta H, \qquad (0.79)$$

where M is the value of the magnetic moment within a field of intensity ΔH, and M_0 the value of this moment in the absence of an external field. The equation may be written:

$$M = M_0(1 + v\Delta H),$$

using the expression

$$v = 1/M_0 \cdot \partial M_0/\partial H. \qquad (0.80)$$

Declassified in Part - Sanitized Copy Approved for Release 2013/01/23 : CIA-RDP81-01043R001600090003-8

Declassified in Part - Sanitized Copy Approved for Release 2013/01/23 : CIA-RDP81-01043R001600090003-8

The term v is the induction coefficient of the magnet which in the general case is a function of the intensity of the external field H. However, over small ranges of the field it may be considered constant and as characterizing one of the properties of a permanent magnet, namely the property of altering the magnetic moment under the action of an external field.

In order to maintain the quantity v constant the magnetization process must be reversible at low values of H.

The conditions under which sucha a process is possible may be attained easily through application of the magnetization curves of ferromagnetic materials.

It is known that magnetization of a sample follows the basic magnetization curve M, and demagnetization follows the hysteresis curve Q, shown in Figure 16.

The hysteresis curve reveals that at least 2 values, J_1 and J_2 correspond to a single value of H.

On the other hand, if magnetization of the sample is interrupted at some point A of the basic curve (Figure 16) and the magnetization cycle is completed from this point at a lower amplitude of magnetizing field, the result is a small hysteresis loop or hysteresis cycle, shown in Figure 16.

This loop is narrower when cycle is short, i.e., the smaller the amplitude of intensity of the magnetic field ΔH. With very small values of ΔH the loop becomes practically a straight line. In such a case hysteresis appears to vanish and the magnetization process becomes reversible. Denoting by ΔJ the increase in magnetization corresponding to the increase ΔH of the external field during such a reversible process, the ratio

Declassified in Part - Sanitized Copy Approved for Release 2013/01/23 : CIA-RDP81-01043R001600090003-8

Declassified in Part - Sanitized Copy Approved for Release 2013/01/23 : CIA-RDP81-01043R001600090003-8

$$x_r = \Delta J / \Delta H \qquad (0.81)$$

is called reversible susceptibility.

The reversible susceptibility of different materials at different points of the hysteresis curve and of the basic magnetization curve is a function of the magnetization J of the sample, and for the same value of J the reversible susceptibility is approximately the same regardless of the portion of the hysteresis curve at which it is taken. The correlation between x_r and J is shown in Figure 17. It is apparent from the latter that the highest value of x_r is at $J = 0$, and that it approaches zero at $J = J_\infty$.

At $J = 0$ the reversible susceptibility is called initial susceptibility, the magnitude of which differs for various types of steel, but it varies inversely with the coercive force.

Study of reversible susceptibility has made it possible to elucidate many questions concerning the stability of permanent magnets.

The maximum amplitude of the magnetizing field ΔH at which the process of magnetization can be considered practicably reversible, also depends upon the composition of the steel, and increases with an increase in coercive force. Therefore, materials having a high value of coercive force are advantageous from the point of view of both the magnetic moment and the permanency of a permanent magnet.

Using the correlation (0.81) it is possible to determine the relationship between the induction coefficient and reversible susceptibility.

Indeed, expressing ΔM_o in equation (0.80) in terms of J, we obtain:

Declassified in Part - Sanitized Copy Approved for Release 2013/01/23 : CIA-RDP81-01043R001600090003-8

Declassified in Part - Sanitized Copy Approved for Release 2013/01/23 : CIA-RDP81-01043R001600090003-8

$$v = 1/M_o \int \Delta J/\Delta H \; dv,$$

whence, in view of equation (0.81):

$$v = 1/M_o \int x_r \, dv,$$

or, on applying the theorem of mean value of integral:

$$v = v/M_o \; x_{r_m} = x_{r_m}/J_m.$$

where x_{r_m} is the mean value of reversible susceptibility and J_m is the mean value of residual magnetization.

From this it follows that v is less at a greater coercive force H_c of the material since x_{r_m} varies inversely with both H_c, and J_m.

Thus for example, for a magnet made of tungsten steel, for which x_r is of the order of 30 at large values of H_c the induction coefficient at $J = 600$, is

$$v = 30/800 = 0.05$$

while in the case of alni or almico alloys, in which x_r is on the order of several units, at the same value of J the induction coefficient will be 10 times less, i.e.,

$$v = 0.005.$$

3. Effect of Temperature. The magnetic moment of a permanent magnet may change in magnitude in the absence of an external field due to the temperature of the medium within which it is located. Assuming that M is a function of temperature, and expanding this function to a series analogously to the foregoing, we obtain

$$M = M_o + \partial M_o/\partial t \; \Delta t,$$

where M is the magnitude of the magnetic moment at a temperature differing from zero by Δt, and M_o is the magnitude of magnetic moment at 0°C.

Declassified in Part - Sanitized Copy Approved for Release 2013/01/23 : CIA-RDP81-01043R001600090003-8

Declassified in Part - Sanitized Copy Approved for Release 2013/01/23 : CIA-RDP81-01043R001600090003-8

Introducing the denotation

$$-\beta = 1/M_0 \cdot \partial M_0/\partial t, \tag{0.82}$$

we have

$$M = M_0(1 - \beta \Delta t). \tag{0.83}$$

The quantity β is called the temperature coefficient. The minus sign indicates that with an increase in temperature the magnetic moment decreases.

Under certain conditions the temperature coefficient, like the induction coefficient, is a constant quantity which characterizes one of the properties of the magnet, the dependence of magnetic moment upon temperature.

The influence of temperature on the magnetic properties of iron and steel was known at the time of Gilbert (1540-1603) who was the first to note that a red hot iron needle is not attracted by a magnet and that the attraction is restored as soon as the needle returns to room temperature. However, quantitative measurements were first undertaken by Coulomb (1736-1806) 200 years after the discovery of Gilbert, and more detailed investigations were conducted by academician Kupfer at Petersburg in 1830-1835.

The results of all the investigations concerning the effect of temperature on magnetic moment of a permanent magnet may be formulated as follows. With rising temperature the magnetic moment decreases; the temperature coefficient defined by equation (0.81) is not a constant in the general case, but depends upon repeated heating, i.e., in the general case the process of changes in the magnetic moment with temperature is irreversible, but after heating and cooling are repeated several times the phenomenon becomes reversible and β is constant.

Declassified in Part - Sanitized Copy Approved for Release 2013/01/23 : CIA-RDP81-01043R001600090003-8

Declassified in Part - Sanitized Copy Approved for Release 2013/01/23 : CIA-RDP81-01043R001600090003-8

The temperature coefficient depends upon the shape and dimensions of the magnet and on the material from which it is made. As a rule, the temperature coefficient decreases with an increase in the coercive force.

The magnitude of the temperature coefficient varies approximately within the limits 0.0008 to 0.0001. Magnets made of cobalt steel, alni and alnico alloys have the lowest, and magnets made of carbon steel have the highest temperature coefficients.

Analogously to expression (0.81) for the induction coefficient, equation (0.82) may be written in the form:

$$= 1/M_0 \int_V \partial J/\partial t \; dv = 1/J_m \, (\partial J/\partial t)_m \cdot \qquad (0.84)$$

In 1935 B. M. Yanovskiy and N. G. Zuyeva [1] investigated the temperature dependence of magnetization of some varieties of steel (tungsten steel and several varieties of cobalt steel). These investigations showed that with an increase in temperature the demagnetization portion of the hysteresis cycle is shifted with the origin of coordinates, as is shown in Figure 18. From these curves the derivative dJ/dt may be obtained as a function of J. The form of a function of this type is shown in Figure 19. Thus the magnitude of the temperature coefficient, similarly to that of the induction coefficient, may be obtained from hysteresis curves derived at different temperatures. From a graph of the function dJ/dt, and also from equation (0.84) it is apparent that the temperature coefficient increases sharply with reduction in the length of the magnet, because this is accompanied by a decrease in J and an increase in dJ/dt.

4. The Effect of Contact of the Magnet with other permanent magnets or with nonmagnetized ferromagnetic bodies is fully analogous

Declassified in Part - Sanitized Copy Approved for Release 2013/01/23 : CIA-RDP81-01043R001600090003-8

Declassified in Part - Sanitized Copy Approved for Release 2013/01/23 : CIA-RDP81-01043R001600090003-8

with the effect of an external magnetic field produced by the second magnet or a ferromagnetic body that is magnetized by contact with the magnet.

Since reversible changes of the magnetic moment take place only in small fields of the order of several oersteds, it is evident that upon contact with a given ferromagnetic body the magnetic moment can change in either direction, i.e., be increased or decreased by a certain quantity. For example, on closing a magnetic circuit by means of an armature the magnetic moment may be increased by several percent.

5. Effect of Impact. The magnetic moment of a permanent magnet may be altered in magnitude under the influence of mechanical effects such as impact, jarring, vibration, etc. This change in the magnetic moment always is a decrease, and steels of high coercive force show a lesser decrease of the magnetic moment than those of a low coercive force.

It has been ascertained experimentally that magnets made of soft steel with coercive force less than 40 Oe lose from 45 to 80% of the total residual magnetization after numerous impacts. With other varieties of steel the losses vary from 1 to 20%.

If the magnet is stabilized in the manner described below it becomes completely insensitive to impacts.

6. Changes of Magnetic Moment with Time. In the early nineteenth century it was noted that the magnetic moment of a permanent magnet which is not subjected to external influence decreases in magnitude with lapse of time, this change taking place very rapidly soon after the magnet is made and decreasing gradually thereafter.

Declassified in Part - Sanitized Copy Approved for Release 2013/01/23 : CIA-RDP81-01043R001600090003-8

Declassified in Part - Sanitized Copy Approved for Release 2013/01/23 : CIA-RDP81-01043R001600090003-8

If a hardened magnet is alternately heated and cooled the magnetization is lost on each heating and is only partially restored on cooling, resulting in a progressive loss of magnetization until the magnet finally reaches a stabilized state in which the magnetization lost on heating is restored on cooling. This led to the idea of artificial aging of newly made magnets by subjecting them to a process analogous to that which occurs under natural conditions but conducted at a higher rate and thus making it possible to convert the magnet to a stable condition rapidly.

This process consists in prolonged heating at a slightly elevated temperature (not exceeding 100° C).

Figure 20 shows the curve which represents changes with time in coercive force following the hardening of tungsten steel. It is apparent that marked changes take place during the first few hours after hardening. The same changes also occur on heating, but at a much more rapid rate.

Thus heating accelerates the natural changes in the physical properties of the steel.

This explains the changes of magnetic moment which have been observed with lapse of time.

Due to changes of the coercive force the configuration of the hysteresis curve is altered, i.e., the magnetic properties of steel change, and since the coercive force decreases with lapse of time the residual magnetization and consequently the magnetic moment of the magnet also decrease.

Declassified in Part - Sanitized Copy Approved for Release 2013/01/23 : CIA-RDP81-01043R001600090003-8

Declassified in Part - Sanitized Copy Approved for Release 2013/01/23 : CIA-RDP81-01043R001600090003-8

7. Magnetic Stabilization. Magnetic stabilization or magnetic aging has the purpose of converting a permanent magnet to a stable, reversible state. The best procedure is partial demagnetization by an alternating magnetic field with an amplitude gradually decreasing to zero. This is done by placing the magnet in an alternating current coil and then it is either slowly withdrawn from the coil, or the alternating current is gradually decreased to zero by means of a rheostat or a transformer without removing the magnet from the coil. The initial amplitude of the demagnetizing field is selected in accordance with the external magnetic fields and other demagnetizing factors which may be selected according to the anticipated conditions of operation of the permanent magnet. In the case of tungsten magnets used in magnitometers to measure the terrestrial field, an initial amplitude of 15-20 Oe is adequate. For cobalt magnets the initial amplitude may be raised to 40-50 Oe, and for alni alloys and other substances the amplitude may be raised to 100 Oe.

During magnetic stabilization the magnet must be disconnected. A magnet stabilized in this manner is found to be entirely insensitive to impact and jarring, has constant temperature and induction coefficients within the temperature range of 20 -50° C and a field intensity range of 1-2 Oe for tungsten magnets, 5-6 Oe for cobalt magnets and 20-30 Oe for alnico alloys magnets.

Increase of the temperature and magnetic field intensity above the stated limits induces irreversible changes of the magnetic moment. Therefore a stabilized magnet must be kept away from other magnets, iron bodies and electric currents, since any contact with another magnet or iron object is equivalent, as was stated above, to

Declassified in Part - Sanitized Copy Approved for Release 2013/01/23 : CIA-RDP81-01043R001600090003-8

Declassified in Part - Sanitized Copy Approved for Release 2013/01/23 : CIA-RDP81-01043R001600090003-8

the action of a magnetic field the intensity of which considerably exceeds permissible limits. In no event should a magnet be provided with an iron armature to conserve the magnetic moment, an iron yoke be used, or should a magnet be stored in contact with the opposite poles of other magnets.

Section 19. Magnetic Materials and Alloys

In modern technology scores of various alloys are used for the production of permanent magnets and the cores of electromagnetic mechanisms. They all differ from each other in their magnetic and technological characteristics and the selection for any particular use is based on a number of factors: cost of the material, magnetic properties, technological characteristics, the purpose for which any given electromagnetic mechanism is to be utilized.

Magnetic materials are subdivided into 2 kinds: hard magnetic and soft magnetic materials, which differ from each other not so much in hardness as in magnetic properties. Hard magnetic materials include steels and alloys the coercive force of which excees 50 Oe, while the coercive force of soft magnetic materials does not exceed several oersteds. As a rule the hardness of hard magnetic materials is of the order of 60-65 Rockwell units, while that of soft magnetic materials is not more than 20-30 units, but certain alloys with a hardness of 45-55 Rockwell units have a coercive force less than one (iron alloys containing 5-6% Al and 8-10% Si) and other alloys of the iron-nickel-copper system have a coercive forve of 400-500 Oe and a low degree of hardness, yet the former are soft magnetic alloys and the latter are hard magnetic alloys.

Hard magnetic materials are used for making permanent magnets

Declassified in Part - Sanitized Copy Approved for Release 2013/01/23 : CIA-RDP81-01043R001600090003-8

Declassified in Part - Sanitized Copy Approved for Release 2013/01/23 : CIA-RDP81-01043R001600090003-8

and soft magnetic materials are used in the production of transformer cores, electromagnets, generator and motor armatures and all kinds of electromagnetic mechanisms.

A. According to the classification of A. S. Zaymovskiy [?] hard magnetic materials may be subdivided into the following groups:

1. Malleable and hot-rolled steels which may be hardened to martensite (martensite is one of the structural components of hardened steel having a spiney microstructure. Martensite is an unstable solid solution of carbon in iron forming a centered-tetragonal lattice).

To this group includes carbon, chromium, tungsten and cobalt steels.

2. Nonmalleable alloys: shaped castings suitable only for grinding, known under the designations alni, alnico, magnico, ticonal and others. The basis of these alloys is the iron-nickel-aluminum system.

3. Malleable iron-nickel-copper or cobalt-nickel-copper alloys suitable for cold rolling and drawing.

4. Malleable iron-cobalt-vanadium alloys suitable for extensive cold rolling and drawing.

5. Alloys based on the iron-platinum and cobalt-platinum systems.

6. Press-worked and sintered magnets from oxides of cobalt and iron.

7. Press-worked magnets from powdered alloys, alni, alnico and of a number of other groups which are not specified herein because of their limited utilization in practice.

Declassified in Part - Sanitized Copy Approved for Release 2013/01/23 : CIA-RDP81-01043R001600090003-8

Declassified in Part - Sanitized Copy Approved for Release 2013/01/23 : CIA-RDP81-01043R001600090003-8

Magnetic properties of hard magnetic materials are characterized, as stated in Section 18 relating to permanent magnets, by the magnitude of residual induction and coercive force, and also by the demagnetization portion of the hysteresis curve.

Table 5 contains information concerning the magnetic properties and chemical composition of the above group of hard magnetic materials.

The table shows that the magnetic properties of modern alloys vary within a very wide range. The coercive force may have values ranging from 60 to 4000 Oe but with an increase in coercive force the residual induction usually decreases, and only magnico alloy, which has a coercive force of 550 Oe does the residual induction increase to 12,500 Gauss or higher. For comparison, the demagnetization portions of the hysteresis curves of the different steels and alloys are shown in Figure 21.

It should be noted that the high value of residual induction of magnico alloy is obtained by allowing the magnets to cool from the Curie point to room temperature within a strong magnetic field. At the same time the magnetic properties perpendicular to the magnetic field are found to be considerably lower.

Magnetic properties of soft magnetic materials are characterized by the basic magnetization curve which makes it possible to determine readily the initial permeability, maximum permeability and saturation of these materials. The characteristics of soft magnetic materials also include the residual induction B_r, coercive force H_c and losses by hysteresis and eddy currents P. Depending on the intended use of the material some of the characteristics acquire primary

Declassified in Part - Sanitized Copy Approved for Release 2013/01/23 : CIA-RDP81-01043R001600090003-8

Declassified in Part - Sanitized Copy Approved for Release 2013/01/23 : CIA-RDP81-01043R001600090003-8

importance, and therefore the requirements which must be met by the soft magnetic materials vary. In geomagnetic measurements a material having a high initial permeability and minimum coercive force is of greatest importance. In other instances the requirements may be different, such as the material for transformers must have very low loss due to hysteresis and eddy currents and must have high induction values in relatively weak fields.

Soft magnetic materials include chemically pure iron, nickel and cobalt free from admixtures. However, because of the difficulty of producting such materials, iron containing small amounts of carbon and silicon, and various alloys of the latter with elements such as nickel and cobalt are used in industry. At present, nickel and cobalt as such are not utilized industrially as magnetic materials.

Soft materials may be classified in several groups, according to their characteristic properties. These groups are the following.

1. Technically pure iron, containing no admixtures except minute traces of carbon and silicon. This group includes armco iron, electrolytic iron and carbonyl iron, which differ according to their method of production. Their magnetic properties are destroyed by low coercive force amounting to several tenths of one oersted and high induction in fields having an intensity of 25-50 Oe.

2. Electrical engineering steel, or alloys containing 2-4% silicon. Soviet domestic industry produces much steel of these varieties, which differ from one another in silicon content as well as in processing methods. These steels are characterized by small losses due to hysteresis and eddy currents and high induction values in fields having an intensity of 25-50 Oe.

Declassified in Part - Sanitized Copy Approved for Release 2013/01/23 : CIA-RDP81-01043R001600090003-8

Declassified in Part - Sanitized Copy Approved for Release 2013/01/23 : CIA-RDP81-01043R001600090003-8

The best properties are found in the KhVP type steel (high permeability, cold rolled), in which hysteresis losses are one-half of those of the best varieties of electrical engineering steel.

3. Alloys having high permeability in weak fields, known as permalloy, mumetal, hypernik and Mo-permalloy.

The principal component of these alloys is nickel, which accounts for 50 to 78% of the composition. The characteristics of these alloys are high permeability in fields having an intensity up to 1 Oe and high initial permeability. Whereas maximum permeability in the first 2 groups does not exceed $20 \cdot 10^3$, it may reach $600 \cdot 10^3$ in the case of permalloys. However, their saturation is almost one-half of that of technically pure iron and electrical engineering steel.

4. Materials having a constant value of permeability include iron, nickel and cobalt alloys showing a constant permeability in fields of up to 1-2 Oe. They include perminvar containing 45% Ni, 25% Co and 30% Fe, the permeability of which is μ = 400-600, and remains constant in fields up to 2 Oe.

5. Alloys of high magnetic saturation attained by combining iron with up to 50% of cobalt. At the present time extensive use is made of the alloy known as permendur, containing 50% Co and 1.8% V, which has a maximum value of $4\pi J$ of 23,800.

Table 6 shows some of the most widely utilized alloys, including their chemical characteristics, magnetic properties and technical uses. Figures 22 and 23 show the basic magnetization curves for fields up to 7 Oe and 300 Oe.

Declassified in Part - Sanitized Copy Approved for Release 2013/01/23 : CIA-RDP81-01043R001600090003-8

Declassified in Part - Sanitized Copy Approved for Release 2013/01/23 : CIA-RDP81-01043R001600090003-8

TABLE 5

MAGNETIC MATERIALS FOR PERMANENT MAGNETS

Group A	Steel or Alloy Designation B	Composition in Percent C	Residual Induction B_r in Gauss D	Coercive Force H_c in Oersted E	Magnet Processing Methods F
I. Hardenable to martensite	carbon	1.0 C, remainder Fe	10,000	58	
		1.5 C, rem. Fe	6,000	67	
	tungsten	0.6 C, 5.5-6.6 W rem. Fe	11,000	65	
	chrome YeKh-2	1.0 C, 1.7-1.6 Cr, 0.4 Si rem. Fe	3,000	58	Hot forging and stamping
	YeKh-3	1.0 C, 2.8-3.8 Cr, 0.4 Si 0.4 mn, rem. Fe	9,000	60	
	low cobalt YeK(Co 5%)	1.0 C, 5-7 Co, 5-10 Cr, 0-15 mn, rem. Fe	9,000	100	
	medium cobalt YeK (Co 15%)	1.0 C, 12-15 Co, 8-10 Cr, 0-1.5 mo, rem. Fe	9,000	180	
	high cobalt YeK (Co 30%)	1.0 C, 30-35 Co, 3-7 Cr, 4-7 W, rem. Fe	9,000	240	
II. Nonmalleable alloys based on iron-nickel-aluminum system	alni	12-14 Al, 2n-32 Ni, rem Fe	5,000	600	
	alnico 1	12 Al, 20 Ni, 5 Co, rem Fe	7,300	440	
	alnico 2	10 Al, 17 Ni, 12.5 Co, 6 Cu, rem. Fe	7,350	[?]	Casting with subsequent grinding
	alnico 4	12 Al, 28 Ni, rem Fe	5,300	730	cold
	magnico	8 Al, 14 Ni, 24 Co, 3 Cu rem Fe	12,500	550	
	Sk alloy	6-9 Al, 15-19 Ni, 18-35 Co, 2-12 Ti, rem Fe	7,000	800-900	

Declassified in Part - Sanitized Copy Approved for Release 2013/01/23 : CIA-RDP81-01043R001600090003-8

Declassified in Part - Sanitized Copy Approved for Release 2013/01/23 : CIA-RDP81-01043R001600090003-8

Table 5 Continued

A	B	C	D	E	F
III. Malleable alloys on copper basis	magneto flax	60 Cu, 20 Ni, 20 Fe	~~5,400~~	550	Forging and drawing, cold
IV. Plastic alloys	vicalloy 1	53 Co, 3.4 V, 0.6 Si rem Fe	8,300	290	
	vicalloy 2	52 Co, 14 V, rem Fe	10,000	500	Cold drawing possible
V. Alloys based on precious metals	platinum-iron	77 Pt, 23 Fe	2,600-4,000	~~11,500~~ ~~14,800~~	
	platinum-cobalt	66 Pt, 23 Co	300-500	~~2,600~~ 4,000	
VI. Pressure-worked magnets	oxidic magnets	Fe_3O_4 and $CoFe_2O_4$	3,500-4,000	550	Pressure working of powder compacts and sintering at 1,000°
	press magnets	Powdered alnico alloy	2,000-3,000	400-500	Bakelitization of powder and compression
	Powder metallurgy magnets	Fine powders of pure iron, nickel and iron-aluminum alloy	5,000	550	Pressure working and sintering in pure hydrogen at 1,300°

Declassified in Part - Sanitized Copy Approved for Release 2013/01/23 : CIA-RDP81-01043R001600090003-8

Declassified in Part - Sanitized Copy Approved for Release 2013/01/23 : CIA-RDP81-01043R001600090003-8

TABLE 6. MAGNETIC CHARACTERISTICS OF SOFT MAGNETIC MATERIALS

Classification I	Designation of Alloy II	Chamical Composition % III	Magnetic Properties: $\mu_o 10^{-3}$ IV	$\mu_m 10^{-3}$ V	$4\pi J \cdot 10^{-3}$ CGS VI	H_c Oe VII	P watt per kg VIII	B · 10^{-3} with H 25 Oe IX	50 Oe X	3,000 Oe XL	Uses XII
Technically pure iron	Armco iron	c < 0.025, Si < 0.05	-			0.8		16.1	16.8	20.4	Magnetic conductors, pole shoes, direct current electromagnets
	Electrolytic	C < 0.025, Si < 0.05	0.5	15.0		0.36			18.0		
	Carbomyl iron	c < 0.025, Si < 0.05	2-3.5	20-21.0		0.08					
Electrical engineering steel	E2B	Si ~ 2					2.6	15.3	16.4	20.1	Motors and generators of medium power, transformers,
	E3A	Si ~ 3					1.6	14.6	15.7	18.9	
	E4AA	Si ~ 4	0.4			0.45	1.2	14.4	15.5	18.7	motors, transformers and motors of all types and heighest quality
	KhVP		0.8			0.12	0.59	18.1	18.9		
Alloys of high permeability in weak fields	Permalloy	Ni-78	10.0	105.0	16.7						Screens, direct current relays, transformers of low and higher frequencies, magnetic screens, measuring instruments, high frequency transformers
	Permalloy S	Ni-78, Mo-2	16.0	5.0							
	Mo-Permalloy	Ni-79.5, Mo-3.8	20.0	75.0	8.5						
	Mumetal	Ni-76, Mr[sic]-08, Cu-6, Cr-2	10-20.0	40-100		0.03					
	Hypernik	Ni-50	4.5	100.0	16.0		0.5-0.6				
	Hypernik 50	Ni-50, Mn-0.3	3.4	28.0							
Materials having constant permeability	1 soperm	Ni-40; Cu-15									Telephone equipment, Pupin coils
	Perminvar	Ni-45; Co-25	0.4-0.6								
	Carbonyl Fe		0.008								
Alloys of high magnetic saturation	Permendur	Co-50, V-1.8		23.8							Telephone diaphragms, electromagnet poles

Declassified in Part - Sanitized Copy Approved for Release 2013/01/23 : CIA-RDP81-01043R001600090003-8

Declassified in Part - Sanitized Copy Approved for Release 2013/01/23 : CIA-RDP81-01043R001600090003-8

PART ONE

THE PERMANENT MAGNETIC FIELD OF THE EARTH

CHAPTER I

DESCRIPTION OF THE MAGNETIC FIELD OF THE EARTH

Section 1. Elements of Terrestrial Magnetism

Direct observations at the earth's surface as well as at a distance from the surface show that the terrestrial globe is located in a magnetic field. Thus, if a magnetic needle is suspended in such a manner that it can rotate freely about its center of gravity, at any point of the earth's surface the needle tends to assume a definite position in space without any appreciable displacement in relation to the earth's surface.

This simple experiment indicates not only the existence of a magnetic field around the earth but also the fact that this field is uniform. However, the same needle experiments show that at points on the earth's surface which are sufficiently remote from one another, its axis is oriented differently, i.e., the magnetic field is not uniform in relation to the entire surface of the earth. The task of the science of terrestrial magnetism includes experimental investigation of this field for the purpose of ascertaining its causes and its relationship to other physical phenomena occurring within the earth and within the surrounding atmosphere.

The characteristic of the earth's magnetic field, as of any magnetic field, is the field intensity H_T and its components. A rectangular system of coordinates usually is used to resolve the vector H_T into its components, in which one of the axes (x) is parallel to the geographical meridian, and the other (y) lies in the direction of the parallels of longitude, the positive direction of the x axis

Declassified in Part - Sanitized Copy Approved for Release 2013/01/23 : CIA-RDP81-01043R001600090003-8

Declassified in Part - Sanitized Copy Approved for Release 2013/01/23 : CIA-RDP81-01043R001600090003-8

facing the north and that of the y axis toward the east. The third axis (z) is vertical and its direction is considered to be from above downward.

Taking the origin of coordinates at the point of observation of the vector of intensity of the terrestrial magnetic field, the vector H_T will have a certain position OH_T (Figure 24) in relation to the system of coordinates. The projection of this vector on the x axis is called the north component and is denoted by X, the projection on the y axis is called the east component Y, and the projection on the z axis the vertical component Z.

The projection of H_T on a horizontal plane is called the horizontal component and is denoted by H.

The vertical plane zOH which contains the vector H_T is called the plane of magnetic meridian, and the angle between the magnetic meridian, and the plane x is the magnetic declination, denoted by D. Finally, the angle HOH_T between the horizontal plane and the direction of vector H_T is called the magnetic dip J. It is readily apparent that at the distribution of coordinate axes shown in the drawing the positive declination will be eastern, i.e., when the vector H is deflected from north to east, and the negative declination is western.

The dip J is positive when the vector H_T is directed downward from the earth's surface which occurs in the northern hemisphere, and it is negative when H_T is directed upward, i.e., in the southern hemisphere.

Declassified in Part - Sanitized Copy Approved for Release 2013/01/23 : CIA-RDP81-01043R001600090003-8

Declassified in Part - Sanitized Copy Approved for Release 2013/01/23 : CIA-RDP81-01043R001600090003-8

The declination D, dip J, horizontal component H, the components vertical Z, north X and east Y, are called the elements of terrestrial magnetism and may be regarded as the coordinates of the tip of vector H_T in different systems of coordinates. Thus X, Y, Z are the coordinates of the tip of vector H_T in the rectangular system of coordinates, Z, H and D the coordinates in a cyclindrical system, and H, D and J are the coordinates in a spherical system.

In each of these 3 systems the coordinates are independent of one another, i.e., one cannot express X in terms of Y and Z, or Z by means of H and D.

To pass from one system of coordinates to another and to define the magnitude of vector H_T, it is readily apparent from Figure 24 that the following correlations obtain:

$$X = H \cos D; \quad Y = H \sin D; \quad Z = H \operatorname{tg} J; \quad H^2 = X^2 + Y^2;$$
$$H_T^2 = H^2 + Z^2; \quad H_T = H \sec J = Z \operatorname{cosec} J; \quad \operatorname{tg} D = Y/X. \tag{1.1}$$

Observations of the magnitudes of these elements show that none of them remains constant in time, and the value of each changes continuously from hour to hour and from year to year. These changes have been designated variations of the elements of terrestrial magnetism. If these variations are observed during a short interval of time, on the order of 24 hours, it is possible to detect that they are of a periodic nature, the periods, amplitudes and phases of which are extremely diversified. If the observations are conducted over a prolonged interval, on the order of several years, it may be readily ascertained that the mean annual values of the elements also undergo changes of a monotonous nature, the periodicity of which may be detected only over a very long period of observations, on the order of several hundred years.

Declassified in Part - Sanitized Copy Approved for Release 2013/01/23 : CIA-RDP81-01043R001600090003-8

Declassified in Part - Sanitized Copy Approved for Release 2013/01/23 : CIA-RDP81-01043R001600090003-8

Thus these variations may be classified into 2 types: rapid variations of periodic nature and slow, or secular variations. Investigations of both types of variations have shown that they differ not only in nature but also in origin. The source of rapid variations are electric currents within the upper strata of the atmosphere, called the ionosphere, whereas the secular variations are associated with sources within the terrestrial globe and probably have the same origin as the magnetic field of the earth.

Therefore it is customary to subdivide the observed magnetic field in 2 parts: the permanent magnetic field and its secular variations, caused by internal sources and the variable magnetic field which is of external origin.

Section 2. Graphic Representation of the Earth's Magnetic Field.

Magnetic Maps

Magnetic observations at different points of the earth's surface provide vast and diversified data concerning the distribution of the elements of terrestrial magnetism over the surface of the terrestrial globe.

This distribution is illustrated by the graphic method of representing the magnetic field, consisting of plotting maps of isolines, i.e., of curves which connect points having equal values of any given element. Thus the curves which connect points of equal declination are called isogons, curves of equal dip are isoclines, and the curves of equal horizontal components are isodynes of horizontal or vertical components. The lines of equal north and east components are called, isodynes of north and east components, respectively.

Declassified in Part - Sanitized Copy Approved for Release 2013/01/23 : CIA-RDP81-01043R001600090003-8

Declassified in Part - Sanitized Copy Approved for Release 2013/01/23 : CIA-RDP81-01043R001600090003-8

Such isolinear maps greatly facilitate investigation of the terrestrial field and also facilitate practical utilization of magnetic survey data. These maps provide a clear picture of the qualitative and quantitative nature of the magnetic field of the terrestrial globe as a whole, and of the individual areas as well.

Since the elements of terrestrial magnetism do not remain constant in time, but change continuously, such a magnetic map relates to some specific point of time. This point of time usually is selected at the middle of a given year, the first of July, and is called the epoch. For example, if a map is drawn for the 1945 epoch the magnitudes of the elements relate to 0 hours 0 minutes of 1 July 1945. At the present time magnetic maps are usually prepared for epochs which are multiples of 5: 1940, 1945, etc.

Magnetic maps are prepared for individual regions, for the entire country, and for the entire terrestrial globe. The latter are called world maps.

It is evident that the smaller the scale of the map, the less accurate is the plotting of isolines and consequently the agreement between actual distribution of the magnetic field and the magnetic field as represented on the map also is less. On small scale maps all the local features of the distribution are levelled off and therefore magnetic maps of this scale, which usually include the world maps and maps of individual countries, must be regarded as representing certain average distribution of the elements of terrestrial magnetism.

Declassified in Part - Sanitized Copy Approved for Release 2013/01/23 : CIA-RDP81-01043R001600090003-8

Declassified in Part - Sanitized Copy Approved for Release 2013/01/23 : CIA-RDP81-01043R001600090003-8

The first magnetic maps of the European portion of Russia were drawn for the 1880 epoch by the astronomer-geodecist A. Tillo [3].

The data available to Tillo in drawing his maps consisted of observations at 894 points, which is an average of one observation point per 7,000-8,000 km^2. It is evident that with such a sparse observation network the maps of Tillo were only a very general representation of the magnetic field of Russia. Nevertheless they were of great practical importance at that time and also played an important part in the history of the development of Soviet science.

During the period 1880 to 1930 the preparation of magnetic maps in Russia was limited to maps of individual regions. Thus Tillo prepared an isolinear map of the north component for Northern Siberia. B. P. Veynberg constructed maps of the 3 elements for the Crimean peninsula for the 1900 epoch, and of Central Asia for the 1925 epoch [4].

The first maps of the entire Soviet Union were prepared by the Institute of Terrestrial Magnetism for the 1925 epoch [5]. Although these maps were based on fairly extensive data the distribution of the data was very uneven. More than two-thirds of the 10,000 observation points pertained to European Russia, with the result that the isolines within the Asian portions of these maps gave only a rough approximation of the distribution of the elements of terrestrial magnetism.

At the present time the amount of data available to the Institute of Terrestrial Magnetism is several times greater than that of 1925, and therefore maps prepared by the Institute for the 1935 subsequent epochs are more accurate representations of the actual distribution of the magnetic field within the USSR.

Declassified in Part - Sanitized Copy Approved for Release 2013/01/23 : CIA-RDP81-01043R001600090003-8

Declassified in Part - Sanitized Copy Approved for Release 2013/01/23 : CIA-RDP81-01043R001600090003-8

The magnetic maps of the world (Figures 25, 26 and 27) provide general ideas of the distribution of the elements of terrestrial magnetism over the surface of the globe. Examination of these maps reveals that the isolines constitute a system of curves which show certain regularities in their configuration. For example, the isogons start from one point of the terrestrial globe and converge at another point which is almost opposite on the globe, recalling in this respect the configuration of the meridians. The only exception is in the eastern portion of the Asian continent where the isogons form closed contours.

The plotting of isogons within the areas of geographic poles (Figure 28) reveals that they converge not at two, but at 4 points in the northern and the southern hemispheres. Two of these points are the geographic poles, and the 2 located near the geographic poles are called the magnetic poles, the one nearest the north geographic pole is called the north magnetic pole, and that nearest the south geographic pole is called the south magnetic pole.

Magnetic poles are characterized by the fact that at these poles the horizontal component is equal to zero and the dip is 90°. A magnetic needle rotating freely in the horizontal plane can come to rest while pointing in any direction, and therefore at a magnetic pole the concept of a magnetic meridian becomes devoid of meaning.

The convergence of isogons at the magnetic poles is caused by the fact that at these points the declination is indefinite and around them it can assume values from 0 to 360°. Since declination is the angle between the geographic and the magnetic meridian, it follows that at the geographic pole where there is a magnetic

Declassified in Part - Sanitized Copy Approved for Release 2013/01/23 : CIA-RDP81-01043R001600090003-8

Declassified in Part - Sanitized Copy Approved for Release 2013/01/23 : CIA-RDP81-01043R001600090003-8

meridian but no geographic meridian the declination is indefinite. The same is true of the magnetic pole, where there is a geographic meridian but no magnetic meridian.

On the other hand, in the area around a geographic pole the geographic meridians change their direction from 0 to 360°, while the magnetic meridian maintains constant direction, with the result that the declination changes from 0 to 360°.

The same also occurs around a magnetic pole, where the geographic meridian is constant and the magnetic meridian is variable.

On transition from the north magnetic pole to the south magnetic pole the horizontal component first increases from zero to a certain maximum and thereafter it decreases again to zero. As is apparent from the map of isolines during this transition maximum value varies at the different meridians. The maximum of greatest magnitude is found in the region of the Sunda Isles where the horizontal component reaches a value of 0.4 Oe.

The smoothest and most regular transition is found on the isoclines which constitute a series of parallel curves extending in the direction of latitude.

The zero isocline circumscribes the terrestrial globe near the equator. On transition from this zero isocline to either magnetic pole the dip increases from zero to 90°. The zero isocline is called the magnetic equator.

Isoclines of the vertical component are analogous to those of the dip. At the magnetic poles the vertical component reaches a maximum value of about 0.6 Oe while at the magnetic equator it is

Declassified in Part - Sanitized Copy Approved for Release 2013/01/23 : CIA-RDP81-01043R001600090003-8

Declassified in Part - Sanitized Copy Approved for Release 2013/01/23 : CIA-RDP81-01043R001600090003-8

equal to zero. On either side of the magnetic equator the vertical component increases toward the poles.

Observations show that the position of magnetic poles as well as those of the isolines does not remain constant but changes continuously from year to year. This is apparent from Table 7 which shows the geographic coordinates of both poles calculated for different epochs on the basis of observational data.

TABLE 7

GEOGRAPHIC COORDINATES OF MAGNETIC POLES FOR DIFFERENT EPOCHS

Epoch	1600	1700	1770	1829	1885	1900	1922	1950
North Pole								
Latitude	78°42	75°51	66°	73°21	69°57	69°18	71°	72°
Longitude	59°00	68°48	104°	93°56	182°45	96°37	96°	96°
South Pole								
Latitude	81°16	77°12	-	72°40	73°45	-	72°25	70°
Longitude	169°30	155°15	-	150°45	153°00	-	154°00	150°

The north magnetic pole was first reached by Captain James Ross in July 1831, who observed that the magnetic dip at 70° 05' 17" latitude and 96°45'48" longitude was 90° in relation to the horizon.

However, because of the imperfect instruments available at that time the position of the magnetic pole discovered by Ross must be regarded as being a rough approximation. Actually, from the standpoint of experimental results the magnetic pole constitutes a certain region wherein the dip has a value of 90° within the limits of experimental error, since in the vicinity of the magnetic poles the dip changes very slowly on passage from one point to another.

Figure 29 shows a map on which the possible location of the north magnetic pole during the 1836 epoch is indicated by a closed line and the position reached by Ross in 1831 is indicated by "X".

Declassified in Part - Sanitized Copy Approved for Release 2013/01/23 : CIA-RDP81-01043R001600090003-8

Declassified in Part - Sanitized Copy Approved for Release 2013/01/23 : CIA-RDP81-01043R001600090003-8

The south magnetic pole still has not been reached by an observer, although Captain Ross came closest to it in 1841.

In addition to isolinear maps, maps sometimes are drawn of the meridians which constitute sets of lines extending at any point of the terrestrial globe through the magnetic axis of a freely suspended needle. Thus the angles between these lines and the geographic meridians represent the declination at any given location. Within each hemisphere the meridians converge at a single point, namely at the magnetic pole.

Figure 30 shows such a map of meridians for the 1950 epoch drawn by V. P. Orlov [6].

On considering magnetic maps drawn for individual regions and even individual countries it may be observed that the regularities in the course of the isolines on world maps are drastically destroyed and the isolines present a diversified and confused appearance. Thus in Figure 31, which shows a map of isogons in one area of the Kursk Oblast, the extent to which the course of the isolines departs from the general regular trend shown on the world map of isogons is apparent. This indicates that near the earth's surface the magnetic field is distributed most irregularly and constitutes a complex function of the coordinates of surface points. The cause of this is the nonuniform structure of the earth's shell and especially of the earth's crust, which is unevenly magnetized because of its different magnetic properties at different areas.

Section 3. Methods of Investigation the Magnetic Field of the Earth. Magnetic Surveys. Magnetic Observatories.

The principal methods of studying the earth's magnetic field are

Declassified in Part - Sanitized Copy Approved for Release 2013/01/23 : CIA-RDP81-01043R001600090003-8

Declassified in Part - Sanitized Copy Approved for Release 2013/01/23 : CIA-RDP81-01043R001600090003-8

direct observation of the distribution of the magnetic field throughout the surface of the earth, and of its changes with lapse of time. Observations of this distribution consist of measurement of the elements of terrestrial magnetism at different points of the earth's surface and are known as magnetic surveys.

Observation of the changes of these elements are carried out at continuously operating magnetic observatories located at different points of the terrestrial globe.

1. Magnetic surveys were initiated at the time when declination was discovered by Columbus. However, during the first 2 centuries (1500-1700) following this discovery the magnetic surveys were of a random nature and were made mostly by navigators for whom determination of the magnitude of declination along their sailing routes was most important. The first systematic survey of declination and dip over the entire globe was carried out at the end of the seventeenth century. This survey made possible the execution of the first magnetic maps of the world in 1700.

At the present time magnetic surveys are conducted by special establishments in every country in most instances cover only the territory of their own country and its colonies.

The first determinations of declination in Russia were carried out in 1586 at the estuary of the Pechera river and from that time to the beginning of the Great October Socialist Revolution only 8,000 observations were made which was equal to an average of one point per 4,500 km^2.

Prior to 1910 magnetic surveys were conducted either by individual

Declassified in Part - Sanitized Copy Approved for Release 2013/01/23 : CIA-RDP81-01043R001600090003-8

Declassified in Part - Sanitized Copy Approved for Release 2013/01/23 : CIA-RDP81-01043R001600090003-8

establishments for their own use (Main Hydrographic Administration, Military Topographic Administration) or were conducted by individual persons on their own initiative. The most extensive work along this line was done by I. N. Smirnov, as was mentioned above.

A systematic magnetic survey of the entire territory of Russia was started by a special commission on Magnetism of the Academy of Sciences [7] in 1910. During 5 years (1910-1914) i.e., to the beginning of World War I, this commission was able to carry out observations at 376 points in the former guberniyas of Petersburg, Novgorod, Bessarabiya, the former Vel'skiy crown land Okrug, situated partially within the former guberniya of Arkchangel'sk and partially within the former guberniya of Vologda. The funds allocated for this purpose permitted the commission to assign not more than 2 or 3 observers to this survey for a period of 3 months. The survey was conducted by the following observers: Ye. A. Kuchinskiy, D. F. Nezdyurov, A. P. Lloydis, Professor N. A. Bulgakov, P. G. Abel's, A. S. Bezikovich, and Z. Yu. Gelin. These observers were under the general direction of the commission, the chairman of which was Academician M. A. Rykachev.

At this rate the execution of magnetic observations throughout all of Russia spaced at 20 km intervals would require more than 100 years.

2. General Magnetic Survey of the USSR. In 1923, after the Great October Revolution a geomagnetic department was established at the initiative of the Main Geophysical Observatory, the main task of which was the preparation and execution of a magnetic survey throughout the territory of the Soviet Union, which had been interrupted by World War I. Preparations for this survey required 7 years of preliminary work by the Geomagnetic department, during which time personnel

Declassified in Part - Sanitized Copy Approved for Release 2013/01/23 : CIA-RDP81-01043R001600090003-8

Declassified in Part - Sanitized Copy Approved for Release 2013/01/23 : CIA-RDP81-01043R001600090003-8

and equipment were acquired, a plan of the survey was prepared and a secular progression service was established. The secular progression service consists of systematic magnetic observations at certain specific points, called field control points. Field control points are spaced 250 to 500 km apart and observations are carried out at these points every 5 years.

Realizing the vast scientific and national economic importance of the results of the magnetic survey, on 21 August 1930 the Council of People's Commissars issued a decree concerning the execution of a general magnetic survey throughout the territory of the entire Soviet Union according to the plan developed by the Geomagnetic Division, and entrusted the conduct of this survey to the Main Geophysical Observatory which set up a special bureau of general magnetic survey.

The bureau initiated the survey in 1931 and fulfilled the planned project within 5 years, covering essentially all of the territory of the USSR.

The plan provided for a total survey of the European portion of the USSR and an itinerary survey of the Asiatic portion. In the total survey the observation points were distributed at intervals of 20-30 km, more or less in checkerboard fashion. The distance between points was the same in the itinerary survey but they were distributed only along communication routes, railroads, country roads and rivers, and along special routes in the deserts of Central Asia.

From 1931 to 1936, inclusive, determinations were made at about 12,000 points, which was one-and-one-half times greater than the number of points at which determinations had been made during the entire period from the discovery of declination to the beginning of

Declassified in Part - Sanitized Copy Approved for Release 2013/01/23 : CIA-RDP81-01043R001600090003-8

Declassified in Part - Sanitized Copy Approved for Release 2013/01/23 : CIA-RDP81-01043R001600090003-8

the general survey. The scale of this operation may be gauged from the fact that in some years as many as 50 parties were engaged simultaneously in the work, whereas from 1910 to 1914 the Academy of Sciences could send out not more than 3 or 4.

Results of the magnetic survey have shown that the magnetic field of USSR is of such topological complexity that the survey scale adopted by the general survey bureau cannot cover all the local anomalies. Notwithstanding this shortcoming the general magnetic survey was of tremendous importance both in the resolution of the problem of terrestrial magnetism and to the national economy of the country. The first close approximation magnetic maps of USSR were prepared as a result of this survey, and they have played an important part in the solution of many scientific and practical problems. The general magnetic survey of 1931-1936 must be regarded as the first stage in the study of spatial distribution of the elements of terrestrial magnetism.

The next stage was the systematic survey which has been conducted from 1937 to the present time by the Institute of Terrestrial Magnetism. The purpose of this survey is to make magnetic maps of the next more accurate approximation, which would permit determination of all the magnetic anomalies within the USSR. For this purpose the survey is conducted on a larger scale. In European USSR the observations are conducted over itineraries along which determinations are made of the vertical component by means of magnetic balance at 1 or 2-km intervals and the usual 3 elements are determined at 20 km intervals. The itineraries are spaced 10 to 20 km apart.

In the Asiatic portion of the USSR a total survey is being conducted according to the former schedule.

Declassified in Part - Sanitized Copy Approved for Release 2013/01/23 : CIA-RDP81-01043R001600090003-8

Declassified in Part - Sanitized Copy Approved for Release 2013/01/23 : CIA-RDP81-01043R001600090003-8

At the beginning of 1950 the total number of points at which the elements of terrestrial magnetism have been determined reached 26,000.

As a rule, magnetic surveys are carried out during the summer from May to September, by magnetic parties each of which consists of an observer, his assistant and a laborer. The party is equipped with a set of instruments with which magnetic and astronomical observations may be made.

The observations consist of a determination of the declination D, horizontal component H, dip J and also determination of the chronometer correction in relation to local time T and the azimuth.

In areas for which large-scale topographic maps are available, latitude φ and longitude λ of the point are taken from the map, while in areas for which no such map is available the geographic coordinates of the point are determined by astronomical observations.

The permissible errors in determination of the elements of terrestrial magnetism which have been adopted for magnetic surveys in the USSR are the following,

$\Delta D = \pm 1'$, $\Delta J = \pm 2'$, $\Delta H = \pm 0.001\ H$,

and for astronomical observations,

$$\Delta \varphi = \pm 1', \quad \Delta \lambda = 1'.$$

The declination and horizontal component are determined by means of a magnetic theodolite by one of the methods described in Part Four. Either the induction inclinometer or the magnetic theodolite with malleable iron rods are used for determining dip.

The magnetic theodolite may be used for astronomical observations

Declassified in Part - Sanitized Copy Approved for Release 2013/01/23 : CIA-RDP81-01043R001600090003-8

Declassified in Part - Sanitized Copy Approved for Release 2013/01/23 : CIA-RDP81-01043R001600090003-8

if it is equipped with a vertical circle, otherwise it is necessary to use a special theodolite. In addition, the set of astronomical instruments must include a half-second chronometer.

3. Magnetic observatories, as was stated above, serve for observation of changes in terrestrial magnetism elements which take place continuously with the lapse of time.

These changes, which have been designated magnetic variations, are recorded at the observatories by means of special automatic instruments, magnetic variometers, which provide a continuous record of the variations in the form of curves traced on a photographic tape. A description of these instruments and of the procedures for using them are presented in Part Four. The magnetic observatory service consists first of maintaining the variometers in working condition so that the absolute value of the elements of terrestrial magnetism may be determined at any time from the recording with an accuracy of ±0.1 for the declination, ±0.0001 H for the horizontal component and ±0.0001 Z for the vertical component. The second function of the service is the primary processing of the recordings of variometers, which consists of converting the hourly coordinates of the recording curves into absolute values, and also calculation of the means monthly values of each element and preparing monthly tables of the hourly deviation of the element from its mean monthly value.

For these purposes the absolute elements of terrestrial magnetism are determined regularly (every week or 2), with an accuracy one order of magnitude higher than those made in the course of magnetic surveys.

Declassified in Part - Sanitized Copy Approved for Release 2013/01/23 : CIA-RDP81-01043R001600090003-8

Declassified in Part - Sanitized Copy Approved for Release 2013/01/23 : CIA-RDP81-01043R001600090003-8

In addition, the value of one division of the graduation scale of the variometer also is determined regularly, but less frequently.

In pre-revolutionary Russia there were only 5 magnetic observatories: at Pavlovsk near Leningrad, at Sverdlovsk, Zuy near Irkutsk, at Tbilisi and at Kazan. After the revolution the USSR magnetic observatory network increased more than 3-fold.

At the present time there are 64 magnetic observatories throughout the world, 16 of which are in the USSR. Alist of all the observatories including thoir coordinates and the values of the elements of terrestrial magnetism is included in the appendix.

CHAPTER II

ANALYTICAL REPRESENTATION OF THE EARTH'S MAGNETIC FIELD

Section 1. The Earth's Magnetic Field as the Field of a Uniformly Magnetized Sphere

One of the first problems in the study of the earth's magnetic field is its representation in the form of an analytic correlation between the components of its intensity and the coordinates of points of terrestrial surface. Such a representation is possible when the causes which induce the magnetic field are known, or as is shown by the theory of potential, when the distribution of the elements of terrestrial magnetism over the surface of the earth is known from observations. If we know the functional correlation between the elements of terrestrial magnetism and the coordinates of the points, we are in a position to solve entire series of scientific and practical problems.

Declassified in Part - Sanitized Copy Approved for Release 2013/01/23 : CIA-RDP81-01043R001600090003-8

Declassified in Part - Sanitized Copy Approved for Release 2013/01/23 : CIA-RDP81-01043R001600090003-8

One of the first attempts at such a representation was a paper of the Russian scientist, I. M. Simonov, a professor at the University of Kazan, published in 1835 in the "Zapiski" [Records] of this University under the title "An Experiment on a Mathematical Theory of Terrestrial Magnetism."

In this paper I. M. Simonov made the assumption, based on observational results available at that time, that the magnetic field of the earth is the field of a uniformly, magnetized sphere, the magnetic axis of which extends through the center of the terrestrial globe parallel to the line which joins the magnetic poles. Thus the solution of the problem required determination of the field of a uniformly magnetized sphere as a function of the coordinates, which was precisely that which was done by I. M. Simonov.

The work of I. M. Simonov is still important because as shown by Gauss and other scientists the greatest portion of the earth's magnetic field constitute the field of a uniformly magnetized sphere, and in the treatment of many problems it still is assumed that the terrestrial globe is uniformly magnetized.

Therefore, the expression of the elements of terrestrial magnetism, assuming that the earth is uniformly magnetized shall be taken into consideration.

In Section 12 of the introduction it was shown that the potential of a uniformly magnetized sphere at point P is expressed by the equation:

$$U = M/r_w \cos \theta, \qquad (2.1)$$

where θ is the angle between the axis of the magnet OQ and the direction of radius vector OP = r (Figure 32), and where the axis of

Declassified in Part - Sanitized Copy Approved for Release 2013/01/23 : CIA-RDP81-01043R001600090003-8

Declassified in Part - Sanitized Copy Approved for Release 2013/01/23 : CIA-RDP81-01043R001600090003-8

rotation of the earth ON forms an angle 90-φ° with the magnetic axis OQ. Connecting the points P, Q and N by great circle arcs, we have in the spherical triangle PQN:

$$\cos\theta = \sin\varphi \sin\varphi_0 + \cos\varphi \cos\varphi_0 \cos(\lambda - \lambda_0)$$

where φ and λ are latitude and longitude of point P, φ_0 and λ_0 are the latitude and longitude of point Q, and consequently

$$U = M/r^2 \,[\sin\varphi \sin\varphi_0 + \cos\varphi \cos\varphi_0 \cos(\lambda - \lambda_0)],$$

The magnetic moment M may be defined as the volume of the sphere multiplied by the magnetization J, i.e.,

$$M = 4/3\ \pi R^3 J$$

where R is the radius of the sphere.

Taking the following formulations:

$$\begin{aligned} g_1^0 &= \tfrac{4}{3}\pi J \sin\varphi_0, \\ g_1' &= \tfrac{4}{3}\pi J \cos\varphi_0 \cos\lambda_0, \\ h_1' &= \tfrac{4}{3}\pi J \cos\varphi_0 \sin\lambda_0, \end{aligned} \qquad (2.2)$$

then

$$U = \frac{R^3}{r^2}\left[g_1^0 \sin\varphi + (g_1' \cos\lambda + h_1' \sin\lambda)\cos\varphi\right]. \qquad (2.3)$$

Since the great circle arc NP is the meridian of point P, the component in the direction NP will be the north component X, the component in the direction of the lesser circle arc PS, which is a parallel, is the east component Y, and finally the component in the direction of radius-vector r is the vertical component Z, then

$$X = \frac{1}{r}\cdot\frac{\partial U}{\partial\varphi}, \quad Y = \frac{1}{r\cos\varphi}\cdot\frac{\partial U}{\partial\lambda}, \quad Z = \frac{\partial U}{\partial r}.$$

Differentiating expression (2.3) with respect to φ, λ and r, and assuming r = R, since point P is situated on the earth's surface, we obtain the following values of the magnetic field:

Declassified in Part - Sanitized Copy Approved for Release 2013/01/23 : CIA-RDP81-01043R001600090003-8

Declassified in Part - Sanitized Copy Approved for Release 2013/01/23 : CIA-RDP81-01043R001600090003-8

$$X = g_1^0 \cos\varphi - (g_1^1 \cos\lambda + h_1^1 \sin\lambda)\sin\varphi,$$
$$Y = -g_1^1 \sin\lambda + h_1^1 \cos\lambda, \qquad (2.4)$$
$$Z = 2[g_1^0 \sin\varphi + (g_1^1 \cos\lambda + h_1^1 \sin\lambda)\cos\varphi],$$

where g_1^0, g_1^1 and h_1^1 are certain constant coefficients which do not depend upon the position of point P on the earth's surface.

φ_0 and λ_0 represent the coordinates of the point of intersection of the magnetic axis with the surface of the terrestrial globe. Taking the meridian which passes through this point as the prime meridian, it follows that $\lambda_0 = 0$, and in view of formula (2.2) $h_1^1 = 0$, hence the components of the terrestrial field are

$$X = g_1^0 \cos\varphi - g_1^1 \cos\lambda \sin\varphi,$$
$$Y = g_1^1 \cos\lambda,$$
$$Z = 2[g_1^0 \sin\varphi + g_1^1 \cos\lambda \cos\varphi].$$

If the magnetic axis is made to coincide with the axis of rotation of the earth the components of the magnetic field assume the form:

$$X = g_1^0 \cos\varphi, \quad Y = 0, \quad Z = 2g_1^0 \sin\varphi,$$

or

$$X = H = \frac{M}{R^3}\cos\varphi, \quad Z = \frac{2M}{R^3}\sin\varphi \qquad (2.5)$$

At the equator, where $\varphi = 0$:

$$Z = 0, \quad H = H_T = \frac{M}{R^3} \qquad (2.6)$$

At the pole, where $\varphi = 90^\circ$:

$$H = 0, \quad Z = H_T = \frac{2M}{R^3}. \qquad (2.7)$$

The ratio Z/H represents the tangent of the angle of dip I.

Therefore, dividing equations (2.5) by each other we obtain:

$$\operatorname{tg} I = 2 \operatorname{tg} \varphi \qquad (2.8)$$

i.e., the tangent of the angle of dip is twice as large as the tangent of the magnetic latitude.

Declassified in Part - Sanitized Copy Approved for Release 2013/01/23 : CIA-RDP81-01043R001600090003-8

Declassified in Part - Sanitized Copy Approved for Release 2013/01/23 : CIA-RDP81-01043R001600090003-8

If one compares the values of the elements of terrestrial magnetism calculated according to these formulas with the actual values, very large discrepancies are found for some of the points but these are not of an order of magnitude to require that the hypothesis of uniform magnetization be rejected altogether. On the contrary, there is observed a certain tendency of coincidence with a field of uniform magnetization.

Thus, for example, the value of field intensity at the magnetic equator is about one-half of that at the magnetic pole (at the pole $H_T = 0.65$ Oe, at the equator $H_T = 0.35$ Oe). Similarly, in many instances the magnetic dip conforms to the law of (2.8).

Therefore, in a rough approximation the magnetic field of the earth may be considered to be the field of a dipole and the theory of I. M. Simonov may be applied in solving problems of a practical nature, such as determining the gradients of terrestrial magnetism and the magnetic moment of the terrestrial globe.

1. Gradients. The gradient of any given element of terrestrial magnetism is its change on moving a unit distance along, or upward from the earth's surface.

To determine the gradients of vertical and horizontal components of altitude and latitude (magnetic) we have:

From equation (2.5):

$$\Delta H/\Delta R = -3H/R; \quad \Delta H/\Delta \varphi = -H \operatorname{tg} \varphi = -Z/2 \sin 1^\circ$$

and

$$\Delta Z/\Delta R = -3Z/R; \quad \Delta Z/\Delta \varphi = Z \operatorname{ctg} \varphi = 2H \sin 1^\circ.$$

Taking the radius of the earth as $R = 6.10^3$ km, and the

Declassified in Part - Sanitized Copy Approved for Release 2013/01/23 : CIA-RDP81-01043R001600090003-8

Declassified in Part - Sanitized Copy Approved for Release 2013/01/23 : CIA-RDP81-01043R001600090003-8

vertical and horizontal components, respectively, at Leningrad as 47,000 γ and 15,300 γ, we obtain:

$\Delta Z/\Delta R = -23.5\,\gamma$/km; $\Delta Z/\Delta\varphi^{\circ} = 250\,\gamma$/degree = 2.5 γ/km;

$\Delta H/\Delta R = -7.5\,\gamma$/km; $\Delta H/\Delta\varphi^{\circ} = 400\,\gamma$/degree = 4.0 γ/km.

i.e., on rising to an altitude of one km the vertical component at Leningrad decreases 23.5γ and the horizontal component decreases 7.5γ. On moving one km in the direction of the north magnetic pole the vertical component increases by 2.5γ and the horizontal component decreases by 4γ.

2. Magnetic Moment of the Earth. The magnetic moment of the terrestrial globe, corresponding to a uniform magnetization, may be determined by raising the equations (2.2) to the second power and adding them, which gives:

$$4/3\,\pi J = \sqrt{g_1^{o2} + g_1^{1^2} + h_1^{1^2}},$$

and on multiplying both sides by R^3 we have:

$$M = R^3\sqrt{g_1^{o2} + g_1^{1^2} + g_1^{1^2}}. \qquad (2.9)$$

The coefficients g_1^o, g_1^1, and h_1^1 are determined from equations (2.4) in which it is only necessary to substitute the numerical values of X, Y and Z for any point of the terrestrial globe where these values are known.

These coefficients have been determined from a series of observations at different points uniformly distributed over the entire surface of the terrestrial globe.

According to the calculations of V. I. Afanas'yeva

$g_1^o = 0.3032$, $g_1^1 = 0.0229$, $h_1^1 = 0.0590$.

hence,

$$M = 8.3 \cdot 10^{25}\ \text{CGS}\mu.$$

Declassified in Part - Sanitized Copy Approved for Release 2013/01/23 : CIA-RDP81-01043R001600090003-8

Declassified in Part - Sanitized Copy Approved for Release 2013/01/23 : CIA-RDP81-01043R001600090003-8

The mean magnetization of the terrestrial globe is

$$J = 3/4\pi\sqrt{g_1^{o2} + g_1^{1^2} + h_1^{1^2}} = 0.072 \text{ CGS}\mu.$$

Assuming that the magnetization of the terrestrial globe is concentrated within its core, the radius of which is about one-half of that of the terrestrial globe, the magnetization of this core must be 8 times greater, i.e.,

$$J = 0.58 \text{ CGS}\mu.$$

For comparison, the residual magnetization of a ferromagnetic sphere depending on the magnitude of residual magnetization and coercive force of the material, ferromagnetic composition, may be calculated.

In Section 9 of the introduction it was shown that the residual magnetization of a sample of any shape is determined by the ordinate of the intersection of the demagnetization part of the hysteresis curve with a straight line drawn from the origin of coordinates at an angle to the y axis, the tangent of which is equal to the demagnetization coefficient N of the sample. Determination of the ordinate of the intersection point requires that the equation of the demagnetization portion of the hysteresis curve be known. Plotting the intensity of the magnetic field on the abscissa axis at a scale so that the magnitude of coercive force H_c plotted on the x-axis is equal to the magnitude of the ordinate corresponding to the residual magnetization J_r, then the demagnetization portion of the curve may be assumed to be very roughly equal to an arc of circumference. The equation of such a circumference will be of the form:

$$J^2 + \beta^2 H^2 = J_r^2 \text{ , wherein } \beta = J_r / H_c,$$

where J and H are the coordinates of some point P of the circumference (Figure 33).

Declassified in Part - Sanitized Copy Approved for Release 2013/01/23 : CIA-RDP81-01043R001600090003-8

Declassified in Part - Sanitized Copy Approved for Release 2013/01/23 : CIA-RDP81-01043R001600090003-8

If point P is the point to be determined, i.e., if its ordinate represents the residual magnetization of the sphere, its abscissa must satisfy the equation:

$$H = NJ.$$

Consequently, the equation of the circumference is of the form:

$$J^2 + \beta^2 N^2 J^2 = J_r^2,$$

and therefore

$$J = \sqrt{J_r / 1 + \beta^2 N^2},$$

or on replacing β by its value, and the coefficient of demagnetization of the sphere by its approximate value, which is 4, we have

$$J = J_r H_c / \sqrt{H_c^2 + 16 J_r^2}$$

Since the coercive force of any industrial material always is smaller or of the same order as the residual magnetization J_r, we may disregard the quantity H_c^2 within the radical sign in the denominator, and in such a case

$$J = H_c / 4$$

i.e., the magnetization of the sphere is 4 times smaller than the coercive force of the material from which it is made. Thus in the case of a sphere made of malleable iron the H_c of which is of the order 1.5-2 Oe, the magnetization cannot exceed 0.25 CGSμ. For a sphere of carbon steel, which has a coercive force of the order of 50 Oe, the magnetization must be of the order of 12 CGSμ. For a sphere of alnico or magnico the residual magnetization may be as high as 150 CGS μ, or higher.

Comparing these values of J with the value of J for the core of the terrestrial globe, it becomes apparent that the core has a J of the same order as the magnetization of a sphere of malleable iron and is many times smaller than the magnetization of a sphere made from modern, high-coercive alloys.

Declassified in Part - Sanitized Copy Approved for Release 2013/01/23 : CIA-RDP81-01043R001600090003-8

Declassified in Part - Sanitized Copy Approved for Release 2013/01/23 : CIA-RDP81-01043R001600090003-8

To produce a spherical magnet having a magnetic moment equal to that of the earth, it would be necessary to make a sphere of modern ferromagnetic alloys (alnico or magnico) having a diameter on the order of 1,000 km.

3. Geomagnetic Poles. Geomagnetic Coordinates. The occurrence of some phenomena of terrestrial magnetism, for example variations during the course of a solar day, depend upon the geomagnetic coordinates or the latitude and longitude. The geomagnetic latitude φ is the complement of the angle between the magnetic axis of the dipole, or axis of uniform magnetization, and the radius-vector extending from the earth's center to the given point. The geomagnetic longitude λ is the angle between the magnetic meridian of the site and the magnetic meridian extending through the geographic pole. The points of intersection on the magnetic axis of the dipole or of a uniformly magnetized sphere are called geomagnetic poles to differentiate them from the magnetic poles which are the points at which dip is equal to zero and where all the isogons converge.

The geographic coordinates φ_o and λ_o of the geomagnetic poles may be determined by the equations of (2.2), from which we obtain:

$$\operatorname{tg}\lambda_o = h_1^1/g_1^1, \quad \operatorname{tg}\varphi_o = g_1^1/\sqrt{(h_1^1)^2 + (g_1^1)^2}.$$

Using the values of coefficients g_1^1 and h_1^1, determined by V. I. Afanas'yeva for the 1945 epoch we obtain for the north pole:

$$\varphi_o = 78.2^\circ, \quad \lambda_o = 68.8\ \text{W}.$$

On comparison with the coordinates of the magnetic pole it is apparent that the geomagnetic pole is located 7° farther to the north and 28° farther to the east, than the magnetic pole.

Formulas for the transition from geographic coordinates to

Declassified in Part - Sanitized Copy Approved for Release 2013/01/23 : CIA-RDP81-01043R001600090003-8

Declassified in Part - Sanitized Copy Approved for Release 2013/01/23 : CIA-RDP81-01043R001600090003-8

geomagnetic coordinates are derived from the spherical triangle PZP_m (Figure 34), where the side PZ represents the complement of the latitude of the site, PP_m the complement of the latitude of the geomagnetic pole, and the side P_mZ the complement of geomagnetic latitude, angle ZPP_m the difference between the longitudes of point Z and the geomagnetic pole, and angle ZP_mP the complement to 180° of the geomagnetic longitude Λ, since the latter based on the south geomagnetic pole.

From the formulas of spherical trigonometry, we have:

$$\sin \theta = \sin \varphi \sin \varphi_0 + \cos \varphi \cos \varphi_0 \cos (\lambda - \lambda_0), \quad (2.10)$$

$$\sin \Lambda = \cos \varphi \sin(\varphi - \varphi_0)/\cos \theta. \quad (2.11)$$

In some problems it is necessary also to know the local magnetic time t_m, which represents the angle between the great circle arc P_mZ and the arc P_mS extending through the sun. (Figure 34). From the spherical triangle PP_mS it is apparent that this angle constitutes the difference between the geomagnetic longitudes of the sun and of the given point Z, which may bedetermined by means of formula (2.11).

At intermediate and low latitudes the magnetic time differs very little from the local solar time and the difference becomes appreciable only at a distance of $15-20^\circ$ from the geomagnetic pole. The difference in latitude depends solely on the longitude of the location.

Table 8 lists observatories located at high latitudes, including their geographic and geomagnetic coordinates.

Declassified in Part - Sanitized Copy Approved for Release 2013/01/23 : CIA-RDP81-01043R001600090003-8

Declassified in Part - Sanitized Copy Approved for Release 2013/01/23 : CIA-RDP81-01043R001600090003-8

TABLE 8

GEOGRAPHIC AND GEOMAGNETIC COORDINATES OF POLAR OBSERVATORIES

Station	φ	λ	φ	Λ
Bukhta Tikhaya	80.3°	52.8°	71.5°	153.3°
Chelyuskin	77.2	104.3	65.9	177.5
Dixon	73.5	80.4	67.0	161.5
Matochkin Shar	73.3	56.4	64.8	146.5
Tromso	69.7	18.9	67.1	116.7
Godkhoven [transliterated]	69.2	306.5	79.8	32.5
Sodankyla	67.4	26.6	63.8	120.0
Uĕlen [transliterated]	66.2	190.2	61.8	237.0
Fairbanks College	64.9	212.0	64.5	255.4
Srednekansk	62.6	152.3	53.2	210.5
Yakutsk	62.0	129.7	51.0	193.8

Section 2. Expansion of Earth's Magnetic Potential to a Series. The Theory of Gauss

The next important step in the analytical representation of the terrestrial magnetic field was the theory proposed by Gauss in 1838 [8]. The purpose of this theory was the representation of earth's magnetic field as a function of the coordinates of a given point without considering the physical causes of the formation of this field. Thus, without providing any explanation of the origin of the magnetic field of the earth and being essentially a formal theory, this theory nevertheless was of great importance and it remains important to the present day in the field of the study of terrestrial magnetism phenomena.

The basis of the theory of Gauss was the assumption that the source of the earth's magnetic field is located inside the terrestrial globe and therefore has a potential.

Declassified in Part - Sanitized Copy Approved for Release 2013/01/23 : CIA-RDP81-01043R001600090003-8

Declassified in Part - Sanitized Copy Approved for Release 2013/01/23 : CIA-RDP81-01043R001600090003-8

Assuming that the terrestrial globe has a residual magnetization J, whichat any given point of the globe has an arbitrary magnitude and direction, let us find the magnitude of the magnetic potential U at point P having coordinates θ and λ, θ being the complement of the latitude and λ the longitude (Figure 35).

The magnetic potential U may be represented as a volume potential in the following form:

$$U = \int\int\int dm/\rho,$$

where dm is the element of magnetic mass at a point M having the spherical coordinates r', θ' and λ' and located at distance ρ from point P. The integration is carried out for the entire volume of the sphere. In the triangle MPO we have:

$$U = \frac{1}{r}\int \frac{dm}{\sqrt{1+\left(\frac{r'}{r}\right)^2 - 2\left(\frac{r'}{r}\right)\cos\gamma}} \qquad (2.12)$$

Since $r > r'$, the function within the integration sign, which may be denoted by $\varphi(r',\gamma)$ may be expanded to a series converging at the power r'/r, by applying the binomial formula of Newton. In fact,

$$\varphi(r',\gamma) = \left\{1+\left[\left(\frac{r'}{r}\right)^2 - 2\left(\frac{r'}{r}\right)\cos\gamma\right]\right\}^{-\frac{1}{2}} = 1-\frac{1}{2}\left[\left(\frac{r'}{r}\right)^2 - 2\left(\frac{r'}{r}\right)\cos\gamma\right] + \frac{3}{8}\left[\left(\frac{r'}{r}\right)^2 - 2\left(\frac{r'}{r}\right)\cos\gamma\right]^2. \qquad (2.13)$$

Eliminating the bracket and assembling the r'/r terms of even power we obtain: $\varphi(r',\gamma) = \sum_{n=0}^{\infty}\left(\frac{r'}{r}\right)^n P_n(\cos\gamma)$,

where $P_n(\cos\gamma)$ are several functions of cos γ of n power, which are called Legendre polynomials. The properties of these polynomials are studied in the theory of spherical functions and one of them, which enables calculation of the polynomial of (n + 1)'-the order when the polynomials of n-the and (n-1)-the order are known, is of the form:

$$P_{n+1}(\cos\gamma) = \frac{2n+1}{n+1}\cos\gamma\, P_n(\cos\gamma) - \frac{n}{n+1}P_{n-1}(\cos\gamma) \qquad (2.14)$$

Declassified in Part - Sanitized Copy Approved for Release 2013/01/23 : CIA-RDP81-01043R001600090003-8

Declassified in Part - Sanitized Copy Approved for Release 2013/01/23 : CIA-RDP81-01043R001600090003-8

The values of the first 2 polynomials are obtained directly on expansion by Newton's binomial. From equation (2.13) we obtain:

$$P_0(\cos\gamma) = 1, \quad P_1(\cos\gamma) = \cos\gamma$$

Hence on applying formula (2.14) we have:

$$P_2(\cos\gamma) = \frac{3}{2}\cos^2\gamma - \frac{1}{2},$$

$$P_3(\cos\gamma) = \frac{5}{2}\cos^3\gamma - \frac{3}{2}\cos\gamma,$$

$$P_4(\cos\gamma) = \frac{35}{8}\cos^4\gamma - \frac{15}{4}\cos^2\gamma + \frac{3}{8}$$

etc.

Consequently, expression (2.12) of the potential may be written as a series:

$$U = \frac{1}{r}\sum_{n=0}^{\infty}\int\left(\frac{r'}{r}\right)^n P_n(\cos\gamma)\,dm.$$

The first term of this series is equal to zero, as is readily ascertained. Indeed, at n = 0 we have $U = \int dm$, an expression representing the sum of all magnetic masses and which is equal to zero in any body. Hence,

$$U = \frac{1}{r}\sum_{n=1}^{\infty}\int\left(\frac{r'}{r}\right)^n P_n(\cos\gamma)\,dm \qquad (2.15)$$

Further, in triangle QNP_1 (Figure 35), according to a formula of spherical trigonometry, we have:

$$\cos\gamma = \cos\theta\cos\theta' + \sin\theta\sin\theta'\cos(\lambda-\lambda'), \qquad (2.16)$$

In the theory of spherical functions it is demonstrated that upon the substitution of $\cos\gamma$ by the Legendre polynomial $P_n(\cos\gamma)$ expression (2.16) assumes the following form:

$$P_n(\cos\gamma) = \sum_{m=0}^{n}\left[c_n^m P_n^m(\cos\theta)\cos m\lambda P_n^m(\cos\theta')\right.$$
$$\left.\cos m\lambda' + c_n^m P_n^m(\cos\theta)\sin m\lambda P_n^m(\cos\theta')\sin m\lambda'\right], \qquad (2.17)$$

where

$$P_n^m(\cos\theta) = \sin^m\theta\,\frac{d^m P_n(\cos\theta)}{d(\cos\theta)^m}$$

$$P_n^m(\cos\theta') = \sin^m\theta'\,\frac{d^m P_n(\cos\theta')}{d(\cos\theta')^m}$$

and c_n^m is a numerical coefficient which at n = 1 is equal to unity.

Declassified in Part - Sanitized Copy Approved for Release 2013/01/23 : CIA-RDP81-01043R001600090003-8

Declassified in Part - Sanitized Copy Approved for Release 2013/01/23 : CIA-RDP81-01043R001600090003-8

The functions $P_n^m(\cos\theta)$ are called associated functions of Legendre and at n = 1 and n = 2 they assume the following values:

$$P_1'(\cos\theta) = \sin\theta;\ P_2' = 3\cos\theta\sin\theta;\ P_2^2 = 3\sin^2\theta;$$

$$P_3' = -\frac{15}{2}\sin^3\theta + 6\sin\theta;\ P_3^2 = 15\cos^2\theta\sin\theta;\ P_3^3 = 15\cos^3\theta.$$

On replacing $P_n(\cos\gamma)$ in equation (2.15) by the expression (2.17) we have:

$$V = \frac{f}{r}\sum_{n=1}^{\infty}\int\left(\frac{r'}{r}\right)^n\sum_{m=0}^{n}\left[C_n^m P_n^m(\cos\theta)\cos m\lambda P_n^m(\cos\theta')\cos m\lambda' + C_n^m P_n^m(\cos\theta)\sin m\lambda P_n^m(\cos\theta')\sin m\lambda'\right]dm$$

Since θ, λ and r remain constant on integration, all the functions depending only on the latter may be taken outside the sign of integration, and therefore:

$$V = \sum_{n=1}^{\infty}\frac{1}{r^{n+1}}\sum_{m=0}^{n}\left[P_n^m(\cos\theta)\cos m\lambda C_n^m\int r'^n P_n^m(\cos\theta')\cos m\lambda' dm + P_n^m(\cos\theta)\sin m\lambda C_n^m\int r'^n P_n^m(\cos\theta')\sin m\lambda' dm\right].$$

Expressions appearing within the sign of integration do not depend on the coordinates of point P and are constant for the given sphere. Therefore on denoting the latter by:

$$A_n^m = C_n^m\int r'^n P_n^m(\cos\theta')\cos m\lambda' dm,$$

$$B_n^m = C_n^m\int r'^n P_n^m(\cos\theta')\sin m\lambda' dm, \qquad (2.18)$$

we obtain:

$$V = \sum_{n=1}^{\infty}\frac{1}{r^{n+1}}\sum_{m=0}^{n}\left[A_n^m\cos m\lambda + B_n^m\sin m\lambda\right]P_n^m(\cos\theta).$$

Introducing the expressions:

$$A_n^m = R^{n+2}g_n^m \qquad B_n^m = R^{n+2}h_n^m, \qquad (2.19)$$

where R is the radius of the sphere; in such a case

$$V = R\sum_{n=1}^{\infty}\left(\frac{R}{r}\right)^{n+1}\sum_{m=0}^{n}\left[g_n^m\cos m\lambda + h_n^m\sin m\lambda\right]P_n^m(\cos\theta). \qquad (2.20)$$

For points located on the surface of the sphere r = R, and therefore:

$$V = R\sum_{n=1}^{\infty}\sum_{m=0}^{n}\left[g_n^m\cos m\lambda + h_n^m\sin m\lambda\right]P_n^m(\cos\theta), \qquad (2.21)$$

Declassified in Part - Sanitized Copy Approved for Release 2013/01/23 : CIA-RDP81-01043R001600090003-8

Declassified in Part - Sanitized Copy Approved for Release 2013/01/23 : CIA-RDP81-01043R001600090003-8

i.e., the magnetic potential produced on the surface of the sphere by magnetic masses located within the sphere is expressed as double sum having an infinite number of terms, and each item constitutes a spherical function $P_n^m(\cos\theta)\cos m\lambda$ of θ and λ, having constant coefficients g_n^m and h_n^m.

Limiting the expansion to terms of order n, the number of constant coefficients g and h is represented by

$$N = n(n + 2)$$

which may be derived readily from expression (2.21), taking into account the fact that m cannot be greater than n, and at m = o all the terms including coefficient h are equal to zero.

The components of field intensity on the coordinate axes X, Y and Z may be determined by differentiation of expression (2.20) with respect to the corresponding coordinate with the inclusion of r = R in the latter, i.e.,

$$\begin{aligned}
Z &= -\partial U/\partial r = \sum_{n=1}^{\infty}\sum_{m=o}^{n}[(n+1)g_n^m\cos m\lambda + (n+1)h_n^m\sin m\lambda]P_n^m(\cos\theta),\\
X &= -1/r\cdot U/\theta = -\sum_{n=1}^{\infty}\sum_{m=0}^{n}(g_n^m\cos m\lambda + h_n^m\sin m\lambda)\,dP_n^m(\cos\theta)/d\theta \qquad (2.22)\\
Y &= -1/r\sin\theta\cdot\partial U/\partial\lambda = \sum_{n=1}^{\infty}\sum_{m=0}^{n}(mg_n^m\sin m\lambda - mh_n^m\cos m\lambda)P_n^m(\cos\theta)/\sin\theta.
\end{aligned}$$

These equations contain essentially the entire Gaussian theory. It is seen this theory permits calculation of the elements of terrestrial magnetism at any point of the earth's surface if the constant coefficients g_n^m and h_n^m are known. Since the right hand portions of these equations are expressed in the form of infinite series, in practical use it is necessary to limit them to a finite number of terms which depends upon the degree of convergence of these series. The question concerning their convergence remains as yet unsolved, but in all probability these series

Declassified in Part - Sanitized Copy Approved for Release 2013/01/23 : CIA-RDP81-01043R001600090003-8

Declassified in Part - Sanitized Copy Approved for Release 2013/01/23 : CIA-RDP81-01043R001600090003-8

converge slowly due to the presence of a large number of local and regional anomalies, which are called "magnetic masses," occurring near the earth's surface. Since with increasing n the number of coefficients g_n^m and h_n^m increases sharply it becomes necessary, in practice, to limit oneself to a number of terms depending not upon the convergence of the series, but upon the number of operations necessary to determine the constant coefficients. In his paper Gauss himself limited the terms of the expansion to those of the fourth order ($n = 4$).

To determine the constant coefficients g_n^m and h_n^m the elements of terrestrial magnetism at certain points of the earth's surface, which should be as uniformly distributed as possible, must be known from observation.

Thus at $n = 4$ the number of coefficients will be 24, and their determination will require at least 24 equations.

Since every point yields 3 equations, it would appear that observations at 8 points would be sufficient to determine all the coefficients.

However, random influences of local anomalies can distort the result greatly, and for greater reliability a larger number of points must be used. In the solution of an even larger number of equations for the same number of unknowns, Gauss himself determined 24 coefficients from observations at 12 points, i.e., he solved 36 equations with 24 unknowns. Such equations are solved by the method of least squares.

It should be noted that the coefficients g_n^m and h_n^m may be

Declassified in Part - Sanitized Copy Approved for Release 2013/01/23 : CIA-RDP81-01043R001600090003-8

Declassified in Part - Sanitized Copy Approved for Release 2013/01/23 : CIA-RDP81-01043R001600090003-8

determined from observations of some single element, for example Z. To do this it is sufficient that the number of points be greater or at least equal to the number of constant coefficients. After Gauss the coefficients have been determined by many scientists as observation data on elements of terrestrial magnetism. The most recent determinations were made for the 1945 epoch and were performed almost simultaneously by V. I. Afanas'yeva at the USSR Institute of Terrestrial Magnetism and by Westein in the USA.

Most of these determinations were carried out up to terms of the fourth order and only Fritsche in 1885 carried out the calculations to the terms of the sixth order which necessitated the determination of 48 coefficients.

To show the accuracy which can be attained in determining the coefficients g and h, and the extent to which they may change from one epoch to another the values of the coefficients of the first 2 orders calculated by different scientists for various epochs, beginning with Gauss and up to the recent calculations of V. I. Afanas'yeva [9] are listed in Table 9.

The table shows that the highest values are those of coefficients g_1^0 and h_1^1 corresponding to terms of the first order. This result is of tremendous importance because it indicates the dipole nature of the terrestrial magnetic field, since the first terms of the Gaussian expansion correspond to a dipole field.

Thus the Gaussian expansion has confirmed the idea of I. M. Simonov concerning a uniform magnetization of the terrestrial globe.

Declassified in Part - Sanitized Copy Approved for Release 2013/01/23 : CIA-RDP81-01043R001600090003-8

Declassified in Part - Sanitized Copy Approved for Release 2013/01/23 : CIA-RDP81-01043R001600090003-8

TABLE 9

VALUES OF THE COEFFICIENTS OF GAUSS' EXPANSION FOR DIFFERENT EPOCHS

Author	Epoch	g_1^0	g_1^1	h_1^1	g_2^0	g_2^1	g_2^2	h_2^1	h_2^2
Gauss	1835	-3235	-311	+625	+ 51	+292	- 2	+ 2	+157
Ehrmann and Petersen	1829	-3201	-284	+601	- 8	+257	- 14	- 4	+146
Adams	1845	-3219	-278	+578	+ 9	+284	+ 4	- 10	+135
Adams	1880	-3168	-243	+603	- 49	+297	+ 6	- 75	+149
Fritsche	1885	-3164	-241	+591	- 35	+286	+ 68	- 75	+142
Schmidt	1885	-3168	-222	+595	- 50	+278	+ 65	- 71	+149
Dayson and Furner	1922	-3095	-226	+592	- 89	+299	+144	-124	+ 84
Westein	1945	-3057	-211	+581	-127	+296	+164	-166	+ 54
Afanas'yeva	1945	-3032	-229	+590	-125	+288	+150	-146	+ 48

Declassified in Part - Sanitized Copy Approved for Release 2013/01/23 : CIA-RDP81-01043R001600090003-8

Declassified in Part - Sanitized Copy Approved for Release 2013/01/23 : CIA-RDP81-01043R001600090003-8

Data relating to the same epochs (1885 and 1945) show that the calculations carried out by 2 investigators using different initial data differ by less than 1% in relation to the principal term g_1^0, while the difference between extreme epochs reaches 6-7%. This indicates that the magnetic field does not remain constant but changes slowly and continuously. Such changes have been designated as secular changes or variations and are described in greater detail in Sections 1 and 2 of Chapter Iv.

Section 3. Physical Meaning of the Terms of Gaussian Series

As we have seen, the expansion of magnetic potential to a series constitute a formal operation which has been named spherical harmonic analysis by analogy with the operation of expansion of a periodic function to a Fourier series, called harmonic analysis. However, its purely formal nature notwithstanding, in spherical analysis the individual terms corresponding to the sequence number n can have a definite physical meaning, as is the case also in harmonic analysis (oscillations of a cord).

The first terms of the expansion corresponding to n = 1 are the most readily interpreted.

Indeed, at n = 1 equations (2.22) assume the form:

$$X = g_1^0 \sin\theta - (g_1^1 \cos\lambda + h_1^1 \sin\lambda)\cos\theta,$$

$$Y = g_1^1 \sin\lambda - h_1^1 \cos\lambda$$

$$Z = 2[g_1^0 \cos\theta + (g_1^1 \cos\lambda + h_1^1 \sin\lambda)\sin\theta.$$

These expressions are fully analogous in form to the expression of the components of field intensity of a field produced by a uniformly magnetized sphere. It is readily shown that these expressions are analogous not only in form but also in essence: to do this

Declassified in Part - Sanitized Copy Approved for Release 2013/01/23 : CIA-RDP81-01043R001600090003-8

Declassified in Part - Sanitized Copy Approved for Release 2013/01/23 : CIA-RDP81-01043R001600090003-8

it is only necessary to determine the values of the constant coefficients g_1^0, g_1^1 and h_1^1.

From equations (2.18), at n = 1, we obtain

$$A_1^0 = \int r' \cos\theta' \, dm, \quad B_1^1 = \int r' \cos\theta' \sin\lambda' \, dm, \quad A_1^1 = \int r' \sin\theta \cos\lambda' \, dm.$$

The expressions appearing within the integration sign represent the projection of radius-vector r' on the rectangular coordinates Z, X and Y, therefore, denoting them by z', x' and y' we have:

$$A_1^0 = \int z' \, dm, \quad B_1^1 = \int x' \, dm, \quad A_1^1 = \int y' \, dm. \tag{2.23}$$

To demonstrate that these expressions represent the projections of magnetic moment M of the terrestrial globe on the axes of coordinates, i.e.,

$$A_1^0 = M_z, \quad B_1^1 = M_x, \quad A_1^1 = M_y.$$

We write one of the equations of (2.23) in the form:

$$A_1^0 = \int pz' \, dv, \tag{2.24}$$

where p is density of magnetic masses and dv is the volume element.

From the theory of magnetic potential it is known that fictitious magnetic masses may be distributed on the surface as well as within a magnetized body, and the density of surface masses p_S is expressed by the correlation

$$p_S = J_n,$$

where J_n is the component of magnetization vector J on the normal to the surface, and the density of volume masses p_v is expressed by the correlation

$$p_v = -\text{div } J.$$

Therefore, replacing p_S and p_v in expression (2.24) by their values, we obtain:

Declassified in Part - Sanitized Copy Approved for Release 2013/01/23 : CIA-RDP81-01043R001600090003-8

Declassified in Part - Sanitized Copy Approved for Release 2013/01/23 : CIA-RDP81-01043R001600090003-8

$$A_1^o = -\int z' \operatorname{div} J \, dv + \int z' J_n dS,$$

where the first integral is taken for the entire volume of the magnetized body and the second for its entire surface.

On the basis of vector analysis formulas we may write:

$$z' \operatorname{div} J = \operatorname{div} (z'J) - (J \operatorname{grad} z') = \operatorname{div} (z' J) - J_z.$$

Therefore,

$$A_1^o = -\int \operatorname{div} (z'J) dv + \int J_z dv + \int z' J_n dS$$

According to the theorem of Ostrogradskiy

$$\int \operatorname{div} (z'J) = \int z' J_n dS,$$

and consequently,

$$A_1^o = \int J_z dv,$$

i.e., A_1^o is the magnetic moment in the direction of the z axis, which was to be demonstrated.

Analogously, it may be demonstrated that

$$A_1^1 = \int J_y dv \qquad \text{and} \qquad B_1^1 = \int J_x dv.$$

Expressing the components of magnetic moment by means of the polar coordinates θ_o and λ_o, and we have:

$$A_1^o = M \cos \theta_o$$
$$B_1^1 = M \cos \theta_o \sin \lambda_o$$
$$A_1^1 = M \sin \theta_o \cos \lambda_o$$

where θ_o is the angle formed by the magnetic axis of the terrestrial globe with the axis of rotation ON (Figure 36), and λ_o is the biplanar angle between the plane of zero meridian and the plane of the meridian extending through the magnetic axis, i.e., the coordinates of the point of intersection of the magnetic axis with the surface of the sphere.

The magnetic moment of terrestrial globe M may be stated in the form:

$$M = 4/3 \pi R^3 Jcp.$$

Declassified in Part - Sanitized Copy Approved for Release 2013/01/23 : CIA-RDP81-01043R001600090003-8

Declassified in Part - Sanitized Copy Approved for Release 2013/01/23 : CIA-RDP81-01043R001600090003-8

where J_{cp} is the mean intensity of magnetization. Therefore, in view of equation (2.19) we have:

$$g_1^0 = 3/4\ \pi J_{cp} \cos \theta_o,\ g_1^1 = 4/3\ \pi J_{cp} \sin \theta_o \cos \lambda_o,$$
$$h_1^1 = 4/3\ \pi J_{cp} \cos \theta_o \sin \lambda_o.$$

Comparing these expressions with the expressions of (2.2) it is apparent that they are identically equal since $\theta_o = 90 - \theta_o$ and at uniform magnetization $J = J_{cp}$. Thus the first term of the Gaussian expansion represents the potential produced by a uniformly magnetized sphere, the magnetic moment of which is equal to the mean moment at nonuniform magnetization.

The next terms of the expansion also may be interpreted as magnetic potentials produced not by one but by several dipoles. Thus, terms corresponding to n = 2 are the potential of a system of 2 antiparallel dipoles called a quadrupole; terms corresponding to n = 3, are the potential of a system of 2 quadrupoles, called a multipole of third order etc.

This interpretation was made first in 1904 by N. A. Umov, professor of physics at the University of Moscow, in his paper "Geometric Representation of Gaussian Potential" [10]. In this work N. A. Umov showed that each of the spherical functions included in the Gaussian potential represents the magnetic potential of a specific distribution having certain axes, the number of which is determined by the order of the functions. In addition, each function has a certain corresponding magnetic moment which may be called the magnetic moment of the same order as that of the function. Through complex mathematical derivations N. A. Umov determined the direction of the axes and the magnitude of these magnetic moments for functions of these and third orders, using the values of constant coefficients g_n^m and h_n^m calculated for the 1885 epoch.

Declassified in Part - Sanitized Copy Approved for Release 2013/01/23 : CIA-RDP81-01043R001600090003-8

Declassified in Part - Sanitized Copy Approved for Release 2013/01/23 : CIA-RDP81-01043R001600090003-8

Let us show that terms of the second order of Gaussian expansion represent the potential of a quadrupole. The name quadrupole is given to a combination of 2 dipoles parallel to each other, but having opposite directions and separated by an infinitely small distance dh_2. This distance dh_2 is assumed to be the distance between the centers of the dipoles, which can have any direction in space.

Consequently the quadrupole has 2 axes, one of which, h_1, coincides with the axis of the dipole and the second h_2 with the distance dh_2.

The magnetic potential U_2 of the quadrupole is expressed as the difference between potentials of the 2 dipoles (Figure 37), i.e.,

$$U_2 = U_1 - U'_1.$$

and because of the small distance between the dipoles

$$U_2 = \partial U_1 / \partial h_2 \, dh_2.$$

But

$$U_1 = M_1/r^2 \cos \theta_1 = M_1 Z/r^3$$

where Z is the projection of vector r on the dipole axis, and therefore:

$$U_2 = M_1 \left[1/r^3 \cdot \partial z/\partial h_2 - 3\, Z/r^4 \cdot \partial r/\partial h_2\right] dh_2.$$

The product $2M_1 dh_2$ is called the moment of quadrupole M_2, and the derivatives $\partial z/\partial h_2$ and $\partial r/\partial h_2$ represent the cosines of the angles between the corresponding directions Z and r, and the quadrupole axis.

Because of this,

$$U = - M_2/r^3 \left[3/2 \cos \theta_1 \cos \theta_2 - 1/2 \cos \theta_{12}\right], \qquad (2.25)$$

where θ_1 and θ_2 are the angles formed by the axes of the quadrupole with the direction r, and θ_{12} is the angle between the quadrupole axes.

Declassified in Part - Sanitized Copy Approved for Release 2013/01/23 : CIA-RDP81-01043R001600090003-8

Declassified in Part - Sanitized Copy Approved for Release 2013/01/23 : CIA-RDP81-01043R001600090003-8

In order to represent the potential U_2 as a function of the coordinates of point P the angles Θ_1, Θ_2 and Θ_{12} must be replaced by spherical coordinates of the directions r, h_1 and h_2. In the spherical triangles h_1ZP, h_2ZP and h_1Ph_2 (Figure 38) we have:

$$\cos\Theta_1 = \cos\varphi_1\cos\varphi + \sin\varphi_1\sin\varphi\cos(\lambda-\lambda_1)$$
$$\cos\Theta_2 = \cos\varphi_2\cos\varphi + \sin\varphi_2\sin\varphi\cos(\lambda-\lambda_2)$$
$$\cos\Theta_{12} = \cos\varphi_1\cos\varphi_2 + \sin\varphi_1\sin\varphi_2\cos(\lambda_1-\lambda_2)$$

Substituting these values in equation (2.25) and through simple transpositions we obtain the following for points located on the surface of a sphere of radius R:

$$U_2 = R\left[g_2^0 P_2^0(\cos\varphi) + (g_2^1\cos\lambda + h_2^1\sin\lambda)P_2^1(\cos\varphi) + (g_2^2\cos 2\lambda + h_2^2\sin 2\lambda)P_2^2\right], \quad (2.26)$$

wherein

$$g_2^0 = \left[\cos\varphi_1\cos\varphi_2 - \tfrac{1}{2}\sin\varphi_1\sin\varphi_2\cos(\lambda_1-\lambda_2)\right]\frac{M_2}{R^4},$$
$$g_2^1 = \tfrac{3}{2}\left[\cos\varphi_1\sin\varphi_2\cos\lambda_2 + \sin\varphi_1\cos\varphi_2\cos\lambda_1\right]\frac{M_2}{R^4},$$
$$h_2^1 = \tfrac{3}{2}\left[\cos\varphi_1\sin\varphi_2\sin\lambda_2 + \sin\varphi_1\cos\varphi_2\sin\lambda_1\right]\frac{M_2}{R^4},$$
$$g_2^2 = \tfrac{3}{4}\sin\varphi_1\sin\varphi_2\cos(\lambda_1+\lambda_2)\frac{M_2}{R^4} \quad (2.27)$$
$$h_2^2 = \tfrac{3}{4}\sin\varphi_1\sin\varphi_2\sin(\lambda_1+\lambda_2)\frac{M_2}{R^4};$$

It is apparent that the potential U_2 actually coincides with the second term of the Gaussian expansion, and in order to determine the magnetic moment of the quadrupole M_2 and the directions of its 2 axes as defined by the spherical coordinates φ_1, h_1, and φ_2, h_2, it is necessary to solve a system of 5 equations (2.27), since we know the coefficients g_n^m and h_n^m. The method for solving these equations is given in the paper of N. A. Umov:

Declassified in Part - Sanitized Copy Approved for Release 2013/01/23 : CIA-RDP81-01043R001600090003-8

Declassified in Part - Sanitized Copy Approved for Release 2013/01/23 : CIA-RDP81-01043R001600090003-8

Thus a "geometric" interpretation, i.e., the likening of each term of the expansion to a certain geometric form (multipole) is fully capable of execution, but the physical explanation of the existence of such forms does not appear possible except for the first term, which corresponds to the potential of a uniformly magnetized sphere and can be visualized as actually existing.

It is of interest to note that 3 terms in expression (2.26) of the potential U_2 correspond to different positions of the axes of the quadrupole. The first term containing the factor $P_2(\cos\varphi)$ corresponds to the potential of the quadrupole in which the axis dh_2 has the same direction as dh_1, i.e., 2 dipoles are shifted in relation to each other along their axis (Figure 39). Assuming the axis of the dipole to be the polar axis we obtain:

$$\varphi_1 = \varphi_2 = 0, \quad \lambda_1 = \lambda_2 = \lambda.$$

Therefore,

$$g_2^1 = 3/2\ M_2/R^4 \cos\lambda,$$
$$h_2^1 = 3/2\ M_2/R^4 \sin\lambda,$$

and

$$g_2^0 = g_2^2 = h_2^2 = 0.$$

Finally, the third term is the potential of a quadrupole in which the axes are perpendicular to each other and are located within the equator plane, i.e., have the coordinates:

$$\varphi_1 = \varphi_2 = 90^\circ \qquad \text{and} \qquad \lambda_1 - \lambda_2 = 90^\circ,$$

and therefore

$$g_2^2 = -\ 3/4\ M_2/R^4 \sin 2\lambda_1,$$
$$h_2^2 = -\ 3/4\ M_2/R^4 \cos 2\lambda_1,$$

while the other coefficients are equal to zero.

Declassified in Part - Sanitized Copy Approved for Release 2013/01/23 : CIA-RDP81-01043R001600090003-8

Declassified in Part - Sanitized Copy Approved for Release 2013/01/23 : CIA-RDP81-01043R001600090003-8

Figure 40 shows the distribution of magnetic masses on the surface of the terrestrial globe corresponding to these quadrupoles, and also to the dipoles parallel to the axes of coordinates.

Section 4. Separation of the Earth's Magnetic Field into "Internal" and "External"

One of the principal results of the theory of Gauss, with respect to knowledge of the essence of terrestrial magnetism, is the possibility of dividing the magnetic field of the earth into a field formed by sources inside the terrestrial globe, and a field formed by sources outside the globe. In his expansion Gauss himself was limited to consideration of only the internal causes. Expansion of a potential, the sources of which are outside of the terrestrial globe, was performed for the first time many years later, in 1885, by Schmidt, when it was shown that such a separation is possible [11].

Assuming that the magnetic masses producing the magnetic field on the surface of the terrestrial globe are located outside of the globe and are concentrated within a certain volume V (Figure 41), let us consider the magnetic potential at point P, produced by an elemental mass associated with point M.

We have $$dU = dm/p$$

where $p = PM$. In the triangle OPM we have

$$p^2 = r'^2 + r^2 - 2rr' \cos\gamma,$$

where $r = OP$, $r' = OM$ and $\gamma = \angle POM$.

Therefore,

$$dU = dm/\sqrt{r^2 + r'^2 - 2rr' \cos\gamma}$$

Transposing r' outside the radical sign, we obtain:

$$dU = dm/r' \sqrt{1 + (r/r')^2 - 2(r/r') \cos\gamma}$$

Declassified in Part - Sanitized Copy Approved for Release 2013/01/23 : CIA-RDP81-01043R001600090003-8

Declassified in Part - Sanitized Copy Approved for Release 2013/01/23 : CIA-RDP81-01043R001600090003-8

Since r' > r, it follows that on expanding the expression within the radical sign to a series by the power r/r', analogously to the expansion in the preceding section, we have

$$dU = \frac{1}{r'} \sum_{n=0}^{\infty} \left(\frac{r}{r'}\right)^n P_n(\cos\gamma)\, dm,$$

while the potential of all the masses concentrated within the volume is expressed as follows:

$$U = \int \frac{1}{r'} \sum_{n=0}^{\infty} \left(\frac{r}{r'}\right)^n P_n(\cos\gamma)\, dm.$$

In the spherical triangle P_1NQ we have:

$$\cos\gamma = \cos\theta\cos\theta' + \sin\theta\sin\theta'\cos(\lambda - \lambda'),$$

therefore, substituting the value of cos γ in the function within the integral sign we obtain, according to formula (2.17):

$$U = \int \frac{1}{r'} \sum_{n=0}^{\infty} \left(\frac{r}{r'}\right)^n \sum_{m=0}^{n} [C_n^m P_n^m(\cos\theta)\cos m\lambda P_n^m(\cos\theta')\cos m\lambda' + C_n^m P_n^m(\cos\theta)\sin m\lambda P_n^m(\cos\theta')\sin m\lambda']\, dm,$$

or

$$U = \sum_{n=0}^{\infty} r^n \sum_{m=0}^{n} \left[\cos m\lambda \int \frac{C_n^m}{r'^{n+1}} P_n^m(\cos\theta')\cos m\lambda'\, dm + \sin m\lambda \int \frac{C_n^m}{r'^{n+1}} P_n^m(\cos\theta')\sin m\lambda'\, dm\right] P_n^m(\cos\theta),$$

where the integration is extended through the entire volume V.

Denoting

$$\int \frac{C_n^m}{r'^{n+1}} P_n^m(\cos\theta')\cos m\lambda'\, dm = C_n^m,$$

$$\int \frac{C_n^m}{r'^{n+1}} P_n^m(\cos\theta')\sin m\lambda'\, dm = D_n^m,$$

we have

$$U = \sum_{n=0}^{\infty} r^n \sum_{m=0}^{n} [C_n^m \cos m\lambda + D_n^m \sin m\lambda] P_n^m(\cos\theta),$$

where C_n^m and D_n^m have the same values for any point P and therefore are constant coefficients.

Denoting further

$$C_n^m = j_n^m R^{-(n-1)}; \quad D_n^m = k_n^m R^{-(n-1)},$$

wherein R is the radius of the terrestrial globe; we have

$$U = \sum_{n=0}^{\infty} \frac{r^n}{R^{n-1}} \sum_{m=0}^{n} [j_n^m \cos m\lambda + k_n^m \sin m\lambda] P_n^m(\cos\theta). \qquad (2.28)$$

Declassified in Part - Sanitized Copy Approved for Release 2013/01/23 : CIA-RDP81-01043R001600090003-8

Declassified in Part - Sanitized Copy Approved for Release 2013/01/23 : CIA-RDP81-01043R001600090003-8

Let us now determine the components Z_e, X_e and Y_e on the coordinate axes at the surface of the globe, where r = R:

$$Z_e = -\frac{\partial U}{\partial r} = -\sum_{n=0}^{\infty}\sum_{m=0}^{n}\left[r g_n^m \cos m\lambda + r h_n^m \sin m\lambda\right] P_n^m(\cos\theta),$$

$$X_e = -\frac{1}{r}\cdot\frac{\partial U}{\partial \theta} = -\sum_{n=0}^{\infty}\sum_{m=0}^{n}\left[g_n^m \cos m\lambda + h_n^m \sin m\lambda\right]\frac{dP_n^m(\cos\theta)}{d\theta}, \qquad (2.29)$$

$$Y_e = -\frac{1}{r\sin\theta}\cdot\frac{\partial U}{\partial \lambda} = \sum_{n=0}^{\infty}\sum_{m=0}^{n}\left[r g_n^m \sin m\lambda - r h_n^m \cos m\lambda\right]\frac{P_n^m(\cos\theta)}{\sin\theta}.$$

Consequently, if there are magnetic masses located outside of the terrestrial globe the components X, Y and Z of the intensity of the field observed at the earth's surface will be expressed as the sum of the components induced by internal causes and of components induced by external causes, i.e.,

$$X = X_i + X_e;$$
$$Y = Y_i + Y_e;$$
$$Z = Z_i + Z_e.$$

It is apparent that the first terms of the expansion Z_e, Y_e and X_e are equal to zero at n = 0, and therefore the summation can be started not with n = 0 but with n = 1. In such a case, on addint the expressions (2.22) and (2.29) term by term, we obtain:

$$Z = \sum_{n=1}^{\infty}\sum_{m=0}^{n}\left\{\left[(n+1)q_n^m - n g_n^m\right]\cos m\lambda + \left[(n+1)h_n^m - n k_n^m\right]\sin m\lambda\right\} P_n^m(\cos\theta),$$

$$X = -\sum_{n=1}^{\infty}\sum_{m=0}^{n}\left[\left(q_n^m + g_n^m\right)\cos m\lambda + \left(h_n^m + k_n^m\right)\sin m\lambda\right]\frac{dP_n^m(\cos\theta)}{d\theta},$$

$$Y = \sum_{n=1}^{\infty}\sum_{m=0}^{n}\left[m\left(q_n^m + g_n^m\right)\sin m\lambda - m\left(h_n^m + k_n^m\right)\cos m\lambda\right]\frac{P_n^m(\cos\theta)}{\sin\theta}.$$

Denoting

$$\begin{aligned} q_n^m + g_n^m &= p'^m_n, \\ (n+1)\,q_n^m - n g_n^m &= p'^m_n, \\ h_n^m + k_n^m &= q'^m_n, \\ (n+1)\,h_n^m - n k_n^m &= q'^m_n, \end{aligned} \qquad (2.30)$$

we may write the following expansion to a series for the components X, Y, Z:

$$X = -\sum_{n=1}^{\infty}\sum_{m=0}^{n}\left(p_n^m \cos m\lambda + q_n^m \sin m\lambda\right)\frac{dP_n^m}{d\theta}(\cos\theta),$$

$$Y = \sum_{n=1}^{\infty}\sum_{m=0}^{n}\left(p_n^m \sin m\lambda + q_n^m \cos m\lambda\right)\frac{m P_n^m(\cos\theta)}{\sin\theta} \qquad (2.31)$$

$$Z = \sum_{n=1}^{\infty}\sum_{m=0}^{n}\left(p'^m_n \cos m\lambda + q'^m_n \sin m\lambda\right)P_n^m(\cos\theta).$$

Declassified in Part - Sanitized Copy Approved for Release 2013/01/23 : CIA-RDP81-01043R001600090003-8

Declassified in Part - Sanitized Copy Approved for Release 2013/01/23 : CIA-RDP81-01043R001600090003-8

The formulas of (2.31) make it possible to determine what portion of the field observed is induced by external causes and what portion is induced by internal causes. By determining the coefficients p'^{m}_{n} and q'^{m}_{n} from observation of one vertical component Z, and p^{m}_{n} and q^{m}_{n} from observation of one component X, by means of the equations of (2.30), we may determine the coefficients g^{m}_{n} and h^{m}_{n} corresponding to a field induced by internal causes and the coefficients j^{m}_{n} and k^{m}_{n} corresponding to the external causes.

The field was separated in this manner for the first time in 1885, when it became possible to determine mathematically what portion of the magnetic field is induced by external and what portion is induced by internal causes. However, more reliable results along this line were obtained in 1922 [12] on the basis of data of a magnetic survey conducted over the entire terrestrial globe. The summary results of calculations for the 1922 epoch are shown in Table 10 where the index i of the component denotes the internal causes and the index e refers to the external causes.

Thus the formal theory of terrestrial magnetism evolved by Gauss not only provided an idea concerning the distribution of the elements of terrestrial magnetism, but also enabled determination of the sources of the magnetic field.

At the present time the actual existence of external sources of the terrestrial field has not been demonstrated, but the existing hypotheses concerning its origin do not conflict with experimental data.

Declassified in Part - Sanitized Copy Approved for Release 2013/01/23 : CIA-RDP81-01043R001600090003-8

Declassified in Part - Sanitized Copy Approved for Release 2013/01/23 : CIA-RDP81-01043R001600090003-8

TABLE 10

VALUES OF THE X AND Z COMPONENTS OF THE EARTH'S MAGNETIC FIELD CORRESPONDING TO INTERNAL AND EXTERNAL CAUSES FOR THE 1922 EPOCH

Value of Component	60°N	40°	20°N	0°	20°S	40°	60°S
X_i	+0.1203	+0.2318	+0.3133	+0.3244	+0.2889	+0.2021	+0.1510
X_e	+0.0113	+0.0058	+0.0043	+0.0045	+0.0042	+0.0033	+0.0013
Z_i	+0.5249	+0.4241	+0.2203	+0.0268	+0.2378	+0.3765	-0.4936
Z_e	-0.0061	-0.0004	-0.0006	+0.0008	+0.0018	+0.0040	+0.0037

Declassified in Part - Sanitized Copy Approved for Release 2013/01/23 : CIA-RDP81-01043R001600090003-8

Declassified in Part - Sanitized Copy Approved for Release 2013/01/23 : CIA-RDP81-01043R001600090003-8

Section 5. Vortical Magnetic Field

In the derivation of formulas (2.31) it was assumed that the magnetic field of the earth has a scalar potential U and its intensity is defined by the equation (0.7):

$$H = -\text{grad } U.$$

If the space within which H is being determined is filled with electric currents of density j, the magnetic field produced by these currents cannot be expressed by means of the scalar potential U, but must be defined by means of the vector-potential of current A, according to the formula

$$H = \text{rot } A$$

and the vector-potential A is expressed by the formula

$$A = \int j/r \, dv,$$

where r is the distance of volume element dv from the point under consideration and the integration applies to the entire volume filled by the currents.

An example is provided by the magnetic field within a conductor through which a current is flowing. In such cases it is said that the magnetic field is of vortical nature.

Thus the condition describing the vortical nature of a magnetic field is the location of a point under consideration within a conductor through which a current is flowing, or to put it differently, the location of a point, a space filled with current.

The expansion of Gauss does not hold for a vortical field, and therefore in the presence of currents flowing within the atmosphere near the earth's surface, application of the Gaussian theory would appear to be impossible. But in view of the fact that the greater portion of the magnetic field is induced by causes situated

Declassified in Part - Sanitized Copy Approved for Release 2013/01/23 : CIA-RDP81-01043R001600090003-8

Declassified in Part - Sanitized Copy Approved for Release 2013/01/23 : CIA-RDP81-01043R001600090003-8

outside of the earth's surface, the vortical portion introduces only a certain distortion in the results of the expansion, affecting the coefficients g and h. In the presence of a vortical portion of the field the coefficients g and h calculated from observations of the north component X_i will differ from the coefficients calculated from observations of the east component Y_i, whereas in the absence of a vortical field the coefficients must be the same in both instances. This enables detection of the presence or absence of a vortical portion of the field, and if there is a considerable difference between the coefficients the magnitude of the intensity of the field produced by the currents and the magnitude of current density also may be determined.

Calculations performed at the beginning of the twentieth century have shown that the density of vortical currents must have a magnitude of the order 0.02 a/km^2. On the other hand, the density of vertical conductivity currents of atmospheric electricity observed directly at the earth's surface has a magnitude of $2 \cdot 10^{-6}$ a/km^2, i.e., is 10,000 times less than the density of currents derived from geomagnetic observations. Such a discrepancy between experimental data and theoretical calculations raises doubts as to the actuality of vertical currents, and one of the causes of this discrepancy must be the inaccuracy of magnetic observations.

Recent investigations based on more extensive data led to the conclusion that current values derived from geomagnetic observations must be distorted due to insufficient accuracy of observations, and primarily to inaccuracies in plotting magnetic data on maps. Therefore the terrestrial magnetic field observed at the earth's surface must be considered a field that is not vortical and which has a scalar potential.

Declassified in Part - Sanitized Copy Approved for Release 2013/01/23 : CIA-RDP81-01043R001600090003-8

Declassified in Part - Sanitized Copy Approved for Release 2013/01/23 : CIA-RDP81-01043R001600090003-8

CHAPTER III

STRUCTURE AND PHYSICAL THEORIES OF THE ORIGIN OF THE EARTH'S MAGNETIC FIELD

Section 1. Structure of the Earth's Magnetic Field.

Examination of world maps of isolines and maps of individual areas, as well as a mathematical analysis of the magnetic field leads to the conclusion that the observed magnetic field at earth's surface is the sum of several fields having different causes. Denoting the intensity by H_T, the magnetic field, it may be described as the sum of the following fields: H_0, produced by uniform magnetization of the terrestrial globe; H_m, induced by internal causes associated with nonuniform structure of the internal strata of the terrestrial globe; H_a, induced by magnetization of the upper strata of the earth's crust; H_e, associated with external causes; and δH, a field of variations the causes of which also are outside the terrestrial globe, i.e.,

$$H_T = H_0 + H_m + H_a + H_e + \delta H.$$

The field induced by the vector H_a is called the anomalous field, that induced by H_m often is called the continental field, because of the vast areas which it covers or the latter also is called the residual field.

Field H_a in turn, may consist of 2 fields: H_a', caused by deeper level rocks and called regional anomaly, and H_a'', caused by rocks of lesser depth and called regional, or local anomaly.

Often the sum of the uniform magnetization, continental, and external fields is called the normal field, the intensity H_n of which is

$$H_n = H_0 + H_m + H_e.$$

Declassified in Part - Sanitized Copy Approved for Release 2013/01/23 : CIA-RDP81-01043R001600090003-8

Declassified in Part - Sanitized Copy Approved for Release 2013/01/23 : CIA-RDP81-01043R001600090003-8

From this point of view, the field under consideration constitutes the sum of normal and anomalous fields, excluding the field of variations, i.e.:

$$H_T = H_n + H_a.$$

Thus, if the distribution of the normal field over the earth's surface is known the anomalous component of the magnetic field may be determined thereby approaching solution of the problem of the geological structure of the upper layers of the earth's crust, which is of extremely great practical importance.

However, depending upon which anomaly is to be isolated, the regional or the local, the term intensity of the normal field must be taken to mean either the sum $H_o + H_m + H_e$ or the sum $H_o + H_m + H_e + H'_a$. Similarly, in the case of the continental or residual field the normal field will be the field of uniform magnetization. Thus the notion of a normal field varies with the purpose for which it is utilized.

Given the magnitude of field intensity at any point, resolution of this value into components corresponding to a given field does not appear possible since in such a case the problem would be indefinite. The normal field may be isolated as the difference between the observed and the anomalous fields by arithmatic or graphic averaging of a series of values observed at different points on the earth's surface.

B. P. Veynberg [13] has shown that mean values of the components of intensity of the anomalous field, taken over the entire area of the anomaly, are very close to zero. Therefore, on averaging the components of the observed field over the area of the anomaly the

Declassified in Part - Sanitized Copy Approved for Release 2013/01/23 : CIA-RDP81-01043R001600090003-8

Declassified in Part - Sanitized Copy Approved for Release 2013/01/23 : CIA-RDP81-01043R001600090003-8

magnetic field of the former vanishes. Usually the averaging is done by levelling off isolines and plotting them on maps of smaller scale. Figures 25, 26 and 27 show maps of the normal magnetic field constructed by the Institute of Terrestrial magnetism for the 1950 epoch, by levelling off isolines. On these maps the isolines correspond to the field which would result if there were no magnetic anomalies, either regional or local.

A more detailed description of each of these fields and of the causes of their formation is presented in the following sections.

Section 2. Continental or Residual Field and Its Theory

The above analytical method of expanding the potential of the earth's magnetic field to a series enables quantitatively separating the observed field into the fields of uniform, and nonuniform magnetization of the terrestrial globe.

Consequently, having calculated the field of uniform magnetization according to formula (2.22), and using maps of the normal magnetic field of the earth the continental, or residual, field may be determined by substracting the former from the latter. This separation of the residual field was first done in 1899 for the 1885 epoch [14]. Since then a vast amount of data relating to the earth's magnetic field has been gathered, enabling the construction of magnetic maps which are closer to the true field of the earth.

In the light of the new data it became necessary to repeat the calculations of the residual field and to construct new maps relating to the current epoch.

The maps for the 1950 epoch shown in Figures 42, 43 and 44 reveal that the surface of the earth is divided by the Z isolines

Declassified in Part - Sanitized Copy Approved for Release 2013/01/23 : CIA-RDP81-01043R001600090003-8

Declassified in Part - Sanitized Copy Approved for Release 2013/01/23 : CIA-RDP81-01043R001600090003-8

into a number of regions of almost circular shape, at the center of which a magnetic needle suspended at its center of gravity comes to rest in a vertical position, with the north end down at some areas, and the south end down at others. This corresponds to the situation which would exist if a magnet were placed vertically in the center of such a region, with the north end up in some regions and the south end up in others. There are 6 of these regions in all, and the region located near the Antarctic is divided in two. The geographic coordinates of the centers of these regions and the values of the vertical component for the 1885 and 1950 epochs are shown in Table 11.

The East Asian region, or the so-called East Asian continental anomaly, has the greatest intensity and most regular shape. It includes all of Asia and a portion of the European continent. The value of the vertical component in this region reaches 30% of the normal field. A somewhat smaller anomaly of opposite sign is located in Western Africa, covering all the continent and a part of the Atlantic Ocean. A large anomaly is found in the Southern Indian Ocean near the Antarctic, but this anomaly, as previously stated, probably is divided into 2 separate anomalies. Therefore in the table the latter is listed as 2 separate regions. The other regions, or anomalies, are of lesser intensity but are clearly defined. If these maps (Figure 42-44) are compared with earlier maps it is seen that the nature of the anomalies and their number are essentially the same as on the maps for the 1885 epoch, but the values of Z at the center of the regions and the positions of these centers differ considerably, which is attributed either to errors in calculation or to actual changes in the anomalies.

Declassified in Part - Sanitized Copy Approved for Release 2013/01/23 : CIA-RDP81-01043R001600090003-8

Declassified in Part - Sanitized Copy Approved for Release 2013/01/23 : CIA-RDP81-01043R001600090003-8

TABLE 11

COORDINATES OF THE CENTERS OF REGIONS OF RESIDUAL FIELD AND VALUES OF THE VERTICAL COMPONENT Z AT THESE COORDINATES

Location of Region	1885 Epoch		1950 Epoch		Value of Z at Center	
	φ	λ	φ	λ	1885 Epoch	1950 Epoch
Eastern Asia	35°N	110°	40°N	100°	+0.139	+0.175
Africa	0	20	0	10	-0.124	-0.155
North America	42	268	40	270	+0.084	+0.066
Northern Pacific Ocean	45	182	50	190	-0.021	-0.030
Iceland	60	0	70	340	-0.106	-0.089
Tasmania	45 S	135	40 S	140	-0.092	-0.105
Southern Indian Ocean	50	325	60	325	+0.164	+0.167
Southern Indian Ocean	-	-	60	33	-	+0.166

Declassified in Part - Sanitized Copy Approved for Release 2013/01/23 : CIA-RDP81-01043R001600090003-8

Declassified in Part - Sanitized Copy Approved for Release 2013/01/23 : CIA-RDP81-01043R001600090003-8

It is most likely that both of the latter causes are involved in this instance, since the earlier maps were drawn from a smaller number of observations and therefore may include greater errors than the more recent maps, especially with respect to the location of the center.

Discrepancies in the values of the vertical component may be attributed mostly to changes of the field during the 1885-1950 period.

Maps of X and Y isolines are not self-contained, but are subordinated to the Z isolines, if the latter are considered basic. This is apparent from the regularity of X and Y isoline distribution in relation to the Z isolines.

Indeed, the X isolines are distributed in closed contours north and south of a Z maximum, with the positive isolines north of the positive, and south of the negative maximum.

Y isolines are located east and west of the maximum, and again their sign depends upon that of the Z maximum. Moreover, if the vectors of the horizontal component are plotted at different points of the map, all of them are directed either toward or away from the center of the anomaly.

This indicates that the central portion of a region of Z isolines constitutes a source of lines of force, and the continental anomalies may be considered as the result of the occurrence, of huge magnetized masses or strong vortical currents beneath their centers.

However, before reaching such a conclusion it must be ascertained whether the continental anomalies are actual facts or are merely the results of a formal processing of observational data.

Declassified in Part - Sanitized Copy Approved for Release 2013/01/23 : CIA-RDP81-01043R001600090003-8

Declassified in Part - Sanitized Copy Approved for Release 2013/01/23 : CIA-RDP81-01043R001600090003-8

The reality of continental anomalies may be verified by proving the reality of uniform magnetization of the terrestrial globe in the form presented by the expansion of Gauss, since the continental field is derived by substraction of this field from the observed field. However, in this instance also there is no direct proof, except for the hypothesis of the magnetization of the terrestrial globe due to its rotation about the axis. An indirect indication is provided by the fact that certain phenomena of terrestrial magnetism and auroras polaris depend upon geomagnetic latitude, the former being associated, as stated earlier, with the axis of uniform magnetization.

For this reason some researchers, such as Academician V. V. Shuleykin [15], and Yu. S. Glebovskiy [16] have expressed the opinion that uniform magnetization coincides with the direction of the axis of the earth's rotation, and that its deflection of 11° is the result of the superposition of continental anomalies. On the basis of such an assumption the continental anomalies must be of another form and their interpretation, i.e., determination of the causes of a given anomaly, also must be different. This assumption was first made by Bauer and his first maps of the residual field were plotted by substracting only the first term of the Gaussian expansion from the normal field, which corresponds to uniform magnetization along the rotation axis. However Bauer himself soon abandoned this assumption because he found that the residual field derived in this manner reveals clearly defined polarization along the equator, as a result of which the local nature of continental anomalies is obliterated to a certain degree. No definite answer has been provided thus far concerning the reality of continental anomalies, but

Declassified in Part - Sanitized Copy Approved for Release 2013/01/23 : CIA-RDP81-01043R001600090003-8

Declassified in Part - Sanitized Copy Approved for Release 2013/01/23 : CIA-RDP81-01043R001600090003-8

the fact that many phenomena depend upon geomagnetic latitude and the sharply manifested local nature of continental anomalies render more probable the assumption of a uniform magnetization of the terrestrial globe parallel to the geomagnetic axis and that the continental anomalies are independent phenomena caused by either magnetization of some types of rock occurring within the areas of the anomalies, or by the presence of vortical current within these areas.

The question as to the depth of occurrence of these rocks or currents also is unsolved. In the opinion of some investigators they occur at a depth on the order of one-half or one-third of the earth's radius, while others assume that they are concentrated in the upper shell of the terrestrial globe, at a depth of several hundred km.

Thus all the theories which have been proposed to explain the continental anomalies may be divided into 2 groups: deep-level and surface theories.

Among the deep-level theories which have been derived most thoroughly is that of Yu. D. Kalinin [17], who endeavored to determine the depth of the center of disturbance through mathematical calculations.

He has shown that a depth level may be selected at which a dipole having a radial direction produces a magnetic field on the earth's surface which agrees with the field of the East Asian anomaly.

Taking a dipole, or center of a spherical rock formation h, having the magnetic moment M, at a distance r_0 from the center of the earth, the direction of which coincides with the radius of the earth,

Declassified in Part - Sanitized Copy Approved for Release 2013/01/23 : CIA-RDP81-01043R001600090003-8

Declassified in Part - Sanitized Copy Approved for Release 2013/01/23 : CIA-RDP81-01043R001600090003-8

then at point P on the surface of the globe the magnetic potential of such a dipole is:

$$U = M \cos \varphi / r^2, \qquad (3.1)$$

where r is the distance from the center of the dipole to the point P and φ the angle ZMP. Denoting the complement of the latitude of point P by θ, and the radius of the terrestrial globe by R, we have in the triangle OMP (Figure 45):

$$r^2 = r_o^2 + R^2 - 2r_o R \cos \theta, \qquad \cos \varphi = r_o - R \cos \theta / r$$

Substituting these values in equation (3.1) we obtain:

$$U = M(r_o - R \cos \theta)/(r_o^2 + R^2 - 2r_o R \cos \theta)^{3/2}$$

and it follows that the components of the vector of field intensity are:

$$X = -\partial U/R \partial \theta = M \sin \theta / r^5 \ (2r_o^2 - Rr_o \cos \theta - R^2), \qquad (3.2)$$

$$Z = -\partial U/\partial R = M/r^5 \ [3Rr_o - 2(R^2 + r_o^2) \cos \theta + Rr_o \cos^2 \theta] \qquad (3.3)$$

In order to calculate X and Z by these formulas and to compare them with data relating to the East Asian anomaly it is necessary to know the depth of occurrence $R - r_o$ and the magnetic moment M. Their values are determined from the anomaly data on the assumption that the East Asian anomaly is caused by a dipole. Thus the depth of occurrence $R - r_o$ may be readily determined if the distance of zero isodyne Z from the center of the anomaly, expressed in units of the arc is known. Equating equation (3.3) to zero, we have

$$r_o = R/4 \cos \theta \ [3 + \cos^2 \theta - \sin \theta \sqrt{9 - \cos^2 \theta}\ ].$$

It is readily apparent that the angle θ in this expression is the angular distance of zero isodyne Z. For the East Asian anomaly θ is of about 40°, which gives $r_o \sim 0.6$ R.

Declassified in Part - Sanitized Copy Approved for Release 2013/01/23 : CIA-RDP81-01043R001600090003-8

Declassified in Part - Sanitized Copy Approved for Release 2013/01/23 : CIA-RDP81-01043R001600090003-8

The value of r_o thus obtained, and the quantities X and Z taken from the map are substituted in equations (3.2) and (3.3) to determine the magnetic moment.

Calculations of this type performed by Yu. D. Kalinin yield a quantity $M = 0.3 \cdot 10^{25}$ CGSμ, which represents about 4% of the magnetic moment of the terrestrial globe.

However, as pointed out by Yu. D. Kalinin better results are obtained with $r_\odot = 0.4$ R.

Table 12 shows the differences between values of Z calculated according to formula (3.3) and those determined from observations for the residual field of the East Asian anomaly.

TABLE 12

DIFFERENCE BETWEEN THEORETICAL AND OBSERVED VALUES OF Z OF THE RESIDUAL FIELD IN CGSμ AT DIFFERENT POINTS OF THE EARTH'S SURFACE

φ \ λ	60°	80°	100°	120°	140°	160°
60°	-0.006	+0.007	+0.012	+0.012	+0.002	-0.032
40	+0.012	+0.018	+0.003	+0.002	+0.000	-0.017
20	-0.017	-0.005	-0.010	+0.003	+0.017	+0.012
0	-0.053	-0.008	-0.025	+0.001	+0.016	+0.025

The fairly good agreement of the calculated and the observed values notwithstanding the existence of a spherical heterogeneity at such a depth appears unlikely. "It is much more natural to assume an inclusion extending more in the horizontal than in the vertical direction," states Yu. D. Kalinin in his publication, and therefore as a second approximation he takes the shape obtained by conformal transformation of the surface of an oblate spheroid by reciprocal radii in relation to a point situated outside of the spheroid on its axis of symmetry.

Declassified in Part - Sanitized Copy Approved for Release 2013/01/23 : CIA-RDP81-01043R001600090003-8

Declassified in Part - Sanitized Copy Approved for Release 2013/01/23 : CIA-RDP81-01043R001600090003-8

The equation of the surface of an oblate spheroid in its parametric form is:

$$x = a \cos \theta, \quad y = b \sin \theta \cos \varphi, \quad z = \sin \theta \sin \varphi.$$

where x, y and z are the rectangular coordinates, θ and φ are parameters representing polar coordinates and a and b are half-axes of the spheroid.

Transforming the space with rectangular coordinates x_1, y_1, z_1, to a space with coordinates u, v, w, the magnitude of the radius-vector extending from the origin of the coordinates is transformed within the new space to a radius-vector having a value inversely proportional to the former, i.e., the following condition is fulfilled:

$$r^2 = u^2 + v^2 + w^2 = k^2/x_1^2 + y_1^2 + z_1^2$$

where k is a certain constant quantity.

In such a case the new coordinates u, v, w are expressed by the coordinates x_1, y_1, and z_1 in the following manner:

$$u = k^2 x_1/r^2, \qquad v = k^2 y_1/r^2, \qquad w = k^2 z_1/r^2.$$

If the origin of coordinates is located on the axis of symmetry of the oblate spheroid, it follows that $x_1 = x + x_o$, $y_1 = y$, $z_1 = z$ and consequently the surface of the oblate spheroid within the new space assumes the form:

$$u = k^2/r^2(a \cos \theta + x_o), \quad v = k^2/r^2 \; b \sin \theta \cos \varphi, \quad w = k^2/r^2 \; b \sin \theta \sin \varphi$$

where

$$r^2 = b^2 \sin^2 \theta + a^2 \cos^2 \theta + 2ax_o \cos \theta + x_o^2.$$

The surface of the body expressed by these equations resembles a mushroom cap and therefore large dimensions in the horizontal direction may be obtained with only slight thickness of the cap.

Magnetization of such a "pseudo-spheroid," According to the

Declassified in Part - Sanitized Copy Approved for Release 2013/01/23 : CIA-RDP81-01043R001600090003-8

Declassified in Part - Sanitized Copy Approved for Release 2013/01/23 : CIA-RDP81-01043R001600090003-8

assumption of Yu. D. Kalinin magnetization of such a "pseudo-spheroid" takes place by induction from the dipole located at the point in relation to which the reciprocal radii transformation is taken.

The results which he obtained with the pseudo spheroid have provided no appreciable improvement in comparison with the dipole or sphere, but the immersion depth of the pseudo-spheroid was found to be about the same as that of the dipole, namely on the order of one-half of the earth's radius. This provided the foundation for Yu. D. Kalinin's assertion that a considerable portion of the residual field is associated not with the crust as was usually assumed, but with much deeper layers of the earth.

Somewhat later an article was published in foreign literature in which another attempt was made to explain the residual field on the basis of selection of a corresponding number of dipoles. According to these calculations it is necessary to place 14 dipoles in the radial direction at a depth of about one-half of the earth's radius in order to explain the residual field in terms of a vertical component. At the same time, the magnitude of magnetic moments of different dipoles also must be different. According to the author's assumption either magnetized lens-shaped regions or systems of equivalent currents may correspond to these dipoles.

Another author arrived at the same results by representing the residual field by a series of spherical harmonics and comparing this field with that of an arbitrary number of dipoles scattered within a spherical layer. Computing the probability of the

Declassified in Part - Sanitized Copy Approved for Release 2013/01/23 : CIA-RDP81-01043R001600090003-8

Declassified in Part - Sanitized Copy Approved for Release 2013/01/23 : CIA-RDP81-01043R001600090003-8

occurrence of any given harmonics in the summative field of these dipoles, he found that to attain a statistical equilibrium between calculated and observed coefficients of the harmonic series it is necessary that the spherical layer in which the dipoles are located be situated at a distance from the center of the earth not exceeding 0.55 of the earth's radius. The result obtained does not depend upon the number of dipoles distributed in this manner.

Thus mathematical calculations appear to confirm the idea that the causes of the residual field must be located at a great depth and consequently are not associated with the structure of the earth's crust.

However, the assumption of a surface origin of the residual field is no less well founded than the "deep-level theories," since without resorting to additional physical considerations it is impossible to demonstrate the correctness of either theory by mathematical procedures. It is known that the converse problem, determination of causes from a given distribution of the field, is multivalent and therefore, in the absence of sufficient physical foundations, the coincidence of calculated and observed results does not constitute confirmation of the fact that the observed field is the result of any given distribution of dipoles upon which the calculations were based. While all the "deep-level" theories are based on purely hypothetical foundations, the theories which associate the residual field with the earth's crust are supported by certain physical facts which indicate some kind of relationship between residual field and other physical and geological phenomena taking place in the earth's crust. Thus D. N. Kazanli [18], on investigating the connection between the distribution of maxima of

Declassified in Part - Sanitized Copy Approved for Release 2013/01/23 : CIA-RDP81-01043R001600090003-8

Declassified in Part - Sanitized Copy Approved for Release 2013/01/23 : CIA-RDP81-01043R001600090003-8

(centers) continental anomalies, found that the centers of anomalies always are located on ascertained or assumed screens or platforms and that the zero isoline of the Z-component extends over geosynclinal zones of a definite type. Moreover, from those investigations Kazanli has ascertained that platforms revealing a tendency of movement in different directions are characterized by residual field maxima which differ in sign.

The coincidence of residual field maxima with platforms indicates that the position of field maxima and the general configuration of the field do not change appreciably with lapse of time. This appears to be confirmed by the fact that the centers of secular range, as will be shown below, move along zero lines of the Z-component.

In 1948 V. I. Pochtarev [19] discovered that changes in the force of gravity and in the residual magnetic field along the parallels of the terrestrial globe are of similar nature. By plotting anomalies of gravity as a dependent function of longitude at different latitudes, and plotting similar graphs of the vertical component of the residual field it is found, as is shown in Figure 46, that these graphs are almost identical. On the other hand, Pochtarev has shown that graphs of gravity anomalies are in good agreement with the structure of earth's crust. Positive anomalies are found over basaltic rock and negative anomalies over granitic rock. This is shown in Figure 47, in which in lieu of gravity anomalies the ordinates represent the excess of geoid over spheroid.

Comparing the graphs of Figures 46 and 47 it is apparent that the magnetic field has a maximum value over basalt, and a minimum value over granite.

Declassified in Part - Sanitized Copy Approved for Release 2013/01/23 : CIA-RDP81-01043R001600090003-8

Declassified in Part - Sanitized Copy Approved for Release 2013/01/23 : CIA-RDP81-01043R001600090003-8

Since basaltic rocks have greater magnetic susceptibility than granite, it is natural to assume that the increase in magnetic field over basalts is caused by magnetization of basalts, and the decrease of the field over granite by the absence of such magnetization.

Assuming the magnetic susceptibility to be 0.1 CGS and taking the residual magnetization J_r of the basaltic layer as 9-fold greater than the inductive, V. I. Pochtarev found by elementary mathematical computations that the intensity of the magnetic field produced by magnetization of a basaltic layer 80 km thick, may vary within the observed range, from -10,000 γ to +10,000 γ, if the basaltic and granitic layers alternate longitudinally as shown in Figure 46. Thus the assumption of a "surface" origin of the residual field not only does not conflict with theoretical calculations, but also has certain physical foundations. However, the correlations and mathematical computations of V. I. Pochtarev cannot be regarded as fully substantiated since the correlation between gravitational and magnetic fields is very general and there are substantial discrepancies in details.

Thus on comparing all the data of theoretical and phenomonological studies of the causes of continental anomalies (residual field), at the present time it is not possible to assert the correctness of any given theory, and the problem of the origin of the continental field still remains unsolved. However, the theory of surface origin is supported by much more factual data.

Section 3. Magnetic Anomalies

Magnetic anomalies are regions in which the earth's magnetic

Declassified in Part - Sanitized Copy Approved for Release 2013/01/23 : CIA-RDP81-01043R001600090003-8

Declassified in Part - Sanitized Copy Approved for Release 2013/01/23 : CIA-RDP81-01043R001600090003-8

field differs appreciably from the field of adjoining areas, and its regular monotonous decrease or increase of the elements of terrestrial magnetism is altered.

This change corresponds to the change in the gradients of terrestrial field components, which in a normal field remain practically constant over a vast area. Thus the basic criterion of the presence of a magnetic anomaly is an appreciable change in the gradients of terrestrial magnetism elements within a given area.

Magnetic anomalies, as stated above, are the result of the presence in a given area of rocks magnetized by the normal field of the earth, producing an additional field which is called an anomalous field.

Since the magnetic field observed on the surface of the earth always is the sum of the normal and anomalous fields, isolation of the anomalous field requires determination of the normal field, which remains unknown.

However, the normal field may be determined using the fact that the magnetic flux through a closed surface surrounding any magnetized body equals zero. To do so it is necessary only to calculate the mean values of the components of the observed field on the area of the anomaly, which will correspond to the normal values.

Taking the case of a uniformly magnetized sphere occurring at a depth z, as an example, it is assumed that the sphere is magnetized in a vertical direction coinciding with the z axis, and that the origin of coordinates is placed at the center of the sphere.

Declassified in Part - Sanitized Copy Approved for Release 2013/01/23 : CIA-RDP81-01043R001600090003-8

Declassified in Part - Sanitized Copy Approved for Release 2013/01/23 : CIA-RDP81-01043R001600090003-8

In view of formula (0.20) the vertical component Z at a point of the earth's surface having the coordinates x, O, z, is

$$Z = M(2z^2 - x^2)/(z^2 + x^2)^{5/2}$$

where M is the magnetic moment of the sphere.

To find the mean value over area S the following integral is solved:

$$Z_{cp} = 1/S \int\int Z \, dS.$$

Taking S as the area of a circle of radius R with its center on the z axis, expressing dS in polar coordinates and substituting Z in the above formula by its expression, we obtain:

$$Z_{cp} = M/\pi R^2 \int_{\theta=0}^{2\pi} \int_{x=0}^{R} 2z^2 - x^2/(z^2 + x^2)^{5/2} \, x \, dx \, d\theta.$$

Performing the integration we obtain:

$$Z_{cp} = 2M/(z^2 + R^2)^{3/2}$$

or, on taking 1/z outside the parentheses and using the denotation R/z = p:

$$Z_{cp} = 2M/z^3 \cdot 1/(1 + p^2)^{3/2}$$

Since $2M/z^3$ represents the maximum value of the vertical component Z_m, it follows that

$$Z_{cp}/Z_m \approx 1/p^3,$$

This correlation shows that the mean value of Z taken over a circle the radius of which exceeds the depth of occurrence by the factor p, is approximately p^3-times smaller than the maximum value Z_m. Thus to determine the normal value of the vertical component with an error not exceeding 1% of the maximum magnitude of the anomalous value, measurements must be taken on the area of a circle the radius of which is 4.5 times greater than the depth of occurrence.

It must be noted, however, that these deductions are correct

Declassified in Part - Sanitized Copy Approved for Release 2013/01/23 : CIA-RDP81-01043R001600090003-8

Declassified in Part - Sanitized Copy Approved for Release 2013/01/23 : CIA-RDP81-01043R001600090003-8

only when the area for which the observational data is averaged contains no anomalies caused by the occurrence of other types of rock. Unique anomalies such as that considered in the above example are rarely encountered in nature. Usually one anomaly is superimposed upon another, and therefore the method of averaging must be applied to very large areas where the normal field no longer can be considered uniform. In such instances it is more convenient to take the normal field as the mean value of observations at several points distant from the center of the given anomaly.

The widespread network of magnetic observations established by the general magnetic survey of the USSR and by the many detailed prospecting surveys have shown that magnetic anomalies are not an accidental occurrence in nature but are rather a normal phenomenon, since in any more or less detailed survey an anomaly of some degree of intensity always is found.

Thus the itinerary magnetic survey conducted in 1930-1931 over the western slopes of the Urals, consisting of points at 1-2 km intervals on itineraries spaced 10-15 km apart, revealed a continuous series of anomalies the existence of which was not known before [20]. The magnetic map of isolines of the vertical component Z_a of one of the districts of this area is shown in Figure 48, from which it is apparent that the maximum value of Z_a in this area does not exceed 1,500γ. However, anomalies are encountered in nature in which the vertical component Z_a reaches 1.5 Oe and greater. The Kursk magnetic anomalies [21], located mostly in Kursk Oblast' and extending into the adjoining Orel, Voronezh and Kharkov oblasts are examples. In area and intensity the Kursk anomalies are the largest

Declassified in Part - Sanitized Copy Approved for Release 2013/01/23 : CIA-RDP81-01043R001600090003-8

Declassified in Part - Sanitized Copy Approved for Release 2013/01/23 : CIA-RDP81-01043R001600090003-8

in the world, since as yet no other anomaly has been found in which the magnitude of the vertical component attains values of 1.0-1.5 Oe over distances of hundreds of km. Figure 49 illustrates the Kursk anomalies, in which the black lines indicate the direction of the axes of anomalies, i.e., of the lines along which the vertical component has maximum values. In Figures 50a, 50b and 50c the isolines of vertical and horizontal components and the declinations of the observed field are shown for one of the sectors near the town of Shchigry [22]. It is seen that the anomalies represent narrow, elongated bands where the isolines are parallel, forming an oval shape within the band. Until the second decade of the current century there was no definite knowledge concerning the origin of such anomalies, although a number of instances in which anomalies were found in conjunction with subterranean iron ore deposits were known. In 1923, drilling at one of the maxima of the Kursk anomalies revealed the presence of iron quartzites containing a large amount pf pure magnetite in the form of interlayers at a depth of approximately 200 m [23]. Drilling within other anomalies also revealed the presence of iron-containing rocks.

Thus at the present time it has been definitely ascertained that the anomalies are caused by rock formations having magnetic properties.

These rocks situated within the earth's magnetic field become magnetized and produce an additional field which has been named an anomalous field. However, the question of the process of rock magnetization is fairly complex and in many instances it remains unresolved. Observations show that magnetization of rocks in most instances considerably exceeds the quantity defined by the equation

$$J = x/1 + xN \quad H_T,$$

Declassified in Part - Sanitized Copy Approved for Release 2013/01/23 : CIA-RDP81-01043R001600090003-8

Declassified in Part - Sanitized Copy Approved for Release 2013/01/23 : CIA-RDP81-01043R001600090003-8

where x is the true susceptibility of the rock determined by laboratory measurements, N is the coefficient of demagnetization of the rock, and H_T is the intensity of the earth's magnetic field. This quantity J, which herein will be refered to as induced, sometimes is several score smaller than the quantity observed for rock formations in their native state. The difference between the observed quantity J and the induced J_a has been termed residual magnetization J_r. In addition the vector J, as a rule, does not coincide in direction with the vector H_T, and in some cases the deflection may reach 180°, i.e., the rock may be magnetized opposite to the terrestrial field.

A slight deflection of 10°-15° of vector J from the vector H_T may be explained by the fact that the coefficient of demagnetization N is of a tensor nature, as was shown in Section 9 of the introduction. Larger angles of deflection have some other causes. The anomalous field may have various directions, depending on the direction of the underlying rock. If the direction of the vertical component of the anomalous field coincides with that of the vertical component of the normal field, the anomaly is considered positive, in the opposite case the anomaly is negative.

Until the third decade of the current century it was assumed that all anomalies are positive because the observation data of that period did not permit an opposite conclusion, and the question of the basic cause of rock magnetization appeared resolved since it was believed that magnetization of rocks is caused by the action of the earth's magnetic field. In 1931, in the Angara-Ilim district of Eastern Siberia, a several-km-sq anomalous strip was discovered in which the direction of Z_a was opposite to the normal field, its value reaching 0.5 Oe and exceeding the normal [24].

Declassified in Part - Sanitized Copy Approved for Release 2013/01/23 : CIA-RDP81-01043R001600090003-8

Declassified in Part - Sanitized Copy Approved for Release 2013/01/23 : CIA-RDP81-01043R001600090003-8

Magnetic maps of the vertical component of this anomaly are shown in Figures 51 and 52. Prospecting operations within the area of this anomaly revealed that it is caused by magnetite veins consisting of a mixture of magnetite and magnesoferrite. Investigation of the magnetic properties of samples of this vein showed that the samples have a residual magnetization opposite to the magnetic field of the earth.

Until recently the Angara-Ilim anomaly was the only negative anomaly and constituted an exception to the general rule. In recent years the similar anomalies have been found in all parts of the world. Thus negative anomalies have been discovered in South Africa north of the town of Pilansberg, where there is a system of dikes of doleritic and dioritic composition with a total length of 300 km. It was found that the dikes are magnetized opposite to the earth's magnetic field and the maximum value of the vertical component reaches 2,000γ. One section of this anomaly is shown in Figure 53.

In 1949 negative anomalies were discovered in northern England over andesite dikes, where the vertical component Z_a has a value of 600γ. Negative anomalies have been found in Germany where the magnitude of Z_a also reaches 2,000γ, and in North and South America.

Thus at the present time negative anomalies must be regarded as a normal rather than an exceptional occurrence. However, the question of their origin still remains unresolved. Most of the explanations of the origin of such anomalies advanced by various authors are untenable and need not be considered. The hypothesis of the magnetization of rocks within negative anomaly areas by electric currents during the periods of the Tectonic processes during which these structures formed is worthy of attention. However, this would necessitate

Declassified in Part - Sanitized Copy Approved for Release 2013/01/23 : CIA-RDP81-01043R001600090003-8

Declassified in Part - Sanitized Copy Approved for Release 2013/01/23 : CIA-RDP81-01043R001600090003-8

complete reformulation of the theory of the magnetization of rocks within areas of positive anomalies.

The current theory of the causes of the existing residual magnetization of rocks causing positive anomalies is based on the assumptions of temperature action during the cooling of rocks within the earth's magnetic field and the effects of resilient stresses which existed at the time of their formation and continue to the present time.

This question is discussed in greater detail in Chapter X concerning the magnetic properties of rock formations.

Section 4. Hypotheses of the Origin of Earth's Magnetic Field

The theory of Gauss being a formal theory could not, and was not intended to provide an answer to the question of the causes of magnetization of the terrestrial globe. Its purpose was to determine the regularities of distribution of the elements of terrestrial magnetism, which constituted merely the first and indispensable step in the study of the nature of the earth's magnetic field, since the development of any theories or hypothesis is impossible without ascertaining these regularities.

Therefore as knowledge of the phenomena of terrestrial magnetism expanded in depth and scope the need arose for physical interpretations of these phenomena and for an explanation of the causes of terrestrial magnetism.

However, notwithstanding the relatively large amount of information on the distribution of the elements of terrestrial magnetism over the earth's surface and the availability of numerous theoretical investigations, the question of the origin of terrestrial

mag

Declassified in Part - Sanitized Copy Approved for Release 2013/01/23 : CIA-RDP81-01043R001600090003-8

Declassified in Part - Sanitized Copy Approved for Release 2013/01/23 : CIA-RDP81-01043R001600090003-8

magnetism has not been resolved. There exists no hypothesis theory which provides a satisfactory explanation of the permanent magnetism of the terrestrial globe.

Enumeration of all the hypotheses which have been advanced and the theoretical considerations evolved in this connection serves no purpose because it would require too much space and would contribute nothing to the understanding of the essence of terrestrial magnetism phenomena, inasmuch as the vast majority of all these hypotheses is of a speculative nature and require further hypotheses and explanations.

However, some of these theories are mentioned below by way of example and to show their inadequacies.

All the existing theories and hypotheses concerning the causes of terrestrial magnetism may be divided into 2 basic groups: hypotheses founded on physical laws, experimentally ascertained by observations carried out at the earth's surface, and hypotheses based on rejection of these laws and assumption of the existence, in connection with the terrestrial globe as a cosmic body, of special laws which are different--out of the ordinary.

The principal facts of terrestrial magnetism which have been ascertained by observations are: an approximately uniform magnetization of the terrestrial globe and close coincidence of magnetic axis of the globe with its rotation axis. Hence it is natural that all the theories primarily have endeavored to explain uniform magnetization and magnetization along the rotation axis.

I. Among the theories of the first group the following will be discussed:

Declassified in Part - Sanitized Copy Approved for Release 2013/01/23 : CIA-RDP81-01043R001600090003-8

Declassified in Part - Sanitized Copy Approved for Release 2013/01/23 : CIA-RDP81-01043R001600090003-8

(1) Theory of rotating charges;

(2) Theory based on the Einstein-Barnett gyroscopic effect.

(3) Theory of drift-currents, and

(4) Theory of vortical currents.

1. The theory of rotating charges [25] assumes the simultaneous existence of 2 charges of equal magnitude but opposite sign, one distributed throughout the entire volume of the earth, and the other over its surface.

The assumption of the presence of either of the charges is in conflict with experimental data since observations of the gradient of electric potential on the surface yield a magnitude of $Q = 5.4 \cdot 10^5$ c for the entire charge of the earth. Whereas a charge 10^8 times greater would be required to explain the earth's magnetic field. If both charges are present their electrostatic fields at the surface mutually cancel each other, while the magnetic fields produced by each are found to be different in absolute magnitude. Therefore, with a corresponding selection of the magnitude of charge Q the calculated magnetic field may be equal to the magnetic field observed. Taking part in the diurnal rotation of the earth, these charges form closed circuits which in turn produce a magnetic field.

Disregarding the fact that the theory thus evolved requires an additional hypothesis concerning the cause of separation of the charges, it still is entirely unsatisfactory because it is in conflict with the principle of relativity, since an observer on the surface of the earth by rotating together with the charges remains stationary in relation to them.

2. In 1916 Barnett was able to demonstrate experimentally the magnetization of a rod by rotation, in connection with the

Declassified in Part - Sanitized Copy Approved for Release 2013/01/23 : CIA-RDP81-01043R001600090003-8

Declassified in Part - Sanitized Copy Approved for Release 2013/01/23 : CIA-RDP81-01043R001600090003-8

assumption of Einstein that every atom of a ferromagnetic body constitutes a gyroscope which in addition to a mechanical moment also possesses magnetic moment, which has the same direction. Therefore, on rotation of a ferromagnetic rod the atom-gyroscopes will have a mechanical moment of rotation which tends to align their axes with the direction of the rotation axis. As a result, the magnetic moments will assume the same direction and the rod will become magnetized. According to the theory this magnetization of the rod must be equivalent to the magnetization due to the action of a field the intensity H of which is given by the equation

$$H = 4\pi\, cm/e \quad n.$$

where e/m is the ratio of the charge of the electron to its mass, n the number of revolutions of the rod per second, and c is the velocity of light. The experiments of Barnett showed that magnetization J of the rod is very close to the theoretical which has the numerical value

$$J = 1.5 \cdot 10^{-6}\ n.$$

Applying this formula to the terrestrial globe, for which $n = 1/8.6 \quad 10^{-4}$, we obtain for the magnetization of the earth the quantity:

$$J = 1.5 \cdot 10^{-6} \quad 1 \cdot 10^{-4}/8.6 = 1.9 \cdot 10^{-11} \quad CGS\Phi.$$

As we have seen, this quantity actually is equal to $8.2 \cdot 10^{-2}$ CGSΦ, i.e., almost 10^{10} times larger.

Thus the attempts to explain magnetization of the earth by the gyroscopic effect are obviously unsatisfactory.

3. The theory of drift currents [26] is based on the assumption of the existence of free charged particles within the terrestrial globe, arising due to high temperatures. If such particles move in a magnetic field in a direction perpendicular to the field, it follows from the

Declassified in Part - Sanitized Copy Approved for Release 2013/01/23 : CIA-RDP81-01043R001600090003-8

Declassified in Part - Sanitized Copy Approved for Release 2013/01/23 : CIA-RDP81-01043R001600090003-8

laws of electrodynamics that their displacement must occur along a circumference the radius r of which is given by the equality of centrifugal and magnetic forces, i.e.,

$$r = cmv/He \qquad (3.4)$$

where v is velocity of the particle, m its mass, e its charge and H the intensity of the magnetic field. If in addition the particle is under the influence of the force of gravity acting perpendicular to the magnetic field and of the velocity v, the movement will take place in loops along trochoids in the direction of the velocity v and the particles therefore will acquire a forward motion (drift) in a direction perpendicular to the magnetic field and to the force of gravity. Since positive and negative particles under the influence of a magnetic field move in opposite directions, their drift under the influence of the force of gravity also will take place in opposite directions.

Such a process of the movement of charged particles is equivalent to an electric current which would be the source of the magnetic field observed on the earth. However to make such a movement possible a small initial magnetic field is necessary which, in the opinion of the authors of this hypothesis, is originated by gravitational separation of charges within the body: the lighter charges -- electrons -- are distributed nearer to the surface, the heavier ones -- the positive charges -- nearer to the center of the earth. Participating in the diurnal rotation of the earth, these charges provide the initial magnetic field which is necessary for the occurrence of drifts. Thereafter on formation of drift currents the magnetic field begins to increase thereby regeneratively increasing the dirft currents and the magnetic field. The principal defects of this hypothesis are first, the fact that it makes no provision for mechanisms which limit the regenerative increase of the magnetic field which, as is shown by

Declassified in Part - Sanitized Copy Approved for Release 2013/01/23 : CIA-RDP81-01043R001600090003-8

Declassified in Part - Sanitized Copy Approved for Release 2013/01/23 : CIA-RDP81-01043R001600090003-8

calculation, must go on continuously to infinity; secondly, the hypothesis leaves unexplained the existence of the initial magnetic field, which cannot be ascribed, as we have seen, to the rotation of the terrestrial globe carrying volume and surface charges.

4. In 1947, Ya. I. Frenkel [27] made the assumption that the inner part of the earth, the core, consists of a liquid metallic medium, the viscosity of which is not much higher than that of water, and that the core contains, the same as the earth's crust, a small amount of radioactive substances. On such assumptions convective movements can occur in the core which are sustained by the energy of disintegration of radioactive elements. These movements arise due to temperature gradients caused by radioactive disintegration during which heat is emitted. However, for the occurrence of convection movements, it is necessary that the condition that the ratio of temperature gradient to gravity acceleration is greater than a certain critical value be fulfilled.

For this it is sufficient that the amount of heat liberated per unit of volume 10^3 less than the amount of heat emitted in the external layers of the earth's crust. Calculations carried out by Ya. I. Frenkel have shown that this condition is fulfilled and consequently there may exist in the core continuous convection movements in the form of closed vortical currents.

In the presence of even a very weak primary magnetic field induction currents arise in the moving metallic masses which with the proper type of convection movement can cause a secondary magnetic field which in turn enhances the primary. This field will gradually increase due to the energy which sustains the convection movement and can increase to a magnitude which is actually observed.

Declassified in Part - Sanitized Copy Approved for Release 2013/01/23 : CIA-RDP81-01043R001600090003-8

Declassified in Part - Sanitized Copy Approved for Release 2013/01/23 : CIA-RDP81-01043R001600090003-8

In such a case the core can be compared to a dynamo operating for self-excitation. The power of such a dynamo will be expanded, accorded to the assumption of Ya. I. Frenkel solely to overcome the ohmic resistance, i.e., Lents-Joule heat, since because of the low viscosity of the core friction is small in comparison with the ohmic resistance.

The question of the origin of the primary magnetic field, in the opinion of Ya. I. Frenkel, is of no physical interest, and he leaves it open.

A quantitative solution of the problem, i.e., determination of the value of the magnetic field under the above stated assumptions could not be achieved by the author because of its extreme complexity. Approximate evaluation of the field yielded a quantity of the order 10^4 Oe, i.e., 10^4 times greater than the observed, but in the opinion of Ya. I. Frenkel, it can be greatly reduced on assuming that the convectional vortical currents are broken up into a series of nuclei as a result of which the mean magnitude of the field is inversely proportional to the square root of the number of such nuclei.

In 1949, Elsasser proposed a theory analogous to that of Ya. I. Frenkel, based on the same assumptions concerning the structure of the core and the occurrence of vortical movements in the core under the influence of the temperature gradient. Elsasser, also, shows that a concentration of one one-thousandth of radioactive substances in the core, compared to the concentration in crust is sufficient to ensure a continuous vortical movement of the metallic mass of the core. However, Elsasser's explanation of the mechanism of the formation of currents in the moving mass is entirely different. Elsasser contends that electric current is generated by action of thermoelectromotive

Declassified in Part - Sanitized Copy Approved for Release 2013/01/23 : CIA-RDP81-01043R001600090003-8

Declassified in Part - Sanitized Copy Approved for Release 2013/01/23 : CIA-RDP81-01043R001600090003-8

force which arises due to a difference in temperature between the eastern and western border of the vortex which, he bases on the following explanation.

Primary convection movement of each mass must be vertical, but under the influence of coriolian force, which is perpendicular to velocity, the turbulent or vortical movement can assume any direction. Therefore let us consider what effect the coriolian force will have on the direction of movement of any given vortex. Taking the origin of coordinates at some point on the vortex and extending the z-axis along the vertical, i.e., in the direction of the earth's radius, the x-axis from west to east and the y-axis from south to north, it is seen that the component of angular moment of earth's rotation P on the x-axis is equal to zero, and on the y axis it is equal to P $\sin\varphi$, where φ is the latitude of the origin of coordinates. Hence the vertical component of coriolian force is expressed as $F_z = 2Pv_x \sin\varphi$, where v_x is the component of linear velocity of turbulent movement. Thus the coriolian force will depend only on the east component of the velocity of movement. If the direction of movement is from west to east the force F_z is directed upward, if movement is from east to west the force F_z is directed downward. Consequently on the average the eastern borders of the vortexes are raised upward and the western are lowered downward. Because of the laws of adiabatic expansion, which is the cause of turbulent movement, the upper portion of the liquid must be warmer and the lower colder, which provides conditions for a constant difference in temperature. However, for formation of thermocurrents a heterogeneous composition of the liquid mass also is necessary. According to the assumption of Elsasser this heterogeneity may arise because of changes in

Declassified in Part - Sanitized Copy Approved for Release 2013/01/23 : CIA-RDP81-01043R001600090003-8

Declassified in Part - Sanitized Copy Approved for Release 2013/01/23 : CIA-RDP81-01043R001600090003-8

pressure on the movement of the liquid mass from upper to lower parts of the core and because of phase conversions of the substance forming the core associated with this movement. According to Elsasser the sloping of the vortical ring toward the equator also explains the difference between the magnetic axis and the axis of rotation of the earth.

In addition to the fact that both these theories remain mathematically undeveloped except for some approximate calculations based on arbitrary assumptions concerning the dimensions of vortical current, they offer no possibilities for derivations which could be verified experimentally, and therefore are purely speculative even though they do not conflict qualitatively with experimental data.

II. In the second group of theories let us consider the hypotheses of Shlomki [transliterated] and Swann [29], and of P. M. Bleket [30].

5. The theory of rotating charges provides no explanation of the separation of charges inside the earth. To meet this difficulty Shlomki and Swann attempted to evolve a theory based on modified laws of electrodynamics, by assuming that the law of Coulomb concerning interaction of electric charges holds only for a rough approximation and should be replaced by a more general law. Shlomki proposed the following expressions to replace the law of Coulomb:

$$f_{++} = (1+\alpha)\, q_+ q_+/r^2,\quad f_{--} = (1+\beta)\, q_- q_-/r^2,\quad f_{+-} = q_+ q_-/r^2,$$

i.e., according to the theory of Shlomki, in lieu of one law there are 3: the first expresses the interaction between 2 positive charges, the second between 2 negative charges and the third between a positive

Declassified in Part - Sanitized Copy Approved for Release 2013/01/23 : CIA-RDP81-01043R001600090003-8

Declassified in Part - Sanitized Copy Approved for Release 2013/01/23 : CIA-RDP81-01043R001600090003-8

and a negative charge. If these laws are valid 2 electrically neutral particles will undergo a certain interaction and, if, in addition, α is not equal to β the charges inside the neutral body must be shifted in relation to each other and will be located at different distances from the center of the body. Consequently, on rotation of such a body a magnetic field must be formed.

According to the theory of Swann the law of Coulomb must be replaced by the following 3 laws:

$$f_{++} = f_{--} = q_+ q_+/r^2, \quad f_{+-} = (1+\alpha)\, q_+ q_-/r^2, \quad f_{-+} = (1-\beta)\, q_- q_+/r^2,$$

i.e., interaction between charges of the same sign coincides with the law of Coulomb, and interaction between charges of different sign differs by the factors $(1+\alpha)$ and $(1-\beta)$, and consequently is not governed by the law of equality of action and counteraction.

The theory of Swann leads to the same conclusions as the theory of Shlomki. By identifying interaction between neutral particles with Newton's force of universal gravitation, and the magnetic field produced on rotation of the earth with the magnetic field observed, Shlomki and Swann were able to determine the value of constant coefficients α and β. According to the theory of Shlomki they were found to be:

$$\alpha = -0.65 \cdot 10^{-19} - 0.4 \cdot 10^{-36}$$

$$\beta = +0.65 \cdot 10^{-19} - 0.4 \cdot 10^{-36}$$

and according to the theory of Swann:

$$\alpha = 1.9 \cdot 10^{-19}$$

$$\beta = -1.9 \cdot 10^{-19} + 7.8 \cdot 10^{-25}.$$

These quantities cannot be checked experimentally.

Although the theories of Shlomki and Swann do not conflict with

Declassified in Part - Sanitized Copy Approved for Release 2013/01/23 : CIA-RDP81-01043R001600090003-8

Declassified in Part - Sanitized Copy Approved for Release 2013/01/23 : CIA-RDP81-01043R001600090003-8

experimental facts in the field of terrestrial magnetism and provide an explanation of its origin, this explanation amounts to assumptions which require new hypotheses.

The purpose of any theory is the reduction of all the observed facts, which at first appear incomprehensible in the light of known facts and laws. If some novel phenomenon does not fit any of the known laws it is the starting point for ascertaining new recurrent regularities which subsequently are verified by experiments. In the present case the authors, being convinced that the phenomena of terrestrial magnetism cannot be explained on the basis of the conventional laws of electrodynamics, attempt to determine new and unusual laws of nature. However, as long as these laws remain valid only for the explanation of the single fact of the earth's magnetic field and cannot be verified in connection with other phenomena, they remain an artificial hypothesis which endeavors to reduce one mysterious natural phenomenon to another that is just as mysterious.

6. The hypothesis of P. M. Bleket. Since none of the theories based on any given physical phenomena occurring within the earth can provide an explanation of the causes of the earth's magnetic field without conflicting with other physical phenomena, the idea was conceived a long time ago that perhaps the magnetic field of the earth is the result of its rotation about its axis, just like a rotating charge causes the formation of a magnetic field.

In 1947 P. M. Bleket made the assumption that irrespective of the presence of charges in a body, any rotating body must have a magnetic moment M proportional to its mechanical moment P, i.e., he formulated a new law of nature not connected with the conventional laws of electrodynamics. The correlation between M and P, according to Bleket is defined by the formula:

Declassified in Part - Sanitized Copy Approved for Release 2013/01/23 : CIA-RDP81-01043R001600090003-8

Declassified in Part - Sanitized Copy Approved for Release 2013/01/23 : CIA-RDP81-01043R001600090003-8

$$M = \beta \sqrt{k/2c}\ P, \qquad (3.5)$$

wherein k is the constant of gravitation, c the velocity of light, and β a numerical coefficient of the order of 0.25.

The basis for such a pronouncement was the fact that the ratio of magnetic moment to rotational moment in the case of 3 heavenly bodies, the earth, the sun and star 78 of the constellation Virgo, was found to be about the same, namely:

	M/P
for the earth	$1.11 \quad 10^{-15}$
for the sun	$0.79 \quad 10^{-15}$
for star 78	$0.81 \quad 10^{-15}$

If the hypothesis of Bleket were correct, that is, if it formulated an actual law of nature, the problem of terrestrial magnetism would be essentially solved, since nonuniform magnetization and also the deflection of the magnetic axis from the axis of rotation could be attributed to the nonuniform structure, and the presence of ferromagnetic rocks and electric currents in the terrestrial globe. For this reason the hypothesis of Bleket, in the form in which it was presented, aroused great interest among magnetologists and among physicists and astronomers, as well. In recent years numerous contributions of theoretical and experimental nature have been published in support of the hypothesis of Bleket.

Direct experimental verification of the magnetic field of rotating bodies is extremely difficult since this would require, as is shown by equation (3.5), the rotation of huge bodies at high angular velocity. Thus to produce a magnetic field having an intensity of several hundredths of one gamma it would be necessary to rotate a copper sphere of 10 m radius at a rate of 10 rpm.

Declassified in Part - Sanitized Copy Approved for Release 2013/01/23 : CIA-RDP81-01043R001600090003-8

Declassified in Part - Sanitized Copy Approved for Release 2013/01/23 : CIA-RDP81-01043R001600090003-8

Therefore, the experiments were aimed at proving those phenomena which follow from this hypothesis [31]. One such phenomenon is the decrease of the horizontal component with depth, whereas according to the dipolar theory of the origin of terrestrial magnetism the horizontal component must increase with depth. These charges are expressed by the formulas:

According to the theory of Bleket: $H_h - H_o = -2(5p_1/p + 1)\ h/R$;

According to the theory of central core (dipolar): $H_h - H_o = 3\ h/R$,

where H_o is the horizontal component at the surface of the earth, H_h the horizontal component at depth h, R the radius of the earth, p_1 density at the surface layer, and p the mean density of the earth.

Thus at a depth h = 1.5 km we have:

$H_h - H_o = -26\gamma$, according to Bleket's theory, and

$H_h - H_o = +11\gamma$, according to the theory of a central core.

The first measurements made in 1947, by means of horizontal balances in mine shafts at a depth of 1.5 km yielded values $H_h - H_o = -26\gamma \pm 4\gamma$, i.e., apparently confirming the theory of Bleket. However, this coincidence was found to be apparent, since the measurements were made without taking into account the effects of local geological structure which could attain 14γ and consequently decrease the absolute value of the difference $H_h - H_o$ to 11γ.

Thus these experiments have yielded no definite answer to the question involved. The principal defect of Bleket's hypothesis is the poor reliability of the results of the determination of magnetic field and moment of rotation of star 78, which also was pointed out by Bleket.

In addition, recent, more accurate determinations of the magnetic field of the sun on the basis of Zeeman's effect have shown that even if

Declassified in Part - Sanitized Copy Approved for Release 2013/01/23 : CIA-RDP81-01043R001600090003-8

Declassified in Part - Sanitized Copy Approved for Release 2013/01/23 : CIA-RDP81-01043R001600090003-8

the magnetic field exists it is several tens of times smaller as a result of which the ratio of magnetic moment to mechanical moment must be smaller by a function equal to the corresponding ratio for the earth. Therefore the hypothesis of Bleket has been found to be just as untenable as all the other hypotheses.

7. It should be mentioned that the first attempt at experimental detection of the magnetic field of rotating bodies was made by the great Russian physicist P. N. Lebedev, in 1911 [39], who in his experiments rotated a ring of 6 cm at 5-6 rpm and measured the magnetic field with sensitive magnetometer.

These experiments yielded negative results although theoretical calculations carried out on the basis of the hypothesis of rotating charges, showed that the sensitivity of the magnetometer is fully adequate for detection of the field involved. The negative result of these experiments did not deter P. N. Lebedev from continuing them, since in his opinion "the above-stated 2 hypotheses do not cover all the possible relationships between moving matter and the formation of magnetic fields which we observe in the case of sun spots and normal geomagnetic phenomena. Other hypotheses which may be advanced in connection with this relationship and which are sufficient to explain the magnetic forces of very large moving bodies lead to the conclusion that under the conditions and at the scale of the above-described experiments only very weak magnetic fields may arise, and which cannot be detected magnetometrically. To verify these hypotheses the scheme of the experiments must be changed in order to attain sufficient sensitivity of measurements, many times greater than that which could be utilized in the above-described preliminary investigations."

New experiments were outlined and developed by P. N. Lebedev but their execution was prevented by his untimely death in 1912.

Declassified in Part - Sanitized Copy Approved for Release 2013/01/23 : CIA-RDP81-01043R001600090003-8

Declassified in Part - Sanitized Copy Approved for Release 2013/01/23 : CIA-RDP81-01043R001600090003-8

8. Explanations of the origin of the terrestrial magnetic field by magnetization of the terrestrial globe also were attempted, leaving open the question of the causes of magnetization. However great difficulties were encountered along this line, also, since in accordance with the facts all ferromagnetic bodies lost their capability of undergoing magnetization above the Curie point, which in the case of iron is 760° C.

Experimental data necessitate the assumption that the temperature inside the earth is considerably above the Curie point of all ferromagnetic bodies. Calculations show that at a depth of 30 km the phenomena of ferromagnetism become impossible. It may be thought that at the pressures which prevail inside the earth the Curie point is shifted to the region of high temperatures. However, experimental attempts at detecting this phenomenon do not permit the contention at the present time that the Curie point is shifted on increased pressure, although theoretical calculations performed by A. A. Leypunskiy [33] and based on the laws of thermodynamics appear to indicate that at an increase Δp in pressure the Curie point is shifted by a value ΔT, expressed by the formula: $\Delta T = 3.3 \cdot 10^{-7} T \Delta p$.
This gives a Curie point for iron inside the earth, of: $T=T_o^{1.89}=4240^{\circ}$ K.
where T_o is the Curie point at normal pressure.

In order to obviate this difficulty attempts have been made to evolve a theory according to which magnetization must be concentrated within the upper 20 to 100 km of the earth's crust, where the temperature is below the Curie point. In such a case, however, the intensity of magnetization must reach the order of 5-10 CGSμ, whereas the observed magnetization surface rocks due to the presence of magnetite amounts to only 0.05-0.1 CGSμ. Therefore it was necessary to assume that the magnetite content increases with depth.

This theory is completely separted from the general explanation of the origin of cosmic magnetism, since it leaves unsolved the question of the cause of the magnetic field of the sun, whereas it is natural to assume that the magnetism of sun and the earth have the same cause.

Declassified in Part - Sanitized Copy Approved for Release 2013/01/23 : CIA-RDP81-01043R001600090003-8

Declassified in Part - Sanitized Copy Approved for Release 2013/01/23 : CIA-RDP81-01043R001600090003-8

8. Explanations of the origin of the terrestrial magnetic field by magnetization of the terrestrial globe also were attempted, leaving open the question of the causes of magnetization. However great difficulties were encountered along this line, also, since in accordance with the facts all ferromagnetic bodies lost their capability of undergoing magnetization above the Curie point, which in the case of iron is 760° C.

Experimental data necessitate the assumption that the temperature inside the earth is considerably above the Curie point of all ferromagnetic bodies. Calculations show that at a depth of 30 km the phenomena of ferromagnetism become impossible. It may be thought that at the pressures which prevail inside the earth the Curie point is shifted to the region of high temperatures. However, experimental attempts at detecting this phenomenon do not permit the contention at the present time that the Curie point is shifted on increased pressure, although theoretical calculations performed by A. A. Leypunskiy [33] and based on the laws of thermodynamics appear to indicate that at an increase Δp in pressure the Curie point is shifted by a value ΔT, expressed by the formula: $\Delta T = 3.3 \cdot 10^{-7} T \Delta p$.
This gives a Curie point for iron inside the earth, of: $T = T_o^{1.89} = 4240°$ K.
where T_o is the Curie point at normal pressure.

In order to obviate this difficulty attempts have been made to evolve a theory according to which magnetization must be concentrated within the upper 20 to 100 km of the earth's crust, where the temperature is below the Curie point. In such a case, however, the intensity of magnetization must reach the order of 5-10 CGS μ, whereas the observed magnetization surface rocks due to the presence of magnetite amounts to only 0.05-0.1 CGS μ. Therefore it was necessary to assume that the magnetite content increases with depth.

This theory is completely separted from the general explanation of the origin of cosmic magnetism, since it leaves unsolved the question of the cause of the magnetic field of the sun, whereas it is natural to assume that the magnetism of sun and the earth have the same cause.

Declassified in Part - Sanitized Copy Approved for Release 2013/01/23 : CIA-RDP81-01043R001600090003-8

Declassified in Part - Sanitized Copy Approved for Release 2013/01/23 : CIA-RDP81-01043R001600090003-8

CHAPTER IV

SECULAR VARIATIONS

Section 1. Phenomena Associated with Secular Variations

As we have seen, secular variations were the first to be discovered. Secular variations are changes in the mean annual values of the elements of terrestrial magnetism with time.

The change of mean annual values of any given element during the course of the year is called the secular range. Thus the secular range represents the difference between mean annual values of the element for 2 epochs divided by the number of years between these epochs. Since the mean annual values of the elements of terrestrial magnetism may be obtained only at observatories and their number is very limited, for a determination of the secular range at other points of the earth's surface somewhat different definition of the secular range is used. In this respect the secular range is taken to mean the difference between mean daily values of the elements for 2 points of time divided by the time interval between these points, expressed in years. The interval in this case is taken not less than 3-5 years. The locations at which repeated determination of the elements of terrestrial magnetism are made at definite intervals of time are called control points.

The means annual values of declination and the magnitude of secular range for several points of the terrestrial globe at which these observations have been made since the discovery of this element are shown in Table 13.

From the table it is apparent that, for example, in London the declination reached a maximum of +11° in about 1580 and then decreased to a minimum of -24°in 1820, which persisted for several years and was followed by an increase which continues to the present time.

Declassified in Part - Sanitized Copy Approved for Release 2013/01/23 : CIA-RDP81-01043R001600090003-8

Declassified in Part - Sanitized Copy Approved for Release 2013/01/23 : CIA-RDP81-01043R001600090003-8

Such cyclic changes in declination and in other elements gave reason for assuming that secular variations are of periodic nature, the period of which is several hundred years long. However, the interval of time over which reliable data concerning the course of the elements of terrestrial magnetism have been available is still too brief to permit a definite determination of the periodic regularities of secular variations.

TABLE 13

DECLINATION AND ITS SECULAR RANGE DURING DIFFERENT EPOCHS

	London		Paris		Rome	
Year	Declination	Secular range	Declination	Secular range	Declination	Secular range
1540	+ 7.2°	--	+ 8.2°	--	--	--
1560	+ 9.6	+ 6'	+ 9.3	+ 3.3'	+ 10.47°	--
1580	+ 10.93	+ 4	+ 9.6	+ 0.9	+ 10.61	+ 0.42'
1600	+ 10.13	- 2.4	+ 8.8	- 2.4	+ 11.41	2.4
1620	+ 7.26	- 8.4	+ 6.9	- 5.7	+ 9.88	- 4.59
1640	+ 3.27	- 12.0	+ 4.42	- 7.4	+ 7.29	- 7.77
1660	- 0.59	- 8.0	+ 0.86	- 10.68	+ 3.86	- 10.29
1680	- 3.89	- 9.9	- 3.47	- 12.49	- 0.01	- 11.55
1700	- 7.03	- 9.6	- 7.99	- 13.56	- 4.01	- 12.00
1720	- 10.97	- 11.6	- 12.27	- 13.44	- 7.77	- 11.28
1740	- 15.30	- 13.0	- 15.83	- 10.68	- 11.02	- 9.75
1760	- 19.57	- 12.8	- 18.76	- 8.78	- 13.63	- 7.83
1780	- 22.65	- 9.2	- 20.87	- 6.33	- 15.51	- 5.64
1800	- 24.07	- 4.3	- 22.12	- 3.75	- 16.64	- 3.39
1820	- 24.09	- 0.06	- 22.40	- 0.84	- 17.06	- 0.96
1840	- 23.22	+ 2.3	- 21.34	+ 3.06	- 16.77	+ 0.87
1860	- 21.55	+ 2.0	- 19.54	+ 5.52	- 15.84	+ 2.79
1880	- 18.73	+ 8.5	- 16.76	+ 8.34	- 14.17	+ 3.21
1890	- 17.57	+ 7.0	- 15.16	+ 9.6	- 11.77	+ 9.00
1900	- 16.5	+ 6.4	- 14.60	+ 3.4	--	

Declassified in Part - Sanitized Copy Approved for Release 2013/01/23 : CIA-RDP81-01043R001600090003-8

Declassified in Part - Sanitized Copy Approved for Release 2013/01/23 : CIA-RDP81-01043R001600090003-8

From Table 13 it is apparent that the secular range is not constant, but changes from year to year. The same nature of the secular range is observed at all points of the terrestrial globe where prolonged series of observations are available. Thus Figures 54 and 55 show the course of mean annual values of the elements of terrestrial magnetism at the Slutsk and Sverdlovsk observatories, indicating clearly that the annual changes of all the elements between 1912 and 1945 altered their values to a fairly appreciable extent.

Until recently the secular range was studied mostly at individual locations, the results of which are shown in the graphs of Figures 54 and 55. In these studies was assumed that the secular range was caused by changes in the total magnetic moment of the earth. The displacement of the magnetic pole along a certain closed contour also was indicated as one of the causes of secular range.

At the present time studies of secular variations have acquired a different nature. The extensive data gathered from observations of the elements of terrestrial magnetism in various countries make it possible to compare the secular ranges of individual observatories, and for numerous individual points as well. Such comparisons are made by means of maps of secular range isolines, i.e., of lines of equal secular range, which have been given the designation isopores. The first maps of isopores for the European part of Russia were drawn by Tillo [3], and world maps were not prepared until 1930, for the 1930 epoch [34]. Figures 56, 57 and 58 show isopore maps for the 1942 epoch [35] from which it is apparent that the secular range exhibits definite regularities in its distribution over the surface of the terrestrial globe. Thus all the isopores are found centered around several areas, called foci of secular range, where these

Declassified in Part - Sanitized Copy Approved for Release 2013/01/23 : CIA-RDP81-01043R001600090003-8

Declassified in Part - Sanitized Copy Approved for Release 2013/01/23 : CIA-RDP81-01043R001600090003-8

variations reach maximum values. From the isopore map of the vertical component it is apparent that at several zones of the surface of the earth the vertical component is increasing and at several zones it is decreasing, i.e., it appears as if within the zones of Z increase of the positive magnetic mass occurs, while in the zones of decrease the negative mass increases.

Examination of the isopores of north and east components reveals that they are not independent but are governed by the isopores of the vertical component, the same as is true in maps of the residual field. Considering the focus of positive values of the secular range as a center of magnetic mass increase, it is possible to determine the distribution of the magnetic field caused by this mass on the earth's surface. Above the center of the magnetic mass the vector of the field must be vertical, while to the side of the center it slopes toward the horizon. Therefore, above the center only the vertical component increases, while around the center the horizontal component δ H also increases but in different directions.

The superimposition of this additional δ H on the horizontal component of the terrestrial field results in either an increase or a decrease of this horizontal component, depending on the direction of δH.

A positive magnetic mass will produce an increase of the north component north of the center and a decrease south of the center. The situation is similar with respect to the east component. The east component increases within areas east of the center having negative δZ and west of the center it decreases, which is what actually take place as is seen from the maps of δX and δY isopores (Figures 57 and 58).

Declassified in Part - Sanitized Copy Approved for Release 2013/01/23 : CIA-RDP81-01043R001600090003-8

Declassified in Part - Sanitized Copy Approved for Release 2013/01/23 : CIA-RDP81-01043R001600090003-8

There are only 5 main foci, where changes of the vertical component attain 100 and more; namely: Indonesian ($\delta Z = -130\gamma$), Iranian, south of the Caspian Sea ($\delta Z = +110\gamma$), South African ($\delta Z = +130\gamma$), Atlantic ($\delta Z = -110\gamma$) and South American ($\delta Z = +160\gamma$).

In addition there are less pronounced foci where δZ has a value of 50-60 γ. These include foci in the Arctic, near Novaya Zemlya, in the Bering Sea, in Canada, and in the Pacific Ocean near the coast of South America. It is probable that there are found many more such foci covering small areas, but on not all of them can be detected on small scale world maps.

Figures 59, 60 and 61 show isopore maps of the Soviet Union drawn by V. P. Orlov for the 1932.5 epoch on the basis of the general magnetic survey data. Plotted from more extensive data than the world maps, these maps give a better representation of the actual distribution of the secular range over the territory of the USSR, but the general regularities are the same as those found on the world maps.

Thus investigations of recent years indicate that secular variations constitute not a "worldwide," but rather a local phenomenon which, however, is localized over vast areas of the terrestrial globe.

Spheric analysis of the earth's magnetic field performed by various investigators for different epochs show that secular changes of the earth's magnetic field cause changes of all the coefficients of the expansion series, including also coefficients g_1^0, g_1^1 and h_1^1 corresponding to a uniform magnetization of the terrestrial globe.

Table 9 in Chapter II shows that from 1885 to 1945 these coefficients have steadily decreased in value within limits exceeding the errors of their determinations. Such changes are associated with a

Declassified in Part - Sanitized Copy Approved for Release 2013/01/23 : CIA-RDP81-01043R001600090003-8

Declassified in Part - Sanitized Copy Approved for Release 2013/01/23 : CIA-RDP81-01043R001600090003-8

change in the magnetic moment of the earth both in magnitude and direction since the magnetic moment and its direction are defined by the coefficients g_1^0, $g^1{}_1$ and h_1^1. Table 14, which is reproduced according to Westein [36], lists the values of the magnetic moment in relative units and the polar angles of the magnetic axis of the dipole corresponding to uniform magnetization for various epochs.

The table shows that during the century the earth's magnetic moment decreased 5% and the magnetic pole was displaced 5° to the West, while the inclination of the magnetic axis in relation to the axis of rotation has remained unchanged since fluctuations of fractions one degree may be ascribed to errors in determination. Thus the magnetic axis undergoes precession about the axis of rotation at an angular rate of 0.05° per year.

A 5% change in the magnetic moment of the earth seems doubtful, and therefore the question arises as to whether it too, may be due to errors in calculation. However, this is opposed by the facts that changes in the magnetic moment during the hundred years were of the same sign as can be seen from the table, and the values of magnetic moments calculated for the same epoch from different initial data differ from by not more than one percent.

Consequently, errors in magnetic moment determinations are substantially smaller than the observed change. Since the time interval over which these changes can be traced is very short, the most probable assumption is that changes of magnetic moment are of a periodic nature, but thus far there are no physical foundations for such an assumption.

Thus the observed secular variations are the result of a change in the earth's magnetic moment and a change of the residual field, the greater portion of the variations observed being variations in the residual field.

Declassified in Part - Sanitized Copy Approved for Release 2013/01/23 : CIA-RDP81-01043R001600090003-8

Declassified in Part - Sanitized Copy Approved for Release 2013/01/23 : CIA-RDP81-01043R001600090003-8

TABLE 14

RELATIVE CHANGES IN THE MAGNETIC MOMENT OF THE EARTH AND OF ITS MAGNETIC AXIS WITH LAPSE OF TIME

Epochs	Mean Epoch	Magnetic Moment M	Mean Value of M	Complement of Latitude θ	Longitude λ	Mean Value of λ
1830		1.061		12.2°	63.5°	
1829	1836	1.047	1.053	11.7	64.7	64.2°
1845		1.052		11.3	64.3	
1880		1.036		11.6	68.0	
1885	1883	1.033	1.035	11.4	67.8	68.4
1885		1.035		11.3	69.5	
1922		1.011		11.6	69.1	
1945	1937	0.989	1.000	11.8	68.8	69.3
1945		0.998		11.4	70.0	

Declassified in Part - Sanitized Copy Approved for Release 2013/01/23 : CIA-RDP81-01043R001600090003-8

Declassified in Part - Sanitized Copy Approved for Release 2013/01/23 : CIA-RDP81-01043R001600090003-8

The next characteristic of the distribution of isopores is their mobility in time. Comparing isopore of different epochs it is noted that foci of secular range are moving continuously over a certain open curve. In accordance with the latter the entire set of isolines surrounding any given focus also is moving. This explains the known fact of a change in the magnitude of secular range at a given observatory with lapse of time.

However, one of the principal characteristics of the distribution of isopores is the concentration of secular range foci within zones of seismic activity.

This was pointed out for the first time by the Soviet magnetologist N. N. Trubyatchinskiy [37], who in 1934 expressed the opinion that "secular variations of field magnetization are localized within a few, but extensive zones of the earth's surface apparently closely associated with physical processes occurring in geosynclines, especially at junctions of geosynclines."

In 1949 A. A. Ol' [38] compared zones of seismic activity and centers of secular range for 5 different epochs by plotting them on a map (Figure 62). The map fully substantiates the idea of N. N. Trubyatchinskiy that most centers of secular range are concentrated either within these zones or near bifurcations or sharp bends of the zones.

Therefore in deriving any theory of secular variations it is impossible to disregard this remarkable fact which under no circumstances may be regarded as being accidental.

Section 2. Theory of Secular Variations

In addition to the phenomena considered in the preceding section

Declassified in Part - Sanitized Copy Approved for Release 2013/01/23 : CIA-RDP81-01043R001600090003-8

Declassified in Part - Sanitized Copy Approved for Release 2013/01/23 : CIA-RDP81-01043R001600090003-8

and which establish a relationship between secular variations and the earth's internal structure, the primary proof of the internal origin of secular variations is provided by spheric analysis. Such an analysis carried out in 1925 on the basis of data obtained at 14 observatories has led to the conclusion that the field of secular variations is a fully "internal" field, i.e., having its sources inside the terrestrial globe.

In 1946 Yu. D. Kalinin [39] essentially confirmed these conclusions but found that there exists also an "external" portion of the field even though it amounts to only one-tenth of the internal field.

Thus at the present time it may be considered fully demonstrated that secular variations are caused by processes occurring inside the terrestrial globe.

However, attempts to determine the depth level at which these processes take place as well as their nature, have yielded no definite results thus far.

Some investigators consider that similar to the case of the residual field this depth is of the order of one-half of the earth's radius, while others place it within the upper shell of the terrestrial globe.

Thus the current theories of secular variations, like the theories of the residual field, may be divided into "deep-level" and "surface" theories. Among the theories advocating the deep-level nature of secular variations are those of McNish, Elsasser, Bullard, and the work of Yu. D. Kalinin which is most thoroughly developed mathematically.

Declassified in Part - Sanitized Copy Approved for Release 2013/01/23 : CIA-RDP81-01043R001600090003-8

Declassified in Part - Sanitized Copy Approved for Release 2013/01/23 : CIA-RDP81-01043R001600090003-8

McNish [40] attempted to represent the field of variations of the vertical component by 13 dipoles of equal magnetic moments located at different points of the terrestrial globe at equal depth amounting to one-half of the earth's radius. Because the calculated values of variations were in fairly good agreement with the observed values McNish contends that the depth of occurrence of the causes of secular variations is of the order of one-half of theearth's radius.

Elsasser [41] associates secular variations with the formation of the overall magnetic field of the earth. As stated previously in the opinion of Elsasser the permanent magnetic field of the terrestrial globe is the result of convection movements within the core, and irregularities of these movements of vortexes lead to the occurrence of secular variations.

Bullard [42], on studying the Atlantic center of secular variations, assumed the presence of a dipole varying with time and located in a horizontal southeast-northwest direction beneath the surface of the core. Calculations have shown that such a dipole is a fairly good representation of the field on the earth's surface, but at great distances from the center of this region the field of this dipole decreases more rapidly than is actually observed, which indicates that placing the dipole on the surface of the core or somewhat higher will not improve, but diminishes the agreement of the calculated values with reality. However, if not one, but several dipoles are placed at the surface of the core in a southeast-northwest direction, better agreement is obtained between calculated and actual values of vertical and horizontal components over a fairly large area of these regions. Therefrom it is concluded that mathematical calculations do not negate the presence of very deep sources of secular variations.

Declassified in Part - Sanitized Copy Approved for Release 2013/01/23 : CIA-RDP81-01043R001600090003-8

Declassified in Part - Sanitized Copy Approved for Release 2013/01/23 : CIA-RDP81-01043R001600090003-8

McNish [40] attempted to represent the field of variations of the vertical component by 13 dipoles of equal magnetic moments located at different points of the terrestrial globe at equal depth amounting to one-half of the earth's radius. Because the calculated values of variations were in fairly good agreement with the observed values McNish contends that the depth of occurrence of the causes of secular variations is of the order of one-half of theearth's radius.

Elsasser [41] associates secular variations with the formation of the overall magnetic field of the earth. As stated previously in the opinion of Elsasser the permanent magnetic field of the terrestrial globe is the result of convection movements within the core, and irregularities of these movements of vortexes lead to the occurrence of secular variations.

Bullard [42], on studying the Atlantic center of secular variations, assumed the presence of a dipole varying with time and located in a horizontal southeast-northwest direction beneath the surface of the core. Calculations have shown that such a dipole is a fairly good representation of the field on the earth's surface, but at great distances from the center of this region the field of this dipole decreases more rapidly than is actually observed, which indicates that placing the dipole on the surface of the core or somewhat higher will not improve, but diminishes theagreement of the calculated values with reality. However, if not one, but several dipoles are placed at the surface of the core in a southeast-northwest direction, better agreement is obtained between calculated and actual values of vertical and horizontal components over a fairly large area of these regions. Therefrom it is concluded that mathematical calculations do not negate the presence of very deep sources of secular variations.

Declassified in Part - Sanitized Copy Approved for Release 2013/01/23 : CIA-RDP81-01043R001600090003-8

Declassified in Part - Sanitized Copy Approved for Release 2013/01/23 : CIA-RDP81-01043R001600090003-8

In 1947, utilizing spheric analysis Westein drew diagrams of currents within the spherical layer which cause the field that is observed, placing them at various depths with a minimum of about 3,000 km. However, it is pointed out by Westein himself that the situation actually is much more complex since the harmonic analysis upon which these evolvements are based is limited to the expansion of n = 6 terms, whereas the effect of higher harmonics must be considerable.

Yu. D. Kalinin, in his 1948 paper "Geomagnetic Secular Variations in the USSR" [39] also supports the theory of a deep level occurrence of the causes of secular variations. He attempted to prove his assumptions by spheric analysis, which method failed to yield good results in earlier works of other investigators due to a slow convergence of the series. The slow convergence of the series, i.e., the effect of higher harmonics, is in turn caused by the local nature of secular variations.

Without resorting to a higher order expansion, Yu. D. Kalinin was able to detect the influence of the spherical harmonics $P_{12}^{9}(\cos\theta)$ and $P_{8}(\cos\theta)$.

Expanding the potential of the secular variation field to terms of the first order corresponding to uniform magnetization and determining the coefficients, he was able to separate the field of uniform magnetization on the basis of the observed values of the field and thus obtained the components of the intensity of the field of secular variations depending upon the terms of higher order.

Since the maxima and minima of the Z component, i.e., the centers of the regions, alternate about every 40°, it may be assumed that the term including the spherical function $P_{n}^{9}(\cos\theta)\cos 9\lambda$ must

Declassified in Part - Sanitized Copy Approved for Release 2013/01/23 : CIA-RDP81-01043R001600090003-8

Declassified in Part - Sanitized Copy Approved for Release 2013/01/23 : CIA-RDP81-01043R001600090003-8

play an important part in the expansion. Considering the fact that the maxima and minima alternate latitudinally every 30° n may be taken equal to 12.

However, the addition of a term including $P_{12}^{9}(\cos\theta)$ to terms of the first order still failed to eliminate the difference between the observed and the calculated values. Therefore on studying the graph of change in secular range depending on latitude, Yu. D. Kalinin arrived at the conclusion that terms containing polynomials of the eighth order $P_8(\cos\theta)$ must be introduced which greatly improved the agreement between the calculated and actual values.

Such an expansion has made it possible to divide the field of secular variations into a field resulting from internal and external causes. In this way it was found that external causes play an appreciable role in the formation of secular variations. In attempting to explain the origin of the internal portion of the field of secular variations Yu. D. Kalinin compares this field with that of a dipole, identifying it with a vortical current located at a certain depth. This comparison enabled determination of the depth of the dipole and its magnetic moment, which at various epochs were found to range from 0.52 to 0.95 of the earth's radius. In the opinion of the author this is explained by the overly simplified assumption concerning the dipole nature of the causes of secular variations.

The "external" field, according to the calculations of Yu. D. Kalinin, is the result of an annular current flowing around the earth, which causes the constant component of the overall field of the earth, and of induced currents in the ionosphere. However, notwithstanding the fairly convincing mathematical calculations of Yu. D. Kalinin, the question concerning the reality of the "external"

Declassified in Part - Sanitized Copy Approved for Release 2013/01/23 : CIA-RDP81-01043R001600090003-8

Declassified in Part - Sanitized Copy Approved for Release 2013/01/23 : CIA-RDP81-01043R001600090003-8

portion of the field of secular variations still remains open, since there are no other foundations or facts in support of such an ascertion.

At present there are no secular variation theories based on the hypothesis of changes in magnetization of the earth's crust and worked out mathematically, as in the case of the deep-level theories. There are, however, a number of pronouncements by various scientists based exclusively upon observed facts. All these facts indicate that the cause of secular variations apparently should be associated with processes occurring within the earth's crust or somewhat deeper, but in any event, not at the surface of the core. At present there are no data except the seismic observations relating to the latter. Hence, the next problem in the development of theories of secular variations should be quantitative computation of their field on the assumption of a surface origin of secular variations.

Upon comparison of all the existing theories and specific pronouncements concerning the causes of secular variations it is apparent that secular variations still remain a problem similar to that of the permanent field of the earth which, also awaits solution. It is also apparent that theories of secular variations cannot be isolated from theories of the permanent magnetic field, especially from its residual portion, since in all probability the causes of residual field and of secular variations are the same.

Declassified in Part - Sanitized Copy Approved for Release 2013/01/23 : CIA-RDP81-01043R001600090003-8

Declassified in Part - Sanitized Copy Approved for Release 2013/01/23 : CIA-RDP81-01043R001600090003-8

PART TWO

VARIABLE MAGNETIC FIELD OF THE EARTH

CHAPTER V

CLASSIFICATION OF VARIATIONS OF THE EARTH'S MAGNETIC FIELD AND METHODS FOR THEIR INVESTIGATION

Section 1. General Information and Classification of Magnetic Variations

Over the permanent magnetic field of the earth, the properties of which were discussed in part one, is superposed the variable field causing changes in the total magnetic field with time. Although the magnitude of these changes is slight in comparison with that of the permanent portion, because the former are associated with other geophysical phenomena in the ionosphere investigation of the variable field yields information concerning these phenomena and their causes. Therefore the study of the variable field and of its regularities is of great scientific and practical interest. Suffice it to state that the audibility of radio transmitting devices depends upon the condition of the ionosphere.

The variable magnetic field of the earth constitutes the geometric difference between the observed intensity of the magnetic field and its mean value over some prolonged interval of time, one month or one year. Observations show that this difference, known as the vector of magnetic variations, changes in a different manner during different days.

Sometimes the changes occur evenly and exhibit definite regularities, while at other times they are irregular, with the periods, amplitudes and phases continuously changing in value. In

Declassified in Part - Sanitized Copy Approved for Release 2013/01/23 : CIA-RDP81-01043R001600090003-8

Declassified in Part - Sanitized Copy Approved for Release 2013/01/23 : CIA-RDP81-01043R001600090003-8

the former case the changes or variations are said to be static or undisturbed and in the latter they are said to be of disturbed nature.

Undisturbed variations are strictly periodic, i.e., they have a fully defined period. Thus for example, if during a disturbance-free day the behavior of a freely rotating, horizontal, magnetic needle is observed at Leningrad, we note that its northern end begins to be deflected toward the east in the morning, reaching a maximum deflection at 8 AM, after which a reverse movement to the west commences, which in turn lasts approximately 14 hours. The amplitude of this oscillation during a 24-hour period at Leningrad does not exceed 16', and therefore may be detected only by careful observation. Consequently the magnetic meridians, and therefore the magnetic declinations as well, undergo continuous change during a 24-hour period. These changes in declination and in all the other elements which occur during a 24-hour period are called solar-day variations and their period is one solar day.

In addition to solar-day variations there are other variations having other periods. Therefore it is convenient to classify undisturbed variations on the basis of their period, especially since they also have different causes. The undisturbed variations include solar-day, lunar-day and annual variations.

The disturbed portion of variations also consists of a series of variations, which are superimposed upon each other, producing summatively irregular oscillations of all the elements of terrestrial magnetism about the median position. Some of these variations have a definite period, others alter their period from one oscillation to the next, and there are also nonperiodic variations.

Therefore the disturbed variations also may be classified on

Declassified in Part - Sanitized Copy Approved for Release 2013/01/23 : CIA-RDP81-01043R001600090003-8

Declassified in Part - Sanitized Copy Approved for Release 2013/01/23 : CIA-RDP81-01043R001600090003-8

the basis of periodicity, as periodic, nonperiodic and irregular fluctuations. The periodic include the disturbed solar-day variations, having a period of one solar day, and the magnetic pulsations, with a period of several minutes. Of the nonperiodic type is the so-called aperiodic disturbed variation, which is observed during magnetic storms and consists of a rapid decrease of the horizontal component, followed by a slow return to the normal state. Irregular fluctuations of the elements of terrestrial magnetism constitute the major portion of the magnetic disturbances and consist of a number of successive changes of the magnetic elements having different period and different amplitude.

In addition, there are variations which cannot be classified under any of these 3 types, since although they involve changes of a regular nature they have no definite period, but at the same time they are not aperiodic. Because of their form these variations have been named bight-like variations, since on magnetograms they appear in the form of a curve which approximates the outline of a sea bay.

Differentiation of the undisturbed, from the disturbed variations and differentiation of their individual forms, with the exception of pulsations and bight-like variations, is possible only by statistical processing methods.

Section 2. Methods for Differentiation of Daily Magnetic Variations Statistical Ppocessing)

Magnetic observatories supply data which require complex processing by statistical methods and also by methods of spheric and harmonic analysis in order to differentiate variations of a given type and to determine the regularities of their occurrence.

Declassified in Part - Sanitized Copy Approved for Release 2013/01/23 : CIA-RDP81-01043R001600090003-8

Declassified in Part - Sanitized Copy Approved for Release 2013/01/23 : CIA-RDP81-01043R001600090003-8

Magnetograms, or curves of continuous correlation of the elements of terrestrial magnetism, reveal that each of the elements consists of complex periodic changes having different periods, amplitudes and phases. Therefore, no correlations in the course of variations may be ascertained from individual magnetograms. However, comparison of the recordings of variations over a prolonged period, viz over a week or month, reveals that in the absence of strong disturbances the curves show a general tendency of duplication every 24 hours, i.e., among the different variations some have a period equal to 24 hours (solar). However, exact determination of these variations requires statistical processing consisting of calculation of the mean diurnal values of variations, utilizing data relating to a fairly long interval of time (month, year). This includes determination, by direct measurements on the magnetograms of the mean hourly values of the ordinates corresponding to variations of any given element. These values are summated for each hour of the 24-hour period, and from this the mean value is derived. An example of such a processing is included in Addendum 2, wherein the mean hourly values of the declination ordinates reckoned from the basis line are listed.

In this processing variations of fortuitous nature, and also those having different periods, mutually compensate each other, provided that the number of items is sufficiently large and therefore the mean value is free from anyother variations except the secular, the period of which is very large in comparison with 24 hours. This proposition is demonstrated in detail below.

Assuming that the magnetogram of some element is free from secular variations and represents the sum of 3 periodic variations of different period, 2 of them being of sinusoidal and one of an arbitrary nature, we have:

Declassified in Part - Sanitized Copy Approved for Release 2013/01/23 : CIA-RDP81-01043R001600090003-8

Declassified in Part - Sanitized Copy Approved for Release 2013/01/23 : CIA-RDP81-01043R001600090003-8

$$S = S_o \sin(w_1 t + \varphi_1) + S'_o \sin(w_2 t + \varphi_2) + S(t), \qquad (5.1)$$

where S_o and S'_o are amplitudes, w_1 and w_2 circular frequencies, φ_1 and φ_2 the phases of harmonic changes of the element, and S(t) is some arbitrary function of periodic nature.

Since the curves represent a continuous series of observations of the quantity S over time t_1 to t_2, upon dividing the interval $t_2 - t_1$ into a series of intervals equal to the period $T_1 = 2\pi/w_1$ it is possible to determine the values of S for the points of time:

$$t,\ t + T_1,\ t + 2T_1, \ldots, t + nT_1.$$

These values will be:

$$S_k = S_o \sin[w_1(t+kT_1)+\varphi_1] + S'_o \sin[w_2(t+kT_1)+\varphi_2] + S_k(t_k).$$

Adding these equalities we obtain:

$$\sum_{k=0}^{n} S_k = S_o \sum_{k=0}^{n} \sin(w_1 t + \varphi_1 + k\pi) + S'_o \sum_{k=0}^{n} \sin(w_2 t + k w_2 T_1) + \sum_{k=0}^{n} S_k(t_k)$$

or

$$\sum_{k=0}^{n} S_k = (n+1)\sin(w_1 t + \varphi_1) + S'_o \sum_{k=0}^{n} \sin(k\alpha + \beta) + \sum_{k=0}^{n} S_k(t_k),$$

where

$$\beta = w_2 t + \varphi_2, \quad k\alpha = w_2 T_1 k.$$

The mean value S_m will be:

$$S_m = \frac{1}{n+1}\sin(w_1 t + \varphi_1) + \frac{S'_o}{n+1} \sum_{k=0}^{n} \sin(k\alpha + \beta) + \frac{1}{n+1} \sum_{k=0}^{n} S_k(t_k).$$

Since the variations S(t) are fortuitous and are not governed by any law, it follows that with a sufficiently large number of observations, individual positive as well as negative values will be encountered in equal amount and therefore the sum will be close to zero. Consequently we may write:

$$S_m = S_o \sin(w_1 t + \varphi_1) + \frac{S'_o}{n+1} \sum_{k=0}^{n} \sin(k\alpha + \beta),$$

or

$$S_m = S_o \sin(w_1 t + \varphi_1) + \frac{S'_o}{n+1}\left(\sin\beta \sum_{k=0}^{n} \cos k\alpha + \cos\beta \sum_{k=0}^{n} \sin k\alpha\right).$$

From trigonometric formulas we have:

$$\sum_{k=0}^{n} \cos k\alpha = \frac{\sin\frac{2n+1}{2}\alpha}{2\sin\frac{\alpha}{2}} + \frac{1}{2}, \qquad \sum_{k=0}^{n} \sin k\alpha = \frac{\sin\frac{n\alpha}{2}\sin\frac{n+1}{2}\alpha}{\sin\frac{\alpha}{2}}.$$

Declassified in Part - Sanitized Copy Approved for Release 2013/01/23 : CIA-RDP81-01043R001600090003-8

Declassified in Part - Sanitized Copy Approved for Release 2013/01/23 : CIA-RDP81-01043R001600090003-8

Substituting these values in the expression for S_m and using simple trigonometric transformations, we have:

$S_m = S_o \sin(w_1 t + \varphi_1) + S'_o / n+1 \operatorname{cosec} \alpha/2 \sin n+1/2 \gamma \sin(n/2 \gamma + \beta)$.

Upon increasing the number of observations n the second term of the right hand portion tends to zero, since at any value of n the numerator remains smaller than the constant quantity $S'_o \operatorname{cosec} \alpha/2$, while the denominator increases with increasing n. Therefore it always is possible to select a number of observations n for which the second term will have a value smaller than the number given beforehand. In such a case

$$S_m = S_o \sin(w_1 t + \varphi_1)$$

i.e., the mean magnitude of variations derived by averaging the values of elements taken at time intervals equal to the period T_1, will be free from fortuitous variations at a sufficiently large number of these intervals, as well as from variations having a period T_2, which is different from T_1.

If the period T_1 is subdivided into K equal intervals of time, and for each point of time $t = t$; $t_1 = t + T_1/n$, $t_2 = t + 2T_1/n$; etc the corresponding mean values S_m^o; S_m^1; S_m^2; ... are calculated by the method described above we obtain a numerical correlation between S and t expressing the variation S of period T_1.

Not only purely sinusoidal variations, but variations of any nature are differentiated in this manner, provided that they recur periodically. Indeed, any periodic function f(t) having period T may be represented as a sum of harmonic functions the period of which is a multiple of T, i.e.,

$$f(t) = \sum_{k=1}^{n} a_k \sin(wkt + \varphi_k), \qquad (5.2)$$

Declassified in Part - Sanitized Copy Approved for Release 2013/01/23 : CIA-RDP81-01043R001600090003-8

Declassified in Part - Sanitized Copy Approved for Release 2013/01/23 : CIA-RDP81-01043R001600090003-8

where k and n are whole numbers. Therefore, replacing the harmonic function $S_o \sin(w_1 t + \varphi_1)$ by the sum (5.2) in equation (5.1) and averaging, we obtain the same function f(t), since the substitution t + kT for argument t in equation (5.2) does not change the function f(t).

Differentiation of secular variations requires needed observations over a long interval of time, one or more years. If some one element is observed continuously during one year and thereafter its mean value for this year is calculated, according to the laws of statistics it will be free from any changes of a periodic nature. Therefore the changes in secular variation are obtained by plotting a graph of the mean annual values over several years.

If the interval of time between observations is large (of several years) only 2 observations are sufficient for forming an opinion of the magnitude of secular variation, since over such an interval the secular variation is considerably greater than the periodic variations, including magnetic disturbances.

By this method not only variations having a period equal to one day (solar day variations) but also variations having a period of one lunar day (lunar day variations), may be calculated for which purpose all the data are subdivided into time intervals of one lunar day.

Section 3. The Method of Spheric and Harmonic Analysis of Variations

After the statistical processing has been completed and curves of the solar-day or lunar-day progression have been obtained from numerous observations further processing consists of determination of the mathematical correlation between the given variation, the time and the coordinates of the point of the earth's surface.

Declassified in Part - Sanitized Copy Approved for Release 2013/01/23 : CIA-RDP81-01043R001600090003-8

Declassified in Part - Sanitized Copy Approved for Release 2013/01/23 : CIA-RDP81-01043R001600090003-8

Since we have no basis for assuming any functional correlation, the only way this correlation may be determined is to represent the variation as a series having constant coefficients which must be determined from observations.

Harmonic Analysis. In view of the fact that diurnal variations (solar and lunar) have a period, they are first expanded to a Fourier series, and for each element of X(north), Y(east) and Z(vertical component) we have:

$$\delta X = \sum_{m=1}^{\infty} \left(a^X_m \cos mt + b^X_m \sin mt \right) + \frac{a^X_0}{2},$$

$$\delta Y = \sum_{m=1}^{\infty} \left(a^Y_m \cos mt + b^Y_m \sin mt \right) + \frac{a^Y_0}{2}, \qquad (5.3)$$

$$\delta Z = \sum_{m=1}^{\infty} \left(a^Z_m \cos mt + b^Z_m \sin mt \right) + \frac{a^Z_0}{2},$$

where δX, δY, δZ are the corresponding variations, a and b are constant coefficients, and t the time expressed in degrees or radians, the day being considered equal to 2π. Harmonic analysis formulas are used to determine the coefficients a and b:

$$a^X_m = \frac{1}{n} \sum_{i=0}^{n-1} \delta X_i \cos mt_i \,; \quad b^X_m = \frac{1}{n} \sum_{i=0}^{n-1} \delta X_i \sin mt_i \qquad (5.4)$$

where n is the number into which the interval T is subdivided, and δX_i is the value of variations at the points of time t_i corresponding to the i-th interval.

Since the values of variations are given for each hour of the day, the number n into which the sum is subdivided may be 24, 12 or 8, depending upon the degree of accuracy desired in determining the coefficients a and b.

The formulas of (5.3) can be written in a somewhat different form more convenient in plotting the graphs, by adding the binomials appearing within the parentheses in accordance with the trigonometric formulas, namely:

Declassified in Part - Sanitized Copy Approved for Release 2013/01/23 : CIA-RDP81-01043R001600090003-8

Declassified in Part - Sanitized Copy Approved for Release 2013/01/23 : CIA-RDP81-01043R001600090003-8

$$X = \frac{a_0}{2} + \sum_{n=1}^{\infty} A_n \cos(nt + \varphi_n),$$

$$Y = \frac{b_0}{2} + \sum_{n=1}^{\infty} B_n \cos(nt + \psi_n),$$

$$Z = \frac{c_0}{2} + \sum_{n=1}^{\infty} C_n \cos(nt + \chi_n), \qquad (5.5)$$

in this case the coefficients A and φ are expressed by a and b, with the corresponding symbols, in the following manner:

$$A = \sqrt{a^2 + b^2}, \quad \operatorname{tg}\varphi = \frac{a}{b} \qquad (5.6)$$

An example of such an expansion is included for solar-day variations observed in 1933 at the Pavlovsk observatory near Leningrad. Table 15 lists the mean values of variations of the 3 elements over the interval 1 May to 1 September, and Table 16 lists the values of coefficients a and b calculated according to formula (5.4), and the values of A and φ calculated by means of formula (5.6).

Figure 63 contains the graphs of variations corresponding to tables 15 and 16. In these graphs the solid curve is empirical and is plotted from the data of Table 15, while the dotted curves represent the result of addition of 2 sinusoids of amplitudes A_1 and A_2 and phases φ_1 and φ_2, in accordance with Table 16.

The satisfactory coincidence of the calculated and empirical curves indicates that on expansion of the solar-day variation to a Fourier series it is sufficient to limit oneself to the first 2 harmonics in order to obtain a result that is in agreement with obeervations.

Declassified in Part - Sanitized Copy Approved for Release 2013/01/23 : CIA-RDP81-01043R001600090003-8

Declassified in Part - Sanitized Copy Approved for Release 2013/01/23 : CIA-RDP81-01043R001600090003-8

TABLE 15

DIURNAL VARIATIONS AT PAVLOV DURING THE SUMMER OF 1933

Hours	1	2	3	4	5	6	7	8	9	10	11	12
δX	7	7	8	5	0	-7	-13	-18	-21	-24	-21	-12
δY	6	10	14	19	22	24	22	12	2	-11	-24	-27
δZ	2	2	2	1	1	1	0	- 2	- 5	- 8	- 8	- 6

Hours	13	14	15	16	17	18	19	20	21	22	23	24
δX	- 5	5	7	8	8	10	10	10	9	9	8	7
δY	-25	-17	-11	- 5	- 4	- 3	- 4	- 2	- 1	0	2	4
δZ	- 2	1	3	4	4	4	3	3	2	1	1	1

TABLE 16

COEFFICIENTS OF FOURIER SERIES

	a_1	b_1	a_2	b_2	A_1	φ_1	A_2	φ_2
δX	13.9	- 6.5	- 7.0	1.6	15.3	- 64.9°	7.2	- 77.1°
δY	4.2	15.9	- 6.3	- 9.0	16.4	+ 14.2	11.0	+ 35.0
δZ	- 3.5	- 0.5	- 3.0	- 1.0	3.5	+ 81.8	3.2	+ 71.0

Declassified in Part - Sanitized Copy Approved for Release 2013/01/23 : CIA-RDP81-01043R001600090003-8

Declassified in Part - Sanitized Copy Approved for Release 2013/01/23 : CIA-RDP81-01043R001600090003-8

Having made such expansions for a large number of observatories distributed over the entire surface of the earth expansion of variations by spheric functions may be undertaken, which permits expression of the variations as functions of 2 variables, latitude and time.

Spheric Analysis. Spheric analysis enables representation of the potential of the field of variations and its first derivatives as functions of 2 variables, local time t and latitude φ, because observations show that solar-day variations are almost independent of longitude, but are of different mature at different latitudes. This is illustrated below.

Assuming that the potential of the field of variations U is a function of local time t and latitude φ, i.e.,

$$U = U(t, \varphi).$$

that variations are due to both internal and external causes, as a result of which the potential U constitutes the sum of 2 potentials produced by these 2 causes, the local time t may be replaced by the longitude in accordance with the formula $t = t_0 + \lambda$, where t_0 is the time at the zero meridian and may be taken equal to zero, the expansion formulas (2.22) and (2.29), derived in Chapter II, may be applied to the potential U and its first derivatives. Therefore, analogously to the equations of (2.31) the following expressions may be written for the components of the potential of variations:

$$\delta X = -\sum_{n=1}^{\infty}\sum_{m=0}^{n}\left(A_n^m \cos mt + S_n^m \sin mt\right)\frac{dP_n^m(\cos\theta)}{d\theta},$$

$$\delta Y = \sum_{n=1}^{\infty}\sum_{m=0}^{n}\left(A_n^m \sin mt - S_n^m \cos mt\right)\frac{mP_n^m(\cos\theta)}{\sin\theta}, \qquad (5.7)$$

$$\delta Z = \sum_{n=1}^{\infty}\sum_{m=0}^{n}\left(\mu_n^m \cos mt + V_n^m \sin mt\right)P_n^m(\cos\theta),$$

Declassified in Part - Sanitized Copy Approved for Release 2013/01/23 : CIA-RDP81-01043R001600090003-8

Declassified in Part - Sanitized Copy Approved for Release 2013/01/23 : CIA-RDP81-01043R001600090003-8

The constant coefficients r, s, u and v of the latter are correlated as follows:

$$\mu_k^m = (n+1) g_n^m - n g_n^m,$$

$$v_k^m = (n+1) f_k^m - n k_n^m,$$

$$\alpha_k^m = \alpha_n^m + J_n^m \qquad \beta_k^m = \beta_k^m + k_n^m,$$

where g_n^m and h_n^m are the coefficients of the expansion of potentials due to interval causes, and J_n^m and k_n^m of those due to external causes. If these coefficients are known the variation at any point of time and at any point of the earth's surface may be determined.

The coefficients r, s, u and v are determined as follows:

As shown above, the variations δ X, δ Y and δ Z at any observatory may be represented by the Fourier series (5.4), the coefficients a_m and b_m of which are known. Hence, comparing the coefficients appearing in these series at cos mt and sin mt with the analogous coefficients of series (5.7) we obtain the following system of equations for each observatory:

$$a_m^k = \sum_{n=1}^{\infty} \cdot \frac{\partial P_n^1}{\partial \theta}, \qquad \alpha_m^k = \sum_{n=1}^{\infty} S_k^m \frac{\partial P_n^1}{\partial \theta}$$

$$b_m^k = \sum_{n=m}^{\infty} \frac{\partial P_n^m}{\sin \theta}, \qquad \beta_m^k = \sum_{n=m}^{\infty} S_k^m \frac{P_n^m}{\sin \theta} \qquad (5.8)$$

$$\gamma_m^k = \sum_{n=m}^{\infty} \mu_k^m P_n^m, \qquad \delta_m^k = \sum_{n=m}^{\infty} v_k^m P_n^m,$$

and following solution of the latter the coefficients r, s, u and v may be determined. However, the solution of these equations requires that the number of equations be equal to the number of unknowns. Therefore the number of observatories evenly distributed over the surface of the earth must be chosen in accordance with the number of unknowns. If expansion by spheric harmonics is limited to terms of the fourth order (n = 4), the total number of coefficients s and r is equal to 24, and the same number holds true for the coefficients

Declassified in Part - Sanitized Copy Approved for Release 2013/01/23 : CIA-RDP81-01043R001600090003-8

Declassified in Part - Sanitized Copy Approved for Release 2013/01/23 : CIA-RDP81-01043R001600090003-8

u and v. As is apparent the equations (5.8), each observatory, yields nine equations for coefficient r and 8 for coefficient S. However, only 9 equations are given for coefficients u and v. Consequently, a minimum of 3 observatories must be available for the determination of all 48 coefficients. However, a much larger number of observatories usually is chosen, so the number of equations exceeds that of the unknowns and the solution is then performed by the procedure of least squares.

With expansion of the curves of diurnal progression to Fourier series of terms of the second order (m = 2), and spherical function expansion to which has been carried out at 5 observatories at different latitudes terms of the fourth order (n = 4) we have the following system of equations for determination of the coefficient r_n^m, set up according to the observations at one of the observatories, the latitude complement of which is θ_1:

$$
\begin{aligned}
a\,x_0 &= n_1 \frac{dP_1}{d\theta_1} + n_2 \frac{dP_2}{d\theta_1} + n_3 \frac{dP_3}{d\theta_1} + n_4 \frac{dP_4}{d\theta_1}, \\
a\,x_1 &= n_1' \frac{dP_1'}{d\theta_1} + n_2' \frac{dP_2'}{d\theta_1} + n_3' \frac{dP_3'}{d\theta_1} + n_4' \frac{dP_4'}{d\theta_1}, \\
a\,x_2 &= n_2^2 \frac{dP_2^2}{d\theta_1} + n_3^2 \frac{dP_3^2}{d\theta_1} + n_4^2 \frac{dP_4^2}{d\theta_1}, \\
0 &= n_3^3 \frac{dP_3^3}{d\theta_1} + n_4^3 \frac{dP_4^3}{d\theta_1}, \\
0 &= n_4^4 \frac{dP_4^4}{d\theta_1} \\
a\,y_1 &= n_1' \frac{P_1'}{\sin\theta_1} + n_2' \frac{P_2'}{\sin\theta_1} + n_3' \frac{P_3'}{\sin\theta_1} + n_4' \frac{P_4'}{\sin\theta_1}, \\
a\,y_2 &= 2n_2^2 \frac{P_2^2}{\sin\theta_1} + 2n_3^2 \frac{P_3^3}{\sin\theta_2} + 2n_4^2 \frac{P_4^2}{\sin\theta_1}, \\
0 &= 3n_3^3 \frac{P_3^3}{\sin\theta_1} + 3n_4^3 \frac{P_4^3}{\sin\theta_1}, \\
0 &= 4n_4^4 \frac{P_4^4}{\sin\theta_1}.
\end{aligned}
\qquad (5.9)
$$

Declassified in Part - Sanitized Copy Approved for Release 2013/01/23 : CIA-RDP81-01043R001600090003-8

Declassified in Part - Sanitized Copy Approved for Release 2013/01/23 : CIA-RDP81-01043R001600090003-8

The equations for the other 4 observatories are set up in the same manner, yielding a total of 45 equations containing 14 unknowns.

To determine the s_n^m coefficients it is necessary to have 40 similar equations in which the known values are coefficients of the Fourier series, b_n^x and b_m^y. To determine the coefficients u_n^m and v_n^m 45 equations will be needed (25 for u_n^m and 20 for v_n^m), in which the coefficients of the Fourier series will be a_m^z and b_m^z.

Having determined above coefficients and substituting them in equation (5.7) we obtain the components of the vector of variation δX, δY, δZ as functions of latitude and time accurate up to terms of the fourth order.

Through expansion of variations to Fourier series and through the use of spheric functions the variation vector may be resolved into 2 components, one of which is due to the internal and the other to the external causes, similarly to the case of a constant field.

Such resolutions show that variations due to internal causes constitute one-third of the total variations and may be explained as resulting from induction currents formed within the terrestrial globe due to the action of external vortical currents.

Section 4. Magnetic Activity

In the analysis of phenomena associated with variations of the magnetic field of the earth, comparison of these with other physical phenomena (auroras polaris, terrestrial currents, propagation of radio waves, occurrence of active formations upon the sun) and in determining correlations between these 2 types of phenomena it is convenient to characterize variations over a definite time interval by means of a

Declassified in Part - Sanitized Copy Approved for Release 2013/01/23 : CIA-RDP81-01043R001600090003-8

Declassified in Part - Sanitized Copy Approved for Release 2013/01/23 : CIA-RDP81-01043R001600090003-8

quantity which expresses the extent of disturbance of the magnetic field. This quantity is called magnetic activity or the state of magnetic disturbance.

If the magnetic field remains unchanged over a period of time the magnetic activity for this period is equal to zero. If on the other hand there are strong changes in the magnetic field, its magnetic activity has a large value. Magnetic activity increases with increase of the amplitude of fluctuation of the elements of terrestrial magnetism and also with an increase in the number of fluctuations per unit time.

While the concept of magnetic activity encounters no difficulties with respect to mensuration or its unit of measurement, there is as yet no rigorous and uniform procedure for its determination since it depends not upon a single parameter, but upon at least 2, the amplitude and the period.

The so-called international geomagnetic characteristics, which are the number 0, 1 and 2, are widely accepted for characterization of the extent of disturbance during each day.

At each observatory the record of daily variations, which are called magnetograms, are characterized by one of these numbers, depending on the nature of the record: the least disturbed are marked by zero and the most violent by the number 2. Naturally, in many instances such characteristics are individual deviations, but on statistical processing the traces of individuality are leveled off and the figures derived as the mean values of data of many observatories may have objective significance. In accordance with an international agreement the results of observatory evaluations are forwarded to the Carnegie Institute in Washington, where they are processed.

Declassified in Part - Sanitized Copy Approved for Release 2013/01/23 : CIA-RDP81-01043R001600090003-8

Declassified in Part - Sanitized Copy Approved for Release 2013/01/23 : CIA-RDP81-01043R001600090003-8

The mean values for all the observatories are printed in a special publication and constitute the international characteristic of a given day.

In the Soviet Union the Institute of Terrestrial Magnetism has an entire network of magnetic observatories, at its disposal, gathers information concerning magnetic activity and derives the mean values, which can fully substitute for the international characteristic figures.

To obviate the individual characteristics of evaluations of the state of the magnetic field many investigators have attempted to represent magnetic activity by means of an objective figure.

One such evaluation is a number proportional to the change in density of magnetic energy during a given interval of time.

The potential energy of a uniform magnetic field within 1 cm^3 is expressed by the equation

$$U = H^2_T/8\pi = H^2 + Z^2/8\pi$$

where H is the horizontal, and Z the vertical component.

The change of this energy δU, at small values of δH and δZ, may be represented in the form

$$\delta U = H\,\delta H + Z\,\delta Z/4\pi$$

A quantity calculated in accordance with this formula, but having a different coefficient usually is taken as the measure of activity, namely

$$\delta U = H\,\delta H + Z\,\delta Z/1{,}000$$

which has been named the numerical characteristic. In this equation H and Z represent the mean monthly values of the vertical and horizontal

Declassified in Part - Sanitized Copy Approved for Release 2013/01/23 : CIA-RDP81-01043R001600090003-8

Declassified in Part - Sanitized Copy Approved for Release 2013/01/23 : CIA-RDP81-01043R001600090003-8

components, while δH and δZ are the differences between the maximum and the minimum values of these elements during the given interval of time (hour, day, etc), expressed in gammas.

Although they are objective, the numerical characteristics still cannot provide a correct idea concerning magnetic activity during any given length of time since δH and δZ are taken as the difference between maximum and minimum values. These differences can be small even though there may be substantial changes during the interval and conversely, the differences can reach large values although the changes during the interval may be of monotonous nature. The intervals of time equal to the periods of random fluctuation of the magnetic field constitute an exception, and may assume values of several minutes or less. But even in these instances this evaluation method has little practical value.

In 1939 the International Association on Terrestrial Magnetism and Electricity adopted the k index for evaluation of the degree of magnetic disturbance and which at the present time is used by the observatories of the Soviet Union. The k index represents the numerical characteristic expressed in points of a scale. Each point of the scale corresponds to the amplitude of oscillations of the magnetic elements over a 3-hour interval, corrected for the undisturbed diurnal progression. The k index scale is made different for each observatory in order to eliminate the effect of latitude, since at any given activity of the sun the degree of disturbance differs at different latitudes.

A very convenient characteristic of the degree of disturbance is the length of the curve during a given interval of time of the magnetogram recording of a given element. Such a characteristic is

Declassified in Part - Sanitized Copy Approved for Release 2013/01/23 : CIA-RDP81-01043R001600090003-8

Declassified in Part - Sanitized Copy Approved for Release 2013/01/23 : CIA-RDP81-01043R001600090003-8

utilized by A. P. Nikol'skiy in his study of variations at high latitudes, in which he measured the length of the curve on recordings of the declination variometer. Although this length does not express any physical quantity, it reproduces very closely the nature of the state of disturbance. Its only flaw is the fact that it does not permit differentiation of monotonous from rapid periodical changes of elements, but it does reveal any change of the elements over any interval of time.

The above measurements of magnetic activity are convenient for characterization of a short interval of time (not exceeding 24 hours) but are of little use in characterization of large intervals such as a month or a year. Therefore in 1932 a specific standard of activity u [43] was proposed, which constitutes the mean magnitude during a month or a year of differences in the successive mean daily absolute values of the horizontal component at or near the magnetic equator. This standard was selected on the basis of the following observed fact. During strong magnetic disturbances the horizontal component undergoes similar changes over the entire terrestrial globe. During the initial period of the magnetic storm the horizontal component decreases everywhere, and thereafter it returns slowly to its normal state. This measurement standard is expressed in units of 10^{-4} Oe.

In addition to standard u, standard u_1 also is used, and is correlated with u by means of the following table:

u =	0.3	0.5	0.7	0.9	1.2	1.5	1.8	2.1	2.7	3.6 and higher
u_1 =	0	20	40	57	79	96	108	118	132	140

The state of magnetic disturbance is a quantity reflecting definite phenomena in the course of magnetic variations and must include regularities which follow from the regularities which govern the phenomena of magnetic variations.

Declassified in Part - Sanitized Copy Approved for Release 2013/01/23 : CIA-RDP81-01043R001600090003-8

Declassified in Part - Sanitized Copy Approved for Release 2013/01/23 : CIA-RDP81-01043R001600090003-8

However, these regularities may be revealed only through statistical processing, since during every day and hour the state of disturbance is of random nature and the extent of this disturbance (magnetic activity) can assume different values during the day, month or year, which do not conform to any regularities. With a sufficiently large number of recurring activity values coinciding with some definite point of time or phenomenon, the mean of these values shows definite regularities. Thus, the mean monthly activity values derived by processing of observational data relating to a period of several years show a clearly manifested yearly progression. The amplitude of this yearly progression increases with an increase in overall magnetic activity, as is apparent from Figure 64 which shows the yearly progression of magnetic activity derived by statistical processing of observational data covering a period of 59 years (from 1872 to 1930). In the processing all the data were subdivided into 3 groups corresponding to years of strong disturbance and years of slight disturbance, and the mean annual and mean monthly values of magnetic activity u were calculated for each group.

The drawing shows that the activity has 2 well-defined maxima coinciding with the equinoctial epochs and 2 minima coinciding with the epochs of solstices. This may be interpreted to mean that in the northern hemisphere magnetic disturbances are more likely to occur during spring and autumn, and are least likely to occur during summer and winter. Therefore the cause of these regularities must be connected with phenomena associated with the relative position of the plane of the terrestrial equator and the plane of the ecliptic.

Such phenomena include the occurrence of sunspots which appear mostly within zones 10^{o} to 30^{o} of northern and southern heliographic

Declassified in Part - Sanitized Copy Approved for Release 2013/01/23 : CIA-RDP81-01043R001600090003-8

Declassified in Part - Sanitized Copy Approved for Release 2013/01/23 : CIA-RDP81-01043R001600090003-8

latitude taken from the plane of the ecliptic, and their maximum number occur from 10° to 15° latitude. Therefore, during equinoctial epochs when the planes of the terrestrial and solar equators are in alignment, the surface of the earth is subjected to the greatest action of radiation emitted by the spots. Consequently, the cause of maximal activity during the equinoctial epochs appears most likely to be due to the maximum radiation emitted by the sun spots during this period.

The relationship between sunspots and magnetic activity manifests itself most characteristically on comparison of the graphs of solar activity and mean annual magnetic activity over a prolonged interval of time. Solar activity usually is taken to mean the sum of the number of sunspots f and of the 10-fold number of groups g of these spots. This standard of measurement of activity is called Wolf's number W and is defined by the formula

$$W = f + 10\,g.$$

Figure 65 shows graphs of solar and magnetic activity for the interval 1830 to 1930. The curves of this drawing indicate that during the years of sunspot maxima the magnetic activity also is at a maximum, and exhibits an 11-year period coinciding with the maximum of sunspots. However the magnetic activity lags somewhat behind the solar, so that on an average this lag amounts to one year for an 11-year period.

Furthermore there is a recurrence of activity after 27 days, corresponding to the period of revolution of the upper layers of the sun about the axis. This periodicity also is associated with the occurrence of spots upon the sun in the following manner. Some sunspots persist during several periods of the sun's rotation and

Declassified in Part - Sanitized Copy Approved for Release 2013/01/23 : CIA-RDP81-01043R001600090003-8

Declassified in Part - Sanitized Copy Approved for Release 2013/01/23 : CIA-RDP81-01043R001600090003-8

when the sun rotates 360° they are found on the side which faces the earth. If the spots did not disappear and remain unchanged there would be a strict periodicity in their appearance every 27 days. But since the spots appear and vanish at irregular intervals, there is only a certain tendency toward the 27-day periodicity of their appearance. M. S. Eygenson [44], on investigating the correlation between the duration of groups of sunspots and the phase of the 11-year cycle, found that on the basis of data of the Greenwich Observatory for the period 1870 to 1932, only 20 or 30 out of 100 sunspots persist longer than one revolution of the sun, with most of these persisting for 2 revolutions, although exceptional spots persist for 7 revolutions of the sun. The spots which appear during the years of maximum occurrence exhibit unstable duration. Observations show that magnetic activity similarly exhibits only a tendency to recur. This tendency is illustrated by the graph of Kri [transliterated] (Figure 66), which shows the progression of the activity during 35 days following, and 5 days prior to a maximum. The graph shows that a second, less pronounced peak occurs 27 or 28 days after the first peak.

The Kri graph is derived in the following manner. Over the periods 1906 to 1911 and 1890 to 1900 a selection was made of the days having the characteristic "2," and the values of activity during the 35 subsequent and the 5 preceding days were written in series, after which each column of these series was summated and the mean values of the activity were determined, which were then plotted on the graph.

This method later was applied to more extensive data on the period from 1906 to 1924. In this case 108 days were taken, right and left, instead of the previous practice of taking 27 days from the

Declassified in Part - Sanitized Copy Approved for Release 2013/01/23 : CIA-RDP81-01043R001600090003-8

Declassified in Part - Sanitized Copy Approved for Release 2013/01/23 : CIA-RDP81-01043R001600090003-8

beginning of the disturbance. It was found that the state of disturbance recurred 4 times at 27-day intervals up to the one hundredth and eighth day. A detailed investigation of this phenomenon was carried out by N. P. Ben'kova on the basis of data of the Pavlovsk observatory. N. P. Ben'kova [45] made a list of the sequences of storms observed at Pavlovsk, assuming that the storms are part of a sequence if the interval between them is 26 to 28 days. As a result it was found that of the 1,073 storms, 576 were part of a sequence, and of these 198 storms were part of 2 simple recurrences, 129 of 3, 72 of 4, 65 of 5, 36 of 6, 49 of 7, 8 of 8, and 20 were part of 10 recurrences.

In order to determine whether these recurrences are accidental or have a physical significance N. P. Ben'kova calculated the probability of an n-fold accidental recurrence of the storms and compared it with her empirical probability results.

This comparison is presented in Table 17 and shows that with the exception of the value Z, the empirical probability greatly exceeds the random distribution probability which indicates a definite regularity in connection with this phenomenon.

TABLE 17

PROBABILITY OF n-FOLD RECURRENCE OF MAGNETIC STORMS

Probability	Number of Recurrences of Storms								
	2	3	4	5	6	7	8	9	10
Empirical	0.370	0.130	0.100	0.053	0.026	0.014	0.006	0.003	0.001
Random	0.260	0.069	0.018	0.05	0.01	$34 \cdot 10^{-5}$	$9 \cdot 10^{-5}$	$2 \cdot 10^{-5}$	$8 \cdot 10^{-6}$

However, a rigorous functional correlation still was not ascertained between magnetic activity, or disturbance state, and the sunspot activity. It is of interest to note that the duration of sunspots over

Declassified in Part - Sanitized Copy Approved for Release 2013/01/23 : CIA-RDP81-01043R001600090003-8

Declassified in Part - Sanitized Copy Approved for Release 2013/01/23 : CIA-RDP81-01043R001600090003-8

the period 1879 to 1932 did not exceed the 7-fold period of sun rotation, while the state of magnetic disturbance can recur at periods up to 10 solar cycles.

In addition to the above regularities, there is a diurnal progression within the course of magnetic activity. Figure 67 shows the progression of this activity over 24 hours, at Kew observatory near London, during winter, summer and the equinoctial epochs on the basis of the international 0-1-2 scale, and also the number of hours having the characteristic "2" during the period 1913 to 1923. It is seen that the minimum of activity occurs at 1,000 to 1,100 hours and the maximum at midnight. This indicates that increased activity during nocturnal hours cannot be caused by wave radiation from the sun, and it is more probable to assume an influence of corpuscular radiation, which under the action of the magnetic field of the earth can penetrate the atmosphere from the nocturnal side.

Declassified in Part - Sanitized Copy Approved for Release 2013/01/23 : CIA-RDP81-01043R001600090003-8

Declassified in Part - Sanitized Copy Approved for Release 2013/01/23 : CIA-RDP81-01043R001600090003-8

CHAPTER VI

MAGNETIC VARIATIONS AND THE AURORA BOREALIS

Section 1. The Solar-Diurnal Variations

The solar-diurnal variations, which we shall denote by the letter S, consist of periodic variations of the elements of terrestrial magnetism with a period equal to the length of the solar day.

A characteristic feature of these variations is their occurrence according to local time. For this reason, at 2 different longitudes, the phases of the fluctuations of one element or another will differ by the difference in longitudes between the 2 points. Thus, if we represent the deviation from its mean value, i. e., the variation, of any element at a given point of the earth's surface in the form of a simple harmonic oscillation:

$$S = S_0 \sin \frac{2\pi t}{T},$$

where S_0 is the amplitude, T are the solar days and t the local time, then the variation at another point whose longitude differs by λ, is represented by the equation:

$$S' = S_0 \sin \frac{2\pi}{T}(t + \lambda).$$

Figure 68 represents the mean annual diurnal march of the declination, the horizontal and vertical components, i. e., the relation of the variations of these elements and the local time during a 24-hour period, according to the observations of the Pavlovsk magnetic observatory.

The mean annual values of the variations of the various elements respectively are plotted along the axis of ordinates and the local time along the axis of abscissas.

Declassified in Part - Sanitized Copy Approved for Release 2013/01/23 : CIA-RDP81-01043R001600090003-8

Declassified in Part - Sanitized Copy Approved for Release 2013/01/23 : CIA-RDP81-01043R001600090003-8

On considering the curve for the variations of the declination, it will be seen that the magnetic needle which remains quiet at night (curve δ D), is deflected in the morning towards the east, and by 0800 hours reaches the maximum deflection, after which it begins to move in the opposite sense, and by 1400 hours it reaches its maximum deviation towards the west. The remaining curves show that the horizontal component (the curve δ H) has a minimum at about 1100 hours and a maximum about 2000 hours, while the vertical component, which remains almost unchanged during the night, begins in the morning to increase, and after noon reaches its maximum value. As shown by observations, the diurnal march of the elements of terrestrial magnetism does not remain constant but varies irregularly from one day to another; in this case the amplitude of fluctuations are mainly subject to change, while the phases themselves remain almost unchanged.

Table 18 gives the values of the differences between the maximum and minimum values of each element at different seasons at Pavlovsk.

TABLE 18

Season	Difference between the maximum and minimum		
	D	H	Z
Winter	4.1'	09 γ	7 γ
Spring	7.9	27	12
Summer	12.0	44	20
Autumn	8.2	36	12

The Table shows that the variations in the diurnal march increase from the winter months, when the declination of the Sun is smallest (to the summer months, when the declination of the Sun is greatest (+ 23.5°).

Declassified in Part - Sanitized Copy Approved for Release 2013/01/23 : CIA-RDP81-01043R001600090003-8

Declassified in Part - Sanitized Copy Approved for Release 2013/01/23 : CIA-RDP81-01043R001600090003-8

The next feature of the solar-diurnal variations is their dependence on the value of the magnetic activity on one day or another. For this reason 2 forms of solar diurnal variations are distinguished: The variations on quiet days when which are obtained by working up the observations only for quiet days, and variations in stormy days, which are called disturbed variations and are obtained by working up the observations on stormy days. The former are denoted by S_d, the latter by S_q.

Variations on stormy days differ markedly from the variations on quiet days. This difference particularly effects the march of the variations of the vertical component, where not only the amplitude but the whole character of the curve changes. In addition, the amplitudes of the quiet diurnal variations S_q vary during the course of the year, taking their maximum value during the summer solstice and their minimum values during the winter solstice. During the epoch of the equinoxes, the amplitude is the mean between the winter and summer and is the same in both hemispheres.

Moreover, observations show that the solar diurnal variation at various points of the earth's surface is of different character. For points located on one and the same parallel, however, the diurnal march is almost the same, but for points located along a meridian, it varies according to a certain definite law. Figure 69 represents the curves of the diurnal march on quiet days at different latitudes for the 3 elements X, Y and Z during the period of the summer solstice in the northern hemisphere (Figure 69, a), for the winter solstice (Figure 69, b), and for the epoch of the equinox (Figure 69, c), both spring and autumn. These curves show that the variations of the northern component S_X have approximately the same character in northern and southern latitudes, since for the individual elements in the southern latitudes, they are inverted on passage across the magnetic equator,

Declassified in Part - Sanitized Copy Approved for Release 2013/01/23 : CIA-RDP81-01043R001600090003-8

Declassified in Part - Sanitized Copy Approved for Release 2013/01/23 : CIA-RDP81-01043R001600090003-8

i. e., they are mirror pictures of the variations in the northern latitudes. On the equator itself, the variations on the eastern and vertical components are close to zero. For the northern component, such a reversibility of the curves takes place at magnetic latitude of about 30° in both southern and northern hemispheres.

The variation of the amplitudes during the course of the year will be clearly seen by comparing Figures 69, a, 69, b, and 69, c.

Figure 70 gives analogous curves of the diurnal march of the variations on stormy days S_d for various latitudes. The ordinates of these curves represent the difference between the variations on stormy days and variations on quiet days ($S_d - S_q$). These curves show that in the low latitudes the differences $S_d - S_q$ are small and, consequently, the S_q variations predominate in them, while in the high latitudes, on the contrary, the variations $S_D = S_d - S_q$, play a predominant part.

The most striking idea of the march of the diurnal variations given by the construction of the so-called vector diagrams which represent the projection of the vector variations S_q on the horizontal and vertical planes.

Such a diagram of the projections of S_q of the horizontal plane is shown in Figure 71 in the period of the equinox for a portion of the earth's surface turned towards the sun and bounded by the geographical latitudes from +60 to -60° and the longitudes from 6 to 18 hours. In this case the longitudes coincide with the local time from 6 to 18 hours.

The following may be noted from this diagram: the vector S_q

Declassified in Part - Sanitized Copy Approved for Release 2013/01/23 : CIA-RDP81-01043R001600090003-8

Declassified in Part - Sanitized Copy Approved for Release 2013/01/23 : CIA-RDP81-01043R001600090003-8

in the northern hemisphere during the daylight hours is always directed towards a certain center located on the forenoon meridian at the parallel $+30^{\circ}$, while in the southern hemisphere it is directed from a center located on the same meridian and the parallel -30°.

Figure 72, a and 72, b show the diagrams of projections of the vector S_q on the vertical planes: one of them on the plane of the principal meridian, and the other on the plane of a great circle making contact with the 30th parallel at the meridian point. Both diagrams show that the centers towards which the S_q vectors are directed lie above the earth's surface roughly above the parallels +30 and -30 near the principal meridian.

Formally, these centers may be identified with the axis of the eddy current whose sense is counterclockwise, viewed from above, in the northern hemisphere, and clockwise in the southern hemisphere. Thus the diurnal variations may be explained by the existence in the atmosphere of a system of closed eddy currents which remain fixed in space, and within which the earth rotates. Since the maximum value of the vector of the variations come during the daylight hours, the maximum current strength must be in the space between the sun and the earth.

The system of electrical currents corresponding to the fields of diurnal variations. The magnetic field of the solar diurnal variations, i. e., the field corresponding to the distribution of the vector of variations must have its sources which most probably may consist of a certain system of electrical currents which most probably may be represented in the form of a certain system of electrical currents. The general distribution of the vector of variations on the earth's surface for a given moment of time,

Declassified in Part - Sanitized Copy Approved for Release 2013/01/23 : CIA-RDP81-01043R001600090003-8

Declassified in Part - Sanitized Copy Approved for Release 2013/01/23 : CIA-RDP81-01043R001600090003-8

represented in Figure 72, a and 72, b, indicates that the system of currents with their center at latitude 30° and on the principal meridian, remains fixed in space between the sun and the earth, and an observer on the earth, in rotating with respect to this system, passes during the course of a 24-hour day through all values of the vector of field strength of these currents, distributed along the parallel of the observer. Since the electric current and its magnetic field are connected by the Biot-Sawra law, the, if we know the field, the current may also be determined, provided that the distances between the current and those points at which the field is known are also known. For this reason to find the system of currents according to an assigned distribution of a magnetic field, we must start out from the law in question or from its consequences.

Such a consequence, which is the most convenient to calculate, is the equivalence of a closed current with a dual magnetic layer. For this reason, by replacing the system of currents by a dual magnetic layer of variable density, disposed on a sphere concentric with the earth's surface and having a radius R greater than the earth's R radius, we find the magnetic potential U of such a layer at the earth's surface. We know from the theory of potential that

$$U = \int\int \mu \frac{\partial}{\partial n}\left(\frac{1}{\rho}\right) dS,$$

where μ is the surface density of the magnetic moment of a double layer corresponding to the element of surface $d\sigma$; p is the distance between the point of the earth's surface where the potential U is sought; n is the direction of the normal to the surface of the sphere coinciding with the radius R, and the integration is taken over the entire surface of the sphere.

Declassified in Part - Sanitized Copy Approved for Release 2013/01/23 : CIA-RDP81-01043R001600090003-8

Declassified in Part - Sanitized Copy Approved for Release 2013/01/23 : CIA-RDP81-01043R001600090003-8

Since $\rho^2 = R^2 + r^2 - 2Rr\cos\gamma$, where γ is the angle between R and r, and $r > R$, then

$$\frac{1}{\rho} = \sum_{n=0}^{\infty} \frac{R^n}{r^{n+1}} P_n(\cos\gamma)$$

and, consequently,

$$U = \iint \mu \frac{\partial}{\partial n} \sum_{n=1}^{\infty} \frac{R^n}{r^{n+1}} P_n(\cos\gamma)\,dS,$$

or

$$U = -\sum_{n=1}^{\infty} (n+1) \frac{R^n}{r^{n+2}} \iint \mu P_n(\cos\gamma)\,dS.$$

It is proved in potential theory that every function of two variables (the latitude θ and longitude λ), assigned for the points of a sphere, may be uniquely expanded into a series in Laplace spherical conditions; and for this reason μ may be represented in the form of the sum:

$$\mu = \sum_{k=1}^{\infty} \mu_k, \quad \text{where } \mu_k = \sum_{m=0}^{k} (a_n^m \cos m\lambda + b_n^m \sin m\lambda) P_n^m(\cos\theta) \quad (6.1)$$

Consequently,

$$U = -\sum_{n=1}^{\infty} (n+1) \frac{R^n}{r^{n+2}} \sum_{k=1}^{\infty} \iint \mu_k P_n(\cos\gamma)\,dS.$$

It is known from the theory of spherical functions that

$$\iint \mu_k P_n(\cos\gamma)\,dS = \frac{4\pi r^2}{2n+1} \mu_n \quad \text{for } k = n,$$

$$\iint \mu_k P_n(\cos\gamma)\,dS = 0, \quad \text{for } k \neq n.$$

For this reason

$$U = -\sum_{n=1}^{\infty} 4\pi \frac{n+1}{2n+1} \left(\frac{R}{r}\right)^n \mu_n. \quad (6.2)$$

On the other hand, the magnetic potential of the field of variations, as we know, is expressed in the form of a series:

$U = R\sum U_n$, where $U_n = \sum (p_n^m \cos m\lambda + q_n^m \sin m\lambda) P_n^m(\cos\theta)$, (6.3)

where the coefficients p_n^m and q_n^m are known from observations and represent the external part of the potential of variations.

Declassified in Part - Sanitized Copy Approved for Release 2013/01/23 : CIA-RDP81-01043R001600090003-8

Declassified in Part - Sanitized Copy Approved for Release 2013/01/23 : CIA-RDP81-01043R001600090003-8

On comparing the expressions 6.2 and 6.3, we find that

$$RU_n = -4\pi \frac{n+1}{2n+1} \left(\frac{R}{r}\right)^n \mu_n,$$

whence

$$\mu_n = -\frac{R}{4\pi} \cdot \frac{2n+1}{n+1} \left(\frac{r}{R}\right)^n U_n,$$

and, by substituting $_n$ in equation 6.1 and replacing U_n by its value, we have

$$\mu = -\frac{R}{4\pi} \sum_{n=1}^{\infty} \frac{2n+1}{n+1} \left(\frac{r}{R}\right)^n \sum_{m=0}^{\infty} (p_n^m \cos m\lambda + q_n^m \sin m\lambda) P_n^m (\cos\theta). \quad (6.4)$$

The density of the magnetic moment μ of the double layer is equivalent to the current strength of a closed circuit, and for this reason the expression for the strength of the current at any point of the surface of the sphere with coordinates θ and λ, will have the same form as equation 6.4.

This equation shows that for the calculation of the current strength at any point of a sphere it is sufficient if we merely multiply each term of the expansion of the potential of order n by the term containing one unknown quantity, the radius of the external sphere through which the current flows. This radius must be determined from any other considerations. In the first paper devoted to the calculations of the currents in the atmosphere, this radius was fortuitously taken at 100 km more than the earth's radius, which corresponds very closely to present-day data on the height of the conducting layer in which the existence of such currents is possible.

At the present time there is ground for holding that the system of currents causing the solar diurnal variations of the magnetic field is located in the E layer of the ionosphere, the height of which, according to observations on deflection of radio waves, varies between 100 and 120 km. For this reason, if we assume the height of the E layer as

Declassified in Part - Sanitized Copy Approved for Release 2013/01/23 : CIA-RDP81-01043R001600090003-8

Declassified in Part - Sanitized Copy Approved for Release 2013/01/23 : CIA-RDP81-01043R001600090003-8

equal to 109 km, as has been done in Ben'kova's paper and t is expressed in thousand amperes, while p_n^m and q_n^m are expressed in gammas, then equation 6.4 takes the form:

$$I = -5{,}0707 \sum_{n=1}^{\infty} \frac{2n+1}{n+1} (1{,}02)^n \sum_{m=0}^{\infty} (p_n^m \cos m\lambda + q_n^m \sin m\lambda) P_n^m(\cos\theta). \qquad (6.5)$$

It is this formula that will serve for the calculation of the system of current. On determining from it the value of I for various values of λ and θ, and plotting these values on a map, we may draw a series of isolines (lines of equal current strength), which will represent current lines, i. e., the lines along which the current flows. The difference between the values of the current strength on two adjacent isolines gives us the value of the current flowing between these lines.

Such a system of currents, correspondent to the solar diurnal variations in the equinoctial period and for heights of 100 km, is shown in Figure 73, while Figure 74 shows the system of currents corresponding to the summer solstice.

The closed curves showing the direction of the currents are drawn in such a way that a current of 1,000 amp flows between two adjacent curves. The currents flow in four main systems of circuits, two northern and two southern. In this case, two systems of contours are located on the lighted hemisphere and the two others on the night hemisphere, the former being more intense.

The total current in the daylight circuit is equal to 62,000 amp during the time of the equinox and 89,000 amp during the time of the solstices.

Declassified in Part - Sanitized Copy Approved for Release 2013/01/23 : CIA-RDP81-01043R001600090003-8

Declassified in Part - Sanitized Copy Approved for Release 2013/01/23 : CIA-RDP81-01043R001600090003-8

As stated in Section 3, about a third of the field of variations is due to internal causes, i. e., to currents flowing within the earth. It may be assumed that these currents are caused by induction of the magnetic field of the external currents in some conducting layer of the earth or perhaps in the entire earth. If the conductivity of the earth were known, then the determination of the system of currents would reduce down to the above mentioned operation, analogous to the operation of calculating the external currents. But we know nothing at all of the conductivity of the interior parts of the earth. We know only the conductivity of the upper stone envelope, which is of the order of 10^{-6} ohm^{-1} cm^{-1} and the conductivity of the oceans, of the order of 4×10^{-2} ohm^{-1} cm^{-1}.

For this reason there have been attempts to calculate the induction current and the magnetic field caused by them under the assumption that the conductivity of the earth is everywhere the same.

It was found that to make the calculated values of the variation agree with the observed values, it would be necessary to assume a conductivity of $\gamma = 3.6 \times 10^{-4}$ ohm^{-1} cm^{-1} for the earth, that is, somewhat less than sea water and more than the conductivity of the upper layers. In addition, it must also be recognized that the upper layer is probably nonconducting down to a depth of 300 km.

The system of currents shown in Figure 73 and 74 has been calculated by equation 6.5 under the assumption that the solar diurnal variations are functions of the geographical latitude at a local time. But a comparison of the observed curves of the diurnal march of the S_q variations with the curves calculated by equation 6.5 in which the arguments are the geographical latitude and the local time, does not yield good agreement. For this reason the S_q variations were expanded into spherical harmonics, taking the geomagnetic latitude and the

Declassified in Part - Sanitized Copy Approved for Release 2013/01/23 : CIA-RDP81-01043R001600090003-8

Declassified in Part - Sanitized Copy Approved for Release 2013/01/23 : CIA-RDP81-01043R001600090003-8

geomagnetic time as the independent variables (Bibl. 16). The agreement between and observed values was now considerably better. Figure 75 shows diurnal march of the northern component at the Huancayo Observatory (South America, $\varphi = -12.0^{\circ}$, $\lambda = 284.7^{\circ}$), observed and calculated by equation 6.5 and by formulas in which φ and λ are geomagnetic. As will be seen the latter curve is in considerably better agreement with the observed curve than the former one.

Figure 76 shows a system of currents corresponding to the expansion in geomagnetic coordinates. Its principal difference from system in Figure 73 is the asymmetry of the currents of the northern and southern hemisphere; the current in the southern hemisphere is two and a half times as great as that in the northern hemisphere. In addition, their centers are also asymmetric with respect to the equator. It is possible to explain this by the fact that the magnetic field is symmetric with respect to the magnetic axis not the geographic axis, which should lead, according to the dynamo theory, to a reduction of current in the northern hemisphere and its weakening in the southern hemisphere (sic). But there are no quantitative calculations.

For a greater approximation of the observed diurnal march to the theoretical, N. P. Ben'kova (Bibl. 47) made a spherical analysis of the diurnal variations of S_q at 47 observatories, including some beyond the Arctic Circle, allowing for the fact that the variation depends not only on the latitude but also on the longitude of the place. In this case the longitude, latitude and time taken were all geomagnetic. No one before Ben'kova has ever performed the expansion with such a formulation of the question, since all of the investigators had considered the diurnal variations to be independent of the longitude.

Since the diurnal analysis assumes the expansion of a function depending only on two coordinates, Ben'kova assumed, in order to calculate

Declassified in Part - Sanitized Copy Approved for Release 2013/01/23 : CIA-RDP81-01043R001600090003-8

Declassified in Part - Sanitized Copy Approved for Release 2013/01/23 : CIA-RDP81-01043R001600090003-8

the third coordinate, longitude, that the S_q variations are the sum of two functions, one of which, S_{q1}, depends on the latitude $\tilde{\Phi}$ and the local time t, while the second one, S_{q2}, depends on the longitude Λ and the latitude, i. e.,

$$S_q = S_{q1}(\tilde{\Phi}, t) + S_{q2}(\tilde{\Phi}, \Lambda), \qquad (6.6)$$

and she performed the expansion separately for the functions S_{q1} and S_{q2}.

The determination of the coefficients of the expansion was performed by the method set forth in Section 3, by equation 5.4 and 5.8. To eliminate the influence of the longitude in the expressions for S_{q1}, the means for the given latitude were taken instead of the coefficients calculated for the separate observatory as the initial coefficients a_x^m etc in equation 5.8.

The original material for the functions S_{q2} was the differences between the mean values of the coefficients a_x^m and those calculated by equation 5.4. As a result of this analysis, performed for a large number of stations, it was found that the main part of the field of variations is represented by the function S_{q1}, i. e., it does not depend on the longitude.

The longitude function exists, but its influence is shown only at low and middle latitudes, so that in the polar regions the introduction of longitude terms does not improve the agreement between the calculated and observed values of the variation.

In accordance with the result of this analysis, Ben'kova constructed a system of points for the summer months (May-August) both for the functions S_{q1}, and for the function S_{q2}. They are shown in Figure 77 and Figure 78. A comparison with the current maps on Figure 76 shows that they are in better agreement with the maps of Figure 73

Declassified in Part - Sanitized Copy Approved for Release 2013/01/23 : CIA-RDP81-01043R001600090003-8

Declassified in Part - Sanitized Copy Approved for Release 2013/01/23 : CIA-RDP81-01043R001600090003-8

than with the maps of Figure 76. The eddy of current located on the daylight side of the northern hemisphere has about the same form as in Figure 73, and is situated at the same latitude, but Ben'kova found the intensity of this eddy to be greater than that of the eddy in Figure 73. As for the intensity of the southern eddy, located on the daylight side, it is, on the contrary, weaker on Ben'kova's map than on the map in Figure 73. In addition, the center of this eddy is at 12 hours 30 minutes, while on Figure 73 it is at 11 hours. Moreover, the night region of negative currents, as will be seen from Figure 77, breaks down into two distinct eddies, while in on the map of Figure 73 it reduces to a single eddy. These differences in Ben'kova's opinion should be ascribed to the difference in the initial data, with which we must reconcile ourselves, since the analysis of Figure 73 was based on the data of 21 observatories located only in middle and southern latitudes, while that of Figure 76 had only 5 observatories, but Ben'kova uses materials of 47 observatories.

The system of currents of the field S_{q2} is represented as shown for four instants of Greenwich time: 0, 6, 12, and 18 hours.

Figure 77 shows that in the equatorial latitudes at local Noon there is a region of positive current. Its development reaches its maximum(20,000 amp) when the 300° meridian is close to the noon meridian. This region almost disappears and is displaced towards the north, when the local meridian lies on the Greenwich meridian. There is a region of negative currents on the night side. They are most distinct at 3 hours on the 300° meridian; and their maximum value in this case is 21,000 amp.

N. P. Ben'kova in her analysis also separated that the part of the field corresponding to internal causes and that part of the

Declassified in Part - Sanitized Copy Approved for Release 2013/01/23 : CIA-RDP81-01043R001600090003-8

Declassified in Part - Sanitized Copy Approved for Release 2013/01/23 : CIA-RDP81-01043R001600090003-8

field (eddy) corresponding to vertical currents. But the latter problems are still controversial, since the value of the vertical currents' strength obtained by Ben'kova from the analysis is many times greater than the value of the currents observed on the earth's surface.

Attempts have recently been made to directly prove the existence in the ionosphere of the currents causing the diurnal variations (Bibl. 48). On 17 March 1949, near the geomagnetic equator ($\varphi = 11^{\circ}$ S, $\lambda = 89^{\circ}$ W) at 1120 hours and at 1720 hours local time, two rockets with magnetic instruments were sent up. These instruments automatically transmitted signals by radio, at definite time intervals, of the value of the magnetic field strength. The height of the rockets at these moments was determined by a radar installation on the ground and by the signals emitted from the rockets. Both rockets reached a height of over 100 km. The first rocket was sent up at a moment when the current density, according to theory (Figure 76), was maximum, and the second when the density was minimum. The results of the worked up observations in Figures 79 a and 79 b. The former relates to the observations at 1720 hours, the second to observations at 1120 hours. The solid lines represent the variations (decrease) of magnetic field strength with height, calculated under the assumption that the earth is uniformly magnetized and that its magnetic moment corresponds to the first term of the Gauss expansion. The dashed lines are the results of direct observations. The points corresponding to the ascent of the rocket are marked by circles and those to the descent by crosses.

The results of these experiments indicate that currents actually do exist at a height of about 105 km, since Figure 79 b has a sharp variation of the magnetic field of these heights, while Figure 79 a, correspondent to the minimum of current such variations are not observed and the experimental curve coincides over its entire length with the theoretical.

Declassified in Part - Sanitized Copy Approved for Release 2013/01/23 : CIA-RDP81-01043R001600090003-8

Declassified in Part - Sanitized Copy Approved for Release 2013/01/23 : CIA-RDP81-01043R001600090003-8

For our final conclusions from these experiments, however, it would be necessary to perform a theoretical calculation of the variation of the field due to currents, and to compare it to the observed values, as well as to have a repeated observation of the same nature.

The noncoincidence of the disagreement between the theoretical and experimental curves near the earth's surface may be explained by the existence of an anomaly in the region of the discharge of the rocket.

Section 2. Lunar-Diurnal Variations

In addition to the variations connected with the positions of the sun with respect to the earth's surface, there also exist variations of periodic character connected with the position of Moon with respect to the horizon. The period of these variations coincides with the time interval between 2 successive crossings of the local meridian by the moon, i. e., with the lunar-half-days.

The lunar diurnal variations are found on working up the records of magnetographs with respect to the lunar days. Since the lunar days differ from the solar days by only 50 min, 28 sec (the lunar days equal 24 hours, 50 min, 28 sec mean solar time) it follows that to eliminate the lunar, that is to isolate the lunar diurnal variations there is no need to work up the magnetograms according to lunar days by taking the ordinates for each lunar hours, but that it is sufficient to use the data obtained in working them up according to solar days and a rearranging of them according to lunar time.

This rearrangement consists in taking the lunar days as equal to 25 hours of solar time, and, for each hour, entering the values of the ordinates from the tables prepared for the solar-diurnal variations. Their values for the 25th hour are taken as equal to the value

Declassified in Part - Sanitized Copy Approved for Release 2013/01/23 : CIA-RDP81-01043R001600090003-8

Declassified in Part - Sanitized Copy Approved for Release 2013/01/23 : CIA-RDP81-01043R001600090003-8

of the first hour of the following day. In this way each successive lunar day begins one hour later than the solar day. The beginning of the lunar day, which is established by the Astronomical Annual Yearbook is taken as the moment of the passage of the moon through the upper meridian (the instant of upper combination). The upper lunar combination does not usually correspond to an even solar hour, but owing to the large number of days being worked up, it is sufficient, without leading to large error, to take the next solar hour as the beginning of the lunar day.

In view of the fact that the lunar day does not contain exactly 25 hours, but is 9 min, 32 sec shorter, every sixth lunar day should have 24 instead of 25 hours; in this case the value of the ordinate for the 25th hour repeats the value for the preceding hour (cf. Appendix 2).

In addition, in order to eliminate the solar diurnal variations, up to the time of the rearrangement its mean monthly value is subtracted from each ordinate. In this way the process of "taking a mean" for the lunar day consists in eliminating all irregular variations. Since the amplitude of the lunar variations is very small by comparison to the nonregular part of the variations, a considerable time interval is required to eliminate those variations. The first detailed study of the lunar-diurnal variations was made by Chapman (Bibl. 49) in 1913. That author worked up by the above method the observation from the observatories at Pavlovsk, Pola, Tsi-Ka-Wei, Manila and Batavia for 7 years (1897 to 1903 inclusive).

The results of the statistical workup, and of the subsequent spherical and harmonical analysis, allowed Chapman to establish a number of regularities in the march of the lunar-diurnal variations, which differed from the regularities of the solar-diurnal.

Declassified in Part - Sanitized Copy Approved for Release 2013/01/23 : CIA-RDP81-01043R001600090003-8

Declassified in Part - Sanitized Copy Approved for Release 2013/01/23 : CIA-RDP81-01043R001600090003-8

The principal regularity is the semidiurnal character in the changes of these variations. The curves of variation of all elements during the course of the lunar day have two maxima and two minima while the time of occurrence of the maximum and minimum vary daily during the course of the lunar months. The mean monthly curve, however, has the form of a regular double wave with maxima at 6 and 18 hours lunar time and minima at 0 and 12 hours for the northern hemisphere. Figure 80 shows the curves of the lunar diurnal variations of the declinations at Batavia and Greenwich for the four phases of the moon, accompanied by the mean monthly curves. The displacement of the extreme values during the course of the month may be clearly seen on the Figure. In addition, the curves for Batavia, which is located in the southern hemisphere, are almost a mirror image of the curves for Greenwich, which is in the northern hemisphere.

Chapman's expansion of the curves of the diurnal march into a harmonic series shows that the harmonics with a semidiurnal period remain constant throughout the course of the entire month, but that the harmonics of the remaining orders change their phase while the amplitude remains unchanged, thus also resulting in the displacement of the extreme values. Thus the change of phase for the first harmonics during the course of the month was -30°, for the third harmonic, $+30^{\circ}$ and for the fourth harmonic, $+50^{\circ}$.

The lunar diurnal variations have annual march depending on the position of the sun. During the time of the summer solstice the amplitude of the lunar days reaches the maximum values in the northern hemisphere and the minimum values in the southern, and in the time of the winter solstice, on the contrary, they reach their

Declassified in Part - Sanitized Copy Approved for Release 2013/01/23 : CIA-RDP81-01043R001600090003-8

Declassified in Part - Sanitized Copy Approved for Release 2013/01/23 : CIA-RDP81-01043R001600090003-8

minimum in the northern hemisphere and their maximum in the southern. For the vertical and horizontal components, the maximum amplitudes reach only 1-2 gammas, while for the declination they reach 40".

The dependence of the lunar diurnal variations on the latitude and longitude are the same character as those of the solar diurnal. Thus, with variation of the latitude, the phases remain constant, but in the northern component, on crossing the parallels $+20^{\circ}$, -20°, they change signs to the opposite. With eastern and vertical components the variation of phase also takes place on the equator. The amplitude of the observations reaches a maximum in the northern component on the equator and at latitude 45°; while the eastern and vertical components' maximum of amplitude is reached at the parallel of 20°.

The lunar diurnal variations are almost independent of the longitude. It is an interesting fact that the amplitude of the lunar variations is dependent on the distance of the moon from the earth; more specifically the amplitude of the variations is about inversely proportional to the cube of this distance. Just as for the solar variations, spherical harmonic analysis allows the lunar diurnal variations to be explained by the existence of horizontal eddy currents, whose distribution for the new moon is shown in Figure 81: the upper figure relates to equinox, the lower to the summer solstice. The meridians correspond to local lunar time and for the new moon the sun and moon are on the meridian 12. The total current flowing in the main circuit reaches 5,300 amp for at equinox and 11,000 amp at solstice.

Section 3. Magnetic Disturbances

Variations without definite periods obtained as a result of

Declassified in Part - Sanitized Copy Approved for Release 2013/01/23 : CIA-RDP81-01043R001600090003-8

Declassified in Part - Sanitized Copy Approved for Release 2013/01/23 : CIA-RDP81-01043R001600090003-8

subtracting the solar diurnal and lunar diurnal variations from the observed variations, and which at first glance appear entirely arbitrary, as a result of their random march, have received the name of magnetic disturbances, and at great intensity, of magnetic storms. While the amplitude of the periodic variations is expressed by a few tens of gammas, they may reach a few hundreds or thousands of gammas during the time of magnetic storms.

Magnetic disturbances may be calssified according to intensity, duration, and spatial distribution, into four types.

The first type includes disturbances of very great intensity, magnetic storms occurring simultaneously over the whole earth. The amplitude of the fluctuations of the elements of the terrestrial magnetism of such storms may reach a few thousand gammas, and their duration, a few days. The second type includes disturbances of local character limited to definite regions, mainly the polar region. Local disturbances may last for one or a few hours and their intensity will exceed hundreds of gammas. While magnetic disturbances of the first type commence simultaneously over the whole earth and proceed in a single phase, disturbances of the second type, even at two nearby points, may proceed entirely differently.

The third type, the bays, is the name given convexities or concavities on the magnetograms, recalling the shape of marine bays. The bay-like disturbances, occurring simultaneously may stretch over the entire earth or may be limited to a certain region near the auroral zone.

Finally, the fourth type of periodic magnetic disturbance consists of the so-called pulsations, which are sinusoidal fluctuations in field strength with an amplitude of the order of few gammas and a

Declassified in Part - Sanitized Copy Approved for Release 2013/01/23 : CIA-RDP81-01043R001600090003-8

Declassified in Part - Sanitized Copy Approved for Release 2013/01/23 : CIA-RDP81-01043R001600090003-8

period of a few minutes. The pulsations may take place simultaneously over the entire earth but may also be limited to individual regions.

In most cases the disturbances of the first and second group usually occur simultaneously, one being superimposed on the other and causing side effects such as, for example, the induction current in the earth which in turn yields an additional component vector of the disturbance.

Figure 82 shows magnetograms of the horizontal component during the time of the magnetic storm of 14 March 1922 according to the records of five observatories located in middle and low latitudes, while Figure 83 shows magnetograms of the horizontal component from the records of observatories in high latitudes during the magnetic storm of 19 February 1933.

The curves show that no complete parallelism is observed in the march of the elements, but that a few maxima and minima do occur simultaneously at all stations. The amplitude of the fluctuations as will be seen from Figure 82, increases with increasing latitude of the station. Thus this storm represents a storm of world-wide character with the superimposition of local disturbances.

Statistical processing of magnetic storms has allowed establishing the existence in them of at least 3 components differing in character and the laws of occurrence and the laws of their course.

The first of them, S_D, representing the difference $S_d - S_q$, of periodic character, with the period of a solar day, has already been considered in Section 1 of this chapter. The second, the aperiodic variation D_{ap} is found as a result of averaging a large number of world-wide storms located in columns during the course of a storm, i. e., when the instant of origin of a storm is taken as the initial moment of time $t = 0$.

Declassified in Part - Sanitized Copy Approved for Release 2013/01/23 : CIA-RDP81-01043R001600090003-8

Declassified in Part - Sanitized Copy Approved for Release 2013/01/23 : CIA-RDP81-01043R001600090003-8

A characteristic feature of most magnetic storms is the suddenness of their appearance. Against the background of a rather quiet magnetic field, almost at one and the same instance of the entire earth all elements of terrestrial magnetism suddenly vary their values, and their subsequent course undergoes very rapid and irregular variations. For this reason it is possible to determine the beginning of a magnetic storm of the magnetograms of all observatories within 1 to 2 minutes.

The third component, which is obtained by subtracting the aperiodic variation and the disturbances of the diurnal variation from the observed ones, is really that magnetic disturbance which we term a magnetic storm and which is manifested in the form of irregular rapid variations of all elements of terrestrial magnetism. This part of the variation is termed, by general agreement, the irregular component, and is denoted by D_i.

The aperiodic disturbed variation D_{ap}. A characteristic feature of this variation is that it is very distinctly manifested in variations of the horizontal component, to a lesser degree in the vertical component, and has entirely no effect on the declination.

The general character of the course of D_{ap} is as follows. The beginning of the disturbance is a short impulse which increases the horizontal component and decreases the vertical one. These variations amount to +20 gammas for the horizontal component and -5 gammas for the vertical one.

The increases of values of the horizontal component lasts only a short time, from 1/2 to 2 hours. There is then a sharp fall in the horizontal component lasting for about 6 hours and going up to 60 gammas, after which begins a long process of return to the normal state, occupying a period of time up to 2 days. This process has received the name of after disturbance.

Declassified in Part - Sanitized Copy Approved for Release 2013/01/23 : CIA-RDP81-01043R001600090003-8

Declassified in Part - Sanitized Copy Approved for Release 2013/01/23 : CIA-RDP81-01043R001600090003-8

The vertical component, after a 5 gamma drop, which likewise lasts from 1/2 to 2 hours, then begins to increase and during the course of the entire storm remains 5γ higher than its normal value.

The declination experiences small deviations (from 1 to 2") from its normal value towards one and the same side, and therefore no regularities in its variation must be spoken of.

The next characteristic feature of D_{ap} is the dependence of these disturbances on the geomagnetic latitude of the place, and their independence of the longitude. The maximum intensity of D_{ap} is found on the magnetic equator, where the variation in the horizontal component reaches 60 gammas and more. To the north and to the south of the equator, the intensity decreases, and at latitude 60° (Pavlovsk) the variation in H amounts to 40 gammas. Further to the north, D_{ap} again begins to increase, reaching a maximum in the zone of maximum aurora.

Figure 84 shows the march of D_{ap} at three latitudes from observations of the observatories at Batavia, Puerto Rico and Honolulu, located at the geomagnetic latitude 0°, Zi-Ka-Wei, San Fernando and Cheltenham, on the latitude 40°, polar, Pavlovsk, Greenwich, and Potsdam, at latitude 60°. The graph of D_{ap} shown on this Figure clearly shows all the regularities in its course that have been pointed out above.

The variations are easily traced up to latitude 60-70°. In the higher latitudes it is still not possible to isolate them so distinctly, owing to the complexity of phenomena that take place there. The local variations of high latitudes are so predominant in influence, that, superimposed on the world-wide magnetic storms, they masked the variations of D_{ap} which are of lesser intensity. This will be taken up in greater detail in the following Section.

Declassified in Part - Sanitized Copy Approved for Release 2013/01/23 : CIA-RDP81-01043R001600090003-8

Declassified in Part - Sanitized Copy Approved for Release 2013/01/23 : CIA-RDP81-01043R001600090003-8

The regularities found in the course of the D_{ap} variation, indicates that their source must be the ring current flowing in the plane of the earth's magnetic equator. In this case the direction of the current in the first phase of the storm must be from east to west, and in the second phase, from west to east.

O. A. Bourdeaux was the first to make a spherical analysis of the disturbances of the diurnal variations. He succeeded in constructing a system of electrical currents in the upper layers in the atmosphere, responsible for the variation S_D. The form of this system is shown in Figure 85a and 85b, 85a represents the system of currents over the entire surface of the earth and Figure 85b a view from the geomagnetic pole. As will be seen, the maximum density of the current lines is reached in the zone of maximum auroral frequency, where the current strength reaches 200,000 amp, while the total current over an area equal to one-quarter of the earth's surface does not exceed 40,000 amp. The strong crowding of the current lines is also observed in the polar regions between the auroral zone and the pole where the total current amounts to 270,000 amp. Figure 85a showed the system of current consists of eight closed currents of which four are located in the eastern hemisphere and four in the western. The system of currents constructed by Bourdeaux is in rather good agreement with the observed diurnal march of the variations. Thus, for example, it reproduces the inversion of the X component of the latitude 55°, the hours of maxima and minima of the X and Y components, and the general march of the variations in high latitudes. There is still no theory of the origin of this system of currents.

The system of currents corresponding to the aperiodic disturbed variation, viewed from the sun and viewed from the pole, is shown in

Declassified in Part - Sanitized Copy Approved for Release 2013/01/23 : CIA-RDP81-01043R001600090003-8

Declassified in Part - Sanitized Copy Approved for Release 2013/01/23 : CIA-RDP81-01043R001600090003-8

Figure 86, from which it is clear that the system forms a current flowing along the surface of a sphere parallel to the equator, its current density declining from the equator to the auroral zone, and increasing on passage through the auroral zone, reaching a maximum between the pole and the zone. The theory of the aperiodic variation has been developed by Chapman and Ferrari; and it will be set forth in the following Section.

Bay shaped variations. As stated above, the bay shaped variations which we shall denote by D_B, have the shape of the shore line of marine bay on the magnetogram records, with an amplitude reaching a few hundred gammas. The bay-shaped disturbances appear most distinctly in the horizontal component. In this case D_B may arise as a solitary disturbance amidst a quiet field, or may be superimposed one on the other, or may also be present in a general magnetic disturbance. Figure 87 shows the character of a record of such disturbances observed at the observatory at Kew, England, in February 1911. Owing to the existence of individual bay-shaped disturbances, undistorted by other variations, in the records of the observatory, their more detailed study was possible. The observations show that D_B, occurring simultaneously at all stations of the world, have a maximum intensity in the auroral zone where the amplitude of the variations of H is tens of times as great as in the low altitudes.

If a graph of the variations of H and Z during bay disturbances is plotted against the latitude, laying off the maximum aplitude of D_B along the axis of ordinates and the latitude of the stations located close to one and the same meridian are laid off on the axis of abscissas, it will take the form shown in Figure 88. This graph is analogous in its shape to the graph of the magnetic field excited by a magnet with its axis parallel to the meridian and its center at latitude 70°.

Declassified in Part - Sanitized Copy Approved for Release 2013/01/23 : CIA-RDP81-01043R001600090003-8

Declassified in Part - Sanitized Copy Approved for Release 2013/01/23 : CIA-RDP81-01043R001600090003-8

In view of the fact that such graphs are followed through simultaneously on other meridians as well, it is necessary, for the formation of D_B to postulate the existence not of a single magnet, but of a series of magnets parallel to each other and located along the parallels, so in the alternative, the existence of an electric current equivalent to it and flowing in a narrow beam which may be taken as a linear current along the 70th parallel.

Indeed, a linear current flowing at a distance R from the earth creates on the earth's surface in a direction perpendicular to the current, a magnetic field determined by the Biot-Sawara law.

The components in this field along the vertical and horizontal will obviously be:

$$\delta H = \frac{2IR}{R^2 + x^2}, \quad \delta Z = \frac{2Ix}{R^2 + x^2}.$$

These formulas coincide with equation 8.45 for a single-pole filament (page 349), the graph at which are given in Figure 167. By comparing these graphs with the curves without the D_B variations in Figure 88, and obtained from observations, it will be seen that they are in close agreement with each other.

If it is postulated that D_B is caused exclusively by current flowing in the upper layers of the atmosphere, then the height at which it flows, and the magnitude of the current strength, can both be easily determined.

The height h of the linear current is found graphically by constructing the field strength vectors at points located along the meridian near the 70th parallel, and producing perpendicular to them. The point of intersection of the perpendiculars will give us the linear current on the scale of the height, since for the linear current

Declassified in Part - Sanitized Copy Approved for Release 2013/01/23 : CIA-RDP81-01043R001600090003-8

Declassified in Part - Sanitized Copy Approved for Release 2013/01/23 : CIA-RDP81-01043R001600090003-8

the direction of the magnetic field is perpendicular to the distance between the linear conductor and the given point of the field.

The current strength I is determined from the Biot-Sawara law for a linear current:

$$\delta H_T = \frac{0.21}{h},$$

where δH_T is the field strength of D_B at the 70th parallel.

Such determinations gave a value of the order of a million amperes for the current strength and a value ranging from 100 km to a few hundred kilometers for the height.

Further refinement showed that the sources of the D_B variations do not consist only of the currents in the atmosphere, but also of induced currents within the earth, which is responsible for about 40% of the entire field of variations.

Magnetic pulsations. Pulsations represent regular fluctuations of the elements of terrestrial magnetism, mainly of the declinations and the horizontal component, with a period from 20 sec to a few minutes and an amplitude of a few gammas. At the usual rate of rotation of the drum of 20 mm per hour, they are found on magnetograms in the form of a sawtooth curve with small peaks. At a higher rate of rotation of the drum, however, (3 mm per minute) they are recorded in the form of a regular sinusoid. A characteristic feature of these variations is that they are observed mainly around midnight, often from 22 to 2 hours of the following day. The usual amplitude of these variations does not exceed a few gammas, although pulsations with larger amplitudes are sometimes observed. Thus, for example, on 12 September 1930 at the observatories of Abisko (Lat = 68.4°, Long = 18.8°), and Troemso (Lat = 69.7°, Long = 18.9°) in

Declassified in Part - Sanitized Copy Approved for Release 2013/01/23 : CIA-RDP81-01043R001600090003-8

Declassified in Part - Sanitized Copy Approved for Release 2013/01/23 : CIA-RDP81-01043R001600090003-8

Norway, pulsations with amplitude as high as 30 gammas were registered. Figure 90 gives the records of these observatories showing the character of the pulsations themselves. Since pulsations are of a sinusoidal form, it has been postulated that they are not, the thought has been expressed that they might perhaps be natural oscillations of the variometer magnets themselves (cf. Chapter XII), due to the seismic vibrations of the soil. But pulsations are also observed with magnets with periods of natural oscillations far from those of seismic vibrations.

An important factor is also that the pulsations are sometimes observed simultaneously at several stations, such as, for example, the pulsations recorded at Abisko and Tromso and shown in Figure 90, which are also observed at a number of other stations. This has given ground for postulating the world-wide character of the causes responsible for pulsations. A more detailed study of the special distribution of pulsations, however, showed that the region which the action of these causes, extends is limited to a radius of not more than 1,000 km. Even such a gigantic pulsation as the one observed on 12 September 1930 at Tromso, which is at a distance of not more than 100 km from Abisko, declines by a factor of several kinds by comparison with Abisko.

A proof that the pulsations constitute a real phenomenon of nature is also their record by instruments based on the conduction principal, i. e., instruments which react to a variation of the magnetic field with time.

In spite of the large number of works devoted to the study of pulsation, their causes have still not been established and there is no theoretical explanation for them.

Section 4. Variations at High Latitudes

The systematic study of the variations in high latitudes began somewhat more than 20 years ago, when in connection with the Second

Declassified in Part - Sanitized Copy Approved for Release 2013/01/23 : CIA-RDP81-01043R001600090003-8

Declassified in Part - Sanitized Copy Approved for Release 2013/01/23 : CIA-RDP81-01043R001600090003-8

International Polar Year (1922-1933) a number of magnetic observatories were opened in these latitudes. The extraordinary complexity of the variational phenomena in these parts of the earth, however, demands for its study a large observational material, both in time and in a number of observatories. For this reason the relatively short period of observation and a small number of observatories still fail to make it possible to establish definite regularity in the course of the magnetic variations at these latitudes, as for the low and middle latitudes, even the material that is available at the present time still allows us to point out certain features and to find regularities of one kind or another in these phenomenon. The most complete material for the past 25 years has been collected by the Arctic observatories of the USSR. This material enabled A. P. Nikol'skiy to find new phenomena in the diurnal march of magnetic activity in high latitudes. Very valuable material was secured during the Second International Polar Year, when a whole system of temporary stations operated on a single common program. The results of the observations of this sphere were worked up by E. Vestine and published in 1947 in the form of many different graphs with explanatory text and a few conclusions.

The results of this workup are the materials which must serve as the foundation for future studies and deductions. But certain conclusions may already be made, even on the basis of this material.

The solar-diurnal variations S_q. One peculiarity of the diurnal variations in high latitudes is their dependence not on the geographical latitude, but on the magnetic. This dependence is manifested with particular sharpness on passage through the zone of maximum aurora frequency. A second peculiarity consists in the considerably higher value of the amplitude and phase variation in the vertical and northern component on passage across certain magnetic parallels.

Declassified in Part - Sanitized Copy Approved for Release 2013/01/23 : CIA-RDP81-01043R001600090003-8

Declassified in Part - Sanitized Copy Approved for Release 2013/01/23 : CIA-RDP81-01043R001600090003-8

Figure 91 shows the mean diurnal course march of the variations on quiet days in the winter and summer months, as well as the mean annual values at the stations of the Second International Polar Year, located in the high latitudes, and at the same time at a few permanently operated observatories in the middle latitudes. These curves clearly indicate the latitudinal dependence of the variations, as well as their dependence on the season. In the winter months the variations are considerably less than in the summer. In addition, our attention is struck by absence of that regularity in the march of the variations which is observed in the middle and low latitudes, which phenomena is probably due to the superimposition of irregular disturbances, since in the high latitudes, disturbances are observed even on the quietest International days.

As a result of this, the variations S_D are of extremely great interest, i. e., the diurnal variations on disturbed days minus those on the quiet days.

Figure 92, showing the mean annual march of the S_D variations, shows that the S_D variations are of more regular character than the S_q. Their peculiarity is the change in phase of the Z component in passing through the zone of maximum aurora frequency, located approximately at the magnetic parallel 68°, and also the maximum value of the amplitude of the X component in this zone. The change of phase in the X component takes place at magnetic latitudes 51°, and then again at latitudes 72°. The eastern component likewise changes its phase twice, once at latitudes of about 60° and afterwards in the auroral zone. The amplitude of all the components reaches values in the auroral zone that many times exceed the values in the middle latitudes.

While the variations S_q have a strong seasonal dependence, the variations S_D remain almost the same throughout the entire year.

Declassified in Part - Sanitized Copy Approved for Release 2013/01/23 : CIA-RDP81-01043R001600090003-8

Declassified in Part - Sanitized Copy Approved for Release 2013/01/23 : CIA-RDP81-01043R001600090003-8

The aperiodically disturbed variation. The least studied variation in the high latitudes is the aperiodic variation (D_{ap}), as a result of which there is still no well established regularity in its course. But the result of the workup of 11 storms registered at the Arctic stations during the second polar year allow us to give a few conclusions. In view of the small number of storms, they have been worked up for a group of stations located close to one and the same magnetic latitude. The result of this workup is given by Figure 93 in the form of graphs, which show that the northern component at the beginning of the storm has a value somewhat lower than normal, and which then during the first 10-12 hours, falls to a minimum, after which it begins gradually to increase to its normal level. The absolute value of the minimum increases on approaching the auroral zone, where it reaches 80 γ. Inside this zone it declines, and at latitude 84° it reaches a value of 30 γ, in this case the character of the curve changes completely and takes on the form of a periodic curve.

The eastern component varies periodically, now increasing, now decreasing, within the range of 10-20 γ, indicating the absence of any definite regularities, and in all probability, also indicating the absence of components of D_{ap} in this direction, since the fluctuations might be caused by the superimposition of random variations.

The vertical component, up to the auroral zone, has the same character and the same value of the amplitude as in the middle latitudes. On passing through the auroral zone, the vertical component, 10 hours after the onset of a storm, begins to increase sharply, reaching a maximum of 60 to 100 gammas within a few hours. The highest value of the maximum is assumed at latitude 71°.

Declassified in Part - Sanitized Copy Approved for Release 2013/01/23 : CIA-RDP81-01043R001600090003-8

Declassified in Part - Sanitized Copy Approved for Release 2013/01/23 : CIA-RDP81-01043R001600090003-8

Magnetic activity or degree of disturbance. The existence of a large number of magnetic disturbances in the Arctic latitudes which, being superimposed on the periodic variations make it impossible to isolate them by an averaging, force us to seek other methods of studying these disturbances than the study of the diurnal variations. Such a method, proposed by A. P. Nikol'skiy (Bibl. 50) in 1938, consists in taking the mean values of the hourly values of some measure of activity, either the international characteristic k, or the characteristic proposed by Nikol'skiy himself, the length of the curve D. The mean value of this activity over a certain time interval was termed the degree of disturbance by Nikol'skiy, who studied it in its relationship to the time, latitude, and longitude of the place, season, and the 11-year cycle of solar activity. These studies yielded new material for the elucidation of the causes of magnetic disturbances, and established a number of new regularities in the course of these variations.

The principal result of Nikol'skiy's work was the establishment of a definite regularity in the diurnal march of the magnetic of the degree of magnetic disturbance, which was as follows: the degree of magnetic disturbance during the course of the 24-hour day has two maxima, one of which comes in the morning hours and occurs according to universal time, the other in the evening hours, and occurs according to local time.

In addition, the instant of onset of the morning maximum in the eastern hemisphere depends linearly on the geomagnetic latitude of the station, while in the western hemisphere this instant of onset takes place at one and the same hour (1530-1630 hours Greenwich mean time).

Figure 94 shows a typical curve of the diurnal march of disturbance at the Tikhaya Bay Observatory (Lat 71.5°, Long = 153.3°) while Figure 95 shows the relation of the morning maximum to universal time (Greenwich mean time). These curves thus give us grounds for asserting the correctness of this regularity.

Declassified in Part - Sanitized Copy Approved for Release 2013/01/23 : CIA-RDP81-01043R001600090003-8

Declassified in Part - Sanitized Copy Approved for Release 2013/01/23 : CIA-RDP81-01043R001600090003-8

On investigating the behavior of these maxima in relation to various parameters, Nikol'skiy found that each of them behaves differently, which gave him reason to enunciate the hypothesis that these maxima were of different nature.

Thus, for example, the value of the morning maximum is almost independent of the season, while the evening maximum has its lowest value in winter and its highest value in summer, which is illustrated by the curves of the diurnal march of disturbance at Tikhaya Bay, worked up by seasons -- winter, summer, and equinoxes (Figure 96).

The value of both maxima of disturbance depends further on the general state of the magnetic field.

With the increase of the general degree of disturbance, the value of the maximum increases but in different ways. Figure 97 shows the diurnal march at Tikhaya Bay for six groups of days with varying degrees of disturbance. It will be seen that at the beginning, when the total disturbance is small, the morning maximum is predominant, but later, with the increase in the total disturbance, both maxima increased, but the night one increases considerably faster and on stormy days is almost twice as large as the morning maximum.

Finally, we point still another peculiarity, the dependence of the value of the maxima on the geomagnetic latitude. This dependence is shown in Figure 98, which indicates that with increasing latitude the maxima also increases, but that the evening maximum reaches its highest value in the auroral zone while the morning maximum reaches it at the geomagnetic pole.

All these facts confirm beyond the doubt the thought that these two maxima are due to different causes. However, attempting to find these causes and to explain the diurnal march of the degree of the

Declassified in Part - Sanitized Copy Approved for Release 2013/01/23 : CIA-RDP81-01043R001600090003-8

Declassified in Part - Sanitized Copy Approved for Release 2013/01/23 : CIA-RDP81-01043R001600090003-8

magnetic disturbance, Nikol'skiy constructs a very simplified scheme of currents postulating that the variations are due to a rectilinear current of corpuscles of different signs, with the morning maximum attributed to a stream of corpuscles of one sign, while the evening maximum is attributed to a stream with the opposite sign, although he adduces no quantitative calculations to confirm this hypothesis.

Nikol'skiy further attempts to cast doubt on the methods of segregating the diurnal and aperiodic disturbed variations, and claims in his work that, at least in the high latitudes, the diurnal variations and aperiodic disturbed variations do not exist as actual processes and that they represent fictitious phenomena obtained as a result of the statistical treatment. It is premature to agree with such theories and conclusions, since they are constructed with no quantitative analysis whatever and are unconfirmed even by elementary mathematical calculations.

Section 5. The Aurora

The magnetic disturbances observed on the earth, and especially in the Arctic regions, are closely connected with the aurora. This connection is not merely external, but is also internal and physical and is due to the common causation of both phenomena. For this reason, in considering the causes of magnetic disturbances they cannot in any case be abstracted from the fact of the aurora, which allows us to understand more clearly and more profoundly the nature of the magnetic disturbances.

1. The forms of the aurora. The aurora may be classified according to its form into two great groups: auroras of nonradial structure and auroras of radial structure. Each of these groups in turn subdivided into a number of subgroups.

Those of nonradial structure include the following:

Declassified in Part - Sanitized Copy Approved for Release 2013/01/23 : CIA-RDP81-01043R001600090003-8

Declassified in Part - Sanitized Copy Approved for Release 2013/01/23 : CIA-RDP81-01043R001600090003-8

1. uniform quiet arcs the lower edge of which is sharply pronounced, while the upper edge is blurred. A dark segment is observed between the lower edge of the arc and the horizon;

2. uniform bands usually extending in the same direction as the arcs, but less regular in form. The lower edge is often sharply defined, but is irregular in form. In most cases the bands are broken up by dark spaces and for this reason have the form of feathery clouds;

3. pulsating arcs, which rhythmically appear and disappear with a period of a few seconds;

4. diffusely luminous surfaces having the form of a veil covering a large part of the sky;

5. pulsating surfaces consisting of diffusely luminous parts of the sky, appearing at one and the same place.

The radial-structure auroras include the following:

1. arcs with a radial structure;

2. bands of radial structure, seemingly uniform, but consisting of a number of streamers;

3. drapery, consisting of a few bands with very long streamers, similar to a folded curtain. The lower edge of the drapery is usually more illuminated. Near the magnetic zenith (the projection of the magnetic pole onto the celestial vault; it has the form of a fane;

4. isolated streamers which may be narrow or wide, short or long, isolated or in the form of beams;

5. a Corona, consisting of streamers, bands, or drapery, converging to a single point near the magnetic zenith.

Declassified in Part - Sanitized Copy Approved for Release 2013/01/23 : CIA-RDP81-01043R001600090003-8

Declassified in Part - Sanitized Copy Approved for Release 2013/01/23 : CIA-RDP81-01043R001600090003-8

2. The direction of the streamers of the aurora. A substantial factor in the observations of the radial structure is a sufficiently close coincidence of the direction of the streamers with the direction of the lines of force of the earth's magnetic field. This fact is one of the basic facts for the construction of the modern theory of the aurora, based on the motion of charged particles in the earth's magnetic fields.

Indeed, by observing visually the streamers of the aurora it may be noted that all of them converge on a single point located near the magnetic zenith. The results of precise determinations of the direction of the streamers by photographing the Corona of the aurora, are given in Table 19 which gives the observed height h and x the azimuth of the point of convergence of the streamers and of the magnetic zenith.

As will be clear, the coincidence between the point of convergence of the streamers and the magnetic zenith is observed within the limits of accuracy of the observations themselves.

Table 19

Station	Observer	Year
Holde	Vegard and Krogness	1914
Oslo	Stoermer	1917-1921

Number of observations	Point of convergence h	Point of convergence a	Magnetic zenith n	Magnetic zenith a
11	75.4°	-2.7°	76.7°	-2.5°
9	70.0	-9.8	70.8	-9.7

Vegard, studying the structure and distribution of the light along a bundle of rays, came to the conclusion that the rays always follow the direction of the lines of force and that the point of their

Declassified in Part - Sanitized Copy Approved for Release 2013/01/23 : CIA-RDP81-01043R001600090003-8

Declassified in Part - Sanitized Copy Approved for Release 2013/01/23 : CIA-RDP81-01043R001600090003-8

intersection corresponds to the magnetic pole, which may be displaced owing to the appearance, during the time of strong auroras, of an additional magnetic field formed by the ring currents around the earth.

3. The height of the aurora. The height and position of the aurora in space may be determined by the simultaneous observation of their coordinates (altitude and azimuths) at two points, the distance between which is known.

The first determinations for this method were made over 200 years ago and they have since been repeated by many investigators, who have given the height within the range of 80 to 200 km. But exact determinations of the height of the aurora became possible with the introduction of the photographic method.

This method was first used by Stoermer (Bibl. 51) in 1910, and in 1913 at the Observatory at Vessekop in Lapland, and is as follows at two stations, working simultaneously and having a telephone connection between them, the aurora is photographed on motion-picture film. Stars are photographed together with the aurora on this film. By determining the position of the aurora among the stars on the film, and knowing the distance between the stations and the azimuth of the aurora, its position in space can be determined with fair accuracy and its height can be calculated. The length of the base, or distance between the stations, was only 4.5 km in 1910, but in 1913 it was as much as 27.5 km, which made it possible to make more exact determinations.

Thanks to the short exposure (half a second or less), this method allowed the observation not only of quiet auroras but also of rapidly pulsating ones.

Declassified in Part - Sanitized Copy Approved for Release 2013/01/23 : CIA-RDP81-01043R001600090003-8

Declassified in Part - Sanitized Copy Approved for Release 2013/01/23 : CIA-RDP81-01043R001600090003-8

The result of the first determinations in 1910-1913 show that the height of the aurora ranges from 87 to 350 km, with two maximum frequencies being observed, one at height 101 and the other at height 106 km.

These results were confirmed in 1920 at the Holder observatory by more systematic determinations of the upper and lower boundaries of various types of aurora.

The results of these determinations are shown in Figure 99 in the form of curves showing the probability of the appearance of the lower boundary of an aurora at one height or another. These curves show clearly that the most frequent lower boundary of the aurora is at height 100-106 km.

During the period from 1910 down to the present, thousands of determinations of the height and positions of the aurora in space have been made. This material has allowed the following conclusions to be drawn. The quiet forms of the aurora, diffuse arcs, bands, and pulsating areas have on the average their lower boundary at a lower height than the pronounced radial structures. Moreover, the mean height of the lower boundary of the quiet forms and drapery is almost independent of the latitude of the place, but for the forms of radial structure the mean height increases from the auroral zone (cf infra) towards lower latitudes. The results of measurements of the lower boundary of various forms of the aurora at various observatories is given by Table 20.

Declassified in Part - Sanitized Copy Approved for Release 2013/01/23 : CIA-RDP81-01043R001600090003-8

Declassified in Part - Sanitized Copy Approved for Release 2013/01/23 : CIA-RDP81-01043R001600090003-8

Table 20

LOWER BOUNDARY OF THE AURORA

Type of aurora	Holder, (Lat 69°56' Long 62°55' Height, km	Number of observations	Tromso (Lat 69°49' Long 16°57' Height, km	Number of observations	Oslo (Lat 60°0' Long 10°40' Height, km	Number of observations
Streamers	113.2	61	117.0	127	146.9	119
Drapery	109.8	409	112.9	1,039		
Drapery-like arcs	106.6	888	106.7	1,175	100.0	150
Pulsating areas	[?]	160	107.3	66	-	-
Diffuse arcs	[?]	409	-	-	118.5	201

Declassified in Part - Sanitized Copy Approved for Release 2013/01/23 : CIA-RDP81-01043R001600090003-8

Declassified in Part - Sanitized Copy Approved for Release 2013/01/23 : CIA-RDP81-01043R001600090003-8

The upper boundary of various types of aurora lies within the limits of 140 to 250 km. The auroras in the form of streamers are the longest. Thus the mean height of the upper boundary of some forms are as follows: streamers, 250 km; drapery, 176.3 km; drapery-like arcs, 174.4 km; diffuse arcs 143.4 km.

Thus the length in a vertical direction is 137 km for the streamers, 68 km for the drapery, and 34 km for the diffuse arcs.

But auroras are also observed in the form of streamers whose lower boundary goes up to a few hundred kilometers and its upper to a thousand.

Thus Stoermer registered on a September 1926 photogram at Oslo an aurora in which the lower boundary lay from 200 to 400 km, and the upper boundary from 1,000 to 1,100 km.

4. The geographic distribution of the aurora. As indicated above, the aurora is observed not only in the Arctic regions but also in the middle latitude and even lower. Thus, for example, in the 1870's an aurora extended to Egypt and even to India. But the frequency of appearance of the aurora (the number of displays per year) is very small in the middle and low latitudes, while in the high latitudes the aurora is observed almost daily.

As early as 1881 (Bibl. 52) a map of the isolines of auroral frequency (isochasms) was prepared and showed that the aurora was most frequent in a region about 23° distant from the geomagnetic pole. This zone has received the name of zone of maximum aurora.

For 60 years from the publication of this map an immense material was accumulated on observations of the aurora, which made it possible in 1947 (Bibl. 53) to construct a new map of the isochasms

Declassified in Part - Sanitized Copy Approved for Release 2013/01/23 : CIA-RDP81-01043R001600090003-8

Declassified in Part - Sanitized Copy Approved for Release 2013/01/23 : CIA-RDP81-01043R001600090003-8

(Figure 100) which on the whole repeats the 1881 map. A similar zone of maximum aurora exists also around the south geomagnetic pole.

On the map, the isochasm corresponding to the maximum frequency is shown by a thicker line. The values of the isochasms are shown in arbitrary units, in percent related to the maximum zone.

Figure 101 is a map of the earth on which the northern and lower zones of magnetic of maximum auroral frequency and the geomagnetic equator corresponding to the uniform magnetization of the earth, are shown.

The following we shall not indicate a few of the most strongest auroras during the last 100 years. The strongest of them was on 4 February 1872 when it was visible at Bombay, Lat 19° N, at a distance of 80° from the magnetic pole. The magnetic zenith of this aurora was observed at Constantinople and Athens. The aurora australis was observed simultaneously at Lat 20° S, at a distance of 72° from the earth's magnetic pole. The next intense aurora was observed on 14-15 May 1921 when the aurora australis reached the Islands of Samoa (13.8° S). This aurora was accompanied by strong magnetic storms.

Strong auroras were also observed in January and April, 1938.

5. The diurnal distribution of the aurora. By observing the aurora daily it may be noted that during the 24-hour day it appeared not at random, but had a tendency to group itself about a certain moment about a certain time. Thus, the observations during the First International Polar Year, 1882-1883, showed that auroras in the form of streamers, draperies and corona have a distinct maximum in the evening hours, and a winter maximum in the morning hours. In this case,

Declassified in Part - Sanitized Copy Approved for Release 2013/01/23 : CIA-RDP81-01043R001600090003-8

Declassified in Part - Sanitized Copy Approved for Release 2013/01/23 : CIA-RDP81-01043R001600090003-8

the moments of maximum appearance of the aurora, according to local time differ at the various stations, depending on the geographical coordinates. Thus at Bossekop station (Lat 69.57° and Long 23.15° E) this maximum was at 2125 hours local time, while at Fort Rae, Lat 62.39°, Long 115°49' W it was at 2400 hours.

If, however, the local magnetic time is taken instead of the local solar time, then the times at maximum auroral frequency will be the same for all stations, and correspond to 23 hours magnetic time. In this case, "by magnetic time" we mean the angle between a plane passing through the magnetic axis through the earth and the sun and the plane passing through the same axis and the given station.

6. The spectrum of the aurora. The spectroscopy of the aurora, owing to its low intensity, requires special spectrographs with a large f number and an exposure measured in tens of hours. For this reason it was long impossible to identify some of the lines observed with the lines of any specific element. In 1912 Vegard succeeded in obtaining 33 lines by the aid of such a spectrograph and an exposure lasting a month.

Subsequent studies showed the presence of a large number of lines in the auroral spectrum in the visible, infrared and ultra-violet regions. Among these lines, the most intense is the green line at 5557.3 A. This line does not correspond to any of those observed under laboratory conditions.

Since this line is observed not only in the spectrum of the aurora but also in the spectrum of the luminescence of the night sky in the absence of the aurora, it gave Vegard cause for enunciating the hypothesis that solid crystaline particles of nitrogen were present in the upper layers in the atmosphere and on bombardment by electrons luminesced and radiated this line.

Declassified in Part - Sanitized Copy Approved for Release 2013/01/23 : CIA-RDP81-01043R001600090003-8

Declassified in Part - Sanitized Copy Approved for Release 2013/01/23 : CIA-RDP81-01043R001600090003-8

But this green line at 5777 A (sic) was later obtained under laboratory conditions from atomic oxygen, and in this way the problem of the origin in this line of the spectra of the aurora and the night sky was solved.

Of the other brightest lines, we may note the lines at 3914, 4278, 4708 and 5225 A, belonging to the ionized nitrogen molecule N_2^+ and the lines 3997 and 4059 A, belonging to the neutral nitrogen molecules.

The discovery of the green line in the spectrum of atomic oxygen permitted the prediction of three red oxygen lines at 6300, 7364 and 6392 A, of which two were found in the auroral spectrum.

Thus the aurora on the whole is the luminescence of atomic oxygen and molecular nitrogen of which the ionosphere is composed.

7. The connection between the aurora and solar activity. The connection between the magnetic disturbances and the aurora was first established as far back as the beginning of the 18th Century, when it was noted that the aurora are accompanied by magnetic storms.

Further observations completely confirm this discovery, but it has still not been possible to establish the essential functional connection between these phenomena. All the studies in this direction lead merely to a statistical correlation which always was found to be high. Thus the regular observations at the magnetic observatory at Tikhaya Bay made in 1932-1933 allowed a Soviet investigator (Bibl. 54) to compare the magnetic characteristics 0 1 2 3 4 with the auroral characteristics 1 2 3 4. In the auroral characteristics, Unit one corresponds to the absence of an aurora on that day, two to the presence of moderate aurora, but without a radial

Declassified in Part - Sanitized Copy Approved for Release 2013/01/23 : CIA-RDP81-01043R001600090003-8

Declassified in Part - Sanitized Copy Approved for Release 2013/01/23 : CIA-RDP81-01043R001600090003-8

structure, three to the presence of bright auroras of radial structures, and four to very bright auroras. The results of these comparisons are given in Table 21, which indicates the number of days with the corresponding auroral and magnetic characteristics.

TABLE 21

COMPARISON OF MAGNETIC ACTIVITY AND AURORAL ACTIVITY FROM OBSERVATIONS AT TIKHAYA BAY DURING THE PERIOD FROM OCTOBER 1932 AND MARCH 1933

Intensity of aurora (characteristics)	Total number of cases	Number of cases when the magnetic characteristics were 0	1	2	3	4	Mean magnetic characteristics
Faint (1)	186	10	114	46	7	3	1.3
Moderate (2)	76	3	27	32	9	5	1.3
Bright (3)	31	0	11	10	5	5	2.1
Very bright (4)	10	0	3	2	2	3	2.5

These results, in general, confirm the absence of magnetic disturbances on those days when aurora are not observed and their appearance with the appearance of the aurora, although there are also exceptions.

Like magnetic activity, the aurora have a tendency to a 27-day cycle, and, finally, also have an 11-year cycle of maximum frequency. Figure 102 gives the curves of a number of sunspots (upper curve) and a number of days in the year with auroral displays (lower curve), observed during the period from 1840 to 1896.

Except for the first cycle, the maxima and minima of the curves are almost in the very same years, which indicates the close connection between these phenomena.

All this forces us to assume that the aurora, the magnetic disturbances, and the appearance of spots on the sun are interrelated.

Declassified in Part - Sanitized Copy Approved for Release 2013/01/23 : CIA-RDP81-01043R001600090003-8

Declassified in Part - Sanitized Copy Approved for Release 2013/01/23 : CIA-RDP81-01043R001600090003-8

CHAPTER VII

THEORY OF MAGNETIC VARIATIONS AND AURORA

Section 1. The Ionosphere and Its Properties

The results of mathematical analysis of the curves of magnetograms give reason for holding that the cause of both solar and lunar diurnal variations is the existence in the upper layers in the atmosphere of a system of electric currents with a distribution that must be roughly about what is shown in Figure 73 and 74. For this reason all theories of diurnal variations, starting out from this proposition, attempt to give the mechanism of origin of these currents, under the assumption that the upper layers of the atmosphere possess a corresponding conductivity. Until the 1920's, the question of the conductivity of the upper layers of the atmosphere remained a pure hypothesis, and consequently the theories of the magnetic variations based on this hypothesis could not claim to be reliable. But observations on the propagation on the radio waves, especially short waves, showed the existence at a height of 100 to 300 km of conducting layers having the ability to reflect radio waves, as occurs with metallic conductors. In this way the hypothesis of the conductivity of the upper layers now has experimental confirmation. The existence of conductivity is explained by the ionization by the atmosphere under the action of the ultraviolet and corpuscular radiation of the sun. This region of the atmosphere has received the name of the ionosphere. Since the ionosphere plays an immense role in the formation of the variations of the magnetic field of the earth, it is necessary, even though only briefly for us to dwell on its properties, and the methods of studying it.

1. The propagation of radio waves in the ionosphere. The dependence of the index of refraction on the density of ionization.

Declassified in Part - Sanitized Copy Approved for Release 2013/01/23 : CIA-RDP81-01043R001600090003-8

Declassified in Part - Sanitized Copy Approved for Release 2013/01/23 : CIA-RDP81-01043R001600090003-8

Let us assume that in an ionized medium located in the magnetic field of the earth, there is propagated a monochromatic plane electromagnetic wave with angular velocity w in the direction of the z axis, which makes the angle B with the direction of the magnetic field H. In this case, under the action of the electric vector E of this wave, the free electrons are put into motion, and the equation of one of them will obviously be:

$$m\frac{d^2r}{dt^2} = -\varepsilon E - \frac{e}{c}\left[\frac{dr}{dt} H\right], \qquad (7.1)$$

if we consider that the electrons do not lose their energy under the action of the collisions, where r represents the vector of displacement under the action of E, and c is the speed of light.

If δ denotes the dielectric constant of the ionized medium, then

$$\varepsilon E = E + 4\pi P,$$

where P is the vector of electric polarization, which may in turn be represented in the following form:

$$P = -Ner,$$

where N is the number of free electrons in 1 cc.

From this, expressing E and r in terms of P, and substituting in equation 7.1, we obtain:

$$-\frac{m}{Ne}\frac{d^2P}{dt^2} = -\frac{4\pi e}{\varepsilon - 1} P + \frac{1}{Nc}\left[\frac{dP}{dt} H\right]. \qquad (7.2)$$

Since the vector E is a harmonic function then $E = E_0 \sin wt$, equation 7.2 allows us to find the value of c connected with the index of refraction, which is as follows:

$$\varepsilon = n^2 = 1 - \frac{2a(1-a)}{2(1-a) - b_x^2 H^2 \pm \sqrt{b_x^4 H^4 + 4b_x^2 H^2 (1-a)^2}} \qquad (7.3)$$

where

$$a = \frac{4\pi Ne}{mw^2} \quad \text{and} \quad b = \frac{e}{mcw}$$

Declassified in Part - Sanitized Copy Approved for Release 2013/01/23 : CIA-RDP81-01043R001600090003-8

Declassified in Part - Sanitized Copy Approved for Release 2013/01/23 : CIA-RDP81-01043R001600090003-8

Let us now consider the case where the magnetic field is absent, or where it may be disregarded. Then, putting H = 0 in equation 7.3, we shall have:

$$\varepsilon = n^2 = 1 - a = 1 - \frac{4\pi Ne^2}{mw^2} . \qquad (7.4)$$

This expression has a physical meaning only for $a < 1$. At $a = 1$, the index of refraction becomes zero, which corresponds to the phenomenon of total internal reflection. Consequently, at constant ionization density, i. e., when N = const., it is always possible to select a frequency of oscillation of the electromagnetic wave w, at which the index of refraction shall be zero. In this case the total internal reflection of the incident wave takes place, and with normal incidence it returns to the place from which it came. It is from the difference between the time of the emission of the signal and time of its arrival that the height of the reflecting layer can be determined. The frequency w_c, at which total internal reflection takes place is termed critical; if we know it we can determine the relation of the density of ionization to the mass of an ionized particle from the equation:

$$\omega_c^2 = \frac{4\pi Ne^2}{m} ; \qquad (7.5)$$

whence

$$\frac{N}{m} = \frac{\omega_c^2}{4\pi e^2} = \frac{\pi f_c^2}{e^2} , \qquad (7.6)$$

where f_c is the critical frequency of the oscillations expressed in cycles per second.

In this way the method of reflection of radio waves of variable frequency from the ionized layer allows us simultaneously to find the height of the reflecting layer and the density of ionization of that layer, provided we know the species of ionized particles. Thus if the particle is an electron whose mass $m = 9 \times 10^{-28}$ g, then

$$N = 1.24 \cdot 10^{-8} f_c^2 .$$

Declassified in Part - Sanitized Copy Approved for Release 2013/01/23 : CIA-RDP81-01043R001600090003-8

Declassified in Part - Sanitized Copy Approved for Release 2013/01/23 : CIA-RDP81-01043R001600090003-8

If, however, the ionized particles are oxygen and nitrogen ions, the means mass of which is m - 3.7×10^{-23} grams, then

$$N = 2.5 \cdot 10^{-4} f_c^2.$$

If an electromagnetic wave of constant frequency penetrates into an ionized layer of gas of variable ionization density, then it may reach a level at which n becomes zero. At this height, then, there is total reflection from the layer.

For the case when the magnetic field is not equal to zero, the index of refraction, as shown by equation 7.3, has two values. For this reason, when an electromagnetic wave passes through an ionized medium, it must be split into two. One of these waves, corresponding to the plus sign in equation 7.3, is called the ordinary wave, while the second, corresponding to the minus sign, is called the extraordinary wave, by analogy with the doubly refracting power of crystals.

If expression 7.3 is equated to zero, then we obtain two equations each of which determines the critical frequency of the ordinary and extraordinary waves.

One of the roots of this equation a = 1, while the second a = 1 ± bH. The first of them corresponds to the ordinary wave, the second to the extraordinary. If we replace a and b by their values and denote the critical frequency of the ordinary wave by w_c and of the extraordinary wave by w_c', then we obtain

$$\omega_a^2 = \frac{4\pi Ne^2}{m}, \quad \omega_c'^2 = \frac{eH}{mc} \quad \omega_c' = \frac{4\pi Ne^2}{m} = \omega_c^2. \tag{7.7}$$

The quantity eH/mc represents the angular velocity of rotation of the charge e about the lines of force of the magnetic field. If we denote it by w_H, we shall have

Declassified in Part - Sanitized Copy Approved for Release 2013/01/23 : CIA-RDP81-01043R001600090003-8

Declassified in Part - Sanitized Copy Approved for Release 2013/01/23 : CIA-RDP81-01043R001600090003-8

$$\omega'^2_c \pm \omega_H \omega'_c - \omega_c^2 = 0,$$

or, passing over to frequencies expressed in cycles per second:

$$f'^2_c \pm f_H f'_c - f_c^2 = 0,$$

whence

$$f_c = f'_c \sqrt{1 \pm \frac{f_H}{f'_c}}.$$

As shown by experience, f_H is always less than f_c, and therefore we may write, approximately:

$$f''_c - f_c = \pm \frac{1}{2} f_H = \pm \frac{1}{4\pi} \frac{eH}{mc},$$

but only the plus sign has a physical meaning, i. e., the frequency of the extraordinary wave is always somewhat higher than the frequency of the ordinary wave.

For a layer of the atmosphere the ionization of which is represented by electrons:

$$f'_c - f_c = 1.4 \text{ H megacycles.}$$

For middle latitudes, where H = 0.5 O_e, the difference in the frequency of the extraordinary and ordinary wave will be of the order of 0.7 megacycle.

But if the ionization is represented by ions, whose mass is a few thousand times as great as the mass of an electron, the f_H, and consequently also the difference $f'_c - f_c$, will likewise be a few thousand times as great, i. e., of the order of a few hundred cycles.

It follows from this that in the presence of double refraction, when the difference between the frequencies of the ordinary and extraordinary rays is of the order of 1-1.5 megacycles, we have an ionized layer represented by electrons. In the absence of double refraction, however, the opposite conclusion cannot be drawn, since the extraordinary ray, after being reflected, may also fail as a result of absorption to reach the earth's surface.

Declassified in Part - Sanitized Copy Approved for Release 2013/01/23 : CIA-RDP81-01043R001600090003-8

Declassified in Part - Sanitized Copy Approved for Release 2013/01/23 : CIA-RDP81-01043R001600090003-8

Equation 7.7 shows that the ordinary wave coincides with a wave that is with the wave propagated in the absence of the magnetic field.

2. Methods of studying the ionosphere. The theory of propagation of radio waves in the ionosphere allows methods to be established by the aid of which it is possible to determine the height of the ionized layers, the density of their ionization and the character of the ionized particles. The principal method in the study of the ionosphere today is the pulse method.

The pulse method is as follows. A radio installation, consisting of a transmitter, receiver, antenna, pulse modulator, relaxation oscillator, and cathode oscillograph (Figure 103) periodically emits short pulses with a duration of the order of 10^{-4} to 10^{-5} seconds. Since the frequency of the oscillations of the transmitter is of the order of a few megacycles, a few hundred oscillations will go into each pulse. The time interval between 2 successive pulses, or in other words the pulse frequency, is so chosen that the radiated impulse shall be able to reach the reflecting layer and return from it before the second impulse begins. With a height of the F_2 layer of the order of 300 km, the travel time t will be 2×10^{-3} seconds. Usually the interval between the pulses is taken ten times as great, i. e., 1/50 seconds. The direct and reflected pulses are received by the antenna and enter the radio receiver, at the output of which an alternating voltage is produced. This voltage is fed to one of the pairs of plates of a cathode oscillograph, while the other pair is connected to the relaxation oscillator of the same frequency as the pulse modulator, 50 cycles.

The relaxation oscillations are synchronized with the pulse modulator in such a way that at the time of minimum amplitude of the

Declassified in Part - Sanitized Copy Approved for Release 2013/01/23 : CIA-RDP81-01043R001600090003-8

Declassified in Part - Sanitized Copy Approved for Release 2013/01/23 : CIA-RDP81-01043R001600090003-8

relaxation oscillations, i. e., when the voltage across the oscillograph plates is at a minimum, the oscillators shall receive a pulse. In that case the reflected pulse arriving after a certain time interval and entering the oscillograph plates, meets the cathode beam deflected in a direction perpendicular to the direction of the oscillations of the pulse, and on the oscillograph screen we shall see two luminous bands a certain distance apart. Since the relaxation oscillations are proportional to time over most of its half-period, the deflection of the reflected beam will likewise be proportional to its time lag. In this way, by measuring the distance between the luminous bands, if we know the time scale, the height of the reflecting layer can be determined.

To photograph these bands, the oscillograph screen is covered by an opaque screen with a narrow slit in the middle, and the photographic film is displaced perpendicularly to this slit. If the height of the reflecting layer is constant, then a series of straight lines, correspondent to a different number of reflections, will be obtained on the film. But if the height varies, we shall obtain a curve showing the relation of the height of the layer to the time.

The pulse method allows us to determine only the height of the reflecting layer corresponding to a given frequency of the transmitter. To find the critical frequencies by this method, the pulse observations and measurements are made with a smooth variation of the transmitter and receiver frequencies from low frequencies up to the frequency which the reflection stops. In modern installations, these variations of frequency are produced automatically, and such an installation has received the name of ionosphere station.

Declassified in Part - Sanitized Copy Approved for Release 2013/01/23 : CIA-RDP81-01043R001600090003-8

Declassified in Part - Sanitized Copy Approved for Release 2013/01/23 : CIA-RDP81-01043R001600090003-8

3. Measurement of the height of the reflecting layer. If the velocity of propagation of waves in the ionosphere did not differ from the velocity of propagation in a neutral medium, i. e., if it were equal to the speed of light c, then the height h_g of the reflecting layer could be calculated by the formula

$$h_g = \frac{1}{2} c \tau,$$

where τ is the time interval between the moment of emission and the moment of arrival of the reflected wave. In view of the existence of dispersion, the velocity for each frequency in the ionosphere will be different and will vary with the variation of the ionization density. For this reason the true height h will differ from the height h_g termed the effective height, and must be calculated by the formula:

$$h = h_0 + \int_{h_0}^{h} u \, dt = h_0 + \int_{h}^{h} dh, \qquad (7.8)$$

where h_0 is the height of the beginning of the layer above the earth's surface and is the velocity of propagation of the waves in the ionosphere layer.

By means of appropriate transformations, equation 7.8 is brought into the following form:

$$h = \frac{2}{\pi} \int_0^{\omega} \frac{h_g d\omega_1}{\omega^2 - \omega_1^2}.$$

Since w_1 is an arbitrary variable, it may be taken as equal to w sin φ, i. e.,

$$\omega_1 = \omega \sin \varphi, \qquad (7.9)$$

and in that case

$$h = \frac{2}{\pi} \int_0^{\pi/2} h_g d\varphi,$$

where h_g is a function of w sin φ. Consequently the true height is

Declassified in Part - Sanitized Copy Approved for Release 2013/01/23 : CIA-RDP81-01043R001600090003-8

Declassified in Part - Sanitized Copy Approved for Release 2013/01/23 : CIA-RDP81-01043R001600090003-8

numerically equal to the area between the curve $h_g = f(\varphi)$ and the axis of abscissas. Since the photograms give us h_g as a function of w, it follows that to find h_g as a function of φ, must be calculated by equation 7.9 for the given frequency w and for various values of w_1, and the values of h_g corresponding to the values of φ must be found from the photogram, and this will in fact give us h_g as a function of φ.

If we now construct a graph of h_g against φ and integrated by a planimeter, we shall find h for the given frequency w.

Observations of the reflections of the radio waves by the critical frequency method, that is, the determination of the frequency at which the reflected wave vanishes, have allowed the existence of three ionized layers at mean heights of 100, 200 and 300 km to be established. These are termed respectively the E, F_1 and F_2 layers.

The critical frequencies corresponding to these layers depend both on the latitude and longitude of the place and on the solar activity and as well as the solar altitude. Table 22 gives the values of the mean annual critical frequencies at noon when the critical frequencies are at maximu, as well as the number of sunspots in the respective years.

The frequencies are expressed in megacycles and are given for various points of the earth, as well as for various epochs within the limits of a single cycle of solar activity.

As indicated by the Table, the critical frequency, and consequently also the ionization density in all layers increases with the solar activity and with decreasing latitude of the places.

Declassified in Part - Sanitized Copy Approved for Release 2013/01/23 : CIA-RDP81-01043R001600090003-8

Declassified in Part - Sanitized Copy Approved for Release 2013/01/23 : CIA-RDP81-01043R001600090003-8

TABLE 22

MEAN ANNUAL CRITICAL FREQUENCIES AND NUMBER OF SUNSPOTS

Point	Latitude φ	Longitude λ	Year	Number of Sunspots	Critical frequency at noon E	F_1	F_2
			1933	6	3.03	3.34	-
			1934	9	3.10	3.28	5.71
			1935	36	3.35	3.49	6.43
			1936	80	3.72	4.34	9.34
Washington	38°50' N	77°0' W	1937	114	3.75	4.61	10.0
			1938	110	3.74	5.21	10.03
			1939	84	3.73	5.26	9.57
			1940	69	3.52	4.58	8.43
			1941	48	3.37	4.43	7.36
Huancayo, Peru	22°3' S	75°20' W	1939	84	4.04	5.46	10.86
Watheroo, Australia	30°19' S	115°53' E	1939	84	4.44	5.16	10.52
Tomsk	56°30' N	84°54' E	1939	84	3.3	5.2	9.5
Tromso, Norway	69°40' N	18°95' E	1939	84	3.07	4.87	7.48

Declassified in Part - Sanitized Copy Approved for Release 2013/01/23 : CIA-RDP81-01043R001600090003-8

Declassified in Part - Sanitized Copy Approved for Release 2013/01/23 : CIA-RDP81-01043R001600090003-8

In exactly the same way, the ionization of the F_1 and E layers, as shown above, depends on the zenith distance of the sun, and therefore has a diurnal and seasonal march. Thus, in the course of a day, the ionization increases from midnight, reaching a maximum at noon, and then symmetrically declines to reach a minimum at midnight again.

The F_1 and E layers are observed only in the daylight hours and at latitudes where the zenith distances of the sun are less than 70°. At great zenith distances, i. e., in the evening and night hours, and also at high latitudes, the F_1 layer disappears, and merges with the F_2 layer.

The region in which layers are observed is termed the F region.

By using equation 7.6 and the data of Table 22, it is easy to obtain the value of the ionization density in the E, F_1 and F_2 layers. Thus, if the ionized particle is considered to have the mass of an electron, then its mean ionization is of the order $N = 1.5 \times 10^5$ for the layer; $N = 3.0 \times 10^5$ for the F_1 layer; and $N = 10 \times 10^5$ for the F_2 layer.

The fact of double refraction in the F_1 and F_2 layers and its absence, in most cases, in the E layer is of importance, for it gives us grounds to hold that the F_1 and F_2 layers consist of electrons while the question of the composition of the ionized particle in the E layer still remains open, since double refraction in the layer is met very seldom, excepting in the high layers.

Figure 104 shows a typical photogram of the height-frequency characteristic with a reflection from the E layer, and from the F_1 and F_2 layers, obtained by means of an automatic record of the reflected waves of various frequencies. The frequencies are plotted along the abscissa

Declassified in Part - Sanitized Copy Approved for Release 2013/01/23 : CIA-RDP81-01043R001600090003-8

Declassified in Part - Sanitized Copy Approved for Release 2013/01/23 : CIA-RDP81-01043R001600090003-8

axis in megacycles, and the effective heights in kilometers on the ordinate axis. As will be seen, the low frequencies are reflected from the lower layer at a height of the order of 100 km (the E layer); at a frequency of about 400 KZ the reflection is interrupted and begins again from a higher layer at a height of about 150-160 km (the F_1 layer). With increasing frequency, the height of the layer increases, and at a frequency of about 5000 KZ a new reflection corresponding to the F_2 layer at a height of 280 km, begins. At a frequency of over 6000 kz, the height of the layer increases sharply, and the curve, by bifurcating, moves upward into branches, and the reflection stops.

The bifurcation of the curve corresponds to the reflection of the ordinary and extraordinary wave. The upper, fainter curve is the result of being twice reflected, as a result of which its ordinate, i. e., its height, is double that of the lower curve.

Figure 105 gives a graph of the ionization density against height obtained by working up a photogram, and indicates the paths of rays of various frequencies emitted from one point of the earth's surface and received at another point.

4. Composition of the ionosphere and formation of ionized layers. On the basis of data on the spectra of the aurora and luminescence of the night sky, it will be assumed that at heights 100-120 km (the E layer) that the ionosphere consists of molecular nitrogen N_2 and molecular oxygen, O_2. Above 120 km, the dissociation of the oxygen begins, and in atomic oxygen, O_1, begins to predominate in the composition of the ionosphere. For this reason it is usually considered that the E layer consists of ionized nitrogen, N_2, when it bifurcates into two layers, layer F_1 consists of N_2 while layer F_2 consists of O_1. In higher regions dissociation of nitrogen begins and atomic nitrogen, N_1 begins to play a role.

Declassified in Part - Sanitized Copy Approved for Release 2013/01/23 : CIA-RDP81-01043R001600090003-8

Declassified in Part - Sanitized Copy Approved for Release 2013/01/23 : CIA-RDP81-01043R001600090003-8

An entirely definite energy (the ionization potential) is required for the ionization of oxygen and nitrogen molecules or atoms. This energy has the following values expressed in electron volts (1eV = 1.59×10^{-12} erg):

gas	O_2	O_1	N_2	N_1
energy	12.5	13.5	15.8	14.5

This energy may be obtained from solar radiations which consist of two forms: corpuscular and waves. The role of the corpuscular radiation, however is very insignificant and is manifested only at moments of enhanced solar activity. On normal days, however, as shown by research, the principal ionizing factor is the wave radiation in its shortwave portion. Indeed, from the condition that the energy of a light quantum $h\nu$ must be not less than the value of the ionization potential above mentioned, it follows that ionizing radiation must have a wavelength between 850 and 1,000 A.

Alongside of ionization the reverse phenomenon also takes place, namely the recombination of ions, which proceeds faster the greater the density of the atmosphere. At a height of the order of 100 km, the equilibrium state between the processes of ionization and recombination is rather rapidly established, and therefore the density of ionization (the number of free electrons per cc) at these heights must be a function of the solar altitude. At great heights, owing to the low density of the atmosphere, there is a lag in the processes of recombination, as a result of which the ionization is shifted in phase with respect to the solar altitude.

Since the density of the atmosphere decreases with increasing height, while the ionizing radiation cannot penetrate into the low layers, the ionization density must reach a maximum at a certain height

Declassified in Part - Sanitized Copy Approved for Release 2013/01/23 : CIA-RDP81-01043R001600090003-8

Declassified in Part - Sanitized Copy Approved for Release 2013/01/23 : CIA-RDP81-01043R001600090003-8

leading to the layered structure of the ionosphere. The existence not of a single layer but of several is explained by the complex composition of the atmosphere and by the different height distribution of different elements.

The principal ionization-recombination equation determining the state of the ionosphere has, as is well known, the following form:

$$\frac{dn_e}{dt} = q - q', \qquad (7.10)$$

where n_e is the density of ionization, q the number of electrons newly formed per second under the action of the ultraviolet radiation, and q' the number of electrons recombining per second.

Obviously the value of q is proportional to the intensity of the incident monochromatic radion W, that is, to the quantity of energy passing per second through $1cm^2$ of surface and normal to the radiation, and to the number of neutral particles $n - n_e$, and is inversely proportional to the quantity of energy w_0 which is necessary for a single event of ionization, i. e.

$$q = \gamma(n - n_e)\frac{W}{w_0}, \qquad (7.11)$$

where γ is the coefficient of photoabsorption, n the number of neutral particles per cc in the unionized atmosphere, and n_e the number of electrons per cc.

The number of q is proportional both to the number of electrons n_e and the number of positive ions n_+, i. e.

$$q' = \chi n_e n_+,$$

where χ is the coefficient of electronic recombination.

Since $n_e \approx n_+$, then

$$q' = \chi n_e^2.$$

Declassified in Part - Sanitized Copy Approved for Release 2013/01/23 : CIA-RDP81-01043R001600090003-8

Declassified in Part - Sanitized Copy Approved for Release 2013/01/23 : CIA-RDP81-01043R001600090003-8

equation 7.10 may thus be written in the form

$$\frac{dn_e}{dt} = q - xn_e^2. \qquad (7.12)$$

In addition to the direct processes of photoionization of electrons and of their recombination, a considerable number of other processes must also exist, as a result of which electrons appear and disappear; these processes include: the adhesion of electrons to a neutral particle, leading to the formation of negative ions; the separation of electrons from negative ions; and the recombination of ions. In reality, therefore, equation 7.12 is more complex in form, but, as shown by calculations, it may be brought into the same form 7.12 if alpha is taken to mean a certain effective coefficient of recombination depending on the coefficient of adhesion, separation, and recombination of ions.

Ya. L. Al'pert gives the following values of q, n_e and alpha for various layers of the ionosphere:

Layer	E in summer	F_1 in summer	F_2 in winter
n_e (electrons) per cc	1.5×10^5	3×10^5	2.5×10^6
a (cc/sec)	10^{-8}	3×10^{-9}	1.5×10^{-10}
q	200	300	800

These values relate to a time close to noon, to maximum solar activity, and measurements in the middle latitude of the northern hemisphere.

To find the height of the layer where ionization is maximum, let us now return to equation 7.11 and substitute in it, for the quantity W, the intensity of radiation beyond the boundaries of the ionosphere. For this purpose, let us consider the passage of radiation at the angle z to the vertical through a plane layer of an atmosphere of thickness dh. The losses of energy in this case will be

Declassified in Part - Sanitized Copy Approved for Release 2013/01/23 : CIA-RDP81-01043R001600090003-8

Declassified in Part - Sanitized Copy Approved for Release 2013/01/23 : CIA-RDP81-01043R001600090003-8

$$dW = \sigma (n - n_e) W \sec \approx dh.$$

On integrating this equation between the limits from height h to infinity, we obtain:

$$W = \frac{W}{\infty} e^{-\sigma \sec \approx [\int_h^{\infty} n\, dh - \int_h^{\infty} n_e dh]}.$$

If we substituted this value in the equation 7.11 we have

$$q = \sigma \frac{W_{\infty}}{W_0} (n - n_e) e^{-\sigma \sec z [\int_h^{\infty} n\, dh - \int_h^{\infty} n_e dh]}. \qquad (7.13)$$

The integrals in the exponent of the power of e represent the total number of neutral particles and electrons in a column 1 sq cm^2 cross section extending in height from level h to infinity.

The maximum number q_m and the height h_m at which this formation takes place, the finding of the maximum number q_m and the height h_m at which such formation takes place is very much simplified if it is assumed that the layer is almost un-ionized, i. e., if we neglect the value of n_e.

In that case:

$$q = \sigma \frac{W_{\infty}}{W_0} n e^{-\sigma \sec z \int_h^{\infty} n\, dh}. \qquad (7.14)$$

The number of neutral particles, n, in this equation, is determined by the barometric formula

$$n = n_0 e^{-ah}, \qquad (7.15)$$

in which the constant a has the value:

$$a = \frac{\mu g}{RT},$$

where μ is the molecular weight of the gas, R the gas constant, g the acceleration of gravity, and T the absolute temperature.

The height h_m at which q reaches its maximum value, is found from the equation

$$\frac{dq}{dh} = 0.$$

Declassified in Part - Sanitized Copy Approved for Release 2013/01/23 : CIA-RDP81-01043R001600090003-8

Declassified in Part - Sanitized Copy Approved for Release 2013/01/23 : CIA-RDP81-01043R001600090003-8

This equation gives

$$h_m = \frac{1}{a} \log \frac{\delta n_e \sec z}{a} . \qquad (7.16)$$

It follows from equation 7.15 that at this height n takes the value:

$$n_m = \frac{a}{e \sec z},$$

on substituting the expressions for h_m and n_m in equation 7.14, we obtain the value of the maximum of q:

$$q_m = \frac{a\, w_{co}}{w_0\, e \sec z} .$$

Equation 7.16 shows that the maximum formation of photoelectrons at a given zenith distance z is determined by the value of τ and the molecular weight μ of the ionized gas, since the coefficient a depends at constant temperature only on μ.

To find the height h_m of the ionized layer at which the maximum formation of electron q_m takes place, the term containing n_e in equation 7.13 must also be taken into account. In that case the condition of the maximum $\frac{\partial q}{\partial h} = 0$ yield:

$$\frac{\partial n}{\partial h} - \delta \frac{\partial n_e}{\partial h} = -\delta (n - n_e)^2 \sec z ,$$

whence as it is from this that we find the value of h_m.

But the maximum number of electrons formed is still insufficient for the appearance of a layer with maximum electron density n_e. For this it is necessary that the disappearance, i. e., the process of recombination, shall not compensate the maximum n_e. The existence of layers with a maximum of density shows that such compensation in reality does not exist.

To find the height of the layer the maximum density of ionization it is necessary to solve the equation 0 with respect

Declassified in Part - Sanitized Copy Approved for Release 2013/01/23 : CIA-RDP81-01043R001600090003-8

Declassified in Part - Sanitized Copy Approved for Release 2013/01/23 : CIA-RDP81-01043R001600090003-8

to h, but for this we must know the function of n_e, and this is found from the ionization-recombination formula of equation 7.12.

It must be borne in mind that the maximum n_e must not by any means coincide with the maximum of q.

But the solution of equation 7.12 meets with difficulties, since up to now the numerical value of the coefficients characterizing one process or another of ionization and recombination has not yet been established. As exactly the same value of the coefficient τ has been established on the basis of quantum calculations, only for atomic oxygen O_1.

5. The conductivity of the ionosphere.

Thanks to the presence of free N ions in the atmosphere, it becomes electrically conductive, and by the electronic theory, its conductivity, γ, is expressed by the relation:

$$\gamma = Ne^2 \frac{l}{2mv}, \qquad (7.17)$$

where l is the mean free path of a particle, v the mean velocity of the thermal motion of the particle, and m its mass. But if the ionized layer is in a magnetic field, then the conductivity in the direction of the field H does not remain the same as in the absence of the field, and in the direction perpendicular to the field, the conductivity γ' now becomes equal to

$$\gamma' = \frac{\gamma}{1 + \left(\frac{l}{r}\right)^2}, \qquad (7.18)$$

where r is the radius of eddying vertical motion of the electrons about the lines of force of the magnetic fields H, determine the equation

$$r = \frac{mv}{He}. \qquad (7.19)$$

Declassified in Part - Sanitized Copy Approved for Release 2013/01/23 : CIA-RDP81-01043R001600090003-8

Declassified in Part - Sanitized Copy Approved for Release 2013/01/23 : CIA-RDP81-01043R001600090003-8

The mean free path of a molecule is determined, according to the kinetic theory of gases, by the relation

$$l\sqrt{2}\pi nd^2 = 1, \qquad (7.20)$$

where n is the number of molecules for 1 cc cm^3 and d the diameter of those molecules.

Table 23 gives the values of n and l for various heights, calculated from equation 7.20 and the barometric formula 7.15.

TABLE 23

NUMBER OF MOLECULES AND MEAN FREE PATH AT VARIOUS HEIGHTS

h, km	60	100	140	200	300
n	9.9×10^{15}	1.6×10^{4}	4.4×10^{12}	2.5×10^{8}	7.7×10^{6}
l, cm	0.03	1.5	57	10^{1}	10^{7}

The radius of vertical motion of the electron depends on the magnitude on the magnetic field strength, and therefore, for particles of the moving at the same velocity, they will differ at different latitudes. It takes the greatest value at the magnetic equator by H = 0.3 0_e. Therefore, for electrons on the equator, r = 1.3 cm, while for ions r = 20 cm.

Consequently the ratio l/r for electrons takes greater values for height over 100 km, and for ions, for heights over 150 km.

Table 24 gives the values of the specific conductivities of various layers, calculated by formulas 7.17 and 7.18 in the CGS system.

It was assumed for this calculation that the velocity of thermal motion of particles v corresponds to the absolute temperature T = 360°, which, as shown by radio measurements, the E layer does have.

Declassified in Part - Sanitized Copy Approved for Release 2013/01/23 : CIA-RDP81-01043R001600090003-8

Declassified in Part - Sanitized Copy Approved for Release 2013/01/23 : CIA-RDP81-01043R001600090003-8

TABLE 24

VALUES OF THE SPECIFIC CONDUCTIVITY IN VARIOUS LAYERS

Layer	N/m	Ye_{11}	Yu_{11}	$Ye_{\perp}$	$Yu_{\perp}$
E	$0.87 \cdot 10^{32}$	$3.66 \cdot 10^{-14}$	$1.25 \cdot 10^{-11}$	$0.83 \cdot 10^{-11}$	$0.62 \cdot 10^{-11}$
F_1	$1.6 \cdot 10^{32}$	$3.3 \cdot 10^{-14}$	$2.48 \cdot 10^{-11}$	$\sim 10^{-22}$	$\sim 10^{-22}$
F_2	$6.4 \cdot 10^{32}$	$12.2 \cdot 10^{-14}$	$9.1 \cdot 10^{11}$	$\sim 10^{-23}$	$\sim 10^{-23}$

At greater heights the temperature in all probability is higher, but the experimental data on the temperature of the upper layers is still inadequate, and therefore it has been taken at one and the same for all layers. This temperature corresponds to a velocity $v = 6.8 \times 10^6$ cm/sec.

6. The sporadic layer.

Besides the E, F_1 and F_2 layers a layer is often observed at the height of the E layer with a critical frequency exceeding the critical frequency of the E layer, and sometimes even the critical frequency of the F_2 layer which points to the existence of reasons with an enhanced degree of ionization in the E layer. Since this layer is not found everywhere nor is it found at different times of the day and year, it has been termed the sporadic layer or E_s layer. The sporadic layer has been found to appear most often in the middle and high latitudes and to have a local character. In the middle latitudes the E_s layer appears more often in summer, from May to September.

Observations show that the waves reflected from the sporadic layer contain both an ordinary and an extraordinary wave. This gives grounds for assuming that the sporadic layer has an electronic structure but the nature of its origin has not yet been elucidated.

7. Tidal phenomena in the ionosphere.

Declassified in Part - Sanitized Copy Approved for Release 2013/01/23 : CIA-RDP81-01043R001600090003-8

Declassified in Part - Sanitized Copy Approved for Release 2013/01/23 : CIA-RDP81-01043R001600090003-8

Observations on the reflection of radio signals from the E layer have allowed the establishment in this layer of the existence of semidiurnal fluctuations at height corresponding to the tidal phenomena caused by the moon. The amplitude of such fluctuations, as shown by the observations, reach 1 km, and the maximum occurs 3/4 hour before the superior combination of the moon, as will be seen from Figure 106 which represents the results of direct observations of the fluctuations of the E layer.

On the earth's surface tidal phenomena of the atmosphere caused by the moon are also observed, but these phenomena are manifested in the form of semidiurnal fluctuations of the atmospheric pressure p with amplitude of about 0.0000115 p.

If the fluctuations of height in the E layer with amplitude $\Delta h = 1$ km are converted into fluctuations of pressure, then, according to the barometric formula of equation 7.15, we obtain

$$\Delta p = pa \Delta h = 0.08\ p,$$

i. e., 7,000 times greater than the relative fluctuations at the earth's surface.

Recent investigations show the existence of such fluctuations not only of height but also of the critical frequency f, i. e., the density of ionization. Figure 107 shows the semidiurnal tidal fluctuations of the equivalent height and critical frequency in the F_2 layer. It will be seen that the amplitude of the fluctuations of height in the F_2 layer are twice those in the E layer, and that in general, as shown by observations, the amplitude of both Δh, and Δf increase with the height of the layer.

The lunar tidal motions of the atmosphere may be regarded as the propagations of plane waves in a medium with a certain coefficient

Declassified in Part - Sanitized Copy Approved for Release 2013/01/23 : CIA-RDP81-01043R001600090003-8

Declassified in Part - Sanitized Copy Approved for Release 2013/01/23 : CIA-RDP81-01043R001600090003-8

of refraction. If such waves at a certain height meet a region of the atmosphere where the index of refraction is equal to zero or has become negative then these waves will be reflected and an oscillatory motion will be set up between the earth's surface and this region. The region of the temperature maximum at a height of the order 15-30 km is believed to be such a reflective region for oscillations at the earth's surface.

To explain the lunar fluctuations in the E layer it is assumed that in addition to the second region of temperature minimum at height 80 km, there is also a third region at height 140-160 km and the fluctuations here take place between the second and third regions.

The existence of fluctuating motions in the ionosphere is very important for the construction of the theory of the diurnal variations of the magnetic field of the earth since one of the possibilities of explaining such variations is the motion of ionized layers in the earth's magnetic field.

Section 2. Theories of the Diurnal Variations

The existence of the conducting layers of the atmosphere at heights of 100 to 300 km gives ground for asserting confidently that cause of the diurnal variations and in general of all the magnetic variations are the electric currents in these layers. But to explain the causes of these currents we still have no well established fact which would allow us to take one explanation or another and consider it correct. All the existing theories of the diurnal variations thus reduce to a choice of the mechanism of the origin of the current each of which may claim a more or less degree of authenticity.

Up to now there have been 3 principal theories of the diurnal variations: the theory of the atmospheric dynamo proposed in 1872

Declassified in Part - Sanitized Copy Approved for Release 2013/01/23 : CIA-RDP81-01043R001600090003-8

Declassified in Part - Sanitized Copy Approved for Release 2013/01/23 : CIA-RDP81-01043R001600090003-8

and worked out in detail somewhat later (1889), the diamagnetic theory (1928), and the theory of drift currents (1929).

Recently in connection with the work of I. Ye. Tamm (cf. infra) the diamagnetic theory has already lost its importance, while the theory of the atmospheric dynamo as a result of the periodic motions movement discovered in the ionosphere has acquired a higher degree of credibility.

The theory of drift currents thanks to the same work of Tamm, has found justification and may on the same level as the theory of the atmospheric dynamo claim a certain standing of credibility. It is therefore necessary to dwell on each of these theories and to point out their shortcomings.

1. The theory of the atmospheric dynamo. This theory proposed by Stewart Shuster (Bibl 55) is based on the principle of the induction of electromotive force on the motion of a conductive in the earth's magnetic field in a manner similar to what takes place in a dynamo and for this reason the theory is called that of the atmospheric dynamo. Since the high layers of the atmosphere possess conductivity, it follows that when they move in the magnetic field of the earth H, an electric field perpendicular to H and to its direction of motion is produced and its strength is determined by the Faraday law:

$$E = [uH],$$

where us is the velocity of motion of the ionized layer. Under the influence of the field E a current whose direction is perpendicular to u and H horizon in the atmosphere while the density j is determined by the equation

$$j = \gamma' E,$$

where γ' is the conductivity determined by equation 7.18 since j is directed perpendicularly to H.

Declassified in Part - Sanitized Copy Approved for Release 2013/01/23 : CIA-RDP81-01043R001600090003-8

Declassified in Part - Sanitized Copy Approved for Release 2013/01/23 : CIA-RDP81-01043R001600090003-8

By substituting for γ' its value taken from equation 7.18 we obtain:

$$j = \frac{Ne^2}{2mv} \cdot \frac{l}{1 + \left(\frac{l}{r}\right)^2} \text{ [uH]}.$$

Shuster assumed that the velocity u was due to the horizontal displacement of the upper layers of the atmosphere under the influence of the diurnal fluctuations of atmospheric pressure observed on the surface of the earth.

Barometric observations show that the pressure has 2 fluctuations during the course of the day: a regular one with a semidiurnal period and an amplitude of 1.2 mm, and a less regular one with a diurnal period and an amplitude of 0.3 mm. The causes of these fluctuations may be either the tidal or the thermal effect. The air currents leaving the high pressure regions located in the meridian at the equator form electric currents of the same character as shown in Figure 73. During the daytime the currents moving northward in the vertical magnetic field Z, create currents directed westward which as a result of the reduction in conductivity in the atmosphere with increasing latitude lead to the formation of closed currents causing the diurnal variations of the magnetic field.

Investigations have shown that the electric currents obtained as a result of the motion of the atmosphere owing to the diurnal variation of barometric pressure although they do in their character coincide with those calculated on the basis of magnetic observations are still markedly different from them in phase. Thus the extreme values of the northern component are observed from 10 to 11 hours (Figure 69) while according to this theory they should occur between 14 and 16 hours.

Such a disagreement may be explained by the horizontal displacements in the upper layers due to the fluctuations of the barometric pressure are assumed to be the same as the displacements observed on the surface of the earth, which might not in reality be the case at all.

Declassified in Part - Sanitized Copy Approved for Release 2013/01/23 : CIA-RDP81-01043R001600090003-8

Declassified in Part - Sanitized Copy Approved for Release 2013/01/23 : CIA-RDP81-01043R001600090003-8

The contradiction with theory was found in the value of the conductivity. If the velocity u is considered a consequence of the diurnal barometric fluctuations, the amplitude of which amounts to 1 mm, then for the equator it should have a value of the order of 30 cm/sec.

On the basis of the current distribution map (Figure 73) the strength of the current flowing through a cross section of the layer 1 cm wide and with the width equal to the thickness of the layer is equal to 3×10^{-5} CGSμ, while the vertical component of the magnetic field Z at latitude 30° equal to 0.3 O_e, and thus the conductivity of a vertical column of the ionosphere 1 cm^2 in cross section and with the height equal to the thickness of the layer is determined by the equation:

$$\gamma = \frac{3 \cdot 10^{-5}}{30 \cdot 0.3} = 3 \cdot 10^{-3} \text{ CGS}\mu.$$

The thickness of the E layer is of the order of 50 km and therefore the specific conductivity of the E layer should be

$$\gamma \sim 10^{-11} \text{ CGS}\mu.$$

On comparing this value with the values for the conductivity in Table 24 we see that they agree with the value of the ionic conductivity but are a thousand times smaller than the electronic conductivity. For this reason in order to reconcile the theory with the observations it would be necessary to assume either the existence of a predominance of ions in the E layer, or the existence of velocities of displacement of the ionized masses of the atmosphere that are many times as great as the velocities observed at the surface of the earth (30 cm/sec).

At the present time neither of these possibilities are excluded, since occasionally we do succeed in observing the splitting

Declassified in Part - Sanitized Copy Approved for Release 2013/01/23 : CIA-RDP81-01043R001600090003-8

Declassified in Part - Sanitized Copy Approved for Release 2013/01/23 : CIA-RDP81-01043R001600090003-8

of a reflected ray in the E layer into 2, an ordinary and an extraordinary with a frequency difference corresponding to the ionic nature of the layer. But the existence of fluctuations of pressure in the E layer 7,000 times as great and the fluctuations at y the surface of the earth give grounds for considering that the velocity of displacement must also be many times greater than 30 cm/sec.

2. The theory of the drift current (Bibl 56). According to this theory the charged particles in the region of long free paths, moving in the magnetic and gravitational fields of the earth must experience a translatory motion (drift) in a direction perpendicular to the force of gravity mg and to the magnetic field H. The velocity of this drift would be:

$$u = \frac{mg}{eH} \sin\phi, \qquad (7.21)$$

where ϕ is the angle between H and the force of the gravity or the vertical. Here H and e must be expressed in absolute electromagnetic units.

Since the magnetic field of the earth may be considered in first approximation as the field of an elementary magnet its field strength H may be represented in the form:

$$H = H_0 \sqrt{1 + 3 \sin^2 \varphi}, \qquad (7.22)$$

where H_0 is the field strength at the equator and φ is the latitude.

Moreover for an elementary magnet the following relation holds true:

$$\cot \varphi = 2 \tan \phi .$$

For this reason expressing sin ϕ in terms of tan ϕ in equation 7.21 and substituting tan ϕ according to the following formula, we shall have

$$u = \frac{mg}{eH} \cdot \frac{\cos \varphi}{\sqrt{1 + 3 \sin^2 \varphi}}.$$

Declassified in Part - Sanitized Copy Approved for Release 2013/01/23 : CIA-RDP81-01043R001600090003-8

Declassified in Part - Sanitized Copy Approved for Release 2013/01/23 : CIA-RDP81-01043R001600090003-8

On substituting for H its expression in equation 7.22, we obtain:

$$u = \frac{mg}{eH_0} \cdot \frac{\cos\varphi}{1 + 3\sin^2\varphi}.$$

Thence the velocity of drift of the electrons at the pole, $u_{90} = 0$, and at the equator $u_0 = 1.2 10^{-4}$ cm/sec, while the drift of the ions of the atmosphere, the mass of which $m = 5 \times 10^{-23}$ g, is zero at the pole and 10.2 cm/sec at the equator.

The current density is obviously expressed as:

$$j = eNu = \frac{mgN}{H_0} \cdot \frac{\cos\varphi}{1 + 3\sin^2\varphi} \text{ CGS } \mu.$$

Since both electrons and ions participate in the formation of the drift currents, it follows that if the number of ions is considered equal to the number of electrons, and the density of ionization in the upper layers $N = 10^{-6}$, we have for the density of the dirft current on the equator the value $j = 1.7 \times 10^{-13}$ CGS μ.

Such a drift, or, to put it differently, displacement of charged particles, produces a current in the direction from west to east, since the magnetic field is directed from south to north. The drift of positive ions to the east causes the accumulation of positive charges on the morning side, while the drift of negative ions causes their accumulation on the evening side. As a result, in the region of long free paths an electrical field arises which is directed toward the west and which, however, may be electrically connected with the lower region of short free paths, since the ions may move freely under the influence of the force of gravity along the lines of force of the magnetic fields, especially around the pole. For this reason, in the lower part of parts currents arise which with a corresponding distribution of activity may form a

Declassified in Part - Sanitized Copy Approved for Release 2013/01/23 : CIA-RDP81-01043R001600090003-8

Declassified in Part - Sanitized Copy Approved for Release 2013/01/23 : CIA-RDP81-01043R001600090003-8

system of currents similar to the one shown in Figure 73. The calculation of the conductivity necessary for the formation of drift currents corresponding to the calculated system of currents shown in Figure 73 indicates that the conductivity may be considered considerably lower than that required by the diamagnetic theory.

The theory of drift currents, however, encounters obstacles in explaining the forenoon extreme extremum of the northern and eastern components, and also in explaining the intensity of the observed variations. In addition some authors have expressed doubts that drift currents could lead to the formation of so complex a system of currents as the theory requires.

I. Ye. Tamm (Bibl. 57) who has given a criticism of the drift current theory and for the first time pointed out the complete unsoundness of this theory if we start out from the same propositions that were established by Chapman. According to Chapman's belief, in an equilibrium system, ionized gas consists of an aggregate of ions which are free and independent in their motion and which may, in the absence of a magnetic field, fall downwards under the action of the force of gravity. In reality, however, in the equilibrium state of the atmosphere, the own weight of the ions is balanced by the partial pressure of the ion gas p', which is defined by the equation

$$p' = kTN,$$

where T is the absolute temperature, N the density of ions, i. e., their number in unit volume, and K is the Boltzman constant. For this reason, in the equilibrium state of the atmosphere, when the density of the ion is determined by the barometric formula, there can be no drift, and, consequently, the Chapman theory, just like the diamagnetic theory, is a simple misunderstanding.

Declassified in Part - Sanitized Copy Approved for Release 2013/01/23 : CIA-RDP81-01043R001600090003-8

Declassified in Part - Sanitized Copy Approved for Release 2013/01/23 : CIA-RDP81-01043R001600090003-8

But in this same work, Tamm also pointed out the possibility of retaining the drift current theory explains the diurnal variation if we start out not from the equilibrium condition of the ionosphere, but from the existence in it of a "nonuniform" distribution of densities that is, of densities varying otherwise than by the barometric formula. Such a distribution, in Tamm's opinion, corresponds more to the real conditions of the state of the ionosphere, which also makes possible the existence of drift currents analogous to those of Chapman. Tamm gives a derivation of the formula for the density of the drift current on thebbasis of a statistical model of the ionosphere obtained by solving the Boltzman kinetic equation. Since in its general form the Boltzman equation is very complex, Tamm introduced 2 assumptions to simplify it: first that the distributions of ions and electrons by velocities in each element of volume of the ionosphere differs little from the Maxwell distribution corresponding to the temperature T, and secondly that the ordered motion of ions of the atmosphere is quasi stationary, that is, at each given moment the motion is determined by the instantaneous distribution of the ion density and the temperature, as a result of which the derivatives of density and temperature with respect to time may be neglected and the density and temperature considered assigned functions of the coordinates.

Under such assumptions, the kinetic equation of the stationary motion of each species of ion will have the form:

$$v \operatorname{grad} f + \left(g + \frac{e}{m} E + \frac{e}{mc} [vH]\right) \operatorname{grad}_v f = \beta f, \qquad (7.23)$$

where v is the velocity of motion of the ions, g the acceleration of gravity, E the electric field strength, H the magnetic field strength, e/m the charge-ratio, f a function of the distribution of ions, which differs from the Maxwell function by the small quantity Φf_o, i. e.,

Declassified in Part - Sanitized Copy Approved for Release 2013/01/23 : CIA-RDP81-01043R001600090003-8

Declassified in Part - Sanitized Copy Approved for Release 2013/01/23 : CIA-RDP81-01043R001600090003-8

$$f = f_0 (1 + \phi),$$

while

$$f_0 = N\beta^3\pi^{3/2} 2_e - \beta^2 v^2, \text{ and } = \frac{m}{2kT}.$$

The term P_f, taking account of the collisions between the ions themselves and with neutral and between ions and neutral molecules, is assumed to be proportional to the deviation of the distribution function f from its equilibrium value f_o, i. e.,

$$Pf \approx \frac{v}{\lambda} (f - f_0) = - \frac{v}{\lambda} f_0 \phi.$$

where λ is the length of the free path.

After substituting the values f, f_0 and P_f, equation 7.23 now takes the form:

$$\left(\frac{e}{mc} [vH] \text{ grad}_r \phi \right) + \frac{\phi}{\lambda} = [vq],$$

where

$$q = \beta^2 (2a - \beta^2 v^2 b);$$

$$a = g + \frac{e}{m} E - \frac{1}{2\beta^2} \text{ grad ln } \left(\frac{N}{T^{3/2}} \right), \quad b = \frac{\text{grad } T}{\beta^2 T}.$$

The solution of this differantial equation is in the following form:

$$\phi = \frac{\lambda \beta}{s^2 + \beta^2 v^2} \left[\beta v (vq_\perp) + \frac{s}{H} v [qH] + \frac{\lambda}{v} (vq_\parallel) \right],$$

where $q_\perp$ is the vector perpendicular to the magnetic field H, $q_\parallel$ is the vector parallel to that field, and H is the ratio between the free path and the diameter of the circular orbit of a particle in the magnetic field, i. e.

$$s = \frac{\lambda}{2r} = \frac{e \lambda H}{2c \sqrt{2mkT}}.$$

The density of the current formed by the motion of charges of one sign is determined by the laws of statistics as:

$$j = e \int v f_0 (1 + \phi) dv_x \, dv_y \, dv_z.$$

Declassified in Part - Sanitized Copy Approved for Release 2013/01/23 : CIA-RDP81-01043R001600090003-8

Declassified in Part - Sanitized Copy Approved for Release 2013/01/23 : CIA-RDP81-01043R001600090003-8

Integration of this expression on substitution of the value of φ is possible only in the 2 limiting cases when $\lambda \ll 2r$ or also, when λ is $\gg 2r$. The former case represents the motion of ions in the lower ionosphere, while the second case represents that motion in the upper ionosphere.

For the case $\lambda \ll 2r$, we obtain:

$$j_{\parallel} = \frac{4e N_4 \sqrt{m}}{3\sqrt{2\pi k T}} \left(g + \frac{e}{m} E - \frac{kT}{m} \cdot \frac{\text{grad } N}{N} \quad \frac{k}{2m} \text{ grad } T\right).$$

For the case, however, where $\lambda \gg 2r$:

$$j_{\perp} = \frac{c}{H^2} [[(Nmg + NeE - \text{grad } (kTN)]H].$$

Since the total current density is equal to the sum of the currents of positive and negative ions, i. e.

$$j = j_+ + j_- ,$$

then

$$j_{\parallel} = \frac{4e^2 N}{3\sqrt{\pi k t}} \left(\frac{\lambda_+}{\sqrt{m_+}} + \frac{\lambda_-}{\sqrt{m_-}}\right) E \quad (\lambda \ll 2r)$$

$$j_{\perp} = \frac{c}{H^2} [[(Nmg - \text{grad } (kTN)] H] \quad (\lambda \gg 2r). \qquad (7.24)$$

In the presence of wind, i. e., the motion of the ion with respect to the earth's surface with the velocity u, the vector $\frac{uH}{c}$, is added to the vector E in the first of these equations, while the second equation remains unchanged.

The factor before E in the first equation represents the electrical conductivity of the ionized gas γ and for this reason the first equation in the presence of wind, may be written as follows:

$$j_{\parallel} = \gamma \left(E + \frac{[uH]}{c}\right) \qquad (\lambda \ll 2r).$$

Declassified in Part - Sanitized Copy Approved for Release 2013/01/23 : CIA-RDP81-01043R001600090003-8

Declassified in Part - Sanitized Copy Approved for Release 2013/01/23 : CIA-RDP81-01043R001600090003-8

It is easy to see that if the term grad p' is rejected in equation 7.24, it then passes over into the Chapman formula for the drift current at $\varphi = 0$, but this is possible in the case when the partial pressure does not vary with the height. For the equilibrium state, however, the weight of ions in unit volume N_{mg} is balanced by the gradient of partial pressure and, consequently $f_{\perp} = 0$.

In Tamm's opinion, the distribution of ions in the rear atmosphere differs so much from the equilibrium distribution that the difference N_{mg} - grad p' can hardly be distinguished from the first term N_{mg} .

In this way, the theory of the drift currents in its modified form, exactly as with the dynamo theory, cannot be refuted and must be accepted for the explanation of the system of currents that cause the diurnal variations, but at the same time it still requires further developments, which Tamm himself admits.

It must be remarked that the Tamm theory enables us to explain the occurrence of the forenoon maximum of the horizontal component, which the Chapman theory could not do. More specfically, although the maximum number and weight of ions in N_{mg} should occur after noon, the maximum current may also occur before noon, since the maximum of the partial pressure of ions at the upper boundary of the upper ionosphere may occur after the maximum of the total ionization of this part of the ionosphere.

On comparing these 2 theories, it may be said that neither of them explains completely all observed facts and in some cases even contradict them. But still owing to the successes that have recently been attained in the experimental study of the ionosphere which have

Declassified in Part - Sanitized Copy Approved for Release 2013/01/23 : CIA-RDP81-01043R001600090003-8

Declassified in Part - Sanitized Copy Approved for Release 2013/01/23 : CIA-RDP81-01043R001600090003-8

led to the establishment in them of periodic horizontal displacements and of the distance of a system of currents at height 100-110 km, and may be assumed that the dynamo affect undoubtedly plays a part in the formation of the system of currents causing the diurnal variations. This, however does not exclude the possibility of the simultaneous existence of the drift current effect as well, which may also participate in the formation of these currents.

The rapid development of our knowledge of the ionosphere will soon make it possible for us to solve the question as to which of these theories is correct and to eliminate the contradictions in them.

Section 3. Basic Propositions of the Theory of the Aurora and Magnetic Disturbance

The close connection of the aurora with magnetic disturbances forces us to seek the causes that might be common to both phenomena. It has been remarked above that the magnetic activity that characterizes the method by which the magnetic disturbances are characterized is well correlated with the solar activity. For this reason all present day theories of the magnetic disturbances are at the same time theories of the aurora as well, and start out with the assumption that their cause is energy radiated by the sun.

Since the energy of the magnetic field w in unit volume (cc) is expressed by the formula

$$w = \frac{H^2_T}{8\pi},$$

then the increment of energy dw when the field strength H_T varies by the small quantity dH_T will obviously be

$$dw = \frac{H_T dH_T}{4\pi}.$$

Declassified in Part - Sanitized Copy Approved for Release 2013/01/23 : CIA-RDP81-01043R001600090003-8

Declassified in Part - Sanitized Copy Approved for Release 2013/01/23 : CIA-RDP81-01043R001600090003-8

Calculations by this formula give a value of $dw = 10^{-5}$ erg/cm^3 for the value of the mean density of the energy. The total value of this energy Δw, however is obtained by multiplying its density by the volume of the earth and the space around the earth, which gives $\Delta w = 3 \times 10^{22}$ ergs. The duration of a storm for which the energy density has been calculated was 28 hours, and therefore, by dividing the value of the total energy Δw by the number of seconds in 28 hours we obtain the increment of the total energy of the magnetic field of the earth per seconds, equal to 3×10^{17} erg/sec. But the energy received by the earth from the sun amounts to 2×10^{24} erg/sec. In this way, only a negligible portion of the total energy radiated by the sun is required for the formation of the energy of the magnetic storms

The reason why this part of the solar energy is converted into magnetic energy only at certain moments of time is connected with the phenomena in the active regions of the sun, such as spots, prominences, etc.

Observations of the sun show that these moments the intensity of the ultraviolet radiation is markedly increased, i. e., it is as though the temperature of the sun were increased. It is therefore assumed that during the periods of increased solar activity, the active regions, where the sunspots are, emit an intense ultraviolet radiation and at the same time eject a large number of charged particles of both signs, electrons, ions, protons, and others.

Thus, for example, if 0.0001 part of the solar surface radiated as a black body at absolute temperature $T = 30.000^{\circ}$, then the solar constant would increase by 0.74%, but the energy at wavelengths 3500, 4000, 5000 and 6000 A would increase respectively by 3.2, 1.7, 0.75 and 0.032%. This additional energy would be entirely sufficient for the formation of the magnetic storms.

Declassified in Part - Sanitized Copy Approved for Release 2013/01/23 : CIA-RDP81-01043R001600090003-8

Declassified in Part - Sanitized Copy Approved for Release 2013/01/23 : CIA-RDP81-01043R001600090003-8

The repetition of magnetic disturbances at intervals of 27 days, equal to the period of rotation of the sun about its axis, furnished reason to assume that the radiation of the active regions takes place either in the form of a narrow beam rotating together with the solar disc, or in the form of a periodically acting wide beam. In this case it must be recognized that it is mainly the corpuscular radiation of the sun that participates in the formation of the magnetic storm and the aurora, although attempts have been made to attribute them mainly to the ultraviolet part of the solar spectrum. Such attempts, however have not led to positive results, and therefore the theory of the aurora based on the ultraviolet radiation of the active regions of the sun has at the present time lost its significance.

Section 4. The Motion of a Charge* in the Magnetic Field of the Dipole

(*ZARYAD, charge, used in this section in the sense of "charged particle." Translator.)

The fact that the aurora takes place mainly in the high latitudes close to the magnetic pole, and the direction of their streamers coincides with the direction of the lines of force from the earth's magnetic field, forces us to seek the course of the aurora in the motion of charges in the high layers of the atmosphere under the action of the earth's magnetic field.

Leaving for the time being the question open as to how and whence these charges appear let us consider the motion of the charges in the earth's magnetic field, having the initial velocity v, under the assumption that the charges do not interact with each other. In this case the problem reduces down to the consideration of the motion of one charge, an electron or a proton. The solution of this problem

Declassified in Part - Sanitized Copy Approved for Release 2013/01/23 : CIA-RDP81-01043R001600090003-8

Declassified in Part - Sanitized Copy Approved for Release 2013/01/23 : CIA-RDP81-01043R001600090003-8

given by Stoermer (Bibl 51) at the beginning of the present century, consists in the solution of the differential equation of motion of a charge in the inhomogenous magnetic field of the earth, taken as the field of a dipole.

The equation of motion of a charged particle in the magnetic field has the form:

$$m \frac{d^2 r}{dr^2} = \frac{e}{c} [\frac{dr}{dr} H], \qquad (7.25)$$

where e is the charge of the particle, m its mass, and r the radius vector produced from the origin of coordinates.

If the origin of coordinates coincides with the center of the dipole, and the axis is directed along the axis of the dipole, the magnetic moment of which is m, then the field strength H is expressed as follows:

$$H = \frac{3Mz}{r^2} r - \frac{M}{r^2}.$$

As a result of this, equation 7.25 takes the form

$$\frac{d^2 r}{dt^2} = \frac{Me}{mcr^3} [\frac{dr}{dt} (3zr - r^2 \frac{z}{z})].$$

Introducing the new variable ds = vdt, where v is the velocity of motion of the charge and denoting Me/mcv = k^2, we obtain the following 3 equations scaler form:

$$\frac{1}{k^2} \cdot \frac{d^2 x}{ds^2} = \frac{3z^2 - r^4}{r^5} \cdot \frac{dy}{ds} - \frac{3yz}{r^5} \cdot \frac{dz}{ds},$$

$$\frac{1}{k^2} \cdot \frac{d^2 y}{ds^2} = \frac{3xz}{r^5} \cdot \frac{dz}{ds} - \frac{3z^2 - r^2}{r^5} \cdot \frac{dx}{ds},$$

$$\frac{1}{k^2} \cdot \frac{d^2 x}{ds^2} = \frac{3z}{r^5} (y \frac{dx}{ds} - x \frac{dy}{ds}).$$

Declassified in Part - Sanitized Copy Approved for Release 2013/01/23 : CIA-RDP81-01043R001600090003-8

Declassified in Part - Sanitized Copy Approved for Release 2013/01/23 : CIA-RDP81-01043R001600090003-8

Multiply the first equation by x and the second by y and add them, term by term; in exactly the same way, multiply this first equation by y and the second by x and subtract one from the other. As a result, the equations now take the following form:

$$\frac{1}{k^2}\left[x\frac{d^2x}{ds^2} + y\frac{d^2y}{ds^2}\right] = \frac{3z^2 - r^2}{r^5}\left[x\frac{dy}{ds} - y\frac{dx}{ds}\right]$$

$$\frac{1}{k^2}\left[y\frac{d^2x}{ds^2} - x\frac{d^2y}{ds^2}\right] = \frac{3z^2 - r^2}{r^5}\left[y\frac{dy}{ds} + x\frac{dx}{ds}\right] - 3z\frac{dz}{ds}(x^2 + y^2),$$

$$\frac{1}{k^2}\frac{d^2z}{ds^2} = \frac{3z}{r^5}\left(y\frac{dx}{ds} - x\frac{dy}{ds}\right). \qquad (7.26)$$

Project the vector r on the plane xy and denote its projection by R. Then

$$r = R\cos\varphi, \quad y = R\sin\varphi,$$

where φ is the angle between R and the x axis (Figure 108). By differentiating this expression with respect to s and performing the subtraction and addition of the derivatives, then, after multiplying them by y and x, and then by x and y, we obtain

$$x\frac{dy}{ds} - y\frac{dx}{ds} = R^2\frac{d\varphi}{ds}; \quad x\frac{dx}{ds} + y\frac{dy}{ds} = R\frac{dR}{ds}.$$

On differentiating a second time with respect to s and performing the same operation of subtraction and addition, we shall have:

$$x\frac{d^2y}{ds^2} - y\frac{d^2x}{ds^2} = \frac{d}{ds}\left(R^2\frac{d\varphi}{ds}\right),$$

$$x\frac{d^2x}{ds^2} + y\frac{d^2y}{ds^2} = R\frac{d^2R}{ds^2} - R^2\left(\frac{d\varphi}{ds}\right)^2.$$

The constant k may be taken as equal to unity since it is equivalent to all lengths being measured in units k.

On substituting these values of the sums and differences in equation 7.26 and setting k = 1, we have:

Declassified in Part - Sanitized Copy Approved for Release 2013/01/23 : CIA-RDP81-01043R001600090003-8

Declassified in Part - Sanitized Copy Approved for Release 2013/01/23 : CIA-RDP81-01043R001600090003-8

$$\frac{\partial^2 R}{\partial s^2} = R\left(\frac{\partial \varphi}{\partial s}\right)^2 - R\,\frac{3z^2 - r^2}{r^5}\,\frac{\partial z}{\partial s},$$

$$\frac{\partial}{\partial s}\left(R^2\,\frac{\partial \varphi}{\partial s}\right) = \frac{3zR^2}{r^5}\cdot\frac{\partial z}{\partial s} - R\,\frac{3z^2 - r^2}{r^5}\cdot\frac{\partial R}{\partial s}, \qquad (7.27)$$

$$\frac{\partial^2 z}{\partial s^2} = \frac{3z}{r^5}\,R^2\,\frac{\partial R}{\partial s}.$$

Remembering that $r^2 = R^2 + z^2$, it is easy to show that the following equations hold:

$$\frac{\partial}{\partial z}\left(\frac{R^2}{r^3}\right) = -\frac{3z\,R^2}{r^5}; \quad \frac{\partial}{\partial R}\left(\frac{R^2}{r^3}\right) = R\,\frac{3z^2 - r^2}{r^5}. \qquad (7.28)$$

The second equation of the preceding system is thus brought into the form:

$$\frac{\partial}{\partial s}\left(R^2\,\frac{\partial \varphi}{\partial s}\right) = -\frac{\partial}{\partial z}\left(\frac{R^2}{r^3}\right)\frac{dz}{ds} - \frac{\partial}{\partial R}\left(\frac{R^2}{r^3}\right)\frac{\partial R}{\partial s}, \qquad (7.29)$$

or, after integration:

$$R^2\,\frac{\partial \varphi}{\partial s} = -\left(2\gamma + \frac{R2}{r^3}\right), \qquad (7.30)$$

where γ is the integration constant varying within the limits from $-\infty$ to $+\infty$.

On substituting the derivative $\frac{\partial \varphi}{\partial s}$ in the first and third equations by the system 7.27 we obtain from equation 7.29 and 7.30

$$\frac{\partial^2 R}{\partial s^2} = \left(\frac{2\gamma}{R} + \frac{R}{r^3}\right)\left(\frac{2\gamma}{R^2} + \frac{3R^2}{r^3} - \frac{1}{r^3}\right),$$
$$\frac{\partial^2 z}{\partial s^2} = \left(\frac{2\gamma}{R} + \frac{R}{r^3}\right)\frac{3Rz}{r^3}. \qquad (7.31)$$

Further, since ds is an element of the arc of the trajectory of the particle, then, by using its expression

$$ds^2 = dR^2 + dz^2 + R^2\,d\varphi^2,$$

we may write

$$1 - R^2\left(\frac{\partial \varphi}{\partial s}\right)^2 = \left(\frac{\partial R}{\partial s}\right)^2 + \left(\frac{\partial z}{\partial s}\right)^2,$$

Declassified in Part - Sanitized Copy Approved for Release 2013/01/23 : CIA-RDP81-01043R001600090003-8

Declassified in Part - Sanitized Copy Approved for Release 2013/01/23 : CIA-RDP81-01043R001600090003-8

or, substituting $\partial\varphi/\partial s$ from equation 7.30:

$$\left(\frac{\partial R}{\partial s}\right)^2 + \left(\frac{\partial z}{\partial s}\right)^2 = 1 - \left(\frac{2\gamma}{R} + \frac{R}{r^3}\right)^2 = Q. \qquad (7.32)$$

It is not hard to show that the righthand sides of equation 7.31 represent respectively the partial derivatives with respect to R and z of the function Q, separated into 2, and thus the system of equations in equation 7.27 may be replaced by the system:

$$\frac{\partial^2 R}{\partial s^2} = \frac{1}{2}\cdot\frac{\partial Q}{\partial R}; \quad \frac{\partial^2 z}{\partial s^2} = \frac{1}{2}\cdot\frac{\partial Q}{\partial z}; \qquad (7.33)$$

$$Q = \left(\frac{\partial R}{\partial s}\right)^2 + \left(\frac{\partial z}{\partial s}\right)^2. \qquad (7.34)$$

Consequently the integration of the system of equation 7.25 reduces down to the integration of equation 7.33 and 7.34.

Equation 7.33 shows that they determine the trajectory of the motion of a charge in the plane passing through the axis z and the radius vector R. The equation 7.34 however determines the rotation of this plane as a whole about the z axis.

Thus the problem of determining the motion of a charge in space reduces to 2 problems: determination of its motion in the plane zR and of the rotation of this plane about the z axis.

However, without solving the problem, but merely using the properties of the function Q, it is easy to find those regions of space in which the charge may move.

Since, according to equation 7.34, Q cannot assume negative values, the coordinates of the charge must always satisfy the inequality:

$$-1 \leqslant \frac{2}{R} + \frac{R}{r^2} \leqslant 1$$

Declassified in Part - Sanitized Copy Approved for Release 2013/01/23 : CIA-RDP81-01043R001600090003-8

Declassified in Part - Sanitized Copy Approved for Release 2013/01/23 : CIA-RDP81-01043R001600090003-8

or, substituting $\partial\varphi/\partial s$ from equation 7.30:

$$\left(\frac{\partial R}{\partial s}\right)^2 + \left(\frac{\partial z}{\partial s}\right)^2 = 1 - \left(\frac{2\gamma}{R} + \frac{R}{r^3}\right)^2 = Q. \tag{7.32}$$

It is not hard to show that the righthand sides of equation 7.31 represent respectively the partial derivatives with respect to R and z of the function Q, separated into 2, and thus the system of equations in equation 7.27 may be replaced by the system:

$$\frac{\partial^2 R}{\partial s^2} = \frac{1}{2} \cdot \frac{\partial Q}{\partial R}; \quad \frac{\partial^2 z}{\partial s^2} = \frac{1}{2} \cdot \frac{\partial Q}{\partial z}; \tag{7.33}$$

$$\dot{\varphi} = \left(\frac{\partial R}{\partial s}\right)^2 + \left(\frac{\partial z}{\partial s}\right)^2. \tag{7.34}$$

Consequently the integration of the system of equation 7.25 reduces down to the integration of equation 7.33 and 7.34.

Equation 7.33 shows that they determine the trajectory of the motion of a charge in the plane passing through the axis z and the radius vector R. The equation 7.34 however determines the rotation of this plane as a whole about the z axis.

Thus the problem of determining the motion of a charge in space reduces to 2 problems: determination of its motion in the plane zR and of the rotation of this plane about the z axis.

However, without solving the problem, but merely using the properties of the function Q, it is easy to find those regions of space in which the charge may move.

Since, according to equation 7.34, Q cannot assume negative values, the coordinates of the charge must always satisfy the inequality:

$$-1 \leqslant \frac{2}{R} + \frac{R}{r^2} \leqslant 1$$

Declassified in Part - Sanitized Copy Approved for Release 2013/01/23 : CIA-RDP81-01043R001600090003-8

Declassified in Part - Sanitized Copy Approved for Release 2013/01/23 : CIA-RDP81-01043R001600090003-8

all the equation

$$\frac{2\gamma}{R} + \frac{R}{r^3} = p, \qquad (7.35)$$

where p is a number less in absolute value than unity.

Consequently, for each value of the arbitrary constant γ_k there exists a region of space bounded on one side by the surface obtained by the rotation of the curve defined by the equation

$$\frac{2\gamma_k}{R} + \frac{R}{r^3} = 1,$$

and by a similar surface defined by the equation:

$$\frac{2\gamma_k}{R} + \frac{R}{r^3} = -1.$$

this space, out of which the charge, at a given value of γ_k, cannot go, was denoted by Q_γ by Stoermer.

The curve defined by equation 7.35 may be represented in polar coordinates if $R = r\cos\varphi$ is substituted in it and it is solved with respect to r, giving:

$$r = \frac{\gamma \pm \sqrt{\gamma^2 + p\cos^2\varphi}}{p\cos\varphi}. \qquad (7.36)$$

Stoermer gives a complete analysis of these curves and the regions corresponding to them. He reached the following conclusions.

If $\gamma > 0$, not a single charge will be able to penetrate into the region near the dipole. If $\gamma < -1$, then for each γ there are 2 regions in which the charges may move, one of them laying outside the region of the dipole so that the charges arriving from an infinite distance do not reach the dipole, while a second, a narrow region, does pass through the dipole. And, finally, if $-1 < \gamma < 0$, then both these regions merge into one and a charge coming from infinite distance may reach the dipole. Figure 109 shows a cross section of these regions in the meridional plane (the white parts of the sketch) and those regions to which the charges cannot penetrate (the black parts).

Declassified in Part - Sanitized Copy Approved for Release 2013/01/23 : CIA-RDP81-01043R001600090003-8

Declassified in Part - Sanitized Copy Approved for Release 2013/01/23 : CIA-RDP81-01043R001600090003-8

The following peculiarity attracts our attention: at $-1<\gamma<0$, there is a torus-like region around the dipole into which a charge from the outside cannot penetrate. The equation of the meridional curve of this torus will obviously be:

$$r = \frac{-\gamma_1 + \sqrt{\gamma_1^2 + \cos^2\varphi}}{\cos\varphi},$$

or, since r is always positive:

$$r = \frac{\cos^2\varphi}{\gamma_1 + \sqrt{\gamma_1^2 + \cos^2\varphi}}$$

where $\gamma_1 = -\gamma$.

A consideration of these regions shows that for aurora only regions for which $-1 < \gamma < 0$ are of importance, since by hypothesis, the charges come to the earth from the sun, i. e., from a practically infinite distance.

But for these values of γ the regions Q_γ make contact with the earth only in a limited part of its surface, close to the north and south magnetic poles, as may be seen from Figure 110. This part of the earth's surface is bounded by a circle which is the result of the section of the surface of the atmosphere by the surface of the torus defined by the equation

$$r = k\frac{\cos^2\varphi}{1 + \sqrt{1 + \cos^2\varphi}}. \qquad (7.37)$$

Here the factor $k = \sqrt{\frac{Me}{mcv}}$ is inserted so as to express r in centimeters.

Let this torus intersect the circumference of the upper layers of the atmosphere at the point P (Figure 111). Let us denote the distance from the center of the earth from the point P by Δ, and the angle zOP by θ. Then from equation 7.37 we obtain:

Declassified in Part - Sanitized Copy Approved for Release 2013/01/23 : CIA-RDP81-01043R001600090003-8

Declassified in Part - Sanitized Copy Approved for Release 2013/01/23 : CIA-RDP81-01043R001600090003-8

$$\Delta\left(1 + \sqrt{1 + \sin^2\theta}\right) = k \sin^2\theta,$$

whence

$$k^2 \sin^2 \theta - \Delta^2 - 2k\Delta = 0$$

and, consequently,

$$\sin \theta = \sqrt{\frac{2\Delta}{k} \quad \frac{\Delta^2}{k^2}}.$$

Since Δ is in practice small by comparison with k, we neglect the higher powers and obtain:

$$\sin \theta = \sqrt{\frac{2}{k}}.$$

Stoermer found that the value of k for the beta-rays of radium is from 1.4×10^6 to 2.2×10^6 km; for the cathode rays, from 4.0×10^6 to 8.9×10^6 km; and for the alpha-rays, from 1.4×10^5 to 1.7×10^5 km.

Therefore the value of the angle θ will be from 4 to 6° for beta-rays, from 2 to 4° for cathode rays, and from 16 to 19° for alpha rays, that is, the maximum deflection of particles from the magnetic pole amounts to 19°, while the maximum zone of the aurora is 23° from the pole and descends in strong magnetic storms to 30°, 40°, and even to 50°.

This contradiction between the theoretical conclusions and the observed facts may be circumvented if we assume the existence of a circular of a ring current in the plane of the magnetic equator at a distance of a few earth-radii. This current will reduce the strength of the earth's magnetic field and thereby will also reduce the value of k. In strong magnetic storms this current will increase, as a result of which the auroral zone expands.

Returning to the consideration of the system of equations 7.33 it must be noted that they are not integrated in simplest functions and therefore require approximate methods for their solution. However, without having recourse to their solution we may still draw certain

Declassified in Part - Sanitized Copy Approved for Release 2013/01/23 : CIA-RDP81-01043R001600090003-8

Declassified in Part - Sanitized Copy Approved for Release 2013/01/23 : CIA-RDP81-01043R001600090003-8

conclusions as to the form of the trajectory in the meridional plane zR. Indeed, if the variable s is identified with time, then Q will represent a force (potential) function. For this reason, by plotting level lines Q at equal intervals on a plane, we can construct the direction of the forces acting on the charge. It is easy to see that when γ becomes negative, the force is equal to zero at the point $R = -\frac{1}{\gamma}$, $z = 0$, as well as on the levelled line $Q = 1$. The point $R = -\frac{1}{\gamma}$, $z = 0$ is a double point of the levelled line. Thanks to such a mechanical interpretation, the analysis of the trajectory is considerably simplified.

Between the trajectories in space and the trajectories in the meridional plane zR, there exists a simple geometrical relation. Let the point M (Figure 108) lie at the same time on the spatial trajectory B and on the trajectory K in the place zR, and let the tangent N to the curve B at point M make the angle θ with the meridional plane. In that case, it follows from geometrical considerations that

$$\sin\theta = R\frac{d\varphi}{ds}, \quad \text{whence} \quad \sin\theta = \frac{2\gamma}{R} + \frac{R}{r^3}.$$

Consequently, $\sin\theta$ is the very same quantity that we denoted by p. Further, on introducing the function Q, we have:

$$\sin\theta = \pm\sqrt{1-Q}, \qquad \cos\theta = \sqrt{Q}.$$

It follows from this that if the curve k intersects the levelled line $Q = 0$, then the tangent to the curve B will be perpendicular to the meridional plane. In this case, since there are always 2 levelled lines $Q = 0$, corresponding respectively to the values $p + 1$ and $p - 1$, and one of them lies within the line $Q = 1$, then on intersecting the line $Q = 0$ inside $Q = 1$ the direction of the charge will coincide with the direction of the increasing values of φ,

Declassified in Part - Sanitized Copy Approved for Release 2013/01/23 : CIA-RDP81-01043R001600090003-8

Declassified in Part - Sanitized Copy Approved for Release 2013/01/23 : CIA-RDP81-01043R001600090003-8

while on its intersection outside the line Q = 1, the motion is opposite to the increase of the angle φ.

However, to find the trajectories of the motion of the charge, besides these general deductions, Stoermer also requires the solution of the system of equation 7.33 and 7.34. These solutions were performed by numerical integration in the form of infinite theories for r and φ.

Thus, for the values: $-1 < \gamma < 0$ and $r < 0.2$, i. e., near the dipole, the following expressions were obtained for r and φ:

$$r = \frac{\cos^2\phi}{2\gamma} + \frac{3}{8}\frac{1}{(2\gamma)^3}\left[\cos^{10}\phi + \cos^{12}\phi + \frac{15}{16}\cos^{14}\phi + \frac{27}{32}\cos^{16}\phi + \ldots\right],$$

$$\varphi = -\frac{180}{\pi}\left[\frac{3}{16}r^2 + \frac{9\gamma}{32}r^3 + \frac{453\gamma^2}{1024}r^4 + \ldots.\right].$$

Figure 112, which represents a wire model of the paths of charged particles near the dipole, shows the form of the curves corresponding to these equations for various values of γ.

Figures 113 and 114 show a number of trajectories coming from infinity into the equatorial plane. Of these, Figure 113 relates to cases where $\gamma < -1$, while Figure 114 relates to cases where γ ranges from -1 to -0.5. It will be seen that all trajectories for which $\gamma < -1$, lie outside the circle corresponding to $\gamma = -1$, while the trajectories having $0 > \gamma > -1$, penetrate inside this circle and consequently may approach the dipole.

On applying the results of the mathematical conclusions directly to the aurora it may be said that, besides giving an explanation of the auroral zone, they also explain the appearance of the aurora in the night hours, since the charges approaching the earth bend around it and

Declassified in Part - Sanitized Copy Approved for Release 2013/01/23 : CIA-RDP81-01043R001600090003-8

Declassified in Part - Sanitized Copy Approved for Release 2013/01/23 : CIA-RDP81-01043R001600090003-8

leave the atmosphere on the opposite side from the sun. In exactly the same way the aurora observed during the daylight hours may be explained; they correspond to trajectories with small values of γ or with values from 0.93 to 1, which when the trajectories bend several times around the earth.

Further, the results of these conclusions form a correct interpretation of the radii form of the aurora. Indeed, in the radio forms of the aurora rapid and considerable variations in the intensity and position of the aurora are observed in a short time, and especially in the case of drapery. If we assume that the radial forms are formed by a narrow beam of charged particles emitted by the sun, then of the entire flux of particles on those which make a definite angle with the direction of the earth's magnetic axis ever reach the earth but since the magnetic axis, owing to the earth's rotation, varies its direction with respect to the trajectory of the particles, the direction of the rays also varies, i. e., some rays are extinguished, while others arise. But the arc-like of the aurora, still remain unexplained by this theory.

Such calculations which threw much light on the formation of the aurora still could not cover the whole group of phenomena observed on their appearance. In exactly the same way they could not give even a functional connection between the motion of the charges near the dipole and the magnetic disturbances, since they indicated merely the qualitative aspect of this correlation, namely the moving charges must produce a magnetic field.

Since the mathematical conclusions are irreproachable, their failure to agree in many cases with the observed facts is explained by the unsoundness of the hypothesis that the electrons do not interact with each other during their motion.

Declassified in Part - Sanitized Copy Approved for Release 2013/01/23 : CIA-RDP81-01043R001600090003-8

Declassified in Part - Sanitized Copy Approved for Release 2013/01/23 : CIA-RDP81-01043R001600090003-8

However, taking into consideration that the trajectories of the charges calculated by Stoermer do in many respects agree with the observed trajectories, and in addition, are confirmed by direct experiments made at various times by various investigators with cathode rays passing by a magnetized sphere, then, without rejecting the mathematical constructions and conclusions it is merely necessary to replace the fundamental hypothesis of a uniform, non-interacting beam of electrons by another, which would allow us to leave the mathematical calculations, on the whole, undisturbed, but considerably supplement it, instead of being contradicted, by the experimental data. The first of these attempts was made by Chapman and Ferraro, and the second by Alfven.

Section 5. The Theory of Chapman and Ferraro.

Stoermer, at the same time as the solution of the problem of the motion of a charge in the magnetic field of the earth, attempted also to explain the formation of charges in the sphere of action of the earth's magnetic field. According to his hypothesis, these charges of a single sign are ejected by the sun in the form of narrow beams, which on reaching the earth's magnetic field begin to move in accordance with the conclusions of this theory.

But elementary calculations show that a uniformly charged beam owing to the electrostatic repulsion of the particles, must be scattered soon after its departure from the sun and therefore could not under any conditions reach the earth.

To avoid this difficulty, Chapman and Ferraro (Bibl 58) constructed a theory on the hypothesis of the motion of a neutral beam.

Declassified in Part - Sanitized Copy Approved for Release 2013/01/23 : CIA-RDP81-01043R001600090003-8

Declassified in Part - Sanitized Copy Approved for Release 2013/01/23 : CIA-RDP81-01043R001600090003-8

According to their hypothesis the sun emits a flux of particles in the form of a cylindrical beam consisting of equal numbers of positive charges of ions and of negative electrons.

Such a beam in diameter of the order of 50 earth-radii is propagated from the sun with a velocity of 1000 km/sec, reaching the earth's orbit and intersecting it at an angle differing somewhat from 90°, since the particles, besides their longitudinal velocity, also have a transverse component equal to the linear velocity of rotation of the surface layers of the sun. The earth moving on its orbit may encounter on its path the lateral surface of the cylinder. Since the dimensions of the earth are small in comparison of the diameter of the cylinder, the lateral surface of the cylinder at the distance of a few earth radii may be taken as a plane and in addition the cylinder may be considered as motionless and the earth itself as a dipole moving at a small angle in the direction of the plane while the axis of the dipole may be taken as parallel to this plane. Since the medium bounded by the surface of the cylinder is conducting it follows that when the dipole moves in it currents arise which will tend by Lenz's law to destroy the magnetic field of the dipole within the conductor.

In addition between the dipole and the conducting medium mechanical forces of repulsive character arise and tend to interrupt to motion of the dipole. Since the conducting medius is not a solid, but in its character rather recalls a gas, the plane surface under the influence of these forces will begin to be pressed in as it approaches the dipole and under certain conditions as shown by Chapman a cavity surrounded by a concave conducting surface may be formed around the dipole.

Declassified in Part - Sanitized Copy Approved for Release 2013/01/23 : CIA-RDP81-01043R001600090003-8

Declassified in Part - Sanitized Copy Approved for Release 2013/01/23 : CIA-RDP81-01043R001600090003-8

Figure 115 shows the gradual distortion of the surface of the cylinder as it approaches the earth and the formation of a hollow space around the earth. In this case the vertex of the hollow, as will be seen from the figure, is turned towards the sun, while on the night side there is free space.

If the ionized stream is an ideal conductor then induction currents will arise only in a thin surface layer and will completely screen the interior of the conductor from the penetration of the magnetic field of the dipole there. As a result of this the magnetic lines of force in space between the dipole and the surface are more closely crowded together and thus cause an increase of the horizontal component in the equatorial plane, since the magnetic axis of the dipoles, by hypothesis, is parallel to the plane of the conductor.

Such an increase in the horizontal component corresponds precisely to the first phase of a magnetic storm.

To explain the principal phase of a magnetic disturbance during the time of which a fall in the horizontal component lasting several hours takes place Chapman and Ferraro postulated that the free space on the night side might be closed off by ions detached from the surface of the cavity, and might form a closed ring current around the earth.

The possibility of the detachment of ions and their closure of the cavity is explained according to Chapman and Ferraro by the following causes. On the surface of the cavity owing to the deflecting action of the earth's magnetic field the charges are separated, and on one side as is shown in Figure 116 the negative charges or electrons appear and on the other side the positive charges or ions.

Declassified in Part - Sanitized Copy Approved for Release 2013/01/23 : CIA-RDP81-01043R001600090003-8

Declassified in Part - Sanitized Copy Approved for Release 2013/01/23 : CIA-RDP81-01043R001600090003-8

The Figure shows the direction of the magnetic axis of the earth (the plus sign) and the direction of the earth's movement, as well as the direction of motion of the positive charges, i. e., the current. These charges produce an electric field on the night side of the earth and under the influence of this field the ions and electrons will be detached from the surface. But a charge detached under the influence of the earth's magnetic fields would have to move along a circle whose radius is determined by the equation

$$r = \frac{mvc}{eH} , \qquad (7.38)$$

Consequently the flying charge might reach the opposite side of the cavity if the radius of its vortex motion r were of the same order as the width of the cavity which according to Chapman's calculation amounts to several earth-radii. Calculations by equation 7.38 that such a value for the vortical motion at a velocity of the charge of the order of 1000 km/sec, could only be possessed by heavy charged particles, i. e., positive ions.

The closed mean current around the earth so formed must have the radius of a ring of the order of a few earth radii and would exist so long as the earth did not pass through the cylindrical beam. Since its diameter reaches 50 earth radii while the orbital velocity of the earth's motion is about 20 km/sec it follows that about 4-5 hours would be required to pass through the beam. During this period the horizontal component would reach a minimum which corresponds to a maximum value of the current.

After passing through the beam, the ring current around the earth would be maintained, but would gradually decline owing to the scattering of the charged particles. In this way, qualitatively the

Declassified in Part - Sanitized Copy Approved for Release 2013/01/23 : CIA-RDP81-01043R001600090003-8

Declassified in Part - Sanitized Copy Approved for Release 2013/01/23 : CIA-RDP81-01043R001600090003-8

Chapman theory would appear almost completely to explain one of the components of the magnetic variations the aperiodic disturbed variation as well as the 27-day cycle of these disturbances since after a complete rotation of the sun its surface which radiates these beams would again turn towards the earth and would again send out these beams to it.

The quantitative calculations made by Chapman and Ferraro however are confined to the ideal schemes which give an order of magnitude corresponding to actuality.

The aurora and S_D disturbances are explained according to this theory by the possibility of detachment of electrons from the surface of the cavity and under proper conditions of their motion along the lines of force from in the magnetic fields in the Arctic regions. From this point of view the electron beams must come not from the sun but from the surface of the cavity, as a result of which they are not able to become scattered during the short time interval and the Stoermer theory might therefore maintain its solidity.

The irregular processes, i. e., the rapid variation of the magnetic field during the magnetic storm may be explained by the varying density of charged particles along the beam as well as by the different velocities of these charged particles.

The principal fault of the Chapman-Ferraro theory is the fact that it is not thoroughly worked out with respect to the aurora and its relation through the magnetic disturbances. While it gives an explanation of the sudden onset of a magnetic storm and the subsequent march of the aperiodic variations it has not been able to explain either the local magnetic disturbances or the diurnal march of the magnetic variation.

Declassified in Part - Sanitized Copy Approved for Release 2013/01/23 : CIA-RDP81-01043R001600090003-8

Declassified in Part - Sanitized Copy Approved for Release 2013/01/23 : CIA-RDP81-01043R001600090003-8

A second fault of the theory is that it fails to give a quantitative relation between the magnetic field and the parameters of the neutral beam: its velocity, the density of the charges, the width of the beam, as well as the relation of these beams with the aurora and with other phenomena. For this reason it may be regarded as the first step in the construction in the theory of the magnetic disturbances and aurora which is not contradicted by the basic observed facts and the fundamental laws of physics.

Section 6. Alfven's Theory

The basic shortcomings of the Chapman-Ferraro theory, the difficulty of explaining the aurora and the local magnetic disturbances as well as the diurnal march of magnetic disturbance, caused the search for somewhat different models of the motion of charged particles and the sun to the earth than those used by Chapman. Such a model was that of Alfven (Bibl 59) who in 1939 postulated that the magnetic field of the sun exerts a substantial influence on the motion of a neutral stream of particles, electrons and ions, while with Chapman and Ferraro, this motion takes place exclusively under the action of the initial impulse. This hypothesis allowed giving a more varied picture of the motion of particles of the magnetic field of the earth and the qualitative explanation of the origin of both their aurora and magnetic disturbances. On considering the question of the extent to which the sun's magnetic field influences the motion of the particles and how it affects their behavior near the earth Alfven resolved the motion of particle in the magnetic field of the sun into the following 4 components:

1. Motion along a circle whose orbit is normal to the lines of the force of the magnetic field.

Declassified in Part - Sanitized Copy Approved for Release 2013/01/23 : CIA-RDP81-01043R001600090003-8

Declassified in Part - Sanitized Copy Approved for Release 2013/01/23 : CIA-RDP81-01043R001600090003-8

2. Oscillations along the lines of magnetic force about the plane of the solar equator owing to the variations in magnetic field strength.

These oscillations along the lines of force result as a necessary consequence from the theory of Stoermer. Since no work is done when a charged particle moves in a magnetic field the change in kinetic energy on oscillatory motion takes place on account of a change in the kinetic energy of the circular motion, as a result of which the particle is unable to deviate far from the equilibrium position and therefore according to Alfven the oscillations are confined to the lower latitudes of the sun.

3. Deflection (in nonuniform drift u_1) of elect [sic] ions towards the east and of positive ions towards the west owing to the inhomogeneity of the magnetic field in a radial direction.

Such a deflection results in the production of space charges at the edges of the stream negative on the eastern side and positive on the western and consequently the appearance of an electric field perpendicular to the magnetic field.

4. The "drift" u_E of electrons in direction perpendicular to both and magnetic fields owing to the simultaneous action of both fields.

The causes of this drift have already been considered in Section 3 of this Chapter. Owing to this drift the particle moves in a radial direction from the sun to the earth.

All these motions are the result of the interaction of a charged particle with magnetic and electric fields and result from the general laws of electrodynamics. For this reason they represent

Declassified in Part - Sanitized Copy Approved for Release 2013/01/23 : CIA-RDP81-01043R001600090003-8

Declassified in Part - Sanitized Copy Approved for Release 2013/01/23 : CIA-RDP81-01043R001600090003-8

nothing new but their isolation from the general motion did allow the behavior of the electrons and ions near the earth to be followed up more graphically.

As they approach the earth the particles use part of their energy which originally according to the Alfven's hypothesis amounted to 10^8 ergs for electrons and somewhat less for the ions. These losses are due to the fact that the nonuniform drift u_1 transfers the particles into regions with a high potential electrical energy where the presence of space charges retards the motion of the particles and they lose parts of their velocity.

The drift u_E is part of the flux into the earth's magnetic field, the radius of action of which by hypothesis is of the same order as the width of the flux. Since the motion of the flux will now take place in an increasing magnetic field the drift u_E due to the inhomogeneity of the magnetic field will become opposite to its earlier drift and the particles owing to this will be transported into a region with a lower potential energy and their magnetic energy will increase. The increase of kinetic energy will lead to an increase of the velocity perpendicular to the magnetic field which evidently becomes the same as the velocity parallel to the magnetic field and the oscillations along the lines of force become small. As a result of this the flux seized by the earth's magnetic field begins to flatten out in its equatorial plane and the nonuniform drift u_1 will tend to transport the positive ions around the earth in a westerly direction and the electrons in an easterly direction. The ratio u_1/u_E is small outside the earth's magnetic field, but at a distance of about 5×10^9 cm from it, u_1 for the electrons is of the same order as u_E, while for the ions u_1 remains small. For this

Declassified in Part - Sanitized Copy Approved for Release 2013/01/23 : CIA-RDP81-01043R001600090003-8

Declassified in Part - Sanitized Copy Approved for Release 2013/01/23 : CIA-RDP81-01043R001600090003-8

reason the electrons will be unable to pass into the "forbidden region" Q, established by Stoermer and must travel around it on the eastern side. The positive particles however freely penetrate it and form a space charge within it. As a result of electrostatic repulsion the charged particles will be scattered and the ions may move along the lines of force of the magnetic fields towards the magnetic poles. At the same time the electron beam E bending around the earth and appearing on its night side, forms a negative space charge there which in turn will also be scattered and electrons are enabled to move along the lines of force to the magnetic poles, but this time from the night side. Figure 117 schematically shows the motion of ions and electrons in the beam near the earth.

Such is the mechanism of motion of charged particles from the sun to the earth according to Alfven hypothesis. But how are magnetic storms and the aurora explained according to this theory?

The aurora is the result of the penetrations of ions and electrons into the Arctic region as a result of their repulsion from the boundary of the forbidden region and the auroral zone represents the projection onto the upper layers of the atmosphere of the lines of force emerging from the boundary of the forbidden region. Since the equation of the lines of force of the dipole in polar coordinates has the form

$$r = R \sin^2 \theta,$$

where R is the value of the radius vector at $\theta = 0^\circ$, then, if we take for R the radius of the boundary of the forbidden region, and for r and θ the solar coordinates of the auroral zone which are known to us, we may find the radius R. If we consider $r \sim 6500$ km and $\theta \sim 20^\circ$, we shall have $R \backsim 5 \times 10^9$ cm.

Declassified in Part - Sanitized Copy Approved for Release 2013/01/23 : CIA-RDP81-01043R001600090003-8

Declassified in Part - Sanitized Copy Approved for Release 2013/01/23 : CIA-RDP81-01043R001600090003-8

At such a distance the strength of the magnetic field of the earth in the plane of its equator, H = 70 γ. This value may correspond to that at which the electron begins to bend around the forbidden region Q.

Alfven then succeeded in explaining the various forms of the aurora including the arcs which were not explained by the Stoermer theory.

The principal phase of the magnetic storm is explained by the motion of electrons inside the forbidden region which motion is equivalent to a closed current while the local disturbances are explained by the appearance of currents in the auroral zone where owing to the penetration of charged particles an accumulation of positive charges takes place in the daylight part and of negative charges in the night part and in this way a potential difference is created.

The quantitative results of this theory depends on 2 unknown parameters, the energy and number of particles emitted by the sun. By a suitable selection of these quantities we may obtain a good agreement with the parameters known to us: the polar distance of the zone of the auroral zone, the energy of the electrons causing the aurora, the time of transit of the ionized beams of the sun to the earth, the duration of the initial phase of the magnetic storm, and the value of the current necessary to explain the storm.

However in spite of the good agreement of certain observed parameters with their calculated values, the theory does not withstand serious criticism with respect to the formation of a flattened stream in the plane of the equator which would be hardly possible.

Declassified in Part - Sanitized Copy Approved for Release 2013/01/23 : CIA-RDP81-01043R001600090003-8

Declassified in Part - Sanitized Copy Approved for Release 2013/01/23 : CIA-RDP81-01043R001600090003-8

As a result of this the formation of a narrow (linear) space charge along the forbidden region likewise becomes hardly possible. However the fundamental factor of the Alfven theory is exactly the presence of such linear charges along the boundary of the forbidden regions. For this reason we must view the Alfven theory as one of the successive steps in the development of the ideas of the Stoermer theory and which although it is not exempt from internal contradictions, still explains a wide circle of phenomena.

PART THREE

PRACTICAL APPLICATIONS OF THE PHENOMENA OF TERRESTRIAL MAGNETISM

CHAPTER VIII

MAGNETIC PROSPECTING

Section 1. The Magnetometric Prospecting Method and Its Development

Of the entire set of magnetic fields which constitute the magnetic field of the earth the best investigated with respect to causation are the fields of magnetic anomalies. As shown in a previous chapter magnetic anomalies regional as well as local, are caused by magnetized rocks occurring within the upper layers of the earth's crust. This fact, which may be regarded as being conclusively proven at the present time, permits utilization of this type of field in the study of the geological structure of the upper layers of the earth's crust and in prospecting for useful minerals. If magnetic anomalies are caused by the presence of maguetized bodies within the earth's crust, the depth of occurrence and the dimensions of the magnetized body may be determined through measurement of the intensity of the anomalous magnetic field and separation of the normal field from the observed field. This also would give answers to the geological problem

Declassified in Part - Sanitized Copy Approved for Release 2013/01/23 : CIA-RDP81-01043R001600090003-8

Declassified in Part - Sanitized Copy Approved for Release 2013/01/23 : CIA-RDP81-01043R001600090003-8

of the structure of the earth's crust. This method, called magnetometric, or simply magnetic prospecting has gained widespread application at the present time in prospecting for a number of valuable minerals (iron, nickel, chromium, gold, patroleum, etc) as well as for geological mapping, i.e., the preparation of geological charts.

Thus, investigation of magnetic anomalies for prospecting purposes must include measurement of the elements of terrestrial magnetism within the area of the anomaly and its interpretation, i.e., a determination of the dimensions and depth of occurrence of magnetized rocks on the basis of these measurement data.

Moreover, for an interpretation of magnetic anomalies in many cases it is necessary to know the magnetic properties of the rocks, and therefore one of the tasks of magnetic prospecting is the investigation of these properties by means of laboratory tests of samples of rocks occurring within anomalous areas.

The procedures used in measuring the elements of terrestrial magnetism within anomalous areas differ somewhat from those utilized in magnetic surveying, and depend upon the nature of the anomaly. At strong anomalies low sensitivity instruments such as the M-1 magnetometer are used, while highly sensitive instruments such as the magnetic balance are used for weak anomalies.

Interpretation of magnetic anomalies may be of either quantitative or qualitative nature. The former necessitates complex theoretical calculations and consists essentially of determination of the sources of the magnetic field on the basis of a given distribution of the field upon the earth's surface, which in this case is considered as being a plane, while the latter requires at least rough knowledge of the geology of a given area or requires the presence of an anomaly in a geologically well investigated area.

Declassified in Part - Sanitized Copy Approved for Release 2013/01/23 : CIA-RDP81-01043R001600090003-8

Declassified in Part - Sanitized Copy Approved for Release 2013/01/23 : CIA-RDP81-01043R001600090003-8

At the present time the magnetometric method of prospecting has become a vast independent branch of knowledge and has been developed by Soviet geophysicists.

The great Russian scientist D. I. Mendeleyev was one of the first to point out the possibility of application of the magnetometric method in prospecting for iron ore deposits. While conducting a survey of the iron industry of the Urals in 1899, he made magnetic observations in this connection in the Blagodat' Magnitnaya and Vysokaya mountains and at the Bakal'sk mine, where iron ore was being mined at that time and the location of the deposits was already known. In his paper "Magnetic Measurements in the Urals" which was published in the symposium Ural'skaya zheleznaya promyshlennost' v 1899 g." [Iron Industry of the Urals in 1899] of which he was editor, he stated: "If our endeavors to increase the number of the most accurate and complete magnetic observations in the Urals will yield nothing more than call attention to the practical advantages which may accrue from a system of accurate and complete magnetic observations within the district of the Urals, especially on the western slopes of the mountains where ore is scarce, I will consider that the efforts made by myself and my associates in this connection have not been in vain." Indeed the work of D. I. Mendeleyev on the development of magnetic prospecting methods has not been in vain. Observations conducted on his personal directions have confirmed his assumption concerning the possibility of outlining iron ore deposits by means of magnetic surveys. In each of the above stated areas appreciable anomalies were detected, reaching 17° in declination and 15,000 γ in the horizontal component.

The first large scale investigation of magnetic anomalies was performed between 1919 and 1926 at the Kursk magnetic anomalies and his

Declassified in Part - Sanitized Copy Approved for Release 2013/01/23 : CIA-RDP81-01043R001600090003-8

Declassified in Part - Sanitized Copy Approved for Release 2013/01/23 : CIA-RDP81-01043R001600090003-8

study was conducted at the instruction of V. I. Lenin by a special commission headed by Academicians P. P. Lazarev and I. M. Gubkin. This work was the actual beginning of magnetic prospecting as a distinct brand of the science of terrestrial magnetism.

The Kursk anomalies were discovered in 1874 by I. N. Smirnov during a magnetic survey of European Russia. While observing the elements of terrestrial magnetism at the town of Belgorod in Kursk guberniya I. N. Smirnov noted that they differed very greatly from the same elements at the adjoining points of Kursk and Khar'kov. For example, he observed that the declination at Kursk was $-4^{\circ}26'$, at Khar'kov $+0^{\circ}59'$, and at Belgorod the declination was $+27^{\circ}51'$. This suggested the existence of a magnetic anomaly at Belgorod. Further study of the Belgorod magnetic anomaly was conducted by a professor of the Moscow University, E. Kh. Leyst, who detected a number of anomalies over a large area of the Kursk Guberniya, for which reason they were designated the Kursk anomalies. E. Kh. Leyst studied these anomalies for more than 20 years (1894-1916), but the material which he had gathered was never published and after his death it was found in Germany. On the initiative of V. I. Lenin in 1919 the Soviet government undertook the investigation of these anomalies, entrusting the study to a special commission of the VSNKh [Supreme Economic Council].

Over a period of 7 years, from 1919 to 1926, the special commission not only made a thorough investigation of the anomalies, but also fully ascertained the causes of their occurrence. At that time the Soviet magnetologists A. I. Zaborovskiy, B. M. Yanovskiy and V. V. Kolyubakin studied the 1921 observation data under the direction of academician P. P. Lazarev and concluded that strongly magnetic rock formations were present at a depth of 180 to 200 m, and which

Declassified in Part - Sanitized Copy Approved for Release 2013/01/23 : CIA-RDP81-01043R001600090003-8

Declassified in Part - Sanitized Copy Approved for Release 2013/01/23 : CIA-RDP81-01043R001600090003-8

could be only magnetite. Drilling at a selected point of the anomaly (near the town of Shchigry) in 1923 revealed the presence of a large stratum of ferrous quartzites containing from 40 to 50% of pure iron at a depth of 180. This was a brilliant achievement for Soviet geophysics because during the end of the nineteenth and the beginning of the twentieth century the most prominent geologists had categorically denied the presence of crystalline rocks in Kursk guberniya at depths less than several thousand meters.

The success attained in the investigation of the Kursk anomalies provided the impetus for further rapid development not only of the magnetometric method, but also of other geophysical prospecting methods. In 1926 the Institute of Applied Geophysics was established at Leningrad under the direction of I. M. Bakhurin, a professor of the Mining Institute. His work on the theory of interpretation of magnetic anomalies has established a new school in the field of magnetic prospecting. As an experiment the Institute of Applied Geophysics carried out a magnetic survey at the salt deposits of Iletskaya station, utilizing the magnetic balance. This experiment yielded completely satisfactory results and demonstrated the suitability of this method in prospecting for rocks with lower susceptibility than the surrounding rock formations.

In 1930 the Leningrad Petroleum Institute first applied the magnetometric method at the petroleum bearing formations within the Western Urals (Second Baku). These operations, which lasted for several years, established a correlation between magnetic anomalies and geological structures and thus widened the applicability of the magnetometric method by showing it to be suitable not only in prospecting for specific deposits, but also for geological mapping.

Declassified in Part - Sanitized Copy Approved for Release 2013/01/23 : CIA-RDP81-01043R001600090003-8

Declassified in Part - Sanitized Copy Approved for Release 2013/01/23 : CIA-RDP81-01043R001600090003-8

A specific achievement of Soviet geophysics is the practical application of the method of aeromagnetic surveying, which was proposed and developed by A. A. Logachev.

The foundation of the theory of magnetometry in the Soviet Union was established by V. I. Bauman (1867-1923) professor at the Leningrad Mining Institute, who provided a number of solutions of the direct and inverse problem in the case of bodies having a simple geometrical shape. This work was the starting point of a large number of theoretical contributions which have enabled utilization of the magnetometric method of prospecting in precise quantitative calculations.

Section 2. Magnetic Properties of Rocks and Minerals.

All the rocks of the earth's crust possess magnetic properties to some extent, but magnetic anomalies are caused only by rocks with magnetic susceptibility greater than a certain definite magnitude. This magnitude can be readily determined by known proposition of magnetostatics, that the normal component of the vector of magnetic induction B_n at the partition surface of 2 media undergoes no discontinuity, i.e.,

$$B_{n_1} = B_{n_2},$$

where index one relates to the first, and index 2 to the second medium.

The induction inside a magnetized body or rock is determined by the equation:

$$B_n = 4\pi J_n + H_n.$$

For a magnetized body H_n is the demagnetizing field NJ_n, where J_n is the magnetization of the rock normal to its surface, and N is the coefficient of demagnetization of the given body or rock. Hence the intensity of the field H_a, produced by this rock at its surface and equal to B_n, will be

Declassified in Part - Sanitized Copy Approved for Release 2013/01/23 : CIA-RDP81-01043R001600090003-8

Declassified in Part - Sanitized Copy Approved for Release 2013/01/23 : CIA-RDP81-01043R001600090003-8

$$H_a = (4\pi - N)J_n.$$

This magnitude is the maximal for the given body or rock and is observed if the rock extends to the surface of the earth. It is evident that this maximum will differ for different shapes of the occurring rock but will not exceed the magnitude $4\pi J_n$.

Thus, in the case of rock having the shape of a sphere the maximum intensity of the field H_m at its surface is expressed by:

$$H_m = (4\pi - 4/3\ \pi) J = 8/3\ \pi J.$$

since the coefficient of demagnetization of a sphere is $N = 4/3\ \pi$.

The same magnitude is obtained with the formula

$$H = 2M/R^3$$

by replacing the magnetic moment of the sphere M with the product of volume by magnetization. Indeed,

$$H = 2 \cdot 4/3\ \pi\ R^3\ J/R^3 = 8/3\ \pi\ J.$$

In the case of rock which outcrops in the form of a plane of large dimensions, the intensity of the field over its center will be

$$H_a = (4\pi - 2\pi)\ J_n = 2\pi\ J_n,$$

because the coefficient of demagnetization of a plane is equal to 2π.

The quantity $4\pi\ J_n$ is the maximum possible magnitude of an anomalous field. Since presently available measuring equipment enables measurement of changes in the vertical component of not less than several tens of gamma (10 to 20), the minimum value of magnetic susceptibility x_m for rock capable of producing an anomalous field is determined by the condition

$$4\pi\ X_m\ H = 20 \cdot 10^{-5}\ \text{Oe}.$$

Since the intensity of the terrestrial field does not exceed 0.5 Oe, it follows that x_m must be not less than $3.2 \cdot 10^{-5}$. This value of

Declassified in Part - Sanitized Copy Approved for Release 2013/01/23 : CIA-RDP81-01043R001600090003-8

Declassified in Part - Sanitized Copy Approved for Release 2013/01/23 : CIA-RDP81-01043R001600090003-8

magnetic susceptibility is the same as that of many paramagnetic bodies, and therefore magnetic anomalies can be caused by rocks which possess not only ferromagnetic, but also antiferromagnetic and paramagnetic properties. This is the reason why it is very important to know the magnitudes of the magnetic susceptibility of rock formations in the interpretation of anomalies.

It is known from experience that many rock formations have ferromagnetic properties although their magnetic susceptibility is of the same order of magnitude as that of paramagnetic bodies. In most cases the ferromagnetism of rock formations is caused by the presence of minerals including some compounds of iron.

Such minerals include: magnetite or magnetic iron ore ($Fe_2O_3 \cdot FeO$), pyrite (FeS_2), pyrrhotite or magnetic pyrites (Fe_nS_{nH}), ilmenite or titaniferous iron ore ($FeO \cdot TiO_2$), limonite or brown iron ore (Fe_2O_3).

The most magnetic and most widely occurring mineral of this type is magnetite, which in most instances causes the ferromagnetic properties of rock formations.

Ferromagnetism is characterized by the magnitude of magnetic susceptibility, the magnitude of residual magnetization J_r and coercive force H_e.

Residual magnetization is found in ferromagnetic rocks as a result of the action at some time of a constant magnetic field on the rocks. Therefore it would appear that rock formations could have no residual magnetization since the magnetic field of the earth was hardly ever greater than it is at the present time. Yet it has been known since the time of ancient China that some rock formations

Declassified in Part - Sanitized Copy Approved for Release 2013/01/23 : CIA-RDP81-01043R001600090003-8

Declassified in Part - Sanitized Copy Approved for Release 2013/01/23 : CIA-RDP81-01043R001600090003-8

such as magnetic iron ore have a large residual magnetization, and which prior to the discovery of Oersted (1820) were used to magnetize steel needles and other permanent magnets.

At the present time it has been ascertained through numerous experiments that all ferromagnetic rocks have some residual magnetization, and that most of the observed anomalies are caused by residual magnetization in rock formations.

The magnetization of rocks caused by the action of the terrestrial magnetic field as will be referred to herein as inductive magnetization, denoted by J_B, while permanent magnetization will be referred to as residual magnetization, denoted by J_r. Thus the total magnetization will be the geometrical sum of J_B and J_r, i.e.,

$$J = J_B + J_r \qquad \text{or} \qquad J = xH + J_r.$$

The magnetic susceptibility of monocrystals depends on the direction of the crystallographic axes. Because rock formations consist of polycrystals this dependence no longer exists and therefore rock formations and minerals may be regarded as being isotropic. However, even in this case x is a function of the direction since the magnetization of bodies depends on their shape and therefore, with the exception of the sphere which is symmetrical in relation to any axis passing through its center, the magnetic susceptibility of any body will differ in different directions. As we have seen in Section 15 of the introduction this relationship is determined by the correlation

$$x' = x/1 + xN,$$

where x is the maximum magnetic susceptibility corresponding to N = 0 and is called true susceptibility, x' is the susceptibility of the given body in some particular direction, and N is the coefficient of

Declassified in Part - Sanitized Copy Approved for Release 2013/01/23 : CIA-RDP81-01043R001600090003-8

Declassified in Part - Sanitized Copy Approved for Release 2013/01/23 : CIA-RDP81-01043R001600090003-8

demagnetization of the body in the same direction; the quantity x' has been designated the apparent magnetic susceptibility.

It follows from the above that the vector of magnetization J of rock formations in general may not coincide with the direction of vector H and may differ from the latter by a certain angle depending upon the shape of the occurring rock.

In the case of rocks with low true magnetic susceptibility, on the order of 10^{-3} or less, the product xN does not exceed 0.01 since the maximum value of the coefficient of demagnetization is $N = 4\pi$ and may be disregarded, and thus

$$x' = x$$

i.e., the apparent susceptibility is equal to the true susceptibility and does not depend upon the direction of magnetization.

Such rocks become magnetized in the direction of the magnetic field and the quantity $J = xH$ has the same value at all points, i.e, the magnetization of the rock is uniform.

On the other hand, rocks having a true magnetic susceptibility greater than 10^{-2} become magnetized nonuniformly since the coefficient of demagnetization N depends not only on direction, but also depends on the position of the point within the body. The coefficient of demagnetization is lowest at the center and highest near the surface. However, in determination of the magnetic field produced by magnetized rocks it may be assumed with an accuracy sufficient for practical purposes that both weakly and strongly magnetic rocks become uniformly magnetized.

Rocks and minerals may be subdivided into 3 principal groups according to their magnetic properties: ferromagnetic minerals,

Declassified in Part - Sanitized Copy Approved for Release 2013/01/23 : CIA-RDP81-01043R001600090003-8

Declassified in Part - Sanitized Copy Approved for Release 2013/01/23 : CIA-RDP81-01043R001600090003-8

igneous rock and sedimentary rock; metamorphic rocks may belong to both the igneous and the sedimentary group.

Ferromagnetic Minerals [60]. As stated above ferromagnetic minerals include magnetite, pyrrhotite, ilmenite, limonite and hematite. Their magnetic properties are characterized by relatively large magnetic susceptibility and the presence of a hysteresis loop. However, the same mineral can have very different values of susceptibility and coercive force, depending on the deposit from which it is obtained. Therefore, it is impossible to characterize the magnetic properties of each of these minerals by a definite value of magnetic susceptibility or a definite hysteresis curve, and it is possible only to state the limits within which these quantities vary.

Pure magnetite is a crystal of the cubic system which, like the crystalline ferromagnetic metals, possesses the properties of magnetic anisotrophy, i.e., the magnetic properties are different along the different axes.

Thus along the diagonal of the cube (triad axis of symmetry) saturation is reached in weak magnetic fields, in the direction of the edges of the cube (tetrad axis) saturation is attained in fields that are 10 times greater, and finally in the direction of the diagonal of the side of the cube (twinning axis) saturation requires an intermediate field. Consequently, the triad axis is the axis of easiest magnetization and the tetrad is the axis of difficult magnetization, whereas in a crystal of pure iron the triad is the axis of difficult magnetization and the tetrad axis that of easiest magnetization.

Figure 118 shows the magnetization curves for different axes of a magnetite crystal at room temperature. It may be seen that saturation along the axis of easiest magnetization is attained in a

Declassified in Part - Sanitized Copy Approved for Release 2013/01/23 : CIA-RDP81-01043R001600090003-8

Declassified in Part - Sanitized Copy Approved for Release 2013/01/23 : CIA-RDP81-01043R001600090003-8

field of approximately 300 Oe intensity and is equal to 430 CGSμ i.e., almost 4 times less than the saturation of iron. Along the axis of difficult magnetization saturation requires a much greater field. The initial magnetic susceptibility of pure magnetite is of the order of 8 CGSμ units, while the residual magnetization is: for the triad axis J_r = 80, for the twinning axis J_r = 70 and for the tetrad axis J_r = 90 CGSμ.

Magnetite ores consisting mostly of magnetite have a polycrystalline structure and therefore their magnetic properties do not depend on the direction of magnetization. Due to the different admixtures of such ores obtained from different deposits their magnetic properties also have different characteristics.

Figures 119 a, b, c and d show the magnetization curves of magnetite obtained from 4 different deposits: Figure 119a relates to a sample obtained from the Kola peninsula, Figure 119b to a sample from the Vysokaya Mountain (Urals), Figure 119c to a sample from the Temir-Tau Mountain (Urals) and Figure 119d to another sample from the Urals the exact origin of which is not known. The first sample contains 45%, the second 40%, the third approximately 60% and the fourth 50% magnetite. The remainder consists of crystalline inclusions of nonmagnetic nature.

Comparison of these curves with the curve of pure magnetite shows the extent to which the magnetic properties of ores vary, depending upon their mineralogical composition. The basic magnetic characteristics listed in Table 25 for the 4 samples of magnetite correspond to these curves.

Declassified in Part - Sanitized Copy Approved for Release 2013/01/23 : CIA-RDP81-01043R001600090003-8

Declassified in Part - Sanitized Copy Approved for Release 2013/01/23 : CIA-RDP81-01043R001600090003-8

TABLE 25

Magnetic Characteristics	Samples No 1	No 2	No 3	No 4
Initial magnetic susceptibility	0.2	0.9	1.9	0.25
Residual magnetization J (CGS μ)	12	20	4.1	7.0
Coercive force in Oesteds	30	20	7.2	40
Saturation (CGS μ)	100	150	-	-

As shown by S. V. Lipin [61] pyrrhotite, the general formula of which is $Fe_n S_{n+1}$ constitutes a solid solution of ferrous sulfide FeS with ferric sulfide Fe_2S_3 or feroso-ferric sulfide Fe_3S_4.

Analyses show that the atomic ratio S:Fe varies from 1.20 to 1.00 assuming all the intermediate values, from approximately Fe_5S_6 to $Fe_{21}S_{22}$.

Crystals of pure pyrrhotite belong to the rhombic system and have the appearance of rectangular prisms, but regardless of the direction of the magnetizing field are magnetized only in a single plane perpendicular to the axis of the prism, called the magnetic plane. Within this plane there is a direction in which magnetization occurs readily (OX). Perpendicularly to the latter (direction OY) magnetization takes place with difficulty. These directions are called the main axes of the crystal. Magnetization perpendicular to the magnetic plane is detected only in very strong fields.

Magnetization curves corresponding to these directions for a sample of pyrrhotine are shown in Figure 120. While saturation along the OX axis takes place at H = 1,000 Oe, saturation along the OY axis is attained in a field H = 7,300 Oe, and for a saturation along the OZ axis a field of approximately 176,000 Oe is required. The magnitude of saturation may vary, depending on the sample, from 17 to 70 CGS μ, and the coercive force may vary from 15 to 30 Oe. Crystals of pyrrhotite

Declassified in Part - Sanitized Copy Approved for Release 2013/01/23 : CIA-RDP81-01043R001600090003-8

Declassified in Part - Sanitized Copy Approved for Release 2013/01/23 : CIA-RDP81-01043R001600090003-8

possess very sharp anistropic characteristics and are of greatest interest from the standpoint of the theory of ferromagnetism.

Because of their polycrystalline structure natural pyrrhotites like the magnetites, lost their anisotropic properties and are magnetically isotropic. Their magnetic properties depend upon the components characteristic of any given deposit. Figures 121a and 121b show the magnetization curves of 2 pyrrhotites, one of which (Figure 121a) was determined by N. I. Spiridovich [62] using a sample containing 7.5% Fe_2O_3 and the other curve was determined by T. N. Roze [63] using a sample containing approximately 20% magnetite and 10% chalcopyrite. In the first sample the residual magnetization was J_r = 1.12 CGS μ and the coercive force H_c = 110 Oe; in the second J_2 = 8 CGS μ and H_c = 46 Oe. The experiments of T. N. Roze have shown that the magnetic properties of pyrrhotites are greatly altered upon heating to temperatures above 270° C. Thus Figure 122 shows the hysteresis curves of pyrrhotite from a deposit located on the Kola peninsula, containing 75% pyrrhotite and 20% magnetite before heating, and after heating above 270°. The experiments have demonstrated that at 270° pyrrhotite is irreversibly converted into a different phase which is retained upon reheating.

The curves show that heating causes a sharp increase in magnetic susceptibility and residual magnetization, while the coercive force has remained almost unchanged. On comparing magnetization curves of natural rocks with those of crystalline pyrrhotite it becomes apparent that the magnetic properties of natural pyrrhotites are intermediate to the properties of the crystalline material along the 3 mutually perpendicular directions corresponding to their polycrystalline structure, in which the axes of easy and difficult magnetization are disposed in every possible direction.

Declassified in Part - Sanitized Copy Approved for Release 2013/01/23 : CIA-RDP81-01043R001600090003-8

Declassified in Part - Sanitized Copy Approved for Release 2013/01/23 : CIA-RDP81-01043R001600090003-8

It was shown by studies of its crystal lattice that hematite (Fe_2O_3) occurs in 2 varieties: α-hematite, which has a rhombohedral system and antiferromagnetic properties, and γ-hematite, which has a cubic system and ferromagnetic properties.

Antiferromagnetics belong to the group of paramagnetic bodies but differ from the latter in specific magnetic properties, namely a specific Curie point below which the magnetic susceptibility depends on the magnetizing field. For α-Fe_2O_3 this point is in the high temperature region, equal to 675° C [64].

Natural hematites always contain admixtures of other minerals and therefore their magnetic property can vary depending on the content of these admixtures, and depending also upon the ratio of magnetic and paramagnetic varieties.

According to the investigations of N. I. Spiridovich and T. N. Roze hematite ores, natural hematite isolated from the ore, and synthetically produced iron oxide have the magnetic characteristics shown in Table 26. It is seen that a specific feature of hematites is low residual magnetization and a high value of coercive force, which becomes greater with increase of the magnetizing field.

Figure 123 shows the hysteresis curve of hematite ore from Tulomozero, determined with a maximum magnetizing field value of 400 Oe. The curve reveals a sharp increase in residual magnetization and coercive force with increase of the magnetizing field.

Ilmenite ($FeO \cdot TiO$) is a mineral component of titanium magnetite ores, i.e., a combination of ilmenite and magnetite at various ratios, and is a paramagnetic mineral with a magnetic susceptibility of approximately $60 \cdot 10^{-5}$ CGS μ and a magnetic field intensity of 2,000 Oe.

Declassified in Part - Sanitized Copy Approved for Release 2013/01/23 : CIA-RDP81-01043R001600090003-8

Declassified in Part - Sanitized Copy Approved for Release 2013/01/23 : CIA-RDP81-01043R001600090003-8

TABLE 26

MAGNETIC CHARACTERISTICS OF HEMATITES

Rocks and Deposits	Chemical Composition Formula	%	H_m Oersted	J_r CGSμ	H_c Oersted	Investigator
Hematite from Kareliya (Tulomozero)	Fe_2O_3	69.8	1,880	0.3	480	N. I. Spiridovid
	FeO	0.8	900	0.037	188	
	TiO_2	0.5				
Iron ore from Mount Magnitnaya	Fe_2O_3	92.76	3,500	0.67	185	T. N. Roze
	FeO	0.98	280		30	
	TiO_2	0.16				
Iron quartzites from an unknown deposit	Fe_2O_3	40.5	3,500	0.24	>185	T. N. Roze
	FeO	0.46	280	< 0.03	40	
	TiO_2	0.02				
Magnetite powder isolated from ore	-	-	400	0.09	130	N. I. Spiridovich
Synthetic Iron oxide	Fe_2O_3	99.98	400	0.03	80.0	

Declassified in Part - Sanitized Copy Approved for Release 2013/01/23 : CIA-RDP81-01043R001600090003-8

Declassified in Part - Sanitized Copy Approved for Release 2013/01/23 : CIA-RDP81-01043R001600090003-8

However in combination with magnetite it acquires strongly manifested ferromagnetic properties which are distinct from those of pure magnetite. A differentiating characteristic of titanium magnetites is a greater coercive force than that of magnetite. This is confirmed by the experiments of N I. Spiridovich and the data of T. N. Roze.

Figure 124 shows the magnetization curves of titanium magnetite samples containing 4% TiO_2 and 50% and 70% Fe_2O_3 according to the data of N. I. Spiridovich and T. N. Roze. The coercive force of the first sample is 31 Oe, and of the second sample 20 Oe, whereas in magnetites it is approximately 10 to 15 Oe. The basic magnetization curve is somewhat lower than that of magnetites and therefore the magnetic susceptibility of titanium-magnetites is somewhat less approximately 0.2-0.4 CGSμ. On this basis it may be asserted that titanium oxide TiO_2 although not magnetic, exercises an influence on the magnetic properties of ferromagnetic minerals.

Limonite ($Fe_2O_3 \cdot nH_2O$) is a hydroxide of iron which forms deposits of brown iron ore widely encountered in nature. Limonite is only slightly magnetic, having a maximum susceptibility of approximately 100-500 $\cdot 10^{-6}$ CGSμ, but has clearly manifested ferromagnetic properties. According to the investigations of N. I. Spiridovich a sample of limonite containing 6% admixtures showed a coercive force of 10 Oe and a residual magnetization of J = 0.011.

Igneous rocks are subdivided into acidic igneous rocks rich in solicic acid, including granites, granodiorites, diorites; basic and ultrabasic rocks containing little solicic acid, including gabbro, diabases, basalts serpentines, peridotites, dunites, porphyrites and others, and rocks rich in alkalies such as syenites. The

Declassified in Part - Sanitized Copy Approved for Release 2013/01/23 : CIA-RDP81-01043R001600090003-8

Declassified in Part - Sanitized Copy Approved for Release 2013/01/23 : CIA-RDP81-01043R001600090003-8

magnetic properties of each of these rocks vary within such wide limits that no definite magnetic susceptibility or definite magnetization curve can be given for them. Their magnetic properties vary sharply, depending on the content of any given mineral components. However, numerous observations by various investigators permit certain definite conclusions. Of the entire series of igneous rocks the most magnetic are the basic and ultrabasic rocks, including gabbro, diabases, porphyrites, serpentines, basalts and periodites. Most granites and granodiorites are practically nonmagnetic. As is shown by observations the magnetic properties of igneous rocks are due to the presence of ferromagnetic minerals, but these properties are not additive since it is most likely that the magnetic properties are affected not only by the amounts of ferromagnetic minerals, but also by the form in which they are included in the rocks, whether they constitute individual inclusions or form an intimate compound.

The experiments of N I. Spiridovich confirm the relationship between the magnetic properties of igneous rocks and the presence in the latter of ferromagnetic minerals. The results of these experiments are listed in Table 27.

This table shows there is no definite regularity between magnetic properties and the content of iron or ferromagnetic material, but there exists a general tendency of increased susceptibility with increasing content of ferromagnetic components. In the absence of ferromagnetics the rock becomes paramgnetic, which is confirmed by one of the samples of metamorphic gabbro.

In view of this fact every known rock may be characterized only by the limits within which its properties may vary, these properties

Declassified in Part - Sanitized Copy Approved for Release 2013/01/23 : CIA-RDP81-01043R001600090003-8

Declassified in Part - Sanitized Copy Approved for Release 2013/01/23 : CIA-RDP81-01043R001600090003-8

being manifested by the magnitude of maximum magnetic susceptibility or merely by a qualitative evaluation as nonmagnetic, slightly magnetic, magnetic, or strongly magnetic.

Table 28 shows the limits of magnetic susceptibility according to the data of various investigators.

Although the magnetic properties of igneous rock are characterized generally by the magnitude of magnetic susceptibility it must be borne in mind that all igneous rocks are ferromagnetic and therefore the susceptibility may vary rather widely for each igneous rock type, depending upon its magnetization. Moreover every type of ferromagnetic rock has hysteresis, as a result of which it may have a residual magnetization. Figures 125, 126 and 127 show magnetization curves and the correlation between magnetic susceptibility and magnetizing field for samples of diabase, gabbronite and gabbrodiabase, according to the data of N. I. Spiridovich. The drawings show that all 3 samples are strongly ferromagnetic

Sedimentary Rocks. Sedimentary rocks include various clays and sandstones, limestones, gipsum, chalk, marls, dolomites, and rock salt. With the exception of some varieties of clay and sandstone, they are all practically nonmagnetic since their susceptibility does not exceed 10^{-5} CGS μ .

Declassified in Part - Sanitized Copy Approved for Release 2013/01/23 : CIA-RDP81-01043R001600090003-8

Declassified in Part - Sanitized Copy Approved for Release 2013/01/23 : CIA-RDP81-01043R001600090003-8

TABLE 27: MAGNETIC PROPERTIES OF IGNEOUS ROCKS

Rocks	Content of Ferro-magnetic mineral in %		Total iron content in %	$X \cdot 10^6$	At H = 400 Oe J_r	H_c
Diabase	magnetite	27.5	30.6	88,000	7.34	75.0
Diabase	magnetite	10.2	12.1	85,000	0.91	89.0
Gabbro diabase	magnetite	6.37	-	5,000	0.23	32.6
Gabbro diabase	magnetite	4.0	12.1	5,100	0.43	57.0
Diabase	hematite FeO	3.83 7.03		3,280	0.02	5.3
Metamorphic diabase	limonite	1.8	-	240	-	-
Gabbronorite	pyrrhotine	3.0	2.5	1,700	0.22	78.0
Metamorphic gabbro	magnetite	12.1	15.0	12,400	0.3	21.3
Metamorphic gabbro	ilmenite	2.12	-	510	0.04	58.0
Metamorphic gabbro	none		C	92	-	-
Pyroxenite	pyrrhotine	2.5	7.7	820	0.05	46.0

Declassified in Part - Sanitized Copy Approved for Release 2013/01/23 : CIA-RDP81-01043R001600090003-8

Declassified in Part - Sanitized Copy Approved for Release 2013/01/23 : CIA-RDP81-01043R001600090003-8

TABLE 28

SUSCEPTIBILITY LIMITS OF IGNEOUS ROCKS

Rocks	VIRG Number of Samples	x · 10^6	Putsikha Number of Samples	x · 10^6	Koenigsberger Number of Samples	x · 10^6
Granite	171	0-4555	3	8-2720	-	4200
Granodiorite	6	200-2000				
Diorite	-	-	1	47		
Diabase	97	0-13820	2	64-106	2	700-2700
Gabbro	33	1000-7470	2	69-2370	4	310-4100
Basalt	43	125-15500				
Peridotite	36	400-72800				
Porrphyrite	136	0-22700	3	45-120		
Syenites	38	0-6590				

Declassified in Part - Sanitized Copy Approved for Release 2013/01/23 : CIA-RDP81-01043R001600090003-8

Declassified in Part - Sanitized Copy Approved for Release 2013/01/23 : CIA-RDP81-01043R001600090003-8

Among sedimentary rocks of significance in magnetic prospecting are certain varieties of clay containing iron oxides, and sandstones containing ore in the form of magnetite granules, or containing other minerals, the magnetic susceptibility of which may reach 10^{-3} CGS μ, and therefore both can cause magnetic anomalies.

Table 29 lists the magnetic susceptibility of some sedimentary rocks recovered from boreholes in the Western Urals based on the data of B. M. Yanovskiy and Ye. T. Chernyshev [65].

TABLE 29

MAGNETIC SUSCEPTIBILITY OF SEDIMENTARY ROCKS

Borehold #	Depth of Occurrence	Rocks	Magnetic Susceptibility x $\cdot 10^6$
701	92.6 - 96.6	Marl, brown, with sandstone interlayers	85
	140.5 -146	Clay, brown, brown-grey	200
	239.6 -241.5	Clay, brown-grey, lime containing	157
	318.1 -320.2	Clay, brown	22
	491.2 -492	Clay, dark brown	19
	588.1 -558.5	Gypsum, white	5
704	182.8 -184.2	Clay, brown, soft and sandy	7.6
	309.8 -310.4	Marl, purple-grey, with calcite inclusions	0
	351.8-353.9	Sandstone, brown, marly	30
	365.4-366.1	Marl, red-brown, dense	19
	513.2-516.9	Marl, pink, dense	10
	553.8-555	Marl, dolomitized	20
	581.6-583.6	Sandstone, reddish brown-grey	43

Section 3. Residual Magnetization of Rock Formations and the Causes of its Occurrence

At the beginning of the preceding section it was stated that most rock formations show magnetization which cannot be explained solely

Declassified in Part - Sanitized Copy Approved for Release 2013/01/23 : CIA-RDP81-01043R001600090003-8

Declassified in Part - Sanitized Copy Approved for Release 2013/01/23 : CIA-RDP81-01043R001600090003-8

by the action of the magnetic field of the earth, since in such a case the magnetization of the rock would change if the rock were rotated 180° in relation to the terrestrial field. Moreover, observations show that the magnitude of residual magnetization sometimes is several score times larger than the magnitude of inductive magnetization $J = xH$. This is apparent from Table 30, which shows the values of residual magnetization J_r, and its ratio to the inductive magnetization for some rocks.

TABLE 30

Rocks	$J_r \cdot 10^3$	J_r/J_B
Diabase	3.2	2.4
Gabbro, post-silurian	2.9	1.4
Gabbro, tertiary	42.0	28.0
Gabbro, tertiary	12	25.5
Basalt metamorphic	14.0	9.3
Granite-porphyry	1.6	6.4
Basalt, tertiary	4.4	3.2

Thus the question naturally arises as to how the rocks could become magnetized if one does not assume the influence of extraneous magnetic fields caused by magnetic fluxes, considering that nothing is known about the latter at the present time.

This problem was first encountered in the interpretation of the Kursk magnetic anomalies. Samples of magnetite from boreholes in the anomalous area showed such a magnitude of residual magnetization which could not be attributed to the action of the terrestrial field. The first attempt to explain this phenomenon was made by P. P. Lazarev, who assumed the existence of a more intensive magnetic field of the earth during the epoch of the formation of these ore deposits.

Declassified in Part - Sanitized Copy Approved for Release 2013/01/23 : CIA-RDP81-01043R001600090003-8

Declassified in Part - Sanitized Copy Approved for Release 2013/01/23 : CIA-RDP81-01043R001600090003-8

However at the present time such a hypothesis is disproved by a large number of facts derived by measurement of residual magnetization of sedimentary and igneous rocks of known age. In all probability the magnetic moment of the earth has undergone hardly any change since the time the Kursk magnetites were formed.

More probable is the hypothesis of the influence of some kind of physical or chemical factors on the process of magnetization of rock formations at the time of their origination. This idea was first expressed by A. F. Ioffe, and the first experiments along this line were conducted in 1926 by A. N. Zaborovskiy, who observed the magnetization of magnetite while it cooled from the Curie point in the earth's magnetic field. T. N. Roze [63] conducted detailed investigations on the influence of temperature in the magnitude of residual magnetization in a large number of rocks. These investigations have shown that any ferromagnetic rock heated to the Curie point and placed in a weak magnetic field acquires a residual magnetization on cooling to room temperature within this field, the magnitude of which is several-fold greater than that corresponding to the given field.

Thus figure 128 shows the correlation between the magnitude of residual magnetization J_r and the magnetizing field when magnetite was listed to the Curie point and then allowed to cool (curve J_{rt}). The same correlation also is given for magnetization at room temperature (curve J_r). Comparison of these curves reveals that the influence of temperature is greatest in weak fields in which J_{rt} is several tens of times greater than J_r.

It is of interest to note that the residual magnetization produced by cooling of the sample in a magnetic field almost coincides

Declassified in Part - Sanitized Copy Approved for Release 2013/01/23 : CIA-RDP81-01043R001600090003-8

Declassified in Part - Sanitized Copy Approved for Release 2013/01/23 : CIA-RDP81-01043R001600090003-8

with the ideal magnetization obtained by the superimposition of a variable with an amplitude decreasing to zero upon a permanent field. Consequently, the action of temperature decreasing from the Curie point is somewhat analogous to the action of a variable field of decreasing amplitude. The same properties also are possessed by some of the present-day alloys used for permanent magnets, such as magnico. The theory of this phenomenon has been developed by D. A. Shturkin and Ya. S. Shur [66].

Figure 129 shows the curves of residual magnetization of a specimen of pyrrhotite from the Temir-Tan deposit, which shows this effect very clearly. From the drawing it is apparent that the ratio J_{rt}/J_r in pyrrhotite has a value of hundreds of units in small fields, i.e., magnetization accompanied by the action of temperature is hundreds of times greater than under the action of the magnetic field alone.

Analogous curves also are obtained for other rocks such as hematite, titanium magnetite, diabase, basalt, gabbro, serpentine, andesite, pyroxene, and druserite, which have been investigated by T. N. Roze.

Another important factor affecting the magnetization of rocks can be mechanical action to which the rock is subjected, such as compression, elongation, vibration or seismic oscillations, which induce internal stresses in the rocks.

The influence of elastic stresses on the magnetic properties of ferromagnetics has long been known and is the subject of numerous investigations, the theoretical foundations of which are found in the work of N. S. Akulov [67]. However, no investigation of rock formations from this point of view has yet been carried out, and therefore no quantitative data are available concerning the effects of mechanical

Declassified in Part - Sanitized Copy Approved for Release 2013/01/23 : CIA-RDP81-01043R001600090003-8

Declassified in Part - Sanitized Copy Approved for Release 2013/01/23 : CIA-RDP81-01043R001600090003-8

action on any given type of rock. M. A. Grabovskiy [68] recently conducted the first investigations of magnetite specimens from the Blagodat' and Vysokaya mountains, including study of the effects of unilateral compression on magnetization curves and on the magnitude of residual magnetization.

The results of his research are contained in Figure 130 which shows the relationship between residual induction and magnetizing field in the case of a specimen not subjected to deformation and of a specimen subjected to the greatest unilateral compression permitted by its durability. It is seen that the residual induction of magnetite decreases on compression, i.e., the magnetite has positive magneto striction, and therefore on elongation the residual induction should increase. However, because of the brittleness of the specimen it was not possible to confirm this conclusion experimentally. Due to the lack of experimental material it is not known whether there are rocks having negative magnetostriction, the residual magnetization of which would increase on compression, but such a possibility is not excluded.

Experimental data on the magnetization of rocks cooling down from the Curie point, and the initial experiments on their magnetization during compression give reason for assuming that the observed high magnetization of rocks is the result of their cooling, following intrusion, in the magnetic field of the earth, since there is every reason for believing that crystallization of the rocks took place on their transition from the liquid to the solid phase. In addition, the magnitude of residual magnetization was undoubtedly affected by mechanical deformations of the rocks induced by uneven compression and bending. Since the earth's crust still is in a state of continuous movement, which is manifested by the slow rising and sinking

Declassified in Part - Sanitized Copy Approved for Release 2013/01/23 : CIA-RDP81-01043R001600090003-8

Declassified in Part - Sanitized Copy Approved for Release 2013/01/23 : CIA-RDP81-01043R001600090003-8

of dry land and by rapid earthquakes or volcanic eruptions, it follows that the mechanical stresses which act upon magnetized rocks are undergoing continuous changes, and consequently the magnetization of the rocks also must change. Therefore one of the causes of secular magnetic variations must be the change in magnetization of rocks due to changing mechanical stresses such as comparison, elongation, etc. These phenomena must be manifested most strongly within seismic areas in which the internal strains in the rocks are suddenly changed during earthquakes. However, because at present there is very little experimental material available on this problem nothing is known of the regularities which are inherent in these phenomena.

Section 4. Effect of Variations on the State of Magnetization of Rocks

Changes in the magnetic field of the earth with lapse of time, i.e., magnetic variations, must have an effect on the state of magnetization of rocks if this magnetization is caused by the action of the terrestrial field. This problem was investigated theoretically and experimentally by the present author [69], in respect to the Kursk magnetic anomalies, which are due to the occurrence of a sharply dipping stratum of quartzites with magnetite interlayers at a depth of several hundred meters.

This stratum may be roughly compared to a rectangular prism (Figure 169), the horizontal side of which (length bb') has infinite dimensions and the vertical side has a (hight ac).

The prism is uniformly magnetized in the vertical direction and its width ab is small in comparison to the height, and thus the influence of the bottom side cd may be disregarded.

Declassified in Part - Sanitized Copy Approved for Release 2013/01/23 : CIA-RDP81-01043R001600090003-8

Declassified in Part - Sanitized Copy Approved for Release 2013/01/23 : CIA-RDP81-01043R001600090003-8

According to the deductions of Section 8 of this chapter the vertical and horizontal components of the intensity of the magnetic field of such a prism will have the form:

$$Z_a = 2J \operatorname{arc\,tg} \frac{2Ra}{R^2 - a^2 + x^2}, \quad H_a = 0.5J \ln \frac{R^2 + (x+a)^2}{R^2 + (x-a)^2}$$

wherein R is the depth of occurrence, i.e., the distance from the earth's surface to the upper side of the prism, a the width of the prism, x the distance from the axis of anomaly and J the magnetization of the prism.

With a change in the magnetic field of the earth the magnetization of the rock J, and consequently the magnitude of the components Z_a and H_a also will change. Therefore, on observing the changes in anomalous field it is possible to ascertain the extent to which variations of the terrestrial field alter the magnitude of magnetization of the rocks, and thus the question whether the magnetization is of residual or inductive origin may be resolved.

Since the anomalous field reaches its highest value at the center of the anomaly the effect of variations must be strongest over its center. Therefore let us consider the variations of the magnetic field over the center of the anomaly. At x = 0:

$$H_a = 0; \quad Z_a = 2J \operatorname{arc\,tg} \frac{2Ra}{R^2 - a^2},$$

and consequently, the variations of the anomalous field will be:

$$\delta H_a = 0, \quad \delta Z_a = Z_a \frac{\delta J}{J}.$$

Since

$$J = J_r + \varkappa Z_n,$$

where J_r is residual magnetization, $\varkappa$ is magnetic susceptibility of the rocks and Z_n is the vertical component of the normal field; hence

$$\delta Z_a = \frac{\varkappa Z_n}{J_r + \varkappa Z_n} \delta Z_n.$$

The observed variation will be the sum of the normal variation δZ_n and the anomalous variation δZ_a, i.e.,

Declassified in Part - Sanitized Copy Approved for Release 2013/01/23 : CIA-RDP81-01043R001600090003-8

Declassified in Part - Sanitized Copy Approved for Release 2013/01/23 : CIA-RDP81-01043R001600090003-8

$$\delta Z = \left[1 + \frac{Z_a}{Z_n\left(1 + \frac{J_r}{x Z_n}\right)}\right] \delta Z_n. \qquad (8.1)$$

Thus the variations of the vertical component over the center of the anomaly must be proportional to the normal variation and as is shown by equation (8.1), the proportionality coefficient always is greater than one, therefore

$$\delta Z > \delta Z_n.$$

If the residual magnetization is small and it may be disregarded, it follows that

$$\delta Z = \left(1 + \frac{Z_a}{Z_n}\right) \delta Z_n.$$

At the Kursk anomalies $Z_a/Z_n \approx 4$, therefore the variation over the center of the anomalies in this case should be 5 times greater than the normal.

On the other hand, if we disregard the inductive magnetization xZ_n, it follows that

$$\delta Z = \left(1 + \frac{x Z_a}{J_r}\right) \delta Z_n.$$

In the case of the Kursk anomalies $Z_a = 1.5$, and according to the findings of N. K. Shchodro the magnetic susceptibility and residual magnetization respectively are $x = 0.1$, and $J_r = 2.5$. Hence

$$\delta Z = (1 + 0.05)\, \delta Z_n,$$

i.e., in this instance variations of the vertical component should be only 5% greater than the variations in the normal field.

Finally, if the susceptibility of the rocks is very small it follows that with any value of residual magnetization J_r:

$$\delta Z = \delta Z_n,$$

i.e., the permanent magnetization of the rocks does not alter the variations of the normal field.

Declassified in Part - Sanitized Copy Approved for Release 2013/01/23 : CIA-RDP81-01043R001600090003-8

Declassified in Part - Sanitized Copy Approved for Release 2013/01/23 : CIA-RDP81-01043R001600090003-8

Observations conducted in 1936 by the present author within one area of the Kursk anomalies have shown that variations within the anomalous area are of the same order as those in the normal field. The observations were carried out simultaneously at 2 stations, one of which was located at the maximum of Z, and the other at the maximum of H. These observations were compared with the observations at the Nizhnedevitsa observatory, located within the normal field approximately 60 km from these stations.

The results of the observations are shown in Figure 131 in the form of graphs of the mean monthly diurnal variations of vertical, north and east components. These curves reveal that the variations of all the components are of the same order both at the stations and at the observatory. There are certain deviations in the amplitude of north and vertical components, but the phases are the same for all the components. However, these deviations must be attributed to errors in measurements rather than to the effect of the variations on the change in magnetization of the rocks. Thus these observations fully confirmed the theoretical deductions that variations of the magnetic field have a very slight effect on the magnitude of the anomalous field, if the latter is caused by residual, and not by inductive magnetization of the rocks. As was shown directly by the experiments the residual magnetization of the rocks of the Kursk anomalies is several score times greater than the inductive magnetization.

Section 5. Methods of Investigation of the Magnetic Properties of Rocks

In view of the great variety of magnetic properties of different types of rocks, procedures for the investigation of magnetic properties also are diversified. Certain methods are applicable in the case of strongly magnetic rocks, while slightly magnetic rocks having paramagnetic properties necessitate the use of other, more sensitive methods.

Declassified in Part - Sanitized Copy Approved for Release 2013/01/23 : CIA-RDP81-01043R001600090003-8

Declassified in Part - Sanitized Copy Approved for Release 2013/01/23 : CIA-RDP81-01043R001600090003-8

In addition, the requirements of practical operations dictate specific prerequisites which necessitate modification of the accepted methods or the development of new methods. Thus there is no single investigative procedure. There are a number of methods and a number of instruments of specific design, the use of which depends on the properties of the rocks as well as on the conditions under which the investigations are carried out.

Investigation of magnetic properties consists of the measurement of magnetic permeability, if it does not depend upon the magnetization J, determination of the basic magnetization and hysterosis curves and determination of the residual magnetization of the rock in its natural state.

The ballistic method is entirely suitable for determination of the hysteresis curve of strongly magnetic rocks such as magnetite, while the magnetometric method is adequate in the case of less magnetic rocks. The magnetometric method is more convenient for determination of residual magnetization.

The method of attraction and repulsion within a nonuniform magnetic field is most convenient for the determination of magnetic susceptibility of para and diamagnetic rocks which are uniform in composition and in which the magnitude of susceptibility is of the order of 10^{-5} to 10^{-6} CGSμ.

However, rocks which are not uniform in composition are more conveniently tested by means of a magnetometer, since in this case the more characteristic quantity is the mean susceptibility of a specimen of large volume, the measurement of which is impossible in principle by the first method.

Declassified in Part - Sanitized Copy Approved for Release 2013/01/23 : CIA-RDP81-01043R001600090003-8

Declassified in Part - Sanitized Copy Approved for Release 2013/01/23 : CIA-RDP81-01043R001600090003-8

The selection of the procedure to be used also depends to a large extent upon the shape of the specimen. In Section 9 of the introduction, it was shown that the magnetization curves of ferromagnetic specimens consisting of the same material, but having different shape differ considerably from one another, and therefore the characteristic of magnetic properties is considered to be the susceptibility, or the magnetization curves of specimens having a closed magnetic circuit. For transition from an open to a closed magnetic circuit the demagnetization coefficient N of the specimen being tested must be known.

In Section 9 it also was stated that the demagnetization coefficients are known only for specimens having the shape of an ellipsoid or cylinder. Therefore the ballistic and magnetometric methods may be utilized only when the magnetic susceptibility of the rocks does not depend upon the shape or where the rocks can be shaped into a cylinder.

The difficulties encountered in working specimens of hard rocks into a regular geometric shape have necessitated the development of specific methods of measurement which do not depend upon the shape of the specimen. However, these attempts have not provided a complete substitute for any of the above measurement methods, in view of the greater accuracy of the latter.

Thus in addition to the approximation methods used mostly under field conditions, the ballistic and magnetometric methods remain the fundamental methods for measuring the magnetic properties of rocks. The method of attraction within a nonuniform magnetic field is used exclusively in the case of rocks having para- and diamagnetic properties.

Declassified in Part - Sanitized Copy Approved for Release 2013/01/23 : CIA-RDP81-01043R001600090003-8

Declassified in Part - Sanitized Copy Approved for Release 2013/01/23 : CIA-RDP81-01043R001600090003-8

1. Ballistic Method. The ballistic method of measurement of the magnetic quantities of a specimen is based on the generator of a current within a conductor surrounding the specimen called the measuring coil, upon variation of the magnetic flux within the specimen from + Φ to - Φ or from + Φ to 0. The induction current is measured by means of a ballistic galvanometer, and for this reason this method is called the ballistic method.

The current intensity I arising within the closed circuit of the measuring coil at some point of time

$$I = E/R = W/R \cdot d\Phi/dt \quad 10^{-8} \text{ a.}$$

where R is the resistance of conductor and galvanometer and W the number of turns of the measuring coil.

Hence the amount of electricity Q flowing through the cross section of the conductor when the flux is changed from + Φ to - Φ, is expressed as the integral

$$Q = \int_0^t I \, dt = 2 \cdot 10^{-8} \, W \, \Phi \, K.$$

If the measuring coil is connected in series to a ballistic galvanometer, upon the passage of Q units of electricity through this coil the pointer or mirror of the galvanometer will be deflected over an angle θ and thus

$$Q = C \theta$$

where C is a constant which depends upon the design of the galvanometer.

Denoting the cross-sectional area of the specimen by S and the magnetic induction in the latter by B, we have

$$B = 10^8 \quad CR/2wS \quad \theta. \qquad (8.2)$$

The constant quantity CR may be determined by measuring the galvanometer deflection θ caused by the change of magnetic flux in a coil with a dual winding, the coefficient of mutual induction of which is known.

Declassified in Part - Sanitized Copy Approved for Release 2013/01/23 : CIA-RDP81-01043R001600090003-8

Declassified in Part - Sanitized Copy Approved for Release 2013/01/23 : CIA-RDP81-01043R001600090003-8

For this purpose one of the windings (secondary) of the coil is connected in series to the ballistic galvanometer and the current intensity in the other (primary) coil is varied from + I to - I.

If the coefficient of mutual induction of the coil M is expressed in Henry's the magnetic flux θ_1 expressed in amperes, contacting the secondary winding of the coil when current I flows through the primary will be

$$\theta_1 = 10^8 \text{ MI} \quad \text{Maxwell}$$

Therefore, on varying the current intensity from + I to - I we obtain through formula (8.2):

$$10^8 \text{ MI} = 10^8 \text{ CR}_1/2\ \theta,$$

where R_1 is the resistance of the secondary winding of the coil and the galvanometer. Usually the secondary winding of the coil is connected in series to the measuring coil which surrounds the specimen. Therefore $R_1 = R$, and hence

$$CR = 2MI/\theta_1$$

The following measurements are possible by this method: (1) determination of the basic magnetization curve, (2) determination of the hysteresis curve, (3) determination of coercive force and residual induction, (4) determination of reversible permeability, and (5) determination of residual flux.

The work diagram of these measurements is shown in Figure 132 in which R_1 and R_2 denote low and high resistance rheostats, respectively, for the regulation of the current in the circuit. A_1 and A_2 are ammeters for measuring the current intensity. A_1 measuring high-intensities and A_2 measuring any current intensity, G is a ballistic galvanometer, K is a magnetizing coil in which the specimen is placed, B is a standard mutual induction coil for calibration of the galvanometer, KB is a variable mutual induction coil for compensation of

Declassified in Part - Sanitized Copy Approved for Release 2013/01/23 : CIA-RDP81-01043R001600090003-8

Declassified in Part - Sanitized Copy Approved for Release 2013/01/23 : CIA-RDP81-01043R001600090003-8

the flux in the air gap between the specimen and the measuring coil, P is the main knife switch, Π_1 is a circuit current direction change-over switch, Π_3 is a change-over switch for the galvanometer circuit, Π_2 is a switch for connecting either the magnetizing coil or the specimen coil, and B_1 is a single pole knife switch for varying current intensity.

In Section 17 of the introduction it was shown that the hysteresis curve and the basic magnetization curve are the characteristics of a magnetic rock when magnetization or magnetic induction relate to a closed magnetic circuit. Induction in a closed circuit can be produced in either of 2 ways: direct observation in the closed circuit, or observation of induction of the specimen in an open solenoid and transference to the closed circuit by means of the demagnetization coefficient, which must be known for the given shape of the specimen.

The first procedure is not applicable in the case of rocks due to the difficulty of obtaining a specimen of necessary shape. Therefore tests of rocks by the ballistic method always are carried out in an open circuit by placing the specimen in a solenoid.

However, in such a case the specimen must be of a definite shape, either a cylinder or a rectangular prism with a length-to-diameter ratio of not less than 15, so that its coefficient of demagnetization may be determined.

2. The Magnetometric Method of measuring magnetic values is based on the interaction of 2 magnets. The specimen NS is suspended from a filament and placed within the horizontal plane inside the magnetizing coil, perpendicularly to the magnetic meridian in the first or second Gaussian position (see below Section 7 of Chapter X) in relation

Declassified in Part - Sanitized Copy Approved for Release 2013/01/23 : CIA-RDP81-01043R001600090003-8

Declassified in Part - Sanitized Copy Approved for Release 2013/01/23 : CIA-RDP81-01043R001600090003-8

to one of the magnets ns (lower) of the astatic system (Figure 133). By an astatic system is meant 2 parallel magnets rigidly fastened at a certain distance l from each other. The magnetic moments of these magnets must be equal and directed in opposite directions. Actually, their magnetic moments differ slightly, both in magnitude and direction.

The astatic system is placed within the magnetic meridian, and under the influence of the specimen NS it is deflected by an angle ϑ, which may be measured, and this the magnetic moment M of the specimen may be determined.

Assuming that the upper magnet is at so great a distance from the astatic magnetic system that the influence of the specimen can be disregarded then, denoting the magnetic moment of one of the magnets of the system by M', the torsion coefficient of the filament by C and the distance between the centers of the specimen and of the magnet of the astatic system by R, we have in accordance with formula (10.35) the following condition of equilibrium for the first and second Gaussian positions

$$n \quad MM'/R^3 \; k \cos \theta = C\theta, \tag{8.3}$$

where n = 2 for the first, and n = 1 for the second Gaussian positions, K is a coefficient greater than unity depending on the coefficients of distribution and different for different positions.

From equation (8.3) it follows that

$$M \; CR^3/nM'k \quad \theta \sec \theta,$$

at small angles of deflection which usually are encountered in practice sec θ may be replaced by the 2 first terms of the expansion, so that

$$M = \xi \theta \; (1 - 1/2 \; \theta^2). \tag{8.4}$$

where the factor ξ, equal to

$$\xi = CR^3/nM'k, \tag{8.5}$$

Declassified in Part - Sanitized Copy Approved for Release 2013/01/23 : CIA-RDP81-01043R001600090003-8

Declassified in Part - Sanitized Copy Approved for Release 2013/01/23 : CIA-RDP81-01043R001600090003-8

represents the value of one division of the magnetometer scale and is constant for any given design.

It is seen that at the given values of C and M' the magnetometer is proportional to the cube of the distance and, therefore, the value of one division may be changed by moving the specimen and thus the sensitivity of the instrument may be varied within wide limits. At a given distance the value of one division is directly proportional to coefficient of torsion of the filament and inversely proportional to the magnetic moment of the magnet of the astatic system. Therefore, it would appear that the sensitivity of the instrument could be increased to any level, but experience shows that every instrument has a limit of sensitivity above which the system becomes unstable and its use impossible.

This is due to the fact that equation (8.3) has meaning under completely astatic conditions of the system and when the magnet of the magnetometer has no influence on the specimen under study. The first condition is never fulfilled in practice and the second is possible only if the specimen is placed at a distance not less than that at which the magnet begins to exercise an influence on the specimen.

The value of a division ξ at both positions is determined by means of a permanent magnet, the magnetic moment M_o of which is known and which is approximately the same size as the specimen under study. Measuring the deflection θ_o of the magnetometer due to the influence of this magnet, we have

$$\xi = M_o/\theta_o(1 - 1/2\ \theta_o^2).$$

To determine the magnetization curve, i.e., the correlation between magnetization J and the magnetizing field H, the specimen under study is given the shape of an elongated ellipsoid or cylindrical rod, the demagnetization coefficients of which are found in tables.

Declassified in Part - Sanitized Copy Approved for Release 2013/01/23 : CIA-RDP81-01043R001600090003-8

Declassified in Part - Sanitized Copy Approved for Release 2013/01/23 : CIA-RDP81-01043R001600090003-8

The specimen is magnetized in a coil at least 3 times larger than the length of the specimen. This is necessary to ensure a uniform field in the middle of the coil, where the specimen is placed. A second, identical coil is placed on the other side of the astatic system so that it is located symmetrically with the first coil and is connected in series with it. A diagram of the connection of these coils is shown in Figure 133.

The second coil serves to compensate the magnetic field produced by the magnetizing coil. This is done by moving the second coil while current is flowing through it, until the astatic system resumes its initial position. This having been done, when the specimen is placed inside the magnetizing coil, deflection of the system is due solely to the action of the magnetized specimen.

Magnetization of the specimen J, corresponding to the magnetizing field H is determined by formula (8.4), in which the product of magnetization J by the volume of the specimen V, is substituted for the magnetic moment, i.e.,

$$J = \xi/V\ \theta\ (1 - 1/2\ \theta^2)$$

The intensity of the magnetizing field is determined by the formula

$$H = H_e - NJ$$

where H_e is the field intensity inside the coil and N is the magnetometric coefficient of the demagnetization of the specimen.

Furthermore, at small distances between the magnetizing and compensation coils the intensity of the field produced by the compensation coil at the place where the specimen is located must be subtracted from H_e.

The magnetometric method in this form enables tests of

Declassified in Part - Sanitized Copy Approved for Release 2013/01/23 : CIA-RDP81-01043R001600090003-8

Declassified in Part - Sanitized Copy Approved for Release 2013/01/23 : CIA-RDP81-01043R001600090003-8

ferromagnetic specimens, the magnetic susceptibility of which is not less than 10^{-4} CGSμ. At lower susceptibility values this method becomes unreliable due to inadequate sensitivity.

As in the ballistic method, the deflection angle θ is observed by means of a mirror connected to the magnet ns, and a graduated scale located at distance L from the mirror. Therefore, the angle θ is replaced by the scale reading n, in accordance with the formula

$$\theta = n/2L\ (1 - n^2/3L^2). \qquad (8.6)$$

Let us consider next the influence of defects in the setup and design of the magnetometer on its readings. This is necessary because in the derivation of equation (8.6) it was assumed that the system was fully astatic and that the second magnet of the system was remote from the specimen.

Influence of the Second (Upper) Magnet. The influence of the upper magnet affects only the value of one division, which in this instance remains a constant quantity independent of the deflection angle. However, this influence varies with different positions of the specimen.

In the first Gaussian position the moment of rotation Q acting on the upper magnet n's' may be readily computed, assuming the specimen to be an elemental magnet (dipole). Indeed, denoting the component of the field of this magnet, in the direction r by H_r, and denoting the component perpendicular to the latter by H_φ, we have:

$$Q = [-M''H_r \cos\varphi + M''H_\varphi \sin\varphi\ ] \cos\theta,$$

where M'' is the magnetic moment of the upper magnet and φ the angle between the axis OO_1 and the direction r (Figure 134a).

Declassified in Part - Sanitized Copy Approved for Release 2013/01/23 : CIA-RDP81-01043R001600090003-8

Declassified in Part - Sanitized Copy Approved for Release 2013/01/23 : CIA-RDP81-01043R001600090003-8

Replacing H_r and H_φ according to the formulas for dipoles, and replacing sin θ and cos θ by the ratio of the sides we obtain:

$$Q = \frac{MM''}{r^5} \cos\theta \left(l^2 - 2R^2\right),$$

and

$$r^2 = R^2 + l^2.$$

It is evident that this moment is equal to zero when

$$R = \frac{l}{\sqrt{2}}$$

at $R > l/\sqrt{2}$ the moment Q is negative, i.e., it is opposite to the moment acting on the lower magnet, and at $R < l/\sqrt{2}$ the moment has a positive value, i.e., the same direction as the moment acting on the lower magnet.

If the magnetic moments M' and M" are equal in magnitude and opposite in direction the equation of equilibrium of the system will be:

$$\left[2\frac{MM'}{R^3} l + \frac{MM'}{r^5}\left(l^2 - 3R^2\right)\right]\cos\theta - C\theta = 0.$$

Solving this equation for M, we obtain

$$M = \frac{R^3 C}{M'\left[l + \frac{R^3}{2R^5}\left(l^2 - 2R^2\right)\right]} \theta \sec\theta. \qquad (8.7)$$

The factor appearing before θ sec θ is constant for a given distance R. Therefore, denoting the former by ε_1, and in view of the smallness of angle θ, denoting sec θ by $1 + 1/2\ \theta^2$ we obtain

$$M = \varepsilon\theta\left(1 + \frac{1}{2}\theta^2\right).$$

Substituting angle θ in accordance with formula (8.6) and assuming $\frac{\varepsilon_1}{2l} = \varepsilon$, we obtain: $M = \varepsilon\left(n - \frac{5}{24}\cdot\frac{n^3}{l^2}\right)$.

The quantity ε is the value of one division of the magnetometer, expressed in units of magnetic moment.

As is apparent from equation (8.7) the value of one division depends on the torque of the filament and the distance between the specimen and the magnetic system.

As is apparent from Figure 134, if the specimen is considered a dipole the moment of rotation Q in the second Gaussian position is given by the equation

Declassified in Part - Sanitized Copy Approved for Release 2013/01/23 : CIA-RDP81-01043R001600090003-8

Declassified in Part - Sanitized Copy Approved for Release 2013/01/23 : CIA-RDP81-01043R001600090003-8

$$Q = \frac{MM'}{r^3}\cos\theta.$$

Consequently, the equation of equilibrium will be of the form

$$\left(\frac{MM'}{R^3} - \frac{MM''}{r^3}\right)\cos\theta = C\theta,$$

Thus

$$M = \frac{CR^3}{M'\left(k - \frac{R^3}{r^3}\right)}\theta\sec\phi,$$

or, analogously to the foregoing,

$$M = \varepsilon_2\theta\left(1 - \frac{1}{2}\theta^2\right), \qquad \text{where} \quad \varepsilon_2 = \frac{CR^3}{M'\left(k - \frac{R^3}{r^3}\right)}$$

In this case the value of one division increases with an increase in R over the entire range from R = 0 to k = ∞, and the increase is more rapid than indicated by formula (8.5).

Influence of Non-Astatic Nature of the System.

We denote the magnetic moments of the 2 magnets by M_1 and M_2 (Figure 135), their geometric sum by M, the horizontal component of the terrestrial field by H, the intensity of the specimen's magnetic field at the site of the lower magnet by H_1, and the intensity of the specimen's field at the site of tbe upper magnet by H_2, with H_1 and H_2 perpendicular to H, the angle of twist of the filament is indicated by φ and C is the constant of torsion.

We denote, further, the angle between M_1 and H by θ_1, the angle between M_2 and H by θ_2 and the angle between M and H by $\theta = \theta_1 + \alpha$, in which case the condition of equilibrium of the magnetic system will be

$$MH\sin(\theta_1 + \alpha) - M_1H_1\cos\theta_1 - M_2H_2\cos\theta_2 = C\varphi \qquad (8.8)$$

A change in magnetization of the specimen produces a change in the intensity of fields H_1 and H_2, as a result of which the condition of equilibrium is disrupted and the system is deflected over a certain angle $d\theta$. Differentiating equation (8.8), and taking into account that H_2 is proportional to H_1, i.e., that $H_2 = kH_1$, we have

Declassified in Part - Sanitized Copy Approved for Release 2013/01/23 : CIA-RDP81-01043R001600090003-8

Declassified in Part - Sanitized Copy Approved for Release 2013/01/23 : CIA-RDP81-01043R001600090003-8

$$dH_1 = \frac{H_1(M_1 \sin\theta_1 + kM_2 \sin\theta_2) + MH\cos\theta - C}{M_1\cos\theta_1 + kM_2\cos\theta_2}\, d\theta$$

Considering kM_2 as a certain magnetic moment M_2', parallel to moment M_2, and considering the geometric sum $M_1 + M'_2$ as a certain moment M', the foregoing expression may be written as:

$$dH_1 = \frac{H_1 M' \sin\theta' + MH\cos\theta - C}{M'\cos\theta'}\, d\theta$$

where θ' is the angle between H and M'.

Disregarding the influence of the specimen on the upper magnet, i.e., assuming k = 0, it follows that $M' = M_1$, and $\theta' = \theta_1$, and therefore

$$dH_1 = \frac{H_1 M_1 \sin\theta_1 + MH\cos\theta - C}{M_1\cos\theta_1}\, d\theta$$

The angle of deflection θ_1 of a magnetometer never exceeds several degrees, and thus cos θ_1 may be replaced by unity, and sin θ_1 may be replaced by the angle θ_1, in which case

$$dH_1 = -\frac{C}{M_1}\left[1 - \frac{H_1 M_1 \theta_1}{C} - \frac{MH}{C}\cos\theta\right] d\theta.$$

If dH, changes at values other than $H_1 = 0$, it follows that at small angles of deflection it may be assumed that $dH_1 = H_1$ and $d\theta = \theta_1$, in which case

$$H_1 = -\frac{C}{M_1}\left[1 - \frac{H_1 M_1 \theta_1}{C} - \frac{MH}{C}\cos\theta\right]\theta_1$$

Since the second and third terms appearing between the brackets are small in comparison with unity, it follows that H_1 in the second term may be replaced by the quantity $H = -C/M'$ and therefore

$$H_1 = -\frac{C}{M_1}\left[1 + \theta_1^2 - \frac{MH}{C}\cos\theta\right]\theta_1. \qquad (8.9)$$

at angles of deflection θ not exceeding 5°, which usually is the case in practice, the second term θ_1^2 is not greater than 0.01, and may be disregarded. In the third term the angle θ may be replaced by the sum $\theta_1 + \alpha$, wherein α is the angle between M and M_1. In this case equation (8.9) becomes:

$$H_1 = -\frac{C}{M_1}\left[1 - \frac{MH}{C}\cos(\theta_1 + \alpha)\right]\theta_1.$$

Declassified in Part - Sanitized Copy Approved for Release 2013/01/23 : CIA-RDP81-01043R001600090003-8

Declassified in Part - Sanitized Copy Approved for Release 2013/01/23 : CIA-RDP81-01043R001600090003-8

Denoting $C/M_1 = \varepsilon$, where ε is the value of one division of the astaticized system, it follows that

$$H_1 = -\ (1 - M/M_1 \cdot H/\varepsilon \cos(\alpha + \theta_1)]\theta_1.$$

Consequently, the value of one division of the astatic magnetometer depends on the angle θ, and the smaller the value of one division, the greater is this dependence. Since α is always close to 90° it follows that at $(\alpha + \theta_1) = \theta_1$ the condition under which this dependence can be disregarded

$$M/M_1 \cdot H/\varepsilon\ \theta_1 < 1,$$

and the value of one division ε must be

$$\varepsilon > M/M_1\ H\ \theta_1.$$

Influence of Non-Parallelism of Magnetizing and Compensation Coils.

If the coils K_1 and K_2 are not parallel to each other, their summative field never is equal to zero, but this field may have no effect on the equilibrium position of the magnetic system and when the current in the coils is switched off the magnetic system may remain at rest. For this it is necessary that the direction of the summative field coincide with the magnetic axis of the lower magnet. With such a system of compensation the value of one division becomes greatly dependent upon the intensity and direction of the current in the coils.

If the intensities of fields H_1 and H_2 produced by the coils at the site of the lower magnet form an angle α between them which is different from 180° (Figure 136), denoting the angle formed by the axis of magnet M_1 with the direction H_1 by φ disregarding the influence on the upper magnet and assuming that the system is fully astaticized, the equilibrium equation of the system will assume the following form

$$M_1 H \cos\theta + M_1 H_1 \sin\varphi + M_1 H_2 \sin(\alpha - \varphi) = C\psi.$$

Declassified in Part - Sanitized Copy Approved for Release 2013/01/23 : CIA-RDP81-01043R001600090003-8

Declassified in Part - Sanitized Copy Approved for Release 2013/01/23 : CIA-RDP81-01043R001600090003-8

where θ is the angle of deflection of the system from the position of equilibrium due to the action of the summative field of intensity H, and ψ is the angle of twist of the filament.

Differentiating this expression and solving for dH, we obtain

$$dH = -C/M_1\ d\theta - [H_2 \cos(\vartheta - \varphi) + H_1 \cos\varphi]\ d\theta.$$

Next, taking $H_1 = H_2$ and transforming the sum of cosines, we have

$$dH = -C/M_1\ d\theta - 2H_1 \cos\vartheta/2 \cos(\vartheta/2 - \varphi)d\theta.$$

The angle $\vartheta/2 - \varphi$ is approximately zero, and therefore its cosine may be replaced by unity, hence

$$dH = -[C/M_1 + 2H_1 \cos\vartheta/2]\ d\theta.$$

Since $2H_1 \cos\vartheta/2$ represents the magnitude of the summative vector $(H_1 + H_2)$, on denoting it by h, we see that the value of one division of the magnetometer ε_1 in this instance is expressed by the sum:

$$\varepsilon_1 = C/M + h.$$

h changes its sign upon a change in direction of current in the coil, and therefore when the magnetometer is deflected in one direction the value of one division will be 2h times greater or smaller than when deflection is in the opposite direction.

In order to avoid this the coil axes must be parallel. This is done as follows: after the coils have been compensated the specimen is placed into the coil. The deflections of the magnetometer are observed when the current flows in either direction, and then one of the coils is rotated around its vertical axis until the deflections are equal in both directions.

Measuring Procedure. To determine the basis curve of magnetization the cylindrical or prismatic specimen is placed inside one of the coils of the magnetometer, and is demagnetized by switching an

Declassified in Part - Sanitized Copy Approved for Release 2013/01/23 : CIA-RDP81-01043R001600090003-8

Declassified in Part - Sanitized Copy Approved for Release 2013/01/23 : CIA-RDP81-01043R001600090003-8

alternating current through the coil, which is gradually decreased to zero. Next, a direct current coinciding with the initial value of the intensity of the magnetic field is passed through the coil. In this operation a completely open rheostat is connected to the coil circuit, and the current is adjusted to the necessary level solely by a gradual decrease of the resistance. After the current has been adjusted the magnetic preparation or repeated reversal of the current is performed, and the last time the current is switched on a reading is taken of the magnetometer.

For determination of subsequent points the current is gradually increased and magnetic preparation is carried out prior to each observation.

There is preliminary demagnetization since in determination of the hysteresis curve, determination of each point begins with the switching on of a maximum current and its gradual decrease to the necessary magnitude corresponding to the intensity of the demagnetizing field.

3. The Magnetometer of B. M. Yanovskiy and Ye. T. Chernyshev. B. M. Yanovskiy and Ye. T. Chernyshev have proposed [65] a more sensitive method which is a variant of the above. The cylindrical specimen A (Figure 137) with diameter not less than 3 cm, is placed several cm (1-3) from the lower magnet of the astatic system M. Large diameter Helmholtz rings K_1 are used for magnetization of the specimen, and on either side of the system so that the specimen and the lower magnet of the system are within the same field. For compensation of this field the upper magnet is placed into small diameter rings K_2, which are connected in series to the large rings. Since the small rings remain stationary final compensation is effected by changing the current in the secondary winding of these rings which is connected in parallel to the large rings.

Declassified in Part - Sanitized Copy Approved for Release 2013/01/23 : CIA-RDP81-01043R001600090003-8

Declassified in Part - Sanitized Copy Approved for Release 2013/01/23 : CIA-RDP81-01043R001600090003-8

Taking the intensity of the field produced by the cylindrical specimen inside the rings as H_o, in such a case the condition of equilibrium of the astatic system will be:

$$H_o M \cos\theta = C\theta \qquad (8.10)$$

because the influence of the specimen on the upper magnet may be disregarded.

The magnitude of H_o is obtained by differentiating equation (0.63) with respect to R:

$$H_o = 2\pi J\left[R + \ell/\sqrt{a^2 + (R + \ell)^2} - R/\sqrt{R^2 + a^2}\right]$$

Substituting this value of H_o in equation (8.10), and replacing angle θ by the reading on the scale n, we obtain:

$$J = \varepsilon n/R + \ell/\sqrt{a^2 + (R + \ell)^2} - R/\sqrt{R^2 + a^2}$$

where $\varepsilon = C/2LM$ is the value of one division of the instrument's scale. The intensity of the field corresponding to magnetization J in the case of the Helmholtz rings is determined in accordance with the usual formula (0.38).

At the experimental shops of the Institute of Physics of the Leningrad State University imeni A. A. Zhdanov a magnetometer has been built which enables measurements to be made by the conventional magnetometric method described on page 302, and by the method of B. M. Yanovskiy and Ye. T. Chernyshev.

It consists (Figure 138) of a base A, on which a suspension tube B, containing the astatic system is mounted. Rigidly attached to the base is the bar C, on which 2 coils K_1 and K_2, the magnetizing and the compensation coil are mounted, each 300 mm long and having an internal diameter of 20 mm. The coils are set in the second Gaussian position. Another bar D is located perpendicular to this bar, on which 2 pairs of square coils K_3 and K_4 with dimensions 250 x 250 mm are mounted.

Declassified in Part - Sanitized Copy Approved for Release 2013/01/23 : CIA-RDP81-01043R001600090003-8

Declassified in Part - Sanitized Copy Approved for Release 2013/01/23 : CIA-RDP81-01043R001600090003-8

At the upper portion of the suspension tube is a pair of Helmholtz rings which compensate the field of the square coils and determine the value of one division of the scale.

The entire instrument rotates through an angle of 30° about the vertical axis for adjustment with respect to the magnetic meridian. Figure 139 shows the circuit diagram of the coils.

The specimen, in the shape of a cylinder up to 20 mm in diameter, or a prism with one side of the base up to 15 mm long, is placed inside the solenoid coil and the basic curve of magnetization and the hysteresis curve are determined by the method described on page 309.

However, in this case magnetization is effected by the 4 sq coils instead of the Helmholtz rings, and therefore the intensity of the magnetizing field at the axis of the coil must be determined for each coil in accordance with the formula:

$$H = \frac{8a^2 wI}{(a^2+x^2)\sqrt{2a^2+x^2}} = f(x)\,wI \qquad (8.11)$$

where 2a is the side of the square, w the number of turns, x the distance from the center of the coil and f(x) is a factor of wI depending on x. The distance between each pair of coils is the same and the magnetic field along the axis is made as uniform by proper selection of the number of turns of the external and internal coils. This ratio must ensure equal intensity at the center of each coil.

The field intensity at the center of the external coil at I = 1, according to formula (8.11) is given by the equation:

$$H = f(0)w_1 + f(x)w_2 + f(2x)w_2 + f(3x)w_1,$$

and at the center of the internal coil:

$$H = f(x)w_1 + f(0)w_2 + f(x)w_2 + f(2x)w_1.$$

Under the condition that the left-hand portions of these equations are equal, we have

$$\frac{w_2}{w_1} = 1 - \frac{f(x) - f(3x)}{f(0) - f(2x)}.$$

Thus, at x = a, $\frac{w_2}{w_1} = 0.57$.

Declassified in Part - Sanitized Copy Approved for Release 2013/01/23 : CIA-RDP81-01043R001600090003-8

Declassified in Part - Sanitized Copy Approved for Release 2013/01/23 : CIA-RDP81-01043R001600090003-8

4. The Method of Attraction and Repulsion in a Non-Uniform Magnetic Field.

This method was proposed by Faraday and is based on measurement of the force F acting on a body of small volume, placed within a non-uniform magnetic field.

The theory shows that the force F is proportional to the magnetic susceptibility x and the volume v of the body, that is

$$F = Axv \tag{8.12}$$

If the coefficient of proportionality A is known and the force F has been measured it is possible to determine the magnitude of magnetic susceptibility. Coefficient A may be determined experimentally by direct measurement of the quantities which constitute this factor, or by measurement of the force acting on a body of known susceptibility. In the former instance the method of measuring the susceptibility is an absolute method, and in the latter it is relative.

In the derivation of formula (8.12) the expression for the potential energy U of a body placed within a magnetic field is used, namely

$$U = -\int xH^2/2 \, dv, \tag{8.13}$$

where H is the intensity of the magnetic field, dv is the element of volume, and the integration applies to the entire volume of the body. According to the laws of mechanics the force F acting on the body is expressed by the gradient of the quantity U preceded by the opposite sign, i.e.,

$$F = \text{grad} \int xH^2/2 \, dv$$

Since for paramagnetic bodies x is a constant quantity, it follows that

$$F = x/2 \int \text{grad } H^2 dv.$$

Declassified in Part - Sanitized Copy Approved for Release 2013/01/23 : CIA-RDP81-01043R001600090003-8

Declassified in Part - Sanitized Copy Approved for Release 2013/01/23 : CIA-RDP81-01043R001600090003-8

If the body is of small dimensions it may be assumed that grad H^2 does not change its magnitude within the boundaries of this body and therefore integration over its volume yields:

$$F = 1/2\ xv\ \text{grad}\ H^2 = xvH\ dH/dr, \tag{8.14}$$

where r is the direction of greatest change in H, and v is the volume occupied by the body. Thus the constant coefficient A of formula (8.12) is the product of the intensity of field H and its gradient.

From equation (8.14) it follows that an equilibrating force must be applied in the direction r to measure force F.

From equation (8.14) we obtain that

$$x = F/H\ dH/dr\ v \tag{8.15}$$

The magnetic susceptibility x, which may be designated as magnetic susceptibility by volume, may be replaced by the specific susceptibility x, i.e., the susceptibility per unit density. Therefore, dividing both sides of equation (8.15) by the density D of the body, we have

$$\chi = x/D = F/H\ dH/dr\ m, \tag{8.16}$$

where m is the mass of the body.

For the case in which the body under study is located in a medium having magnetic susceptibility x_o (viz air, a liquid, etc) equation (8.13) must be corrected as follows:

$$U = -\int x\text{-}x_o/2\ \ H^2\ dv.$$

Thus in the general case formula of susceptibility (8.15) is:

$$x = \kappa_o + F/H\ dH/dr\ v,$$

or, substituting volume for susceptibility thefollowing is obtained for the specific susceptibility:

$$\gamma = \chi_o D_o/D + F/mH\ dH/dr, \tag{8.17}$$

Declassified in Part - Sanitized Copy Approved for Release 2013/01/23 : CIA-RDP81-01043R001600090003-8

Declassified in Part - Sanitized Copy Approved for Release 2013/01/23 : CIA-RDP81-01043R001600090003-8

where D_o is the density of the medium (air), and D the density of the substance being measured.

This method has very high sensitivity, enabling measurement of sensitivity up to 10^{-10} CGSμ. Indeed, from equation (8.16) it follows that at $H = 2 \cdot 10^4$ Oe and $dH/dr = 10^4$, which is readily attained by means of electromagnets, and at an attraction force F = 0.01 dyne, which is registered by a beam balance, x is approximately 10^{-10}CGSμ.

However, despite its high sensitivity as an absolute method this method has a substantial flaw in its low degree of accuracy, and for this reason it has been used mainly as a relative method. Formula (8.17) shows that for determination of χ the field intensity H and its gradient in the direction r must be measured in addition to direct measurement of the force F and of the mass m of the body being tested. Although the measurement of H involves no great difficulties, the measurement of dH/dr is very difficult, especially in the case of a large gradient. Both these quantities are eliminated with the use of a relative method and the problem is limited to direct measurement of F and m. Indeed, taking equation (8.17) for 2 bodies having specific susceptibilities x_1 and x_2, densities D_1 and D_2, masses m_1 and m_2 and placed within similar fields having the identical gradients, we have

$$\chi_1 = \chi_0 \frac{D_0}{D_1} + \frac{F}{m_1 H \frac{dH}{dr}}, \quad \chi_2 = \chi_0 \frac{D_0}{D_2} + \frac{F'}{m_2 H \frac{dH}{dr}}$$

Transposing the first terms of the right half of the equation to the left half and dividing one equation by the other, we obtain

$$\frac{\chi_1 - \chi_0 \frac{D_0}{D_1}}{\chi_2 - \chi_0 \frac{D_0}{D_2}} = \frac{F}{F'} \cdot \frac{m_2}{m_1},$$

hence,

$$\chi_1 = \chi_0 \frac{D_0}{D_1} + \left(\chi_2 - \chi_0 \frac{D_0}{D_2}\right) \frac{F}{F'} \cdot \frac{m_2}{m_1}. \qquad (8.18)$$

Declassified in Part - Sanitized Copy Approved for Release 2013/01/23 : CIA-RDP81-01043R001600090003-8

Declassified in Part - Sanitized Copy Approved for Release 2013/01/23 : CIA-RDP81-01043R001600090003-8

From this formula it is apparent that in the case of a relative method for determining x, the attraction forces F and F' acting on both the test specimen and on the standard specimen, and the masses m_1 and m_2 of these specimens are measured directly. The intensity of the field H and its gradient dH/dr can remain entirely unknown.

An electromagnet with tapered pole shoes N-S, as shown in Figure 140 usually is used to produce a non-uniform field. If the axis of the pole shoes AB is directed horizontally, it follows from the conditions of symmetry that the greatest variations of the quantity H in the vertical direction will occur along the CD axis which is perpendicular to AB and extends through the center of the pole shoes. Therefore if the equilibrating force is applied in the vertical direction, the point of application of this force must be on the axis CD, otherwise the specimen will be subjected to the influence of an additional force perpendicular to the axis.

The force of attraction which acts on the specimen may be counterbalanced by the force of gravitation, by a torsion force, or by an electromagnetic force. In the first case the body a under study is placed on one arm of the balance between the poles of the electromagnet (somewhat higher) and the force of its attraction is counterbalanced by counter-weights placed on the other arm (Figure 141). In such a case $F = M_g$ and $F' = M_1 g$, where M and M_1 are the masses of the counter weights used to counterbalance the force of attraction of the test body and of the standard body, so that formula (8.18) becomes

$$\chi_1 = \chi_0 \frac{D_0}{D_1} + \left(\chi_2 - \chi_0 \frac{D_0}{D_2}\right) \frac{M}{M_1} \cdot \frac{m_2}{m_1} \qquad (8.19)$$

In the second instance the specimen under study is suspended from the arm of a torsion balance and is placed laterally of the gap

Declassified in Part - Sanitized Copy Approved for Release 2013/01/23 : CIA-RDP81-01043R001600090003-8

Declassified in Part - Sanitized Copy Approved for Release 2013/01/23 : CIA-RDP81-01043R001600090003-8

between the poles. The attractive force F_x is counterbalanced by the torsion of the filament, which is twisted a certain angle θ. Since according to the condition of equilibrium

$$FL = C\,\theta$$

where L is the arm of the balance beam and C the coefficient of torsion, it follows that:

$$X_1 = X_o D_o/D_1 + (X_2 - X_o D_o/D_2)\,\theta/\theta_1 \cdot m_2/m_1. \qquad (8.20)$$

Among the defects of Faraday's method as a relative method, is the variation of the quantity H dH/dr in the direction r. The formulas of magnetic susceptibility (8.19) and (8.20) are derived on the assumption that the product H dH/dr remains constant on equilibration of force F, as well as of force F', since the specimen under study and the standard specimen are placed at the same distance from the pivot. Actually, complete coincidence cannot be attained in practice, and the slightest displacement of the body under study causes a sharp change in the force of attraction, since the product H dH/dr changes very rapidly with a change in the distance from the poles of the electromagnet. At point O, on the axis of the pole shoes (Figure 140) the gradient is dH/dr = O, and consequently the product is H dH/dr = O.

Upon vertical displacement along the axis r the product H dH/dr increases, reaches a maximum, and then gradually approaches zero. The curves representing H dH/dr as a function of r, in the case of symmetrically located pole shoes are shown in Figure 142. It is seen that the curve increases very rapidly from the point O, reaches a sharp maximum, and thereafter tends asymptotically to the ordinate axis. It is apparent from the curve that the most advantageous condition for measurement of x is obtained by placing the test body at a point where the quantity H dH/dr is at a maximum, since on either side of the maximum the function H dH/dr changes very slowly.

Declassified in Part - Sanitized Copy Approved for Release 2013/01/23 : CIA-RDP81-01043R001600090003-8

Declassified in Part - Sanitized Copy Approved for Release 2013/01/23 : CIA-RDP81-01043R001600090003-8

Figure 143 shows a diagram of a typical arrangement of a torsion balance. The balance beam AA is suspended from a metallic filament F which can be twisted by means of knob G. At one end of the beam is suspended the glass flask B containing the specimen being tested, and at the other end are the counter-weight E and mirror Z, which is used to observe deflection. The system is damped by means of an oil damper H. To prevent the effects of air oscillations the entire apparatus is enclosed by a sealed housing.

5. Cylinder Method.

Another variant of the method of attraction in a non-uniform field is based on measurement of the force acting on prism AB or on a cylinder, one end of which is placed within a uniform field H, and the other end within a uniform field H_o. This is called the cylinder method (Figure 144).

The attraction of such a cylinder may be regarded as the resultant of the attraction of each elemental volume dv = Sdz, where S is the cross-sectional area of the cylinder and dz its height. According to the preceding paragraph the force acting on such an elemental volume is

$$dF = 1/2\ \chi S\ \text{grad}\ H^2\ dz.$$

The vertical component is

$$df_z = \chi SH\,\partial H/\partial z\ dz,$$

or

$$dF_z = \chi SHdH.$$

Hence the total force in the direction z is:

$$F_z = \chi S \int_{H_o}^{H} H\ dH = \chi S/2(H^2 - H_o^2), \qquad (8.21)$$

where H is the intensity of the field between the poles and H_o the intensity of the field at the lower end of the cylinder.

Declassified in Part - Sanitized Copy Approved for Release 2013/01/23 : CIA-RDP81-01043R001600090003-8

Declassified in Part - Sanitized Copy Approved for Release 2013/01/23 : CIA-RDP81-01043R001600090003-8

If the axis of the cylinder is half way between the poles, i.e., coincides with the vertical symmetry axis of the poles, it follows that $\partial H/\partial x = 0$ and therefore the horizontal force is absent. However, upon the slightest deflection of the cylinder axis from the symmetry axis a horizontal attraction force arises. In the following it is assumed that the cylinder axis coincides with the symmetry axis, and consequently there are no forces other than the vertical forces F_z. Thus from equation (8.21) we have:

$$x = 2F_z/S(H^2 - H_o^2) \qquad (8.22)$$

The force F_z may be counterbalanced as in the Faraday method, either by means of a beam balance, placing the test cylinder at one end, and the pan holding the counter-weights at the other end of the beam, or some other method may be used.

In the former which is the most widely used method, the force F_z will be equal to the product of mass m of the counter-weights and the acceleration due to gravity, i.e.:

$$F_z = mg$$

hence,

$$\chi = 2mg/SD(H^2 - H_o^2)$$

where D is the density of the substance being tested.

Since the test usually is performed in the air, it follows from deductions analogous to those pertaining to the Faraday method, that corrections must be made for the susceptibility of the air, and the formula will be:

$$\chi = \chi_o D_o/D + 2mg/SD(H^2 - H_o^2). \qquad (8.23)$$

Thus we see that the cylinder method necessitates that the body under study be of a specific shape, either cylindrical or prismatic,

Declassified in Part - Sanitized Copy Approved for Release 2013/01/23 : CIA-RDP81-01043R001600090003-8

Declassified in Part - Sanitized Copy Approved for Release 2013/01/23 : CIA-RDP81-01043R001600090003-8

which leads to great difficulties in measuring the susceptibility of solids. Therefore this method is limited mostly to liquids, solutions of solids in liquids, and powders.

The liquid or solution is poured into a length of cylindrical glass tubing which is twice as long as the liquid column, to eliminate the influence of the magnetic field on the glass tubing. By placing the tubing between the poles of the electromagnet so that its center is at the center of the pole shoes the top and bottom ends of the tubing will be equidistant from the center of the electromagnet, and the action of the magnetic field on each half of the tubing will be equal but opposite. A diagram of the cylinder method, using a beam balance, is shown in Figure 145.

6. Astatic Magnetometer of S. Sh. Dolginov [70]

The principle upon which S. Sh. Dolginov's method is based was proposed by N. I. Spiridovich [71].

Dolginov's method differs from that of N. I. Spiridovich in that the former incorporates an astatic system of small dimensions, with the result that it can be utilized under field conditions. Also, the instrument proposed by S. Sh. Dolginov is absolute, whereas that of N. I. Spiridovich is relative.

Let us assume that a specimen of random shape and of small volume compared to is placed in the same plane, and at a certain distance from the dimensions of the magnet the center of one of the magnets of the astatic system.

If the radius-vector r (Figure 146) forms an angle other than 90° with the axis of the magnet a torque caused by the interaction between specimen and magnet will act on the magnet. This torque is

Declassified in Part - Sanitized Copy Approved for Release 2013/01/23 : CIA-RDP81-01043R001600090003-8

Declassified in Part - Sanitized Copy Approved for Release 2013/01/23 : CIA-RDP81-01043R001600090003-8

proportional to the product of magnetic moments of specimen M' and magnet M and inversely proportional to the cube of the distance, and is counterbalanced by the twisting moment of the filament when the filament is twisted through the angle φ, i.e.,

$$C\varphi = k\, MM'/r^3, \tag{8.24}$$

where k is the proportionality coefficient and C the coefficient of torsion of the filament. The coefficient k is smaller than unity and depends on the mutual positions and on the dimensions of the specimen and the magnet.

The magnetic moment M' is due to the action of the magnet and is roughly approximated by the expression:

$$M' = xHv, \tag{8.25}$$

where x is the apparent magnetic susceptibility of the specimen, H is the intensity of magnetic field produced by the magnet, and v is the volume of the specimen. The quantity H may be written in the form:

$$H = k'\, M/r^3, \tag{8.26}$$

where k' is a coefficient depending on the angle between r and M. Therefore, replacing M' in equation (8.24), from the values derived from equations (8.25) and (8.26), we obtain

$$kk'M^2v/r^6 = C\varphi$$

Taking the same equation for another specimen of volume V_o and magnetic susceptibility x_o, and dividing one equation by the other, we have:

$$x = x_o\, V_o/v \cdot \varphi/\varphi_o$$

Therefore if the volume and magnetic susceptibility of a specimen are known, the magnetic susceptibility may be determined by observing the angles φ and φ_c through which the magnetic needle is deflected by the action of the test specimen and that of a specimen of known susceptibility.

Declassified in Part - Sanitized Copy Approved for Release 2013/01/23 : CIA-RDP81-01043R001600090003-8

Declassified in Part - Sanitized Copy Approved for Release 2013/01/23 : CIA-RDP81-01043R001600090003-8

If this instrument is used for absolute measurements the specimens must be cylindrically shaped to enable calculation of the intensity of the magnetic field produced by the magnetized specimen. Moreover, the instrument must be calibrated by means of a cylindrical coil, the diameter and length of which are about equal to those of the specimen under study.

According to equation (0.62) the intensity of the magnetic field produced by a specimen of cylindrical shape at a distance R from its base will be:

$$H = 2\pi J \left[\frac{R+l}{\sqrt{(R+l)^2+a^2}} - \frac{R}{\sqrt{R^2+a^2}} \right] \qquad (8.27)$$

where l is the length of the specimen, and a is its diameter. The magnetization of the specimen is $J = \chi H_m$, where H_m is the intensity of the magnetic field of the astatic system. If 2 identical cylinders are placed on either side of one of the magnets of the astatic system, as shown in Figure 147, the torque to which the magnet of this system is subjected is equal to MH, and the equilibrium equation is:

$$MH = C\varphi,$$

or

$$2\pi\chi M H_m \left[\frac{R+l}{\sqrt{(R+l)^2+a^2}} - \frac{R}{\sqrt{R^2+a^2}} \right] = C\varphi .$$

In place of the magnets, 2 coils of length l and diameter a having w turns are installed, and at a current intensity I the field intensity at distance R will be expressed analogously to formula (8.27):

$$H_{coil} = 0.2\pi\omega I \left[\frac{R+l}{\sqrt{(R+l)^2+a^2}} - \frac{R}{\sqrt{R^2+a^2}} \right],$$

and the equation of equilibrium of the magnets will be

$$H_{coil} M = C\varphi_{coil}$$

Therefore

$$\chi = \frac{\omega I \varphi}{10 H_m \varphi_{coil}} .$$

Declassified in Part - Sanitized Copy Approved for Release 2013/01/23 : CIA-RDP81-01043R001600090003-8

Declassified in Part - Sanitized Copy Approved for Release 2013/01/23 : CIA-RDP81-01043R001600090003-8

In order to determine the magnetic susceptibility of the specimen, in addition to recording the angles φ and φ_{coil}, the intensity of the magnetic field H_M produced by the magnet of the astatic system also must be known. The intensity H_M is determined by rotating a small coil of known area and number of turns at a definite rate of speed and measuring the emf.

Because this instrument permits measurement of only the apparent magnetic susceptibility, the error in measurements due to the shape of the specimen increases in the more magnetic rocks. Thus in the case of specimens having a susceptibility of about 0.1 CGSμ the error may reach 20% or more. An appreciable error is introduced by the great dependence of the instrument readings on the position of the specimen under study since the angle φ is inversely proportional to r^6 and the coefficients k and k' are not constant, but depend upon the mutual positions of specimen and magnet. However, with careful positioning of the test specimen and the coil, the author estimates the error in measurements to be 6 or 7%.

The advantages of this instrument include its small size and the convenience and simplicity of the measurements, which permit its use under field conditions.

7. The Method of T. N. Roze [72]

Among the methods which permit a large number of determinations of magnetic susceptibility to be made without requiring knowledge of the demagnetization coefficient of the specimen is the method proposed by T. N. Roze. This method is based on the change in residual induction of a permanent magnet when a specimen having a magnetic susceptibility other than unity is placed into its interpolar gap.

This method is embodied in an instrument consisting of a permanent

Declassified in Part - Sanitized Copy Approved for Release 2013/01/23 : CIA-RDP81-01043R001600090003-8

Declassified in Part - Sanitized Copy Approved for Release 2013/01/23 : CIA-RDP81-01043R001600090003-8

horseshoe magnet M (Figure 148), with a winding K consisting of several thousand turns of fine, insulated wire at its bend, and a ballistic galvanometer O.

The winding is connected to the galvanometer, and the oblong specimen A is placed between the poles of the magnet.

Under the influence of the field of the permaent magnet the specimen becomes magnetized in the transverse direction, increasing the magnetic flux cutting through the winding k. When the specimen is removed from the interpolar space the flux decreases and the galvanometer will show a deflection proportional to the change in flux $\Delta \Phi$.

Denoting the cross sectional area of the specimen by S, the intensity of magnetic field in the interpolar gap by H, and the number of turns on the magnet by w, we have

$$\Delta \Phi = 4\pi x' HSw$$

where x' is the apparent magnetic susceptibility of the specimen. The change in flux $\Delta \Phi$ corresponds to a galvanometer deflection α which is proportional to $\Delta \Phi$, and thus

$$4\pi x'HSw = C\alpha,$$

where C is the galvanometer constant.

In the case of a specimen of known magnetic susceptibility x_o and cross sectional area S_o, we have:

$$4\pi X_o HS_o w = C \alpha_o$$

Dividing one equation by the other, we have

$$X' = X_o S_o \alpha / S \alpha_o$$

Consequently, in order to determine the susceptibility of some rock a specimen with known susceptibility x_o and cross sectional area S_o is needed and 2 observations must be made by removing the

Declassified in Part - Sanitized Copy Approved for Release 2013/01/23 : CIA-RDP81-01043R001600090003-8

Declassified in Part - Sanitized Copy Approved for Release 2013/01/23 : CIA-RDP81-01043R001600090003-8

specimen under study and then the specimen of known susceptibility from the interpolar gap. Although the shape of the specimen is unimportant in these measurements its middle portion must be prismatic or cylindrical inorder that the cross sectional area of the specimen may be measured.

As in the preceding case this method yields not the actual but the apparent susceptibility, and thus specimens with low magnetic susceptibility must be used, in which the apparent approximates the actual magnetic susceptibility. With proper selection of the number of turns, galvanometer constant, and dimensions of the permanent magnet this method may be used for the determination susceptibility of the order of 10^{-5} CGS μ.

For susceptibility values of several tenths and higher in addition to the influence of the demagnetizing field, the magnitude of magnetization of the magnet itself is affected by the magnetization of the specimen, which causes an increase in $\Delta \Phi$ and also in x.

8. Contact Magnetometer for Measuring the Magnetic Properties of Rocks and Materials of Small Volume

All the above methods for measuring the magnetic properties of rocks involve determination of the mean value of some magnetic quantity of the tested specimen.

Mean values are quite adequate for interpretation of magnetic anomalies, and therefore measurement procedures were developed for the purpose of obtaining these values. Yet, the mean values of magnetic properties do not permit correlation of these properties with the mineralogical composition of rocks necessary for thorough understanding of the geological nature of anomalies. It is also difficult to determine which of the materials included in the composition of the rock cause its magnetic properties.

Declassified in Part - Sanitized Copy Approved for Release 2013/01/23 : CIA-RDP81-01043R001600090003-8

Declassified in Part - Sanitized Copy Approved for Release 2013/01/23 : CIA-RDP81-01043R001600090003-8

In recent years A. S. Semenov and A. P. Ochkur have designed an instrument called a contact magnetometer, which makes possible determination of the magnetic susceptibility of individual particles ingrained in rock, thus enabling determination of its mineralogical composition.

The instrument consists of a magnetic needle M (Figure 149) 6 or 7 cm long and one mm in diameter suspended on a horizontal filament C. The ends of the filament are held in clamps P and Q, with which the filament may be twisted to adjust the position of the needle. With the needle in an oblique position, if a magnetic specimen is brought near one end of the needle the latter will be drawn toward the specimen with a force of attraction proportional to the magnetic susceptibility of the specimen. Therefore, by measuring this force in arbitrary units the magnitude of magnetic susceptibility also may be determined by twisting the filament C through an angle equal to that which separates the needle from the specimen. The magnitude of this angle provides a measure of the magnetic susceptibility.

To measure the magnetic susceptibility of individual particles it is necessary only to bring visually identified particles on a plane polished surface of the specimen close to the tip of the magnet. It has been ascertained by tests that the average diameter of these particles must be not less than 5 mm in the case of slightly magnetic, and not less than 0.5 mm for strongly magnetic minerals. This instrument permits measurement of magnetic susceptibilities from $x = 10^{-2}$ to $x = 1$ CGS μ. The measurement error is in the range of several percent.

Section 6. Magnetometric Procedures

In conducting magnetometric operations the primary prerequisites

Declassified in Part - Sanitized Copy Approved for Release 2013/01/23 : CIA-RDP81-01043R001600090003-8

Declassified in Part - Sanitized Copy Approved for Release 2013/01/23 : CIA-RDP81-01043R001600090003-8

are congruence between the number of points and nature of the anomaly, and correct choice of a sufficiently accurate observation procedure for determination of the values of anomalous components of the intensity of the magnetic field. Since the choice of procedure also depends upon the nature of the anomaly the maximum values of the anomalous field components and their gradients must be determined, or approximated first. Also, for correct distribution of the observation point network it is necessary to determine the trend of the anomaly, that is, the direction of the axis of the anomaly and the approximate area it covers.

Such determinations are made by preliminary reconnaissance of the anomaly and recording the points of maximum value of the vertical component on a map or marking these points on the terrain.

If the anomaly has a longitudinal trend, i.e., the maximum vertical component values are distributed along a straight line, such as at the Kursk magnetic anomalies, the points of observation are distributed over lines or profiles perpendicular to the line of maxima or, as it is called, crosswise to the trend of the anomaly. This distance between the profiles and the distances between observation points along the profiles are selected according to the magnitude of variation of the gradient of the vertical component. If the gradient, i.e., dZ/dx, over the distance x_2-x_1 remains constant it is sufficient to carry out observations at points x_1 and x_2 in order to ascertain the magnitude of Z at any point situated between x_1 and x_2. If the gradient within this interval is not constant the measurements at terminal points x_1 and x_2 do not permit determination of the values of Z within this interval. Thus for a true picture of the distribution of the magnetic field of the anomaly the distance between points must be chosen in a manner which assures a linear change in the vertical component over this distance.

Declassified in Part - Sanitized Copy Approved for Release 2013/01/23 : CIA-RDP81-01043R001600090003-8

Declassified in Part - Sanitized Copy Approved for Release 2013/01/23 : CIA-RDP81-01043R001600090003-8

For this, the nature of the magnetic field within the area under investigation must be roughly determined during the preliminary reconnaissance.

The location of the observation points is determined by topographical methods, by tying the points in with topographical control points selected beforehand at the center of the anomaly, Usually these points, indicated by tall stakes or pyramids, are distributed along the axis of the anomaly. The geographical coordinates of these markers are determined either by tying them in with the nearest topographical points or by means of a large-scale map.

For ready tying in of the observation points with the control points, the former are distributed along straight profiles perpendicular to the main line, i.e., the line connecting 2 control points, if the main line follows the axis of the anomaly. If the main line departs from the axis of the anomaly it is more convenient to plot the profiles at a certain angle to the main line, so that they are perpendicular to the trend of the anomaly. Distances between points of observation are measured with a tape and the angles between the main line and the profile are measured with an angle-measuring instrument (theodolite). If the nature of the terrain makes the plotting of straight profiles impossible they can be laid out as broken lines, but in such a case the angle of deflection must be determined at each bending point. Such a distribution of points and the method of tying them in with the control points is illustrated in Figure 150.

In the investigation of magnetic anomalies the accuracy of magnetic observations must correspond with the accuracy of determination of the coordinates of the observation points. Regardless of how accurately the elements of terrestrial magnetism have been measured,

Declassified in Part - Sanitized Copy Approved for Release 2013/01/23 : CIA-RDP81-01043R001600090003-8

Declassified in Part - Sanitized Copy Approved for Release 2013/01/23 : CIA-RDP81-01043R001600090003-8

if the position where these observations were made is unknown, or is known only very approximately, these measurements are without value since they cannot be utilized for interpretation purposes.

The same is true of the converse situation, in which the position of a point has been determined exactly but measurement of the elements of terrestrial magnetism are approximate.

The proper correspondence of accuracy is determined by an equation correlating a change in some element of terrestrial magnetism and a change in location on passing from one point to another. In the case of the vertical component this equation is

$$\Delta Z = \partial Z/\partial x \times \Delta x,$$

where $\partial Z/\partial x$ is the gradient of Z in the direction x.

If Δx represents the error involved in determining the distance between points, ΔZ will be the error due to inadequate knowledge of the precise position of the point, and consequently it will be the minimum error beyond which any measurement is meaningless.

For example, in the region of the Kursk anomalies the gradients of Z attain 200 γ /m, while the error in determination of distances was within one meter, consequently the error in measurement of the vertical component had to be not more than ± 200 γ. This actually was the case, since the measurements were made by means of a deflector magnetometer, in which the error is approximately of this order of magnitude.

Section 7. Aerial Magnetic Surveying

During the past 10 years the aeromagnetic method of investigating the magnetic field of the earth has been used extensively in geological prospecting. This method, which was developed and put into practical use by A. A. Logachev [73], has been termed aeromagneti surveying.

Declassified in Part - Sanitized Copy Approved for Release 2013/01/23 : CIA-RDP81-01043R001600090003-8

Declassified in Part - Sanitized Copy Approved for Release 2013/01/23 : CIA-RDP81-01043R001600090003-8

Aeromagnetic surveying consists of continuous measurement of the vertical component by means of a semi-automatic instrument, called an aeromagnetometer, installed in an aircraft. Because of the high speed of aircraft this method enables a several hundred-fold increase in the productivity of magnetic survey operations. While the use of a magnetic balance in magnetic survey ground operations enables a single observer to complete a detailed survey of area during a summer season (100 km^2), the aeromagnetic survey method covers 30 to 40,000 km^2 in the same period with the same intervals between itineraries. The aeromagnetic survey has the additional advantage of covering areas inaccessible to conventional ground survey operations (mountains, tayga, deserts, etc).

Aeromagnetic survey has been applied in locating iron ore deposits, and in geological mapping. During recent years a number of large deposits of iron ore which are of great industrial significance have been discovered by aeromagnetic survey.

At the present time this method still does not equal the accuracy of ground instrument surveying which is necessary for exact determination of the boundaries and depth of occurrence of rocks. Therefore, when an anomalous area has been discovered by aeromagnetic survey, instrument surveying is necessary for its interpretation. However there are no fundamental hindrances to increasing the accuracy of magnetic measurements and tying them in with landmarks and it may be expected that in the near future new aeromagnetometers will be developed which will completely supplant ground surveying operations.

It should be noted that the idea of a survey conducted by an observer in continuous motion and the first practical application of this method must be credited to E. I. Val'skiy [74], an associate of

Declassified in Part - Sanitized Copy Approved for Release 2013/01/23 : CIA-RDP81-01043R001600090003-8

Declassified in Part - Sanitized Copy Approved for Release 2013/01/23 : CIA-RDP81-01043R001600090003-8

the Department of the Physics of the Earth's Crust, of the Leningrad State University. In 1930 Val'skiy made the first observations from a railroad train in the area of the Kursk magnetic anomalies, using an instrument of his own design, the magnetron.

Because of the specificity of the conditions under which aeromagnetic survey is conducted, namely the high speed and considerable altitude of the observer, this method may be utilized to investigate only anomalies which exceed a certain minimum size and intensity. Thus, for example, operational practice shows that the time required for visual measurements cannot be less than 4-5 seconds, which at an air speed of 100-120 km per hour corresponds to an anomaly with diameter not less than 150 m. It is known also from experience that the minimum vertical component which can be detected in aeromagneti survey is 500 γ.

Aeromagnetic survey is conducted over straight itineraries perpendicular to the course of the principal local geological structures. However, because of the availability of landmarks for tying in itineraries, the course of the flight path may be altered with respect to the direction dictated by geological factors. The lateral interval between itineraries is determined by the altitude of flight, which in turn is chosen in accordance with the depth of occurrence of the rock formations which cause the anomalies. To discover an anomaly it is sufficient to trace the change of the vertical component within the limits of one-half of its maximum value, i.e., from $-Z_m/2$ to $+ Z_m/2$.

In the case of monopolar occurrences such as a vertical cylinder or a vertical stratum of very great length, the distance between $- Z_m/2$ and $+ Z_m/2$ is equal to twice the depth of occurrence of the upper pole.

Declassified in Part - Sanitized Copy Approved for Release 2013/01/23 : CIA-RDP81-01043R001600090003-8

Declassified in Part - Sanitized Copy Approved for Release 2013/01/23 : CIA-RDP81-01043R001600090003-8

In the case of a spherical deposit or a cylindrical deposit of infinite length, the axis of which is parallel to the earth's surface, this distance is equal to the depth of occurrence of the sphere center or cylinder axis.

In the case of rocks having a finite course in the vertical direction, i.e., having poles at a finite distance, the distance between - $Z_m/2$ and + $Z_m/2$ is greater than the depth of occurrence and less than twice its value.

Therefore, if the flight altitude is great in comparison with the depth of occurrence of the pole, and the altitude may be considered equal to the distance between the pole and the aircraft, in order to discover the anomaly it is necessary that the distance between itineraries be not greater than twice the flight altitude.

However, the depth of occurrence of any given type of rock within an uninvestigated area is not known and may be only estimated on the basis of geological factors. Thus the altitude must be selected in accordance with geological data relating to the area under study and the problems involved in carrying out the aeromagnetic survey.

The results of an aeromagnetic survey are plotted on the map in the form of the graphs of Z as a function of itinerary distance for each of the itineraries. The plotting of the itineraries is based on local landmarks over which the aircraft will travel. Such landmarks may be road intersections, river bends, inhabited localities, summits of hills or mountains, etc.

As an example Figure 151 shows a map of the magnetic field in the area of the Krasnokamen iron ore deposit (Eastern Sayans), plotted by A. A. Logachev on the basis of the results of an aeromagnetic

Declassified in Part - Sanitized Copy Approved for Release 2013/01/23 : CIA-RDP81-01043R001600090003-8

Declassified in Part - Sanitized Copy Approved for Release 2013/01/23 : CIA-RDP81-01043R001600090003-8

survey. The shaded areas between the curves and the directions of the itineraries represent the positive values of anomalous vertical component and the solid black areas represent negative values.

While it has no particular advantages over the isoline method with respect to clarity of representation of the magneti field, this graphic procedure does have the advantage that it requires less time and effort in reproduction, and for this reason it has been generally adopted for both aeromagnetic and ground surveys.

Figure 152 shows a geological map of the same area of the Krasnokamen deposit to illustrate the practical importance of the results of aeromagnetic survey. Comparison of the magnetic and geological maps reveals that the regions of increased vertical component are in good agreement with the areas of occurrence of igneous rocks: gabbrodiabases, prophyrites, syenites, etc, which exhibit increased magnetic susceptibility. It is this fact which permits utilization of the results of aeromagnetic surveys in geological mapping.

At the present time large areas of many regions of the USSR have been covered by aeromagnetic survey and numerous magnetic anomalies have been discovered, which in addition to enabling identification of the geological structure of these areas has also resulted in the discovery of a number of iron ore deposits.

Section 8. The Main Problem of Magnetometry. Magnetic Fields of Regularly Shaped Bodies.

The main problem of magnetometry is the determination of the magnetic field produced by magnetized rocks of different shapes. Although the infinite variety of shapes of rock occurrences does not permit their expression by any one equation, still in many instances each of them can be generally likened to some geometrically regular shape (sphere, prism, etc).

Declassified in Part - Sanitized Copy Approved for Release 2013/01/23 : CIA-RDP81-01043R001600090003-8

Declassified in Part - Sanitized Copy Approved for Release 2013/01/23 : CIA-RDP81-01043R001600090003-8

This is based on the fact that at distances much greater than the dimensions of the rock formation involved the magnetic field is equivalent to the field of a uniformly magnetized sphere.

Indeed, from the expansion of the magnetic potential to a series by spherical functions [equation (2.20)] it follows that on recession of the point P at which the potential is being considered the terms of higher order become small in relation to the initial terms and may be disregarded. The first term of the expansion, on the other hand, represents the potential of a uniformly magnetized sphere.

The regular geometric shapes of importance in magnetic prospecting are: the sphere, circular cylinder, rectangular prism, ellipsoid of rotation, ellipsoidal cylinder and plane plate, since most deep rocks which cause anomalies can be likened to one of these shapes.

Therefore let us calculate the components of the magnetic field of the above bodies, assuming that they are magnetized uniformly over one of their geometric axes.

The solution of the main problem is based on the formulas and laws which were set forth in the introduction. In many instances use will be made of the law of Coulomb, assuming that the magnetized rocks contain magnetic charges.

The assumption that the rocks are uniformly magnitized is quite tenable since their magnetic susceptibility in most cases is of the order of 10^{-2} to 10^{-3} and changes slightly, depending on magnetization. Indeed, according to the deductions of Section 15 of the introduction, magnetization at any point of the rock is defined by the equation:

Declassified in Part - Sanitized Copy Approved for Release 2013/01/23 : CIA-RDP81-01043R001600090003-8

Declassified in Part - Sanitized Copy Approved for Release 2013/01/23 : CIA-RDP81-01043R001600090003-8

$$J = \frac{\chi}{1 + \chi N} H$$

Since x is small, and the value N of most rocks is smaller than unity, the product xN may be disregarded, in which case

$$J = \chi H$$

If x is a constant quantity, J also will be constant for all points of a body.

1. Sphere. In accordance with the decutions of section 1 of chapter II the potential of a uniformly magnetized sphere at any point of its surrounding space having the spheric coordinates r, θ and λ, taking the origin of coordinates at the center of the sphere, is expressed by the equation $U = M/r^2[\cos\theta \cos\theta_0 + \sin\theta \sin\theta_0 \cos(\lambda - \lambda_0)]$ where θ_0 and λ_0 are the coordinates of the magnetic axis of the sphere and M its magnetic moment.

Since we are concerned with the distribution of the magnetic field over a plane, the spheric coordinates must be replaced by rectangular coordinates. Taking the z axis perpendicular to the plane involved (Figure 153) and the x-axis the line O'P extending through point P, denoting the coordinates of point P by x, y, z, the coordinates of the point of intersection of the magnetic axis with the plane, by x_0, y_0, z_0, and the distance from the center of the sphere to the origin of coordinates by R, it follows that,

$$\cos\theta = \frac{R}{r}, \quad \cos\theta_0 = \frac{R}{r_0}, \quad \sin\theta = \frac{x'}{r}, \quad \sin\theta_0 = \frac{x'}{r_0}$$

and consequently

$$U = \frac{M}{r^2}\left[\frac{R^2}{r_0} + \frac{xx'}{r_0}\cos(\lambda - \lambda_0)\right],$$

where $x' = O'Q$, $r_0 = OQ$ and, as is readily apparent from the drawing

$$x'^2 = x_0^2 + y_0^2, \quad r_0^2 = R^2 + x_0^2 + y_0^2 \text{ and } r^2 = x^2 + y^2 + R^2.$$

For practical purposes it is sufficient to consider only the magnetic field along the line O'Q, which constitutes the intersection of the vertical plane extending through the magnetic axis of the sphere

Declassified in Part - Sanitized Copy Approved for Release 2013/01/23 : CIA-RDP81-01043R001600090003-8

Declassified in Part - Sanitized Copy Approved for Release 2013/01/23 : CIA-RDP81-01043R001600090003-8

with the horizontal plane. In such a case, the angle $\lambda - \lambda_0 = 0$, and the coordinate y = 0, therefore

$$U = \frac{M}{R^3} \frac{R^2 + xx_0}{r_0}$$

The components of the intensity of the magnetic field on the x axis and the z axis, i.e., the horizontal and the vertical components, denoted by H and Z, respectively, are as follows:

$$H = -\frac{\partial U}{\partial x} = \frac{M}{R^5 r_0}\left(3R^2 x + 2x^2 x_0 - R^2 x_0\right),$$
$$Z = -\frac{\partial U}{\partial R} = \frac{MR}{R^5 r_0}\left(2R^2 + 3xx_0 - x^2\right). \qquad (8.28)$$

Since the magnetic moment of a uniformly magnetized sphere is the product of the sphere volume V by its magnetization J, the right-hand portions of equations (8.28) are functions of zero order and therefore do not depend on the scale used to measure the quantities R, x, x_0 or the radius of the sphere. Therefore, taking the distance R as the unit of length and expressing M in terms of the sphere radius a and the magnetization J, we have:

$$H = \frac{4}{3}\pi J a^3 \frac{-3x\cos\theta_0 + 2x^2\sin\theta_0 - \sin\theta_0}{(1+x^2)^{\frac{5}{2}}}$$
$$Z = \frac{4}{3}\pi J a^3 \frac{2\cos\theta + 3x\sin\theta_0 - x^2\cos\theta_0}{(1+x^2)^{\frac{5}{2}}} \qquad (8.29)$$

In this form the equations in which a and x are expressed in R units, with a given angle of inclination θ_0, are independent of both the depth of occurrence of the sphere and its dimensions, and the graphs plotted in accordance with these formulas will hold for any dimensions of the sphere and any depth of occurrence.

Thus, for example, when the depth of occurrence increases n-fold, and on retention of the same graph, i.e., retention of the same values of x, z and H, it is necessary only to increase the radius by n. When the radius of the sphere is changed n-fold and the same graph is retained J must be changed in reverse proportion by the factor n^3.

Declassified in Part - Sanitized Copy Approved for Release 2013/01/23 : CIA-RDP81-01043R001600090003-8

Declassified in Part - Sanitized Copy Approved for Release 2013/01/23 : CIA-RDP81-01043R001600090003-8

Graphs corresponding to formulas (8.29) for an angle $\theta_0 = 30^0$ are shown in Figure 154, where the x distances are plotted on the abscissa axis and the corresponding values of H and Z are plotted on the ordinates axis.

From the graphs it is apparent that the horizontal component has one maximum and one minimum, and the vertical component has one maximum and 2 minima, with one of the minima having greater absolute magnitude than the other and is disposed opposite to the inclination of the magnetic axis in relation to the horizon. On the other hand the maximum of the vertical component is shifted from the origin of the coordinates in the direction of the dip of the magnetic axis.

Simpler expressions for H and Z are obtained when the magnetic axis of the sphere is perpendicular to the earth's surface, i.e., when magnetization of the sphere is directed along the vertical. In such a case $X_0 = 0$ and $r_0 = R$, and consequently:

$$H = \frac{3MRx}{r^5}, \qquad Z = \frac{M(2R^2 - x^2)}{r^5} \tag{8.30}$$

The H and Z graphs (Figure 155) in this case will be analogous to those of Figure 154, but will be symmetrical in relation to the ordinate axis, i.e., the maximum of Z will be at x = 0, and the minima will be at equal distances X_m from the origin of coordinates and equal to each other in absolute magnitude.

It is readily apparent that

at x = 0 $Z_{max} = \frac{2M}{R^3}$, $H = 0$;

at x = 2R $Z_{min} = \frac{Z_{max}}{25\sqrt{5}}$;

at x = R/2 $H_{max} = \frac{24 Z_{max}}{25\sqrt{5}}$.

It is also of interest to note that in the case of a sphere the magnetization of which is parallel to the horizontal plane, i.e., $x_0 = \infty$, $r_0 = \infty$ and $\frac{x_0}{r_0} = 1$,

Declassified in Part - Sanitized Copy Approved for Release 2013/01/23 : CIA-RDP81-01043R001600090003-8

Declassified in Part - Sanitized Copy Approved for Release 2013/01/23 : CIA-RDP81-01043R001600090003-8

the components are

$$H = \frac{M}{r^5}(2x^2 - R^2), \qquad Z = \frac{3MRx}{r^5}$$

i.e., the nature of their change with distance x will be the same as the nature of the change of Z and H respectively, with vertical magnetization.

2. Cylinder Having a Small Diameter-to-Length Ratio, Magnetized in the Direction of Its Geometric Axis. The natural occurrence of intrusion stock with small cross sectional area may be compared to this geometric type.

Because of the small transverse dimensions of the cylinder in comparison with the depth of occurrence the magnetic charges distributed over the end surfaces of the cylinder may be considered as concentrated at 2 points, at the ends of the cylinder. The magnitude of these charges evidently is equal to the product of magnetization by the area of the cylinder base, i.e.,

$$m = JS$$

Magnets in which the charges may be considered concentrated at 2 points (poles) are called schematic magnets. The magnetic potential of a schematic magnet is determined by the law of Coulomb:

$$U = \frac{m}{r_1} - \frac{m}{r_2},$$

wherein r_1 and r_2 are the distances of the poles from point P (Figure 155).

As with a sphere, in practice it is sufficient to consider the distribution of the field along a horizontal line extending through the projections of the poles + m and - m. Taking this line as the x axis, denoting the coordinates of the poles + m and - m by x_1, R_1 and x_2, R_2, respectively, and the coordinates of point P by x, R, we have:

$$H = -\frac{\partial U}{\partial x} = m\left[\frac{x - x_1}{r_1^3} - \frac{x - x_2}{r_2^3}\right],$$

$$Z = -\frac{\partial U}{\partial R} = m\left[\frac{R - R_1}{r_1^3} - \frac{R - R_2}{r_2^3}\right].$$

Declassified in Part - Sanitized Copy Approved for Release 2013/01/23 : CIA-RDP81-01043R001600090003-8

Declassified in Part - Sanitized Copy Approved for Release 2013/01/23 : CIA-RDP81-01043R001600090003-8

Placing the origin of coordinates at one of the poles of the schematic magnet, i.e., assuming $x_1 = 0$, $R_1 = 0$ and $x_2 = x_0$, $R_2 = -R_0$, we obtain:

$$H = m\left[\frac{x}{r_1^3} - \frac{x - x_0}{r_2^3}\right]; \quad Z = m\left[\frac{R}{r_1^3} - \frac{R + R_0}{r_2^3}\right], \tag{8.31}$$

and

$$r_1^2 = R^2 + x^2, \quad r_2^2 = (R + R_0)^2 + (x - x_0)^2.$$

Analogously to the preceding example, the right-hand portions of these equations are functions of zero order, since the magnetic charge may be represented as the product of magnetization by the cross-sectional area of the center.

Therefore, with given values of cylinder length and angle of inclination of the axis in relation to the horizon, a graph in which the abscissas are plotted at a scale of depth of occurrence of the upper pole will relate to any depth of occurrence of the cylinder and any dimensions of the cross sectional area, provided that the dimensions of this area are small in comparison with the length of the cylinder and the depth of occurrence.

The graphs of these functions are shown in Figure 157. In essence they are analogous to the graphs of a sphere with magnetic axis inclined in relation to the horizon.

The difference resides in the relationships between the maxima of H and Z, the maximum and minimum of Z and in the distance of the extreme values of H and Z from the origin of coordinates.

In the particular instance when the axis of the schematic magnet is vertical, i.e., when $x_1 = x_2 = 0$ and $R_2 = l$, the length of the schematic magnet, we have:

$$H = mq\left[\frac{1}{r_1^3} - \frac{1}{r_2^3}\right]; \quad Z = m\left[\frac{R}{r_1^3} - \frac{R + l}{r_2^3}\right] \tag{8.32}$$

Declassified in Part - Sanitized Copy Approved for Release 2013/01/23 : CIA-RDP81-01043R001600090003-8

Declassified in Part - Sanitized Copy Approved for Release 2013/01/23 : CIA-RDP81-01043R001600090003-8

These functions are symmetrical in relation to the z axis (Figure 158).

In the special instance in which the lower end of a magnet or stock is located at a very great depth in comparison with its upper end, so that the influence of the lower pole may be disregarded, we have:

$$H = \frac{mx}{(R^2+x^2)^{\frac{3}{2}}} \quad \text{and} \quad Z = \frac{mR}{(R^2+x^2)^{\frac{3}{2}}}. \qquad (8.33)$$

The graph of these functions is shown in Figure 159.

From equation (8.33) it is apparent that at x = 0 the vertical and horizontal components assume the value

$$Z_{max} = \frac{m}{R^2}, \quad H = 0,$$

and at $x = \frac{R}{\sqrt{2}}$ they assume the values

$$H_{max} = \frac{2\sqrt{3}}{9} Z_{max}$$

Let us determine the conditions under which the 2-pole magnet can be replaced by a single-pole magnet, i.e., the case in which the field of a 2-pole magnet coincides with that of a single-pole magnet within the limits of observational error. If, in the equations (8.32) and (8.33), the vertical component of a 2-pole magnet is denoted by Z_1 and that of a single-pole magnet denoted by Z_2 expressing x and l in R units and Z_1 and Z_2 in units of their maximum values, i.e., taking $Z_{m_1} = 1$ and $Z_{m_2} = 1$, it follows that:

$$\frac{Z_1 - Z_2}{Z_1} = \frac{(Z_0-1)\left[(1+l)^2+x^2\right]^{\frac{3}{2}} + (1+l)(1+x^2)^{\frac{3}{2}}}{Z_0\left[(1+l)^2+x^2\right]^{\frac{3}{2}}} \qquad (8.34)$$

where Z_0 is the value of Z_2 at x = 0, i.e.,

$$Z_0 = 1 - \frac{1}{(1+l)^2}.$$

Thus the relative difference of the vertical components of 2-pole and single-pole magnets depends not only on the distance between the pole l, but also on the coordinate x of the point where the observations are carried out. The further the point of observation is from the maximum Z_m,

Declassified in Part - Sanitized Copy Approved for Release 2013/01/23 : CIA-RDP81-01043R001600090003-8

Declassified in Part - Sanitized Copy Approved for Release 2013/01/23 : CIA-RDP81-01043R001600090003-8

the greater is this distance. The values of this difference, expressed in percent, for the different values of l and x are shown below.

x \ l	4	6	8	10
0	0.0	0.0	0.0	0.0
1	6.8	3.4	1.9	1.3
2	37	2035	14.0	8.9

The table shows that only at a value of l more than 10 times greater than the depth of occurrence of the upper pole the difference over the length 2R will not exceed several percent, and therefore the formulas for a single-pole magnet may be utilized only at $l > 10$ R, in which an error of several percent is committed in the determination of Z. However, for determination of the depth of occurrence it is sufficient to have a portion of the curve, of length equal to the depth of occurrence, and in such a case the replacement is possible with $l > 6R$.

Another problem of practical importance is the ratio of radius of vertical cylinder to the depth of occurrence of its upper surface at which the cylinder may be considered as a 2-pole or as a single-pole magnet. Determination of the magnetic field of a cylinder with a finite base radius is a complex mathematical problem, and therefore the solution is obtained by the approximation methods described on page 361. This method shows that the relative difference in percent, between the vertical component Z_2 of a cylinder, the depth of occurrence of the upper base of which is 4 times greater than the radius of the cylinder, and the vertical component Z_1 of a punctal pole at the center of the anomaly, does not exceed 7% and remains almost the same over an area equal to the depth of occurrence. Therefore, if the upper base of the cylinder is located at a depth no greater than 4 times the radius of the

Declassified in Part - Sanitized Copy Approved for Release 2013/01/23 : CIA-RDP81-01043R001600090003-8

Declassified in Part - Sanitized Copy Approved for Release 2013/01/23 : CIA-RDP81-01043R001600090003-8

cylinder the cylinder may be considered a punctal magnet. In such a case the vertical component has no negative values.

3. Ellipsoid. Among the ellipsoids with different axial ratios the 2-axis compressed ellipsoid is of significance in magnetometry. Rocks occurring in the form of lenses parallel to the earth's surface are of this type. An elongated ellipsoid (according to the theory) of great focal length is equivalent, with a high degree of approximation, to a schematic magnet the poles of which coincide with the foci of the ellipsoid. Therefore, complex calculation of the potential, such as by formulas of the potential of the ellipsoid and its first derivatives is unnecessary since the potential may be calculated in accordance with the simpler formulas relating to a schematic magnet with accuracy adequate for practical purposes.

Ellipsoids of small focal length obviously are equivalent to spheres. The magnetic field of a compressed ellipsoid having a large axis ratio has no simpler analogy, and therefore its potential must be calculated and practically utilized. The magnetic potential of a 3-axis ellipsoid is expressed by equation (0.67). If we take a = b this equation becomes

$$U = \frac{\pi a^2 c}{a_1 c_1}\left[J_z N_1 z + (J_x x + J_y y) Z_1\right].$$

and assuming that a > c and that the ellipsoid is magnetized along the z axis, then

$$U = \frac{a^2 c}{a_1 c_1} N_1 J_z z, \qquad (8.35)$$

and the constant coefficient N_1 is of the form:

$$N_1 = 2\pi a_1^2 c_1 \int_0^\infty \frac{d\theta}{(a^2+\theta)(c_1^2+\theta)^{\frac{3}{2}}}$$

or, after integration,

$$N_1 = 4\pi a_1^2 c_1 \left[\frac{1}{q^2 c_1} - \frac{1}{q^3} \operatorname{arc\,tg} \frac{q}{c_1}\right], \qquad (8.36)$$

where $q = a_1^2 - c_1^2$. Noting that $4/3\ \pi a^2 c\ J$ represents the magnetic moment of ellipsoid M, and substituting N_1 from equation (8.36) in equation (8.35) we obtain:

$$U = 3M\left[\frac{1}{q^2 c_1} - \frac{1}{q_1^3} \operatorname{arc\,tg} \frac{q}{c_1}\right] z. \qquad (8.37)$$

Declassified in Part - Sanitized Copy Approved for Release 2013/01/23 : CIA-RDP81-01043R001600090003-8

Declassified in Part - Sanitized Copy Approved for Release 2013/01/23 : CIA-RDP81-01043R001600090003-8

Assuming the ellipsoids are co-focal and that the point P, with coordinates x, θ and z, is located on the surface of the ellipsoid with axes a_1 and c_1 we have:

$$a_1^2 - c_1^2 = a^2 - c^2 = q^2; \quad \frac{x^2}{a_1^2} + \frac{z^2}{c_1^2} = 1,$$

and solving these equations we obtain:

$$a_1^2 = \frac{1}{2}(x^2+z^2+q^2) + \frac{1}{2}\sqrt{(x^2+z^2-q^2)^2 + 4z^2q^2},$$

$$c_1^2 = \frac{1}{2}(x^2+z^2-q^2) + \frac{1}{2}\sqrt{(x^2+z^2-q^2)^2 + 4z^2q^2}.$$

Denoting the coordinate z by R the components of the intensity of the magnetic field are determined from equation (8.37):

$$H = -\frac{\partial U}{\partial x} = 3\frac{MR}{a_1^2 c_1} \cdot \frac{x}{t},$$

$$Z = -\frac{\partial U}{\partial R} = 3M\left[\frac{R^2}{t^3} - \frac{1}{q^2}\left(\frac{1}{c_1} - \frac{1}{q}\operatorname{arc\,tg}\frac{q}{c}\right)\right], \tag{8.38}$$

where

$$t = \sqrt{(x^2+R^2-q^2)^2 + 4R^2q^2}.$$

Taking the unit of length equal to one-half the focal distance, i.e., if we set q = 1, the ratios H/M and Z/M will be independent of the dimensions of the ellipsoids and the ratios of their axes, since a_1 and c_1 depend only on the focal distance 2q and the coordinates of point P.

Therefore, to keep H and Z constant at any dimensions of the ellipsoid the magnetization must be changed by the corresponding factor. Figure 160 shows the graphs of functions (8.38) for q = 1 (1) and q = 2 (2) with R = 1. These graphs show the degree of change in the Z and H curves corresponding to a change in the horizontal axis of the ellipsoids (q = 1 and q = 2). From the curves it is apparent that the ratio of maximum H_m to maximum Z_m, when q = 1, is 0.46, and when q = 2 it is 0.56. The minimum of the vertical component is only slightly more than 0.02 of the maximum when q = 1 and when q = 2. These, as well as the preceding graphs are characterized by the slow change of horizontal and vertical components. The curves

Declassified in Part - Sanitized Copy Approved for Release 2013/01/23 : CIA-RDP81-01043R001600090003-8

Declassified in Part - Sanitized Copy Approved for Release 2013/01/23 : CIA-RDP81-01043R001600090003-8

become wider with increase of the horizontal axis or, what amounts to the same thing, with increasing eccentricity of the ellipsoid.

The graphs also show that the maximum and minimum of the horizontal component occur almost over the foci of the ellipsoid.

4. Infinitely Long Circular Cylinder Magnetized Perpendicularly to the Axis

Many of observed anomalies are narrow regions elongated in one direction, exemplified by the Kursk anomalies. Such anomalies are produced by extremely long bodies of rock with transverse dimensions very small in comparison with their length. Their geometrical images are infinitely long bodies parallel to the earth's surface and in cross section resembling a circle, ellipse, rectangle or parallelogram. In the first instance the rock body may be considered an infinitely long cylinder, in the second an elliptic cylinder and in the third and fourth instances infinitely long prisms.

The magnetic field of any such body is uniform along a line parallel to its axis, i.e., does not depend on one of the 3 coordinates. Therefore the problem of determining the magnetic field of such bodies is called a plane or 2-dimensional problem, since its solution consists of finding the potential within a plane perpendicular to the axis of these bodies.

We will seek to determine the magnetic potential of a uniformly magnetized cylinder by means of the theorem of Poisson

$$U = -(J \text{ grad } V), \qquad (8.39)$$

in this case the vector J must be perpendicular to the axis of the cylinder.

The quantity V, which is proportional to the gravitation potential,

Declassified in Part - Sanitized Copy Approved for Release 2013/01/23 : CIA-RDP81-01043R001600090003-8

Declassified in Part - Sanitized Copy Approved for Release 2013/01/23 : CIA-RDP81-01043R001600090003-8

is determined from the equation of Laplace, which in the case of a 2 dimensional problem with cylindrical coordinates is of the form

$$\frac{\partial^2 V}{\partial r^2} + \frac{1}{r} \cdot \frac{\partial V}{\partial r} + \frac{1}{r^2} \cdot \frac{\partial^2 V}{\partial \varphi^2} = 0,$$

where r and φ are the cylindrical coordinates of point P (Figure 161).

Since the cylinder has a constant density the gravitation potential must be symmetrical in relation to the axis of the cylinder, and therefore independent of the coordinate φ, as a result the above equation becomes:

$$\frac{\partial^2 V}{\partial r^2} + \frac{1}{r} \cdot \frac{\partial V}{\partial r} = 0, \text{ или } \frac{d}{dr}\left(r \frac{dV}{dr}\right) = 0.$$

Integrating this equation twice, we obtain

$$V = C_1 \ln r + C_2,$$

where C_1 and C_2 are arbitrary integration constants.

Substituting this value of V into equation (8.39) we have:

$$U = C_1 \frac{(Jz)}{r^2} = \frac{C_1 J}{r} \cos\theta. \qquad (8.40)$$

An expression analogous in form is obtained for the magnetic potential of 2 infinitely long filaments having opposite charges and separated by an infinitely small distance.

Indeed, considering such charged filaments as a combination of an infinitely large number of dipoles parallel to one another, the axes of which are perpendicular to the filaments, their magnetic potential may be represented as an infinite sum of the potentials of each of the dipoles, or at the limit, as the integral of the dipole potential, i.e.,

$$U = \int_{-\infty}^{+\infty} \frac{d\mu}{r'^2} \cos\varphi,$$

However, the magnetic moment of the dipole may be expressed as the product of magnetic moment μ of the unit of length of such a filament, by the element of its length dl, i.e., $d\mu = \mu\, dl$, while the distance r' and angle φ may be expressed as the distance r (Figure 162), and angles θ and α may be expressed by the formulas

Declassified in Part - Sanitized Copy Approved for Release 2013/01/23 : CIA-RDP81-01043R001600090003-8

Declassified in Part - Sanitized Copy Approved for Release 2013/01/23 : CIA-RDP81-01043R001600090003-8

$$r'^2 = r^2 + l^2;$$

$$\cos\varphi = \cos\theta\cos\alpha$$

Substituting these values, we have:

$$U = 2\mu\cos\theta\int_0^\infty \frac{\sin\alpha\,dl}{r^2+l^2}. \qquad (8.41)$$

which, when integrated gives

$$U = \frac{2\mu}{r}\cos\theta. \qquad (8.42)$$

Since expression (8.40) for the potential does not depend upon the magnitude of the cylinder radius, it follows that by reducing the radius to infinitely small dimensions, we arrive at a 2-pole filament. Comparing expressions (8.40) and (8.41) we find that

$$C_1 J = 2\mu,$$

hence

$$C_1 = \frac{2\mu}{J} = 2S,$$

where S is the cross sectional area of the cylinder, i.e., the area of a circle.

Thus a cylinder uniformly magnetized in the direction of its diameter is equivalent to a 2-pole filament, the magnetic moment per unit length of which is equal to the magnetic moment per unit length of the cylinder.

Assuming that the magnetization of the cylinder forms an angle φ_0 with the vertical axis (Figure 161), and the radius-vector r forms an angle φ with the same axis, then $\theta = \varphi - \varphi_0$ and therefore

$$U = \frac{2\mu}{r}(\cos\varphi\cos\varphi_0 + \sin\varphi\sin\varphi_0).$$

Transposing from polar to rectangular coordinates, we obtain

$$U = 2\mu\left(\frac{R\cos\varphi_0}{R^2+x^2} - \frac{x\sin\varphi_0}{R^2+x^2}\right),$$

whence we have

$$H = \frac{2\mu(R^2-x^2)\sin\varphi_0 + 2Rx\cos\varphi_0}{(R^2+x^2)^2}$$

$$Z = 2\mu\,\frac{(R^2-x^2)\cos\varphi_0 - 2Rx\sin\varphi_0}{(R^2+x^2)^2}$$

The graphs of these functions are shown in Figure 163.

At $\varphi = 0$, i.e., with vertical magnetization we have

$$H = \frac{4\mu Rx}{(R^2+x^2)^2}; \quad Z = \frac{2\mu(R^2-x^2)}{(R^2+x^2)^2}$$

Declassified in Part - Sanitized Copy Approved for Release 2013/01/23 : CIA-RDP81-01043R001600090003-8

Declassified in Part - Sanitized Copy Approved for Release 2013/01/23 : CIA-RDP81-01043R001600090003-8

The corresponding graphs are shown in Figure 164. These graphs are analogous in form to the graph of a sphere or dipole, but the correlation of extreme values of H and Z is somewhat different, thus;

at x = 0 $H = 0, \quad Z_{max} = \frac{2\mu}{R^2}$,

at x = $\sqrt{3}R$ $Z_{min} = -\frac{1}{8} Z_{max}$,

at x = $1/\sqrt{3}$ R $H_{max} = \frac{9}{8\sqrt{3}} Z_{max}$.

5. Elliptical Cylinder of Infinite Length, Magnetized along the Major Axis of the Ellipse.

An infinitely long elliptical cylinder constitutes an ellipsoid, one of the axes of which is infinitely long. Considering the case in which the major axis of the ellipse of section is vertical and the magnetization coincides with this axis, then according to formula (0.67) the magnetic potential of an ellipsoid, for one axis of which $a = \infty$, will be: $U = \frac{abc}{b_1 c_1} J N_1 z$;

Since $a = a_1$, N_1 will be $N_1 = 2\pi b_1 c_1 \int_0^\infty \frac{d\theta}{(\theta + b_1^2)\sqrt{(b_1^2+\theta)(c_1^2+\theta)}}$,

Integration is effected by the substitution $\theta = c_1^2 \operatorname{tg}^2 \varphi$,

which gives: $N_1 = 4\pi \frac{b_1}{b_1 + c_1}$

and as before, b_1 and c_1 are determined from the equations $c_1^2 - b_1^2 = q^2, \quad \frac{y^2}{b_1^2} + \frac{z^2}{c_1^2} = 1$.

Substituting the value of N_1 in the equation of U_1 we have: $U = 4\pi abc \frac{J}{c_1(b_1+c_1)} = \frac{4\mu}{c_1(b_1+c_1)}$,

where μ is the magnetic moment per unit length of the elliptic cylinder.

By simple differentiation of potential U the following values are obtained for the components of the intensity of the magnetic field:

$$H = 4\mu \frac{y}{b_1 c_1 t}, \quad Z = 4\mu \frac{1}{c_1}\left(\frac{z^2 b_1}{c_1^2 t} - \frac{1}{b_1 + c_1}\right), \qquad (8.43)$$

where $t = \sqrt{(y^2+z^2-q^2)^2 + 4y^2q^2}$,

$b_1^2 = \frac{1}{2}(y^2+z^2-q^2) \pm \frac{t}{2}, \quad c_1^2 = \frac{1}{2}(y^2+z^2+q^2) \pm \frac{t}{2}$,

Declassified in Part - Sanitized Copy Approved for Release 2013/01/23 : CIA-RDP81-01043R001600090003-8

Declassified in Part - Sanitized Copy Approved for Release 2013/01/23 : CIA-RDP81-01043R001600090003-8

Figure 165 contains the graphs for q = z = 1, showing H and Z as functions of y, and the graphs of an infinitely long vertical plate of width 2q. From comparison of these graphs it is apparent that the magnetic field of an infinitely long cylinder differs very little from the field of this type of plate, and therefore in practice it is entirely permissible to utilize formulas relating to an infinitely thin plate. This enables determination of the position of the upper and lower ends of the plate, which are equivalent to the foci of an elliptical cylinder. This is substantiated by the fact that the dimensions of an ellipsoid with semi-axes a and b and given q can be of any magnitude, as is apparent from equation (8.43).

6. A Thin and Infinitely Long Plate Magnetized in Width.

Suppose that a rock layer having the shape of a thin plate is located parallel to the earth's surface, forming an angle φ with the vertical OO_1 (Figure 166), and the magnetization J coincides with the side ab = l of the rectangle abcd of the transverse section of the plate.

With uniform magnetization of the upper and lower surfaces of the plate magnetic charges of surface density J will be formed, and for each unit length the magnitude of this charge m will be m = J $\overline{bc}$.

Disregarding the width $\overline{bc}$, the magnetic mass concentrated at some point Q, may be represented as m dy, where dy is the element of length of the plate. At any point of space P this mass produces a magnetic field with intensity

$$dH_T = m\, dy/p^2 ,$$

where p is the distance between the elemental mass and the point P.

The components dX, dY, dZ on the coordinate axis are obtained

Declassified in Part - Sanitized Copy Approved for Release 2013/01/23 : CIA-RDP81-01043R001600090003-8

Declassified in Part - Sanitized Copy Approved for Release 2013/01/23 : CIA-RDP81-01043R001600090003-8

by multiplying dH_T by the corresponding cosines of the angles between PQ and the coordinate axes.

The x axis is extended through point P perpendicularly to the length of the plate, the z axis is placed in a vertical position, and the origin of coordinates is placed at some random point of the upper surface of the plate.

In this case the coordinates of point P will be x, o and R, the coordinates of point Q will be o, y, o, and therefore

$$\rho^2 = x^2 + y^2 + R^2.$$

The components of vector dH_T are expressed by the equations:

$$dX = \frac{x\,dy}{\rho^3}, \quad dY = \frac{y\,dy}{\rho^3}, \quad dZ = \frac{R\,dy}{\rho^3} \qquad (8.44)$$

Integrating these expressions within the limits $-\infty$ to $+\infty$ we obtain:

$$X = H = \frac{2mx}{x^2+R^2}; \quad Z = \frac{2mR}{x^2+R^2} \qquad (8.45)$$

These equations show that the magnetic field of an infinitely long charged, or single pole line does not depend upon the coordinate y which is parallel to this line.

Similar expressions for H and Z are obtained in relation to the lower surface of the plate, the coordinates of which are

$$x_1 = x - l\sin\varphi; \quad R_1 = R + l\cos\varphi.$$

Therefore, the magnetic field of the entire plate is defined by components H and Z, which are of the following form:

$$H = \frac{2mx}{R^2+x^2} - \frac{2m(x-l\sin\varphi)}{(R+l\cos\varphi)^2+(x-l\sin\varphi)^2},$$
$$Z = \frac{2mR}{R^2+x^2} - \frac{2m(R+l\cos\varphi)}{(R+l\cos\varphi)^2+(x-l\sin\varphi)^2} \qquad (8.46)$$

With a vertical position of the plate, at $\varphi = 0$:

$$H = 2mx\left(\frac{1}{R^2+x^2} - \frac{1}{(R+l)^2+x^2}\right),$$
$$Z = 2m\left(\frac{R}{R^2+x^2} - \frac{R+l}{(R+l)^2+x^2}\right). \qquad (8.47)$$

Declassified in Part - Sanitized Copy Approved for Release 2013/01/23 : CIA-RDP81-01043R001600090003-8

Declassified in Part - Sanitized Copy Approved for Release 2013/01/23 : CIA-RDP81-01043R001600090003-8

Graphs, corresponding to equations (8.46) and (8.47) are shown in Figure 167, and the graphs of equations (8.45) are shown in Figure 165.

In view of (8.45) the maximum values H_m and Z_m in the case of a single-pole line will be:

$$H_m = m/R, \qquad Z = 2m/R$$

i.e., the maximum Z_m is twice H_m.

The geometric image intermediate between a single-pole and a dipole formation is that of a 2-pole magnet (schematic) and thus a thin plate is the intermediate geometrical image between a linear pole and a dipole filament equivalent to a cylinder magnetized along the diameter. Indeed, with l approaching infinity we have the field of a single-pole filament or line, and with l approaching zero formulas (8.46) and (8.47) describe a cylinder. To demonstrate this, it is sufficient to reduce equations (8.46) and (8.47) to a common denominator and in the resulting expressions equate $l = 0$ and $ml = \mu$.

The conditions under which a 2-pole plate may be replaced by a single-pole plate are analogous to those of a 2-pole magnet, and are derived in the same manner as the conditions expressed by the ratio (8.34).

In such a case the relative difference between the vertical components, which must be less than a certain quantity, will be defined by the following expression:

$$z_1 - z_2/z_1 = (z_0 - 1)\,[(1 + l)^2 + x^2\,] + (1 + l)\,(l + x^2)/$$
$$z_0\,[1 + l)^2 + x^2\,]$$

where

$$z_0 = l/1 + l.$$

However the depth at which the second pole of the plate must be

Declassified in Part - Sanitized Copy Approved for Release 2013/01/23 : CIA-RDP81-01043R001600090003-8

Declassified in Part - Sanitized Copy Approved for Release 2013/01/23 : CIA-RDP81-01043R001600090003-8

located will be considerably greater than the depth of the second pole of the magnet. The following table shows the magnitude of the relative difference of the vertical components in percent, for various distances l between the poles, and for various values of the coordinate x, assuming the depth value of the upper pole is equal to unity.

x \ l	5	10	20
0	0	0	0
0.5	3.9	2.3	1.2
1	18	8.8	4.8

The table shows that the depth of occurrence of the second pole must be not less than 10 times the depth of the upper pole, for the plate to be considered monopolar, assuming that the relative error in the determination of Z is of the order of 6 to 8%.

7. Infinitely Long Rectangular Prism, Magnetized Vertically. Vertical Stratum. A rectangular prism of infinite length with its upper side parallel to the earth's surface may be considered as being composed of infinitely great number of infinitely thin plates, and its magnetic potential is calculated as the sum of the potentials of such plates. In this calculation linear density of magnetic charge of the thin plate must be formulated as the product of the surface density of magnetism σ concentrated at the upper side, and the width of the infinitely small plate dx_0. Using the same system of coordinates described above the horizontal and vertical components of the magnetic field produced by the charges of the upper side of the prism are expressed by the following integrals:

$$H = 2\sigma \int_{-a}^{+a} \frac{(x_1 - x)\,dx_0}{R^2 + (x_0 - x)^2}; \quad Z = 2\sigma R \int_{-a}^{+a} \frac{dx_0}{R^2 + (x_0 - x)^2} \qquad (8.48)$$

Declassified in Part - Sanitized Copy Approved for Release 2013/01/23 : CIA-RDP81-01043R001600090003-8

Declassified in Part - Sanitized Copy Approved for Release 2013/01/23 : CIA-RDP81-01043R001600090003-8

where x is the abscissa of point P at which the field is being considered, x_0 is the abscissa of the element of length dx_0, and 2a is the width of the prism.

Integration gives:

$$H = 2\sigma \ln \frac{R^2 + (x+a)^2}{R^2 + (x-a)^2} \qquad (8.49)$$

$$Z = 2\sigma\left(\operatorname{arctg}\frac{x+a}{R} - \operatorname{arctg}\frac{x-a}{R}\right) = 2\sigma \operatorname{arctg}\frac{2Ra}{R^2 - a^2 + x^2} \qquad (8.50)$$

If the radius-vectors r_1 and r_2 are plotted from point P to the edges of the prism (Figure 168), and denoting the angles which they form with the z-axis by α_1 and α_2, it is apparent from the drawing that

$$r_1^2 = R^2 + (x+a)^2,$$

$$r_2^2 = R^2 + (x-a)^2,$$

and

$$\operatorname{tg}\alpha_1 = \frac{x+a}{R},$$

$$\operatorname{tg}\alpha_2 = \frac{x-a}{R},$$

therefore

$$H = 2\sigma \ln \frac{r_1}{r_2},$$

$$Z = 2\sigma(\alpha_1 - \alpha_2) = 2\sigma\alpha, \qquad (8.51)$$

where α is the angle at which the upper side of the prism is seen from point P. It is evident that the charges of the lower side of the prism will produce an analogous field, and its components will be expressed by analogous formulas in which the distance R_1 to the lower side appears in lieu of the distance R. Hence the expressions for H and Z for entire prism will be:

$$H = 2\sigma\left(\ln\frac{r_1}{r_2} - \ln\frac{r_3}{r_4}\right) = 2\sigma \ln\frac{r_1 r_4}{r_2 r_3}, \quad Z = 2\sigma(\alpha - \beta),$$

where the values r_3, r_4 and β are apparent from the drawing.

If the longitudinal dimensions of the prism are large in comparison to the depth of occurrence of the upper side, the influence of the lower side may be disregarded. In such a case the magnetic field will be defined by formulas (8.49) and (8.50), the graphs of which are shown in Figure 169. The graphs relate to 2 instances: when the width

Declassified in Part - Sanitized Copy Approved for Release 2013/01/23 : CIA-RDP81-01043R001600090003-8

Declassified in Part - Sanitized Copy Approved for Release 2013/01/23 : CIA-RDP81-01043R001600090003-8

of the prism is equal to its depth of occurrence, and when its width is twice the depth. The graphs show that in the case of a prism with width equal to depth of occurrence the H and Z curves almost coincide with the curves relating to a thin plate, and the deviation is apparent only in the case of a prism the width of which is twice its depth of occurrence. The ratio of the maxime H_{max} to Z_{max} is approximately equal to 0.5, increasing somewhat with an increase in width 2a. In addition, the maximum H is shifted to the right of the z axis.

The curves H and Z of the prism represent a sum of an infinitely large number of H and Z curves of thin plates which compose the prism. However, with an error that is admissible in practice they can be represented as the sum of a finite number of curves of thin plates disposed at a finite distance from each other. Thus the curves of a prism with width 2a = 2R differ only slightly from the curves representing the magnetic field of 2 plates disposed symmetrically in relation to the z axis at a distance R from each other. The curves corresponding to the latter case are shown in dotted lines in Figure 169. Therefore, given the H and Z curves derived from observation it cannot be deduced whether they represent the magnetic field of a prism or the sum of the fields of 2 or several plates, if no additional geological or geophysical information concerning the nature of the occurrence of the rocks is available.

8. A Thin, Horizontal, Infinitely Long Plate. Thin Horizontal Stratum.

A thin, vertically magnetized plate or a stratum infinitely thin in comparison with the depth of occurrence, constitutes a combination of a large number of linear dipoles, the magnetic field of which was discussed in section 2 of the present paragraph. The potential of such a plate is represented by the integral

$$V = 2\mu \int_{-a}^{+a} \frac{P\, dx_0}{P^2 + (x_0 - x)^2}$$

Declassified in Part - Sanitized Copy Approved for Release 2013/01/23 : CIA-RDP81-01043R001600090003-8

Declassified in Part - Sanitized Copy Approved for Release 2013/01/23 : CIA-RDP81-01043R001600090003-8

where the expression within the integration sign is the potential of a linear dipole or infinite cylinder with linear magnetic moment μdx_0. Further, x is the abscissa of point P at which the potential is being considered, and 2a is the width of the plate.

After integration, we have:

$$U = 2\mu \left(\operatorname{arc\,tg} \frac{x+a}{R} - \operatorname{arc\,tg} \frac{x-a}{R} \right),$$

which is differentiated with respect to the corresponding coordinates, yielding the following values for horizontal and vertical components:

$$H = \frac{4\mu Rx}{[R^2+(x-a)^2][R^2+(x+a)^2]}, \qquad (8.52)$$

or

$$Z = \frac{2\mu(R^2-x^2+a^2)}{[R^2+(x-a)^2][R^2+(x+a)^2]},$$

$$H = \frac{4\mu Rx}{r_1^2 r_2^2} \quad \text{and} \quad Z = \frac{2\mu(R^2+a^2-x^2)}{r_1^2 r_2^2}$$

where r_1 and r_2 have the same values as in the preceding instance of a prism (Figure 168).

The same correlations are obtained for the components of the magnetic field of 2 infinitely long rectilinear currents distributed along the edges of the plate, since the magnetized plate constituting a double magnetic layer is equivalent in its properties to such currents. From this it follows that if the width of the plate is large in comparison with the depth of its occurrence, or if the distance between the currents is large, the magnetic field over the edge of the plate will be greater than over its center.

Indeed, upon analyzing equation (8.52) it can be readily shown that if a $< \sqrt{3}R$ the vertical component Z has one maximum at x = 0, and if a $> \sqrt{3}R$, 2 maximum values are obtained at $x_{1,2} = \pm\sqrt{(R^2+a^2) - 2R\sqrt{R^2+a^2}}$ and 3 minimum values are obtained if $x_1 = 0$ at $x_{1,2} = \pm\sqrt{(R^2+a^2) + 2R\sqrt{R^2+a^2}}$

Figure 170 shows the Z and H graphs for a = 1/2 R and a = 3R. In the first instance, a $< \sqrt{3}R$, we actually obtain one maximum and 2 minima of

Declassified in Part - Sanitized Copy Approved for Release 2013/01/23 : CIA-RDP81-01043R001600090003-8

Declassified in Part - Sanitized Copy Approved for Release 2013/01/23 : CIA-RDP81-01043R001600090003-8

Z, and in the second instance, when $a > \sqrt{3}R$ the Z curve shows 2 maxima and 3 minima.

In addition, it is characteristic of bodies of this kind that with an increase in the width of the plate 2a the maximum of the horizontal component increases, while at a width exceeding a certain value the maximum of H becomes greater than the maximum of Z and is located over the edge of the plate.

Further, on comparing the curves for a = 1/2 R with the curves of a linear dipole or cylinder (Figure 165), it is seen that they differ only slightly, i.e., the magnetic field of a thin plate, the width of which is less than the depth of occurrence, practically does not differ from a linear dipole.

9. Semi-Infinite Horizontal Stratum.

Let us suppose that the rock formation is horizontal stratum of constant thickness and infinite area in a horizontal plane, but bound on one side by a vertical plane. Such a stratum will be called semi-infinite. The limiting plane is called the contact plane, since at this plane the stratum contacts other rocks. If such a stratum is magnetized vertically it is evident that at a distance from the contact the magnetic field underneath it will be constant and close to zero, and appreciable gradients and an appreciable magnitude are found only above the contact.

The components of the magnetic field intensity of such a stratum are determined by expressions (8.48) for H and Z, corresponding to the upper and lower side of an infinitely long prism, and only the limits of integration are changed, namely:

$$H = 2\delta \int_0^{\infty} \frac{(x_0 - x)\,dx_0}{l^2 + (x_0 - x)^2} - 2\delta \int_0^{\infty} \frac{(x_0 - x)\,dx_0}{(R + l)^2 + (x_0 - x)^2}$$

$$Z = 2\delta K \int_0^{\infty} \frac{dx_0}{l^2 + (x_0 - x)^2} - 2\delta K \int_0^{\infty} \frac{dx_0}{(R + l)^2 + (x_0 - x)^2}.$$

Declassified in Part - Sanitized Copy Approved for Release 2013/01/23 : CIA-RDP81-01043R001600090003-8

Declassified in Part - Sanitized Copy Approved for Release 2013/01/23 : CIA-RDP81-01043R001600090003-8

After integration, we have

$$H = 5 \ln \frac{x^2 + (R+l)^2}{x^2 + R^2} \qquad (8.53)$$

$$Z = 2\sigma \left(\operatorname{arc\,tg} \frac{x}{R} - \operatorname{arc\,tg} \frac{x}{R+l} \right) = 2\sigma \operatorname{arc\,tg} \frac{xl}{R^2 + x^2 + Rl} \qquad (8.54)$$

It is readily apparent that above the contact, where x = 0 and Z = 0, H has a maximum value, and at $x \gg l$ both components H and Z approach zero.

Maximum and minimum values of the component Z occur at $x = \pm \sqrt{R(l+R)}$, and their magnitude is

$$Z_m = \pm 2\sigma \operatorname{arc\,tg} \frac{l}{2\sqrt{R(l+R)}}$$

The curves for R = 1 and $l = 4$, based on formulas (8.53) and (8.54), are shown in Figure 171.

10. Vertically Magnetized Sloping Stratum of Infinite Length.

Let us assume that a sloping stratum of rock has a vertical plane section shaped like a parallelogram (Figure 172) one of the sides of which is parallel to the earth's surface and the opposite side is located at a great depth, which we will assume to be equal to infinity. With a uniform vertical magnetization magnetic charges will be found at the upper side ab, having surface density σ, while at the lateral side bc the density is $\sigma \cos \varphi$, where φ is the angle of inclination of the stratum in relation the the horizon. At the opposite side ad the charge density is $-\sigma \cos \varphi$.

In accordance with the deductions of section 7 the components H_1 and Z_1 of the magnetic field at point P on the upper side will be:

$$H_1 = 2\sigma \ln \frac{r_2}{r_1}, \quad Z_1 = 2\sigma\alpha, \qquad (8.55)$$

where α, r_1 and r_2 have the values shown in Figure 172.

If the origin of coordinates is placed at point P and a new x'

Declassified in Part - Sanitized Copy Approved for Release 2013/01/23 : CIA-RDP81-01043R001600090003-8

Declassified in Part - Sanitized Copy Approved for Release 2013/01/23 : CIA-RDP81-01043R001600090003-8

axis is drawn parallel to the side bc, in accordance with equation (8.48), the components H' and Z' of the sides bc and ad, in relation to the new system of coordinates, will be:

$$H' = -2\delta \cos\varphi \ln\frac{r_2}{r_1},\quad Z' = -2\delta\cos\varphi(\theta - \theta_2) = -2\delta\alpha\cos\varphi. \tag{8.56}$$

In the former system of coordinates the components H_2 and Z_2 are determined in accordance with the transition formulas

$$H_2 = H'\cos\varphi - Z'\sin\varphi;\quad Z_2 = H'\sin\varphi + Z'\cos\varphi \tag{8.57}$$

The expression for the components of the entire stratum are determined by adding expressions (8.55) and (8.57), i.e.,

$$H = 2\delta\ln\frac{r_2}{r}(1-\cos^2\varphi) + 2\delta\alpha\sin\varphi\cos\varphi;$$

$$Z = 2\delta\alpha - 2\delta\sin\varphi\cos\varphi\ln\frac{r_2}{r_1} - 2\delta\alpha\cos^2\varphi,$$

or, in accordance with formulas (8.49) and (8.50), replacing α, r_1 and r_2 by their values, we have:

$$\mu = 2\delta\sin\varphi\left[\cos\varphi\operatorname{arctg}\frac{2R\alpha}{R^2 - a^2 + x^2} + \frac{1}{2}\sin\varphi\ln\frac{(x-a)^2+z^2}{(x+a)^2+z^2}\right],$$

$$Z = 2\delta\alpha\left[\sin\varphi\operatorname{arctg}\frac{2R\alpha}{R^2 - a^2 + x^2} - \frac{1}{2}\cos\varphi\ln\frac{(x-a)^2+z^2}{(x+a)^2+z^2}\right].$$

From Figure 173, which shows the Z and H curves in the case of a stratum with an inclination of 60° in relation to the horizon, it is apparent that the inclination causes asymmetry of voth curves although the lower boundary is at infinity. In comparison with a vertical position of the stratum (Figure 169), the value Z of which is nowhere negative, the slanting stratum has a vertical component which passes through zero at values of X approximately twice as large as the depth of occurrence of the upper side, and at $x > 2R$ it assumes negative values. Further, the maximum value of the horizontal component increases sharply with an increasing angle of inclination, which also is a characteristic feature of rock occurrences of this kind.

Declassified in Part - Sanitized Copy Approved for Release 2013/01/23 : CIA-RDP81-01043R001600090003-8

Declassified in Part - Sanitized Copy Approved for Release 2013/01/23 : CIA-RDP81-01043R001600090003-8

It must be noted that in the case of a sloping stratum which extends deep into the earth but is magnetized along its axis, the magnetic field will be identical with the field of a vertical stratum, i.e., in the case of axial magnetization the inclination of the stratum is of no significance.

11. The Method of Cards for Solving the Main Problem of Magnetometry

In cases in which exact determination of the potential is impracticable, the conventional methods of approximate calculations may be used if they enable the preparation of suitable cards for determining the magnetic field of some group of bodies. In geophysics the term cards is used to designate transparent sheets on which systems of curves or straight lines derived by theoretical calculations are plotted. In many instances the superposition of such a card over the experimental curve enables the necessary result to be obtained without resorting to additional calculations. Thus D. S. Mikov has proposed a card for determining the magnetic field of infinitely long horizontal cylindrical bodies, the cross section of which may be a plane figure of any shape, and which are uniformly magnetized perpendicularly to their axis [75]. Due to the uniform magnetization the magnetic field of such a cylinder may be regarded as the field of an infinitely large number of elemental cylinders the magnetic potential of which may be expressed according to equation (8.41) as follows:

$$dU = 2dM/r \cos\theta.$$

The field intensity components in the direction of the radius-vector r and perpendicular to the latter will be:

$$dH_r = 2dM/r^2 \cos\theta \qquad \text{and} \qquad dH_\theta = 2dM/r^2 \sin\theta.$$

Projecting these components on the magnetic axis of the cylinder and on the axis perpendicular to the latter, we obtain the components in these directions, which we shall denote by $dH_\parallel$ and $dH_\perp$. It is readily apparent that:

Declassified in Part - Sanitized Copy Approved for Release 2013/01/23 : CIA-RDP81-01043R001600090003-8

Declassified in Part - Sanitized Copy Approved for Release 2013/01/23 : CIA-RDP81-01043R001600090003-8

$$dH_{\parallel} = \frac{2\,dM}{r^2}\cos 2\theta, \quad dH_{\perp} = \frac{2\,dM}{r^2}\sin 2\theta \tag{8.58}$$

The elemental magnetic moment dM may be replaced by $dM = \mu\,dS$, and the elemental surface may be expressed by the polar coordinates $dS = r\,dr\,d\theta$.

Then, replacing dM in equation (8.58) and integrating over the entire area of the cylinder cross section we obtain:

$$H_{\parallel} = \mu\int\cos 2\theta\int\frac{dr}{r}\cdot L = 2\mu\int\sin 2\theta\,d\theta\int\frac{dr}{r}. \tag{8.59}$$

Since in these expressions the integrals do not depend upon the magnetization of the rock and their values are determined solely by the position of point P and the shape of the cylinder cross section, the integrals may be calculated once for all definite shapes of cross sectional areas found at different distances r from the point P. It is most convenient to determine the dimensions of areas of segmentary shapes, which produce at point P a field intensity component equal to unity.

For segments limited by radii r_n and r_{n+1} and the angles θ_m and θ_{m+1}, the equations (8.59) assume the form:

$$H_{\parallel} = \mu(\sin 2\theta_{m+1} - \sin 2\theta_m)\ln\frac{r_{n+1}}{r_n},$$
$$H_{\perp} = \mu(\cos 2\theta_{m+1} - \cos 2\theta_m)\ln\frac{r_{n+1}}{r_n} \tag{8.60}$$

Taking $\mu = 100$ CGSμ and equating each of the equations equal to one gamma (1.10^{-5} CGSμ), we obtain 2 equations and 3 unknown differences. Therefore one of them must be arbitrarily taken equal to a certain constant quantity. D. S. Mikov assumed

$$\sin 2\theta_{m+1} - \sin 2\theta_m = 0.125,$$

in which case the natural logarithm of the ratio was found to be

$$\ln\frac{r_{n+1}}{r_n} = 0.080,$$

and the common logarithm

$$\lg\frac{r_{n+1}}{r_n} = 0.0347.$$

Declassified in Part - Sanitized Copy Approved for Release 2013/01/23 : CIA-RDP81-01043R001600090003-8

Declassified in Part - Sanitized Copy Approved for Release 2013/01/23 : CIA-RDP81-01043R001600090003-8

Hence the values of angle θ and radius r which limit the segment areas are:

$\theta = 0^{\circ}; 3.6^{\circ}; 7.2^{\circ}; 11.0^{\circ}; 15.0^{\circ}; 19.3^{\circ}; 24.3^{\circ}; 30.5^{\circ}; 45^{\circ};$

$r = 1.00 ; 1.08; 1.17; 1.27; 1.38; 1.49,$ etc.

The angles of the next octant will be symmetrical with the angles of the first octant.

If radius-vectors are drawn from some point P at angle θ and limited by the radii r we obtain a grid consisting of a number of segments, each of which produces at point P a component $H_{\parallel}$ equal to $1 \cdot 10^{-5}$ CGS $\int$. It is evident that the direction of $H_{\parallel}$ coincides with the radius vector corresponding to $\theta = 0$. Having drawn such a card, if we wish to calculate the magnetic field of a cylinder having the cross section shown in Figure 174 the center of the card is placed over the point P at which the component $H_{\parallel}$ is to be determined and the card is adjusted so that the zero radius-vector extends in the direction of magnetization of the cylinder. The number of areas thus brought within the contour will correspond to the magnitude of $H_{\parallel}$. From the equations of (8.60) it is apparent that to determine $H_{\perp}$ it is sufficient to turn the card through an angle of 45°. When $H_{\parallel}$ and $H_{\perp}$ are known it is not difficult to switch to the components Z and H, which are determined by means of the equation

$$Z = H_{\parallel} \cos i - H_{\perp} \sin i; \quad H = H_{\perp} \cos i + H_{\parallel} \sin i;$$

where i is the angle between the vertical and the vector J.

Instead of counting the areas it is more convenient to count the points found at the center of each area. An example of such a card is shown in Figure 175.

T. N. Roze [76] used the same card method to calculate the vertical

Declassified in Part - Sanitized Copy Approved for Release 2013/01/23 : CIA-RDP81-01043R001600090003-8

Declassified in Part - Sanitized Copy Approved for Release 2013/01/23 : CIA-RDP81-01043R001600090003-8

component of semi-infinite vertical cylindrical bodies, the upper base of which is limited by any contour. In this process it is assumed that the cylinder is uniformly magnetized in the vertical direction.

In the case of such a cylinder, the upper base of which is located at a depth h, the vertical component of magnetic field intensity at point P (Figure 176) is expressed by the equation:

$$Z = hJ \int dS/(h^2 + r^2)^{3/2},$$

where J is magnetization of the cylinder, r the distance from the element of surface dS to the vertical axis extending through point P, and the integration is carried out over the entire surface of the cylinder base. If dS is expressed in polar coordinates, it follows that

$$Z = hJ \int r\, dr\, d\theta/(h^2 + r^2)^{3/2}.$$

As in the previous case the base of the cylinder is divided into segments of such area that each of them produces a vertical component of one γ, at point P. The dimensions of these segments must satisfy the equation:

$$J(\theta_{m+1}-\theta_m)(h/\sqrt{h^2 + r_n^2} - h/\sqrt{h^2 + r_{n+1}^2}) = 1 \cdot 10^{-5}.$$

Having calculated and plotted θ_m and r_m in accordance with this formula the contour is divided into a number of areas limited by radius-vectors and circumference arcs. The number of these areas will be equal to the magnitude of the vertical component expressed in gammas. Since the dimensions of these areas are independent of the magnitude of J, they may be plotted beforehand for all the values from $r = 0$ to $r = \infty$ and from $\theta = 0$ to $\theta = 2\pi$ and may be used as a card for the calculation of the Z of any plane figure.

To prepare such a card it is necessary to assume values for the interval $\theta_{m+1}-\theta_m$ and for the quantity J.

Declassified in Part - Sanitized Copy Approved for Release 2013/01/23 : CIA-RDP81-01043R001600090003-8

Declassified in Part - Sanitized Copy Approved for Release 2013/01/23 : CIA-RDP81-01043R001600090003-8

Assuming $J = 10^{-3}$, $\theta_{m+1} - \theta_m = 10^{\circ}$ and replacing the terms appearing between the second parentheses by the cosines of angles φ (Figure 176), we have:

$$(\cos\varphi_n - \cos\varphi_{n+1}) = 0.0573$$

assuming $\cos\varphi_{n+1} = 0$, which corresponds to $r = \infty$, we obtain $\cos\varphi_n = 0.0573$ or $\varphi_n = 86.7^{\circ}$. Then, adding 0.0573 to each value of the cosine in succession, we obtain all the following values. The last value of the cosine will be 0.9738.

When φ_n is known, the radius r may be determined according to the formula $r_n = h \operatorname{tg} \varphi_n$.

The last value $\varphi_o = 0.9738$ corresponds to an area with radius $r_o = 0.23\ h$, for which the quantity Z is determined according to the formula

$$Z = 2\pi J(1 - h/\sqrt{h^2 + r_0^2}).$$

A card plotted in this manner will have the appearance of rays drawn from a single point at intervals of 10°, and of a number of concentric circumferences having the radii $r_0 = 0.23\ h$, $r_1 = 0.44\ h$, $r_2 = 0.60\ h$, etc.

To determine Z at some point P the center of the card is placed over the point P and the number of areas included within the contour is counted.

This kind of card also may be used for determination of the vertical component produced by a body of any shape, magnetized in the vertical direction. To do this the body is divided into layers by horizontal planes at equal intervals and the card is used to determine the Z for a number of plane surfaces: S_1, $S_2 - S_1$; $S_3 - S_2$, etc where S_1 is the surface produced by intersection with the first plane, S_2 that of the second section, etc (Figure 177).

Declassified in Part - Sanitized Copy Approved for Release 2013/01/23 : CIA-RDP81-01043R001600090003-8

Declassified in Part - Sanitized Copy Approved for Release 2013/01/23 : CIA-RDP81-01043R001600090003-8

Since the depth of occurrence of each sectional surface is different, the center of the card must be moved every time so that the ratio of the distance of point P from the epicenter 0, to the depth of the corresponding layer is always the same.

The card for determination of the horizontal component is somewhat different in appearance. Within each sector having an angle at the base equal to 10^{o}, the radii of circumferences r_n have different values for the same values of h, since in this case r_n depends upon the angle θ_n.

12. Experimental Method of Solving the Main Problem

Both theoretical calculation of magnetic fields and the card method include many assumptions, such as the uniform magnetization of the rock strata and the geometric regularity of their shape, which actually are never encountered. Furthermore, in many instances both methods lead to fairly complex and laborious calculations as a result of which they are poorly adapted for practical use.

Therefore, in such cases it is more appropriate to determine the magnetic field by means of direct measurements of the field over rock formations of different shape, produced artificially in the form of models. From the very formulas for the components of intensity of a magnetic field produced by bodies of regular shape, it follows that with a proportional change of their dimensions, i.e., retention of the similarity, the intensity of the magnetic field will remain the same if the distance to the center of the body is changed in the same proportion. However this characteristic of similarity in the topography of the field of such bodies also is retained in the case of bodies of any shape, and therefore permits utilization of the method of models for determination of the magnetic field of rock formations of any shape.

Declassified in Part - Sanitized Copy Approved for Release 2013/01/23 : CIA-RDP81-01043R001600090003-8

Declassified in Part - Sanitized Copy Approved for Release 2013/01/23 : CIA-RDP81-01043R001600090003-8

The experiment consists of the preparation of a corresponding model and measurement of Z and H at different points of space around this model. Because of the small dimensions of the model in comparison with the naturally occurring rocks, the gradients of the magnetic field become very large, with the result that the volume of space within which the field may be considered uniform is very small. Hence the measuring instrument must be of very small dimensions. This requirement is met by the magnetometer of A. G. Kalashnikov, which is called a field meter. The field meter consists of a direct current generator, the principal part of which is a coil provided with a 5 mm-long and 1.5 mm diameter permalay core wound with thin enamel-coated wire 0.03 mm in diameter. The coil is connected to a synchronous motor by a long rod which rotates the coil in the magnetic field to be measured at a speed of 25 revolutions per second, and the induction current produced as a result of this rotation is measured by means of a galvanometer. With the above dimensions the coil measures the mean value of the field within a spherical space 3 mm in diameter. This is quite sufficient if the dimensions of the model are chosen accordingly.

The coil and the motor can be moved a certain distance in vertical and horizontal directions.

Using this type of a field meter A. G. Kalashnikov and S. S. Fonton [77] carried out measurements of the fields over models of faults consisting of 2 rectangular plates 120 to 500 mm long and 20 to 120 mm thick, which were given various vertical displacements.

The models were made of magnetite powder mixed with an equal weight of plastelin, giving the product a susceptibility of approximately 10^{-2} CGS μ.

Declassified in Part - Sanitized Copy Approved for Release 2013/01/23 : CIA-RDP81-01043R001600090003-8

Declassified in Part - Sanitized Copy Approved for Release 2013/01/23 : CIA-RDP81-01043R001600090003-8

Figures 178 and 179 show the characteristic graphs of Z and H over faults of different types, Figure 178 relating to a fault in which both branches extend over a large distance while Figure 179 relates to a fault in which length is commensurate with thickness. A characteristic feature of these graphs is the inflection of the Z curve, and also the occurrence of an H maximum over the boundary of the fault.

The results of these measurements have demonstrated the possibility of wide utilization of the experimental method in the solution of the main problem of magnetometry, which in the case of structures such as faults is extremely complex in its theoretical aspects.

Section 9. The Possibility of Utilizing the Plane Problem

A boundless expanse of rocks does not occur in nature. A rock occurrence always is limited in the horizontal as well as in the vertical direction. Hence the question arises as to the practical instances in which it is possible to apply the formulas derived in the preceding section for bodies or rocks having boundless dimensions in the horizontal direction, i.e., when is it possible to apply the plane problem. To answer this question the magnetic field of the rock or body having an unlimited expanse must be compared with a body of finite dimensions. Therefore, as an example we will consider the magnetic field of a single-pole line and of a linear dipole of finite length.

Since for mathematical interpretation of anomalies of limited area it is sufficient to know the magnetic field along the profile extending through the middle and through the cross section of its area it follows that without departing from the general nature of the problem we can seek to determine the magnetic field through the middle, and perpendicular to the single-pole line and to the linear dipole.

Declassified in Part - Sanitized Copy Approved for Release 2013/01/23 : CIA-RDP81-01043R001600090003-8

Declassified in Part - Sanitized Copy Approved for Release 2013/01/23 : CIA-RDP81-01043R001600090003-8

In accordance with equation (8.44) the components of field intensity of a single pole line of finite length may be represented by the following integral expressions:

$$X_l = nx \int_{-l}^{+l} \frac{dz}{(z^2+y^2)^{\frac{3}{2}}}, \quad Y_l = ny \int_{-l}^{+l} \frac{dz}{(z^2+y^2)^{\frac{3}{2}}}, \quad Z_l = nR \int_{-l}^{+l} \frac{dz}{(z^2+y^2)^{\frac{3}{2}}}$$

where the limits of integration are the positive and negative values of the half-length of the pole line. The values of the other symbols are the same as on page 349. The symbol l appearing next to X, Y and Z is used to differentiate these components from those of a line of infinite length.

Integrating within the above limits, we obtain the following expressions:

$$X_l = H = \frac{2nx}{R^2+x^2} \cdot \frac{l}{\sqrt{l^2+r^2}}, \quad Y_l = 0,$$

$$Z_l = \frac{2nR}{R^2+x^2} \cdot \frac{l}{\sqrt{l^2+r^2}}.$$

At the same time, we have $r^2 = R^2 + x^2$.

Comparing these expressions with the expressions of (8.45) for an infinite line, we see that:

$$X_l = X \frac{l}{\sqrt{l^2+r^2}}, \quad Z_l = Z \frac{l}{\sqrt{l^2+r^2}}$$

Therefore, in order that X_l approximate X and Z the half-length of the pole line must be considerably greater than r. To evaluate the magnitude of the ratio r/l, at which the pole line may be considered equivalent to an infinite line the numerator and denominator of the right hand portion are divided by l and disregarding the terms of higher order, we obtain $X_l = X\left[1 - \frac{1}{2}\frac{r^2}{l^2}\right]$, $Z_l = Z\left[1 - \frac{1}{2}\frac{r^2}{2l^2}\right]$.

whence we have

$$\frac{X - X_l}{X} = \frac{Z - Z_l}{Z} = \frac{1}{2}\frac{r^2}{l^2}. \qquad (8.61)$$

Declassified in Part - Sanitized Copy Approved for Release 2013/01/23 : CIA-RDP81-01043R001600090003-8

Declassified in Part - Sanitized Copy Approved for Release 2013/01/23 : CIA-RDP81-01043R001600090003-8

Assuming the limit of error does not exceed 3% in the determination of H and Z over a profile 3 times the depth of occurrence (X >3R) this equality may be used to determine the length of the pole line $2l$, which is equivalent to an infinite line. Indeed, from equation (8.61) we obtain

$$\frac{1}{2}\left(\frac{9R^2+R^2}{l^2}\right. = 0{,}03$$

and therefore

$$\frac{2l}{R} \sim 25$$

i.e., the length of the pole line must be 25 times greater than the depth of occurrence.

The same result is obtained for a horizontal cylinder magnetized along the diameter. In accordance with formula (8.41) the magnetic potential U_l of a cylinder of finite length $2l$, is:

$$U_l = 2\mu \cos\theta \int_0^{\alpha} \frac{\cos\alpha\, d\alpha}{r^2 + l^2},$$

where the meaning of the letters is the same as in formula (8.41). On integration, we obtain

$$U_l = \frac{2\mu}{r} \cos\theta \cos\alpha \quad \text{i.e.,} \quad U_l = U\cos\alpha.$$

At small values of angle α, i.e., when $l \gg r$ we have, with a sufficient degree of accuracy,

$$H_l = H\cos\alpha, \qquad Z_l = Z\cos\alpha,$$

or

$$H_l = H\frac{r}{\sqrt{l^2+r^2}}, \qquad Z_l = Z\frac{l}{\sqrt{l^2+r^2}}$$

Since we know neither the depth of occurrence nor the length of the occurring rock formations, deductions concerning the ratio of these 2 factors can be made only on the basis of maps of isolines of the vertical component which are based on magnetic surveys. Therefore, let us consider how the vertical component changes along the length and breadth of a rock formation, depending on the ratio of the depth of occurrence to the length of the formation and, assuming that the deposit is shaped in thin plate with a single line of poles.

Declassified in Part - Sanitized Copy Approved for Release 2013/01/23 : CIA-RDP81-01043R001600090003-8

Declassified in Part - Sanitized Copy Approved for Release 2013/01/23 : CIA-RDP81-01043R001600090003-8

The component Z_l at any point of the surface is:

$$Z_l = m \cos\theta \int_{l_1}^{l_2} \frac{\cos\alpha \, dl}{r^2 + l^2},$$

where l_1 and l_2 are the distances from the ends of the cylinder to a plane extending through the point P and perpendicular to the line of the poles.

Expressing l_1 and l_2 by means of the angles α_1 and α_2 and performing the integration, we obtain:

$$Z_l = \frac{m \cos\theta}{r} (\cos\alpha_1 + \cos\alpha_2).$$

For points located over the ends of the pole line, r = R, $\theta = 0, \alpha_1 = 90^\circ$ and $\cos\alpha_2 = \frac{2l}{\sqrt{R^2 + 4l^2}}$,

therefore: $$Z_l = \frac{2m}{R} \frac{l}{\sqrt{R^2 + 4l^2}};$$

and over the center of the pole line

$$Z_{l_0} = \frac{2m}{R} \frac{l}{\sqrt{R^2 + l^2}},$$

Comparing these expressions, we obtain:

$$\frac{Z_{l_0}}{Z_l} = \sqrt{\frac{R^2 + 4l^2}{R^2 + l^2}}$$

Since [l] must be approximately 12 times greater than R, on replacing $l = 12R$, we have

$$\frac{Z_{l_0}}{Z_l} \sim 2, \qquad (8.62)$$

i.e., an isodynamic line having a value one-half of that above the center of the anomaly must extend over the center of the pole line. Let us determine further the distance x from the center, along the perpendicular to the axis of the anomaly, this isodynamic line is encountered. From equation (8.45) we have: $\frac{2mR}{R^2 + x^2} = \frac{mR}{R^2}$.

hence x = R, i.e., at a distance equal to the depth of occurrence the vertical component has the same value as over the end of the pole line. It follows from the latter that if the longitudinal dimensions of the

Declassified in Part - Sanitized Copy Approved for Release 2013/01/23 : CIA-RDP81-01043R001600090003-8

Declassified in Part - Sanitized Copy Approved for Release 2013/01/23 : CIA-RDP81-01043R001600090003-8

isodynamic line Z, equal to one-half of the maximum value, are 12 times smaller than the transverse dimensions, the anomaly may be regarded as being of infinite length.

Section 10. The Inverse Problem of Magnetometry.

In direct contrast with the main problem, the inverse problem of magnetometry consists of determination of the depth, shape and dimensions of the occurring rock formation from a given distribution of the magnetic field on the surface of the earth.

However, simultaneous determination of the shape, dimensions and depth of occurrence of the rock by analytical methods is impossible due to extreme mathematical difficulties, and therefore the inverse problem is subdivided into 2 separate problems: (1) Determination of shape, and (2) Determination of depth and dimensions of the occurring rock.

1. Determination of the Shape of a Rock Formation

Before undertaking the quantitative calculations concerning the depth of occurrence and the dimensions of a rock formation, it is necessary first to determine its shape, since it is only under this condition that the problem becomes entirely definite. Determination of the shape consists of finding a geometrical body which upon uniform magnetization will produce the same magnetic field as that of the occurring rock. Therefore solution of the problem will consist of comparison of the observed magnetic field with the fields of bodies of a regular shape. The latter have been derived in the preceding section and are represented in the form of graphs of Z and H as functions of the x coordinate.

In order to compare the observed Z and H curves with theoretical curves the 2 sets of curves must be plotted at the same scale. Ascertaining the value of the units on the ordinate axis involves no difficulties,

Declassified in Part - Sanitized Copy Approved for Release 2013/01/23 : CIA-RDP81-01043R001600090003-8

Declassified in Part - Sanitized Copy Approved for Release 2013/01/23 : CIA-RDP81-01043R001600090003-8

since in plotting the theoretical curves the maximum value of the Z component, which is always known from observation usually is taken as the unit of field intensity. A convenient unit for the abscissa axis, as we have seen in solving the main problem, is the depth of occurrence of the rock which, however, is not known in this case. Therefore a preliminary determination of the depth of occurrence of the rocks must be made, or a unit which does not depend on the depth of occurrence must be selected for both the theoretical and observational curves. Accordingly, there are 2 procedures of comparing the curves for a subsequent interpretation of the anomaly.

In the first, a determination is made of the depth of occurrence, which is then taken as the unit of length and the graphs of Z and H are plotted as functions of the distance.

In the second, the distance between some characteristic points of the Z or H curve, for example the distance between the maximum and minimum of H, the distance between the points of intersection of the H and Z curves, must be taken as the unit of length and the graphs of the observed and of the theoretical curves are prepared at this scale.

In practice, however, the distance between points on the Z curve with ordinates equal to one-half of the maximum of Z is a more useful quantity.

These points nearly coincide with an inflection of the Z curve, and therefore they are among the most characteristic points of this function.

In both cases the magnitude of Z maximum must be taken as the unit of magnetic field intensity.

Declassified in Part - Sanitized Copy Approved for Release 2013/01/23 : CIA-RDP81-01043R001600090003-8

Declassified in Part - Sanitized Copy Approved for Release 2013/01/23 : CIA-RDP81-01043R001600090003-8

For convenience of utilization of the theoretical curves it is necessary to have an atlas of these curves plotted at 2 different scales: the depth of occurrence scale, and the scale of the distance between the inflection points of the Z curve. A complete atlas of all the curves is at present unavailable, however, for some bodies of regular shape which are encountered most frequently in practice tables compiled by T. N. Roze of Z and H values as a function of distance, in which the depth of occurrence as well as the distance between the inflection points is taken as the unit of length are available. Using these tables graphs may be plotted easily at any scale. Addendum 3 are tables of this type, which were used in plotting the graphs of Figures 153-170, and which provide an example of such an atlas.

In order to determine the shape of a rock formation a graph of the observed values of Z_m first must be plotted as a function of x and from this graph the distance x_o between points of the curve corresponding to Z values equal to one-half of the maximum value are determined. Thereafter a second graph is plotted at the same scale as the theoretical curves as a function of x/x_o, and by successive superposition of this graph upon the theoretical graphs one of the latter is selected as the closest approximation of the observation graph.

Having established such a coincidence of curves it can be assumed that the shape of the occurring rock will be the same as that of the geometrical body corresponding to the theoretical graph.

However, it must be noted that this procedure of ascertaining the shape of the occurring rock formation is possible only in those cases in which the vertical component is symmetrical in relation to the ordinate axis, or when the asymmetry is not too pronounced. Hence this

Declassified in Part - Sanitized Copy Approved for Release 2013/01/23 : CIA-RDP81-01043R001600090003-8

Declassified in Part - Sanitized Copy Approved for Release 2013/01/23 : CIA-RDP81-01043R001600090003-8

procedure is unsuitable in the case of faults or when the rock is magnetized horizontally. In such cases the unit of length must be taken as the distance between points of the H curve at which H has a value of one-half of the maximum, provided that the H curve is symmetrical in relation to the ordinate axis.

In many cases the shape of the occurring rock may be ascertained merely on the basis of the external appearance of the curves of isolines, and the Z and H graphs. Thus, if the isolines are closed curves approximating circumferences, the occurring rock must be either a sphere or a shaft with a cross sectional form of a cylinder, prism, etc. On the other hand, if the isolines form elongated ovals it is clear that the occurring rock is a body elongated in the longitudinal direction, such as a horizontal cylinder, horizontal plate, etc. Further, inferences concerning the inclination of the rock formation may be made from the appearance of the Z and H curves. With a symmetrical appearance of the Z and H curves in relation to the ordinate axis the rock formation is disposed vertical and in the case of asymmetry the rock must be inclined in relation to the horizon.

Similarly, from the absence of a minimum of the Z curve it follows that the rock extends to great depth and may be considered as a single-pole occurrence. Faults and contacts of one rock with another also are readily ascertained from the form of the Z and H graphs, since in such cases these graphs have a characteristic appearance shown by the curves of Figures 171, 178 and 179.

Specific mention should be made of the fact that all these methods are applicable when the distribution of the magnetic field over a horizontal surface is known, i.e., when the results of the magnetic survey pertain to terrain where differences in elevation are small

Declassified in Part - Sanitized Copy Approved for Release 2013/01/23 : CIA-RDP81-01043R001600090003-8

Declassified in Part - Sanitized Copy Approved for Release 2013/01/23 : CIA-RDP81-01043R001600090003-8

in comparison with the depth of occurrence of the rock. If the survey is conducted over mountain slopes and the depth of the occurring rock is approximately the differences in elevation between observation points the observation curves must be compared with theoretical graphs plotted for sloping profiles, or to reduce all the observations to a horizontal plane. Thus if the observations were made on a surface inclined at an angle δ in relation to the horizon, the reduced values Z_{red} and H_{red} are correlated with the observed values Z_{obs} and H_{obs} by the following formulas:

$$Z_{red} = Z_{obs} \cos \delta + H_{obs} \sin \alpha ,$$

$$H_{red} = Z_{obs} \sin \delta + H_{obs} \cos \alpha .$$

2. Multiple-Valued Nature of the Inverse Problem of Magnetometry.

While the main problem of magnetometry, namely determination of the potential of the magnetic field and its components in accordance with a given distribution of magnetization J or of magnetic charges within a definite volume is uniquely defined, i.e., only one definite field corresponds to a given distribution of magnetization J or of charges, the inverse problem, consisting of determination of the volume (magnitude and spatial disposition) and of the distribution of charges when the distribution of the potential or of its first derivatives over some surface is known yields a multiple-valued solution. An infinitely large number of bodies of different volume having different distributions of magnetization or charges therein may correspond to a given distribution. This theorem may be easily demonstrated in particular instances. For example, in a case in which the distribution of the magnetic field on a level area corresponds to that of a uniformly magnetized sphere, if the potential or its first derivatives are known we can determine only the distance to the center of the sphere and its magnetic moment. Yet the volume of the sphere can be

Declassified in Part - Sanitized Copy Approved for Release 2013/01/23 : CIA-RDP81-01043R001600090003-8

Declassified in Part - Sanitized Copy Approved for Release 2013/01/23 : CIA-RDP81-01043R001600090003-8

of any magnitude. This is apparent from the fact that the horizontal H component and the vertical Z component of the magnetic field intensity of a uniformly magnetized sphere are expressed by the equations:

$$H = 3MxR/(R^2 + x^2)^{5/2}, \qquad Z = M(2R^2 - x^2)/(R^2 + x^2)^{5/2},$$

where H and Z are known for different values of x.

By solving these equations we can determine only M and R, since the volume does not appear in the equation in an explicit form.

The same can be demonstrated in the case of a uniformly magnetized cylinder.

An example of the general instance is the expansion of the magnetic potential to a series by spherical functions.

Indeed, if the distribution of potential over the surface of the sphere is known, the constant coefficients of this series also are known. In Section 3 of Chapter II we saw that each term of n-th order represents the potential of a multipole of 2n-th order. Its coefficients A_n^m and B_n^m, from m = o to m = n, determine the magnetic moment of the multipole and n determines the directions of its axes. Thus, given the coefficients of the expansion, we can determine only the moments of the multipole, which represent the functions of the distribution of charges and volume of the body. But the volume of the bodies corresponding to the multipoles remains indefinite.

As a result, this interpretation of magnetic anomalies which requires the solution of the inverse problem cannot be effected in an uniquely defined manner if no additional data other than the results of magnetic measurements are available, or if no assumptions are made concerning the nature of the occurring rock. The most important information in this case is knowledge of the geological make-up

Declassified in Part - Sanitized Copy Approved for Release 2013/01/23 : CIA-RDP81-01043R001600090003-8

Declassified in Part - Sanitized Copy Approved for Release 2013/01/23 : CIA-RDP81-01043R001600090003-8

of the given area, i.e., its structure and the type of rock present. This information helps in limiting the range of shapes as well as of the dimensions of the rock which cause the given anomaly.

3. Analytical Methods of Solving the Inverse Problem.

If the shape of the occurring rock has been ascertained the mathematical problem is reduced to a determination of certain elements of occurrence, such as depth of the punctal or linear pole, depth of the center of symmetry of the occurring rock, the magnetic moment or magnetic mass of the rock, distance between the poles, angle of inclination of the magnetic axis of the rock in relation to the horizon, and others. This is obtained by solving the equations derived in Section 8 (in solving the main problem of magnetometry) and which establish the correlations between components of magnetic field intensity and the coordinates of the observed point, i.e., solving equations of the form:

$$H = f_1(R, x), \qquad Z = f_2(R, x),$$

since for each value of x we know the values of H and Z. However, the solution of these equations is difficult since in the majority of cases it becomes necessary to solve either algebraic equations of higher order (sixth, eighth, tenth) or to solve transcendental equations containing unknowns within the sign of the logarithm and tangent.

Let us consider the solution of this problem in connection with several examples (sphere, schematic magnet, pole lines, and several others).

Sphere. In the general case in which the magnetic axis of the sphere forms a certain angle with the vertical this problem consists in solving the equations of (8.28) in which the unknowns are: M -- magnetic moment of the sphere, R -- depth of occurrence of its center, and x_o --

Declassified in Part - Sanitized Copy Approved for Release 2013/01/23 : CIA-RDP81-01043R001600090003-8

Declassified in Part - Sanitized Copy Approved for Release 2013/01/23 : CIA-RDP81-01043R001600090003-8

the distance from the origin of coordinates to the point of intersection of the magnetic axis with the earth's surface. However, one of these unknowns (M) is readily eliminated on dividing the equations of (8.28) by each other.

Since for each value of x the components H are known from observation, it follows that on selecting 2 values x_1 and x_2 with their corresponding values of H and Z, and using the denotation H/Z = q, we obtain the following 2 equations, containing 2 unknowns R and x_0,

$$q_1 = \frac{3R^2x_1 + x_1^2x_0 - R^2x_0}{2R^3 + 3x_0x_1 - x_1^2}, \qquad q_2 = \frac{3R^2x_2 + 3x_2^2x_0 - R^2x_0}{2R^3 + 3x_0x_2 - x_2^2}$$

These equations are reduced to an equation of the sixth order with respect to R, the numerical solution of which is obtained by higher algebraic operations.

The solution is simplified if the magnetic axis is vertical. Indeed, from the equations of (8.30) it follows that

$$q_1 = \frac{3Rx_1}{2R^2 - x_1^2},$$

hence

$$R = 3x_1 + \sqrt{9x_1^2 + 8x_1^2q_1^2}$$

If we select a value of X_1 for which H = Z, it follows that

$$R = \frac{3+\sqrt{17}}{4}\,x_1 \sim 1.75x_1.$$

But in this case the depth of occurrence is determined still more conveniently from the correlation between depth of occurrence and the coordinate X_m corresponding to the maximum value of H, namely

$$R = 2x_m,$$

i.e., the depth of occurrence is equal to the distance on the graph between the 2 extreme values of H.

Having determined R we determine the magnetic moment of the sphere:

$$M = \frac{R^3Z_{max}}{2}.$$

Declassified in Part - Sanitized Copy Approved for Release 2013/01/23 : CIA-RDP81-01043R001600090003-8

Declassified in Part - Sanitized Copy Approved for Release 2013/01/23 : CIA-RDP81-01043R001600090003-8

To find the radius of the sphere it is necessary to know its magnetization, which may be determined if we know the type of rock of which the sphere is composed.

Schematic Magnet. In the general case in which a schematic magnet is equivalent to a thin cylinder or prism, has a finite length and is inclined at an arbitrary angle in relation to the horizon, the determination of the depth of occurrence, dimensions and angle of inclination is very complex, since it becomes necessary to deal with 3 equations of the seventh order containing 3 unknowns.

Therefore in practice this problem is solved by approximate methods, by transition from a particular to a more general instance.

Thus in an instance in which the influence of the lower pole may be disregarded the depth of occurrence of the upper pole R is obtained directly from the equation (8.33):

$$R = x\ Z/H$$

When R is known, it is easy to determine the magnetic mass m:

$$m = Z_{max}\ R^2.$$

However, the fact that this mass is known does not resolve the question concerning the dimensions of the area over which it is distributed and which is equal to the cross sectional arc S of the rock. For the given m it can have any value not greater than that at which the influence of the transverse dimensions of the rock begins to manifest itself. Thus this example also shows the multiple-valued nature of the inverse problem.

As in the case of a sphere, it is necessary to know the magnetization of the rock to find the value of S.

In the case of a vertical magnet of finite length the depth of

Declassified in Part - Sanitized Copy Approved for Release 2013/01/23 : CIA-RDP81-01043R001600090003-8

Declassified in Part - Sanitized Copy Approved for Release 2013/01/23 : CIA-RDP81-01043R001600090003-8

occurrence of the upper pole may be determined approximately by the same procedure, assuming that x is a very small quantity. To do this the equations of (8.32) are divided into each other, and denoting $R_o = x\,Z/H$, we obtain:

$$R_o = R - l\,(R^2 + x^2)^{3/2}/[(R + l)^2 + x^2]^{3/2} - (R^2 + x^2)^{3/2}. \qquad (8.63)$$

When x approaches zero the right hand portion of this equation approaches a definite limit, and therefore the left hand portion also has a limit, i.e.,:

$$R_o = R - l R^3/(R + l)^3 - R^3 = R - l/3\,l/R + 3(l/R)^2 + (l/R)^3.$$

Therefore at values of l considerably greater than R this limit is equal to the depth of occurrence of the upper pole R_o. At values of l approximating R the limit will be somewhat smaller than R. Thus at $l = R$:

$$R - R_0 = 1/7\ R.$$

At $l = 2R$ this difference amounts to 1/13 R, i.e., approximately 8%, and at $l = 0$ the difference is less than 1%.

To find this limit it is sufficient to calculate the quantity $x = Z/H$ for different values of x and to extrapolate graphically to the value for $x = 0$.

The quantity R obtained in this manner increased within a limit of 10% may be considered with an approximation sufficient for practical purposes, to be the depth of occurrence of the upper pole.

Having determined R it is not difficult also to determine l approximately by means of equation (8.63). Indeed, the quantity x, if in the denominator of the right hand portion of this equation, is disregarded in comparison with $R + l$, we have an equation of third order with respect to l, which may be solved by elementary operations. On the other hand, if x is small in comparison with $R + l$, R must be

Declassified in Part - Sanitized Copy Approved for Release 2013/01/23 : CIA-RDP81-01043R001600090003-8

Declassified in Part - Sanitized Copy Approved for Release 2013/01/23 : CIA-RDP81-01043R001600090003-8

determined for values of x not very far from the center of the anomaly, i.e., from the maximum.

In the general case of an oblique magnet the depth of occurrence of the upper pole is first determined approximately, in the same manner as in the case of a vertical magnet, and then an approximate determination is made of the length of the magnet l and of the mass m, after which, with the values of R, l, and m known, the formulas of (8.31) are used to calculate Z and H for different angles of inclination of the magnet, i.e., for the different values of the coordinate x_0, and the angle of inclination is determined by comparing the calculated graphs with the observational graphs.

Horizontal Cylinder of Infinite Length. The solution of this problem is analogous to the solution in the case of a sphere. Indeed, from the equations of item 4 of Section 8, it follows that:

$$(R^2 - x^2) \operatorname{tg} \varphi_0 + 2Rx/(R^2 - x^2) - 2Rx \operatorname{tg} \varphi_0 = H/Z. \qquad (8.64)$$

Taking various values of x for which the ratio H/Z is known we can obtain 2 equations of the third order with 2 unknowns, R and $\operatorname{tg} \varphi_0$. The combined solution of these equations results in an equation of the fourth order containing a single unknown.

However, it must be remembered that the origin of coordinates of the curves of observed H and Z is taken not on the axis of the cylinder, but at the point of maximum Z_m, since with an oblique magnetization the position of the cylinder axis is not known. The same applies to a sphere, the magnetic axis of which is inclined in relation to the horizon. Therefore, using the theoretical formulas derived in item 4 of Section 8, we introduce an error in our calculations. However, in view of the fact that the distance between the point of the maximum and the origin of coordinates of the theoretical curve is small (not more than 0.2R) at angles

Declassified in Part - Sanitized Copy Approved for Release 2013/01/23 : CIA-RDP81-01043R001600090003-8

Declassified in Part - Sanitized Copy Approved for Release 2013/01/23 : CIA-RDP81-01043R001600090003-8

of declination of the magnetic axis from the vertical not exceeding 30°, in practice this error may be disregarded, provided that the chosen distances x from the maximum Z_m are not too small.

With a vertical magnetization of the cylinder, when $\varphi_0 = 0$ equation (8.64) becomes:

$$2Rx/R^2 + x^2 = q, \qquad (8.65)$$

hence

$$R = x + x\sqrt{1 + q}$$

If x is chosen so that q = 1, it follows that

$$R = x\,(1 + \sqrt{2}) \sim 2.41\,x.$$

As in the case of a sphere, the depth of occurrence of the cylinder axis may be determined from the value of the coordinate x_m at which H has the maximum:

$$R = \sqrt{3}\,x_m.$$

In this case formula (8.65) can serve as control of the correctness of selection of the shape of the occurring rock. The ratio of maximum to minimum values of the vertical component also can serve as a similar control. As was shown under items 1 and 4 of Section 8, in the case of a cylinder this ratio is 8, and in the case of a sphere it is approximately 50.

Thin Plate of Infinite Length (Single-Pole and Two-Pole Lines). In the general instance when the plate is disposed at an angle φ with the vertical, the solution of the equations of (8.46) is extremely complex, and therefore the approximate method described in the case of a 2-pole magnet (page 374) is preferred.

Disregarding the influence of the lower pole, from equation (8.45) we obtain:

$$R = H/Z\,x$$

which is analogous to the formula for a single-pole magnet. When H = Z

Declassified in Part - Sanitized Copy Approved for Release 2013/01/23 : CIA-RDP81-01043R001600090003-8

Declassified in Part - Sanitized Copy Approved for Release 2013/01/23 : CIA-RDP81-01043R001600090003-8

it follows that R = x. It should be noted that at this point in addition to an equality of H and Z, the horizontal component has a maximum, which is a criterion of the proper selection of the shape of a single-pole line.

Further transition from a single-pole to a 2-pole line is the same as in the case of a 2-pole magnet.

Solution of the inverse problem in the form described above is possible only if the curves of observed H and Z differ only slightly from the shape of one of the theoretical graphs (Section 8).

In many cases the dependence of H and Z upon the coordinates of the points of observation is found to be so complex that comparison of the observation curves with the theoretical curves is impossible. Therefore attempts have been made to solve the inverse problem in the most general form without resorting to a search for some definite shape of the occurring rock. These attempts include the work of K. B. Veynberg, A. P. Kazanskiy, B. A. Andreyev, and D. S. Mikov. It should be mentioned that they all relate to the solution of the plane inverse problem, i.e., the determination of the shape and depth of occurrence of the cross section of a cylinder of infinite length.

On the basis of the fact that the intensity of the magnetic field must satisfy the equations div H = 0 and rot H = 0, K. B. Veynberg [78] has proposed that from the given distribution of vector H over the earth's surface, its value at a number of parallel surfaces below the given surface be determined, after which, the direction of vector H at each point of such a surface may be plotted. From the convergence of these vectors an opinion can be formed concerning the depth of occurrence and the approximate shape of the body.

In the case of a plane problem the equations assume the form:

Declassified in Part - Sanitized Copy Approved for Release 2013/01/23 : CIA-RDP81-01043R001600090003-8

Declassified in Part - Sanitized Copy Approved for Release 2013/01/23 : CIA-RDP81-01043R001600090003-8

$$\frac{\partial H}{\partial x} + \frac{\partial Z}{\partial z} = 0, \quad \frac{\partial H}{\partial z} - \frac{\partial Z}{\partial x} = 0.$$

Since H and Z are known at every point of the earth's surface, their derivatives $\partial H/\partial x$ and $\partial Z/\partial x$ also are known.

Therefore it is possible to find the increases ΔZ and ΔH of H and Z at a distance Δz from the earth's surface:

$$\Delta Z = -\frac{\partial H}{\partial x}\Delta z \text{ and } \Delta H = \frac{\partial Z}{\partial x}\Delta z,$$

and therefore the values Z_1 and H_1 at these surfaces will be:

$$Z_1 = Z + \Delta Z \text{ and } H_1 = H + \Delta H.$$

At the next surface, it is evident that

$$\Delta Z_1 = -\frac{\partial H_1}{\partial x}\Delta z \text{ and } \Delta H_1 = \frac{\partial Z_1}{\partial x}\Delta z.$$

and so forth, until the increases are equal to zero.

In the case of anomalies caused by horizontal rock formations in the shape of long cylinders or prisms with any cross sectional shape the inverse problem may be solved by the method of A. P. Kazanskiy [79] which enables determination of the depth of occurrence of the center of gravity of the plane figure of the cylinder section and the magnetic moment per unit of length of the occurring rock.

The method is based on integrating the expression of the horizontal component twice and the expression of the vertical component along the x axis 3 times.

Using the expressions of (8.58) for dH and dZ, r is substituted in accordance with the formula r = R sec θ (Figure 180) and we integrate section S over the entire area of the cylinder:

$$H = 2\int_S \frac{\sin 2\theta \cos^2\theta}{R^2}\,dM, \quad Z = 2\int_S \frac{\cos 2\theta \cos^2\theta}{R^2}\,dM,$$

where dM is the magnetic moment corresponding to the elemental area dS at point Q and equal to J dS and the direction of magnetization J is assumed to be parallel to the z axis.

Declassified in Part - Sanitized Copy Approved for Release 2013/01/23 : CIA-RDP81-01043R001600090003-8

Declassified in Part - Sanitized Copy Approved for Release 2013/01/23 : CIA-RDP81-01043R001600090003-8

Next we multiply both sides of these expressions by dx and integrate the first integral from x = x to x = ∞ , and the second from -x to +x, replacing the variable x by θ in accordance with the formula x = R tg θ:

$$\int_{x}^{\infty} H\,dx = 2\int_{\theta}^{\pi/2}\int_{S} \frac{\sin 2\theta}{R}\,d\theta\,dM,$$

$$\int_{-x}^{+x} Z\,dx = 2\int_{-\theta'}^{\theta}\int_{S} \frac{\sin 2\theta}{R}\,d\theta\,dM,$$

where θ' is the angle corresponding to the coordinate -x.

Since on integration with respect to x R remains constant, it follows that on denoting the first of these intervals by U and the second by Φ, and changing the order of integration, we obtain

$$U = \int_{x}^{\infty} H\,dx = 2\int_{S} \frac{\cos^2\theta}{R}\,dM \qquad (8.66)$$

$$\Phi = \int_{-x}^{+x} Z\,dx = 2\int_{S}\left(\frac{\sin 2\theta}{R} + \frac{\sin 2\theta'}{R}\right)dM \qquad (8.67)$$

However, it is not difficult to see that U is nothing else but the magnetic potential at the earth's surface at a point having the coordinate x, while Φ is the magnetic flux passing through an area the earth's surface limited by a rectangle of length 2x and a width equal to unity.

Placing the origin of coordinates at point 0 (Figure 180) and denoting the coordinates of point P by x, o, the coordinates of point Q by ξ , R and the distance PQ = r, then replacing the polar coordinates in equation (8.67) by rectangular coordinates we have:

$$\Phi = 4\int_{S}\left(\frac{x-\xi}{(x-\xi)^2+R^2} + \frac{x+\xi}{(x+\xi)^2+R^2}\right)dM$$

This equation shows that Φ is a function of x, and at high values of x it approaches zero.

Further, on multiplying both integrals (8.66) and (8.67) by dx, integrating the first from $-\infty$ to $+\infty$, and the second from zero to x, and expressing dx by dθ and dθ', we have:

Declassified in Part - Sanitized Copy Approved for Release 2013/01/23 : CIA-RDP81-01043R001600090003-8

Declassified in Part - Sanitized Copy Approved for Release 2013/01/23 : CIA-RDP81-01043R001600090003-8

$$\int_{-\infty}^{+\infty} U\,dx = 2\int_S dM \int_{-\pi/2}^{+\pi/2} d\theta = 2\pi M, \quad \int_0^{\pi} \Phi\,dx = 2\int_S dM \tag{8.68}$$

$$\left[\int_{\theta_0}^{\theta} tg\,\theta\,d\theta + \int_{-\theta_0}^{\theta'} tg\,\theta'\,d\theta'\right] = -2\int_S \left(\ln\frac{1}{\cos^2\theta} + \ln\frac{1}{\cos^2\theta'} - 2\ln\frac{1}{\cos^2\theta_0}\right) dM, \tag{8.69}$$

where θ_0 is the value of angle θ, and $-\theta_0$ is the value of angle θ', with $x = 0$ (Figure 180).

It is seen that the equation (8.68) enables determination of one of the parameters of occurrence, namely the magnetic moment per unit length of the occurring cylinder, provided the distribution of the potential or its first derivative (H) along the perpendicular to the cylinder axis is known.

Equation (8.69) is used to find the second parameter, the depth of occurrence of the rock, which requires a second integration along the x-axis.

However, a direct integration with infinitely large values of x leads to infinitely large numbers since the function $\int_0^x \Phi dx$ at $x = \infty$ is converted to infinity. Therefore in order to avoid infinitely large numbers equation (8.69) must be transformed by replacing the function Φ with another function:

$$\Phi_1 = \Phi - \frac{2\sin\theta_1}{R_1} M = \Phi - \frac{4Mz}{x^2+z^2}, \tag{8.70}$$

where R_1 and θ_1 are the coordinates of point P in relation to the new origin of coordinates O_1 (Figure 180). In such a case

$$\int_0^x \Phi_1\,dx = \int_0^x \Phi\,dx - 2M\int_0^x \frac{\sin\theta_1}{R_1}\,dx,$$

since at $x = 0$ the angle $\theta = 0$. Having performed the integration and denoting the left hand portion of this expression by ψ we get:

$$\psi = -2\int_S \left(\ln\frac{\cos^2\theta_1}{\cos^2\theta\cos^2\theta'} - 2\ln\frac{1}{\cos^2\theta_0}\right) dM.$$

Since $\cos\theta_1 = R_1/r_1$, $\cos\theta = R/r$ and $\cos\theta' = R/r'$, where $r_1 = O_1P$ and $r' = QP'$, it follows that

$$\psi = -2\int_S \left(\ln\frac{R^4}{R^4}\cdot\frac{r^2r'^2}{r_1^4} - 2\ln\frac{1}{\cos^2\theta_0}\right) dM \tag{8.71}$$

Declassified in Part - Sanitized Copy Approved for Release 2013/01/23 : CIA-RDP81-01043R001600090003-8

Declassified in Part - Sanitized Copy Approved for Release 2013/01/23 : CIA-RDP81-01043R001600090003-8

From this equation it is apparent that at x = ∞ the function ψ tends to a limit ψ_∞, which is

$$\psi_\infty = 2\int_S \ln\frac{R^4}{R_1^4\cos^2\theta_0}\,dM \qquad (8.72)$$

Let us take the difference $\psi_\infty - \psi$ and integrate with respect to x from 0 to ∞, in which case

$$\int_0^\infty (\psi_\infty - \psi)\,dx = 2\int_S dM \int_0^\infty \ln\frac{r^4}{r^2 r'^2}\,dx.$$

On integrating by parts we obtain:

$$\int_0^\infty (\psi_\infty - \psi)\,dx = 2\int_S x\ln\frac{r^4}{r^2 r'^2}\,dM\Big|_0^\infty + 2\int_S dM \int_0^\infty x\left(\frac{x-\xi}{r^2} + \frac{x+\xi}{r'^2} - 2\frac{x}{r_1^2}\right)dx.$$

Upon substitution of the limits the first term of this expression becomes zero. To determine the second we substitute in accordance with the formulas: $x = r_1\sin\theta_1$, $x - \xi = r\sin\theta$, $x + \xi = r'\sin\theta'$, $R_1 = r_1\cos\theta_1$, $R = r\cos\theta$, $R' = r'\cos\theta'$, then, on denoting the left hand portion of the preceding expression by Q, we have:

$$Q = 2\int_S dM \int_0^\infty x\left(\frac{\sin\theta\cos\theta}{R} + \frac{\sin\theta'\cos\theta'}{R} - 2\frac{\sin\theta_1\cos\theta_1}{R_1}\right)dM$$

Further, on replacing the variable x in the first term of this expression by the formula x = R tg θ + ξ, in the second by the formula x = R tg θ' − ξ, and in the third by the formula $x = R_1$ tg θ_1, we have:

$$Q = 2\int_S dM \int_0^\infty \left[\sin^2\theta + \sec^2\theta' - 2\sec^2\theta_1 + \frac{\xi}{R}(\sin\theta\cos\theta - \sin\theta'\cos\theta')\right]dx,$$

or, expressing the sines in terms of cosines:

$$Q = 2\int_S dM \int_0^\infty \left[\cos^2\theta_1 + \cos^2\theta_1 + \frac{\xi}{R}(\sin\theta\cos\theta - \cos\theta'\sin\theta')\right]dx$$

Since $dx = R_1\sec^2\theta_1 d\theta_1 = R\sec^2\theta d\theta = R\sec^2\theta' d\theta'$, upon integration we obtain: $Q = 2\int_S dM[\pi R - \pi R_1] = 2\pi\int_S R\,dM - 2\pi R_1 M.$

The expression $\int RdM/M$ represents the coordinate z of the center of gravity of our area S, i.e., the depth of occurrence, and denoting it by R_c, we have:

$$R_c = \frac{Q}{2\pi M} - R_1. \qquad (8,73)$$

Declassified in Part - Sanitized Copy Approved for Release 2013/01/23 : CIA-RDP81-01043R001600090003-8

Declassified in Part - Sanitized Copy Approved for Release 2013/01/23 : CIA-RDP81-01043R001600090003-8

It follows that determination of the quantities U, Φ, M, Ψ and Q, expressed as definite integrals, must be replaced by determination of the areas between the x-axis and the corresponding curves since in practice the correlation between H and Z and the distance x is given in the form of curves.

Thus in accordance with formulas (8.66) and (8.68) in order to find M the areas limited by the abscissa axis, the H curve and the ordinates of various values of x from x = 0 to x = ∞ are determined with the aid of a planimeter or by simple summation of the ordinates of the H curve at equal intervals Δ X, which yields a number of values of U for the different values of X. Having plotted in accordance with these data of the curve showing the correlation between U and x, it is necessary, also, to determine the entire area limited by this curve and the abscissa axis and dividing this area by 2π we obtain the quantity M.

To determine R_c in accordance with equation (8.67) the areas corresponding to different values of x which are limited by the Z curve and the abscissa axis first are found according to the above method, and the curve of Φ is plotted as a function of x. In accordance with equation (8.70) subtracting from this curve the curve defined by the equation

$$\Phi' = 4Mx/x^2 + R_1^2, \qquad (8.74)$$

and plotting the new curve representing the correlation between $\Phi_1 = \Phi - \Phi'$ and x, it is necessary to find the areas limited by this curve, the abscissa axis and the values of ordinates corresponding to different values of x, which will yield a number of values for the function Φ_1. Finally, having plotted the third curve of Ψ as a function of x and determined the entire area limited by this curve, we obtain the quantity R_c from equation (8.73).

It is best to select a value of R_1 at which the function Φ_1 reaches

Declassified in Part - Sanitized Copy Approved for Release 2013/01/23 : CIA-RDP81-01043R001600090003-8

Declassified in Part - Sanitized Copy Approved for Release 2013/01/23 : CIA-RDP81-01043R001600090003-8

zero more rapidly, since on this condition the integral in equation (8.71) will approach a limit. From equation (8.74) it follows that function Φ' reaches a maximum at $x = R_1$. Therefore, taking R_1 as the abscissa of a point of curve Φ, somewhat greater than the abscissa corresponding to the maximum of Φ', we get a function Φ' which rapidly brings the difference $\Phi-\Phi'$ to zero.

As an example let us calculate the magnetic moment and depth of occurrence of a circular cylinder, the distribution of Z and H of which is defined by the formulas appearing on page 346, and is represented graphically in Figure 181a for the case in which the magnetic moment of the unit of length $M = 1/2$ and the depth of occurrence $R = 2$.

Figure 181b shows a curve of the correlation between U and x wherein each ordinate of this curve corresponding to the abscissa x represents the area between curve H of Figure 181a and the segment of the abscissa from $x = -\infty$ to $x = x$. Thus, for example, the ordinate corresponding to $x = -1$, is equal to the shaded portion of area S_1 of Figure 180a.

Having determined the shaded area between curve U and the abscissa axis we obtain the quantity $2\pi M$. Numerically, this area is approximately 3, and therefore the magnetic moment per unit length $M = 1/2$.

The correlation between functions Φ and x is shown in Figure 181c, where each ordinate corresponding to the abscissa x is equal to the area between curve Z (Figure 181a) and the segment of the abscissa axis from x to -x. Thus the ordinate at $x = 0.5$ represents the shaded portion of area S_2, shown in Figure 181a.

Declassified in Part - Sanitized Copy Approved for Release 2013/01/23 : CIA-RDP81-01043R001600090003-8

Declassified in Part - Sanitized Copy Approved for Release 2013/01/23 : CIA-RDP81-01043R001600090003-8

In the drawing the ordinates of curve Θ_1, represent the difference between the ordinates of curve Θ and the function Θ' (8.70) in which R_1 is taken as 2.

Next, the Ψ curve (Figure 181d) is plotted, the ordinates of which are the areas between the Θ_1 curve and the corresponding x abscissa. This curve, as is shown by the drawing, tends asymptotically to a certain value Ψ_ω which is defined by formula (8.72) and is indicated in the drawing by a dotted line. The area Q between this asymptote and the Ψ curve, which is equal to approximately 9, gives us the magnitude of R_c, which according to formula (8.73) is 2.

The Method of Cards. One of the procedures for solving the inverse problem in the geophysics of prospecting, especially in gravimetry and electrometry, is the method of cards. In magnetometry, however, this procedure has not been utilized extensively, although in principle it has the same potentialities in this, as in the other branches of geophysics.

To show the nature of this procedure let us consider the card of D. S. Mikov [80], the theory behind the preparation of which is as follows.

Since a uniformly magnetized body constitutes a combination of elemental magnets (dipoles) having magnetic moments of equal magnitude and same direction, the observed magnetic field may be considered as consisting of the sum of the magnetic fields produced by such dipoles. Therefore, by substracting the fields of the dipoles from the observed magnetic fields until the observed field is compensated, we determine the disposition of the dipoles which comprise the given magnetized body. Although this principle is applicable to a body of any shape, in practice

Declassified in Part - Sanitized Copy Approved for Release 2013/01/23 : CIA-RDP81-01043R001600090003-8

Declassified in Part - Sanitized Copy Approved for Release 2013/01/23 : CIA-RDP81-01043R001600090003-8

it may be utilized only in the case of plane bodies, i.e., bodies in which the longitudinal dimensions are large in comparison with the transverse dimensions, since the disposition of dipoles at different distances from the boundary of a surface is most readily effected on a plane. Therefore the card of D. S. Mikov relates to the determination of the depth of occurrence and shape of infinitely long horizontal bodies.

The card (Figure 182) consists of a drawing on transparent paper, of isolines of vertical and horizontal components of the intensity of the magnetic field of a linear dipole defined by the formulas of (8.58).

This card is prepared as follows: the values of H and Z for the different values of r and θ are calculated according to the formulas of (8.58) and these values are plotted on transparent paper, a definite scale being used for the distances r. In calculating H and Z the magnitude of the magnetic moment of the dipole remains arbitrary, and was taken by D. S. Mikov as $dM = 100$ CGS/A.

Since the linear dipole may be replaced by a circular cylinder or a small quadrangular prism 1 cm^2 in cross sectional are it is evident that $dM = J$, i.e., the magnetization of the rock.

On the card the isolines which run upward from the AB axis relate to the vertical component Z, and those to the right of the CD axis relate to the horizontal component H.

The procedure for utilizing the card in the case of vertically magnetized bodies is as follows. On a sheet of mm graph paper a straight line is drawn corresponding to the profile which is perpendicular to the trend of a given anomaly, and the numerical values of

Declassified in Part - Sanitized Copy Approved for Release 2013/01/23 : CIA-RDP81-01043R001600090003-8

Declassified in Part - Sanitized Copy Approved for Release 2013/01/23 : CIA-RDP81-01043R001600090003-8

vertical and horizontal components are marked on this profile. In this the scale of distances along the profile must be the same as that of the card.

Next the card is placed on the mm graph paper in such a manner that its AB axis is parallel to the profile and its center is brought to coincide, successively, with the centers of the cm squares located below the profile, and at the points of observational determinations notations are made of the values of Z found on the card, which then are substracted from the observed values. This superposition is repeated until the anomalies are fully eliminated, whereupon the total area of the squares gives the position, depth of occurrence and shape of cross section of the body causing the given anomaly.

However, in order to use such a card it is necessary to know the magnetization of the rock and the observed values of Z and H must be reduced to a magnetization of 100 CGS M, which is the scale of the card. To do this it is necessary to multiply all the values of Z and H by a constant factor -- $p = 100/J$. This is one of the defects of the method of cards since the magnetization of the rock is not known and it must be tentatively assumed.

The second defect resulting from the multiple-valued nature of the inverse problem is the arbitrary alignment of the center of the card with the centers of the cm-squares. It is possible to compensate the anomalous values of Z and H by placing the center at a small body of squares at a shallow depth, but overall compensation is effected by equating the center of the card to a large number of squares located at great depth.

Therefore in the application of this method it becomes necessary to rely upon data of other investigations, especially of geological

Declassified in Part - Sanitized Copy Approved for Release 2013/01/23 : CIA-RDP81-01043R001600090003-8

Declassified in Part - Sanitized Copy Approved for Release 2013/01/23 : CIA-RDP81-01043R001600090003-8

studies, in addition to magnetic data in order to know the approximate possible depth of occurrence and magnetization of the rocks.

For calculations with respect to the horizontal component the card must be turned 45°, i.e., its CD axis must be set parallel to the profile.

If the axis of magnetization of the rock forms an angle i with the vertical the card must be rotated through an angle θ, which is determined on the basis of the correlation

$$\text{tg } i = \text{tg } 2\theta \quad \text{or} \quad \theta = i/2.$$

The Method of B. A. Andreyev. In Section 2 of the present chapter it was shown that the intensity of the magnetic field Z over a plane surface is determined by the equation $Z = 2\pi J_n$, where J_n is the normal component of magnetization.

This equation shows that Z and J_n are equivalent to each other and their magnitude differs only by the factor 2π.

Thus we are justified in considering any surface which is intersected by a magnetic flux as a surface covered by fictitious magnetic charges having a surface magnetic density of $1/2\pi$ Z.

In such a case the magnetic potential of the field U_p at an external point P (Figure 183) is defined on the basis of Coulomb's law as:

$$U_p = 1/2\pi \int \bar{Z}\, dS/r,$$

where r is the distance of point P from the surface element dS at point M, and the integration is carried out over the entire infinite plane. The line over Z indicates that the value of Z is taken at the plane.

If a derivative is taken of the normal component on both sides of this equality, we have:

$$\frac{\partial U_p}{\partial n} = Z = -\frac{1}{2\pi} \int \frac{\bar{Z}}{r^2} \cdot \frac{dr}{dn}\, dS.$$

Declassified in Part - Sanitized Copy Approved for Release 2013/01/23 : CIA-RDP81-01043R001600090003-8

Declassified in Part - Sanitized Copy Approved for Release 2013/01/23 : CIA-RDP81-01043R001600090003-8

Since $r^2 = R^2 + x^2 + y^2$, where R is the distance from point P to the plane, x the distance P_0M and y the coordinate of point P on the y axis, it follows that

$$dr/dn = -dr/dR = -R/r$$

since n and R have opposite directions, and consequently,

$$Z = R/2\pi \int \overline{Z}\, dS/r^3. \qquad (8.75)$$

In the plane problem, when the magnetic field remains constant in one direction, for example in the direction of the y axis, expression (8.75) becomes:

$$Z = R/2\pi \int_{-\infty}^{+\infty} \overline{Z}\, dx \int_{-\infty}^{+\infty} dy/(R^2 + x^2 + y^2)^{3/2}$$

Upon integration, we obtain:

$$Z = R/\pi \int_{-\infty}^{+\infty} Z\, dx/R^2 + x^2. \qquad (8.76)$$

Thus if the distribution of the normal component of intensity along the profile or crosswise to the trend of the anomaly is known the component in the same direction may be determined at any point over the profile where there are no sources of a magnetic field.

Since

$$\int_{-\infty}^{+\infty} dx/R^2 + x^2 = \pi/R,$$

it follows that on substracting a constant quantity from both portions of equality (8.76), for example the value $\overline{Z}_0$ at point P_0, which is the projection of point P upon the plane (Figure 183) we obtain:

$$Z - \overline{Z}_0 = R/\pi \int_{-\infty}^{+\infty} (\overline{Z} - Z_0)dx/R^2 + x^2. \qquad (8.77)$$

This formula is more convenient in practical use than formula (8.76) since it does not require knowledge of the absolute values of the vertical component along the profile. It is sufficient to know only the difference in vertical components between any point and the point P_0 having the coordinate x, the same as for point P at which the value of Z is to be determined.

Declassified in Part - Sanitized Copy Approved for Release 2013/01/23 : CIA-RDP81-01043R001600090003-8

Declassified in Part - Sanitized Copy Approved for Release 2013/01/23 : CIA-RDP81-01043R001600090003-8

Formula (8.77) may be modified by replacing the difference $\bar{Z} - \bar{Z}_0 = \delta Z$ by a sum of 2 differences:

$$\delta \bar{Z} = [\bar{Z}(x) - \bar{Z}_0] + [\bar{Z}(-x) - \bar{Z}_0] = \bar{Z}(x) - \bar{Z}(-x) - 2\bar{Z}_0,$$

where $\bar{Z}(x)$ and $\bar{Z}(-x)$ are the values of $\bar{Z}$ at equal distances x on either side of point P_0. In such a case the formula (8.77) becomes

$$Z - \bar{Z}_0 = \frac{R}{\pi} \int_0 \frac{\delta \bar{Z}}{R^2 + x^2} dx. \qquad (8.78)$$

The integral (8.78) may be calculated approximately by the method of trapeziums, for which it is more convenient to divide the profile AB (Figure 183) into 2n equal parts and to determine the quantity $\bar{Z}_k$ at each point of k-th in which case formula (8.78) becomes

$$\bar{Z} - \bar{Z}_0 = \frac{R \Delta x}{\pi} \left[\sum_{k=1}^{n-1} \frac{\delta \bar{Z}_k}{R^2 + x_k^2} + \frac{1}{2} \frac{\delta \bar{Z}_n}{R^2 + x_n^2} \right], \qquad (8.79)$$

where $\delta \bar{Z}_k = \bar{Z}_k(-x) - 2\bar{Z}_0$.

The expressions (8.78) and (8.79) may be utilized to determine the depth of occurrence of rocks having a great length along the y axis. This possibility was first demonstrated by B. A. Andreyev [81]. The method of B. A. Andreyev is based on equation (8.79) and consists of solving this equation by the method of successive approximations, considering Z and R as known quantities.

The usefulness of the method of successive approximations is due to the fact that equation (8.79) holds true when point P, at which the quantity Z is to be determined, is located over the profile AB.

To determine Z at points below this profile, for example on profile CD (Figure 183), it is necessary to know the distribution of Z on an even lower level. Therefore, let us assume that the distribution along the CD profile is known, and let us seek to determine the value of Z at point P_0, which is external in relation to the profile CD. In such a case, denoting the magnitude of the vertical component at point P_0 by Z, and at point P_1 by $\bar{Z}_0$, we have the same expression (8.79)

Declassified in Part - Sanitized Copy Approved for Release 2013/01/23 : CIA-RDP81-01043R001600090003-8

Declassified in Part - Sanitized Copy Approved for Release 2013/01/23 : CIA-RDP81-01043R001600090003-8

for the determination of Z, but the unknown in this equation must be considered to be $\bar{z}_0$. Therefore, changing the sign in equation (8.79) and denoting $\bar{z}_0 - z$ by Δ^1_1, we obtain:

$$\Delta^1_1 = -\frac{R\Delta x}{\pi}\left[\sum_{k=1}^{n-1}\frac{\delta \bar{z}_k}{R^2 + x^2_k} + 1/2 \quad \frac{\delta \bar{z}_n}{R^2 + x^2_n}\right] \qquad (8.80)$$

The method of successive approximations consists in taking the values of $\delta \bar{z}_k$ in expression (8.80) as being roughly equal to the values of Z at the corresponding points on the profile AB. Having thus calculated the values Δ^1_m for the different points of profile CD, we obtain a series of values $\Delta^1_1, \Delta^1_2, \ldots, \Delta^1_n$, which represent the value of the difference δz_k on the profile CD, i.e., $\Delta^1_1 = \delta \bar{z}_1$, $\Delta^1_2 = \delta \bar{z}_2$ ... substituting the latter in equation (8.80) we obtain a closer approximation Δ^2_1, i.e.,

$$\Delta^2_1 = -\frac{R\Delta x}{\pi}\left[\sum \frac{'k}{R^2 + x^2_k} + \frac{1}{2} \quad \frac{\Delta^1_n}{R^2 + x^2_n}\right].$$

The values $\Delta^2_1, \Delta^2_2, \ldots, \Delta^2_n$ serve in arriving at a third approximation, and so forth, until the series

$$\Delta^1_l, \quad \Delta^2_l, \quad \Delta^3_l, \ldots\ldots, \quad \Delta^n_l \qquad (8.81)$$

where $l = 1, 2 \ldots$, reaches a definite limit indicating the absence of magnetic charges at depth R, and consequently indicating the presence of an occurring rock. By gradually increasing the depth R and performing the above calculations for each value of R, it is possible to find a value at which the series (8.81) is divergent, which constitutes proof of the presence of magnetic charges at this depth, and consequently also, the presence of an occurring rock formation.

Thus if for a depth R_1 the series (8.81) is found to be convergent, and for the next depth R_2 it is found to be divergent, the occurring rock is found at a depth greater than R_1 but less than R_2.

This procedure for determining the depth of occurrence, the same

Declassified in Part - Sanitized Copy Approved for Release 2013/01/23 : CIA-RDP81-01043R001600090003-8

Declassified in Part - Sanitized Copy Approved for Release 2013/01/23 : CIA-RDP81-01043R001600090003-8

as the procedure of Kazanskiy, necessitates extensive calculations without yielding the same degree of accuracy attainable by using the formulas for bodies of regular geometrical shape. Errors in determination of depth by the method of Kazanskiy and the method of Andreyev, can attain considerable magnitude, and therefore these methods must be regarded as being of an orientative nature and are to be utilized in thos instances when the shape of the occurring rock cannot be identified with any of the simple geometric bodies.

Section 11. Procedures of Interpreting Magnetic Anomalies

The interpretation of magnetic anomalies consists of determination of the causes which bring about any given anomaly. Since anomalies are caused by rocks having enhanced magnetic properties, the problem is reduced to identification of the composition of these rocks and determination of their dimensions and depth of occurrence. Thus the interpretation of anomalies involves not only solution of the inverse problem of magnetometry but also determination of the rocks which cause the anomaly.

While the first part of this general problem is geophysical the second part is purely geological. Therefore, for interpretation of magnetic anomalies it is necessary to know not only the results of geophysical investigations, but also the geology of the given area.

In the absence of geological data the interpretation always will be purely physical and limited to determination of the depth of occurrence of the disturbance-inducing rocks and of their dimensions, without yielding any information as to their composition. Thus, in the investigation of the Kursk magnetic anomalies, until drilling operations revealed the geological structure of the anomalous area only various assumptions could be made concerning the composition of the rocks which cause the anomalies. A borehole was sufficient to change the interpretation

Declassified in Part - Sanitized Copy Approved for Release 2013/01/23 : CIA-RDP81-01043R001600090003-8

Declassified in Part - Sanitized Copy Approved for Release 2013/01/23 : CIA-RDP81-01043R001600090003-8

of all the anomalies from theoretical , a physical, and also a geological nature, revealing the actual causes of their occurrence.

At the present time a tremendous amount of experimental material relating to investigation of magnetic anomalies over various structures and useful mineral deposits has been amassed which permits identification of some characteristic features of each of them. The knowledge of these data and their comparison with the geological characteristics of the area are indispensable to any person undertaking practical prospecting operations. However, a discussion of these questions is beyond the scope of the present text, which is of a purely physical nature. Therefore, in the subsequent discussion of examples of interpretation attention is focused on the physical aspects of the phenomena, i.e., elucidation of the physical causes which bring about a given anomaly.

As the first example of interpretation we will consider one of the sections of the Kursk magnetic anomalies situated south of the village of Saltykovka. The nature of the anomaly in this area is shown in Figure 184a in the form of the anomalies of the vertical component Z and horizontal component H, and is taken from the atlas of the Kursk magnetic anomalies. Figure 185a also contains a graph (solid line curves A and B) of theresults of measurement of Z and H along the profile AB (Figures 184a and b) perpendicular to the isolines of the vertical component.

It is seen that the H and Z isolines form almost rectilinear shapes, which indicates large longitudinal dimensions of the occurring rock. At the same time, the longitudinal dimensions of the Z isodyne corresponding to one-half of the maximum value 1.4 Oe, are more than 12 times greater than the transverse dimensions. Therefore, on the

Declassified in Part - Sanitized Copy Approved for Release 2013/01/23 : CIA-RDP81-01043R001600090003-8

Declassified in Part - Sanitized Copy Approved for Release 2013/01/23 : CIA-RDP81-01043R001600090003-8

basis of the conclusions found in Section 9 of the present chapter, we may consider the occurring rock as being of infinite length and the formulas for infinitely long bodies may be applied in the solution of the inverse problem.

Further, upon comparison of the Z and H graphs of Figure 185a with the theoretical curves it is noted that they correspond to the curves of a linear pole or a thin plate extending deep inside the earth. This is indicated first of all by the absence of negative values of Z, and secondly by the ratio of Z_m to H_m. In the case of a linear pole, as was shown under item 6 of Section 8, this ratio is $Z_m/H_m = 2$. Approximately the same ratio is obtained on the basis of the observational data represented by the curves of Figures 184a and b.

Therefore, assuming that the magnetic anomaly of this sector is caused by a linear pole, the depth of occurrence of the pole is immediately determined as approximately equal to the depth of occurrence of the upper boundary of the rock. In the given instance this determination is very clearly derived by plotting the lines of force (Figure 185a).

From the equation (8.45) it follows that $R/x = Z/H = \text{tg } J$. i.e., the ratio of depth of occurrence to the distance along the profile is equal to the tangent of the angle of inclination. Consequently the direction of the diagonal of the quadrangle with sides Z and H will coincide at some point with the direction of the line of force. Since in the case of a single pole the lines of force are straight lines, upon extending a series of values plotted at different points on their intersection, we obtain the position of the magnetic pole, the distance of which from the surface will be on the same scale as the distance x.

Declassified in Part - Sanitized Copy Approved for Release 2013/01/23 : CIA-RDP81-01043R001600090003-8

Declassified in Part - Sanitized Copy Approved for Release 2013/01/23 : CIA-RDP81-01043R001600090003-8

From Figure 185a it is apparent that the lines of force of the right hand side and from the more remote points of the left hand side of the drawing converge almost to a single point at a distance of 260 m from the surface. On the other hand, the lines of force from the middle of the left side intersect at greater depth. Assuming the depth of occurrence of the pole is 260 m, it is possible to find the linear density of magnetic masses and to plot the theoretical Z and H curves in accordance with the formulas of (8.45). The curves thus plotted are shown in Figure 185a as the dotted lines C and D, which show that the right hand branches of the observation curves are in good agreement with the theoretical curves, while the left branches show large deviations. The cause of these deviations must be sought in the presence of secondary sources of the magnetic field occurring to the left of the Z maximum. To find them (these secondary sources) the additive property of magnetic fields may be utilized by finding the difference between the observed, and theoretical curves of Z and H. These differences are represented by the dotted lines E and F in Figure 185a. The shape of these curves fully corresponds to the curves of a linear pole and therefore the depth of the second linear pole may be found by same method of graphical representation of the lines of force. This graphic representation, shown in Figure 185a, indicates the depth of occurrence of this pole as 220 m, and its distance along the x axis from the first pole as 310 m.

For comparison of theoretical curves corresponding to 2 linear poles located at a depth of $R_1 = 260$ m and $R_2 = 220$ m and separated by a distance $x = 310$ m, the linear magnetic densities σ_1 and σ_2 for the first and second pole are determined by the equations

$$Z_m = 2\sigma_1/R_1 + 2\sigma_2 R_2/R_2^2 + x_o^2 \quad , \quad Z'_m = 2\sigma_2/R_2 + 2\sigma_1 R_1/R_1^2 + x_o^2$$

Declassified in Part - Sanitized Copy Approved for Release 2013/01/23 : CIA-RDP81-01043R001600090003-8

Declassified in Part - Sanitized Copy Approved for Release 2013/01/23 : CIA-RDP81-01043R001600090003-8

where Z_m is the observed maximum value of the vertical component corresponding to pole O_1, and Z'_m is the maximum value corresponding to pole O_2. The calculated graphs of Z and H corresponding to these values of σ_1 and σ_2 are indicated by dotted lines in Figure 185b. The summative curves of H and Z, i.e., curves in which the ordinates represent the sum of the ordinates of the dotted line curves, are shown in the same drawing by broken lines, and the component observational curves are shown as solid lines.

It is clearly apparent that in this case the theoretical curves approximate the observation curves much more closely than in Figure 185a, especially over their extreme portions. In the central part the apparent slight deviations of H as well as Z may be attributed to errors in observations and calculations.

Thus the given sector of the Kursk anomalies may be attributed to the presence of 2 narrow vertical strata, the upper edges of which are at a depth of 260 and 220 m, and have different degrees of magnetization making their lower edges considerably deeper. The width of these strata cannot be determined from magnetic observations. The question of their mineralogical composition must be resolved on the basis of geological data. Before it became known that large formations of intrusion rocks are present in the area of the Kursk anomalies the only possible interpretation was that the Kursk anomalies are caused by narrow strata of rocks having high magnetic susceptibility and occurring at a definite depth. Such an interpretation was provided by Kh. E. Leyst. At the present time it has been ascertained as a result of drilling that similar strata in other areas of the anomalies are composed of iron-ore quartzites, hence it may be assumed that iron-ore quartzites occur also in the area covered by the above interpretation.

Declassified in Part - Sanitized Copy Approved for Release 2013/01/23 : CIA-RDP81-01043R001600090003-8

Declassified in Part - Sanitized Copy Approved for Release 2013/01/23 : CIA-RDP81-01043R001600090003-8

Drilling operations carried out within this area of the Kursk anomalies have shown that iron-ore quartzites actually occur in a series of parallel narrow strata over a distance of several hundred meters.

The example of interpretation of the Kursk anomalies is one of the simplest and at the same time one of the most convincing as concerns the possibility of utilizing the magnetometric method in prospecting for valuable minerals. However, most magnetic anomalies have a more complex structure of magnetic field and their interpretation necessitates more involved calculations. Nevertheless, the general principle upon which these calculations are based is the same, namely: the magnetic field of any anomaly must be compared with the field of a uniformly magnetized body, the intensity of the magnetic field of which can be computed either theoretically or by means of cards, graphs, etc.

Let us consider still another example of interpretation of an anomaly which differs in nature from the Kursk anomalies. An example of this type is provided by one of the sectors in which large numbers of anomalies are observed between the Urals and the middle Stretch of the Volga. The map of isolines of anomalous values of the vertical component over such a sector, shown in Figure 186, indicates that the isolines over this area form closed curves of almost circular form. This fact indicates that the occurring rocks have equal longitudinal and transverse dimensions.

Thus, from the very nature of the isolines certain conclusions are possible concerning the shape of the occurring rocks: namely, that the rocks which cause the anomalies must have the shape of spheres or vertical cylinders.

Declassified in Part - Sanitized Copy Approved for Release 2013/01/23 : CIA-RDP81-01043R001600090003-8

Declassified in Part - Sanitized Copy Approved for Release 2013/01/23 : CIA-RDP81-01043R001600090003-8

Since all the regions of closed isolines (Figure 186) surrounding the 4 maxima of Z are of the same nature it is sufficient for their interpretation to consider some single region for example the region Z_1, for which special observations of the vertical and horizontal component have been carried out over the profile AB. The results of these observations are shown in Figure 187a in the form of graphs of H and Z, in which the abscissa axis is marked off in km, and the ratios of H and Z to the maximum value Z_m, which is equal to Z = 3630 γ are plotted on the ordinate axis.

Upon examination of these graphs it may be noticed that the ratio of maxima H_m to Z_m is equal to 0.43 and closely approximates the ratio of the same quantities in the case of the vertically magnetized sphere, which was discussed on page 335. Therefore, assuming at the first approximation that the occurring rock has the shape of a sphere magnetized in the vertical direction, we may determine the depth of occurrence of the center of the sphere R from the correlation $R = 2x_m$ which was derived on page 373, and in which X_m denotes the abscissa corresponding to the maximum value H_m. This correlation gives R ~2 km.

Calculating H and Z for this depth of occurrence in accordance with the formulas of (8.45) and plotting the former on the same graph (Figure 187a) for the purpose of comparison, we see that while the left hand branches of both curves H and Z are in good agreement with the observational curves, the right hand branches show considerable deviation.

This deviation must be attributed to an inclination of the magnetic axis, which we have assumed to be vertical whereas the lack of symmetry of the Z curve in relation to the axis of ordinates indicates it is oblique in relation to the vertical. Therefore, taking the angle of inclination of the magnetic axis of the sphere as equal to 15° and increasing the depth of occurrence to 2.5 km, we repeat the calculations

Declassified in Part - Sanitized Copy Approved for Release 2013/01/23 : CIA-RDP81-01043R001600090003-8

Declassified in Part - Sanitized Copy Approved for Release 2013/01/23 : CIA-RDP81-01043R001600090003-8

of H and Z with these parameters and plot the new graphs shown in Figure 187b, together with the observational curves. Comparing the newly plotted theoretical curves with the observational curves we find that they very nearly coincide. Hence the anomaly under study may be attributed to the presence of a spherical magnetized rock formation, the center of which is at a depth of 2.5 km.

When the depth of occurrence and the absolute value of the vertical component which is equal to 0.0363 Oe are known, the magnetic moment of this rock may be determined (see page 373): $M = R^3 Z_m / 2 = 0.283$ Oe km^3.

To determine the volume of the rock it is necessary to know its magnetic susceptibility, which requires some idea of the mineralogical composition of the rock. The geological structure of the area involved is such that at a depth of the order of 1-2 km crystalline rocks must occur. Hence it is quite probable that the anomalies in this area are caused by igneous rocks containing magnetites.

Such rocks include basalts, gabbro and diabases, the residual magnetization of which as is shown in Table 39, is within the range from 0.003 to 0.001 CGSμ.

Assuming that the magnitude of magnetic susceptibility is 0.02 CGSμ the volume of the rock is $V = M/X = 14.1$ km^3,

and therefore the radius of the sphere is $a = 1.5$ km.

Therefore the depth of occurrence of the upper boundary of the sphere is one km, which is entirely possible within this area.

In more complex instances, when the observed H and Z curves cannot be identified with any of the theoretical curves, one of the above graphical methods of computation, i.e., the method of Kazanskiy, Andreyev or Mikov, must be used for determining the depth and shape of the occurring rock formation.

Declassified in Part - Sanitized Copy Approved for Release 2013/01/23 : CIA-RDP81-01043R001600090003-8

Declassified in Part - Sanitized Copy Approved for Release 2013/01/23 : CIA-RDP81-01043R001600090003-8

CHAPTER IX

Ship's Magnetic Compass Deviation

1. The Basic Equations of a Ship's Magnetic Field

One of the first applications of the compass was to determine the ship's position at sea.

In the first half of the nineteenth century an iron type ship was limited because it tended to become a part of the magnetic field causing compass deviation. In order to compensate for this deviation a whole new science was developed known as compass deviation, consisting of methods of determining deviation and correcting it.

Some of the forerunners in the field of magnetic deviation were Russian Naval officers, such as I. P. Belavents and I. P. Dekolong who developed methods of correcting deviation which were adapted not only by the Russian fleet but subsequently by all fleets.

In order to obtain an uniformly magnetized body with J equal to the intensity of magnetization, the following equation with the magnetic potential equal to U in some point P is illustrated:

$$J = -(J \text{ grad } V) \text{ and } V = [\text{illegible}]$$

where = the distance from the magnetic element to point P.

Let us take the coordinate axes fixed to the ship, placing axis x fore and aft, with axis z placed vertically. Correspondingly, axis y will run athwartships.

The components of magnetic field intensity called Xa, Ya and Za, are obtained by differentiating this equation and changing sign, i. e.,

Declassified in Part - Sanitized Copy Approved for Release 2013/01/23 : CIA-RDP81-01043R001600090003-8

Declassified in Part - Sanitized Copy Approved for Release 2013/01/23 : CIA-RDP81-01043R001600090003-8

$$Xa = J_x \frac{d^2V}{dx^2} + J_y \frac{d^2V}{dx\,dy} + J_z \frac{d^2V}{dx\,dz},$$
$$Ya = J_x \frac{d^2V}{dy\,dx} + J_y \frac{d^2V}{dy^2} + J_z \frac{d^2V}{dy\,dz}, \qquad (9.1)$$
$$Za = J_x \frac{d^2V}{dz\,dx} + J_y \frac{d^2V}{dz\,dy} + J_z \frac{d^2V}{dz^2}.$$

The vector of magnetization J is the sum of a constant vector or residual magnetization Jr and the vector of the temporary magnetization J, induced by the external field H and equal to xH. Therefore, generally speaking the following is written:

$J = Jr + xH$

whereas for components of vector J:

$Jx\ 2\ x_1\ X + Jrx$; $Jy = x_2\ Y + Jry$; $Jz = x_3\ Z + Jrz$

Here x_1, x_2 and x_3 denote magnetic susceptibility of the ship in the direction of the axes x, y and z. Therefore, in substituting the terms in equations (9.1) Jx, Jy and Jz can be written:

$$Xa = aX + bY + cZ + P,$$
$$Ya = dX + eY + fZ + Q, \qquad (9.2)$$
$$Za = gX + hY + kZ + R.$$

Coefficients a, b, c, d, e, f, g, h, k, P, Q and R have the following values:

$$a = x_1 \frac{d^2V}{dx^2}, \quad b = x_2 \frac{d^2V}{dx\,dy}, \quad c = x_3 \frac{d^2V}{dx\,dz},$$
$$P = Jrx \frac{d^2V}{dx^2} + Jry \frac{d^2V}{dx\,dy} + Jrz \frac{d^2V}{dx\,dz}, \text{ etc}$$

therefore, coefficients a, b, c, ..., are products of corresponding magnetic susceptibility and second derivatives of potential V, which depends on the size and shape of the ship, magnetic properties of the material used in constructing the ship, etc. P, Q and R are constant components of the field intensity, depending on the ship's magnetization.

Declassified in Part - Sanitized Copy Approved for Release 2013/01/23 : CIA-RDP81-01043R001600090003-8

Declassified in Part - Sanitized Copy Approved for Release 2013/01/23 : CIA-RDP81-01043R001600090003-8

The (9.2) equations are known as Poisson's equations and are the basis of all theoretical and practical deviations of a ship's magnetic compass. These equations make it possible to attain a great degree of precision in determining magnetic forces acting on the compass needle and can be used for solving problems of deviation correction.

2. Transformation of Poisson's Equations

A still better method of correcting deviation is by simple transformation of the equations shown in (9.2) consisting of adapting coefficients X and Y in the first equation and Y and X in the second equation. To fulfill this operation it is necessary to add and deduct the corresponding terms in each equation of (9.2), which gives:

$$Xa = \frac{a+e}{2}X + \frac{a-e}{2}X + \frac{b+d}{2}Y + \frac{b-d}{2}Y + cZ + P,$$

$$Ya = \frac{b+d}{2}X - \frac{b-d}{2}X + \frac{a+e}{2}Y - \frac{a-e}{2}Y + fZ + Q,$$

or, after transposing some terms:

$$Xa = \frac{a+e}{2}X + \frac{a-e}{2}X + \frac{b+d}{2}Y + \frac{b-d}{2}Y + cZ + P, \qquad (9.3)$$

$$Ya = \frac{a+e}{2}Y - \frac{a-e}{2}Y + \frac{b+d}{2}X - \frac{b-d}{2}X + fZ + Q, \qquad (9.4)$$

As $H^2 = X^2 + Y^2$, where H = the horizontal component, in vector form these equations read as follows:

$$Ha = \frac{a-e}{2}Hh_1 + \frac{a-e}{2}Hh_2 + \frac{b+d}{2}Hh_3 + \frac{b-d}{2}Hh_4 + (cZ+P)k + (fZ+Q)e,$$

where h_1, h_2, h_3, h_4 are unit vectors corresponding to vectors, components of which are located in the first, second, etc columns, k equals a unit vector along axis x and e along axis y. It is not difficult to see that the direction of vector h_1 coincides with the direction of the horizontal component. Then designating the angle between vectors H and axis x by φ, and the angles between vectors h_2, h_3 and h_4 and the same axis by α_2, α_3 and α_4, one obtains according to equations (9.3) and (9.4):

Declassified in Part - Sanitized Copy Approved for Release 2013/01/23 : CIA-RDP81-01043R001600090003-8

Declassified in Part - Sanitized Copy Approved for Release 2013/01/23 : CIA-RDP81-01043R001600090003-8

$$tg\alpha_2 = -tg\zeta, \; tg\alpha_3 = ctg\,\zeta, \; tg\alpha_4 = -ctg\,\zeta,$$
$$\alpha_2 = -\zeta, \; \alpha_3 = 90^\circ - \zeta, \; \alpha_4 = 90^\circ + \zeta$$

or

$$\alpha_2 = -\zeta, \; \alpha_3 = 90^\circ - \zeta, \; \alpha_4 = 90^\circ + \zeta.$$

In this manner, the magnetic force Ha, caused by the reaction of the ferromagnetic materials on the compass, can be replaced by the action of 6 independent forces, each of which produces its own declination. In order to represent the disposition of these forces more clearly, a graph showing these forces in a form of a polygon, with a horizontal component included is illustrated.

Assuming that ON is the direction of the magnetic meridian (Figure 188) and H is the horizontal component, the first force $\frac{a+e}{2}$ H, is plotted in the same direction as segment Oh_1. The second force $\frac{a-e}{2}$ H, is directed to an angle ζ to axis x, and consequently, is plotted clockwise at an angle 2ζ to the magnetic meridian, as segment h_1h_2. The third force, $\frac{b+d}{2}$H is perpendicular to the second force and is therefore represented by segment h_2h_3; the fourth force, $\frac{b-d}{2}$ H, is perpendicular to the magnetic meridian and is represented by segment h_3h_4, whereas of the last two, one is parallel to axis x, and the other parallel to axis y; these are represented by segments h_4h_5 and h_5h_6.

The resultant force, F, will be the closing segment OH_6, in whose direction the compass needle aligns itself. Consequently, angle NOh_6 is the compass deviation δ. Angle ζ' is the ship's magnetic course and angle ζ' is equal to xOH_6 between axis X and the direction of the compass needle or the compass course. Therefore,

$$\zeta = \zeta' \delta.$$

Declassified in Part - Sanitized Copy Approved for Release 2013/01/23 : CIA-RDP81-01043R001600090003-8

Declassified in Part - Sanitized Copy Approved for Release 2013/01/23 : CIA-RDP81-01043R001600090003-8

3. Determination of Deviation

In order to determine deviation δ, project all the forces acting on the compass, first in the direction of the magnetic meridian and then in the direction perpendicular to it, resulting in the following 2 equations:

$$F\cos\delta = H + Oh + h_1h_2\cos 2\zeta + h_2h_3\sin 2\zeta + h_4h_5\cos\zeta + h_5h_6\sin\zeta ,$$

$$F\sin\delta = h_1h_2\sin 2\zeta + h_2h_3\cos 2\zeta + h_3h_4 - h_4h_5\sin\zeta + h_5h_6\cos\zeta ,$$

or,

$$F\cos\delta = H + \frac{a+e}{2}H + \frac{a-e}{2}H\cos 2\zeta + \frac{c+d}{2}H\sin 2\zeta + (cZ + P)\cos\zeta + (fZ + Q)\sin\zeta .$$

$$F\sin\delta = -\frac{a-c}{2}H\sin 2\zeta + \frac{c+d}{2}H\cos 2\zeta + \frac{c-d}{2}H - (cZ + P)\sin\zeta + (fZ + Q)\cos\zeta .$$

Let us introduce the following notation:

$$f\frac{Z+Q}{H} = C\lambda , \frac{cZ+P}{H} = B\lambda , \frac{c+d}{2} = E\lambda , \frac{a-e}{2} = D\lambda , \frac{c-d}{2} = A\lambda ,$$

$$\frac{a+e}{2} + 1 = \lambda . \qquad (9.5)$$

Dividing the second equation by the first the following is obtained:

$$\tan\delta = \frac{A - B\sin\zeta + C\cos\zeta - D\sin 2\zeta + E\cos 2\zeta}{1 + B\cos\zeta + C\sin\zeta + D\cos 2\zeta + E\sin 2\zeta} \qquad (9.6)$$

Coefficients A, B, C, D and E cannot be obtained theoretically, and consequently their values are determined by experience, observing deviation δ of different courses where coastal lines exist with known magnetic azimuths.

However equation (9.6) can be simplified if coefficients A, B, C, D and E are small, which is always the case since deviation is corrected on each ship before a voyage, i. e., the compensation of magnetic forces caused by the ship's iron. This compensation is effected by the use of permanent magnets and iron bars.

Declassified in Part - Sanitized Copy Approved for Release 2013/01/23 : CIA-RDP81-01043R001600090003-8

Declassified in Part - Sanitized Copy Approved for Release 2013/01/23 : CIA-RDP81-01043R001600090003-8

As it is impossible to compensate all the forces, the deviation does not revert to zero but remains at a few degrees. In this case in equation (9.6) the tangent of the angle can be replaced by the angle itself, and the right side of the equation can be expanded into Fourier series. Therefore, equation (9.6) can be replaced by the following approximation:

$$\delta = A + B \sin \xi + C \cos \xi + D \sin 2\xi + E \cos 2\xi \qquad (9.7)$$

In order to determine coefficients A, B, C, D and E, the above method is used, i. e., different course deviations are observed and 8 of them are used. Then, by solving 8 equations with 5 unknowns by the least squares method, the sought coefficients are obtained and used to calculate the deviation of 24 courses, through every 15°.

Table 31 illustrates a typical deviation table used in navigation.

4. Elimination of Deviation

In order to correct deviation it is necessary to compensate for the ship's magnetic forces acting on the compass. The theoretical basis of this operation is Poisson's equation in its transformed shape.

In the equation (9.5) one discovers that forces $cZ + P = \lambda HB$ and $fZ + Q = \lambda HC$ are independent of the ship's course and when Z is constant the forces are constant. Therefore, to correct them, it is necessary to create forces of opposite direction by placing permanent magnets close to the compass. As force λHB is directed along axis x, i. e., from stem to stern, the permanent magnet NS should be placed in the same direction, on the vertical line through the center of the compass needle. Then, the intensity of the magnetic field -- magnetic force H_1, created by such a magnet would be:

Declassified in Part - Sanitized Copy Approved for Release 2013/01/23 : CIA-RDP81-01043R001600090003-8

Declassified in Part - Sanitized Copy Approved for Release 2013/01/23 : CIA-RDP81-01043R001600090003-8

$$H_1 = \frac{2M_1}{R_1^3}\left[1+\frac{P'}{R_1^2}\right],$$

where M_1= the magnetic moment of the magnet,

R_1= the distance of the magnet to the compass

and P_1= constant coefficient.

Moving the magnet NS vertically it is possible to find the distance R_1 in which $H_1 = \lambda$ HB. To correct force λ HC it is necessary to place the second magnet vertically, perpendicular to the first magnet. Moving the magnet in a vertical line it is possible to find distance R_2, in which the intensity of the field H_2, produced by it, compensates λ HC, i. e., gives the following equation:

$$H_2 = \frac{2M_2}{R_2^3}\left(1+\frac{P_2}{R_2^2}\right) = \lambda \text{ HC}.$$

Forces λ DH and λ EH as shown in (9.5) and Figure 188, change their direction relative to X-axis with changes in the ship's course, and therefore it is impossible to compensate the forces by permanent magnets.

To correct these forces it is necessary to produce a magnetic field, constant in size, but changing in direction according to the ship's course.

To find a source of such a magnetic field it is necessary to determine how forces λ DH and λ EH originate.

From equations (9.5) one obtains: $H_\lambda D = \frac{a-e}{2} H$, λ EH $= \frac{b+d}{2} H$.

These forces as shown in equation (9.1), are the components: the first of force $\sqrt{a^2 X^2 + e^2 Y^2} = H_1$, and the second of force $\sqrt{b^2 Y^2 + d^2 X^2} = H_2$. Consequently, the reason for their origin is the same as the reasons for the origin of forces H_1 and H_2.

Declassified in Part - Sanitized Copy Approved for Release 2013/01/23 : CIA-RDP81-01043R001600090003-8

Declassified in Part - Sanitized Copy Approved for Release 2013/01/23 : CIA-RDP81-01043R001600090003-8

It is not difficult to see that H_1 is caused by the iron bars that are located symmetrically in relation to the compass, where one of them is parallel to axis x, i. e., located fore and aft, and the others parallel to axis y, i. e., located athwartships. Let us assume that one of the bars is parallel to axis x, and the second bar is parallel to axis y and with the compass set in point 0 or the center of the bars; the field, then, produced by one of the bars at point 0 would be parallel to axis x, whereas the other would be parallel to axis y, and the intensity of Hx and Hy would be expressed as $Hx = c_1J_1$ and $Hy = c_2J_2$ where J_1 and J_2 are the intensities of magnetization of the bars, and c_1 and c_2 are the coefficients of proportionality. But $J_1 = x_1X$, and $J_2 = x_2Y$, where x_1 and x_2 equal magnetic susceptibility of the bars. Consequently, $Hx = aX$ and $Hy = eY$.

In this instance a and e will be negative as the field created by the bars is opposed to the magnetizing force. If the bars are placed in line with the compass needle, perpendicular to the axis of the needle, then a and e will be positive.

Therefore, to correct force λ DH, it is necessary to take soft iron bars in the form of cylinders or prisms and place one of them fore and aft and the rest athwartships, symmetrically located in relation to the compass. Usually 4 bars are used, i. e., 2 lengthwise and 2 laterally as shown in Figure 189.

As demonstrated in practice on all ships with rare exceptions, force λ DH is positive; therefore, to correct this force it is necessary to produce a negative force $-\lambda$ DH which is accomplished by placing the bars either under the compass or on the sides of the compass. Instead of bars iron spheres can be used, placed on the side of the compass.

Declassified in Part - Sanitized Copy Approved for Release 2013/01/23 : CIA-RDP81-01043R001600090003-8

Declassified in Part - Sanitized Copy Approved for Release 2013/01/23 : CIA-RDP81-01043R001600090003-8

In order to correct force λ EH, which is always perpendicular to force λ DH, it is sufficient as is demonstrated by theory, to turn the whole system of soft iron bars at an angle B + Y, where B = arc tg $\frac{AE}{D}$ and Y = arc tg A.

Force λ AH is always perpendicular to the magnetic meridian and produces a constant deviation, equal to angle γ, and therefore, cannot be corrected, but as this deviation is ordinarily very small and is part of the residual deviation, it is determined by observation.

It is necessary to mention the established terminology used in the fleet in reference to compass matters. Deviation, produced by constant forces λ BH and λ CH, is called semicircular because it assumes maximum values every 180°, whereas deviation caused by forces λ DH and λ EH is known as quarter deviation as its maximum occurs every 90°. This is explained by equation (9.7). The quarter deviation λ DH is called symmetrical and deviation λ EH is asymmetrical because the first is produced and corrected by iron bars located symmetrically in relation to the compass, whereas the second calls for iron bars located asymmetrically in relation to the compass.

5. Deflection Magnetometer of Dekolong

In order to solve various problems concerning the calculation of deviation coefficients it is necessary to know besides deviation, the direction of magnetic forces which maintain the compass needle in the meridian. This was finally accomplished by the invention of a magnetometer which was capable of measuring intensity and direction of magnetic forces.

In Russia the forerunner in this field was I. P. Dekolong who devised the deflection magnetometer. Upon the suggestion of A. N. Krylov,

Declassified in Part - Sanitized Copy Approved for Release 2013/01/23 : CIA-RDP81-01043R001600090003-8

Declassified in Part - Sanitized Copy Approved for Release 2013/01/23 : CIA-RDP81-01043R001600090003-8

this instrument was adapted as the basis for measuring elements of the earth's magnetism during observations made by the magnetic anomalies in the area of Kursk.

The principle of measuring horizontal and vertical forces of the earth's field by a deflection magnetometer means that one or the other force is compensated by the aid of a permanent magnet located near the compass needle freely rotating in a horizontal or vertical plane.

If the horizontal component is compensated then the moment of rotation around the vertical axis becomes equal to zero and the needle will occupy any bearing depending on the magnetitic meridian or will be found in a neutral position.

In order to compensate for either component it is necessary to set the compensating magnet which is known as the deflector in a definite position in relation to the needle. In order to compensate for the horizontal component it is best to install a deflector magnet in the magnetic meridian so that its center is on a vertical line, perpendicular to the axis of the needle, going through its center. In order to compensate for the vertical component, the deflector magnet is set vertically so that its axis goes through the center of the needle.

The intensity of the magnetic field produced by a deflector magnet can be calculated by formulas if the magnetic moment M of the deflector magnet and the distance between its center and center of the needle are known. If there is full compensation the amount of field intensity equals the amount of intensity of the horizontal or vertical components.

Declassified in Part - Sanitized Copy Approved for Release 2013/01/23 : CIA-RDP81-01043R001600090003-8

Declassified in Part - Sanitized Copy Approved for Release 2013/01/23 : CIA-RDP81-01043R001600090003-8

In measuring the horizontal component the deflector magnet is set at a distance R from the needle so that its axis takes a position corresponding to the direction of the perpendicular magnet, i. e., from E to W.

Measuring the vertical component means finding the distance between the deflection magnet and needle which is set in a horizontal position.

The deflection magnetometer (Figure 190) consists of the following parts: binnacle, magnetic needle, compass card and deflector.

The binnacle is a large brass bowl with a diameter of 18 or 12.5 cm, depending on the purpose of the instrument. A lead cylinder is welded to the outside surface of the binnacle which holds the axis when the binnacle is suspended in gimbal rings. Magnetometers built for field use contain 3 screws for raising the binnacle and have no lead cylinders.

A column with screwed-up sharp pin is set in the exact center inside the bowl.

The column can be centered in the binnacle by screws. The binnacle has well ground top c representing a graduated circle holding a glass plate. The center of the glass plate supports bearing finder K which is used to adjust deflector D. The bearing finder, acting as an alidade is a plate containing 2 sliding sights a and b located on opposite ends for sighting distant objects.

The deflector is a bar mounted on the bearing finder containing a circular base and 2 plates on which the carriage slides. One of the

Declassified in Part - Sanitized Copy Approved for Release 2013/01/23 : CIA-RDP81-01043R001600090003-8

Declassified in Part - Sanitized Copy Approved for Release 2013/01/23 : CIA-RDP81-01043R001600090003-8

plates contains graduations with one side of the plate used for the horizontal force and the other for the vertical force. The base of the bar has 2 openings for a third perpendicular magnet for determining N, and a mechanism containing a rack for precise adjustment of the deflection magnet.

The compass card (Figure 191) consists of a system of 6 small magnets mounted on an aluminum frame, a graduated paper disc securely attached to it, and a magnetic needle.

Determining the horizontal component by means of a deflection magnetometer consists of the following operation:

After adjusting the deflection magnetometer, the prism of the range finder is set to S on the compass card with the reading recorded on the horizontal circle.

After this operation, the deflector is adjusted by having magnet M^1 (Figure 190) pointing its north seeking end north. As the bearing finder does not have reinforcement screws it can be thrown off while adjusting the deflector, following which it is necessary to verify the direction according to the horizontal circle and bring the bearing finder to its former position.

In adjusting the deflection magnet upward and downward on the bar it is necessary to have E or W of the compass card appear under the prism, obtaining readings on the left side of the deflector scale.

In order to decrease the amount of chance errors it is necessary to perform this operation several times.

Finally the perpendicular magnet is reset to 180° and E instead of W or W instead of E is brought under the prism.

Declassified in Part - Sanitized Copy Approved for Release 2013/01/23 : CIA-RDP81-01043R001600090003-8

Declassified in Part - Sanitized Copy Approved for Release 2013/01/23 : CIA-RDP81-01043R001600090003-8

Sighting a vertical component is carried out in the absence of a perpendicular magnet and by the deflection magnet in a vertical position with its northern end facing upwards.

The deflector is adjusted and the compass card steadied by sliding the magnet upward and downwards until the compass card needle assumes an horizontal position, after which readings are taken on the right side of the deflector scale. The operation of bringing the needle into a horizontal position is performed several times.

PART FOUR

METHODS AND APPARATUS FOR MEASUREMENT OF THE ELEMENTS OF TERRESTRIAL MAGNETISM

CHAPTER X

MEASUREMENT OF THE ELEMENTS OF TERRESTRIAL MAGNETISM

Section 1. Classification of Measurement Methods and of Measuring Apparatus

Measurement is a physical experiment consisting of a number of procedures that enable comparison of the quantity being measured with the unit of measurement.

By measuring apparatus is meant the combination of technical means which make these comparisons possible. Measuring apparatus may be subdivided into 2 groups: the group of measures and the group of measuring instruments.

By the term measure is meant the physical body or device which reproduces a given unit or subdivision of a unit of measurement. An example is any weight used in conjunction with a balance, and by any ruler divided into cm or m which reproduce respectively the unit of mass and the unit of length.

Declassified in Part - Sanitized Copy Approved for Release 2013/01/23 : CIA-RDP81-01043R001600090003-8

Declassified in Part - Sanitized Copy Approved for Release 2013/01/23 : CIA-RDP81-01043R001600090003-8

A measuring instrument is a technical device which enables comparison of a quantity with a measure in a direct or indirect manner.

In measuring the elements of terrestrial magnetism the entire measuring apparatus consists only of measuring instruments, since at present there are no measures which reproduce the unit of intensity of the magnetic field.

The measurement procedures may be divided into 2 fundamental forms: direct, and indirect measurements.

Direct measurement includes comparison of a quantity with a measure either directly or by means of measuring instruments graduated in the proper units. Thus, weighing on a balance or an ammeter reading are typical examples of measurements of this kind.

Indirect measurement consists of a number of direct measurements of several quantities which are functionally correlated with the quantity being measured. Thus the quantity under consideration is determined in accordance with mathematical formulas which define these functional correlations.

Measurements of this kind include all magnetic measurements of the elements of terrestrial magnetism, with the exception of the measurement of variations of these elements, which are measured directly.

Both direct and indirect measurements may be further subdivided into absolute and relative classes.

In the class of absolute measurements all the direct measurements consist of measuring length, angles, mass or time. Relative measurements are those in which directly measured quantities are compared.

Declassified in Part - Sanitized Copy Approved for Release 2013/01/23 : CIA-RDP81-01043R001600090003-8

Declassified in Part - Sanitized Copy Approved for Release 2013/01/23 : CIA-RDP81-01043R001600090003-8

In magnetic measurements absolute methods are used in determining the declination, dip and horizontal component. At present the vertical component is determined mostly by relative procedures. Absolute magnetic measurements are performed exclusively under observatory conditions, and only relative methods are used under field conditions. In relative measurements the observed quantity A usually is calculated by the formula

$$A = \varepsilon N$$

where N is the number of divisions of a scale (linear or circular) which is read directly on the instrument, and ε is a constant which depends upon the design of the instrument.

If the scale is not uniform, i.e., if ε has different values depending upon N, the following differential formula is used:

$$dA = \varepsilon\, dN.$$

where dN is the difference between 2 readings corresponding to a small change in the quantity A.

In the case of a uniform scale the constant factor is expressed by the ratio:

$$\varepsilon = A/N,$$

and in the case of a nonuniform scale it is expressed by the ratio

$$\varepsilon = dA/dN$$

and is called the value of one division of the instrument.

The inverse quantity, i.e.,

$$S = N/A \quad \text{or} \quad S = dN/dA$$

is called the sensitivity of the instrument.

The following paragraphs describe the procedures and apparatus used in measuring the elements of terrestrial magnetism, namely: declination, dip, and horizontal and vertical components. The other

Declassified in Part - Sanitized Copy Approved for Release 2013/01/23 : CIA-RDP81-01043R001600090003-8

Declassified in Part - Sanitized Copy Approved for Release 2013/01/23 : CIA-RDP81-01043R001600090003-8

elements, namely the north and east components, and the total force of terrestrial magnetism, are not measured directly and these values are determined by means of the corresponding mathematical formulas.

Section 2. The Principle of Measuring Declination.

Declination is the angle between the plane of the magnetic meridian and the plane of the geographic meridian, and therefore the problem of determining the declination consists in finding points on the horizontal circular scale of the instrument which are intersected by magnetic and geographical meridians extending through the center of the instrument. If the magnetic meridian intersects the horizontal circle at a point corresponding to the division n_M (Figure 192), and the geographic meridian at the point n_A corresponding to the division n_A, the declination D is expressed as follows:

$$D = n_M - n_A \qquad (10.1)$$

The positive direction of the meridians is taken from N toward S, and the readings increase in the clockwise direction.

In the determination of the geographical meridian an astronomical procedure for determining the azimuth of some remote object, called the mire, is utilized. The determinations usually are based on the sun when it is located near the primary vertical or are based on the North Star. Taking a as the azimuth of the mire, reading from S toward N over W as determined by astronomical observations, and n the reading of the horizontal circular scale when the axis of the sighting device, telescope or sight is aligned with the mire. (Figure 192), then the position of the geographic meridian on the circular scale will be

$$n_A = n - a \qquad (10.2)$$

In the determination of the magnetic meridian a permanent magnet freely rotating about a vertical axis which extends through the center

Declassified in Part - Sanitized Copy Approved for Release 2013/01/23 : CIA-RDP81-01043R001600090003-8

Declassified in Part - Sanitized Copy Approved for Release 2013/01/23 : CIA-RDP81-01043R001600090003-8

of the horizontal circle of the instrument is used. When the magnet is in equilibrium its magnetic axis coincides with the magnetic meridian; therefore the reading n_M is obtained from the position of this axis with respect to the horizontal circle. From equations (10.1) and (10.2) it follows that:

$$D = n_M - n + a.$$

The difference $n - n_M$ is called the magnetic azimuth of the mire and is denoted by the symbol a_m. Therefore the declination D may be expressed as the difference between the geographic and magnetic azimuths of the mire, i.e.,

$$D = a - a_m.$$

Instruments for Determination of Declination. There are 2 types of instruments for determination of declination: compasses equipped with a sighting device, and declinators which utilize a magnetic system on a pivot or on a filament. A compass with a sight consists of a magnetic system on a pivot, rotating within a cylindrical casing the top of which is graduated in degrees. The magnetic meridian is determined by reading the division on the scale which is in line with the tip of the needle. The mire sight consists of a slotted rear sight and a front sight and is located above the compass. Instruments of this type include the deflection magnetometer and the M-1 magnetometer. In the former the sight, called the direction finder is located on the azimuth circle, and the prism is below the slot of the direction finder.

When measuring declination with the deflection magnetometer (Figure 193) the sighting plane of the direction finder [illegible], i.e., a plane extending through the hairline A and slot B, is aimed at the mire and a reading is taken on the horizontal circle. Next, the south and north poles of the compass card are aligned with the prism so that the hairline of the direction finder coincides with the zero or 180° division of the card, and another reading is taken on the horizontal circle.

Declassified in Part - Sanitized Copy Approved for Release 2013/01/23 : CIA-RDP81-01043R001600090003-8

Declassified in Part - Sanitized Copy Approved for Release 2013/01/23 : CIA-RDP81-01043R001600090003-8

In the M-1 magnetometer (Figure 194) the sight D is located underneath the compass B, so that the sighting plane extends through the zero division of the compass card, and the front sight consists of the sharp edge of holes C drilled through a plate. In measuring the declination the sighting plane is aligned with the mire and the magnetic azimuth of the mire is directly indicated by the tip of the needle, since when the needle is set at the zero division of the compass the sighting plane extends through the magnetic axis of the needle.

In the declinators either the collimator, or mirror methods are used for aligning with the needle. The sighting device in these instruments is an astronomical telescope.

In the collimetor method the magnet M is a cylindrical tube with an optical system, called a collimator, consisting of an objective and a glass plate provided with either a cross hair or a single hair line P, within the main focal plane of the objective L. The optical axis of this system should be parallel to the magnetic axis of the needle (Figure 195).

On leaving the lens the diffused pencil of light issuing from mark P_1, illuminated with diffused light by means of mirror S is propagated along the optic axis of the collimetor as a parallel beam T. An astronomical telescope, the objective L_1 of which faces the objective of the collimetor is located within the path of this beam. If the optic axis of the instrument is parallel to the optic axis of the collimetor the parallel beam of light T passing through lens L_1 is gathered within the main focal plane of the telescope, which is provided with a reticle, and will give a true image of collimator mark P, which is seen by the eye through the occular L_2.

Declassified in Part - Sanitized Copy Approved for Release 2013/01/23 : CIA-RDP81-01043R001600090003-8

Declassified in Part - Sanitized Copy Approved for Release 2013/01/23 : CIA-RDP81-01043R001600090003-8

Thus when the astronomical telescope is sighted at magnet M so that at the intersection of the reticle and the true image of the collimator mark are in focus, the optical axis of the telescope will coincide with the direction of the magnetic axis of the magnet.

When mirror readings are to be utilized a plane mirror P is fastened to the magnet M (Figure 196), and the normal to the mirror should be parallel to the magnetic axis of the magnet.

The telescope through which the reflected image of the hair lines is sighted is a conventional astronomical telescope the ocular of which is provided with a glass plate inclined at an angle of 45° and having a reticle within the main focal plane of the objective. The pencil of rays passing through the aperture of the ocular is partially reflected by the plate P_1 and illuminates the reticle. Under this illumination the reticle diffuses the light, becoming similar to a source of light, and each hair line, for instance C, produces a diverging pencil, which on passing the objective reaches the mirror of the magnet P as a parallel beam and impinges on the mirror at a certain angle. After being reflected from the mirror it passes again through the objective and is gathered within the principal focal plane FF' at point C'. Therefore, on looking through the ocular the observer sees both the illuminated hair line C and the mirror reflection of the hairline C', which constitutes a real image of hairline C. If the magnet is deflected by a certain angle the mirror P also is deflected and the image of the reticle is displaced by twice this angle.

When the direct and reflected reticle images coincide the optical axis coincides with the normal to the surface of the mirror, and thus also with the magnetic axis.

Declassified in Part - Sanitized Copy Approved for Release 2013/01/23 : CIA-RDP81-01043R001600090003-8

Declassified in Part - Sanitized Copy Approved for Release 2013/01/23 : CIA-RDP81-01043R001600090003-8

These special instruments, declinators, are seldom used outside of observatories and magnetic theodolites designed for measuring the horizontal component are more widely used.

Thus in the "combine" instrument, which is described below, a special magnetic system is used for measuring declination, consisting of 2 rigidly fixed parallel magnets M_1 and M_2 (Figure 197), between which is a mirror P perpendicular to the axis of the magnet. At the opposite side of the mirror is a weight q for counterbalancing the system in a horizontal position.

Errors in Declination Measurements. The sources of error in the mirror and collimator methods of sighting may be the following: the collimator axis or the normal to the mirror surface may not be parallel to the magnetic axis of the magnet, and the filament from which the magnet is suspended may be twisted. The former, which is called collimation error, is eliminated by turning the magnet 180° around its longitudinal axis, and the latter error cannot be excluded from any of the observation procedures and can be only decreased or reduced to a minimum by careful untwisting of the filament.

Assuming that the magnetic axis of magnet NS forms an angle α with the normal to the surface of the mirror B (Figure 198). In such a case the optic axis of the telescope, when the direct and reflected images of the reticle coincide, will coincide with the normal to the mirror and the corresponding reading on the horizontal circle, is designated θ_1. After the magnet has been rotated 180° the magnetic axis of the magnet will be in the same position, while the mirror will assume a position P', which is symmetrical in relation to the magnetic axis. Therefore in order to bring about coincidence of the direct and reflected images the axis of the telescope must be directed normal to

Declassified in Part - Sanitized Copy Approved for Release 2013/01/23 : CIA-RDP81-01043R001600090003-8

Declassified in Part - Sanitized Copy Approved for Release 2013/01/23 : CIA-RDP81-01043R001600090003-8

the mirror, i.e., the telescope must be rotated through an angle 2δ. The new reading will be $\theta_1 \pm 2\delta$. The average of these 2 readings will be in accord with the direction of the magnetic axis of the magnet, i.e., free from the collimation error.

If the filament is twisted through an angle φ the magnetic axis of the magnet, in the position of equilibrium, will be deflected from the magnetic meridian by an angle β, which is defined by the equation $MH \sin \beta = C\varphi$ or $\sin \beta = C\varphi/MH$. where M is the magnetic moment of the magnet. Consequently, in order to have angle β be as small as possible a magnet of greatest possible magnetic moment must be suspended from a filament having the least possible coefficient of torsion C. Moreover, the filament first is untwisted so that angle φ will be as small as possible. When these conditions are fulfilled the angle β usually can be made less than the permissible error for the determination of declination.

The error due directly to the reading depends upon the accuracy of graduation of the horizontal azimuth circle and to the error in sighting the magnet.

The magnetic field theodolite usually may be read with an accuracy of from 1' to 30" and the sighting error is somewhat lower, therefore with an untwisted filament the error in determination of the declination should not exceed 1'.

The Sequence and Record of Observations of Declination. From the foregoing it follows that the determination of declination requires the performance of the following operations.

(1) Determination of the astronomical azimuth of the mire in relation to the sun.

(2) Untwisting the filament.

Declassified in Part - Sanitized Copy Approved for Release 2013/01/23 : CIA-RDP81-01043R001600090003-8

Declassified in Part - Sanitized Copy Approved for Release 2013/01/23 : CIA-RDP81-01043R001600090003-8

(3) Sighting the mire and taking a reading on the horizontal circle.

(4) Suspending the magnet and sighting the telescope at the magnet, taking a reading on the circle.

(5) Rotating the magnet 180° and taking another reading.

(6) Repeating, as a check, the observations of the magnet in reverse order, i.e., after the last sighting, moving the telescope and resetting the magnet in relation to the axis of the telescope, then rotating the magnet 180° and adjusting it to the initial position.

(7) Sighting the mire.

To untwist the filament a copper dummy of the same mass as the magnet and about the same shape is suspended from the filament. If the filament is twisted the dummy in equilibrium will be deflected from the sighting plane, and by using the twisting knob the filament is twisted in the opposite direction until the dummy assumes the direction of the sighting plane axis, coinciding with the axis of the telescope. Since the directing force of the filament is very slight the oscillation period of the dummy is very large (of the order of several minutes and longer) and the equilibrium position of the dummy is determined with great difficulty. Hence untwisting the filament requires much time and is affected by the method of successive approximations, since after the first twisting of the knob the filament usually is not untwisted or is found to be twisted in the opposite direction.

The record of observations made by means of the theodolite is shown in Table 32.

The method of measuring declination described above is an absolute method since in this case the entire set of direct measurements consists in the measurement of angles and the result of these measurements is the value of declination expressed in absolute units.

Declassified in Part - Sanitized Copy Approved for Release 2013/01/23 : CIA-RDP81-01043R001600090003-8

Declassified in Part - Sanitized Copy Approved for Release 2013/01/23 : CIA-RDP81-01043R001600090003-8

TABLE 32

RECORD OF OBSERVATIONS OF DECLINATION AT SLUTSK

7 April 1938, Magnetic Theodolite: Combine No 15, Mire:

Church Steeple, Erickson Chronometer

Correction of Mean Local Time: + 2 min. 30 sec.

Time of Observation	Sighted at	Position of Magnet Mark	Horizontal Circle Reading	Average	Calculations
	mire		209° 49'		
10 h. 25 m.	magnet	toward E	135 34		
	magnet	toward W	135 48		a_a = 78° 59'
	magnet	toward W	135 47		a_m = 74 08
10 h. 31 m.	magnet	toward E	135 35	135° 41'	
	mire	-	209 49	209 49	D = 4° 51'

Section 3. Astronomical Observations during Magnetic Surveys.

In the preceding section it was shown that the determination of declination requires knowledge of either the geographic meridian or the azimuth of a mire, which are determined by means of astronomical observations. Even though astronomical observations have nothing in common with magnetic observations and the procedures relating to the former are described in texts on astronomy it is fitting to give a brief description of the theoretical foundations of, and the practical procedures utilized in conjunction with magnetic measurements, especially because the high degree of precision required in astronomy is not essential for a magnetic survey.

Since the true local time must be known in determining the azimuth of the mire (if the longitude of the point is unknown or is not exact) it is necessary, in addition to observation of the azimuth of the mire, to carry out observations for determining the local chronometric correction.

Declassified in Part - Sanitized Copy Approved for Release 2013/01/23 : CIA-RDP81-01043R001600090003-8

Declassified in Part - Sanitized Copy Approved for Release 2013/01/23 : CIA-RDP81-01043R001600090003-8

Since magnetic observations are conducted during daytime, astronomical observations also are carried out during the day. However, the only planet upon which observations may be based during daytime is the sun, and therefore only the solar observation methods will be discussed below, and those relating to other planets will be omitted. Detailed instructions on astronomical observations are found in specific texts of spherical astronomy.

Determining the Azimuth of Planets in Accordance with the Hour Angle. Let us describe about some arbitrary point, for example the eye of the observer, a sphere of arbitrary radius is called the celestial sphere, and let us plot upon this sphere a planet s, the zenith Z, and the direction from the center of the sphere parallel to the terrestrial axis OP. The point P is called the world pole. On connecting these 3 points of the sphere by arcs of great circles we obtain a spheric triangle sPZ which is called in astronomy the parallactic triangle (Figure 199). It is readily apparent that the sides of this triangle represent, respectively: Zs — the zenithal distance z of the planet, Ps is the complement of the planet declination $90^\circ - \delta$, since the arc sT is the distance of the planet from the plane of the equator OQ, which is called the declination of the planet; and PZ is the complement of the latitude of the point $90^\circ - \varphi$, since the arc ZQ is the latitude φ. The angle ZPs is called the hour angle of the planet t.

If the planet s is the sun, the hour angle is the true local time.

Angle PZs is the complement of the azimuth of planet s to 90°. In the triangle PZs we have, in accordance with the formulas of spheric trigonometry

$$\sin\delta = \sin\varphi \cos z - \cos\varphi \sin z \cos a, \qquad (10.3)$$

$$\sin z/\sin t = \cos\delta/\sin a, \qquad (10.4)$$

$$\cos z = \sin\varphi \sin\delta + \cos\varphi \cos\delta \cos t. \qquad (10.5)$$

Declassified in Part - Sanitized Copy Approved for Release 2013/01/23 : CIA-RDP81-01043R001600090003-8

Declassified in Part - Sanitized Copy Approved for Release 2013/01/23 : CIA-RDP81-01043R001600090003-8

Substituting sin z and cos z in the first formula with the values of the second and third and solving the resulting equation with respect to the azimuth a, with simple transformations we obtain:

$$\operatorname{tg} a = \sin t / \sin \varphi \cos t - \cos \varphi \operatorname{tg} \delta . \qquad (10.6)$$

Thus if the local latitude φ and the declination of the sun δ are known the azimuth a of the sun may be calculated for any time t.

Determination of the Azimuth of the Mire by the Sun. The azimuth of the more a_m is determined in the following manner. The vertical hairline of the theodolite telescope is sighted at the rim of the sun and the chronometer time T and the reading n on the horizontal circle of the theodolite are recorded.

Similar sightings usually are performed several times for both rimssof the sun to increase the accuracy of the determinations. This is done with the vertical circle to the right and to the left of the observer, recording the chronometer readings T_1, T_2..., and the horizontal circle readings n_1, n_2...

Next, the vertical hairline of the telescope is sighted at the mire, taking the corresponding reading n_0 on the horizontal circle. Calculation of the sun's azimuths a_1, a_2... a_k for each point of time T_1, T_2,...T_k we obtain the mire azimuth a_m as the mean value in accordance with the equations:

$$A_m = N_0 - a_i \quad (i = 1, 2, \ldots, k)$$

The chronometer readings must be reduced to true local solar time. The difference between the chronometer readings and the true solar time, called the chronometer correction, is determined as above from observations of the sun.

Let us calculate the most advantageous conditions of observation

Declassified in Part - Sanitized Copy Approved for Release 2013/01/23 : CIA-RDP81-01043R001600090003-8

Declassified in Part - Sanitized Copy Approved for Release 2013/01/23 : CIA-RDP81-01043R001600090003-8

and the permissible error in the determination of chronometer corrections and the local latitude upon which the error in determination of the mire azimuth depends.

In field measurements the permissible error of magnetic declination is approximately $\pm 1'$. Hence the error in mire azimuth must not exceed this magnitude.

For this purpose equations (10.5) and (10.3) are differentiated, considering δ and φ as constants, in which case

$$\sin z\, dz = \cos\varphi \cos\delta \sin t\, dt - (\sin z \sin\varphi \pm \cos z \cos\varphi \cos a)\, dz \pm \sin z \cos\varphi \sin a\, da = 0.$$

Substituting in the last equation the value of dz from the first equation, and replacing $\sin t \cos\delta = \sin z \sin a$, from equation (10.4) we have:

$$da = (\sin\varphi \pm \cos\varphi \operatorname{ctg} z \cos a)\, dt$$

Since φ and z can range from 0 to 90°, the least error is committed in the determination of the azimuth when $a = 90^\circ$ or $z = 90^\circ$, i.e., when the sun is at the primary vertical or when it is at the horizon. The maximum error occurs when $a = 0$, i.e., when the sun is at the meridian, in which case

$$da_{min} = \sin\varphi\, dt$$

$$da_{max} = \sin z \sin\varphi \pm \cos\varphi \cos z/\sin z\, dt =$$

$$\sin\varphi \sin(\varphi - \delta) \pm \cos\varphi \cos(\varphi - \delta)/\sin(\varphi - \delta)\, dt =$$

$$\cos\delta /\sin(\varphi - \delta)\, dt,$$

since at the meridian $z = \varphi - \delta$.

Thus, for example, with a latitude of $\varphi = 60^\circ$ and $\delta = \pm 23.5^\circ$ we have: $\Delta a_{min} = 0.87'$, $\Delta a_{max} = 1.54'$. From these correlations it follows that when the sun is observed at the horizon the error which may be involved in the ascertaining true local time must satisfy the following condition:

$$\Delta t = \Delta a/0.87 = 1'/0.87 = 1.15' \approx 4 \text{ seconds}.$$

Declassified in Part - Sanitized Copy Approved for Release 2013/01/23 : CIA-RDP81-01043R001600090003-8

Declassified in Part - Sanitized Copy Approved for Release 2013/01/23 : CIA-RDP81-01043R001600090003-8

Consequently the chronometer correction must be known within the same limits of error.

When the sun is observed near the meridian the error Δt must be decreased 2-fold.

Tables 33 and 34, which contain the recorded data and calculations, reveal in detail the sequence of observations and the method of their processing.

TABLE 33

CHART OF OBSERVATIONS FOR DETERMINATION OF

THE MIRE AZIMUTH BY THE HOUR ANGLE

30 July 1916

Correction of the Chronometer in Relation to the True Local Time:

$\neq$ 12 min. 9 sec.

Circle	Sighted at	Chronometer Readings	Horizontal Circle Readings: Vernier I	Vernier II	Average
R	mire		203° 04'	03'	203° 03.5'
L	mire		23 03	02	23 02.5
L	0	9 h. 24 m. 15 s.	357 34	32	357 33.0
L	0	25 50	358 44	43	358 43.5
R	0	28 25	179 35	34	179 34.5
R	0	29 12	179 07	05	179 05.0
R	0	29 58	179 18	17	179 17.5
R	0	31 16	180 24	24	180 24.0
L	0	34 09	1 8.5	7.5	1 08.0
L	0	35 06	0 44	44	0 44.0
L	mire		23 03	03	23 03.0
R	mire		203 04	03	203 03.5

Declassified in Part - Sanitized Copy Approved for Release 2013/01/23 : CIA-RDP81-01043R001600090003-8

Declassified in Part - Sanitized Copy Approved for Release 2013/01/23 : CIA-RDP81-01043R001600090003-8

TABLE 34

CHART OF MIRE AZIMUTH CALCULATIONS

φ = 60°11.0'

δ = 18°32.6'
$\Delta\delta$ = +2.4'
δ = 18°35.0'

$r_\odot$ = 15.8'
$z_\odot$ = 48°14'

Chronometer (A)	9 h. 24 m. 15 s.	9 h. 25 m. 50 s.	9 h. 28 m. 25 s.
True Time (B)	9 36 24	9 37 59	9 40 34
t hour (C)	-2 23 36	-2 22 01	-2 19 26
t° (D)	- 35° 54.0'	- 35° 30.2'	-34° 51.5'
lg cos t (E)	9.90851	9.91067	9.91411
lg cos t sin φ (F)	9.84684	9.84900	9.85244
cos t sin φ (G)	0.70280	0.70631	0.71194
cos t cos φ - cos φ tg δ (H)	0.53563	0.53914	0.54477
lg sin t (I)	9.76817	9.76798	9.75705
tg (cos t cos φ - cos φ tg δ) (J)	9.72886	9.73170	9.73621
lg tg a (K)	0.03931	0.03229	0.02084
-a (L)	- 47°35.3'	47°07.6'	46° 22.5'
Horizontal circle reading (M)	177 33.0	178 43.5	179 34.5
r_0 cosec z (N)	+ 21.2	-21.2	-21.2
Corrected reading (O)	357 54.2	358 22.3	359 13.3
a (P)	312 24.7	312 54.4	313 37.5
Position of South (Q)	45 29.5	45 29.9	45 35.3

Mean position of south 45° 32.4'

To the mire 203 03.1

Azimuth of mire 157° 36.9' from S toward W.

Declassified in Part - Sanitized Copy Approved for Release 2013/01/23 : CIA-RDP81-01043R001600090003-8

Declassified in Part - Sanitized Copy Approved for Release 2013/01/23 : CIA-RDP81-01043R001600090003-8

Table 34 Continued

$\lg r_\odot = 1.1987$		$\lg \cos\varphi = 9.69655$		
$\lg \operatorname{cosec} z = 0.1273$		$\lg \operatorname{tg}\delta = 9.52661$		
$\Sigma = 1.3260$		$\Sigma = 9.22316$		
$r_\odot \operatorname{cosec} z = 21.2'$		$\cos\varphi \operatorname{tg}\delta = 0.16717$		$\lg \sin\varphi = 9.93833$
(A) 9 h. 29 m. 52 s.	9 h. 29 m. 58 s.	9 h. 31 m. 16 s.	9 h. 34 m. 09 s.	9 h. 36 m. 06 s.
(B) 9 41 21	9 42 07	9 43 25	9 46 18	9 47 15
(C) -2 18 49	-2 17 53	-2 16 35	-2 13 42	-2 12 45
(D) $-34^\circ 39.8'$	$-34^\circ 28.2'$	$-34^\circ 08.8'$	$-33^\circ 25.5'$	$-33^\circ 11.2'$
(E) 9.91514	9.91615	9.91782	9.92148	9.92267
(F) 9.85347	9.85448	9.85615	9.85981	9.86700
(G) 0.71360	0.71530	0.71805	0.72412	0.72610
(H) 0.54643	0.54813	0.55088	0.55695	0.55893
(I) 9.75492	9.75580	9.74920	9.74103	9.73828
(J) 9.73754	9.73888	9.74114	9.74582	9.77736
(K) 0.01739	0.01391	0.00815	9.99521	9.99092
(L) $46^\circ 08.8'$	$45^\circ 55.1'$	$45^\circ 32.2'$	$44^\circ 41.3'$	$44^\circ 24.1'$
(M) 179 06.0	179 17.5	180 24.0	181 08.0	180 44.0
(N) +21.2	+21.2	-21.2	-21.2	+21.2
(O) 359 27.2	359 38.7	0 02.8	0 46.8	1 05.2
(P) 313 51.2	314 04.9	314 27.8	315 18.7	315 35.9
(Q) 45 36.0	45 38.8	45 35.0	45 28.1	45 29.3
(R)				
(S)				

Determination of Chronometer Correction by Absolute Altitude of the Sun. In the parallactic triangle PZs at the Zs side we have the following formula

$$\cos z = \sin\varphi \sin\delta + \cos\varphi \cos\delta \cos t. \quad (10.7)$$

The zenithal distance of the sun z may be replaced by the altitude above the horizon h, and cos t may be substituted to the trigonometric formula $1 - \cos t = 2 \sin^2 t/2$, in which case

$$\sin h = \cos(\varphi - \delta) - 2 \cos\varphi \cos\delta \sin^2 t/2,$$

and, solving this equation with respect to $\sin^2 t/2$, we find the correlation between the hour angle t of the sun and its altitude h is:

Declassified in Part - Sanitized Copy Approved for Release 2013/01/23 : CIA-RDP81-01043R001600090003-8

Declassified in Part - Sanitized Copy Approved for Release 2013/01/23 : CIA-RDP81-01043R001600090003-8

$$\sin^2 t/2 = \cos(\varphi - \delta)/2 \cos\varphi \cos\delta \left[1 - \sin h/\cos(\varphi - \delta)\right]$$

This formula serves to determine the true local time from observations of the absolute altitude of the sun.

The actual process of observation consists in sighting the horizontal hairline of the theodolite telescope at the upper or lower rim of the sun and noting this point of time by reading the chronometer, and also taking readings on the vertical circle of the theodolite. In order to be able to find the absolute altitude of the center of the sun on the basis of readings of the vertical circle of the instrument it is necessary that the optic axis of the telescope be rotated to extend through the zenith, and that the position of the zenith on the circle be known. Moreover, the observed altitudes must be corrected for refraction, parallax of the sun, magnitude of the half-diameter of the sun and inclination of the level of the vertical circle.

Corrections for refraction r and parallax p are found in the Navigation Tables, and for the half-diameter of the sun are found in the Astronomical Yearbook.

In view of the fact that refraction at the sun altitudes less than 15° is not known with a sufficient degree of accuracy it is recommended that observations not be conducted at these altitudes.

To calculate errors in the determination of the hour angle t and the effects of errors in the determination of latitude φ and measurement of angle h, and also to determine the most advantageous conditions, equation (10.7) is differentiated, considering δ to be constant, in which case

$$\cos h\, dh = (\cos\varphi \sin\delta - \sin\varphi \cos\delta \cos t)\, d\varphi - \cos\varphi \cos\delta \sin t\, dt.$$

Declassified in Part - Sanitized Copy Approved for Release 2013/01/23 : CIA-RDP81-01043R001600090003-8

Declassified in Part - Sanitized Copy Approved for Release 2013/01/23 : CIA-RDP81-01043R001600090003-8

whence

$$dt = \cos\varphi \sin\delta - \sin\varphi \cos\delta \cos t/\cos \cos \sin t \; d\varphi - \cos h/\cos\varphi \cos \sin t \; dh.$$

In view of formula (10.6) for tg a, and formula (10.4), the above equation assumes the form:

$$dt = dh/\cos \sin a + d /\cos \operatorname{tg} a.$$

This expression shows that the least error in the determination of t depending upon errors in local latitude and in the altitude of the sun is obtained when the solar azimuths a approximate 90°, i.e., when the sun is close to the primary vertical. At $a = 90^\circ$

$$dt_{min} = dh/\cos$$

i.e., the error dt in this case is independent of the error d . The error of direct measurements of altitude h by a magnetic theodolite amounts to $\pm 30''$, and therefore the minimum error in the case of latitude $\varphi = 60^\circ$ will be:

$$dt = \pm 4 \text{ seconds.}$$

We have seen that for observation of the mire azimuth the chronometer correction must be known within an error of ± 4 seconds, therefore, the ascertained error $dt = 4$ seconds is entirely acceptible for determination of the azimuth.

Having calculated the hour angle t for the given altitude h of the sun and knowing the chronometer time T when the sun was sighted, the chronometer correction u relative to the true local time may be determined in accordance with the formula

$$u = t - T.$$

Tables 35 and 36 show the observation record charts and their processing, which illustrates the entire processing of the observations. To determine the location of the zenith on the vertical circle of the instrument the horizontal hairline of the theodolite telescope is sighted at some object with the circle at the right, and with the circle at the left. The average of these 2 readings gives the position of the zenith.

Declassified in Part - Sanitized Copy Approved for Release 2013/01/23 : CIA-RDP81-01043R001600090003-8

Declassified in Part - Sanitized Copy Approved for Release 2013/01/23 : CIA-RDP81-01043R001600090003-8

whence

$$dt = \cos\varphi \sin\delta - \sin\varphi \cos\delta \cos t/\cos\varphi \cos\delta \sin t \; d\varphi - \cos h/\cos\varphi \cos\delta \sin t \; dh.$$

In view of formula (10.6) for tg a, and formula (10.4), the above equation assumes the form:

$$dt = dh/\cos\varphi \sin a + d\varphi/\cos\varphi \operatorname{tg} a.$$

This expression shows that the least error in the determination of t depending upon errors in local latitude and in the altitude of the sun is obtained when the solar azimuths a approximate 90°, i.e., when the sun is close to the primary vertical. At $a = 90^\circ$

$$dt_{min} = dh/\cos\varphi$$

i.e., the error dt in this case is independent of the error $d\varphi$. The error of direct measurements of altitude h by a magnetic theodolite amounts to $\pm 30''$, and therefore the minimum error in the case of latitude $\varphi = 60^\circ$ will be:

$$dt = \pm 4 \text{ seconds.}$$

We have seen that for observation of the mire azimuth the chronometer correction must be known within an error of ± 4 seconds, therefore, the ascertained error $dt = 4$ seconds is entirely acceptible for determination of the azimuth.

Having calculated the hour angle t for the given altitude h of the sun and knowing the chronometer time T when the sun was sighted, the chronometer correction u relative to the true local time may be determined in accordance with the formula

$$u = t - T.$$

Tables 35 and 36 show the observation record charts and their processing, which illustrates the entire processing of the observations. To determine the location of the zenith on the vertical circle of the instrument the horizontal hairline of the theodolite telescope is sighted at some object with the circle at the right, and with the circle at the left. The average of these 2 readings gives the position of the zenith.

Declassified in Part - Sanitized Copy Approved for Release 2013/01/23 : CIA-RDP81-01043R001600090003-8

Declassified in Part - Sanitized Copy Approved for Release 2013/01/23 : CIA-RDP81-01043R001600090003-8

TABLE 35

CHART OF OBSERVATIONS FOR DETERMINATION OF CHRONOMETER CORRECTION BY THE ABSOLUTE ALTITUDE OF THE SUN

25 August 1920, position of zenith 98°20'

Approximate Chronometer Correction Relative to Mean Greenwich Time: 2 minutes 37 seconds, temperature $\vartheta = 14°$ C, pressure $p = 765$ mm. Value of one division of the level: 1'.

Position of Circle	Sighted at	Chronometer Readings	Level Readings	Vertical Circle Readings Vernier I	Vernier II	Average
L	$\overline{\odot}$	12 h.50m.14s.	+ 1.1	162° 32.5'	33.5	126° 33.0'
R	$\underline{\odot}$	12 57 15	0	33 48.0	42.5	33 42.7
R	$\underline{\odot}$	13 01 39	- 0.6	33 58	54.5	33 58.7
L	$\overline{\odot}$	13 07 12	+ 1.2	163 0.5	04.5	163 04.7

The declination of the sun is taken from the "Astronomical Yearbook" for the mean point of time of observations. Hence it is necessary to know the chronometer correction relative to mean Greenwich time and the local longitude. Temperature and pressure of the air are needed for determination of the refraction.

Determination of the Azimuth by Zenithal Distances of the Sun. A very convenient method for determination of the azimuth utilizes the zenithal distances of the sun and does not require separate determination of the chronometer correction.

In this case the observations consist of sighting the telescope of the sun in such a manner that the lower or upper rim of the solar disk is tangent to the horizontal hairline, and its right or left rim is tangent to the vertical hairline, i.e., is inscribed in the angle between the horizontal and the vertical hairlines of the

Declassified in Part - Sanitized Copy Approved for Release 2013/01/23 : CIA-RDP81-01043R001600090003-8

Declassified in Part - Sanitized Copy Approved for Release 2013/01/23 : CIA-RDP81-01043R001600090003-8

telescope. The observations are made by taking readings on the horizontal and vertical circles, and on the level; chronometer readings are not indispensible in this procedure if the chronometer corrections need not be determined for other purposes, such as determination of the local latitude. In order to be in a position to determine the declination of the sun from the "Astronomical Yearbook" the time need be determined within an accuracy of one minute.

Since the zenithal distance of the sun is known in this method of observation the azimuth of the sun may be determined by formula (10.3), which gives:

$$\cos a = \cos z \sin\varphi - \sin\delta / \sin z \cos\varphi$$

Adding or substracting unity from both halves of this equation and replacing $1 - \cos a$ and $1 + \cos a$ by $\cos^2 a/2$ and $\sin^2 a/2$, following simple transformations we obtain:

$$\sin^2\frac{a}{2} = \frac{\sin\frac{z-\varphi+\delta}{2}\cos\frac{z-\varphi-\delta}{2}}{\sin z \cos\varphi},$$

$$\cos^2\frac{a}{2} = \frac{\sin\frac{z+\varphi-\delta}{2}\cos\frac{z+\varphi+\delta}{2}}{\sin z \cos\varphi}$$

The first of these formulas is used when the absolute values of a/2 are less than 45°, and the second when they are greater than 45°.

The navigation tables contain the logarithms of $\sin^2 a/2$ and $\cos^2 a/2$, therefore, having found the logarithm of the right-hand portion, it is possible to find a from the logarithm.

As in the preceding instances the observations are carried out with the circles R and L and with different positions of the sun in relation to the hairlines, for example with the 4 positions indicated in the chart: $\frac{L}{10}$, $\frac{R}{10}$, $\frac{R}{01}$, $\frac{L}{01}$.

Declassified in Part - Sanitized Copy Approved for Release 2013/01/23 : CIA-RDP81-01043R001600090003-8

Declassified in Part - Sanitized Copy Approved for Release 2013/01/23 : CIA-RDP81-01043R001600090003-8

TABLE 36

CHART OF CALCULATIONS OF THE CHRONOMETER CORRECTION BY ABSOLUTE ALTITUDE OF THE SUN

φ = 69 43.2'
λ = 66'43' o of Greenwich

r = - 2.0 φ δ = 58°54.8'
p = + 0.1
r-p = - 1.9

Mean point of time 12 h 58 m δ = 10°47.0'
- 2 37 + 1.4
10 h 21 m 10°48.4'

lg cos(φ - δ) = 9.71292
lg secφ = 9.46016
lg secδ = 0.00775
lg o.5=9.69897
Σ = 9.87980

Circle readings	162°33.0'	33°42.7'	33°58.7'	163°04.7'
Correction for level	+1.1	0.0	+0.6	+1.2
	162 34.1	33 42.7	33 58.1	163 05.9
Zero point correction	-8-20.20	-8 20	-8 20	-8 20
	154 14.1	25 22.7	25 38.1	154 45.9
Observed altitude	25 45.9	25 22.7	25 38.1	25 14.1
Correction for refraction and parallax	25 44.0	25 20.8	25 36.2	25 12.2
Correction for half-diameter of sun	+15.9	+15.9	-15.9	-15.9
Corrected altitude h	25 59.9	25 36.7	25 20.3	24 56.3
lg sin h	9.64181	9.63575	9.63141	9.62495
lg sin h/cos (φ - δ)	9.92889	9.92283	9.91849	9.91203
R= lg 1-lg sin h/cos (φ - δ)	0.07111	0.7717	0.08154	0.08797
Δ1	0.820911	0.78834	0.76655	0.75670
lg$\sqrt{1-\sin h/\cos(\varphi - \delta)}$	9.17906	0.21166	0.23375	0.26330
lg $\sin^2$ t/2	9.05886	9.09146	9.11325	9.14310
t	2 h 38 m 14 s	2 h 44 m 33 s	2 h 48 m 57 s	2 h 55 m 08 s
Chronometer T	12 12 50	14 12 57 15	13 01 39	13 07 12
u = t - T	1 48 0	1 47 18	1 47 18	1 47 56

Mean .... u = - 1 h 47 m 38 s.

As is shown by differentiation of equation (10.3), the observation conditions wherein the sun is at the primary vertical, or near the horizon are the most advantageous. In these instances the error in determination of the azimuth is given by the correlation:

$$\Delta a = \operatorname{tg}\varphi \, \Delta z$$

Declassified in Part - Sanitized Copy Approved for Release 2013/01/23 : CIA-RDP81-01043R001600090003-8

Declassified in Part - Sanitized Copy Approved for Release 2013/01/23 : CIA-RDP81-01043R001600090003-8

On approaching the meridian this error increases rapidly, and with azimuths of less than 30° the observations cannot be carried out.

A chart of the observations and computations is shown in tables 37 and 38.

TABLE 37

CHART OF AZIMUTH OBSERVATIONS BY THE ZENITHAL DISTANCES OF THE SUN

25 August 1920

Chasselon theodolite No 85; chronometer correction relative to Greenwich time: 2 hours 37 minutes

Circle and Sighting at	Vertical Circle Readings				Horizontal Circle Readings		
	Level	Vernier I	Vernier II	Mean	Vernier I	Vernier II	Mean
R mire					56°21.5'	21.0'	56°21.2'
L mire					236 20.0	20.0	236 20.0
L ☉	-0.1/2.3	162°32.5'	33.5'	162°33.0'	275 01.5	0.10	275 01.2
R ☉	-1.2/1.1	34 43.0	42.5	33 42.7	97 04.0	03.0	97 03.5
R ☽	-1.9/0.7	33 58.0	59.5	33 58.7	98 47.5	47.0	98 47.2
L ☽	-0.0/2.4	163 05.0	04.5	163 04.7	280 03.5	03.0	280 03.2
L mire					236 20.0	20.0	236 20.0
R mire					56 20.5	20.5	56 20.5

[See Table 38 on the following page]

Declassified in Part - Sanitized Copy Approved for Release 2013/01/23 : CIA-RDP81-01043R001600090003-8

Declassified in Part - Sanitized Copy Approved for Release 2013/01/23 : CIA-RDP81-01043R001600090003-8

TABLE 38

CHART OF CALCULATION OF MIRE AZIMUTH BY ZENITHAL DISTANCES OF THE SUN

φ = 69°43.2'; λ = 10°48.4'; $\varphi - \lambda$ = 40°15.8'; $\varphi + \lambda$ = 29°27.4'.

Vertical Circle Readings	162°33.0'	33°42.7'	33°58.7'	163°4.7'
Correction for level	01.1	0.0	-0.6	01.2
z	64 14.1	64 37.3	64 21.9	64 45.9
Refraction + parallax	01.9	01.9	01.9	01.9
R ⊙	-15.9	-15.9	-15.9	-15.9
z	64 00.1	64 23.3	65 39.7	65 03.7
z/2	32 00.0	32 11.6	32 19.9	32 31.8
$(z - \varphi + \delta)$: $2 = S_1$	2 32.6	2 44.2	2 52.5	3 04.4
$(z - \varphi - \lambda)$: $2 = S_2$	8 15.8	8 04.2	7 55.9	7 44.0
lg sin S_1	8.647138	8.678933	8.700333	8.729500
lg cos S_2	9.995467	9.995677	9.995825	9.996032
lg sin S_1 cos S_2	8.642605	8.674610	8.696158	8.725532
lg sin z	9.953666	9.955083	9.956071	9.957490
lg cos φ	9.539840	9.539840	9.539840	9.539840
lg sin z cos φ	9.493506	9.494923	9.495911	9.497330
lg $\sin^2$ a/2	9.149099	9.179687	9.200247	9.228202
a/2	22°03.1'	22°53.2'	23°28.0'	24°16.6'
a	44 06.2	45 46.4	46 56.0	48 33.2
Horizontal circle reading	95 18.7	97 21.0	98 29.7	99 45.2
Position S	51 12.5	11 34.6	51 33.7	51 12.5

Section 4. Measurement of Dip with a Needle Inclinator.

The underlying principle of the measurements. In a uniform magnetic field, such as the terrestrial magnetic field, a permanent magnet in the absence of additional external forces assumes a position in which its magnetic axis is aligned with the direction of the lines

Declassified in Part - Sanitized Copy Approved for Release 2013/01/23 : CIA-RDP81-01043R001600090003-8

Declassified in Part - Sanitized Copy Approved for Release 2013/01/23 : CIA-RDP81-01043R001600090003-8

of force of the magnetic field. Therefore if its center of gravity coincides with the rotation axis a freely rotating magnetic needle within the plane of the magnetic meridian will assume a position in which its magnetic axis is parallel to the direction of the lines of force of the terrestrial field. Thus, with the plane of rotation of such a needle set within the plane of the magnetic meridian the dip is determined by measuring the angle between the magnetic axis and the horizontal plane. The instrument based upon this principle is called a needle inclinator.

Description of the instrument. The inclinator, which is shown in Figure 200, is composed of a horizontal circle with 3, adjusting screws, and a vertical circle which together with the arm, rotates about the vertical axis. The axis of the vertical circle has horizontal agate bearings a which support the axis c and c_1 of the magnetic needle M. The needle has the shape of a narrow blade with pointed tips (Figure 201). To guard against air vibrations the needle is contained within a wooden housing, the front and rear walls of which are made of glass. The alidade of the vertical circle has a microscope at either end, which are used in sighting the tips of the needle.

The needle is aligned with the axis of the vertical circle and is dampened by means of a checking device consisting of 2 pins which may be raised to engage the axis of the needle, thereby centering it. The vertical and horizontal circles have division marks at 30' intervals, and readings are taken by means of verniers. The zero marks of the vertical circle are at the horizontal axis and the scale division of the vertical circle run in both directions, i.e., up and down to 90°.

Setting the inclinator along the magnetic meridian. To obtain correct readings of a needle inclinator the plane of oscillation of the

Declassified in Part - Sanitized Copy Approved for Release 2013/01/23 : CIA-RDP81-01043R001600090003-8

Declassified in Part - Sanitized Copy Approved for Release 2013/01/23 : CIA-RDP81-01043R001600090003-8

needle is set parallel to the magnetic meridian. This is done by taking advantage of the fact that when the plane of oscillations coincides with the plane perpendicular to the magnetic meridian the needle assumes a vertical position. Therefore, when the needle comes to rest with respect to vertical circle a reading is taken on the horizontal circle and then the plane of the vertical circle is rotated 90°, thereby setting it along the magnetic meridian.

In theoretical substantiation of the above method let us assume that the plane of rotation of the needle, i.e., the plane of the vertical circle, forms an angle φ with the plane of the magnetic meridian.

In such a case the forces acting upon the needle include the vertical component Z and a projection of the horizontal component upon this plane, H cos φ. The second component H sin φ is counterbalanced by the reaction of the support. Therefore, in the triangle OZH_T (Figure 202) the angle I which the magnetic axis of the needle forms with the horizontal plane is defined by the following equation:

$$\operatorname{tg} I' = Z/H \cos \varphi . \qquad (10.8)$$

Hence it follows that at $\varphi = 0$

$$\operatorname{tg} I' = Z/H = \operatorname{tg} I,$$

where I is the dip, i.e., when the plane of oscillations coincides with the plane of the meridian the angle between the magnetic axis of the needle and the horizon coincides with the dip I.

At $\varphi = 90^{\circ}$ the tangent of the angle of dip is equal to infinity, and consequently $I' = 90^{\circ}$, i.e., the needle assumes a vertical position.

Errors in measurement. Let us determine first the error which may result in the determination of dip I, when the plane of rotation of the needle forms an angle $\Delta\varphi$ with the magnetic meridian.

Declassified in Part - Sanitized Copy Approved for Release 2013/01/23 : CIA-RDP81-01043R001600090003-8

Declassified in Part - Sanitized Copy Approved for Release 2013/01/23 : CIA-RDP81-01043R001600090003-8

To do this we differentiate equation (10.8) and obtain:

$$\frac{\Delta I'}{\cos I' \sin 1'} = -\operatorname{tg} q \, \Delta\varphi,$$

hence, at $I = I'$: $\Delta I = -\sin I \cos I \operatorname{tg} q \, \Delta\varphi$

But it has been specified that $q = \Delta I$, therefore, in view of the smallness of ΔI, upon replacing the tangent by the angle, we obtain: $\Delta I = -\sin I \cos I \sin 1' \Delta\varphi^2 = -\frac{\sin 2I}{2} \sin 1' \Delta\varphi^2$,

where ΔI and $\Delta\varphi$ are expressed in minutes of arc.

At $I = 72^\circ$, which is at the magnitude of dip at Leningrad:

In order that the error in determination of ΔI does not exceed a predetermined quantity ΔI the plane of rotation of the needle must parallel the magnetic meridian within an error $\Delta\varphi$ not exceeding

$$\Delta\varphi \leq \sqrt{\frac{\Delta I}{0.000086}} = 108 \sqrt{\Delta I}$$

Thus, for example, at $\Delta I = 1'$ the error $\Delta\varphi = 108' \sim 2^\circ$, i.e., the error in setting the inclinator in the plane of the magnetic meridian may be as high as $\pm 2^\circ$ when the error in determination of I is within $\pm 1'$.

In addition to the error ΔI caused by departure of the plane of needle oscillation from the plane of the magnetic meridian several other errors may arise in the use of the needle inclinator due to imperfections in the instrument itself. These include: (1) the axis of rotation of the needle does not coincide with the center of the circle, (2) the horizontal axis of the vertical circle does not coincide with the horizontal plane, (3) the magnetic axis of the needle does not coincide with its geometric axix, (4) the center of gravity of the needle does not coincide with the axis of rotation (5) friction between the needle axis and the agate bearings, and (6) non-cylindrical shape of the needle axis.

Declassified in Part - Sanitized Copy Approved for Release 2013/01/23 : CIA-RDP81-01043R001600090003-8

Declassified in Part - Sanitized Copy Approved for Release 2013/01/23 : CIA-RDP81-01043R001600090003-8

The first 3 errors can be fully eliminated by proper combination of observations, and the fourth may be eliminated by observing certain rules, but the last 2 cannot be eliminated under any conditions and only one of them, friction, may be reduced by a sufficient number of observations.

The non-coincidence of the axis of rotation of the needle with the center of the vertical circle, or eccentricity, is eliminated by observation of both the upper and lower tips of the needle.

The error due to the fact that the horizontal axis of the vertical circle does not coincide with the horizontal plane may be eliminated by rotating the plane of the vertical circle 180° about the vertical axis, since upon such rotation the inclination of the axis in relation to the horizon is changed in the opposite direction.

The error due to the fact that the center of gravity does not coincide with the axis of rotation may be partially or fully eliminated by changing the magnetization of the needle and carrying out observation before and after the change in magnetization.

The theory shows that error due to the difference between the center of gravity of the needle and its axis of rotation does not exceed ± 1' if the difference in readings before and after change in magnetization does not exceed 2°, provided further that the magnetic moment of the needle before and after change in magnetization is the same. This condition is most readily fulfilled if the magnetism is reversed to complete saturation for every observation of the needle.

To magnetize the needle it is placed into the socket of a special wooden support and rubbed with the tips of 2 permanent magnets

Declassified in Part - Sanitized Copy Approved for Release 2013/01/23 : CIA-RDP81-01043R001600090003-8

Declassified in Part - Sanitized Copy Approved for Release 2013/01/23 : CIA-RDP81-01043R001600090003-8

of opposite polarity (Figure 203). The needle is rubbed by circular movements from the middle of the needle toward one end and then the other.

Errors due to friction at the needle axis due to noncylindrical shape of the axis cannot be eliminated and are included in their entirety in the results of the observations. To reduce this error the axis pivots of the magnetic needle are made in the shape of circular cylinders, which roll in the agate bearings and thus produce rolling friction, which is considerably less than sliding friction. Additional care must be taken that the pivots and bearings are always clean and free from dust or moisture. For this purpose the needle and bearing should be wiped off before observations are performed.

The magnitude of the error induced by friction varies from one to several minutes depending upon the quality of the needle pivots. Therefore the maximum accuracy with which dip may be determined by means of a needle inclinator does not exceed $\pm 2'$.

Sequence of observations. In accordance with the foregoing, observation by means of a needle inclinator is performed in the following basic stages. Determination of the magnetic meridian on the horizontal circle for the purpose of setting the plane of the vertical circle parallel to the meridian; determination of the dip after magnetization of the needle and again after changing the magnetization of the needle. To eliminate the errors described above the observations of dip and determination of the meridian must be performed consecutively and in accordance with a definite system which is shown as an example in Table 39.

Declassified in Part - Sanitized Copy Approved for Release 2013/01/23 : CIA-RDP81-01043R001600090003-8

Declassified in Part - Sanitized Copy Approved for Release 2013/01/23 : CIA-RDP81-01043R001600090003-8

TABLE 39

ORDER OF OBSERVATIONS USING A NEEDLE INCLINATOR, KOLGUYEV ISLAND, ESTUARY OF GUSINA RIVER

4 August 1920, Inclinator No 195, Needle No 3

DETERMINATION OF THE MERIDIAN

Position of Vertical Circle	Position of Needle Mark	Horizontal Circle Readings: Upper tip of needle	Lower tip of needle	Mean
N	N	34°06'	31°51'	30°58.5'
S	S	34 05	35 21	32 43.0
S	N	31 26	30 12	30 49.0
N	S	31 36	32 47	32 11.5
			Mean	31°40.5'

DETERMINATION OF DIP

Chronometer No 2423. Chronometer correction to local mean time +38"

	Time by chronometer	Position of vertical circle	Position of needle mark	Vertical Circle Readings: upper tip	lower tip	Mean
Needle magnetized A-up	16 h 17 m	E	E	77°53'	78°14'	77°63.5'
		W	W	77 26.5	77 17	77 21.7
	16 24	W	E	78 01.5	77 52	77 56.7
		E	W	77 15.5	77 37.5	77 26.5
Needle magnetization reversed A-down	16 32	E	E	77 25.5	77 53.5	77 38.0
		W	W	77 59.4	77 47	77 53.0
	16 38	W	E	77 40.5	77 31	77 35.8
		E	W	77 30	77 53	77 41.5
				Mean		I = 77°42'

Section 5. Measurement of Dip by Means of an Induction Inclinator.

Underlying Principle of the Measurements. Measurement of dip by means of the induction inclinator is based upon the phenomenon of induction within a closed circuit rotating in a uniform magnetic field.

According to Faraday's Law the electromotive force of induction $\mathcal{E}$ (e.m.f.) generated within the circuit is:

$$\mathcal{E} = - d\Phi / dt, \qquad (10.9)$$

Declassified in Part - Sanitized Copy Approved for Release 2013/01/23 : CIA-RDP81-01043R001600090003-8

Declassified in Part - Sanitized Copy Approved for Release 2013/01/23 : CIA-RDP81-01043R001600090003-8

where Φ is the magnetic flux passing through the circuit and t is time. As is shown below, the emf is equal to zero if the rotation axis of the circuit coincides with the direction of the lines of force of the magnetic field. Therefore, by rotating a circular circuit in the magnetic field of the earth, the current in the circuit, which is registered by a galvanometer, may be made equal to zero by changing the position of the rotation axis. In such a case the angle between the axis of rotation of the circuit and the horizontal plane will be equal to the angle of dip.

Design of the Induction Inclinator. The principle of operation of the induction inclinator is shown in Figure 204. The horizontal circle A has 2 supports B and B' on which the horizontal axis aa' of the circular ring C is set in bearings. Perpendicular to the axis aa' is a second axis bb' around which a closed circuit flows through a circular coil K, the center of which coincides with the center of ring C. The supports BB' can rotate over the horizontal circle and around the vertical axis ZZ'. At one of the supports is a vertical circle D, through the center of which the axis aa' passes.

To bring the axis of coil bb' parallel to the lines of force of the magnetic field of the earth by means of a compass the horizontal axis aa' is first set perpendicularly to the magnetic meridian, then by changing the slant of axis bb', i.e., by turning the slanting ring C around the horizontal axis and rotating the coil K, which is connected in series to the galvanometer, an adjustment is made so that the galvanometer registers no current. The angle of inclination of the axis of rotation bb' corresponding to the absence of current and equal to I, is measured on the vertical circle D.

Figure 205 shows an external view of the instrument.

Declassified in Part - Sanitized Copy Approved for Release 2013/01/23 : CIA-RDP81-01043R001600090003-8

Declassified in Part - Sanitized Copy Approved for Release 2013/01/23 : CIA-RDP81-01043R001600090003-8

Theory of the Induction Inclinator. First, let us demonstrate that the current in the circuit is equal to zero if its axis of rotation coincides with the direction of the magnetic field.

We circumscribe a sphere of arbitrary radius around the inclinator, the center of which coincides with the center of coil K and ring C, taking the plane of ring C as the plane of the drawing, and taking the axis bb' as intersecting with the sphere at points b and b' (Figure 206).

In such a case the vertical plane extending through the rotation axis bb' will intersect our sphere along the great circle arc bZb', which at point b will form a 90° angle with the plane of the drawing, and the vertical axis extending through the center will intersect the sphere at point Z, located on the great circle arc bZb'.

Further, we draw a plane extending through the circuit K and intersecting our sphere along the great circle arc bKb'. The normal to the plane of the circuit, extending through the center of the coil, will intersect the sphere at the point n located on the great circle arc MKnN which is perpendicular to the plane of the drawing, and the arc Kn = 90°. Finally, we draw the line OF through the center of the sphere, which is parallel to the lines of force of the magnetic field.

Next, the points b, n and F are connected by arcs of great circles, forming spheric triangle nbF, in which the side bn = 90°. In accordance with the definition the magnetic flux Φ passing through the coil is expressed as follows:

$$\Phi = H_T S w \cos(n, H_T), \qquad (10.10)$$

where H_T is the intensity of the earth's magnetic field coinciding with

Declassified in Part - Sanitized Copy Approved for Release 2013/01/23 : CIA-RDP81-01043R001600090003-8

Declassified in Part - Sanitized Copy Approved for Release 2013/01/23 : CIA-RDP81-01043R001600090003-8

the direction OF, S is the area of the circuit, W the number of windings and n the normal to the plane of the circuit.

The cosine of the angle between normal n and intensity H_T is determined from the spheric triangle nbF:

$$\cos(n, H_T) = \sin\gamma \cos\varphi, \qquad (10.11)$$

where γ is the angle between the rotation axis bb' and the direction H_T, and φ is the dihedral angle formed by plane γ and the plane extending through normal n and the axis bb'.

We denote by α the angle MbK between the plane of the inclination ring MbN and the plane of the coil circuit bKb'; and by ε the angle ZbF between the vertical plane extending through the coil rotation axis bb' and the plane of angle γ.

Then, since angles MbZ and Kbn are equal to 90°, angle φ may be expressed as follows:

$$\varphi = 90° + \alpha - (90° - \varepsilon) = \alpha + \varepsilon, \qquad (10.12)$$

where ε is a constant quantity, and α a variable which indicates how far the plane of the coil has turned away from the stationary plane of the inclination ring.

By means of equations (10.10), (10.11) and (10.12) we find:

$$\Phi = H_T Sw \sin\gamma \cos(\varepsilon + \alpha).$$

Substituting this value in equation (10.9) we obtain:

$$E = H_T Sw \sin\gamma \sin(\varepsilon + \alpha)\, d\alpha/dt$$

where $d\alpha/dt$ is the angular velocity of rotation of the coil K, which may be replaced by the number of revolutions per second N by using the correlation

$$d\alpha/dt = 2\pi N.$$

Declassified in Part - Sanitized Copy Approved for Release 2013/01/23 : CIA-RDP81-01043R001600090003-8

Declassified in Part - Sanitized Copy Approved for Release 2013/01/23 : CIA-RDP81-01043R001600090003-8

and the angle α may be replaced by a constant speed of rotation, in accordance with the formula $\alpha = 2\pi Nt$.

Hence

$$\mathcal{E} = 2\pi H_T SwN \sin\gamma \sin(\varepsilon + \alpha) = 2\pi H_T SwN \sin\gamma \sin(2\pi Nt + \varepsilon). \qquad (10.13)$$

Consequently the electromotive force of induction $\mathcal{E}$ on rotation of the coil varies in accordance with the sinusoidal law depending on time t, since all the quantities in formula (10.13), except t, are constants.

From equation (10.13) it follows that $\mathcal{E} = 0$ when $\gamma = 0$, i.e., when the axis of rotation of coil K coincides with the direction of field H_T, which was to be demonstrated.

The angle γ between the axis of rotation of the coil and the direction of the magnetic field OF, may be divided into 2 angles, the angle formed by the axis of rotation with the horizontal plane, which we shall denote by I_k, and the angle of deflection A of the vertical plane bZb'O in relation to the plane of the magnetic meridian OZF.

The difference between the angle of dip I and the angle I_k, i.e., $I-I_k$, represents the error in setting the rotation axis B parallel to the plane of the magnetic meridian, and angle A is the error in setting the plane of rotation within the magnetic meridian i.e., the azimuthal error of the setting.

The effect of each error upon the measurement error differs, and to find this difference angle γ must be expressed by angles I_k and A in equation (10.13).

In the spheric triangle ZbF, where the arc ZF represents the intersection of the plane of the magnetic meridian with the sphere and is equal to the complement of the angle of dip I, while the arc $Zb = 90^\circ - I_k$, we obtain:

Declassified in Part - Sanitized Copy Approved for Release 2013/01/23 : CIA-RDP81-01043R001600090003-8

Declassified in Part - Sanitized Copy Approved for Release 2013/01/23 : CIA-RDP81-01043R001600090003-8

$$\sin\gamma\sin\varepsilon = \cos A\cos I,$$
$$\therefore I = \cos\gamma\sin I_k + \sin\gamma\cos I_k\cos\varepsilon,$$
$$\cos\gamma = \sin I\sin I_k + \cos I\cos I_k\cos A \qquad (10.14)$$

From the second equation we have $\sin\gamma\cos\varepsilon = \dfrac{\sin I - \cos\gamma\sin I_k}{\cos I_k}$,

or, on substituting for $\cos\gamma$ its value taken from the third equation:

$$\sin\gamma\cos\varepsilon = \sin I\cos I_k - \cos I\sin I_k\cos A \qquad (10.15)$$

Equation (10.13) is further transformed by substitution of the constant factor $2\pi H_0 S w N = Q$ and expanding $\sin(\varepsilon + \alpha)$ in accordance with trigonometric formulas, so that

$$\mathcal{E} = Q[\sin\gamma\cos\varepsilon\cos\alpha + \sin\gamma\cos\varepsilon\sin\alpha]$$

Substituting their values from equations (10.14) and (10.15) for $\sin\gamma\sin\varepsilon$ and $\sin\gamma\cos\varepsilon$ we obtain

$$\mathcal{E} = Q[\sin A\cos I\cos\alpha + (\sin I\cos I_k - \cos I\sin I_k\cos A)\sin\alpha]$$

At $A = 0$, i.e., when the axis of rotation is within the plane of the magnetic meridian: $\mathcal{E} = Q\sin(I_k - I)\sin\alpha$

If the difference $I_k - I$ is not large for the largest value of α we obtain the expression: $\mathcal{E}_{max} = Q\sin 1'(I_k - I)$. (10.16)

At $I_k = I$, i.e., when the angle between the axis of rotation and the horizontal plane is equal to the dip, but is displaced on the azimuth by an angle $A = \angle A$, we have

$$\mathcal{E} = Q[\sin\Delta A\cos I\cos\alpha + \sin I\cos I(1-\cos\Delta A)\sin\alpha].$$

If ΔA is not large it follows that $\sin\Delta A = \angle A \sin 1'$ and $\cos\angle A = 1$, hence the maximum value $\mathcal{E}_{max}$ is expressed:

$$\mathcal{E}_{max} = Q\cos I\sin 1'\Delta A \qquad (10.17)$$

Consequently, at $\angle A = I - I_k$ the electromotive forces have different values.

From correlations (10.16) and (10.17) we obtain the necessary accuracy with which the axis of rotation must be set within the magnetic meridian in order that the error due to incorrect setting in the determination of I does not exceed $\Delta I = I_k - I$. Dividing equations (10.16) and (10.17), term by term, we obtain

$$\Delta A = \Delta I\sec I, \qquad (10.18)$$

Declassified in Part - Sanitized Copy Approved for Release 2013/01/23 : CIA-RDP81-01043R001600090003-8

Declassified in Part - Sanitized Copy Approved for Release 2013/01/23 : CIA-RDP81-01043R001600090003-8

i.e., the error in azimuth setting can be sec I-times greater than the error permissible in the measurement of I. The greater the value of I, the larger is the permissible error ΔA. At $I = 72^{\circ}$ we have sec $I = 4$, and therefore $\Delta A \quad 4 \cdot \Delta I$.

Equation (10.17) makes it possible to determine the least magnitude of error in measurement of I caused by error in measuring the electromotive force $\mathcal{E}$. We have $\Delta I = \frac{\mathcal{E} \cdot \ldots}{\ldots}$,

or, expressing $\mathcal{E}_{max}$ in volts: $\Delta I = \frac{\mathcal{E}}{\ldots}$

The smallest electromotive force that can be measured by means of a galvanometer is approximately 10^{-5} v. Therefore, in the case of a 2,000-turn coil 10 cm in diameter and rotating at a rate of 10 rps, considering that $H_T = 0.5$ Oe, we have: $\Delta I = 0.\ldots$

To increase the accuracy of the measurement of I the direct method is replaced by an indirect method, in which the absence of current, and not an electromotive force is the factor observed. However, in view of the fact that the current induced in the coil is an alternating current, and the instruments which measure an alternating current are not sufficiently sensitive, this current must be rectified.

The method most extensively used is that of academician Vil'd, who utilized a commutator for this purpose, consisting of 2 cylindrical casings set on the axis of the coil. Each casing is connected to the ends of the coil and the casings are insulated from each other. The casings are in contact with stationary brushes. When the brushes pass from one casing to the other the direction of the current in the external circuit changes.

Because of the presence of a commutator and the fact that due to the self-induction and capacitance of the circuit the current in

Declassified in Part - Sanitized Copy Approved for Release 2013/01/23 : CIA-RDP81-01043R001600090003-8

Declassified in Part - Sanitized Copy Approved for Release 2013/01/23 : CIA-RDP81-01043R001600090003-8

the coil does not coincide in phase with the electromotive force, different conditions arise for the absence of a current in the circuit, and in certain instances the current in the circuit is equal to zero although the axis of rotation forms an angle γ with the direction of the lines of force of the magnetic field.

Let us consider this question from a theoretical point of view. Taking the plane of commutation as the plane which through the generatrixes of the cylindrical casings described by the contact between brushes and commutator, and the angle between the plane of inclination and the plane of commutation is taken as the angle of shift of the brushes, denoted by β.

We shall assume further that the casings of the commutator are secured on the cylindrical axis of rotation in such a manner that a diameter drawn through the gaps between the casings is parallel to the plane of the windings of the coil.

The intensity of the alternating current i, in the absence of self-induction and capacitance of the circuit, is given by the formula:

$$i = \frac{\varepsilon}{R} = \frac{G}{R} \omega \gamma \sin(\alpha - \varepsilon)$$

If the brushes are shifted through an angle β, switching over will take place at: $\alpha = \beta \quad \beta + \pi, \quad \beta + 2\pi$ and so forth.

Therefore the mean intensity of the alternating current i_m which flows through the galvanometer between 2 consecutive switch overs will be:

$$i_m = \frac{1}{\pi} \int_{\beta}^{\beta+\pi} i \, d\alpha = \frac{2G}{\pi R} \omega \gamma \cos(\beta + \varepsilon),$$

or, expanding the cosine in accordance with trigonometric formulas:

$$i_m = \frac{2Q}{\pi R} (\omega \gamma \cos\varepsilon \cos\beta - \omega \gamma \sin\varepsilon \sin\beta).$$

We replace $\sin\gamma\cos\varepsilon$ and $\sin\gamma\sin\varepsilon$ by their expressions derived from equations (10.14) and (10.15), and obtain:

$$i_m = \frac{2Q}{\pi R} [\omega (I \cos I_K - \cos I \sin I_K \cos A) \cos\beta - \cos I \sin A \sin\beta]. \quad (10.19)$$

Declassified in Part - Sanitized Copy Approved for Release 2013/01/23 : CIA-RDP81-01043R001600090003-8

Declassified in Part - Sanitized Copy Approved for Release 2013/01/23 : CIA-RDP81-01043R001600090003-8

Hence it is apparent that i_m can be equal to zero not only at $A = 0$ and $I = I_k$, but also when

$$\cos I \cos I_k - \cos I \sin I_k \cos A = \cos I \sin A \operatorname{tg} \beta.$$

Since $I_k - I$ and A usually are small, it follows that on substituting $\sin A = \leq A \sin 1'$ $\sin(I - I_k) = \Delta I \sin 1'$, and $\cos A \; 1 - \frac{1}{2} A^2 \sin^2 1'$, we obtain the following formula, in which ΔA and ΔI are expressed in minutes of arc:

$$\Delta I = \cos I \operatorname{tg} \beta \Delta A - \tfrac{1}{4} \sin 2I \sin 1' \Delta A^2, \qquad (10.20)$$

that is, in the absence of a current in the galvanometer the measured angle between the axis of rotation and the horizontal plane can differ from the angle of dip by the quantity ΔI, which depends upon the angle of shift of the brushes β, and on the incorrectness in setting with respect to the magnetic meridian.

If the angle of shift of the brushes $\beta = 0$, it follows that:

$$\Delta I = -\tfrac{1}{4} \sin 2I \sin 1' \Delta A^2 \qquad (10.21)$$

In this case the difference ΔI between the measured and the true angle of dip depends only on the incorrectness in setting the axis of rotation within the plane of the magnetic meridian.

In this derivation the capacitance C and self-induction L of the circuit of the coil and galvanometer were not taken into account. Their existence causes a shift in the current relative to the electromotive force by an angle φ, which is called the phase difference and is determined by means of a correlation that is derived in the theory of alternating currents:

$$\operatorname{tg} \varphi = \frac{\omega L}{R} - \frac{1}{CR\omega},$$

where w is the angular velocity of coil rotation.

An analogous effect would be obtained if the coil had neither capacitance nor self-induction, but the brushes were shifted through

Declassified in Part - Sanitized Copy Approved for Release 2013/01/23 : CIA-RDP81-01043R001600090003-8

Declassified in Part - Sanitized Copy Approved for Release 2013/01/23 : CIA-RDP81-01043R001600090003-8

an angle $\beta \neq \varphi$. Consequently, in the presence of capacitance and self-induction the angle I_k corresponding to an absence of current in the galvanometer, may differ by a quantity ΔI determined by equation (10.20), in which it is necessary only to replace the angle β by an angle $\beta \neq \varphi$.

Errors of an Induction Inclinator and their Elimination. Theory shows that the sources of error in measurement of the dip by means of an induction inclinator can be the following: (1) the plane extending through the axis of rotation does not coincide with the plane of the magnetic meridian, (2) the presence of an angle of shift of the commutator brushes, (3) the presence of capacitance and self-induction in the circuit, (4) the horizontal axis of the vertical circle does not coincide with the horizontal plane, (5) the axis of rotation is not perpendicular to the horizontal axis of the circle, and (6) thermoelectric current.

The first error is eliminated by setting the axis of rotation within the plane of the magnetic meridian within an error limit which ensures the absence of a permissible error in determination of the dip I.

From equation (10.21) we have: $\Delta A' = \pm 2' \sqrt{\frac{\Delta I}{\sin 2I \ldots}}$ ', at $\Delta I = 0.1'$ and $I = 72°$:

whereas in measuring the electromotive force the error in setting the axis of rotation equal to the azimuth must not exceed $\pm$ 0.4' [see (10.18)].

The setting along the meridian is done with the aid of a compass at an error of $\pm$ 0.1°, and fully ensures that no error will occur in the determination of the dip I.

Declassified in Part - Sanitized Copy Approved for Release 2013/01/23 : CIA-RDP81-01043R001600090003-8

Declassified in Part - Sanitized Copy Approved for Release 2013/01/23 : CIA-RDP81-01043R001600090003-8

The error caused by the shift of the brushes is eliminated by turning the axis of rotation 180° about the horizontal axis, i.e., by carrying out observations at 2 different positions of the commutator: with the commutator upward and with the commutator downward. If at one position of the commutator the angle of shift was β, on turning the axis of rotation 180° the sign of the angle β will change, and in one instance the error will be

$$I - I_k = \Delta I = \cos I \operatorname{tg} \beta \cdot A,$$

and in the other instance

$$I - I'_k = \Delta I = -\cos I \operatorname{tg} \beta \cdot A.$$

The mean of the 2 readings I and I_k will be free from the error Δ I, since

$$I_k + I'_k/2 = I.$$

The above method of turning the axis to eliminate error caused by self-induction and capacitance fails to produce the desired result since the corresponding shifts in current phase will be $\beta + \gamma$ and $-\beta + \gamma$, and consequently the error determined by equation (10.20) in the presence of angle γ is not eliminated. To eliminate this error observations of the angle I_k on turning the coil in 2 opposite directions, clockwise and counter-clockwise, are used, since this results in opposite signs for angle γ, as is apparent from equation (10.20).

The effects caused by the non-perpendicular position of the rotation axis, and the condition in which the horizontal axis of the vertical circle does not coincide with the horizontal plane are eliminated by carrying out observations at 2 positions of the vertical circle, one to the E and the other to the W.

During rotation of the coil the brushes become heated due to friction against the commutator and a thermoelectric current may be generated in the circuit, which may distort the observational results.

Declassified in Part - Sanitized Copy Approved for Release 2013/01/23 : CIA-RDP81-01043R001600090003-8

Declassified in Part - Sanitized Copy Approved for Release 2013/01/23 : CIA-RDP81-01043R001600090003-8

The effect of the thermoelectric current may be eliminated by rotating the coil clockwise and counter-clockwise. According to equation (10.19), taking $\beta = 0$, $A = 0$ and $\sin (I - I_k) = (I - I_k) \sin 1'$:

$$i_m = 2Q/\pi R (I - I_k) \sin 1'.$$

If there is no current in the galvanometer and there is a thermocurrent i_o in the circuit $i_m + i_o = 0$

that is: $$2Q/\pi R (I-I_k) \sin 1' + i_o = 0.$$

With a change in the direction of rotation the sign of Q changes since it comprises the angular velocity $2\pi N$. Therefore, on measuring the angle I'_k with the new direction of rotation we obtain:

$$-2Q/\pi R (I-I_k) + i_o = 0$$

Adding term by term, we obtain: $I = I_k + I'_k/2$

that is, the mean value of the 2 measured dips I_k and I'_k is free from the effect of the thermal current.

Order of Observations and Table. After levelling the instrument by means of a superposed level the inclinator is set parallel to the magnetic meridian. For this purpose the compass needle is placed parallel to the horizontal axis of the inclination ring, and by turning the horizontal circle first one and then the other tip of the needle is aligned with the middle division of the compass scale, and readings of the horizontal circle are taken. The same operation is performed after turning the horizontal circle 180° and moving the compass accordingly, in order to eliminate the error due to non-parallel positions of the magnetic axis of the compass and the horizontal axis of the inclination ring. The instrument then is turned 90°, thereby setting the vertical plane extending through the axis of rotation of the coil within the plane of the magnetic meridian, and the dip is determined.

Declassified in Part - Sanitized Copy Approved for Release 2013/01/23 : CIA-RDP81-01043R001600090003-8

Declassified in Part - Sanitized Copy Approved for Release 2013/01/23 : CIA-RDP81-01043R001600090003-8

The process of the observation of the angle of dip I_k consists of the following operations. The coil is rotated by means of a flexible shaft connected to a gear transmission, at a constant angular velocity (10 rps). The inclincation of the ring, and therefore also the axis of rotation of the coil is gradually altered, until the oscillations of the galvanometer, connected in series with the coil, become equal to zero, after which a reading of the vertical circle is taken by means of the 2 microscopes.

To eliminate the systemic errors enumerated above the observations of the angle I_k are carried out in the following sequence.

TABLE 40

DETERMINATION OF DIP

Time	Vertical Circle	Position of Commutator	Direction of Rotation	Microscope Readings on Vertical Circle I	II	Mean	I_K
1158	E	Down	→	108°22.15'	21.2	108°21.68'	71°38.3'
1200	E	Down	←	23,05	22.0	22.52	37.4
0006	E	Up	→	288 22.10	21.1	288 21.60	38.4
0008	E	Up	←	22.10	21.1	21.65	38.3
0014	W	Up	→	251 38.40	37.7	251 38.05	38.0
0015	W	Up	←	37.05	32.2	36.63	36.6
0018	W	Down	→	71 37.55	36.6	71 37.08	37.0
0023	W	Down	←	36.00	35.2	35.60	35.6
						Mean	71°37.5'

Section 6. Measurement of Dip by the Method of Induction in Soft Iron.

The Principle of the Measurements. Both of the above described methods for measuring dip obviously are absolute methods. The induction method described in the present section is a relative method since it requires calibration of the instrument by observation at points where the dip had been determined by an absolute method.

Declassified in Part - Sanitized Copy Approved for Release 2013/01/23 : CIA-RDP81-01043R001600090003-8

Declassified in Part - Sanitized Copy Approved for Release 2013/01/23 : CIA-RDP81-01043R001600090003-8

The gist of this method is that a rod of soft magnetic material (See Section 19 of the Introduction), which is placed in a vertical position becomes magnetized due to the action of the vertical component of the terrestrial magnetic field, and causes deflection of a magnetic needle placed near one end of the rod. The angle of deflection θ of the magnet depends upon both the magnitude of magnetization of the rod, which in turn is proportional to Z, and upon the magnitude of the horizontal component. Theory shows that the ratio Z/H, i.e., the tangent of the angle of dip, is proportional to the sine of the angle of deflection θ. Thus the dip I may be determined by measuring the angle θ.

The Theory of the Method. Let us indicate by NS a rod of soft magnetic material, capable of becoming magnetized in a weak magnetic field and fixed in vertical position within the terrestrial field (Figure 207). Under the influence of the vertical component Z the rod is magnetized, and the magnitude of magnetization J at some point P of the rod is:

$$J = x'Z, \qquad (10.22)$$

where x' is the apparent magnetic susceptibility of the specimen at point P. Let us assume further that a magnet ns is freely suspended in the horizontal plane extending through one end of the rod at a distance R from the rod. Under the influence of the magnetic field produced by the rod NS the magnet will be driven from the position of the magnetic meridian and the condition of its equilibrium will be:

$$H \sin \theta = H_1, \qquad (10.23)$$

where θ is the angle of deflection from the magnetic meridian and H_1 is the horizontal component of the intensity of the magnetic field produced by the rod. At the same time the vector R must be perpendicular to the magnet ns, which is accomplished by rotating the rod around the magnet.

Declassified in Part - Sanitized Copy Approved for Release 2013/01/23 : CIA-RDP81-01043R001600090003-8

Declassified in Part - Sanitized Copy Approved for Release 2013/01/23 : CIA-RDP81-01043R001600090003-8

For the sake of simplicity let us assume that the rod is magnetized uniformly along its axis, i.e., that magnetization J is the same at all points and is directed along the length of the rod.

In such a case magnetic masses m = JS are formed at the ends of the rod, where S is the cross sectional area of the rod NS.

The horizontal intensity H_1 of the magnetic field at point O will be: $H_1 = m/R^2 - m/R^2 + l^2 \cos \varphi$

where l is the length of the rod and φ is the angle between R and the direction from the center of the magnet to the pole S. Since

$$\cos\varphi = R/\sqrt{R^2 + r^2}$$

it follows that

$$H_1 = JS/R^2 \left[1 - R^3/(R^2 + l^2)^{3/2}\right]$$

or, in view of (10.22):

$$H_1 = x'SZ/R^2 \left[1 - R^3/(R^2 + l^2)^{3/2}\right]. \qquad (10.24)$$

The apparent magnetic susceptibility x' is expressed by means of the true susceptibility x of the material in accordance with formula (0.77).

Since x depends upon the intensity of the field, i.e., in this instance upon Z, in order to have a constant x' the rod must be made of a material with the greatest possible magnitude of x, and the ratio of S to l of the rod should give a product xN which is large in comparison with unity. Thus, disregarding unity we obtain:

$$x' = 1/N.$$

Substituting this value into formula (10.24) we obtain:

$$H_1 = S/NR^2 \left[1 - R^3/(R^2 + l^2)^{3/2}\right] Z.$$

With the exception of Z, all the quantities appearing in this expression are constants, and therefore denoting the factor of Z by the constant number C^{-1}, we have: $H_1 = Z/C$

Declassified in Part - Sanitized Copy Approved for Release 2013/01/23 : CIA-RDP81-01043R001600090003-8

Declassified in Part - Sanitized Copy Approved for Release 2013/01/23 : CIA-RDP81-01043R001600090003-8

or, replacing H_1 in this equation by the expression (10.24) we obtain:

$$H \sin \theta = Z/C.$$

Since $Z/H = \operatorname{tg} I$, it follows that

$$\operatorname{tg} I = C \sin \theta \qquad (10.25)$$

Consequently, given the constant quantity C, which is determined experimentally by observing the angle θ at a point where Z is known, we can determine the dip I.

Differentiating equation (10.25), we have:

$$\Delta I = 1/2 \sin 2I \operatorname{ctg} \theta \, \Delta\theta.$$

at $\theta > 45^\circ$ all the factors of $\Delta\theta$ in the right hand portion of this equation are less than unity, and therefore when the angle of dip is changed by some quantity ΔI the angle of deflection θ must change by a quantity which is as many times greater than the quantity ΔI as the factor of $\Delta\theta$ is smaller than unity.

Thus the advantages of this method over the method of direct measurement of the angle of dip are first, the fact that the quantity being measured is the horizontal angle of deflection of the magnet and is free from errors due to friction, and secondly, the error ΔI due to error in measurement of the angle θ is several times less than the error $\Delta\theta$. Thus a change of 1' in the angle of dip at $\theta = 60^\circ$ and $I = 70^\circ$, corresponds to a 4' change in the angle of deflection.

Description of the Instrument. There is no special instrument for the determination of I by this method. The instruments for measurement of the horizontal component according to the Gauss-Lamont method often are used for this purpose. For example, in the "combine" instrument 2 bars of transformer steel, for which $\chi \sim 50$, are set vertically on the bars provided for holding the deflecting magnet, with one bar above, and the other below the magnet being deflected, as is shown in Figure 208.

Declassified in Part - Sanitized Copy Approved for Release 2013/01/23 : CIA-RDP81-01043R001600090003-8

Declassified in Part - Sanitized Copy Approved for Release 2013/01/23 : CIA-RDP81-01043R001600090003-8

The Sequence and Table of Observations. To eliminate a number of systemic errors, which will not be discussed here, the angle of deflection is observed at several different positions of the rods.

At first the rods are set arbitrarily in such a manner that one is directed upward and the other downward in relation to the suspended magnet, and the magnet being deflected is set by rotating the entire instrument perpendicularly to the direction of the bar. Next, the rods are rotated 180° so that the one which was directed upward now is directed downward and the one which was directed downward is now directed upward, and the magnet again is set perpendicularly to the bar. After each setting of the magnet a reading is taken on the horizontal circle. The difference between 2 readings gives the double angle of deflection 2θ.

The 2 rods then are interchanged and the observations are repeated in the same order and the double angle of deflection again is recorded. The table of observations is shown in Table 41.

TABLE 41

TABLE OF OBSERVATIONS BY THE INDUCTION METHOD

Slutsk, 3 May 1938, "combine" No 13, Chronometer 1857; Chronometer correction + 3 seconds relative to local mean time

Time of observations	Rod No 1	Rod No 2	Horizontal Circle Readings	2θ	θ
12 hrs 35 m	Up E	Down W	135°43'		
	Down E	Up W	92 22	43°21'	21°40.5'
	Down W	Up E	92 32	43 16	21 38
12 hrs 50 m	Up W	Down E	135 48		

Mean θ = 21°39.2'

Declassified in Part - Sanitized Copy Approved for Release 2013/01/23 : CIA-RDP81-01043R001600090003-8

Declassified in Part - Sanitized Copy Approved for Release 2013/01/23 : CIA-RDP81-01043R001600090003-8

Section 7. Measurement of the Horizontal Component. The Absolute Method of Gauss.

Theoretical Foundations. The absolute method of measuring the horizontal component was proposed by Gauss. It is based on the laws of interaction between a magnetic field and permanent magnets, and the method consists of direct measurement of the period of oscillation of the magnet in the horizontal plane, and observation of the angle of deflection which this magnet imparts to another magnet which occupies a definite position. It is demonstrated below that a magnet placed in a uniform magnetic field of intensity H_T can exhibit oscillations, the half-period T of which is defined by the equation:

$$T = \pi \sqrt{\frac{K}{MH + C}\left(1 + \frac{1}{4}\sin^2\frac{\alpha}{2}\right)}, \qquad (10.26)$$

where K is the moment of inertia of the magnet, M is the magnetic moment, α is the amplitude of oscillation of the magnet, and C is the constant of filament torsion.

In measuring the horizontal component H the magnet is suspended from a thin filament so that its axis coincides with the horizontal plane, and the half-period T of its oscillation is determined by direct observation.

In view of equation (10.26) we may write:

$$MH = \frac{\pi^2 K}{T^2}\left(1 + \frac{1}{4}\sin^2\frac{\alpha}{2}\right) - C \qquad (10.27)$$

This equation makes it possible to determine the product of the horizontal component and the magnetic moment MH of the magnet since all the quantities in the right hand portion of the equation may be measured directly.

In order to determine the horizontal component H and the magnetic moment M separately a second equation which contains M and H as a sum, difference, ratio, etc, but not as a product, is necessary.

Declassified in Part - Sanitized Copy Approved for Release 2013/01/23 : CIA-RDP81-01043R001600090003-8

Declassified in Part - Sanitized Copy Approved for Release 2013/01/23 : CIA-RDP81-01043R001600090003-8

For this purpose a magnet with a predetermined period of oscillation is used as the deflecting magnet in the first position of Lamont (Figure 209c) and the angle of deflection θ of a second magnet, called the deflected magnet is measured. The magnetic moment of this magnet we shall denote by M'. The condition of equilibrium of the deflected magnet is defined by the equation

$$M'H \sin\theta = Q. \qquad (10.28)$$

where Q is the moment of rotation to which the deflected magnet is subjected due to the action of the deflecting magnet. This moment is

$$Q = \frac{2MM'}{R^3 \cos\theta}\beta,$$

where R is the distance between the centers of the magnets, and β is a certain constant coefficient close to unity, which depends upon the dimensions and shape of the magnets and also upon the distribution of the vector of magnetization J within the magnets.

Consequently

$$\frac{M}{M'} = \frac{2\beta}{R^3 \cos\theta}. \qquad (10.29)$$

Multiplying and dividing equations (10.27) and (10.29) by each other we obtain after evolution:

$$H = \frac{A}{T\sqrt{2\cos\theta}}\left(1 + \frac{1}{4}\sin^2\theta\,\frac{\alpha}{2} - \frac{1}{2}\,\frac{C}{MH}\right); \qquad (10.30)$$

$$M = \frac{B\sqrt{\cos\theta}}{T}\left(1 + \frac{1}{4}\sin^2\theta\,\frac{\alpha}{2} - \frac{1}{2}\,\frac{C}{MH}\right); \qquad (10.31)$$

$$A = \pi\sqrt{\frac{2K}{R^3}\beta} \quad \text{AND} \quad B = \pi\sqrt{\frac{2K}{\beta}R^3}. \qquad (10.32)$$

These expressions show that the horizontal component H and the magnetic moment M can be determined in a system of absolute units, since all the measurements of quantities in the right half of the equation can be reduced to direct measurement of length, mass and time. For this reason the method of determination of the horizontal component and the magnetic moment, based on observations of the period of oscillation of the magnet and the angle of deflection is an absolute method.

Declassified in Part - Sanitized Copy Approved for Release 2013/01/23 : CIA-RDP81-01043R001600090003-8

Declassified in Part - Sanitized Copy Approved for Release 2013/01/23 : CIA-RDP81-01043R001600090003-8

We shall now undertake the derivation of formulas (10.27) and (10.29).

Determination of the Period of Oscillation (Theory). The period of oscillation of the magnet may be determined on the basis of the equation for the motion of the magnet:

$$K\ d^2\theta/dt^2 = \sum_i M_i,$$

where θ is the angle formed by the axis of the magnet and the magnetic meridian, and $\sum_i M_i$ is the sum of the moments of rotation acting upon the magnet.

In this case these moments are the torsional moment of the filament $M_1 = -C\theta$, and the moment of rotation induced by the horizontal component, $M_2 = -MH \sin\theta$.

Hence the preceding equation assumes the form:

$$\frac{d^2\theta}{dt^2} + \frac{MH}{K} \sin\theta = \frac{C}{K}\theta = 0.$$

Since the torsion of the filament C is very small and the angle θ does not exceed several degrees, it may be replaced, without appreciable error, by the sine, and we have:

$$\frac{d^2\theta}{dt^2} + \frac{MH + C}{K} \sin\theta = 0,$$

or

$$\frac{d^2\theta}{dt^2} + n^2 \sin\theta = 0, \tag{10.33}$$

where

$$n^2 = \frac{MH + C}{K}.$$

Multiplying this equation by $d\theta$ and integrating term by term, we obtain:

$$\frac{1}{2}\left(\frac{d\theta}{dt}\right)^2 - n^2 \cos\theta = C.$$

If we take as the initial point of time the time of greatest deflection of the magnet when $\theta = \alpha$ and $d\theta/dt = 0$, the constant of integration $C = -n^2 \cos\alpha$ and consequently the equation assumes the form:

$$\frac{d\theta}{dt} = n\sqrt{2}\left[\cos\theta - \cos\alpha\right].$$

Separating the variables and integrating a second time from $+\alpha$ to $-\alpha$, we obtain:

$$\int_{+\alpha}^{-\alpha} \frac{d\theta}{\sqrt{\cos\theta - \cos\alpha}} = \sqrt{2}\, nT,$$

Declassified in Part - Sanitized Copy Approved for Release 2013/01/23 : CIA-RDP81-01043R001600090003-8

Declassified in Part - Sanitized Copy Approved for Release 2013/01/23 : CIA-RDP81-01043R001600090003-8

or, replacing θ and α by the half-arcs:

$$T = \frac{1}{\pi} \int_0^{\alpha} \frac{d\theta}{\sqrt{\sin^2\frac{\alpha}{2} - \sin^2\frac{\theta}{2}}},$$

where T is the half-period of oscillation of the magnet.

Introducing a new variable φ in accordance with the formula $\sin\theta/2 = \sin\alpha/2 \sin\varphi$, $\sin\frac{\theta}{2} = k\sin\varphi$, we obtain:

$$T = \frac{2}{\pi} \int_0^{\frac{\pi}{2}} \frac{d\varphi}{\sqrt{1 - k^2\sin^2\varphi}}.$$

The integral in the right-hand portion of this expression is a complete elliptical integral of the first type. To determine this integral of the first type it is necessary to expand the function within the sign of integration to a series in the Newton binomial and to integrate each term of this series.

Considering only the first term of the expansion, we obtain:

$$T' = \frac{\pi}{\eta}\left(1 + \frac{1}{4}\sin^2\frac{\alpha}{2}\right),$$

and replacing n by its value in accordance with (10.33):

$$T' = \pi\sqrt{\frac{K}{MH + C}}\left(1 + \frac{1}{4}\sin^2\frac{\alpha}{2}\right),$$

or, in view of the smallness of the coefficient C in comparison with MH:

$$T = \pi\sqrt{\frac{K}{MH}}\left(1 - \frac{1}{2}\frac{C}{MH} + \frac{1}{4}\sin^2\frac{\alpha}{2}\right),$$

and

$$MH = \frac{\pi^2 K}{T^2}\left(1 - \frac{C}{MH} + \frac{1}{2}\sin^2\frac{\alpha}{2}\right).$$

Interaction of Two Magnets. Of all the possible positions relative to each other of magnets in space, only 4 are used in practical magnetic measurements: 2 Gaussian and 2 Lamontian positions, in which the magnets are located within a single horizontal plane.

In the first Gaussian position one of the magnets NS is fixed perpendicular to the magnetic meridian and the other ns is free to rotate about the vertical axis through its center, and is placed with its center at the extension of the axis of the magnet NS (Figure 209a).

In the second Gaussian position the magnet ns is located with

Declassified in Part - Sanitized Copy Approved for Release 2013/01/23 : CIA-RDP81-01043R001600090003-8

Declassified in Part - Sanitized Copy Approved for Release 2013/01/23 : CIA-RDP81-01043R001600090003-8

its center on a line perpendicular to the axis and through the center of the fixed magnet (Figure 209b).

In the first Lamontian position at the instant of equilibrium of the rotating magnet its axis is perpendicular to that of the stationary magnet and its center is on the extension of the axis of the magnet NS (Figure 209c). The second Lamontian position differs from the first in this, that the axis of the movable magnet ns coincides with a line perpendicular to the axis and through the center of the magnet NS (Figure 209d).

In measuring the horizontal component of the magnetic field of the earth the magnets usually placed in the first Lamontian position, and therefore in deriving the formula for the forces of interaction between 2 magnets, we shall limit discussion to the first Lamontian position and calculate the forces of interaction between the 4 poles, i.e., assume that the magnets are schematic. Although such an assumption is not in accord with the actual situation the formulas thus obtained are of the same form and do not differ in principle from those which are based on the actual distribution of magnetic masses within the magnet.

In the first Lamontian position we designate the poles of the deflecting magnet by $+ m$ and $- m$, and the poles of the deflected magnet by $+ m'$ and $- m'$ (Figure 210). We denote the length of the deflecting magnet by 2L, and that of the deflected magnet by 2l; the distance between poles $+ m$ and $+ m'$ by r_1 and the distance between the poles $- m$ and $- m'$ by r_2.

In view of the symmetrical disposition of the magnets it is evident that the distance between $+ m$ and $- m'$ also is equal to r_1, and the distance between $- m$ and $+ m'$ is equal to r_2.

Declassified in Part - Sanitized Copy Approved for Release 2013/01/23 : CIA-RDP81-01043R001600090003-8

Declassified in Part - Sanitized Copy Approved for Release 2013/01/23 : CIA-RDP81-01043R001600090003-8

According to Coulomb's law 2 forces of the deflecting magnet will act on the pole + m': $F_1 = \frac{mm'}{r_1^2}$ and $F_2 = -\frac{mm'}{r_2^2}$, the first in the direction from + m to + m', and the second in the direction from m' to - m'. In an analogous manner 2 forces act on the pole - m': $F_3 = \frac{mm'}{r_1^2}$ and $F_4 = \frac{mm'}{r_2^2}$, of which F_3 is directed from - m' to + m, and F_4 is directed from - m to - m'. It is apparent that in magnitude, $F_1 = F_3$ and $F_2 = F_4$.

The projections of forces F_1 and F_2 on the axis of the deflected magnet, which is made to coincide with the x-axis, and on the perpendicular to the y axis, will be:

$$f_1 = \frac{mm'}{r_1^2}\sin\alpha; \quad f_1' = \frac{mm'}{r_1^2}\cos\alpha;$$

$$f_2 = \frac{mm'}{r_2^2}\sin\beta; \quad f_2' = -\frac{mm'}{r_2^2}\cos\beta.$$

The projections of forces F_3 and F_4 upon the same axes will be:

$$f_3 = \frac{mm'}{r_1^2}\sin\alpha; \quad f_3' = \frac{mm'}{r_1^2}\cos\alpha;$$

$$f_4 = -\frac{mm'}{r_2^2}\sin\beta; \quad f_4' = \frac{mm'}{r_2^2}\cos\beta$$

where α and β are the angles formed by the vectors F_1 and F_2 with the y axis.

The sum of projections on the x-axis will give the total magnitude of the force acting on the deflected magnet:

$$F = f_1 + f_2 + f_3 + f_4 = 2mm'\left(\frac{\sin\alpha}{r_1^2} - \frac{\sin\beta}{r_2^2}\right).$$

The projections upon the y axis form 2 pairs, the moment Q_1 and Q_2 of which are: $Q_1 = \frac{2lmm'}{r_1^2}\cos\alpha$; $Q_2 = \frac{2lmm'}{r_2^2}\cos\beta$.

The total moment is

$$Q = Q_1 + Q_2 = 2lmm'\left(\frac{\cos\alpha}{r_1^2} - \frac{\cos\beta}{r_2^2}\right).$$

It is readily apparent from geometrical considerations (Figure 210) that $\cos\beta = \frac{R+L}{r_2}$, $\sin\alpha = \frac{l}{r_1}$, $\sin\beta = \frac{l}{r_2}$, $\cos\alpha = \frac{R-L}{r_1}$, where R is the distance OO between the centers of the magnets.

Declassified in Part - Sanitized Copy Approved for Release 2013/01/23 : CIA-RDP81-01043R001600090003-8

Declassified in Part - Sanitized Copy Approved for Release 2013/01/23 : CIA-RDP81-01043R001600090003-8

Therefore:

$$F = 2\ell m m' \left[\frac{1}{[(R-L)^2+\ell^2]^{\frac{3}{2}}} - \frac{1}{[(R+L)^2+\ell^2]^{\frac{3}{2}}} \right]$$

$$Q = 2\ell m m' \left[\frac{R-L}{[(R-L)^2+\ell^2]^{\frac{3}{2}}} - \frac{R+L}{[(R+L)^2+\ell^2]^{\frac{3}{2}}} \right]$$

In the numerator and denominator of the right-hand portion, R^3 is removed outside the parentheses, R-L and R+L are raised to the square and, noting that $2m'\ell$ is equal to the magnetic moment M' of the deflected magnet, we have:

$$F = \frac{M'm}{R^3}\left[\left(1 + \frac{L^2+\ell^2}{R^2} - 2\frac{L}{R}\right)^{-\frac{3}{2}} - \left(1 + \frac{L^2+\ell^2}{R^2} + 2\frac{L}{R}\right)^{-\frac{3}{2}}\right];$$

$$Q = \frac{M'm}{R^2}\left[\left(1-\frac{L}{R}\right)\left(1 + \frac{L^2+\ell^2}{R^2} - 2\frac{L}{R}\right)^{-\frac{3}{2}} - \left(1+\frac{L}{R}\right)\left(1 + \frac{L^2+\ell^2}{R^2} + 2\frac{L}{R}\right)^{-\frac{3}{2}}\right].$$

Since L and ℓ usually are small in comparison with R, by expansion of the expressions appearing within the parentheses to a series in powers of L/R and ℓ/R and considering the terms up to the second order in the case of F, and up to the fourth order in the case of Q we obtain:

$$F = \frac{3MM'}{R^4}\left[1 + \frac{\frac{10}{3}L^2 - \frac{5}{2}\ell^2}{R^2}\right];$$

$$Q = \frac{2MM'}{R^3}\left[1 + \frac{2L^2 - 3\ell^2}{R^2} + \frac{3L^4 - 15\ell^2L^2 + \frac{45}{8}\ell^4}{R^4}\right].$$

Introducing the denotations:

$$\frac{10}{3}L^2 - \frac{5}{2}\ell^2 = \rho', \quad 2L^2 - 3\ell^2 = \rho, \quad 3L^4 - 15\ell^2L^2 + \frac{45}{8}\ell^4 = q, \quad 1 + \frac{\rho}{R^2} + \frac{q}{R^4} = \beta, \tag{10.34}$$

we obtain for the schematic magnets:

$$F = \frac{3MM'}{R^4}\left(1 + \frac{\rho'}{R^2}\right),$$

$$Q = \frac{2MM'}{R^3}\left(1 + \frac{\rho}{R^2} + \frac{q}{R^4}\right) = \frac{2MM'}{R^3}\beta. \tag{10.35}$$

The numerical value of force F in the case of magnets found in conventional instruments is of the order of one dyne, since the magnetic

Declassified in Part - Sanitized Copy Approved for Release 2013/01/23 : CIA-RDP81-01043R001600090003-8

Declassified in Part - Sanitized Copy Approved for Release 2013/01/23 : CIA-RDP81-01043R001600090003-8

moments of magnets M and M' are of the order of 1,000 and 250 CGS/ respectively, and the distance R= 30 cm.

Due to the influence of such a force the magnet will become displaced in the direction of its axis by a distance of approximately 12 .

Therefore, in the first Lamontian position when the distance between the magnets is large in comparison with the length of the magnets it may be assumed that only one couple of the deflecting magnet, the moment of which is defined by formula (10.35), acts on the deflected magnet.

The actual magnets in which the magnetic mass is distributed throughout their entire volume may be replaced by quasi-schematic magnets and the same equations (10.34) may be used for p and q, provided that the distances 2L and 2 between the poles are determined in accordance with the equations:

$$L^2 = \frac{\int \rho_1^3 P_3(\cos\theta_1)\,dm_1}{M_1}, \qquad \ldots = \frac{\int \rho_2^3 P_3(\cos\theta_2)\,dm_2}{M_2} \tag{10.36}$$

$$L^4 = \frac{\int \rho_1^5 P_5(\cos\theta_1)\,dm_1}{M_1}, \qquad \ldots = \frac{\int \rho_2^5 P_5(\cos\theta_2)\,dm_2}{M_2} \tag{10.37}$$

where M_1 and M_2 are the magnetic moments of the 2 magnets, ρ_1 and θ_1 are the polar coordinates of elemental mass dm_1 of the first magnet, ρ_2 and θ_2 are the polar coordinates of the second magnet, and P_3 and P_5 are Legendre's polynomials of third and fifth order. The 2 integrals encompass the volume of the 2 magnets.

Obviously, an actual magnet cannot be fully replaced by a schematic magnet since the distances between the poles in the case of the coefficient must be taken in accordance with formulas (10.36) and in the case of the coefficient q in accordance with the formulas of (10.37).

Declassified in Part - Sanitized Copy Approved for Release 2013/01/23 : CIA-RDP81-01043R001600090003-8

Declassified in Part - Sanitized Copy Approved for Release 2013/01/23 : CIA-RDP81-01043R001600090003-8

The integrals of equations (10.36) and (10.37) may be solved only under conditions of uniform magnetization and regular geometric shape of the magnets. These conditions are fulfilled if the magnets are shaped like ellipsoids, and therefore the coefficients p and q may be determined for these magnets according to the formulas based on geometric dimensions.

In the case of magnets of cylindrical, or any other shape, the coefficients p and q may not be determined in accordance with these formulas and must be used.

In the case of magnets of an ellipsoidal shape, solution of the integrals of equations (10.36) and (10.37) yields the following values for p and q:

$$p = 6/5\ (a_1^2 - b_1^2) - 9/5\ (a_2^2 - b_2^2),$$
$$q = 9/7\ (a_1^2 - b_1^2)^2 - 27/5\ (a_1^2 - b_1^2)(a_2^2 - b_2^2) + 135/36\ (a_2^2 - b_2^2)^2, \qquad (10.38)$$

where a and b are the half-axes of the ellipsoids.

The equations of (10.38) make it possible to find the correlation between the dimensions of the ellipsoids for which the coefficient q is equal to zero. Thus taking the second equation of (10.38) as equal to zero and disregarding the terms $(b_1/a_1)^2$ and $(b_2/a_2)^2$, we have

$$9/7\ a_1^4/a_2^4 - 27/5\ a_1^2/a_2^2 + 135/36 = 0$$

Solution of this equation yields

$$a_1/a_2 = 1.93$$

Consequently, in order to be able to disregard the coefficient q the deflecting magnet must be twice as long as the deflected magnet. The same result also may be obtained for the schematic magnets. In such a case $q = 3l_1^4 - 15 l_1^2 l_2^2 + 45/8\ l^4$.

Declassified in Part - Sanitized Copy Approved for Release 2013/01/23 : CIA-RDP81-01043R001600090003-8

Declassified in Part - Sanitized Copy Approved for Release 2013/01/23 : CIA-RDP81-01043R001600090003-8

Equating this expression to zero, we obtain an equation for $\frac{l_1}{l}$, the solution of which is: $\frac{l_1}{l} = 2.1$.

In the more general instance where the deflecting magnet forms an angle φ with the line joining the centers of the magnets (Figure 211), the moment of rotation Q will depend not only upon R, but also upon the angle φ. At $\varphi = 0$ this correlation is determined by equation (10.35), while with a sufficiently large value of R it must assume the form $Q \simeq 2MM'/R^3 \cos\varphi$.

These conditions lead to the fact that in the general case the moment of rotation Q must have the following expression

$$Q = 2MM'/R^3 \cos\varphi\left[1 + p(\varphi)/R^2 + q(\varphi)/R^4\right]$$

where $p(\varphi)$ and $q(\varphi)$ are certain functions of φ.

It is clear that Q is a periodical function with a period equal to 2π, therefore upon expanding Q to a Fourier series we obtain:

$$Q = 2MM'/R^3 \sum_{k=0}^{\infty} a_k \cos k\varphi.$$

Furthermore, it is apparent that all the coefficients a_k having even-valued subindices must become zero since at $\psi = 90^\circ$ the moment of rotation Q is equal to zero. Therefore, retaining 5 terms of the expansion, we obtain:

$$Q = 2MM'/R^3(a_1\cos\varphi + a_3\cos 3\varphi + a_5\cos 5\varphi). \qquad (10.39)$$

At $\varphi = 0$, i.e., in the first Lamontian position:

$$Q = 2MM'/R^3(a_1 + a_3 + a_5).$$

Comparing these expressions with expression (10.35), we find that

$$1 + p/R^2 + q/R^4 = a_1 + a_3 + a_5 = \beta. \qquad (10.40)$$

Introduction of Correction Terms. Formulas (10.30) and (10.31) hold on the condition that all the quantities appearing in these equations are independent of any external factors which may change during the course of the observations. Actually each of them is a function

Declassified in Part - Sanitized Copy Approved for Release 2013/01/23 : CIA-RDP81-01043R001600090003-8

Declassified in Part - Sanitized Copy Approved for Release 2013/01/23 : CIA-RDP81-01043R001600090003-8

of some quantity. Thus the moment of inertia K and the distance R depend upon temperature; the magnetic moment M depends on the temperature and intensity of the field in which the magnet is located; the period of oscillation T depends on the daily rate of the chronometer; the horizontal component H depends on the variations of the earth's magnetic field, etc. Hence it is necessary to correct formulas (10.30) and (10.31) to take into account the influence of all these factors. Since these effects are small the corrections may be made in the form of correction terms of the first order.

The magnetic moment M, the distance R between the magnets, and the moment of inertia K may be represented as functions of the temperature by means of the following linear correlations [See formula (0.83)]:

$$\begin{aligned} M_t &= M_{20}[1 - \mu(t - 20)], \\ R_t &= R_{20}[1 + \beta(\tau - 20)], \\ K_t &= K_{20}[1 + 2\varepsilon(t - 20)], \end{aligned} \tag{10.41}$$

where the subindices of M, R and K indicate the temperature at which each of the quantities is determined; μ is the temperature coefficient of the magnet; δ and ε are the coefficients of expansion of the magnet and the bar upon which the magnet is placed; t is the mean temperature during the oscillation of the magnet and τ is the mean temperature during the observation of the deflections.

In addition, the magnetic moment of the deflecting magnet M depends upon the intensity H of the magnetic field in which it is located, and in view of the small changes of the magnetic moment this correlation may be expressed as a linear formula:

$$M_H = M_0(1 + \nu H), \tag{10.42}$$

where ν is the induction coefficient of the magnet, M_0 is the magnetic moment in the absence of a field and M_H is the magnetic moment during the action of a field of intensity H upon the magnet.

Declassified in Part - Sanitized Copy Approved for Release 2013/01/23 : CIA-RDP81-01043R001600090003-8

Declassified in Part - Sanitized Copy Approved for Release 2013/01/23 : CIA-RDP81-01043R001600090003-8

During the oscillations the magnet is subjected to the action of the horizontal component H, and therefore the magnetic moment of the magnet is expressed by formula (10.42). During deflection the magnet is subjected to the action of the projection of the horizontal component H sin θ (Figure 212) the direction of which is opposite to the direction of the magnetic moment, with the result that the magnetic moment during deflection will be:

$$M'_H = M_0(1 - \gamma H \sin \theta). \qquad (10.43)$$

Observations of the half-period of oscillation T are carried out with the aid of a chronometer, which always has a certain daily rate $\pm$S seconds, i.e., during the mean solar day it is too fast (plus sign) or too slow (minus sign) by S seconds. Therefore the half-period T measured according to the chronometer will differ from the half-period determined in relation to the mean solar time by a quantity Δ T, which is:

$$\Delta T = S/24 \cdot 60 \cdot 60 \quad T = bST \text{ seconds}, \qquad (10.44)$$

and therefore in the equation (10.30) the function T must be replaced by the quantity $T(1 \pm bS)$.

The horizontal component H during the time of observation does not remain constant, but changes continuously. Therefore it may have one value during determination of the period of oscillation and another value during determination of the angle of deflection. Denoting it in the former instance by H, and in the latter by $H \pm \delta H$, the quantity H in equation (10.29) must be replaced by the quantity $H \pm \delta H$.

The change of the horizontal component δ H during the time interval between the mean instant of observation of oscillation and the mean instant of observation of the deflection angle is determined either by direct observation or is determined from the recordings n_1 and n_2 of variation instruments for these instants and the quantity δH then is calculated according to the formula:

Declassified in Part - Sanitized Copy Approved for Release 2013/01/23 : CIA-RDP81-01043R001600090003-8

Declassified in Part - Sanitized Copy Approved for Release 2013/01/23 : CIA-RDP81-01043R001600090003-8

$$\delta H = \varepsilon_H (n_1 - n_2),$$

where ε_H is the constant of the instrument recording the variation. Therefore

$$H + \delta H \simeq H[1 + k(n_1 - n_2)], \qquad (10.45)$$

where

$$k = \varepsilon_H / H.$$

Substituting the values of M, R, k, T and H taken from equation (10.41) through (10.45) into the equations (10.30) and (10.31), and performing algebraic operations with an accuracy up to the terms of first order, we obtain the following formulas for H and M:

$$H = \frac{A_{20}}{T\sqrt{\varepsilon_1}\,\theta}\left[1 + \mu(t-\tau) + 6(t-20) - \frac{3}{2}\beta(\tau-20) - \frac{H}{2}(1+\mu\sin\theta) - \frac{c}{2MH} - \frac{S}{4} + \frac{1}{4}\sin^2\frac{\alpha}{2}\right], \qquad (10.46)$$

$$H = \frac{B_{20}\sqrt{\varepsilon_1}\,\theta}{T}\left[1 + \mu(t+\tau-40) + 6(t-20) + \frac{3}{2}\beta(\tau-20) - \frac{c}{2MH} - \frac{H}{2}(1-\varepsilon_1\sin\theta) - \frac{S}{4} + \frac{1}{4}\sin^2\frac{\alpha}{2}\right], \qquad (10.47)$$

and at the same time,

$$A_{20} = \pi\sqrt{\frac{2K_{20}\left(1 + \frac{\varepsilon_2}{2} + \frac{q}{4}\right)}{2K_{20}R_{20}^5}}\,R_{20}^5, \qquad B_{20} = T\sqrt{\frac{1}{1 + \frac{\varepsilon_2}{2} + \frac{q}{4}}}, \qquad (10.48)$$

It must be noted however that these formulas do not take into account a number of sources of errors, such as: (1) non-coincidence of the axes of the deflecting and the deflected magnets with the horizontal plane; (2) non-coincidence of the geometric center of the inertial body with the axis of rotation; (3) presence of magnetic susceptibility of the materials from which the instrument is made, and others. If not eliminated in the manufacture of the instrument and during its setting while carrying out the observations these sources of error must be reduced to a minimum so that the errors which they engender will be less than the error permissible in the determination of H and M.

Declassified in Part - Sanitized Copy Approved for Release 2013/01/23 : CIA-RDP81-01043R001600090003-8

Declassified in Part - Sanitized Copy Approved for Release 2013/01/23 : CIA-RDP81-01043R001600090003-8

Section 8. Sequence of Observations of the Absolute Method

If the constants of the instrument: conversion factor A, induction and temperature coefficient μ and γ are known, the observation of the horizontal component is reduced to determination of the angle of deflection, the period of oscillation of the magnet T, and the torsion of the filament Δ.

To observe the angle of deflection the smaller deflected magnet is suspended within the magnet housing by a filament, while the deflecting magnet is set upon one of the bars with its north and to the east or to the west. By turning the instrument around its vertical axis, it is set in such a manner that the axis of the telescope coincides with the axis of the deflected magnet (which is done by aligning the vertical hairline of the eyepiece with the image reflected from the mirror of the magnet), and a reading is taken on the horizontal circle. The deflecting magnet then is turned on the bar with its north end toward west or toward the east and the instrument again is set parallel to the axis of the deflected magnet and a second reading of the horizontal circle is taken. The difference between the 2 readings corresponds to the double angle of deflection.

As was stated above, the error caused by non-coincidence of the center of the magnet with the geometric center is eliminated by rotating the deflecting magnet on the bar.

To eliminate the error caused by non-coincidence of the center of the deflecting magnet with the axis of rotation of the instrument the deflecting magnet is transferred to the opposite bar and repeated observations of the deflection angle are performed as described above.

Declassified in Part - Sanitized Copy Approved for Release 2013/01/23 : CIA-RDP81-01043R001600090003-8

Declassified in Part - Sanitized Copy Approved for Release 2013/01/23 : CIA-RDP81-01043R001600090003-8

Thus the angle of deflection is determined on the basis of 4 readings of the horizontal circle at 4 positions of the deflecting magnet.

Upon completion of these observations, observations of the filament torsion are carried out to determine the angle Δ. For this purpose the deflecting magnet is suspended in the magnet housing and is set to coincide with the magnetic meridian. The twisting knob which carried the filament then is turned clockwise 360°, and after the magnet has come to rest a second reading is taken on the horizontal circle. Next, the twisting knob is turned counterclockwise 720° and a third reading is taken. Finally, the magnet is returned to its initial position by turning the knob clockwise 360° and a fourth reading is taken.

Next, observations are made of the period of oscillation of the deflecting magnet to determine the torsion of the filament while the magnet remains within the housing. A preliminary determination with an accuracy within 1 or 2 seconds for 10 or 20 oscillations in order to determine the number of oscillations during which the observations may be recorded and chronometer readings may be taken. Approximately 20 seconds is sufficient for the recording, and therefore if one oscillation lasts 4 seconds, the observations thereafter are made at intervals of 5 oscillations.

The number of intermediate oscillations always must be an odd number.

The observation of the period of oscillation of the magnet consists of the following operations. The starting chronometer time is noted and, counting the seconds by listening to the ticking of the chronometer, the time when the reflected hairline mark of the oscillating magnet passes over the eyepiece hairline is noted. This

Declassified in Part - Sanitized Copy Approved for Release 2013/01/23 : CIA-RDP81-01043R001600090003-8

Declassified in Part - Sanitized Copy Approved for Release 2013/01/23 : CIA-RDP81-01043R001600090003-8

instant is determined with an accuracy within one-tenth of a second by interpolating the instant of the passage between 2 consecutive ticks of the chronometer. Thus if during the tick of the chronometer corresponding to the time 2 hours 31 minutes 40.5 seconds the reflected hairline occupies the position ab in the eyepiece (Figure 213), and during the next tick, i.e., one-half second later, it is seen at cd, then if AB is the vertical hairline of the eyepiece the instant corresponding to the passage of the reflected hairline mark over the hairline AB will be 2 hours 31 minutes 40.7 seconds, since the distance OO_1 in relation to the distance O_1O_2 can be evaluated by eye at 0.4 or 0.2 seconds.

After the instant of the first passage is recorded in a notebook the duration of 5 oscillations (about 20 seconds) is added to obtain the approximate instant of the next passage. To observe the second passage the counting of seconds, using the chronometer, is continued uninterruptedly, and the instant of the actual passage is awaited. The tenth, fifteenth, etc passages are observed in the same manner.

After a series of such observations an interval of time corresponding to 100, 200 or 300 oscillations is allowed to elapse before another series of observations is made.

Prior to observation of the oscillation the magnet is moved by means of a small magnet from the position of equilibrium to a distance corresponding to several degrees, after which it begins to oscillate. To make corrections for amplitude α and temperature t the angle of deflection of the magnet and the temperature are noted at the beginning and at the end of the oscillation trial, and from these readings the mean values of α and t are calculated.

Declassified in Part - Sanitized Copy Approved for Release 2013/01/23 : CIA-RDP81-01043R001600090003-8

Declassified in Part - Sanitized Copy Approved for Release 2013/01/23 : CIA-RDP81-01043R001600090003-8

After determination of the period of oscillation the observations of the deflection are repeated as described above .

The observations of the horizontal component according to the method of Gauss are recorded as shown in Table 42.

Determination of the Period by Means of the Synchronous Clock. The visual or subjective procedure of determining the period of oscillation of the magnet as well as of any pendulum is limited by a definite accuracy of measurement which cannot be increased due to the inadequacy of the organs of hearing and sight. Therefore a long time ago the question arose concerning replacement of the subjective method by an objective method which would make it possible to increase the accuracy of measurements within wide limits. However, until recently this problem remained at the stage of development of various systems of photoelectric cells and chronographs which, while yielding somewhat more accurate results than the visual method, necessitated fairly complex and laborious processing of data.

Recently, the practical use of alternating current generators of very constant frequency has enabled highly accurate measurement of short intervals of time and this method has been applied to measurement of the oscillations of pendulums. At the present time the absolute frequency of such a generator may be determined within an error of 10^{-8} of the measured magnitude by comparison with a standard frequency transmitted through the atmosphere and over wires by the All Union Scientific Research Institute of Metrology imeni D. I. Mendeleyev.

Thus the alternating current generator can serve as a source of time signals transmitted at definite time intervals, the magnitude of which is known within an error that is several-fold less than the error involved in the same interval as determined by the best

Declassified in Part - Sanitized Copy Approved for Release 2013/01/23 : CIA-RDP81-01043R001600090003-8

Declassified in Part - Sanitized Copy Approved for Release 2013/01/23 : CIA-RDP81-01043R001600090003-8

chronometers. Therefore, the principal part of an instrument used to measure the period of oscillation of a magnet by the objective method consists of a device which converts the frequency of an alternating current into time signals which are easily registered either visually or photographically. This device has been named the synchronous clock.

A synchronous clock is essentially a clock or stopwatch in which the hands have been replaced by 2 concentric moving dials, i.e., disks provided with division marks. The inner, smaller disk completes one revolution per minute, while the larger, outer disk completes 10 revolutions per minute. Each disk is divided into 100 parts and the divisions of the outer disk are further subdivided into 5 parts. The divisions of the inner disk adjoin those of the outer disk and bear numerical markings: the outer from 0 to 99 and the inner from 0 to 9, with each numeral appearing 10 times on the inner disk as is shown in Figure 214.

Both disks are covered by an opaque screen which is provided on the right side of the axis of rotation with a small window A with a pointer mark B in the form of a thin line. The size of the window is such that at any position of the disks a number may be seen on both disks.

Because of the speed of movement of the dial (one division of the inner disk passes the window pointer every 0.6 second, and one division of the outer disk passes every 0.06 second) the eye cannot directly perceive the reading. Therefore to take a reading at a given point of time a neon tube briefly illuminates the scale seen through the window. The duration of the neon tube illumination is of the order of 10^{-4} second, with the result that the illuminated scale

Declassified in Part - Sanitized Copy Approved for Release 2013/01/23 : CIA-RDP81-01043R001600090003-8

Declassified in Part - Sanitized Copy Approved for Release 2013/01/23 : CIA-RDP81-01043R001600090003-8

appears stationary to the observer, who thus is able to read the numerical markings of the scale.

It is readily apparent that the first numeral visible through the window, reading from left to right, corresponds to 0.1 of a second, the second to 0.01 and the third to 0.001, while each division of the outer disk corresponds to 0.0002 second. Thus the instant of ignition of the neon tube can be read within an error of ± 0.0002 second.

To facilitate reading of the synchronous clock the disks are made of a transparent material and the neon tube is placed behind the window.

In determining the period of oscillation of the magnet the synchronous clock is included in an apparatus utilizing photoelectric cell combined with an amplifier, the block diagram of which is shown in Figure 215. Light rays from source S pass through lens L and in a converging beam reach the mirror of the oscillating magnet P. The reflected beam also oscillates, and when the magnet passes through the position of equilibrium the reflected beam strikes the photoelectric cell F. E. in which an impulse current is generated. This impulse passes through amplifier Y to the grid of a thyratron, in the anodic circuit of which is the neon tube which at this instant illuminates the scale of the synchronous clock S. Ch.

In addition, the synchronous clock arrangement includes an impulse counter which enables the number of passages of the magnet through the position of equilibrium to be counted.

The process of observation by means of the synchronous clock consists of reading off the points of time when the magnet passes through

Declassified in Part - Sanitized Copy Approved for Release 2013/01/23 : CIA-RDP81-01043R001600090003-8

Declassified in Part - Sanitized Copy Approved for Release 2013/01/23 : CIA-RDP81-01043R001600090003-8

the position of equilibrium. In this, the instants of passage following the initial 10 or 20 oscillations are determined, followed by determination of the passages between the 100th and either the 110th or 125th oscillations. Since the readings of the synchronous clock show only decimal or smaller fractions of a second, the period of oscillation of the magnet is determined beforehand within 0.5 second with the use of a stopwatch, and this period, multiplied by the passage number, is added to the reading.

The sequence of recordings and calculations is shown in Table 43. Comparing Table 43 with the table of visual observations, it is seen that the error involved in determinations using the synchronous clock is more than one-hundred times less than of the visual method.

It was established by preliminary experiments that the duration of 10 oscillations is approximately 34.5 seconds. Therefore the duration of 50 oscillations must be approximately 172.5 seconds. Measurements using the synchronous clock gave not the figure 5, but 975 after the decimal point, and consequently the more precise value of the period must be:

$$T \simeq 172.975/50 \simeq 3.45950 \pm 0.00004 \text{ seconds.}$$

/See following pages for Tables 42 and 43/

Declassified in Part - Sanitized Copy Approved for Release 2013/01/23 : CIA-RDP81-01043R001600090003-8

Declassified in Part - Sanitized Copy Approved for Release 2013/01/23 : CIA-RDP81-01043R001600090003-8

TABLE 42

TABLE OF RECORDINGS OF OBSERVATIONS OF THE HORIZONTAL COMPONENT BY THE METHOD OF GAUSS

Slutsk, 4 November 1939. Instrument: Vil'd- Freynberg No 1.

A. Observations of Deflection

I. Prior to Observations B and C

Time	Bar	No of Magnet	t	Horizontal Circle Vernier I	Vernier II	Mean	$2\theta_1$
8 h 35 m	E	E	9.2°	69°60'04"	50'08"	69°50'06"	54°16'36"
39	W	E	9.2	15 33 28	33 32	15 39 30	
42	W	W	9.1	15 22 16	22 20	15 22 18	54°51 52"
45	E	W	9.1	70 14 08	14 12	70 14 10	

Mean t = 9°15'

Mean θ_1 = 27°17'07"

Correction for declination +11"

θ_1 = 27°17'18"

II. After Observations B and C

Time	Bar	No of Magnet	t	Horizontal Circle Vernier I	Vernier II	Mean	$2\theta_2$
9 h 22 m	E	W	9.2°	70°11'44"	11'50"	70°11'47"	54°50°62"
26	W	W	9.2	15 20 52	20 56	15 20 55	
28	W	E	9.2	15 32 30	32 34	15 32 32	54 15 42
30	E	E	9.2	69 48 12	48 16	69 48 44	

Mean t = 9.2

Mean θ_2 = 27°16'41"

Correction for declination - 2"

θ_2 = 27°16'39"

$\theta = \theta_1 + \theta_2/2 = 27°16'58"$

B. Torsion

Angle of Torsion	Time	Horizontal Circle Vernier I	Vernier II	Mean	Δ
0	8 h 40 m	52°53'56"	53'60"	52°53'58"	23'14"
+ 360°	50	53 17 10	17 16	53 17 13	
- 360°	52	53 27 04	27 10	52 07 07	26'43"
0°	53	52 53 48	53 52	52 53 50	

Mean Δ = 25'00"

Declassified in Part - Sanitized Copy Approved for Release 2013/01/23 : CIA-RDP81-01043R001600090003-8

Declassified in Part - Sanitized Copy Approved for Release 2013/01/23 : CIA-RDP81-01043R001600090003-8

Table 42 Continued

C. Duration of Oscillations

$\alpha = 33.8$

No of Oscillation	Time of Passage	No of Oscillation	Time of Passage	Duration of 200 Oscillations
0	8 h. 56 m. 01.0 s.	200	9 h. 10 m. 43.5 s.	14 m. 42.5 s.
10	45.0	210	27.7	42.7
20	39.1	220	11.8	42.7
30	13.2	230	56.0	42.8
40	57.2	240	40.1	42.9
50	41.3	250	24.1	42.8
60	25.6	260	08.2	42.6
70	09.7	270	52.4	42.7
80	03.9	280	36.4	42.5
90	08.0	290	20.6	42.6
5	22.8	205	05.5	42.7
15	07.1	215	49.7	42.6
25	51.1	225	33.9	42.8
35	35.2	235	18.0	42.8
45	19.4	245	02.2	42.8
55	03.6	255	46.1	42.5
65	47.7	265	30.4	42.7
75	21.8	275	14.5	42.7
85	16.1	285	58.7	42.6
95	02.0	295	42.8	42.6

$t = 10.7^{\circ}$

Mean 200 T = 14 m. 42.68 s.

T = 4.4135 s.

Declassified in Part - Sanitized Copy Approved for Release 2013/01/23 : CIA-RDP81-01043R001600090003-8

Declassified in Part - Sanitized Copy Approved for Release 2013/01/23 : CIA-RDP81-01043R001600090003-8

TABLE 43

DETERMINATION OF THE PERIOD OF OSCILLATION OF A PENDULUM BY MEANS OF A SYNCHRONOUS CLOCK

No of Oscillation	Instant of passage of the magnet	No of Oscillation	Instant of passage of the magnet	Difference	Deviation from mean value of Δ	Δ^2
0	0.465	50	0.447	982	7	49
2	383	52	360	997	12	144
4	304	54	278	974	4	16
6	220	56	196	976	1	1
8	147	58	117	970	5	25
10	070	60	944	974	1	1
12	995	62	070	975	0	0
14	913	64	880	967	8	64
16	827	66	797	970	5	25
18	747	68	712	965	10	100

Mean: 0.975 ± 0.002.

Section 9. Determination of the Constant Coefficients

Determination of the Moment of Inertia K. Observations of the period of oscillation without and with the load of an additional body of regular geometric shape called the inertia body are used in the determination of the moment of inertia of a magnetic system.

Denoting the period of oscillation in the former case by T, and in the latter by T_k we have, without correction for temperature, variations, etc

$$T = \frac{4\pi^2 K}{MH}; \quad T_K = \frac{4\pi^2 (K + K_0)}{MH},$$

where k is the moment of inertia of the magnetic system and k_o the moment of inertia of the additional body.

Solving these equations for k, we obtain

$$K = K_0 \frac{T^2}{T_K^2 - T^2}. \qquad (10.49)$$

Declassified in Part - Sanitized Copy Approved for Release 2013/01/23 : CIA-RDP81-01043R001600090003-8

Declassified in Part - Sanitized Copy Approved for Release 2013/01/23 : CIA-RDP81-01043R001600090003-8

The moment of inertia of the additional body K_0, usually in the shape of a cylinder or ring of rectangular cross section is determined by formulas based on geometric dimensions.

In the case of a cylinder the moment of inertia in relation to a line through the center and perpendicular to its axis, is expressed by the formula

$$K_0 = \frac{m}{12}(3r^2 + h^2), \qquad (10.50)$$

where m is mass, r is the radius, and h is the length of the cylinder.

In the case of a ring of rectangular cross section the moment of inertia relative to its axis is of the form:

$$K_0 = \frac{m}{2}(r_1^2 + r_2^2),$$

where r_1 and r_2 are the external and internal radii of the ring.

Determination of the Coefficient b. The coefficient b may be determined by 2 methods, depending on whether it is expressed in terms of the coefficients of distribution p and q, or in terms of the coefficients of the Fourier series a_1, a_3 and a_5, in accordance with equation (10.40).

In the former case, equation (10.28) for the equilibrium of a magnet in the first Lamontian position is written in the form:

$$H \sin\theta = \frac{2M}{R^3}\left[1 + \frac{p}{1^2} + \frac{q}{6R^2}\right],$$

and in the latter case it is:

$$H \sin\theta = \frac{2M}{R^3}[a_1 \cos\alpha + a_3 \cos 3\alpha + a_5 \cos 5\alpha]. \qquad (10.51).$$

The first method, proposed by Lamont in the last century, consists in observing the angles of deflection θ with various distances R between the magnets. Thus, having determined by observation the angles θ_1, θ_2 and θ_3 corresponding to the distances R_1, R_2 and R_3, and substituting them into expression (10.28) we obtain 3 equations, the solution of which yields the values of p and q and consequently, also the magnitude of b.

Declassified in Part - Sanitized Copy Approved for Release 2013/01/23 : CIA-RDP81-01043R001600090003-8

Declassified in Part - Sanitized Copy Approved for Release 2013/01/23 : CIA-RDP81-01043R001600090003-8

However, as is revealed by theoretical calculation and practical observation, the error in determination of p and q by this method considerably exceeds the permissible error for the absolute determinations of H.

The second method, which is based on equation (10.51) is more precise. This method was evolved by the well-known Russian geophysicist Academician B. B. Golitsin, and consists in observation of the angles of deflection θ with the same distance R between the magnets but with different values of the angle α of the deflecting magnet (Figure 211).

Assuming that angles θ_1, θ_2 and θ_3 have been measured at $\alpha = 0^\circ$, 30° and 60°, then by substituting these values into equation (10.51) and using the denotation $HR^3/2M = A$, we obtain 3 equations:

$$a_1 + a_3 + a_5 = A \sin \theta_1 .$$

$$\sqrt{\frac{3}{2}}(a_1 - a_5) = A \sin \theta_2 .$$

$$\frac{1}{2}(a_1 - a_3 + \frac{1}{2} a_5) = A \sin \theta_3 .$$

Solving these equations for a_1, a_3 and a_5, we have:

$$a_1 = \frac{A}{3}(\sin \theta_1 + \sqrt{3} \sin \theta_2 + \sin \theta_3),$$

$$a_3 = \frac{A}{3}(\sin \theta_1 - 2 \sin \theta_3),$$

$$a_5 = \frac{A}{3}(\sin \theta_1 - \sqrt{3} \sin \theta_2 + \sin \theta_3).$$

Since a_3 and a_5 are small in comparison to a_1, and the coefficient a_1 is close to unity, with a rough approximation a_1 may be equated to unity in which case

$$A = \frac{3}{\sin \theta_1 + \sqrt{3} \sin \theta_2 + \theta_3}$$

and consequently,

$$\beta = a_1 + a_3 + a_5 = \left[1 + \frac{2 \sin \theta_1 - \sqrt{3} \sin \theta_2 - \sin \theta_3}{\sin \theta_1 + \sqrt{3} \sin \theta_2 + \sin \theta_3}\right]. \qquad (10.51a)$$

As an example Table 44 lists the mean values of the observed θ angles at 30° intervals of the position of the deflected magnet, and also the results of calculation of the coefficient β.

Declassified in Part - Sanitized Copy Approved for Release 2013/01/23 : CIA-RDP81-01043R001600090003-8

Declassified in Part - Sanitized Copy Approved for Release 2013/01/23 : CIA-RDP81-01043R001600090003-8

TABLE 44

CALCULATIONS OF THE COEFFICIENT b

θ_1	34°37'00"	$2 \sin \theta_1$	1.136162
θ_2	28 59 21	$\sqrt{3} \sin \theta_2$	0.839420
θ_3	15 46 02	$2 \sin \theta_1 - \sqrt{3} \sin \theta_2 - \sin \theta_3$	0.025020
$\sin \theta_1$	0.568081	$\sin \theta_1 + \sqrt{3} \sin \theta_2 + \sin \theta_3$	1.679226
$\sin \theta_2$	0.484457	$1 - b$	0.01489
$\sin \theta_3$	0.271728	δ	1.01489

The relative error in the determination of δ by this method, depending upon error in the measurement of angle θ, is determined by means of equation (10.51). Differentiating with respect to θ on the assumption that the errors of θ_1, θ_2 and θ_3 are equal, we have:

$$\frac{\Delta(1-\beta)}{1-\beta} = \left[\frac{2\cos\theta_1 + \sqrt{3}\cos\theta_2 + \cos\theta_3}{\sin\theta_1 - \sqrt{3}\sin\theta_2 - \sin\theta_3} \quad \frac{\cos\theta_1 + \sqrt{3}\cos\theta_2 + \cos\theta_3}{+\sin\theta_1 + \sqrt{3}\sin\theta_2 + \sin\theta_3}\right] \Delta\theta.$$

Substituting the numerical values of the angles from Table 44, we obtain:

$$\frac{\Delta(1-\beta)}{1-\beta} = 1.00 \sin 1'' \Delta\theta''.$$

The error in measurement of angle θ is of the order of $\pm 5''$, therefore:

$$\frac{\Delta(1-\beta)}{1-\beta} = 3 \cdot 10^{-3}.$$

Determination of the Temperature Coefficient. Upon observation of the period of oscillation of the magnet at different temperatures, temperature coefficient may be determined. At temperature t_1 we have:

$$HM_{20}[1-\mu(t_1-20)] = \frac{\pi^2 K_{20}[1+26(t_1-20)]}{T_1^2},$$

and at temperature t_2:

$$HM_{20}\left(1+\frac{\delta H}{H}\right)[1-\mu(t_2-20)] = \frac{\pi^2 K_{20}[1+26(t_2-20)]}{T_2^2},$$

where δH is the change in the horizontal component during the time between measurement of the periods T_1 and T_2.

Dividing one equation by the other, we obtain:

$$\frac{1-\mu(t_1-20)}{[1-\mu(t_2-20)]\left(1+\frac{\delta H}{H}\right)} = \frac{T_2^2}{T_1^2} \cdot \frac{1+26(t_1-20)}{1+26(t_2-20)},$$

Declassified in Part - Sanitized Copy Approved for Release 2013/01/23 : CIA-RDP81-01043R001600090003-8

Declassified in Part - Sanitized Copy Approved for Release 2013/01/23 : CIA-RDP81-01043R001600090003-8

or

$$1+(\mu+2\delta)(t_2-t_1)=\frac{T_2^2}{T_1^2}\left(1-\frac{\delta H}{H}\right),$$

hence

$$\mu+2\delta=\frac{T_2^2\left(1-\frac{\delta H}{H}\right)-T_1^2}{T_1^2(t_2-t_1)}.$$

Using the denotation

$$T_2^2\left(1-\frac{\delta H}{H}\right)=T'^2_2, \qquad (10.52)$$

we have

$$\mu+2\delta=\frac{T'^2_2-T_1^2}{T_1^2(t_2-t_1)}.$$

Since the periods T_1 and T_2 differ from each other only slightly, we may equate

$$\frac{T_1+T_2}{2}=T_1;$$

in which case

$$\mu+2\delta=\frac{2(T_2-T_1)}{T_1(t_2-t_1)}. \qquad (10.53)$$

This formula, together with formula (10.52), makes it possible to determine the sum $(\mu+2\delta)$, and consequently the temperature coefficient μ, since the coefficient of expansion δ can be taken from tabulated data.

In addition, the temperature coefficient may be determined also from observations of the angle of deflection at different temperatures T_1 and T_2, for which we have:

$$H=\frac{2M_{20}[1-\mu(T_1-20)]\beta}{R_{20}^3[1+3\beta(T_1-20)]\sin\theta_1},$$

$$H+\delta H=\frac{2M_{20}[1-\mu(T_2-20)]\beta}{R_{20}^3[1+3\beta(T_2-20)]\sin\theta_2}.$$

Dividing one equation by the other, we obtain:

$$1+\frac{\delta H}{H}=\frac{[1-\mu(T_2-20)][1+3\beta(T_1-20)]\sin\theta_1}{[1+3\beta(T_2-20)][1-\mu(T_1-20)]\sin\theta_2},$$

or

$$1+(\mu+3\beta)(T_2-T_1)=\frac{\sin\theta_1}{\sin\theta_2\left(1+\frac{\delta H}{H}\right)}.$$

Using the denotation

$$\sin\theta_2\left(1+\frac{\delta H}{H}\right)=\sin\theta'_2, \qquad (10.54)$$

we obtain:

$$\mu+3\beta=\frac{\sin\theta_1-\sin\theta'_2}{\sin\theta_2(T_2-T_1)},$$

or, in view of the slight difference between angles θ_1 and θ'_2:

$$\mu+3\beta=-\frac{\operatorname{ctg}\theta_2\sin 1'(\theta'_2-\theta_1)}{T_2-T_1}. \qquad (10.55)$$

Declassified in Part - Sanitized Copy Approved for Release 2013/01/23 : CIA-RDP81-01043R001600090003-8

Declassified in Part - Sanitized Copy Approved for Release 2013/01/23 : CIA-RDP81-01043R001600090003-8

Since there is only slight difference between θ_2 and θ'_2 formula (10.54) may be written in the form: $(\theta'_2 - \theta_2) \sin 1'' = \mu \sin \theta_2 \frac{\delta H}{H}$,

hence $\theta'_2 = \theta_2 + \frac{\delta H}{H} \cdot \frac{\mu \theta_2}{\sin 1''}$.

Substituting this value into equation (10.55) we obtain:

$$\mu + 3\beta = \frac{\theta_1 - \theta_2}{\tau_2 - \tau_1} \operatorname{ctg} \theta_2 \sin 1'' - \frac{\delta H}{H} \operatorname{ctg} \theta_2 .$$

an expression which is more convenient in practical use.

Determination of the Induction Coefficient. The induction coefficient ν is determined from observation of the angle of deflection on the action of magnetic fields of different intensity upon the deflecting magnet. The method of determination depends upon the manner in which this action is effected. Lamont has proposed a method for determining ν by means of setting the deflecting magnet vertically, first with the north end upward, then downward, in such a manner that the entire magnet is located either above or below the plane of the deflected magnet (Figure 216).

In the first instance the action of the vertical component Z is opposite to the magnetization of the magnet, while in the second case this action is in the direction of the magnetization, so that the magnet moment in the first case is $(M - \nu Z)$ and in the second case is $(M + \nu Z)$.

If a vertical plane extending through the deflecting magnet and through the center of the deflected magnet is perpendicular to its axis, the conditions of equilibrium for both cases are formulated as follows: $H \sin \theta_1 = f(R, l) M (1 - \nu Z)[1 - \mu (t_1 - 20)]$,

$H\left(1 + \frac{\delta H}{H}\right) \sin \theta_2 = f(R, l) M (1 + \nu Z)[1 - \mu (t_2 - 20)]$,

where $f(R, l)$ is a certain function of the distance R between the magnets and of the length l of the deflecting magnet.

Declassified in Part - Sanitized Copy Approved for Release 2013/01/23 : CIA-RDP81-01043R001600090003-8

Declassified in Part - Sanitized Copy Approved for Release 2013/01/23 : CIA-RDP81-01043R001600090003-8

Dividing one equation by the other, we obtain:

$$\frac{\sin\theta_1}{\sin\theta_2\left(1+\frac{\delta H}{H}\right)} = \frac{1-\nu Z}{1+\nu Z}\left[1+\mu(t_2-t_1)\right],$$

or

$$\frac{\sin\theta_1}{\sin\theta_2\left[1+\frac{\delta H}{H}+\mu(t_2-t_1)\right]} = \frac{1-\nu Z}{1+\nu Z}.$$

Using the denotation

$$\sin\theta_2\left[1+\frac{\delta H}{H}+\mu(t_2-t_1)\right] = \sin\theta_2',$$

we have:

$$\frac{\sin\theta_1}{\sin\theta_2'} = \frac{1-\nu Z}{1+\nu Z}, \qquad (10.56)$$

where, analogously to the deductions of the preceding section,

$$\theta_2' = \theta_2 + \operatorname{tg}\theta_2\frac{\delta H}{H} + \operatorname{tg}\theta_2\,\mu(t_2-t_1).$$

Solving equation (10.56) for ν, we obtain:

$$\nu = \frac{1}{2}\cdot\frac{\sin\theta_2'-\sin\theta_1}{\sin\theta_1+\sin\theta_2'} \quad \text{or} \quad \nu = \frac{1}{2}\cdot\frac{t_1\dfrac{\theta_2'-\theta_1}{2}}{\operatorname{tg}\dfrac{\theta_2'+\theta_1}{2}}.$$

B. M. Yanovskiy has proposed a procedure in which the deflecting magnet is placed in a solenoid, the field of which serves to change the magnetic moment. The solenoid is set in the first Gaussian position in relation to the deflecting magnet, a second, identical solenoid, connected in series to the latter, is placed on the opposite side to compensate the action of the field of the solenoid on the deflected magnet (Figure 217).

Denoting by α the angle through which the magnet is deflected when the current is absent in the solenoid, the condition of equilibrium of the magnet will be: $\frac{2M}{R^3} = H\operatorname{tg}\alpha$.

When current flows through the solenoid the magnetic moment M will change and the new condition of equilibrium will be:

$$\frac{2M(1+\nu H_1)}{R^3} = H\operatorname{tg}\alpha_1,$$

where H_1 is the intensity of the field of the solenoid, equal to kI, in which I is current intensity and K is the constant of the solenoid.

Declassified in Part - Sanitized Copy Approved for Release 2013/01/23 : CIA-RDP81-01043R001600090003-8

Declassified in Part - Sanitized Copy Approved for Release 2013/01/23 : CIA-RDP81-01043R001600090003-8

Dividing the first equation by the second we obtain:

$$1 + \nu H_1 = \frac{\bar{\eta}\alpha_1}{\bar{\eta}\alpha},$$

hence

$$\nu = \frac{\bar{\eta}\alpha_1 - \bar{\eta}\alpha}{\lambda I \bar{\eta}\alpha},$$

Section 10. Errors in Determination of H Caused by Incidental Errors of Direct Observations

From the theory of errors it is known that the mean square error in the determination of H is expressed in the following form:

$$\frac{\Delta H}{H} = \pm \sqrt{\frac{1}{4}\left(\frac{\Delta K}{K}\right)^2 + \frac{9}{4}\left(\frac{\Delta \lambda}{\lambda}\right)^2 + \left(\frac{\Delta T}{T}\right)^2 + \frac{1}{4}\sigma_\eta^2 \delta\alpha^2 + \mu^2[\alpha(t-\tau)]^2} \quad (10.57)$$

This formula makes it possible not only to calculate the magnitude of error $\Delta H/H$ depending upon the magnitude of error of each argument, but also to determine the permissible error in the measurement of these arguments with a previously given error in determination of H.

The numerical values of errors in the determination of the horizontal component H depending upon the error in any argument, and also the permissible values of errors in individual arguments with a given accuracy of determination of H are shown in Table 45.

The last column of this table shows that for the determination of the horizontal component with an error not exceeding 10^{-4} the greatest difficulty in the measurement of individual arguments is encountered in the measurement of the moment of inertia K, and of temperatures t and τ, which must be determined within an error of 0.008 g · cm^2 and 0.1°, respectively.

Let us consider the conditions which must obtain in order to keep the error in measurement of the moment of inertia below 0.008 g · cm2.

From equation (10.49) we have:

$$\frac{\Delta K}{K} = -\frac{\Delta[T_K^2 - T^2]}{T_K^2 - T^2} + \frac{2\Delta T}{T} + \frac{\Delta K_0}{K_0},$$

Declassified in Part - Sanitized Copy Approved for Release 2013/01/23 : CIA-RDP81-01043R001600090003-8

Declassified in Part - Sanitized Copy Approved for Release 2013/01/23 : CIA-RDP81-01043R001600090003-8

and from equation (10.50), assuming that the inertia body is cylindrical, $\frac{\Delta K_0}{K_0} = \frac{\Delta m}{m} + \frac{\Delta(3r^2 + h^2)}{3r^2 + h^2}$.

Therefore $\frac{\Delta K}{K} = -\frac{\Delta(T_K^2 - T^2)}{T_K^2 - T^2}\Delta T_K + \frac{2T}{T_K^2 - T^2}\Delta T + \frac{2\Delta T}{T} + \frac{\Delta m}{m} + \frac{6r\Delta r}{3r^2 + h^2} + \frac{2h\Delta h}{3r^2 + h^2}$,

or, upon differentiation:

$$\frac{\Delta K}{K} = -\frac{\Delta(T_K^2 - T^2)}{T_K^2 - T^2} + \frac{2\Delta T}{T} + \frac{\Delta m}{m} + \frac{\Delta(3r^2 + h^2)}{3r^2 + h^2}$$

Since r usually is small in comparison to h, the term $3r^2$ of the denominator may be disregarded. Thus, after certain transformations we obtain:

$$\frac{\Delta K}{K} = -\frac{T_K^2}{T_K^2 - T^2}\cdot\frac{\Delta T_K}{T_K} + \frac{2T^2}{T_K^2 - T^2}\cdot\frac{\Delta T}{T} + 2\frac{\Delta r}{r} + \frac{\Delta m}{m}.$$

The relative errors in the determination of the periods T and T_k are equal, therefore on transition to the mean square error we have:

$$\frac{\Delta K}{K} = \pm\sqrt{4\left(\frac{T_K^2 + T^2}{T_K^2 - T^2}\right)^2\left(\frac{\Delta T}{T}\right)^2 + 36\left(\frac{\Delta r}{r}\right)^2 + 4\left(\frac{\Delta h}{h}\right)^2 + \left(\frac{\Delta m}{m}\right)^2} \quad (10.58)$$

Table 46 lists the values of permissible error in the measurement of the period of oscillation T, radius r, length h and mass m, of the inertia body when $K \leq 125$ g • cm^2 and $\Delta K = 0.008$ g • cm^2.

Thus it is apparent that the greatest difficulty is encountered in measuring the period of oscillation, in which the error must not exceed ± 0.000012 sec. However, the use of the synchronous clock eliminates this difficulty and such a degree of accuracy is entirely feasible in the determination of the period of oscillation. Although the measurement of the other quantities r, h and m presents no difficulties, the preparation of the inertia body is a complex task since it requires a homogeneous material and exact shape and dimensions.

See Tables 45 and 46 following pages

Declassified in Part - Sanitized Copy Approved for Release 2013/01/23 : CIA-RDP81-01043R001600090003-8

Declassified in Part - Sanitized Copy Approved for Release 2013/01/23 : CIA-RDP81-01043R001600090003-8

TABLE 45

NUMERICAL VALUES OF ERRORS IN THE MEASUREMENT OF H BY THE ABSOLUTE METHOD OF GAUSS

Errors 1	Formulas showing the correlation between error $\Delta H/H$ and the error of each argument 2	Adopted values of each argument and its error 3
ΔR	$\Delta H/H = 3/2\ \Delta R/R$	$R = 30$ cm; $\Delta R = 1$ mm
ΔK	$\Delta H/H = 1/2\ \Delta K/K$	$K = 150$ g · cm^{-2}; $\Delta K = 1$
ΔT	$\Delta H/H = \Delta T/T$	$T = 3$ seconds; $\Delta T = 0.0001$ sec.
$\Delta \theta$	$\Delta H/H = 1/2$ ctg θ sin 1' $\Delta \theta$	$\theta = 45^\circ$; $\Delta \theta = 1'$
Δp	$\Delta H/H = 1/2\ \Delta p/R^2$	$R = 30$ cm; $\Delta p = 1$
$\Delta \mu$	$\Delta H/H = t - \tau/2\ \Delta \mu$	$t - \tau = 1^\circ$; $\Delta \mu = 10^{-4}$
$\Delta \nu$	$\Delta H/H = H/2(1 \neq \sin \theta)\ \Delta \mu$	$H = 0.153$ Oe; $\theta = 45^\circ$; $\Delta \nu = 10^{-3}$
Δt	$\Delta H/H = \mu \neq 2\varepsilon/2\ \Delta t$	$\mu \neq 2\varepsilon/2 \cdot 4 \cdot 10^{-4}$; $\Delta t = 1^\circ$
$\Delta \tau$	$\Delta H/H = \mu \neq 3\beta/2\ \Delta \tau$	$\mu \neq 3\beta/2 = 4 \cdot 10^{-4}$; $\Delta \tau = 1^\circ$
ΔH	$\Delta H/H = 1/2(1 \neq \sin \theta)\Delta H$	$\nu = 0.01$
$\Delta \Delta$	$\Delta H/H = a/2 \cdot \Delta \Delta$	$a/2 = 2.3 \cdot 10^{-5}$; $\Delta \Delta = 1'$
ΔS	$\Delta H/H = b \Delta S$	$b = 1.2 \cdot 10^{-5}$; $\Delta S = 1$ second
$\Delta \alpha$	$\Delta H/H = \sin^2 1'/8\ \alpha \cdot \Delta \alpha$	$\alpha = S$; $\Delta \alpha = 1^\circ$
$\Delta \delta H$	$\Delta H/H = 1/2 \cdot \Delta \delta H/H$	$H = 0.15$ Oe; $\delta H = 1\gamma$

Declassified in Part - Sanitized Copy Approved for Release 2013/01/23 : CIA-RDP81-01043R001600090003-8

Declassified in Part - Sanitized Copy Approved for Release 2013/01/23 : CIA-RDP81-01043R001600090003-8

Table 45 Continued

Magnitude of the error $\Delta H/H$ at the value and error of argument stated in column 3	Permissible values of error in the measurement of each argument at $\Delta H/H = 10^{-4}$, assuming	
	Error of all other arguments equal to zero	Errors of all arguments of equal possibility
4	5	6
0.00495	20μ	6μ
0.00333	0.03	0.008 g · cm
0.00033	0.0003	0.0001 seconds
0.00014	0.71	10"
0.00056	0.18	0.05
0.000015	0.0002	0.00005
0.00005	0.0002	0.0013
0.00020	0.5°	0.1°
0.00020	0.5°	0.1°
0.0085	0.010 Oe	0.0030 Oe
0.00002	5'	1.5'
0.00001	10 seconds	3 seconds
0.00017	0.6°	0.2°
0.00003	3γ	1γ

TABLE 46

Errors	Values	Permissible Errors Relative	Absolute
Δ T	T = 3 seconds	0.0000043	0.000012 seconds
Δ r	r = 4 mm	0.0080	32 microns
Δ h	h = 10 cm	0.000016	1.6 microns
Δ m	m = 40 g	0.000032	1.3 mg

Declassified in Part - Sanitized Copy Approved for Release 2013/01/23 : CIA-RDP81-01043R001600090003-8

Declassified in Part - Sanitized Copy Approved for Release 2013/01/23 : CIA-RDP81-01043R001600090003-8

Section 11. Systemic Errors Caused by Imperfections of the Instruments.

Formulas (10.46) and (10.47), which define H and M, do not take into account certain imperfections of the instruments which can cause systemic errors in the determination of these quantities. Let us consider some most important sources of these errors.

Noncoincidence of the Center of Deflected Magnet with the Axis of the Deflecting Magnet. Let us assume that the center of the deflected magnet O_1 is located somewhat lower than the axis of the deflecting magnet M (Figure 218).

We draw a radius-vector from the center of the deflecting magnet to the center of the deflected magnet and denote the angle formed by this radius-vector with the axis of the magnet M by α. Considering the magnet M as an elemental, the components of the intensity of field h produced by the magnet at the point O will be

$$h_R = \frac{2M}{R_1^3}\cos\alpha \quad \text{and} \quad h_\theta = \frac{M}{R_1^3}\sin\alpha$$

where h_R is the component in the direction of radius-vector R, h_θ is the component in the direction perpendicular to the latter, and R_1 is the distance OO_1.

The field intensity h_1 acting upon magnet M' within the horizontal plane is:

$$h_1 = \frac{2M}{R_1^3}\cos^2\alpha - \frac{M}{R_1^3}\sin^2\alpha = \frac{M}{R_1^3}(3\cos^2\alpha - 1).$$

Upon calculating the horizontal component H we assume that a field of intensity h_o is acting on the magnet M, expressed by the formula

$$h_o = 2M/R^3,$$

where $R = OO_2 \approx R_1\cos\alpha$.

Since the horizontal component H is proportional to the magnitude of intensity h_1, the relative error in determination of H is equal to the relative error in the determination of h_1, i.e.,

Declassified in Part - Sanitized Copy Approved for Release 2013/01/23 : CIA-RDP81-01043R001600090003-8

Declassified in Part - Sanitized Copy Approved for Release 2013/01/23 : CIA-RDP81-01043R001600090003-8

$$\Delta H/H = h_1 - h_0/h_0$$

or

$$\Delta H/H = \cos^3 \alpha \ (3 \cos^2 \alpha - 1) - 2/2 = 3 \cos^5 \alpha - \cos^3 \alpha - 2/2.$$

Since the angle α usually is small, $\cos \alpha$ may be expanded to a series retaining the terms of second order, hence

$$\Delta H/H = 3/2(1 - \alpha^2/2)^5 - 1/2(1 - \alpha^2/2)^2 - 1$$

or, on expanding to a series of terms of the second order in accordance with the binomial formula:

$$\Delta H/H = -3\alpha^2.$$

Replacing the angle α by the ratio of O_1O_2 to R, we obtain:

$$\Delta H/H = -3 \ \overline{O_1O_2}^2/R^2.$$

Consequently, in order that the displacement of magnet M in relation to axis OO_1 will introduce no error greater than 0.0001 H, in the determination of H, the displacement O_1O_2 must not exceed the quantity $\sqrt{3R}/300$.

To eliminate such an error by means of observations does not appear possible, hence the only thing that can be done, is to set the deflected magnet in the horizontal plane through the axis of the deflected magnet with the degree of accuracy stated above. This setting is obtained by observation of the angles of deflection at different positions of the deflected magnet in relation to the horizontal plane OO_2. From the formula for h_1 it follows that with an increase in angle α or of distance O_1O_2 the intensity of the magnetic field h_1 which is produced by the deflecting magnet M decreases (minus sign), as a result of which the angle of deflection θ decreases with an increase of O_1O_2. Therefore, having carried out the observations, having plotted the graph representing the correlation between angle of deflection θ and distance O_1O_2 measured on the vertical scale, we obtain a parabola, the maximum of which will correspond to the position of the magnets when they are in a single horizontal plane.

Declassified in Part - Sanitized Copy Approved for Release 2013/01/23 : CIA-RDP81-01043R001600090003-8

Declassified in Part - Sanitized Copy Approved for Release 2013/01/23 : CIA-RDP81-01043R001600090003-8

Non-coincidence of Geometrical Centers of Deflected and Deflecting Magnets with their Magnetic Centers. Since the positions of the magnetic centers of the magnets are unknown the distance R between the magnets is measured between their geometrical centers, and thus a systemic error is knowingly introduced in the determination of H due to an error in the measurement of R. Since the distance between the geometric and magnetic centers may be several mm, at R $\simeq$ 300 mm the error in determination of H may reach several tenths of one percent and higher.

However, in the case of values of ΔR not exceeding a certain magnitude this error may be completely eliminated by observation of the angle of deflection at different positions of the deflecting magnet.

Thus, if the magnetic center of the deflecting magnet is shifted to the left in relation to the geometric center by a quantity $O_1O \simeq \Delta R$ (Figure 219) and the geometric and magnetic centers of the deflected magnet coincide, disregarding the correction terms, we have:

$$H \sin \Theta_1 \simeq 2M/(R + \Delta R)^3$$

where Θ_1 is the angle of deflection.

Rotating the deflecting magnet 180° around the geometric center the magnet M' will be deflected in the opposite direction by a certain angle Θ_2, and the preceding equation becomes:

$$H \sin \Theta_2 \simeq 2M/(R - \Delta R)^3$$

Adding these 2 equations term by term and dividing by 2, we obtain:

$$H \sin \frac{\Theta_1 + \Theta_2}{2} \cos \frac{\Theta_1 - \Theta_2}{2} = M\left[\frac{1}{(R+\Delta R)^3} + \frac{1}{(R-\Delta R)^3}\right].$$

Declassified in Part - Sanitized Copy Approved for Release 2013/01/23 : CIA-RDP81-01043R001600090003-8

Declassified in Part - Sanitized Copy Approved for Release 2013/01/23 : CIA-RDP81-01043R001600090003-8

Expanding $(R \pm \Delta R)^{-3}$ and $(R - \Delta R)^{-3}$ to a series with an accuracy up to terms of the second order, and introducing the denotations $\frac{\theta_1 + \theta_2}{2} = \theta_m$ and $\frac{\theta_1 - \theta_2}{2} = \gamma$, we have:

$$H \sin \theta_m \cos \gamma = \frac{M}{R^3}\left[1 + 3\frac{\Delta R^2}{R^2}\right];$$

since $\cos \gamma = 1 - \frac{\gamma^2}{2}$, this equation becomes, with an accuracy up to terms of the second order

$$H = \frac{2M}{R^3 \sin \theta_m}\left[1 + \frac{\gamma^2}{2} + 3\frac{\Delta R^2}{R^2}\right].$$

But since

$$3\frac{\Delta R}{R} = -\gamma \operatorname{ctg} \theta_m,$$

it follows that

$$H = \frac{2M}{R^3 \sin \theta_m}\left[1 + \left(\frac{1}{2} + \frac{1}{3}\operatorname{ctg}^2 \theta_m\right)\gamma^2\right].$$

Thus if the second term in parentheses is smaller than the given error the quantity H may be calculated according to the usual formula, taking the value of the angle θ as the mean of 2 observations when the north end of the deflecting magnet is placed successively in opposite directions.

At $\theta_m = 45^\circ$ the greatest permissible value of angle $\Delta\theta$, i.e., the greatest deflection will be $\gamma \leq 0.009$ or, measured in degrees, $\gamma \leq 32'$, with an accuracy of the H determination equal to 0.01%.

In exactly the same manner the error due to noncoincidence of geometric and magnetic centers of the deflected magnet is eliminated by observation of 2 angles of deflection when the deflecting magnet is placed on either side of the deflected magnet. Thus the errors caused by noncoincidence of geometric and magnetic centers of both magnets can be completely eliminated if the angle of deflection is taken as the mean value of 4 observations and if the distance R istaken as one-half of the distance between geometric centers of the deflecting magnet when it is placed on either side of the deflected

Declassified in Part - Sanitized Copy Approved for Release 2013/01/23 : CIA-RDP81-01043R001600090003-8

Declassified in Part - Sanitized Copy Approved for Release 2013/01/23 : CIA-RDP81-01043R001600090003-8

magnet, and if at the same time the difference between angles θ_1 and θ_2 does not exceed a definite magnitude. With an accuracy of 0.01% this difference must not exceed 64'.

Non-Perpendicularity of the Axes of Deflecting and Deflected Magnets in the First Lamontian Position. The axes of magnets in the first Lamontian position must be perpendicular to each other, and if not, formula (10.29) for finding the deflection must be replaced by a more general formula which takes into account the angle between the axes of the magnets.

Let us assume that the deflecting magnet M_1 (Figure 220) forms an angle α with the line OO_1 joining the centers of both magnets and the deflected magnet M_2 forms an angle β with the perpendicular to this line. If in a rough approximation both magnets are considered elemental, the condition of equilibrium of the deflected magnet will be of the form:

$$H_r \cos\beta + H_\alpha \sin\beta = H \sin\theta$$

where H_r and H_α are the components of the magnetic field produced by the elemental magnet M parallel and perpendicular to the direction of axis OO_1. Replacing H_r and H_α by the values (2.6) and (2.7) we obtain:

$$H = 2M_1/R^3 [\cos\alpha \cos\beta + 1/2 \sin\alpha \sin\beta]$$

In view of the smallness of angles α and β this equation may be written in the following form:

$$H = 2M_1/R^3 \sin\theta (1 - \alpha^2/2 - \beta^2/2 + \alpha\beta/2).$$

Consequently, in order that the non-perpendicularity of the magnets should not affect the quantity H, which is being determined with an accuracy of 0.01%, the values of α and β must satisfy the following conditions:

$$\alpha^2 \leq 0.0001 \quad \text{and} \quad \beta^2 \leq 0.0001 \quad \text{or}$$

$$\alpha \leq 35' \text{ and } \beta \leq 35'.$$

Declassified in Part - Sanitized Copy Approved for Release 2013/01/23 : CIA-RDP81-01043R001600090003-8

Declassified in Part - Sanitized Copy Approved for Release 2013/01/23 : CIA-RDP81-01043R001600090003-8

These conditions always can be met without special difficulty in building and adjusting the instrument, and therefore when carrying out observations this error may be disregarded.

Non-coincidence of the Center of Inertia Body with the Rotation Axis. In the discussion of the determination of the moment of inertia of the magnet it was assumed that the inertia body used to load the magnet was set in such a manner that its center of inertia coincides with the rotation axis. Let us find the error in the determination of the moment of inertia of the magnet which is caused by non-coincidence of the center of inertia with the rotation axis. The moment of inertia K, relative to any axis, is expressed by means of the moment of inertia K_c in relation to the axis extending through the center of inertia, in the following manner:

$$K = K_c + mr^2$$

where m is the mass of the body and r the distance between the center of inertia and the axis of rotation. Consequently the relative change in the moment of inertia due to displacement r of the center of inertia of the body relative to the rotation axis will be:

$$\Delta K_c/K_c = mr^2/k_c$$

For an inertia body having the shape of a cylinder this expression becomes: $\Delta K_c/K_c = 12/3R^2 + h^2 \quad r^2$

Assuming that the permissible error in the determination of the moment of inertia is $\Delta K_c = 0.008$ g · cm^2 for $K_c \geq 125$ g · cm^2, then $\Delta K_c/K_c = 0.000064$, and therefore the permissible displacement r of the center of inertia must satisfy the inequality:

$$r/h \leq \sqrt{0.0000053} \quad 2.9 \cdot 10^{-3}$$

At $h \geq 100$ mm the distance $r \leq 0.29$ mm.

Declassified in Part - Sanitized Copy Approved for Release 2013/01/23 : CIA-RDP81-01043R001600090003-8

Declassified in Part - Sanitized Copy Approved for Release 2013/01/23 : CIA-RDP81-01043R001600090003-8

Consequently a system upon which the magnet and the inertia body is suspended must permit adjustment of the center of the inertia body with an error not exceeding the above quantity.

Effect of Air Masses Entrained by the Magnetic System during Oscillation. During observation of the period of oscillation of the magnet the air surrounding the magnetic system is entrained by the moving body and takes part in its oscillatory motion. For this reason the moment of inertia of the magnetic system increases, and provides an additional source of error in the determination of H.

If on leading of the magnetic system with the inertia body the entrainment of air masses remained the same as in its absence, the moment of inertia of the system calculated according to formula (10.49) would represent the entrained air masses, and as a result the error would be equal to zero. But since the amount of entrained air mass depends upon the period of oscillation and on the shape of the system, it follows that the loading of the system with the inertia body changes its shape as well as the period of oscillation, and therefore the mass of entrained air also is changed.

Let us consider one of the instances when loading of the magnetic system with the inertia body does not change its shape; namely, the case when the magnet is a hollow cylinder and the inertia body is a cylinder which is inserted into the magnet, completely filling its internal space. In the oscillation of the magnetic system without the inertia body it may be assumed that the air inside the magnet fully participates in the oscillatory motion. Therefore the moment of inertia K of the oscillating system consists of the moment of inertia of the magnetic system K_1, the moment of inertia of a cylindrical column of air inside the magnet K_2, and the moment of inertia of the air mass K_3 surrounding the magnet and being entrained by the system, i.e.,

$$K = K_1 + K_2 + K_3.$$

Declassified in Part - Sanitized Copy Approved for Release 2013/01/23 : CIA-RDP81-01043R001600090003-8

Declassified in Part - Sanitized Copy Approved for Release 2013/01/23 : CIA-RDP81-01043R001600090003-8

When loaded with the inertia body the moment of inertia of the oscillating system K' is expressed by the sum:

$$K' = K_1 + K_0 + K_3$$

where K_0 is the moment of inertia of the body, since in lieu of the air there will be a cylinder having the moment of inertia K_0 inside the magnet. For the sake of simplicity it is assumed that the mass of entrained air around the magnetic system remains the same in both instances.

Adding and subtracting K_2, we obtain:

$$K' = K + (K_0 - K_2)$$

According to formula (10.49), taking K_0 as the moment of inertia of the inertia body when calculating the moment of inertia of the system K, we introduce a systemic error

$$\Delta K/K = \Delta K_0/K_0 = K_2/K_0$$

since $\Delta K_0 = K_2$.

In view of the fact that the cylinder of air and the inertia body have the same shape the ratio K_2/K_0 is equal to ratio of their masses or densities, i.e.,

$$K_2/K_0 = D_2/D_0$$

where D_2 is the density of air, 0.0013 g/cm^3, and D_0 is the density of the inertia body, 8.0 g/cm^3, hence

$$\Delta K/K = 0.00016 .$$

For $K = 125$ g/cm^2, $\Delta K = 0.02$ g/cm^2, whereas the permissible error in the determination of K must not exceed 0.008.

Thus the influence of this factor on the error of the results, even when the shape of the magnetic system remains constant, can be of considerable magnitude, exceeding the permissible values of the error.

Declassified in Part - Sanitized Copy Approved for Release 2013/01/23 : CIA-RDP81-01043R001600090003-8

Declassified in Part - Sanitized Copy Approved for Release 2013/01/23 : CIA-RDP81-01043R001600090003-8

To eliminate this influence the observations must be performed in a medium containing no air or, having determined the error due to the air masses, a constant correction must be made.

Section 12. Absolute Electric Method of Determining the Horizontal Component.

The absolute method of Gauss based upon the interaction of permanent magnets within the magnetic field of the earth meets the principal requirement of the independence of absolute measurements from any quantities other than length, mass and time, but has the disadvantage that the error in measurement cannot be reduced below 0.01%, whereas the error of absolute measurement of electrical quantities, current intensity and resistance, does not exceed 0.001%. Therefore, concurrently with improvements in procedures and equipment of the absolute method of Gauss, during the last century electrical methods were developed for measuring the horizontal component of the terrestrial field. Electrical methods of measurement are based upon the interaction of a conductor carrying a current, with a permanent magnet located within the magnetic field of the earth.

If, in observing the angle of deflection by the Gauss method the deflecting magnet is replaced by a coil carrying an electric current of corresponding magnitude, we have a sine-galvanometer electrical method. Denoting the intensity of the magnetic field produced by the coil by H_0, the equilibrium equation of the deflected magnet as defined by equation (10.28) is written in the form:

$$H \sin \Theta = H_0$$

or, since H_0 always is proportional to the current intensity I:

$$H \sin \Theta = kI. \qquad (10.59)$$

The coefficient of proportionality K constitutes a certain function of the geometric dimensions of the coil. By measuring the

Declassified in Part - Sanitized Copy Approved for Release 2013/01/23 : CIA-RDP81-01043R001600090003-8

Declassified in Part - Sanitized Copy Approved for Release 2013/01/23 : CIA-RDP81-01043R001600090003-8

angle of deflection Θ and the intensity of current I in the coil we may determine the magnitude of the horizontal component H, provided the coefficient of proportionality K is known.

In modern instruments the deflecting coil consists of Helmholtz rings, and the magnet to be deflected is placed at the center of the rings. The size of the magnet should enable it to fit entirely within the uniform portion of the magnetic field of the rings. From Table 1 in Section 7 of the introduction, it is apparent that over a distance equal to 0.05 of the radius of the ring the field is uniform within 10^{-6} of the magnitude of its intensity. Therefore, if the length of the magnet is less than 0.1 of the ring radius R the field may be considered uniform and its intensity is calculated according to formula (0.40) without correction terms, but taking into account the term which depends upon the dimensions of the ring cross section, i.e.,

$$H_o = 4\pi IwR^2/(R^2 + d^2)^{3/2} (1 - b^2/R^2)$$

since an exact correspondence between radius R and distance d between the rings cannot be attained.

Consequently the coefficient of proportionality K in the case of Helmholtz rings is of the form:

$$K = 4\pi wR^2/(R^2 + d^2)^{3/2} (1 - b^2/R^2) \qquad (10.60)$$

In order to impart a regular geometric shape to the Helmholtz rings, i.e., to maintain their coaxial disposition and definite separation the rings are made in the shape of a circular cylinder of quartz or pyrex, on the surface of which are wound several turns of uninsulated wire, a second, identical ring is located at a distance equal to the radius of the cylinder. The turns are placed into a previously cut helical groove in order to maintain uniform pitch of the winding and to prevent contact between the turns.

Declassified in Part - Sanitized Copy Approved for Release 2013/01/23 : CIA-RDP81-01043R001600090003-8

Declassified in Part - Sanitized Copy Approved for Release 2013/01/23 : CIA-RDP81-01043R001600090003-8

This design of the rings ensures rigorous coaxiality and constant diameter of the turns with an accuracy within a few microns at a diameter of 30-40 cm.

The diameter and distance between rings are measured by means of special machines which enable measurements to be made within an error of decimal fractions of a micron.

The current intensity I is measured by means of a potentiometer, which includes a standard cell and a standard resistance and makes it possible to determine I with an error of $5 \cdot 10^{-6}$ of the measured magnitude.

From equations (10.59) and (10.60) it follows that the relative error of measurement of the horizontal component, depending upon the errors of the direct measurements, is defined by the correlation:

$$\left(\frac{\Delta H}{H}\right)^2 = 0.16\left(\frac{\Delta R}{R}\right)^2 + \left(\frac{\Delta I}{I}\right)^2 + ctg^2\theta\,\Delta\theta^2 + \left(\frac{\Delta w}{w}\right)^2 + 0.36\left(\frac{\Delta d}{R}\right)^2,$$

on the condition that the distance d between the rings differs from the radius R by a small quantity.

The relative error Δ w/w may be replaced by the relative change in length of winding, or a multiple of the number of turns, i.e.,

$$\frac{\Delta w}{w} = \frac{\Delta l}{2\pi w R},$$

where Δl is the distance between 2 generatrixes of the cylinder, one of which extends through the beginning of the winding and the other through its end.

At R =15 cm, w =10, θ =45° and $\Delta\theta = \pm 1''$, assuming $\Delta R = \Delta d = \pm 1\mu$, $\frac{\Delta I}{I} = 5 \cdot 10^{-6}$ and $\Delta l = \pm 0.1$ mm we have

$$\frac{\Delta H}{H} = \pm 8.4 \cdot 10^{-6},$$

which at Leningrad, where H is approximately 0.15 Oe, amounts to

$$\Delta H = \pm 0.12\ \gamma.$$

Declassified in Part - Sanitized Copy Approved for Release 2013/01/23 : CIA-RDP81-01043R001600090003-8

Declassified in Part - Sanitized Copy Approved for Release 2013/01/23 : CIA-RDP81-01043R001600090003-8

a quantity which is almost one order of magnitude lower than the error in measurement by the method of Gauss.

Section 13. Absolute Magnetic Theodolite of VNIIM.

Of all the known magnetic theodolites intended for the absolute determination of the horizontal component, let us consider the theodolite designed at the magnetic laboratory of the All-Union Scientific Research Institute of Metrology imeni D. I. Mendeleyev (VNIIM) [82]. A diagram of this theodolite is shown in Figure 221 and external views are shown in Figures 222 and 223.

The principal characteristic of the VNIIM theodolite which differentiates it from all others is that it has 2 pairs of Helmholtz rings, which enable measurement of the horizontal component H both by the method of Gauss and by the electrical method, and also enables reproduction of the unit of intensityy of the magnetic field and magnetic flux.

The first pair of rings K_2 (Figure 221) consist of a single layer winding of uninsulated wire on a pyrex cylinder 300 mm in diameter, with 10 turns spaced at a distance of 150 mm on each ring.

This arrangement of the rings enables the necessary accuracy to be maintained in their manufacture, both in measuring the diameter and the distance between the windings.

The second pair of rings K_1, are 500 mm in diameter and consist of 2 multiple layer coils of rectangular section. The distance between the center planes of these coils is 250 mm. The first pair of rings is used to measure the horizontal component H by the electrical method described above.

For the determination of H by the method of Gauss the theodolite

Declassified in Part - Sanitized Copy Approved for Release 2013/01/23 : CIA-RDP81-01043R001600090003-8

Declassified in Part - Sanitized Copy Approved for Release 2013/01/23 : CIA-RDP81-01043R001600090003-8

is provided with a bar PQ, on which the deflecting magnet is placed. At the ends of the bar are horizontal circles with division marks which serve for determination of the coefficients of distribution, whereas with conventional theodolites, the coefficient of distribution p is determined from observation of the angle of deflection at 3 different distances of the deflecting magnet, with the VNIIM theodolite p determined repeatedly at the same distance, but at different angles between the axis of the magnet and the axis of the bar. For this purpose the deflecting magnet M is placed on the horizontal circle, and by rotating it the magnet M may be positioned at any angle to the axis of the bar.

The horizontal circle L of the instrument, which is 270 mm in diameter, has divisions at intervals of $1/6^{o}$, and with an accuracy within 2" readings are taken by means of the microscopes F_1 and F_2.

The magnet housing B consists of a cylindrical wooden box, with 110 mm inside diameter. The deflected magnet carrying a mirror at the end is suspended inside the box from a metal filament. The 400 mm-long suspension tube C, has a twisting knob P at the top which permits the filament to be twisted or untwisted, moved vertically, or in 2 mutually perpendicular directions within the horizontal plane in order to adjust the magnetic center of the deflected magnet at the intersection of the vertical axis of the instrument with the axis of the deflecting magnet.

The reading telescope D is provided with a Gaussian eyepiece and serves for observation of the angles of deflection.

The distance between the deflected and the deflecting magnets is measured by a comparing device consisting of 2 measuring microscopes and a cylindrical arm bearing 2 pairs of linear marks 600 and 800 mm apart.

Declassified in Part - Sanitized Copy Approved for Release 2013/01/23 : CIA-RDP81-01043R001600090003-8

Declassified in Part - Sanitized Copy Approved for Release 2013/01/23 : CIA-RDP81-01043R001600090003-8

By special supports the arm is carried to a position parallel to the bars, so that the linear marks of the arm are aligned with the linear marks on the deflecting magnets when these magnets are placed on the horizontal circles. Since the distance between the linear marks of the arm is known, the double distance between the centers of the deflecting and the deflected magnets is determined by measuring the difference between linear marks on the arm and linear marks on the magnets by means of the microscopes.

The period of oscillation and the moment of inertia are determined in a special glass housing, the external appearance of which is shown in Figure 224. The housing is of cylindrical shape, 200 mm long, and has a suspension tube. During observations the air is evacuated from the housing to eliminate the effect of the masses of air which oscillate with the magnet.

Thus the VNIIM theodolite makes it possible to determine H in absolute units by 2 independent methods, and thus to obtain a reliable evaluation of the magnitude of the absolute error of measurements.

The second pair of rings, together with a third coil of cylindrical shape, serves to reproduce the unit of magnetic flux and thus constitutes a standard of magnetic flux.

The cylindrical coil consists of a marble cylinder 20 mm in diameter and 20 mm long, with a single-layer winding of wire 1/10 mm in diameter. The coil is placed at the center of the Helmholtz rings in lieu of the magnet housing, which is first removed, and the axis of the coil must coincide with the axis of the rings.

The intensity of the field of the second pair of Helmholtz

Declassified in Part - Sanitized Copy Approved for Release 2013/01/23 : CIA-RDP81-01043R001600090003-8

Declassified in Part - Sanitized Copy Approved for Release 2013/01/23 : CIA-RDP81-01043R001600090003-8

rings is determined by comparison with the field of the first pair, through observation of the period of oscillation of the magnet in the field of the first and in the field of the second pair of rings, or by observation of the angles of deflection.

If the field intensity of the second pair of rings at a current intensity of I_2 is denoted by H_2, the magnetic flux permeating the cylindrical coil will be:

$$\Phi = \pi/4 \; d^2 H_2 \; w$$

where w is the number of turns of the cylindrical coil, from which it follows that the flux corresponding to a unit of current intensity or, to put it differently, the mutual inductance of the 2 coils will be:

$$M = 1/I_2 \cdot \pi/4 \; d^2 H_2 \; w.$$

Since the right hand portion of this equation consists of quantities which can be measured directly, M also is determined directly in absolute units. When M is known we can determine the magnitude of mutual inductance of any pair of coils.

Section 14. The Relative Method of Gauss for Determination of the Horizontal Component

The method which Gauss had proposed as an absolute method has been utilized extensively as a relative method in magnetic surveys of the terrestrial globe. During the entire nineteenth and up to the third decade of the twentieth century this was the only method used in Russia, the USSR and abroad. In view of the fact that this method has not lost its importance up to the present time it deserves discussion in this text.

The principle and theory of this method are the same as those of the absolute method and the only difference is the procedure used in determining the constant factor A, which for relative measurements

Declassified in Part - Sanitized Copy Approved for Release 2013/01/23 : CIA-RDP81-01043R001600090003-8

Declassified in Part - Sanitized Copy Approved for Release 2013/01/23 : CIA-RDP81-01043R001600090003-8

is determined by observation of the half-period T and the angle θ at an observatory where the horizontal component H is known, i.e.,

$$A = HT \sqrt{\sin \theta} / [1 + \Sigma]$$

where Σ is the sum of all the correction terms.

Consequently, with the relative method the distance between the magnets R, the moment of inertia K of the magnet, and the coefficients of distribution p and q need not be measured. It is necessary only that during the observations the magnet always must be set at the same distance and for determination of the half-period T it always must be suspended in the same position in order that R and K will be constant.

The sequence of observations and the formulas for calculation of H remain the same as in the absolute method.

The error in determination by the relative method is determined merely by differentiation of the formula (10.30) i.e.,

$$\frac{dH}{H} = \frac{dA}{A} - \frac{dT}{T} - \frac{1}{2} \operatorname{tg} \theta \, d\theta + d\Sigma (1 + \Delta),$$

or

$$\left(\frac{\Delta H}{H}\right)^2 = \left(\frac{\Delta A}{A}\right)^2 + \left(\frac{\Delta T}{T}\right)^2 + \frac{1}{4} \operatorname{tg}^2 \Delta\theta + \sum \Delta^2, \quad (10.61)$$

where $\sum \Delta^2$ is the sum of the squares of errors caused by the correction terms.

Thus it is apparent that in order to attain a relative error in the determination of H not exceeding a given magnitude, the relative error in the determination of the magnet constant A must be several times smaller than this magnitude. Therefore the determination of A at an observatory is based on several independent observations, the number of which depends upon the predetermined accuracy of the measurement of H.

Declassified in Part - Sanitized Copy Approved for Release 2013/01/23 : CIA-RDP81-01043R001600090003-8

Declassified in Part - Sanitized Copy Approved for Release 2013/01/23 : CIA-RDP81-01043R001600090003-8

The required accuracy of determination of the horizontal component under field conditions is about 10 times less than the accuracy of absolute observations at observatories. Therefore, the permissible errors of direct measurements of all the quantities appearing in formula (10.61) can be 10 times greater than those set forth in Table 45.

Section 15. Measurement of the Horizontal Component by the Method of Deflections (Abridged Method of Gauss)

At the present time the deflection method, an abridgement of the method of Gauss employing observations of the angle of deflection only, frequently is used for determination of the horizontal component under field conditions.

Therefore the theory and the observational procedure remain the same as in the method discussed in the preceding paragraph.

The formula for calculating the horizontal component in accordance with observations of the angle of deflection is of the form [see equation (10.29)]: $H = 2M/R^2 \sin\theta\,[1 + \Sigma]$, where Σ is the sum of correction terms for temperature, induction action of terrestrial field etc.

The correction terms are readily determined through the use of the general formula (10.46), in which it is necessary to retain only those terms which depend upon the processes of observation of the angle of deflection and to raise them to the square, i.e., multiplying by 2, since in the derivation of formula (10.46) we extracted the square root of expression (10.29). Hence,

$$H = \frac{2M}{R^3 \sin\theta}\,[1 + (\mu + 3\beta)(t - 20) - \nu H \sin\theta].$$

Taking M and R as constants, and using the denotation $\frac{2M}{R^3} = B'$, we have:

$$H = \frac{B'}{\sin\theta}\,[1 + (\mu + 3\beta)(t - 20) - \nu H \sin\theta].$$

Declassified in Part - Sanitized Copy Approved for Release 2013/01/23 : CIA-RDP81-01043R001600090003-8

Declassified in Part - Sanitized Copy Approved for Release 2013/01/23 : CIA-RDP81-01043R001600090003-8

The product H sin Θ, at first approximation, is a constant quantity and therefore the correction term ν H sin Θ is constant.

Therefore, denoting the constant quantity $B'(1 - \nu H \sin \Theta) = B$, we obtain the final formula for H:

$$H = \frac{B}{\sin \theta}\left[1 + (\mu + 3\beta)(t - 20)\right].$$

The coefficient B is called the conversion factor and is determined from observations of the angle Θ at an observatory where H is known. If we denote the magnitude of the horizontal component at the observatory by H_0, and the deflection angle by Θ_0, it follows that

$$B = H_0 \sin \theta_0 \left[1 - (\mu + 3\beta)(t - 20)\right].$$

Thus the error in determination by the method of deflections is expressed by the formula

$$\left(\frac{\Delta H}{H}\right)^2 = \left(\frac{\Delta B}{B}\right)^2 + \operatorname{ctg}^2 \theta \Delta\theta^2 \sin^2 1' + (\mu + 3\beta)^2 \Delta t^2 + (t - 20)^2 \Delta\mu^2 \quad (10.62)$$

As stated above, the acceptable error in field observations for the determination of H is of the order of $\pm$ 0.001. Therefore, considering the errors of H due to each term of the expression (10.62) as being equal, we obtain the following values for permissible errors of direct measurements of Θ and t, and in the determination of B and μ at $\theta = 45^\circ$, $\mu = 0.0004$ and $t = 15$:

$$\frac{\Delta B}{B} \leq 0.001, \quad \Delta\theta \leq 1.8', \quad \Delta t \leq 1.2^\circ \quad \Delta\mu \leq 0.0001$$

The sequence of observations and the table of recordings are the same as in the method of Gauss for the observation of the deflection angle.

It must be stated that the deflection method can yield correct results only in the case when the quantity B remains within 0.001 of its magnitude during the entire period of field observations. The constant nature of B, in turn, depends on the constant nature of the magnetic moment of the deflecting magnet. Therefore, for the observation of H by the method of deflections it is necessary to have a

Declassified in Part - Sanitized Copy Approved for Release 2013/01/23 : CIA-RDP81-01043R001600090003-8

Declassified in Part - Sanitized Copy Approved for Release 2013/01/23 : CIA-RDP81-01043R001600090003-8

well stabilized deflecting magnet made from a material of great coercive force (cobalt or nickel-aluminum steel).

Section 16. The Relative Electric Method of Measurement of H.

Under field conditions the electric method described in Section 12 is used as a relative method , i.e., the quantity H_0 in equation (10.59) is determined from observation of the angle of deflection at an observatory where the horizontal component is known. In such a case it is necessary that the current intensity I used during the field observations equal that used within an accuracy of the order of 0.001 of its magnitude.

Therefore the primary problem of the electric method is that of maintaining a constant current intensity within the above stated limit of accuracy during the entire period of field observations. This is attained by regulating the current in a compensation circuit which is described below.

Two resistances r and r_π in the principal circuit are connected in series with the coil K (Figure 225), one of which, r, can be regulated while the other, r_π, is constant. An auxiliary circuit consisting of a standard cell E_π and galvanometer G is connected in parallel with the constant resistance r_π. If the current intensity over the sector Ea is equal to I', is equal to I over ab, and is equal to I" over aGb, according to the laws of Kirchhoff it follows that:

$$I = I' + I'' \text{ or } E_\pi = I r_\pi + I'' r, \qquad (10.63)$$

where r is the resistance of aGb.

In order that the current will be the same everywhere within the circuit EabK it is necessary that $I'' = 0$, and this is possible if

$$E_\pi = I r_\pi ,$$

Declassified in Part - Sanitized Copy Approved for Release 2013/01/23 : CIA-RDP81-01043R001600090003-8

Declassified in Part - Sanitized Copy Approved for Release 2013/01/23 : CIA-RDP81-01043R001600090003-8

i.e., if the drop in potential over ab is equal to the electromotive force of the standard cell $E_{\text{н}}$. On this condition

$$I = E_{\text{н}}/r_{\text{ab}}.$$

Since the electromotive force of a standard cell is a constant quantity and the resistance r_{ab} also is constant it follows that when no current flows through the galvanometer we always have the same value of current intensity in the circuit of the coil. To attain this it is necessary to adjust the current intensity in the circuit EabK by means of rheostat r in such a manner that the galvanometer G is not actuated.

In the event that the galvanometer shows any deflection the current intensity I in the circuit of the coils will be expressed by the formula (10.63):

$$I = E_{\text{н}} - I'''r_G/r_{\text{ab}}$$

or, since $I''' = \Delta n \varepsilon$, where Δn is the deflection of the galvanometer and ε the value of one division of the galvanometer scale,

$$I = E_{\text{н}} - \varepsilon r_G \Delta n/r_{\text{ab}}.$$

Design of the Instrument. The magnetic theodolite "combine" /kombayn/ which, as may be seen in Figure 226, is equipped with Helmholtz rings K, utilizes the electric method. The magnet used in the method of deflections also serves as the deflected magnet in this instrument.

This magnet also constitutes the movable part of the galvanometer, consisting of 2 coils 5 cm in diameter, with this magnet located at the center of the coils.

The Helmholtz rings are provided with terminals for switching on the galvanometer current. When H is measured by the electric

Declassified in Part - Sanitized Copy Approved for Release 2013/01/23 : CIA-RDP81-01043R001600090003-8

Declassified in Part - Sanitized Copy Approved for Release 2013/01/23 : CIA-RDP81-01043R001600090003-8

method the theodolite "combine" is supplemented with a potentiometer in a special box. The diagram of the potentiometer is shown in Figure 225. It includes a standard cell, a standard and an adjustable resistance, a disconnecting switch, a change-over switch and a storage battery.

Sequence of Observations. The sequence of observations and the table of data are similar to those of the method of deflections described above.

After the magnet has been set to coincide with the magnetic meridian the current to the Helmholtz rings is switched on and the plane of the coil is rotated until the magnetic axis of the magnet assumes a position parallel to the plane of the coils. While observing the behavior of the magnet through the telescope the coils of the galvanometer are switched on and the current in the Helmholtz rings is regulated until the magnet ceases to react to the switching-on and -off of the current in the galvanometer coil.

Next, the plane of the Helmholtz rings is set exactly coincidentally with the axis of the magnet, and a reading is taken of the horizontal circle.

Following repetition of the operation with an opposite direction of the current in the Helmholtz rings a second reading is taken. The difference between the readings gives the double angle of deflection.

The potentiometer usually has 2 standard cells. Therefore the observations are repeated with a switch-over to the second standard cell.

Declassified in Part - Sanitized Copy Approved for Release 2013/01/23 : CIA-RDP81-01043R001600090003-8

Declassified in Part - Sanitized Copy Approved for Release 2013/01/23 : CIA-RDP81-01043R001600090003-8

Section 17. The "Combine" Magnetic Theodolite

The "combine" theodolite (Figure 226) is used in the measurement of the elements of terrestrial magnetism: declination, horizontal component, and dip under field conditions.

The "combine" is a relative instrument and enables determination of the horizontal component by 2 methods: the method of deflection and the electric method.

The instrument consists of a horizontal circle A with divisions at intervals of 0.5° and with readings of 0.1', a magnet housing B in the form of a rectangular box, a suspension tube C, Helmholtz rings K, reading telescope T and 2 bars P and Q for holding the deflecting magnet M. A characteristic feature of the "combine" magnetic theodolite is the absence of both a magnet housing for oscillation, and of the corresponding device for observation of the oscillation of the deflecting magnet. Therefore with this instrument the method of Gauss may be utilized only in an abridged form, to observe the angle of deflection.

To ensure a constant magnetic moment the deflecting magnet is made from either cobalt steel or nickel-aluminum steel. For control measurements, observations can be made by the electric method, in which case the Helmholtz rings supplied with current from a 3 to 4 volt battery serve as the deflecting factor.

On the one side of the magnet housing is a round port hole with a plane-parallel glass pane through which the magnet is sighted by the reading telescope, and on the other side is a door for placing the magnet into the housing.

Declassified in Part - Sanitized Copy Approved for Release 2013/01/23 : CIA-RDP81-01043R001600090003-8

Declassified in Part - Sanitized Copy Approved for Release 2013/01/23 : CIA-RDP81-01043R001600090003-8

The deflecting magnet M is placed on a special carrier which may be moved along the bar, and thus may be set at a definite distance corresponding to a deflection angle of 30° to 40°.

Inside the housing is a second pair of small diameter rings, the axis of which extends through the center of the deflected magnet. These rings serve as the fixed coils of a pointer galvanometer in measuring the horizontal component by the electric method.

The bar with the carrier can rotate 90° around the horizontal axis for positioning the vertical rods in measuring dip by the induction method (see Section 6).

Section 18. Measurement of the Horizontal Component by Means of the Quartz Magnetometer

Recently an instrument called the quartz magnetometer, which is essentially designed for comparing observatory instruments has been used extensively for the purpose of measuring the horizontal component. This instrument is a magnetic theodolite in which the magnet is deflected through the torsion of a quartz filament from which the magnet is suspended.

Theory of the Method. Let us assume a magnet of moment M is suspended by a filament the torsion coefficient of which is C, and let β be the initial angle of twist of this filament. In the position of equilibrium the magnet will form a certain angle α (Figure 227) with the magnetic meridian, and the condition of equilibrium will be:

$$MH \sin\alpha = C\beta. \qquad (10.64)$$

If the filament is twisted through an angle $2k\pi$, where k

Declassified in Part - Sanitized Copy Approved for Release 2013/01/23 : CIA-RDP81-01043R001600090003-8

Declassified in Part - Sanitized Copy Approved for Release 2013/01/23 : CIA-RDP81-01043R001600090003-8

is an integer, the magnet will be deflected from the initial position by an angle θ_1, and the new condition of equilibrium will be:

$$MH\sin(\alpha+\theta_1) = C(2k\pi+\beta). \qquad (10.65)$$

If the filament is twisted $2k\pi$ in the opposite direction the condition of equilibrium in the new position will be analogous to that of equation (10.65):

$$MH\sin(\alpha-\theta_2) = -C(2k\pi-\beta). \qquad (10.66)$$

Replacing $C\beta$ in equations (10.65) and (10.66) by the quantity $MH\sin\frac{\beta}{2}$, in accordance with equation (10.64), we have:

$$H\sin(\alpha+\theta_1) = \frac{-2k\pi C}{M} + H\sin\alpha, \qquad (10.67)$$

$$H\sin(\alpha-\theta_2) = \frac{2k\pi C}{M} + H\sin\alpha. \qquad (10.68)$$

These equations make it possible to determine the value of H from observation of the angles of deflection θ_1 and θ_2, given the constant coefficient:

$$A = \frac{-2k\pi C}{M}. \qquad (10.69)$$

To do this it is sufficient to subtract one equation from the other, as a result of which we have:

$$H = \frac{4k\pi C}{M}\cdot\frac{1}{\sin(\alpha+\theta_1)-\sin(\alpha-\theta_2)}.$$

Replacing the difference of sines in the denominator in accordance with trigonometric formulas and replacing the constant factor $4\pi kC/M$ by A, we have:

$$H = \frac{A}{\sin\frac{\theta_1+\theta_2}{2}\cos\left(\frac{\theta_1-\theta_2}{2}+\alpha\right)}. \qquad (10.70)$$

The magnitude of angle α may be determined by adding equations (10.67) and (10.68) term by term; in which case

$$\sin(\alpha+\theta_1)+\sin(\alpha-\theta_2) = 2\sin\alpha$$

or, on expanding the sines according to trigonometric formulas:

$$\sin\alpha(\cos\theta_1+\cos\theta_2)+\cos\alpha(\sin\theta_1-\sin\theta_2) = 2\sin\alpha$$

and therefore,

$$\operatorname{tg}\alpha = \frac{\sin\theta_1-\sin\theta_2}{2-(\cos\theta_1+\cos\theta_2)}, \quad \text{or} \quad \operatorname{tg}\alpha = \frac{\sin\frac{\theta_1-\theta_2}{2}\cos\frac{\theta_1+\theta_2}{2}}{1-\cos\frac{\theta_1+\theta_2}{2}\cos\frac{\theta_1-\theta_2}{2}}.$$

Declassified in Part - Sanitized Copy Approved for Release 2013/01/23 : CIA-RDP81-01043R001600090003-8

Declassified in Part - Sanitized Copy Approved for Release 2013/01/23 : CIA-RDP81-01043R001600090003-8

When α is close to zero, i.e., when the filament is untwisted, the difference between θ_1 and θ_2 is very slight, and therefore in equation (10.70) $\cos\left(\frac{\theta_1 - \theta_2}{2} + \alpha\right)$ may be equated to unity. In such a case

$$H = \frac{A}{\frac{\theta_1 + \theta_2}{2}} = \frac{A}{\sin\varphi}, \tag{10.71}$$

where $\varphi = \frac{\theta_1 + \theta_2}{2}$.

It is apparent that equation (10.71) is fully analogous to the equation for the determination of H by the method of deflections.

For comparison of observatory instruments by this method the coefficient A must be constant. Yet from equation (10.69) it is apparent that A is a function of the quantities C and M, which in turn depend upon temperature and the induction influence of the terrestrial field.

In order to eliminate these influences correction terms must be introduced in the usual manner, i.e., to write coefficient A in the following form:

$$A = \frac{-\lambda \cdot C_0 [1 + \mu_c (t - t_0)]}{M_0 [1 - \mu_m (t - t_0)][1 + \nu H \cos\varphi]}$$

or

$$A = A_0 [1 + \mu (t - t_0) - \nu H \cos\varphi],$$

where μ_c is the temperature coefficient of the torsion of the filament, μ_m is the temperature coefficient of the magnet, ν is the induction coefficient, C_0 and M_0 are the values of C and M at initial temperature t_0 and in the absence of field H, and μ is the temperature coefficient of the instrument, equal to $\mu_c + \mu_m$.

Substituting the derived value of coefficient A into equations (10.70) and (10.71), at $\alpha > 0$ we finally obtain:

$$H = \frac{A_0 [1 + \mu (t - t_0) - \nu H \cos\varphi]}{\sin\frac{\theta_1 + \theta_2}{2} \cos\left(\frac{\theta_1 - \theta_2}{2} + \alpha\right)} \tag{10.72}$$

At $\alpha = 0$:

$$H = \frac{A_0 [1 + \mu (t - t_0) - \nu H \cos\varphi]}{\sin\varphi} \tag{10.73}$$

Declassified in Part - Sanitized Copy Approved for Release 2013/01/23 : CIA-RDP81-01043R001600090003-8

Declassified in Part - Sanitized Copy Approved for Release 2013/01/23 : CIA-RDP81-01043R001600090003-8

Errors in the Determination of H. Upon differentiating equation (10.72), we obtain:

$$\Delta H = -H \operatorname{ctg} \Delta\varphi + H \operatorname{tg}\left(\frac{\varphi_1 - \varphi_2}{2} + \alpha\right)\Delta\left(\frac{\varphi_1 - \varphi_2}{2} + \alpha\right) + H\mu\,\Delta t.$$

Since Δ usually is small, it follows that assuming

$$\frac{\varphi_1 - \varphi_2}{2} = \frac{\varphi_1 - \varphi}{2} + \alpha = \psi,$$

we obtain

$$\Delta H^2 = H^2 \operatorname{ctg}^2\varphi\,\Delta\varphi^2 + H^2 \operatorname{tg}^2\psi\,\Delta\psi^2 + H^2 \operatorname{tg}^2\psi\,\Delta\alpha^2 + (H\mu\,\Delta t)^2.$$

If φ, ψ and α are expressed in minutes of arc, we have

$$\Delta H^2 = H^2 \operatorname{ctg}^2\varphi \sin^2 1' \Delta\varphi'^2 + H^2 \operatorname{tg}^2\psi \sin^2 1' \Delta\psi'^2 + H^2 \operatorname{tg}^2\psi \sin^2 1' \Delta\alpha'^2 + \ldots + (H\mu\,\Delta t)^2.$$

At $\alpha = 0$ this expression assumes the form:

$$\Delta H^2 = H^2 \operatorname{ctg}^2\varphi \sin^2 1' \Delta\varphi^2 + (H\mu\,\Delta t)^2.$$

Thus we see that the error in determination of H by this method is of the same order as in the determination by the method of deflections.

With an angle of deflection $\varphi = 45$ and H = 15700 γ:

$$\Delta H = \mp 4.36\,\Delta\varphi',$$

or, an error of 1' in the measurement of the angle will cause an error of 4.36 γ in the determination of H.

Description of the Instrument. The characteristic feature of a quartz magnetometer based upon this principle is the absence of a horizontal circle. Since the instrument is designed for comparison of observatory instruments, it is always possible to utilize the circle of an observatory instrument and to set the quartz magnetometer at the center of this circle.

The instrument consists of a cylindrical housing (Figure 228) approximately 40 mm in diameter 50 mm high, and a suspension tube K approximately 160 mm long and 20 mm in diameter. The housing has 2 circular windows, a and b. A telescope is attached to one window by a threaded connection, and at the opposite side is a counterweight.

Declassified in Part - Sanitized Copy Approved for Release 2013/01/23 : CIA-RDP81-01043R001600090003-8

Declassified in Part - Sanitized Copy Approved for Release 2013/01/23 : CIA-RDP81-01043R001600090003-8

The dimensions of magnet M are approximately 1 x 1 x 15 mm, and the magnetic moment is 2 CGSμ. To lock it in position during transportation the rod to which the magnet is fastened is clamped between 2 plates by means of a perpetual screw N.

To prevent the filament from breaking on locking, on top of the rod is cone-shaped, which when clamped between the plates causes the magnet to rise slightly, thus slackening the filament. The magnet is suspended by a quartz filament l.

Sequence of Operations. The quartz magnetometer is set on the horizontal circle of some instrument and is attached to it with a light cement. If it is found that the filament is twisted over a large angle the filament is untwisted to $2k\pi$ by turning the horizontal circle the required number of times. The twisting knob is used to untwist an angle smaller than $2k\pi$. After untwisting, the axis of the telescope is sighted at the mirror of the magnet and a reading of the circle is taken. The filament then is twisted to $2k\pi$ by corresponding rotation of the horizontal circle, and a second reading of the circle is taken. The difference between the readings gives the angle θ_1. Analogous twisting in the opposite direction over $4k\pi$ yields the angle θ_2.

Section 19. Double Compass for Measuring H.

The methods for measuring the horizontal component H described in the preceding sections are intended for conducting magnetic surveys on land and become entirely impracticable at open sea where the instruments must be installed on a continuously oscillating ship deck. Hence the measuring procedures at open sea must be entirely different.

The most convenient instrument for measurement of the horizontal

Declassified in Part - Sanitized Copy Approved for Release 2013/01/23 : CIA-RDP81-01043R001600090003-8

Declassified in Part - Sanitized Copy Approved for Release 2013/01/23 : CIA-RDP81-01043R001600090003-8

component is a so-called double compass, consisting of 2 marine compasses positioned along the same vertical line (one above the other) at a distance which is adjusted in such a manner that the interaction between the compass needles is of the same order as the interaction between the magnetic field of the earth and each of the needles.

The Principle of Measurement is based upon the fact that due to the interaction between the magnets they tend to assume an antiparallel position, while the terrestrial field tends to position them parallel to each other in the direction of the magnetic meridian. Therefore the magnets are at equilibrium when the angle between the magnets is other than 0° or 180°.

With a given distance between the compasses this angle must be a function of the horizontal component, and therefore on measuring this angle and knowing the functional correlation, it is possible to determine the magnitude of the horizontal component.

Theory of the Instrument. Let us place 2 magnets having the magnetic moments M_1 and M_2 at a distance R along the same vertical and let the direction of the magnetic meridian coincide with the x-axis (Figure 229). Denoting by φ_1 the angle between the axis of the upper magnet and the magnetic meridian at the state of equilibrium, and the corresponding angle for the lower magnet by φ_2 the condition of equilibrium of the upper magnet is defined by the equation

$$\frac{M_1 M_2}{R^3}\beta \sin(\varphi_1+\varphi_2) = M_1 H \sin\varphi_1, \qquad (10.74)$$

and that of the lower magnet by

$$\frac{M_1 M_2}{R^3}\beta \sin(\varphi_1+\varphi_2) = M_1 H \sin\varphi_2, \qquad (10.75)$$

where β denotes the correction coefficient which is close to unity and depends upon the dimensions of the magnets.

Declassified in Part - Sanitized Copy Approved for Release 2013/01/23 : CIA-RDP81-01043R001600090003-8

Declassified in Part - Sanitized Copy Approved for Release 2013/01/23 : CIA-RDP81-01043R001600090003-8

Adding these equations term by term and solving the resulting equation for H, using the denotations $\varphi_1 + \varphi_2 = \varphi$ and $M_1 + M_2 = M$ we obtain:

$$H = \frac{MB}{R^3} \sec \frac{\varphi_1 - \varphi_2}{2} \cos \frac{\varphi}{2} \qquad (10.76)$$

Equating the left hand portions of equations (10.74) and (10.75) we obtain $\frac{\cos \varphi_1}{\cos \varphi_2} = \frac{M_1}{M_2}$,

or

$$\frac{\cos \varphi - \sin \varphi_2}{\cos \varphi_1 - \sin \varphi_2} = \frac{M_1 + M_2}{M_1 - M_2} \qquad (10.77)$$

Using the denotation $M_1 - M_2 = \Delta M$ and solving equation (10.77) we obtain: $\frac{\varphi_1 - \varphi_2}{2} = 1 + \tg \frac{\varphi}{2} \cdot \frac{\Delta M}{M}$

The magnetic moments of the magnets are selected to be almost equal, and therefore Δ M is very small in comparison with M. Thus, expanding the right hand portion of this equation to a series and substituting it into equation (10.76) we obtain:

$$H = \frac{MB}{R^3} \cos \frac{\varphi}{2} \left(1 + \frac{1}{2} \tg^2 \frac{\varphi}{2} \cdot \frac{\Delta M^2}{M^2}\right). \qquad (10.78)$$

The factor MB/R^3 is constant and is determined from measurements of angle φ in a known field.

From equation (10.78) it is apparent that the correction term in parentheses may be disregarded if the difference between the magnetic moments is less than a definite quantity. Thus, upon determination of H within an error of 0.1% at $\varphi/2 = 45°$, the relative difference between the magnets must not exceed 2%, which is readily attained in practice.

Therefore the correction term usually may be disregarded and expression (10.78) assumes a simple form:

$H = A \cos \frac{\varphi}{2}$, and at the same time $A = \frac{H_0}{\cos \frac{\varphi}{2}}$

Declassified in Part - Sanitized Copy Approved for Release 2013/01/23 : CIA-RDP81-01043R001600090003-8

Declassified in Part - Sanitized Copy Approved for Release 2013/01/23 : CIA-RDP81-01043R001600090003-8

Description of the Instrument. The instrument consists of a cylindrical casing K (Figure 230) inside of which magnets M_1 and M_2, having the shape of disks and made from a high coercity alloy, rotate on the pivots O and O_1 which are located on the same vertical. The pointers i_1 and i_2 are rigidly attached to the magnets. Within the same plane pointer i_2 is a ring S which is marked off in a graduated scale. The ring is attached to the casing of the instrument. At the upper part of the casing is a plate i_o, which provided with a thin line mark and is located within the same plane as pointer i_1. Between magnets M_1 and M_2 is a convex lens L for viewing the marks of ring S.

By means of a locking device A the magnets may be lifted and removed from the pivots. Observations are made from above, through the glass window P.

A convenient feature of the instrument is the fact that it requires no setting either in relation to the horizon or azimuth. The horizontal position of the instrument is ensured by a universal joint, and spatial orientation is effected automatically by the magnets. The setting of the instrument consists of rotating the instrument around its vertical axis until the line marks of pointer i_1 of the upper magnet and plate i_o are brought into alignment as shown in Figure 231, which is a plan view of the instrument as seen through the window.

Observation with such a position of the upper magnet consists in reading the scale division opposite pointer i_2; to facilitate computations the divisions of the scale represent units proportional to H, and the zero mark is located on the side opposite to the i_o mark.

Declassified in Part - Sanitized Copy Approved for Release 2013/01/23 : CIA-RDP81-01043R001600090003-8

Declassified in Part - Sanitized Copy Approved for Release 2013/01/23 : CIA-RDP81-01043R001600090003-8

Section 20. Measurement of Vertical Component by the Electric Method

The electric method of measuring the horizontal component described in Section 15 of the present chapter also may be utilized to measure the vertical component. For this purpose the coils, in the form of Helmholtz rings, which serve to compensate the magnetic field, must be disposed horizontally and an indicating device showing the absence of a magnetic field is placed at their center. In such a case, at the instant of compensation we have the following equation: $Z = kI$,

where k is the constant of the coils which is determined from observations in a known field, and I is the current intensity, which is measured directly.

The instrument based on this principle was first designed by B. Ye. Bryunelli [83] in 1936 and now is utilized in practical magnetic measurements.

The base of the instrument is circle 3 (Figure 232), which is set on leveling screws. On top of the circle is casing 2, which contains the Helmholtz rings 1. An oscillating coil 4 serves as an indicator, and consists of a system of Helmholtz rings, the frame of which is attached to quartz prism 5 which rests on agate bearings. Current is supplied to the rings by means of the mercury contacts 6, and by means of mirror 7 the movements of the system are observed. On compensation, that is when $Z = kI$, a current flowing through the system causes no deflection, which constitutes the criterion of compensation.

The screws 8 are used to remove the mercury contacts from the instrument when observations are not to be carried out. The motion of the system of oscillating coils is observed by means of

Declassified in Part - Sanitized Copy Approved for Release 2013/01/23 : CIA-RDP81-01043R001600090003-8

Declassified in Part - Sanitized Copy Approved for Release 2013/01/23 : CIA-RDP81-01043R001600090003-8

an optical system consisting of light bulb 9, from which beams of light pass through prism 10 and through the objective to the mirror of indicator 7. The reflected beam passes through the objective and through the prism, and is focussed upon the scale attached to the frame of the instrument.

Current intensity I in the stationary rings is measured by means of a special potentiometer.

CHAPTER XI

METHODS OF MEASUREMENT USED DURING INVESTIGATION OF MAGNETIC ANOMALIES

Section 1. Introduction

The methods utilized in the investigations of local and regional magnetic anomalies differ somewhat from the methods which have been described in Chapter X and therefore require special consideration.

As was stated in Section 3 of Chapter I, the magnetic measurement procedures described in Chapter X are used mostly in observatory operations and in general magnetic surveying, the purpose of which is investigation of the total magnetic field of the earth.

Magnetic anomalies, both local and regional, encompass relatively small areas and therefore even when they are of comparitively small intensity their magnetic field gradients considerably exceed those of the normal field. For this reason the density of magnetic network, i.e., the number of observation points per unit area must be considerably higher in these areas. Whereas in a general magnetic survey observation points are spaced several km apart in the investigation of magnetic anomalies these distance sometimes are reduced to several meters. This fact alone necessitates modification of the measurement procedures to shorten the duration of observations.

Declassified in Part - Sanitized Copy Approved for Release 2013/01/23 : CIA-RDP81-01043R001600090003-8

Declassified in Part - Sanitized Copy Approved for Release 2013/01/23 : CIA-RDP81-01043R001600090003-8

Further, the intensity of magnetic anomalies which may be characterized by the maximum intensity of the anomalous magnetic field can change within fairly wide limits, from several tens or hundreds of gammas to hundreds of thousands of gammas, as a result of which the procedures for investigation of anomalies of low intensity must differ from those used to investigate strong anomalies, such as the Kursk anomalies.

Thus the general requirements which must be met by instruments used within anomalous areas are simplicity of handling and minimum expenditure of time for effecting the observations, and for setting up and transporting the instruments. In addition, instruments used to investigate weak anomalies must be highly sensitive, while those used for strong anomalies must have lower sensitivity.

The magnetic balance known as the M-2 magnetometer meets the high-sensitivity requirements of the former type.

The low-sensitivity instruments include: the M-1 magnetometer and the deflector magnetometer which also is used in navigation for determination of anomalies caused by the ship iron.

The instruments which meet all the requirements of maximum speed observations include the aeromagnetometers, with which measurements are carried out in an aircraft in flight.

Section 2. M-1 Field Magnetometer

During the investigation of strong magnetic anomalies such as the Kursk and Krivoy Rog anomalies the M-1 magnetometer is used which permits rapid and sufficiently accurate measurement of all 3 elements: declination, and the horizontal and vertical components. At one time it was the only instrument utilized for practical purposes,

Declassified in Part - Sanitized Copy Approved for Release 2013/01/23 : CIA-RDP81-01043R001600090003-8

Declassified in Part - Sanitized Copy Approved for Release 2013/01/23 : CIA-RDP81-01043R001600090003-8

namely, prospecting for iron ore deposits. The simplicity of handling and minimal observation time (observation of the 3 elements requires 2 to 5 minutes) have ensured its widespread utilization in magnetometric practice at the sites of strong anomalies. However, all these advantages are limited by the low sensitivity of this instrument, because of which it may be used only within areas of strong anomalies where the magnetic field differs from the normal by not less than 10 or 20%.

Principle of Measurement of the Horizontal Component. Measurement of the horizontal component by this instrument is based on the method of deflection in the first Gaussian or first Lamontian positions. We have seen that the deflection angle caused by the action of the deflecting magnet depends on the horizontal component, and therefore by measuring this angle it is possible to form an opinion concerning the magnitude of the horizontal component.

The Principle of Measurement of the Vertical Component resides in the fact that a magnet free to rotate in the vertical plane alters the angle of inclination between its axis and the horizontal plane upon a change in the vertical component. Hence, if this angle is known, it is possible to determine the vertical component in accordance with the corresponding formulas.

Theory of the Measurement Method. Let us assume that the magnetic needle (compass) rotating freely in the horizontal plane is under the action of a permanent magnet located at a distance R from the needle in the first Gaussian or the first Lamontian position. Under the condition of equilibrium the needle will form a certain angle θ with the magnetic meridian which for the first Gaussian position is defined by the equation

$$H \tan \theta_1 = \frac{2M}{R^3}\left[1 + \frac{r_1}{R_1}\right],$$

and for the first Lamontian position by the equation

$$H \tan \theta_2 = \frac{2M}{R^3}\left[1 + \frac{r_2}{R_2}\right],$$

Declassified in Part - Sanitized Copy Approved for Release 2013/01/23 : CIA-RDP81-01043R001600090003-8

Declassified in Part - Sanitized Copy Approved for Release 2013/01/23 : CIA-RDP81-01043R001600090003-8

where M is the magnetic moment of the deflecting magnet, H is the horizontal component, and p is the distribution coefficient.

Since in the instrument the distance R remains constant during the entire period of the magnetic survey it follows that the right hand portion of both equations may be considered as constant. Denoting the latter by A and B we have:

$$H = A \operatorname{ctg} \theta_1 \quad \sim \quad H = B \operatorname{ctg} \theta_2. \tag{11.1}$$

The deflection angles Θ_1 and Θ_3 are measured directly on the instrument, while the constant factors A and B are determined from observation of the angles Θ_{01} and Θ_{02} at a point where H is known. Denoting the horizontal component at this point by H_0, we have:

$$A = H_0 \operatorname{tg} \theta_{01}, \quad B = H_0 \operatorname{tg} \theta_{02}. \tag{11.2}$$

For measuring the vertical component the plane of oscillation of the magnet is set within a plane perpendicular to the magnetic meridian and the axis of rotation of the magnet is shifted slightly laterally in relation to the center of gravity. In this position the magnet is subjected to the action of: the vertical component with moment $M_z = MZ \cos i$, where i is the angle between the axis of the magnet and the horizontal plane, and the force of gravity p-mg the moment of which relative to the axis of rotation is $Mp = mgl \cos \Theta$, where l is the distance between the center of gravity and the rotation axis, and Θ is the angle between the horizontal plane and the vector L (Figure 233).

With the magnet in equilibrium these moments will be equal and opposite, i.e.,

$$MZ \cos i = mgl \cos \theta.$$

Denoting by α the angle between the vector l and the axis of the magnet, it is apparent from the drawing that

$$\theta = \alpha + i$$

Declassified in Part - Sanitized Copy Approved for Release 2013/01/23 : CIA-RDP81-01043R001600090003-8

Declassified in Part - Sanitized Copy Approved for Release 2013/01/23 : CIA-RDP81-01043R001600090003-8

therefore, expanding cos Θ in accordance with trigonometric formulas and dividing both sides by M cos i, we obtain:

$$Z = \frac{mgl}{M}\cos\alpha - \frac{mgl\sin\alpha}{M}\operatorname{tg} i$$

Since m, g, l, α and M are constant for a given instrument, it follows that on using the denotation

$$\frac{mgl\cos\alpha}{M} = A, \qquad -\frac{mgl\sin\alpha}{M} = B,$$

where A and B are certain constants, we have

$$Z = A + B\operatorname{tg} i. \tag{11.3}$$

Consequently, given the constant coefficients A and B, by measuring the angle i between the axis of the magnet and the horizontal plane we can determine Z.

To determine the constant A the angle i_0 must be measured at a point where the vertical component Z_0 is known. In such a case it follows from equation (11.3) that

$$A = Z_0 + B\operatorname{tg} i_0.$$

Substituting this value into equation (11.3) we obtain:

$$Z = Z_0 + B(\operatorname{tg} i - \operatorname{tg} i_0) \tag{11.4}$$

The constant B is determined from observations of the angle of deflection i'_1 caused by the additional field Z' of the deflecting magnet which is located at a certain vertical distance R from the magnetometer, as shown in Figure 234.

From equation (11.3) we have:

$$Z + Z' = A + B\operatorname{tg} i'_0.$$

Subtracting equation (11.3) from the latter, we obtain:

$$B = \frac{Z'}{\operatorname{tg} i'_0 - \operatorname{tg} i}$$

The intensity of the additional field Z' is determined according to the formula $Z' = \frac{2M_0}{R^3}$,

where M_0 is the magnetic moment of the deflecting magnet, which must be known.

Declassified in Part - Sanitized Copy Approved for Release 2013/01/23 : CIA-RDP81-01043R001600090003-8

Declassified in Part - Sanitized Copy Approved for Release 2013/01/23 : CIA-RDP81-01043R001600090003-8

Errors in Measurement of the Horizontal Component. To determine the error in determination of the horizontal component by means of the M-1 magnitometer the constants A and B in equation (11.1) are replaced by their values according to equation (11.2) after which the equation is logarithmized and differentiated. In such a case, for the first Gaussian position

$$\frac{dH}{H} = \frac{2\,d\theta_0}{\sin 2\theta_0} - \frac{2\,d\theta}{\sin 2\theta},$$

and for the first Lamontian position:

$$\frac{dH}{H} = \operatorname{ctg} \theta_0\, d\theta_0 - \operatorname{ctg} \theta\, d\theta,$$

or, considering the errors:

$$\left(\frac{\Delta H}{H}\right)^2 = \frac{4}{\sin^2 2\theta_0}\,\Delta\theta_0^2 + \frac{4}{\sin^2 2\theta}\,\Delta\theta^2$$

and

$$\left(\frac{\Delta H}{H}\right)^2 = \operatorname{ctg}^2 \theta_0\,\Delta\theta_0^2 + \operatorname{ctg}^2 \theta\,\Delta\theta^2.$$

Thus it is apparent that the least error $\Delta H/H$ for the first Gaussian position is obtained at value of angles θ_0 and θ close to 45°, and for the first Lamontian position when θ_0 and θ are approximately 90°.

If we assume that $\Delta\theta_0$ and $\Delta\theta$ are equal, the minimum error for the first Gaussian position will be: $\frac{\Delta H}{H} = \sqrt{2}\sin 1^\circ \Delta\theta$,

wherein $\Delta\theta$ must be expressed in degrees.

The direct readings of the M-1 magnitometer are obtained with an error of $\pm 0.25^\circ$, therefore: $\frac{\Delta H}{H} = \pm 0.012 \sim \pm 1.2\%$

At Leningrad, where H = 15 300 γ, the error of measurement may attain 180 γ. Hence the least difference in horizontal components which can be detected with the M-1 magnetometer in the Leningrad area is approximately 180 γ.

In the first Lamontian position the greatest angle at which measurements still are possible is of the order of 70°. Hence the least error of H measurements will be

$$\frac{\Delta H}{H} = \pm\sqrt{2}\operatorname{ctg} 70^\circ \sin 1^\circ \Delta\theta = 0.009\,\Delta\theta,$$

Declassified in Part - Sanitized Copy Approved for Release 2013/01/23 : CIA-RDP81-01043R001600090003-8

Declassified in Part - Sanitized Copy Approved for Release 2013/01/23 : CIA-RDP81-01043R001600090003-8

that is, of the same order as in the first Gaussian position.

Errors of Measurement of the Vertical Component. Upon differentiating equation (11.4), taking therein B as constant, we obtain:

or, on considering the errors and assuming $di_0 = di$:

$$\Delta Z^2 = C^2 \left[\frac{1}{\cos^4 i_0} + \frac{}{} \right] \Delta i^2$$

From this correlation it is apparent that the minimum error occurs when $i = i_0 = 0$.

Usually the angle i does not exceed 30°. Therefore the greatest magnitude of error ΔZ_m assuming $i'_0 = 30°$, $i = 0$ and $B = 0.1$, will have the value:

$$\Delta Z_m = \pm \quad \gamma$$

i.e., an error of 1° in the measurement of the angle of deflection causes an error of 280 γ in the determination of the vertical component.

Since direct readings of angle i within an accuracy of 1/4% are not very difficult, the absolute magnitude of error in measurement of the vertical component with the M-1 magnetometer is of the order of 70-100 γ.

Description of the Instrument. The instrument (Figures 235 and 194) consists of support A with ball and socket joint for levelling by means of 2 screws a and b, frame B with 2 bearings p and q, and sights c and bar D for setting the deflecting magnet.

The removable compass, which can be set in either the horizontal or vertical plane, is mounted on the bearings. A special ring-shaped tapper r serves to shake the compass slightly in order to overcome friction at the pivots of the needle when the latter turns in the vertical plane.

At the outer end of the bar is a sight with 5 apertures for observing the mire azimuth, the sharp edges of which serve as front sights.

Declassified in Part - Sanitized Copy Approved for Release 2013/01/23 : CIA-RDP81-01043R001600090003-8

Declassified in Part - Sanitized Copy Approved for Release 2013/01/23 : CIA-RDP81-01043R001600090003-8

The carrier onto which the magnet is placed can be set at different distances from the needle and secured in position by means of a screw S. The compass turns around a horizontal axis and the entire frame B turns around a vertical axis.

The needle of the compass has at one side a small pivot carrying a weight to give the instrument the necessary sensitivity with respect to the vertical component.

At the tips of the needle there are movable weights for adjusting it in the horizontal position.

The circle is divided at intervals of one degree, which are marked every 10° from 0 to 90° according to the compass points; the line EE corresponding to the marking EW and extending parallel to the axis of rotation of the compass. A clamp is provided for locking the needle.

Sequence of Observations of the Horizontal Component. The determination of H by the method of tangents (first Gaussian position) is effected as follows. After levelling the compass the instrument is turned around the vertical axis until the needle assumes a position along the NS line with the north end opposite the 90° N mark. Then the magnet is placed on the carrier S with its north end toward E, and the reading indicated by the needle on the compass scale is recorded.

Since the divisions of the circle read from W to N, the angle θ through which the magnet is deflected from the magnetic meridian is obtained by subtracting the reading from 90°.

To eliminate systemic errors the observation is repeated with the north end of the magnet turned toward W, which is done by turning the magnet 180° on the carrier and taking a reading on the horizontal circle.

Declassified in Part - Sanitized Copy Approved for Release 2013/01/23 : CIA-RDP81-01043R001600090003-8

Declassified in Part - Sanitized Copy Approved for Release 2013/01/23 : CIA-RDP81-01043R001600090003-8

The magnet then is removed and the needle again is adjusted along the NS line, with its north end facing the 90° S mark. Next, the magnet is placed on the carrier and the angle θ is observed at 2 positions of the magnet.

In observing the horizontal component according to the method of sines (first Lamontian position) the magnet is first placed on the carrier and the compass needle is set along the NS line. Then the magnet is removed and a compass reading is taken. As above, the observations are repeated 4 times at different positions of the magnet.

Sequence of Observations of the Vertical Component. To observe the vertical component the magnet is withdrawn and with the compass in horizontal position the needle is adjusted along the NS line with its north end opposite the 90° mark.

Next, the compass is turned 90° around the horizontal axis so that the plane of oscillation of the needle is vertical (Figure 235). After the needle comes to rest a reading is taken on the compass. To reduce friction at the needle pivots the compass is tapped with a tapper r. The observation is repeated after setting the needle at the 90° S mark in the horizontal position.

Section 3. M-2 Magnetic Balance

The magnetic balance was utilized extensively in the practice of magnetic measurements in the early 1920's. In contrast with the M-1 magnetometer the magnetic balance is used in the investigation of weak anomalies where the magnetic field exceeds the normal only by several percent or by fractions of one percent. However, it also can be utilized successfully at stronger anomalies. Hence, when the balance was made available it was used in prospecting for deposits

Declassified in Part - Sanitized Copy Approved for Release 2013/01/23 : CIA-RDP81-01043R001600090003-8

Declassified in Part - Sanitized Copy Approved for Release 2013/01/23 : CIA-RDP81-01043R001600090003-8

associated with weak anomalies. At the present time the magnetic balance is used in prospecting for deposits of petroleum, manganese and chromium ores, in prospecting for gold, etc.

The balance for field measurements is a modification of the balance used for measuring variations of the vertical component (see Section 5 of Chapter XII). It differs from the latter only in the method of measuring the deflection angle of the magnet. In addition, the principle of the balance is utilized in this instance for the horizontal as well as the vertical component.

Because of its high sensitivity the magnetic balance is used not only in prospecting but also in measuring the normal field when its difference at 2 points is small. At the present time it is one of the principal instruments used in the study of terrestrial magnetism.

The Principle of Measurement, of the vertical and horizontal components by means of the magnetic balance is based on counterbalancing the moment of rotation of the magnet, caused by the action of the terrestrial magnetic field, with the moment of gravitation acting upon the same magnet.

When the magnet is set in a horizontal position the greatest torque is caused by the vertical component, and therefore in this position the balance is most sensitive to changes in the latter and is called a vertical balance. When the magnet is set in a vertical position the balance is most sensitive to changes in the horizontal component and therefore can be used to measure this component. In the latter instance it is called a horizontal balance.

Since the attraction of gravity within the limited boundaries

Declassified in Part - Sanitized Copy Approved for Release 2013/01/23 : CIA-RDP81-01043R001600090003-8

Declassified in Part - Sanitized Copy Approved for Release 2013/01/23 : CIA-RDP81-01043R001600090003-8

of the earth's surface area under study usually is assumed to be the uniform, the changes in the angle will depend only upon changes in the intensity of the terrestrial magnetic field. By measuring the angles θ_1 and θ_2 at 2 different points of the earth's surface we can determine the difference in values of vertical or horizontal components.

If the magnetic balance is used to measure the vertical component of the normal field over large areas where the acceleration of gravity g cannot be considered constant, it becomes necessary to make corrections, in accordance with the corresponding formulas, for changes in g. In order to do this it is necessary to know the magnitude of the acceleration of gravity at each observation point with an accuracy within decimal fractions of one %.

The Theory of a Vertical Magnetic Balance for measurements under field conditions differs in no way from the theory of the balance used for the observation of variations described in Chapter XII, which deals with variation instruments. Hence we shall not discuss it here, and will utilize only those deductions of this theory which are needed in the description presented below.

1. To eliminate the dependence of the balance readings upon the horizontal component, the plane of oscillation of the magnet must be perpendicular to the magnetic meridian.

2. The difference in values of the vertical component at 2 points Z_1-Z_2 is proportional to the difference between 2 readings n_1-n_2 taken at these points, i.e.,

$$Z_1 - Z_2 = \varepsilon_z(n_1 - n_2), \qquad (11.5)$$

on the condition that the axis of the magnet is deflected from the horizon over the small angles θ_1 and θ_2.

Declassified in Part - Sanitized Copy Approved for Release 2013/01/23 : CIA-RDP81-01043R001600090003-8

Declassified in Part - Sanitized Copy Approved for Release 2013/01/23 : CIA-RDP81-01043R001600090003-8

3. The coefficient of proportionality ε_z (value of one division) is expressed by the formula

$$\varepsilon_z \approx mgz_0/2MR$$

where m is the mass of the magnet, M is its magnetic moment, z_0 is the distance from the center of gravity to the axis of the magnet extending through the oscillation axis, g is the acceleration due to gravity and R is the distance between the mirror of the magnet and the scale, equal to the principal focal length of the telescope objective.

4. A change in the value of one division (sensitivity), in the horizontal setting of the magnet and in the temperature compensation of the magnet are effected by the same procedures as in the case of a balance for observation of variations.

The Theory of the Horizontal Balance will be presented also in Section 5 of Chapter XII, where it is shown that if the axis of the magnet closely approximates the vertical and if the plane of oscillation of the magnet coincides with the plane of the magnetic meridian, its deflections are caused only by changes in the horizontal component H, and the correlation between angle of deflection of the magnet from vertical and the change ΔH is expressed by equation (12.36), from which we obtain:

$$H_1 - H_2 = \mp (Z - mgx_0/M)(\theta_1 - \theta_2).$$

The plus sign in the above equation corresponds to the setting of the oscillation plane along the magnetic meridian when $\varphi = 0$, and the minus sign corresponds to $\varphi = 180°$, where φ is the angle formed by the plane of the magnet with the plane of the magnetic meridian. This equation can be written:

$$H_1 - H_2 = \frac{1}{k}(n_1 - n_2), \qquad (11.6)$$

Declassified in Part - Sanitized Copy Approved for Release 2013/01/23 : CIA-RDP81-01043R001600090003-8

Declassified in Part - Sanitized Copy Approved for Release 2013/01/23 : CIA-RDP81-01043R001600090003-8

where n_1 and n_2 are readings of the scale expressed in mm, and ε_H is the value of a division of the horizontal balance defined by the equation:

$$\varepsilon_H = 1/2R(Z - mgx_c/M). \qquad (11.7)$$

Since the value of this division cannot be a negative quantity it follows that in equation (11.6) the minus sign must be discarded, and consequently observation of the angle θ can be carried out only at one position of the magnet, when the center of gravity is north of the axis of rotation. By turning the rotation axis 180° the state of equilibrium of the magnet is disrupted since the moment of gravity and the moment MH have the same direction. The horizontal balance is differentiated from the vertical balance by the dependence of the value of any one division upon the vertical component, whereas in a vertical balance, when this balance is set perpendicularly to the magnetic meridian, the value of one division is a constant quantity.

In order to ascertain the limits within which changes of the vertical component are permissible, assuming that the value of one division is a constant quantity, let us determine the variation in $\Delta\varepsilon_H$ with a change ΔZ. In view of equation (11.7), we have

$$\Delta\varepsilon_H = 1/2R\ \Delta Z.$$

The value of one division may be considered constant if $\Delta\varepsilon/\varepsilon$ does not exceed 0.01 of its value; hence

$$\Delta Z \leqslant 2R\varepsilon_H \cdot 0.01\ \gamma.$$

If we adopt the values $\varepsilon_H = 20\ \gamma$/division and R = 800 divisions, which usually is the case in practice, it follows that

$$\Delta Z \leqslant 320\ \gamma.$$

Consequently, the change in vertical component must not exceed the order of 300 γ, and if it does exceed this value the value of one division must be determined when Z is measured at intervals of 300 γ.

Declassified in Part - Sanitized Copy Approved for Release 2013/01/23 : CIA-RDP81-01043R001600090003-8

Declassified in Part - Sanitized Copy Approved for Release 2013/01/23 : CIA-RDP81-01043R001600090003-8

Determination of the Value of One Division. In order to be in a position to determine the differences in vertical and horizontal components ΔZ and ΔH according to formulas (11.5) and (11.6) value of one division of the vertical and horizontal balances, i.e., the quantities ε_Z and ε_H must be known. In view of equations (11.5) and (11.6), we have:

$$\varepsilon_Z = \frac{\Delta Z}{\Delta \theta} \quad \text{or} \quad \varepsilon_H = \frac{\Delta H}{\Delta \theta} \qquad (11.8)$$

Consequently, in order to determine ε_Z and ε_H it is necessary to measure the change in the angle of inclination $\Delta\theta$ of the magnet due to the action of the additional vertical component ΔZ and the additional horizontal component ΔH, the values of which must be known.

To produce these additional fields ΔZ and ΔH 2 methods, the magnetic and the electric methods are used.

In the magnetic method the vertical component ΔZ and the horizontal component ΔH are produced by means of a permanent magnet M_0, which is called a deflector, and which is set in the vertical position to produce ΔZ, so that the extension of its axis coincides with the center of the magnetic system of the balance M (Figure 236). To produce the horizontal component ΔH the magnet M_0 is placed in a horizontal position and the extension of the axis of the magnetic system of the balance M must coincide with the center of the magnet M_0.

In the former case $\Delta Z = \frac{2M_0}{R^3}$,

and in the latter $\Delta H = \frac{M_0}{R^3}$,

where M_0 is the magnetic moment of the deflector magnet and R is the distance between the magnets.

Substituting these values into equation (11.8) we obtain:

Declassified in Part - Sanitized Copy Approved for Release 2013/01/23 : CIA-RDP81-01043R001600090003-8

Declassified in Part - Sanitized Copy Approved for Release 2013/01/23 : CIA-RDP81-01043R001600090003-8

$$\varepsilon_Z = \frac{2M_0}{R^3 \Delta\theta} \qquad \text{and} \qquad \varepsilon_H = \frac{M_0}{R^3 \Delta\theta}.$$

If M_0 is expressed in absolute electromagnetic units and R in cm, ε_Z and ε_H are obtained in oerstads per unit of angle. In practice the value of one division is expressed in gammas per division of the instrument. Therefore in order to obtain ε_Z and ε_H in these units, it is necessary to multiply the right hand portions of the equations by 10^5, and in lieu of the difference in angles $\Delta\theta$ the difference in readings is expressed in terms of Δn. In such a case

$$\varepsilon_Z = \frac{2M_0 \cdot 10^5}{R^3 \Delta n}\ \gamma/\text{div.}, \qquad \varepsilon_H = \frac{M_0 \cdot 10^5}{R^3 \Delta n}\ \gamma/\text{div.}$$

When the electric method is used ΔZ and ΔH are produced by the Helmholtz rings.

Each ring has the same number of turns through which the current flows. If we denote by w the number of turns in one ring, by p the radius of mean turn, and by I the current intensity in amperes, the field intensity H_0 at the center of the rings is expressed by the formula:

$$H_0 = 0.9 \frac{w}{p} I \quad ,$$

where p must be expressed in centimeters.

The direction of field H_0 coincides with the axis of the rings. The constant factor 0.9 w/p is called the constant of Helmholtz rings and is denoted by the symbol K. Therefore

$$H_0 = kI.$$

If the axis of the rings is vertical and the center of the magnetic system of the vertical balance is placed at the center of the rings an additional vertical component ΔZ, expressed by the formula

$$\Delta Z = kI$$

will be acting upon the system, and consequently

$$\varepsilon_Z = \frac{kI}{\Delta n}.$$

Declassified in Part - Sanitized Copy Approved for Release 2013/01/23 : CIA-RDP81-01043R001600090003-8

Declassified in Part - Sanitized Copy Approved for Release 2013/01/23 : CIA-RDP81-01043R001600090003-8

To determine the value of a division on a horizontal balance the axis of the coil is placed horizontally in the direction of the magnetic meridian, and the magnetic system of the horizontal balance is positioned at the center of the coils. In such a case

$$\Delta H = kI \qquad \text{and} \qquad \varepsilon_H = kI/\Delta n.$$

Description of the Instrument. Three types of balances are manufactured: a vertical balance for measuring the vertical component, a horizontal balance for measuring the horizontal component, and a universal balance for measuring both components. The present section contains a description of the universal balance, since the horizontal and vertical balances differ only slightly from the universal balance, and therefore if one is familiar with the universal balance the practical operation of either a horizontal or a vertical balance is easily learned.

The universal balance, the general appearance of which is shown in Figure 237, consists of a cylindrical housing A, in which the magnetic system is located, a reading telescope B, the horizontal circle C attached to the tripod T, and a vertical bar carrying the deflector magnet M for the determination of the value of one division.

The principal part of the balance is the magnetic system which consists of 2 plane magnets M_1 and M_2 (Figure 238) held by a square frame R.

In the universal balance there are 2 magnetic systems, one of which serves to measure the vertical component (Figure 238a) and the other serves for measuring the horizontal component (Figure 238b). The latter differ in the fact that for the vertical component the magnets are set in horizontal position while for the horizontal component they are set in vertical position.

Declassified in Part - Sanitized Copy Approved for Release 2013/01/23 : CIA-RDP81-01043R001600090003-8

Declassified in Part - Sanitized Copy Approved for Release 2013/01/23 : CIA-RDP81-01043R001600090003-8

The rotation axis about which the system oscillates is the edge of a quartz prism Q, which near the center of gravity is perpendicular to the plane of the magnets. For the vertical component the side opposite the edge upon which the system is placed is parallel to the axis of the magnet, while for the horizontal component it is perpendicular to the axis.

The system is adjusted in the horizontal or vertical position by means of 2 pins a and b, on which 2 moveable weights p and q are mounted by means of a screw-threaded engagement.

In the arrangement for determining the vertical component these pins are parallel to the axis of the magnets, while in the arrangement for determining the horizontal component they are perpendicular to the axis.

To vary the sensitivity there is provided a small weight r at the lower part of frame R which is moved up and down over a screw thread, thus altering the position of the center of gravity in the vertical direction. A mirror P is mounted on the upper side of frame R, by means of which the angle of inclination of the magnetic system is observed.

The telescope B (Figure 237) is provided with a reading device for measuring the angle of inclination of the magnetic system. It is a conventional astronomical telescope with a Gaussian eyepiece and a reticle in the principal focal plane of the objective. The principle of measurement of the angle of inclination is as follows: a shaft of light passing through the aperture of the eyepiece a (Figure 239) is reflected from the glass plate p, set at a 45° angle to the optic axis of the telescope AA_1, and illuminates the reticle q which is in the focal plane of eyepiece l.

Declassified in Part - Sanitized Copy Approved for Release 2013/01/23 : CIA-RDP81-01043R001600090003-8

Declassified in Part - Sanitized Copy Approved for Release 2013/01/23 : CIA-RDP81-01043R001600090003-8

Under the influence of the diffused pencil of rays the reticle acts as a light source and any line-mark of the reticle, for example C, produces a divergent band which passes through objective L and reaches the mirror P as a parallel band, incident to the mirror at a certain angle. After being reflected from the mirror it passes again through the objective and is gathered within the principal focal plane FF_1 at the point C'. Therefore, on looking through the eyepiece we see both the illuminated reticle and the reticle q reflected from the mirror, which is a real image of reticle q. If the magnet, and consequently the mirror, are deflected over a certain angle the reflected image of the reticle will be displaced by the double angle in accordance with the laws of reflection, and the 2 reticles will be shifted in relation to each other. This shift is read on the reticle scale and constitutes the measurement of the angle of deflection.

Figure 240 shows the positions of the scales as seen through the eyepiece. The fixed scale ab has 40 divisions, every fifth and tenth of which is indicated by a longer line mark. The central line, which is considered the zero mark, either has a dot, as is shown in the drawing, or is differentiated by a greater length.

The reflected scale cd is parallel to the fixed scale and is placed at such a distance from the latter that the 2 sets of line marks do not overlap. The shifting of the reflected, in relation to the fixed scale, or in other words, the reading, is equal to the number of divisions between the zero-lines of the fixed and reflected scales. The divisions on one side of zero are considered positive and those on the other side negative. If the zero line of the reflected scale is outside of the field of the eyepiece the reading is taken on the terminal line mark of the reflected scale to which 20 divisions are added. The reading shown in Figure 240 is equal to $\pm$ 2.0.

Declassified in Part - Sanitized Copy Approved for Release 2013/01/23 : CIA-RDP81-01043R001600090003-8

Declassified in Part - Sanitized Copy Approved for Release 2013/01/23 : CIA-RDP81-01043R001600090003-8

Sequence of Observations. The following operations must be performed to determine the vertical component.

(1) Set the horizontal circle and level it by means of the circular level.

(2) Place the compass in position and orient the horizontal circle along the EW line, securing it in position by means of the set screw.

(3) Remove the compass and replace it by the housing containing the magnetic system, which then is levelled off by means of 2 levels.

(4) Release the locking clamp, and after the magnetic system comes to rest take simultaneous readings of the scale and of the temperature and level, repeating this operation several times.

(5) Rotate the housing 180° and repeat the observations listed under No 4, above.

Section 4. The Aeromagnetometer of A. A. Logachev.

The aeromagnetometer of A. A Logachev [73] used in conducting surveys from aircraft, is based on the principle of current induction in a revolving loop located within a magnetic field. In the instrument the loop is placed within a coil to which a direct current is supplied and the field of which compensates the terrestrial field, with the result that no current is generated in the loop during its rotation. By measuring the current in the coil, and knowing the constant of the coil, it is possible to determine the magnitude of the component of the terrestrial field which is compensated by the coil. The absence of a current in the loop is determined by means of a galvanometer which is connected in series to the loop.

The instrument of A. A. Logachev permits measurement of the

Declassified in Part - Sanitized Copy Approved for Release 2013/01/23 : CIA-RDP81-01043R001600090003-8

Declassified in Part - Sanitized Copy Approved for Release 2013/01/23 : CIA-RDP81-01043R001600090003-8

vertical component, which is of greatest importance in the interpretation of magnetic anomalies.

The characteristic design features of the aeromagnetometer of A. A. Logachev include its semi-automatic recording arrangement. Since the conductivity of the loop and galvanometer circuit is proportional to current intensity, and consequently also to the intensity of the field of the coil, the quantity measured is not the current intensity, but is the conductivity or the resistance of the circuit, which in turn is proportional to the length of the rheostat wire. Therefore, if the slide of the rheostat is moved while compensating the current in the loop, the length over which it is moved is an indication of the intensity of the field of the coil. The rheostat slide is provided with a pen, and when the slide is moved the pen traces a curve on a moving paper tape which indicates the changes of the magnetic field.

Theory of the Aeromagnetometer. In Section 7 of Chapter X it was shown that when any closed circuit is rotated within a magnetic field an alternating emf is generated in the latter which when rectified by means of a commutator produces a current, the mean intensity of which is defined by equation (10.19):

$$i_m = \frac{4Sw}{R} N H_T [(\cos I \cos I_k - \sin I \sin I_k \cos A)\cos\beta - \sin I \sin\beta],$$

since $H_T \sin I = Z$ and $H_T \cos I = H$ it follows that

$$i_m = \frac{4Sw}{R} N [(Z \cos I_k - H \sin I_k \cos A)\cos\beta - H \sin A \sin\beta].$$

where I_k represents the angle between the horizontal plane and the rotation axis; A is the magnetic azimuth of the vertical housing within which the axis of rotation is located, and β is the angle of shift of the commutator brushes.

If the axis of rotation is positioned horizontally, then $I_k = 0$ and

$$i_m = \frac{4Sw}{R} N [Z - H \sin A \sin\beta].$$

Declassified in Part - Sanitized Copy Approved for Release 2013/01/23 : CIA-RDP81-01043R001600090003-8

Declassified in Part - Sanitized Copy Approved for Release 2013/01/23 : CIA-RDP81-01043R001600090003-8

This equation shows that the intensity of current in the circuit is proportional to the vertical component when A = 0 or β = 0. Since it is not possible to align the axis of rotation of the coil with magnetic meridian under flight conditions the simplest solution is to bring the plane of commutation into coincidence with the plane of the turns of the coil. Consequently, at β = 0

$$i_m = 4SwN/R \quad Z,$$

i.e., the intensity of the rectified current is proportional to the vertical component and the axis of the coil may have any direction within the horizontal plane.

The vertical component Z is compensated by the field of the coil, the intensity H_k of which is defined by the formula

$$H_k = kI,$$

where I is the current intensity in the coil and k the coil constant.

Upon compensation the current in the loop becomes equal to zero and we have

$$Z = kI,$$

or, replacing the current intensity in accordance with Ohm's law:

$$Z = kU/R_o + R$$

where U is the voltage of the feed battery, R_o the constant portion and R is the variable portion of the circuit resistance.

To obviate large values of the current intensity in the compensation coil a considerable portion of the vertical component is compensated by the field of permanent magnets.

Arrangement of the Aeromagnetometer. The aeromagnetometer (Figure 241) consists of a rotating loop or inductor 1 placed inside the compensation coil, a galvanometer and recorder 2 with a control panel, and the current-supplying battery 3. All 3 component parts are connected to an overall system as shown in the diagram of Figure 242.

Declassified in Part - Sanitized Copy Approved for Release 2013/01/23 : CIA-RDP81-01043R001600090003-8

Declassified in Part - Sanitized Copy Approved for Release 2013/01/23 : CIA-RDP81-01043R001600090003-8

The inductor is a drum 80 mm in diameter and 140 mm long having 2 grooves, each of which holds 1,200 turns of wire 0.5 mm in diameter. The drum is mounted on the same axis with the commutator, to which both ends of the drum winding are connected. The drum is rotated at a speed of 50 rpm by an electric motor mounted on the same axis.

The recorder consists of a tape-moving mechanism, a recording device, and a rheostat connected to the circuit of the compensation coil. At the upper part is a control panel.

The tape-moving mechanism is actuated by a separate 3.4 watt motor which moves the tape at a rate of 4-5 cm/minute.

The recording is traced by a pen, which upon change in the resistance of the rheostat moves perpendicularly to the direction of travel of the tape.

The galvanometer is a magnetoelectric needle galvanometer, one division on the scale of which corresponds to $2 \cdot 10^{-7}$ a.

The inductor is placed in a hermetically sealed container and is suspended from a cable inside the cabin of the aircraft so that the axis of the drum always remains horizontal, regardless of the flight altitude of the aircraft. The diagram of the aeromagnetometer is shown in Figure 242.

Section 5. Magnetically Saturated Sondes

With the development of alloys of high magnetic permeability, of the permalloy type, it has become possible to utilize the method of induction in soft magnetic cores for the measurement of small values of magnetic field intensity. This method was first used for measuring the dip and magnetic variations of the vertical component,

Declassified in Part - Sanitized Copy Approved for Release 2013/01/23 : CIA-RDP81-01043R001600090003-8

Declassified in Part - Sanitized Copy Approved for Release 2013/01/23 : CIA-RDP81-01043R001600090003-8

and is described in Section 6 of Chapter X and Section 8 of Chapter XII. Although this method, in the described form, yields fully satisfactory results in the measurement of variations, permalloy was found to be unsuitable for the measurement of dip and other elements of terrestrial magnetism due to erratic readings of the instruments. With the same value of dip the instruments showed readings which varied within a range of several minutes. These scattered readings are due to the fact that in an open circuit the permeability of permalloy depends to a larger extent upon mechanical action than a metal such as soft iron. Experiments have shown that on the slightest impact or light tapping of the instrument the magnetization of permalloy plates increases sharply and causes deflection of the suspended magnet.

Therefore, in order to eliminate this phenomenon it would be necessary to bring the plates to a state of greatest magnetization by means of repeated tapping within a given magnetic field. However, while such a procedure of imparting a stable magnetic condition to the plates is impractical, it may be replaced by the action of an alternating magnetic field which is equivalent to the action of mechanical percussions.

In addition, the use of the induction effect of an alternating magnetic field has made it possible to replace observation of the angle of deflection of a permanent magnet by observation of emf, that is, to replace the magnetometric method of observation by electric methods.

Since with the superposition of an alternating magnetic field upon a permanent magnetic field the permalloy plates reach a state of saturation they have been named magnetically saturated sondes.

Declassified in Part - Sanitized Copy Approved for Release 2013/01/23 : CIA-RDP81-01043R001600090003-8

Declassified in Part - Sanitized Copy Approved for Release 2013/01/23 : CIA-RDP81-01043R001600090003-8

The method of superposing an alternating magnetic field over a permanent field was employed for the first time in 1942-1943 by P. A. Khalileyev in the course of magnetic prospecting ground operations. In recent years magnetically saturated sondes have been used in aerial magnetic surveying.

The principle of utilizing emf for measuring the intensity of a magnetic field is based on the fact that the permeability of a permalloy plate with respect to the alternating field is a function of the intensity of the magnetic field in which it is located. Therefore when an alternating current passes through the primary winding of the plate an emf is induced in the secondary winding which depends upon the intensity of the magnetic field.

The current-supplying systems and the measurement systems vary, and therefore the instruments which compose magnetically saturated sondes differ from one another.

Instruments in which the emf in the secondary winding is produced by secondary harmonics formed by the action of a permanent field upon the specimen are extensively utilized. In the absence of a permanent field and with a sinusoidal voltage applied to the primary winding, only harmonics of odd numbers can occur in the secondary winding. Indeed, disregarding hysteresis, the magnitude of induction in the speciment does not depend upon the direction of the applied magnetic field, and therefore with a 180° change in phase of the alternating field in the primary winding the magnitude of induction must remain the same while its sign changes to the opposite. This is possible in the instance when upon expansion of the induction to a Fourier series this series includes no terms containing harmonics of the fourth order.

When a permanent field is superimposed the induction in the

Declassified in Part - Sanitized Copy Approved for Release 2013/01/23 : CIA-RDP81-01043R001600090003-8

Declassified in Part - Sanitized Copy Approved for Release 2013/01/23 : CIA-RDP81-01043R001600090003-8

specimen is determined concurrently by the action of this field and by the component of the alternating field. It is clear that the summative field during different directions of the alternating current will be different, and consequently the induction in the specimen also will differ, i.e., with a 180° change in the phase of the alternating field the induction changes in both sign and magnitude, which in turn is possible only with even-number harmonics.

Another convenience of the use of even-number harmonics is the fact that upon a change in the sign of the permanent field the even-number harmonics also change their sign, which makes it possible to measure the intensity of the permanent magnetic field and to determine its direction, as well.

These propositions can be readily demonstrated mathematically in the particular instance when the basic curve up to the point of inflection can be represented by an equation of the third order, which is very close to the actual facts, namely:

$$B = aH^3 + cH$$

Therefore, if

$$H = H_0 \cos \omega t,$$

it follows that

$$B = aH_0^3 \cos^3 \omega t + cH \cos \omega t,$$

or

$$B = \frac{1}{4} aH_0^3 \cos 3\omega t + \left(\frac{3}{4} aH_0^3 + c\right) \cos \omega t \qquad (11.9)$$

Upon superimposition of a permanent field H_1 the induction B will be expressed by the equation

$$B = a(H_0 \cos \omega t + H_1)^3 + c(H_0 \cos \omega t + H_1),$$

or, following corresponding transformations,

$$B = \frac{1}{4} aH_0^3 \cos 3\omega t + \frac{3}{2} aH_1 H_0^2 \cos 2\omega t + \left(\frac{3}{4} aH_0^3 + 3aH_1^2 H_0 + cH_0\right) \cos \omega t + \frac{3}{2} H_1 H_0^2 + H_1. \qquad (11.10)$$

Declassified in Part - Sanitized Copy Approved for Release 2013/01/23 : CIA-RDP81-01043R001600090003-8

Declassified in Part - Sanitized Copy Approved for Release 2013/01/23 : CIA-RDP81-01043R001600090003-8

Equations (11.9) and (11.10) show that in the absence of the permanent field H_1 the induction consists of harmonics of first and third order, with the superimposition of a permanent field harmonics of the second order appear, and on a change of the sign of H_1 the odd-numbered harmonics remain the same while the even-numbered harmonics change their sign.

Therefore, if we replace the third order equation (11.9) by an equation of n-th order and perform the same operations, we will obtain an analogous result which differs only to the extent that in the expression (11.9) for B harmonics of higher odd orders will beepresent in addition to harmonics of first and third order, while in expression (11.10) even numbered harmonics also will be present.

In all the existing systems the emf of even numbered harmonics is not measured directly but serves merely as an indication of the fact that the permanent field being measured is compensated by the field of the coil in which the permalloy plate (sonde) is placed. Thus the quantity that is being measured is the current intensity of the compensating coil, which is proportional to the intensity of the magnetic field. In the course of this measurement compensation is effected automatically.

The simplest block diagram of the use of secondary harmonics is shown in Figure 243. From an alternating current generator T having a frequency of about 1,000 Hertz the current passes through filter F-I, and flows to the winding W_1 of the sonde at a definite frequency f. The self-induced emf of doubled frequency 2f produced at the terminals of this winding passes through filter F-II tuned to frequency 2f to the input of amplifier YC. Voltage from the generator is transmitted at the same frequency 2f to the same input. After

Declassified in Part - Sanitized Copy Approved for Release 2013/01/23 : CIA-RDP81-01043R001600090003-8

Declassified in Part - Sanitized Copy Approved for Release 2013/01/23 : CIA-RDP81-01043R001600090003-8

amplification the current is rectified and passes into the compensation winding W_2, the magnetic field of which compensates the terrestrial field being measured.

At the instant of compensation even numbered harmonics are absent, and therefore only the voltage from the generator will pass to the amplifier input. On a change in the magnitude of the field the compensation is disrupted, secondary harmonics appear, and their emf will pass to the input of the amplifier and change the current at its output. Such a change will take place until the current in winding W_2 restores the compensation.

A second system extensively utilized in modern instruments is that shown in Figure 244, which utilizes 2 sondes. Alternating current is switched on through 2 windings in series carried by each of the sondes. The windings are connected in such a manner that their magnetic fields are directly opposite, and consequently in the absence of an external field the total magnetic moment of the 2 sondes is equal to zero.

The secondary winding usually covers both sondes at the same time and therefore the emf of induction occurs in the sondes only in the presence of an external magnetic field, when a constant summative induction B is imparted to the sondes. Due to the opposite phases of the alternating current in the primary windings, the induction in each of the rods will change by the same quantity but in opposite directions and the difference ΔB will oscillate at a frequency 2f. As a result of this an emf of frequency 2f is generated in the secondary winding. Indeed, according to equation (11.10), for one of the sondes all the terms of the expression defining the induction will have positive signs, while for the other sonde, in view of the reverse direction

Declassified in Part - Sanitized Copy Approved for Release 2013/01/23 : CIA-RDP81-01043R001600090003-8

Declassified in Part - Sanitized Copy Approved for Release 2013/01/23 : CIA-RDP81-01043R001600090003-8

of the amplitude of alternating field H_1, the odd numbered harmonics will have negative signs and the even numbered harmonics will have positive signs. Hence the difference in induction ΔB in the sondes is defined by the equation

$$\Delta B = 3aH_1H_0^2 \cos 2 wt \neq H_1,$$

and the emf by

$$\mathcal{E} = 6 awH_1H_0^2 \sin 2 wt. \qquad (11.11)$$

These equations show that the amplitude of the emf is proportional to the intensity of the permanent field being measured.

Finally, a third system which is used in magnetometers may be mentioned. This system employs large alternating saturation. It is essentially the same system as that shown in Figure 244, but in this system the sondes are subjected to the action of a high amplitude alternating field.

As a result of this, the magnetization of the primary windings on each change in the direction of the current reaches saturation before the alternating field attains its maximum value. Thus during each half-period there are intervals of time during which the induction in the sondes assumes a constant value corresponding to the saturation, while the emf during this length of time becomes equal to zero, and therefore the correlation between emf and time will appear graphically as a series of peak-shaped curves alternating within the positive and negative portions of the plane and divided from each otherby zero values of ordinates. These curves, as is shown by oscillographic recordings, are asymmetrical because the rise of emf from zero to a certain maximum occurs gradually, while the return to zero occurs very rapidly. This asymmetry is due to eddy currents within the core which prevent a rapid increase of induction in the sonde.

Declassified in Part - Sanitized Copy Approved for Release 2013/01/23 : CIA-RDP81-01043R001600090003-8

Declassified in Part - Sanitized Copy Approved for Release 2013/01/23 : CIA-RDP81-01043R001600090003-8

In order to show this analytically, we will express the basic magnetization curve by a tangensoid, assuming that the tangents are plotted on the abscissa, and the arcs are plotted on the ordinate. Such a representation is entirely permissible, as is apparent from comparison of the basic curve of magnetization of armco (1) with a tangensoid (2), shown in Figure 245.

The equation of a basic curve corresponding to a tangensoid may be expressed as: $B = \frac{2}{\pi} B_m \operatorname{arc\,tg} \frac{H}{\pm H_0}$, (11.12)

where B_m is induction corresponding to $H = \infty$, and H_0 is the intensity of the magnetic field corresponding to $B = B_m/2$.

If only an alternating field is acting on the specimen, it follows that $B = \frac{2}{\pi} B_m \operatorname{arc\,tg} \left(\frac{H_m}{H_0} \cos \omega t \right)$.

Using the denotation $\frac{H_m}{H_0} = h$, $\omega t = \tau$ and denoting the cross sectional area of the specimen by S, we have for the magnetic flux Φ the expression $\Phi = \frac{2}{\pi} B_m S \operatorname{arc\,tg} \frac{h \cos \tau}{1 + h^2 \cos^2 \tau}$,

and the emf in volts is represented by the equation

$$\mathcal{E} = 10^{-8} \frac{2}{\pi} B_m S \omega \frac{h \sin \tau}{1 + h^2 \cos^2 \tau} \quad (11.13)$$

The maximum value of $\mathcal{E}$ corresponding to phase $\tau = 90°$ will be

$$\mathcal{E} = 10^{-8} \cdot \frac{2}{\pi} B_m S \omega h, \quad (11.14)$$

which, in the case of the given sonde, is proportional to the magnitude of saturation B_m, frequency w and the ratio H/H_0.

Figure 246 shows curves corresponding to equation (11.13) for 3 different parameters $h = 5$, 10 and 20, from which it is apparent that the curves are peak-shaped with an increase of the parameter h, i.e., with an increasing amplitude of the alternating field the amplitude $\mathcal{E}$ increases and the width of the peak decreases.

Declassified in Part - Sanitized Copy Approved for Release 2013/01/23 : CIA-RDP81-01043R001600090003-8

Declassified in Part - Sanitized Copy Approved for Release 2013/01/23 : CIA-RDP81-01043R001600090003-8

Upon superimposition of a permanent field of intensity H_1, the expfession (11.12) for the induction becomes

$$B = \frac{2}{\pi} B_m \operatorname{arc\,tg} \frac{H + H_1}{H_0},$$

and expression (11.13) for the emf becomes

$$\mathcal{E} = 10^{-8} \cdot \frac{2}{\pi} S\omega \frac{h \sin \omega t}{1 + (h \cos \tau + h_1)^2}, \qquad (11.15)$$

where $h_1 = \frac{H_1}{H_0}$.

In this case the maximum value of $\mathcal{E}$ will be obtained not at $\tau = 90^\circ$ but at a somewhat different value which satisfies the equation:

At the same time, if h_1 is negative the maximum occurs at $\tau < 90^\circ$, and if h_1 is positive the maximum occurs later, i.e., there is a shift in phase equal to $\tau - 90^\circ$.

From this it follows that if in the absence of a permanent field the total emf in the secondary winding of both sondes is equal to zero, when the field is present the sum of the emf will become different from zero due to the phase shift and its magnitude will increase with the increase in phase shift and in the intensity of the permanent field.

The above applies to the instance when the specimen (sonde) has poor resistance and contains no eddy currents. Actually, however, on application of an alternating current eddy currents arise within the specimen and during the first quarter of the phase retard the increase of induction and hence also of emf, and during the second phase tend to retain it. Consequently, the emf curve is asymmetrical in relation to the y-axis. Figure 247 shows the appearance of actual curves obtained on oscillograms. Of these the curves a correspond to the case when the external permanent field is absent and curve b corresponds to the instance when a permanent field is superimposed on the alternating field. The summative magnitude of emf in the former case will be equal to zero and in the latter case will be represented by curve c. As is apparent,

Declassified in Part - Sanitized Copy Approved for Release 2013/01/23 : CIA-RDP81-01043R001600090003-8

Declassified in Part - Sanitized Copy Approved for Release 2013/01/23 : CIA-RDP81-01043R001600090003-8

the asymmetry is manifested more sharply when the positive amplitudes greatly exceed the negative ones. On a 180° change in the direction of the permanent field the curves of the emf in the primary windings are shifted in the opposite direction, as a result of which the summative curve assumes the form shown in the same drawing under the letter d, wherein the negative amplitudes become predominant. For this reason this system permits measurement of the intensity of the permanent field, and identification of its direction as well.

However this system has the disadvantage that it requires a completely identical core for the sonde and for its windings, since the slightest difference in geometric dimensions of the sondes or in magnetic characteristics of the cores produces considerable voltage impulses at the output of the secondary winding even in the absence of an external field. Therefore, in practice systems with an initial detuning are used in which one of the primary windings is shunted with a resistance, and thus both cores deliberately are made identical. The form of the curves for the emf induced by the primary windings is shown in Figure 248 (curve a).

Since the amplitude of impulses of the primary and secondary windings are not equal in the absence of an external field impulse with opposite sign but equal amplitude, curve b, occur at the output of the secondary winding. On superimposition of a permanent field one of the amplitudes becomes smaller and the other larger (curve c). Upon a change in polarity of the magnetic field the picture is altered in the opposite direction (curve d).

Thus with detuned sondes also, the effect of a permanent field will manifest itself in a manner fully analogous to that with

Declassified in Part - Sanitized Copy Approved for Release 2013/01/23 : CIA-RDP81-01043R001600090003-8

Declassified in Part - Sanitized Copy Approved for Release 2013/01/23 : CIA-RDP81-01043R001600090003-8

identical sondes, and therefore the measurement procedure remains the same while the manufacture and tuning of the sondes are greatly simplified.

At the present time magnetically saturated sondes are extensively utilized in measuring weak magnetic fields and in compass studies. Their threshold of sensitivity, with a good stability, reaches 0.1-1.0 γ. Thin wires of permalloy or mumetal 30 to 60 mm long and with a diameter-to-length ratio not greater than 0.01 are used as cores. This diameter-to-length ratio is necessary, since otherwise their apparent susceptibility becomes inadequate for attaining large values of induction, and consequently also of voltage, at the output of the sonde.

Magnetic sondes are especially important in aeromagnetic surveying. Aeromagnetometers in which the measuring element is a magnetically saturated sonde are highly sensitive and permit complete automation of measurement of the magnetic field. Therefore we shall consider only the aeromagnetometer system among all the various measuring systems.

Aeromagnetometers with magnetically saturated sondes, in contrast with the aeromagnetometer of Logachev, measure the total magnitude of field intensity H_T instead of the vertical componont of the terrestrial field. This is due to the fact that the sonde is much more easily aligned with the direction of the lines of force of the magnetic field, and moreover, a deviation of the axis of the sonde from the direction of the lines of force causes less error in the determination of H_T than an equal deviation of the vertical position during determination of the vertical component Z.

Declassified in Part - Sanitized Copy Approved for Release 2013/01/23 : CIA-RDP81-01043R001600090003-8

Declassified in Part - Sanitized Copy Approved for Release 2013/01/23 : CIA-RDP81-01043R001600090003-8

Indeed, from the equation $Z = H_T \sin I$,

where I is dip, we obtain:

$$\Delta Z = H_T \cos I \Delta I, \qquad (11.16)$$

i.e., the error in determination of the vertical component is proportional to the cosine of the angle of dip, and therefore when the axis of the sonde is directed along the lines of force $Z = H_T$ and the error in the determination of H_T becomes close to zero.

Assuming that in measuring the vertical component corresponding to dip I, an error has occurred in the adjustment of the axis of the sonde amounting to a quantity ΔI, let us determine the quantity ΔI_1 by which the sonde may become deflected during the measurement of H_T in order that the errors in determination of Z and H_T will be equal.

From equation (11.16) we have:

$$H_T \cos I \Delta I = H_T \cos (90 - \Delta I_1) \Delta I_1,$$

hence

$$\Delta I_1^2 = \cos I \Delta I.$$

If the measurements are carried out at Leningrad, where $I = 72^\circ$, we find that at $\Delta I = 1'$ the error is $\Delta I' = 32'$, ie., the alignment of the axis of the sonde with respect to the direction of the lines of force can be more than 30 times less accurate than its setting in the vertical direction.

The alignment of the axis of the sonde in the H_T direction is effected by means of 2 mutually perpendicular sondes which are perpendicular to the measuring sonde, and are called tracing sondes. The secondary windings of these sondes are connected through amplifiers to servomotors which are actuated if the sonde is not perpendicular to the lines of force of the magnetic field, i.e., if a component of the terrestrial field is acting upon the sonde the rotation of the motor is transmitted to the system of the sondes and they turn until they assume

Declassified in Part - Sanitized Copy Approved for Release 2013/01/23 : CIA-RDP81-01043R001600090003-8

Declassified in Part - Sanitized Copy Approved for Release 2013/01/23 : CIA-RDP81-01043R001600090003-8

a position perpendicular to the terrestrial field. At that instant the impulses in the secondary circuit cease and the motors stop. As soon as the plane within which the tracing sondes are located departs from the plane perpendicular to the direction of the lines of force the servomotor is actuated and returns it to its former position. Thus the measuring sonde always is maintained in the direction of the lines of force of the field. The deflection of its axis from this direction does not exceed 15', which causes an error in the measurement of ΔZ not exceeding 1 %. However the total error in measurement of ΔZ by means of a sonde aeromagnetometer reaches $\pm$ 5 %.

The compensation of the magnetic field of the earth also is done automatically. The direct current in the compensation coil within which the sonde is placed is regulated by rheostats which are automatically controlled by means of motors and is transmitted to the automatic recording device. The motors are actuated until a complete compensation of the magnetic field has been attained.

The aeromagnetometer records not the total quantity H_T but only the algebraic difference ΔH_T between initial and terminal values.

Current is supplied to the primary windings of all 3 sondes from a sinusoidal current generator having a frequency of 400 Hertz and stabilized as to frequency and amplitude. A storage battery supplies current for the compensation windings. Figure 249 shows a block-diagram of an aeromagnetometer of thin type. Measuring sondes and tracing sondes with servomotors are mounted within a streamlined gondola which is towed by the aircraft at the end of a 50 m cable.

The direct and alternating current generators, the amplifiers and the automatic recording device are set up in the cabin of the aircraft.

Declassified in Part - Sanitized Copy Approved for Release 2013/01/23 : CIA-RDP81-01043R001600090003-8

Declassified in Part - Sanitized Copy Approved for Release 2013/01/23 : CIA-RDP81-01043R001600090003-8

CHAPTER XII

Variation Instruments

Variation instruments used to register magnetic variations of the earth's field are based for the most part of the interaction between the magnetic field and permanent magnet. As the earth's magnetic field within the instrument's range can be considered uniform, the interaction produces a moment of rotation turning the magnetic axis in the direction of the field. The amount and direction of rotation M is determined by the formula $M = [M_m H_T]$, where M_m = magnetic moment of the permanent magnet and H_T = intensity of the magnetic field.

In variation instruments moment M is counteracted by moment M^1, produced by mechanical forces such as: gravity, torque action of the thread, etc; therefore, the equilibrium of a permanent magnet, comprising the basic part of variation instruments takes the form of: $M^1 [M_m H_T] = 0$ (12.1).

In changing vector H_T to δH_T, the initial conditions of equilibrium (12.1) are disturbed and the new conditions will be characterized by the fact that moment M^1 will change to δM^1 and the magnet will take a new position, i. e., vector M_m will change to δM_m. In the differentiation of equation (12.1), one finds the relationship between the variations of vectors H_T and M_m and variation of vector M^1, namely: $\delta M^1 + [M_m \delta H_T] + [\delta M_m H_T] = 0$ (12.2)

This relationship represents the basic equation of variation instruments and enables one to determine the variation of vector H_T, or its variation δH, if the direct measurements of variations of moments δM_m and δM^1 are known.

Declassified in Part - Sanitized Copy Approved for Release 2013/01/23 : CIA-RDP81-01043R001600090003-8

Declassified in Part - Sanitized Copy Approved for Release 2013/01/23 : CIA-RDP81-01043R001600090003-8

All variation instruments are constructed in such a way that the rotation of the permanent magnet will take place only in one surface, horizontal or vertical. Therefore M and M^1 moments can only have one component perpendicular to the surface's axis of rotation.

For example if the axis of rotation called the Z-axis is set vertically, the x-axis is directed along the geographical meridian (Figure 250) and the angles formed by the x-axis with the magnetic meridian and the axis of the magnet are designated D and θ, respectively, then equation (12.1) in a scalar form assumes the following form:

$$M\frac{r'}{z} + My\,X - MxY = 0 \qquad (12.3)$$

where

$My = M_m \sin \theta;$

$Mx = M_m \cos \theta;$

$X = H \cos D;$

$Y = H \sin D;$

in which H is the horizontal component.

Substituting values for the components in equation (12.3);

$$M^1_z - M_m H \sin \vartheta = 0 \qquad (12.4)$$

where $\vartheta = \theta - D.$

Correspondingly the equation (12.2) can be written in this form:

$$\delta M^1 - Mx\delta Y + My\delta X - Y\delta Mx + X\delta My = 0,$$

or in this form (12.5)

$$\delta M^1 = M_m \sin\vartheta\,\delta H + H \sin\vartheta\,\delta M_m + M_m H \cos\vartheta\,\delta\theta - M_m H \cos\vartheta\,\delta D.$$

The first of these equations can be represented in several different ways, substituting Mx and My by M_m and θ, namely:

$$\delta M = M_m \cos\theta\,\delta Y - M_m \sin\theta\,\delta X + (Y\cos\theta - X\sin\theta)\,\delta M_m - M_m (Y\sin\theta + X\cos\theta)\,\delta\theta. \qquad (12.6)$$

Declassified in Part - Sanitized Copy Approved for Release 2013/01/23 : CIA-RDP81-01043R001600090003-8

Declassified in Part - Sanitized Copy Approved for Release 2013/01/23 : CIA-RDP81-01043R001600090003-8

Equation (12.6) establishes the link between the angle of declination of magnet $\delta\theta$ and variations of the northward and eastward parts of components δX and δY; equation (12.5) establishes the link between $\delta\theta$, variations of horizontal component δH, and the variation of the declination δD.

From these equations it is evident how the magnet should be set in relation to the coordinate axes so that the magnet declinations depend on the variations of one of the components of the earth's magnetic field intensity.

Therefore, if in equation (12.5) one assumes that θ = zero, i. e., placing the magnet along the geographical meridian, then

$$\delta M_z = M_m \delta Y + Y \delta M_m - M_m X \delta\theta \qquad (12.7)$$

if one assumes $\theta = 90^\circ$, i. e. setting the magnet along a parallel,

$$\delta M_z = -M_m \delta X - X \delta M_m - M_m Y \delta\theta \qquad (12.8)$$

In the first case the declination of the magnet will produce variations of the eatward component, whereas in the second case, it will produce variations of the northward component.

Furthermore, if in equation (12.6) the angle is equal to zero or 90°, i. e., if the magnet is set along the magnetic meridian or perpendicular to it, the equation would assume the following respective forms:

$$\begin{aligned} \delta M_z &= M_m H \delta\theta - M_m H \delta D, \\ \delta M_z &= M_m \delta H + H \delta M_m. \end{aligned} \qquad (12.9)$$

The first equation gives the connection between the declinations of the magnet and the variation, δD, of the declination, whereas the second equation gives the connection between the declination and variation of the horizontal component.

Declassified in Part - Sanitized Copy Approved for Release 2013/01/23 : CIA-RDP81-01043R001600090003-8

Declassified in Part - Sanitized Copy Approved for Release 2013/01/23 : CIA-RDP81-01043R001600090003-8

If the axis of rotation is horizontal assuming that it is axis y, equation (12.1) will be written in form:

$$M'_y - Mx\,Z + Mz\,X = 0$$

as $Mx = Mm \cos \theta$; $Mz = Mm \sin \theta$,

where θ will be the angle in a vertical plane between the magnetic axis of the magnet and axis x (Figure 251), therefore

$$M'_y = Mm\,Z \cos \theta - Mm\,X \sin \theta, \tag{12.10}$$

whereupon

$$\delta M'_y = (Z \cos \theta - X \sin \theta)\delta Mm + Mm \cos \theta \delta Z - Mm \sin \theta \delta X - (Z \sin \theta + X \cos \theta)\delta \theta.$$

Assuming that $\theta = 0$ in this equation, i. e., adjusting the magnet in a horizontal line one obtains:

$$\delta M'_y = Z\delta Mm + Mm\delta Z - Mm\,X\delta\theta. \tag{12.11}$$

The last equation indicates the connection between the variation δZ, of the vertical component and the declination $\delta\theta$ of the magnet, produced by this variation.

Equations (12.7) and (12.11) represent a scaler expression of the basic equation (12.2) applicable to any variation instrument, based on the interaction of magnetic field with a permanent magnet. The following instruments belong to the category: the unifilar, used to register variations of the horizontal component and declinations; magnetic balances and the Z-variometer, used to register variations of the vertical component. The difference between them consists in the different arrangement of the axis rotation of the permanent magnet and in the different system of counteracting moment M[1].

Declassified in Part - Sanitized Copy Approved for Release 2013/01/23 : CIA-RDP81-01043R001600090003-8

Declassified in Part - Sanitized Copy Approved for Release 2013/01/23 : CIA-RDP81-01043R001600090003-8

2. Variometers

The unifilar is an instrument whose main part is permanent magnet M, suspended by a thread (Figure 252) which possesses a constant torsion coefficient. For this purpose the most satisfactory thread is either made of quartz or metal. The suspension system is built so that the magnet can freely rotate only in a horizontal plane, which causes the direction of moment of rotation to coincide with the vertical axis. The counteracting moment of rotation in this case will be the thread torque which is proportional to its angle φ, i. e.,

$$M' = C\varphi, \tag{12.12}$$

or as φ coincides with axis z,

$$M'_z = C\varphi,$$

where C = torsion coefficient of the thread.

The twisting of the thread is carried out by the attachment K (Figure 252) which ordinarily contains graduations.

Let us assume that the thread is initially untwisted. In this case the axis of the magnet coincides with the direction of the magnetic meridian NS (Figure 253). If the torsion knob K (Figure 252) is turned through an angle ψ, the thread will twist through an angle ϑ, and the magnet will deflect from magnetic meridian by an unknown angle . Therefore, it can be seen that the angle through which the thread is equal to the difference between angles ψ and ϑ, i. e., $\varphi = \psi - \vartheta$.

If according to the foregoing, θ is designated the angle between the axis of the magnet and axis x, coinciding with the geographical meridian, then $\vartheta = \theta - D$, where D = the declination and correspondingly

$$M'_z = C(\psi - \theta + D),$$

and

$$\delta M'_z = -C\delta\theta + \varphi\delta C \tag{12.13}$$

Declassified in Part - Sanitized Copy Approved for Release 2013/01/23 : CIA-RDP81-01043R001600090003-8

Declassified in Part - Sanitized Copy Approved for Release 2013/01/23 : CIA-RDP81-01043R001600090003-8

According to equation (12.4), $MH \sin\vartheta = C\varphi$, then $\delta M'_z = -C\delta\theta + Mm H \sin\vartheta$.

Substituting the derived value $\delta M'_z$ in equation (12.5) and assuming that $\vartheta = 0$ and $90°$, one obtains, removing subscript m from M:

$$\delta\theta = \frac{MH}{MH+C}\,\delta D \qquad (12.14)$$

$$\delta\theta = -\frac{M}{C}\,\delta H - \frac{H}{C}\cdot\frac{\delta M}{M} + \frac{M+C}{C}\cdot\frac{\delta C}{C} \qquad (12.15)$$

(a) Let us examine a case when a unifilar operates as a variometer of declination.

Equation (12.14) demonstrates that the readings of the unifilar which is fixed on the magnetic meridian are proportional to the variation of declination and are not dependent on the variations of the magnetic moment of the unifilar and the torque factor.

In view of the fact that variations M and H are insignificant, the coefficient of proportionability with δD given can actually be considered a constant value which can be called susceptibility of the unifilar; the inverse value $\frac{MH+C}{H+M}$ is called the constant of the instrument or scale value. In showing the scale value of the declination variometer by ε_D, one can write:

$$\delta D = \varepsilon_D \cdot \theta \qquad (12.16)$$

Normally, the readings of the unifilar are not angular measurements but scale divisions (mm) with the scale located at a distance R from the mirror of the magnet (Figure 254).

If δn is the number of scale divisions by which the reflected image of light S declines from zero, then: $\frac{\delta n}{R} = \text{arc tg } 2\delta\theta$, or in view of the small value of δn as compared to R: $\delta\theta = \frac{\delta n}{2R}$.

Declassified in Part - Sanitized Copy Approved for Release 2013/01/23 : CIA-RDP81-01043R001600090003-8

Declassified in Part - Sanitized Copy Approved for Release 2013/01/23 : CIA-RDP81-01043R001600090003-8

In this case equation (12.14) takes the form: $\delta n = \frac{2RMA}{MH+C} \delta D$.

If δD in this equation is expressed not in radius, but in minutes of the arc, it is necessary to multiply the right side of this equation by sin 1', therefore:

$$\delta n = \frac{2RMH \sin 1' \delta D'}{MH+C}$$

or

$$\delta D' = \varepsilon'_D \delta n \qquad (12.17)$$

where ε'_D = scale value, expressed in minutes per 1 mm and determined by equation:

$$\varepsilon'_D = \frac{MH+C}{2R \sin 1' MH} \qquad (12.18)$$

In this case when the value of the thread torque can be disregarded (c = 0):

$$\varepsilon'_D = \frac{1}{2R \sin 1'}$$

i. e., the scale value of the unifilar which is set along the meridian is inversely proportional to the distance of the mirror from the scale and does not depend on other values. Therefore for example in order to obtain the scale value ε'_D = 1' per 1 min it is necessary to adjust the scale in relations to the mirror of the unifilar at a distance R = $\frac{1}{\sin 1'}$ = 1718 mm.

An interesting circumstance occurs when the magnet of the unifilar is set in opposition to the magnetic meridian (ϑ = 180°). In this case, $\delta\Theta$ and δD in equations (12.5) and (12.13) should be linked by the ratio:

$$\delta D = - \varepsilon_D \delta\Theta \qquad (12.19)$$

where ε_D = scale value of the variometer, expressed by formula:

$$\varepsilon_D = \frac{C-MH}{MH} \qquad (12.20)$$

The minus sign in formula (12.19) indicates that the variometer readings $\delta\Theta$ and the declination variations δD are in opposition. Therefore,

Declassified in Part - Sanitized Copy Approved for Release 2013/01/23 : CIA-RDP81-01043R001600090003-8

Declassified in Part - Sanitized Copy Approved for Release 2013/01/23 : CIA-RDP81-01043R001600090003-8

if initially the magnetic axis of the unifilar is pointed in the direction OM in opposition to the magnetic meridian NS (Figure 255), during the variation of the declination from angle δ D to E, the magnet deflects by angle $\delta\theta$ in the opposing direction.

Formula (12.20) shows that the scale value of the variometer with the magnet pointed in opposition to the magnetic meridian can take any value from zero to infinity, depending on the value of torsion coefficient C of the thread.

With C = MH, the scale value $\varepsilon_D = 0$ and the susceptibility becomes infinity.

With C < MH it is impossible to adjust the magnet of the unifilar in opposition to the magnetic meridian as in this case the magnet is in an unstable condition, i. e., with the smallest declination of the magnet axis from the SN direction, the magnet turns in the direction of the magnetic meridian NS.

Actually, with ϑ 180° the magnet can be in an unstable condition, first when the thread is entirely untwisted, i. e., $\varphi = 0$, as the following conditions have to be fulfilled: MH sin 180° = C φ secondly, when with the smallest declination of the magnet from this position by angle "a," the counteracting moment exerted by the thread will be greater than the moment acting on the magnet, i. e., when MH sin (180± a) $\leq \pm$ Ca.

With small angles sin a = a, therefore, MH $\leq$

Let us examine the second case when the unifilar is a horizontal component variometer.

Declassified in Part - Sanitized Copy Approved for Release 2013/01/23 : CIA-RDP81-01043R001600090003-8

Declassified in Part - Sanitized Copy Approved for Release 2013/01/23 : CIA-RDP81-01043R001600090003-8

The (12.15) equation shows that in pointing the magnet perpendicular to the magnetic meridian achieved by a corresponding twist of the thread the declinations become a linear function of the 3 parameters: variations of the horizontal component δ H, variations of the magnetic moment δ M and variations of the thread torque δ C. Therefore in order to obtain magnet declinations independent of variations it is necessary to have the magnetic moment M and torsion coefficient C constant; this is achieved by suitable compensating devices, discussed below:

Let us assume that these conditions are fulfilled, i. e., M = const and C = const, in this case with = 0° or 270°

$$\delta\,\theta = \pm \frac{M}{C}\,\delta\,H \qquad (12.21)$$

i. e., the declinations of the unifilar are proportional to the horizontal component and the coefficient of proportionality represents the susceptibility of the unifilar, while the inverse value relating to the angle

$$\varepsilon_{H} = \frac{C}{M} \qquad (12.22)$$

is the scale value of the unifilar.

The minus sign with $\vartheta = 90^{\circ}$ indicates that angle θ increases with the decrease of the horizontal component and conversely.

If one expresses the scale value in units of field intensity per one scale division, then, similarly, the derivatives of the foregoing paragraph can be written:

$$\varepsilon_{H} = \frac{C}{2MR} \qquad (12.23)$$

This equation shows that the scale value of the horizontal component variometer at a given distance from the scale to the mirror of the magnet can take any values from zero to infinity in relation to the value of the torsion coefficient C, of the thread and magnetic

Declassified in Part - Sanitized Copy Approved for Release 2013/01/23 : CIA-RDP81-01043R001600090003-8

Declassified in Part - Sanitized Copy Approved for Release 2013/01/23 : CIA-RDP81-01043R001600090003-8

moment M. The torsion coefficient depends on the daimeter, length and elastic properties of the thread. This function for wire and thread of round cross-section is in conformity with the theory of elasticity and is expressed by the following ratio:

$$C = \frac{\pi G d^4}{32 \ell} \qquad (12.24)$$

where d = diameter of the wire or thread;

ℓ = its length and

G = shear (modulus) of the material

Quartz and bronze are considered the best materials for use in unifilars as they possess the greatest tensil strength and a small shear modulus.

Substituting the value for C from equation (12.24) in the equation (12.23) one obtains:

$$H = \frac{\pi G d^4}{64 \ell MR} \qquad (12.25)$$

i. e., the scale value of the horizontal component variometer is proportional to the fourth power of the thread diameter and inversely proportional to its length.

Formula (12.25) makes it possible to calculate the thread diameter and its length at a given scale value of the variometer. For example, in order to obtain scalevalues $\varepsilon H = 1\gamma$ per 1 mm, at a distance R = 100 cm from the mirror to the cylinder with the magnetic moment M = 10 CGS$_M$ and thread length l = 20 cm, it is necessary to have a quartz thread with a diameter: $d = \sqrt[4]{\frac{64\ CMR}{\pi G}} = 34$ mk as the shear modulus of quartz is $G = 3 \cdot 10^{11}$ dyne/cm^2.

3. The Influence of Temperature on the Unifilar Readings: Methods of Compensation

In the foregoing paragraphs in obtaining a formula for the

Declassified in Part - Sanitized Copy Approved for Release 2013/01/23 : CIA-RDP81-01043R001600090003-8

Declassified in Part - Sanitized Copy Approved for Release 2013/01/23 : CIA-RDP81-01043R001600090003-8

declination of an unifilar one assumes that the magnetic moment and thread torque are constant. Besides it is well known that the 2 values are related to the temperature and, therefore, all the temperature changes will be reflected by the unifilar readings.

It was shown in Chapter I that the influence of the temperature upon the value of the magnetic moment at small temperature changes δt can be expressed

$$\delta_M = -\mu_M \delta_t,$$

where μ = temperature coefficient of the magnet. The temperature influence on the coefficient of the thread torque C can be determined by using formula (12.24), which when it is differentiated by t yields:

$$\frac{1}{C} \cdot \frac{\delta C}{\delta t} = \frac{1}{G} \cdot \frac{\delta G}{\delta t}$$

i. e., the relative change of torque C with the temperature equal to the relative change of the shear coefficient G which will be designated by "a."

In this case, $\delta_C = aC\delta t$.

Substituting these values for δ_M and δ_C in formula (12.15) and assuming that $\delta_H = 0$ one obtains the expression for an unifilar declination depending on the temperature changes δt: $\delta\theta = \frac{MH}{C}(a + \mu)\delta t$.

As the factor M/C represents the inverse value of the scale value H, therefore, expressing the factor in gammas per division, one obtains: $\delta n = \frac{H}{H}(a + \mu)\delta t$.

The value $\mu_H = \frac{H}{H}(a + \mu)$ (12.26)

is called the temperature coefficient of an unifilar or variometer and is the declination of the variometer, expressed in units of field intensity with temperature changes of 1°.

Declassified in Part - Sanitized Copy Approved for Release 2013/01/23 : CIA-RDP81-01043R001600090003-8

Declassified in Part - Sanitized Copy Approved for Release 2013/01/23 : CIA-RDP81-01043R001600090003-8

A general formula expressing the declination of an unifilar with variations δ H and temperatures δ t, can be written thus:

$$\delta n = \frac{1}{H}\,\delta H - \frac{A\pi}{H}\,\delta t \qquad (12.27)$$

from which in solving for δ H, one obtains:

$$\delta H = H\,\delta n + k A \delta t$$

i. e., in order to compute the variation δ H according to the declination of a unifilar δ n it is necessary after converting δ n into units of intensity (gammas) to add the temperature correction equal to μ H δ t. Let us calculate the order of magnitude of the temperature coefficient of the variometer assuming that H = 15300γ, $H = 2\gamma/\mu$. The value of the temperature coefficient of the magnet is ordinarily μ = 0.0002, whereas the value of the temperature coefficient of shear for quartz thread equals a = - 0.00014. Therefore substituting these values in equation (12.26) one obtains the value μ H for an unifilar with quartz thread: μ H = 5.1γ /degrees which has a great deal of significance in the operation of magnetographs and, therefore, determining the temperature coefficient.

If the influence of the temperature on the readings of the unifilar cannot be eliminated completely it has to be kept to a minimum. This operation is known as temperature compensation. However, the more widely used compensation systems in modern instruments are the magnetic or calmalloy type.

The magnetic system is used in order instruments which simply means that a second magnet is placed in a stationary position at a certain distance from the suspended magnet. In temperature changes, the magnetic moment of this magnet varies and produces a declination of the unifilar equal to the declination produced by the variations of the magnetic moment of the suspended magnet, but in an opposite direction. The calmalloy method proposed by B. M. Yanovskiy and employed in

Declassified in Part - Sanitized Copy Approved for Release 2013/01/23 : CIA-RDP81-01043R001600090003-8

Declassified in Part - Sanitized Copy Approved for Release 2013/01/23 : CIA-RDP81-01043R001600090003-8

Soviet instruments at the present time, consists of a ferromagnetic plate made of calmalloy which is placed on the suspended magnet. This plate acts as a rotor and by cutting off the magnetic flux of the magnet decreases its magnetic moment. With an increase in temperature the permeability of calmalloy is decreased and the cutting off of the magnetic flux becomes less. As a consequence there is an increase in the magnetic moment which compensates for the decrease caused by heating.

In the magnetic system as shown above compensation is accomplished with the aid of a magnet which is located at a certain set distance from the movable magnet. If the distance between both magnet centers is R the magnets will be perpendicular to each other in a vertical plane with the centers resting in a vertical line. Let us designate the magnetic moment of the stationary magnet by M_0, and the temperature coefficient of it by $\mu 0$, then the field intensity H_0 produced by this magnet in the center of the suspended magnet will be: $H_0 = M_0 f(R)$, where $f(R)$ = a certain function of distance R. The direction of vector H_0 will be in an opposite direction to H (Figure 256).

During temperature changes the field intensity H_0 will vary and in the initial approach this change δH_0 can be expressed as

$$\delta H_0 = f(R)\,\delta M_0 = \mu 0\, M_0 + (R)\,\delta t = -H_0\, \mu 0\, \delta t,$$

i. e., the change of intensity is proportional to the temperature change δt.

The variation δH_0 together with the change of the magnetic moment of the suspended magnet will produce a declination of the unifilar through δn, expressed, according to equation (12.27) by the ratio:

$$\delta n = \frac{1}{H} (H_0 \mu 0 - \mu H) \delta t.$$

as the direction of field H_0 is opposite to field H.

Declassified in Part - Sanitized Copy Approved for Release 2013/01/23 : CIA-RDP81-01043R001600090003-8

Declassified in Part - Sanitized Copy Approved for Release 2013/01/23 : CIA-RDP81-01043R001600090003-8

In view of this fact the condition of temperature compensation is written in the following manner:

$$\mu H = H_o \mu_0.$$

This ratio can always be fulfilled by means of selecting the corresponding distance R between the suspended and compensated magnets.

If the compensated magnet M_o is set in a vertical plane passing through the suspended magnet, then the value of the vector H_o in the initial approach will be expressed as $H_o = \frac{M_o}{R^3}$, and condition of temperature compensation will be

$$\mu H = \frac{M_o}{R^3} \mu_0.$$

It is evident that this condition is possible with any value μ_0.

Let us assume that $\mu H = 5\Gamma$ at 1^o, $\mu_0 = 0.0002$ and magnetic moment $M_o = 50$, then one can find the distance R on which magnet M_o is set so that the temperature compensation can be carried out. Substituting these values in the foregoing ratio and solving it in relation to R one obtains:

$$R \sqrt[3]{\frac{M_o \, 0}{H}} = 6.2 \text{ cm.}$$

The magnetic system of temperature compensation possesses one essential deficiency which can be called heat inertia. In order to obtain complete compensation simultaneous heating or cooling at the same temperature as the suspended and compensated magnets are necessary. Actually because of the temperature gradient, inequalities in the mass of a magnet and other reasons, magnets are not heated or cooled simultaneously and therefore in places where the temperature is not constant but varies magnetic compensation is ineffective. The application of magnetic compensation is possible only in a static condition when the temperature of a space changes slowly or passes from one constant to another.

Declassified in Part - Sanitized Copy Approved for Release 2013/01/23 : CIA-RDP81-01043R001600090003-8

Declassified in Part - Sanitized Copy Approved for Release 2013/01/23 : CIA-RDP81-01043R001600090003-8

This deficiency is linked with heat inertia and is almost completely absent in compensation methods using calmalloy. As stated above this method consists of a calmalloy plate which is placed directly on the magnet forming one whole plate. Under the influence of the magnetic field of the magnet which is in opposition to its magnetic moment the plate magnetizes and acquires a magnetic moment in opposition to the magnet. In this manner the total magnetic moment of the suspended magnet M will be the difference: $M = M_0 - M_1$, where M_0 = the magnetic moment of the suspended magnet and M = the magnetic moment of the plate.

The variation of the magnetic moment is expressed $\delta M = \delta M_0 - \delta M_1$.

If this value substituted in equation (12.15) assuming that $\delta H = 0$, then one obtains: $\delta\varphi = \frac{MN}{C}\left(\frac{\delta M_0}{M} - \frac{\delta M_1}{M} - \frac{\delta C}{C}\right)$,

this expression represents the declination of the unifilar during variations of the magnetic moment and thread torque. If these variations are caused by the temperature it is possible to write:

$$\delta\theta = \frac{MN}{C}\left(\frac{1}{M}\cdot\frac{\delta M_0}{\delta t} - \frac{1}{M}\cdot\frac{\delta M_1}{\delta t} - \frac{1}{C}\cdot\frac{\delta C}{\delta t}\right)\delta t$$

Temperature compensation is possible when the t coefficient is equal to zero: $\frac{1}{M}\cdot\frac{\delta M_0}{\delta t} - \frac{1}{M}\cdot\frac{\delta M_1}{\delta t} - \frac{1}{C}\cdot\frac{\delta C}{\delta t} = 0$,

or

$$\frac{M_0}{\delta t} = -M_0\mu_0\cdot\frac{1}{C}\cdot\frac{\delta C}{\delta t} = a, \quad \text{т.е.} \quad \frac{M_0}{M}\mu_0 + a + \frac{1}{M}\cdot\frac{\delta M_1}{\delta t} = 0$$

As the ratio M_0/M is close to unity the calmalloy plate alters the magnetic moment of the magnet to a small degree therefore the conditions of temperature compensation can be written

$$\mu_0 + a + \frac{1}{M}\cdot\frac{\delta M_1}{\delta t} = 0 \qquad (12.28)$$

Calmalloy possesses properties that decrease its magnetic susceptibility x with an increase in temperature, almost according to the linear law whereupon the Curie point in which x = 0 remains at about 100° C.

Declassified in Part - Sanitized Copy Approved for Release 2013/01/23 : CIA-RDP81-01043R001600090003-8

Declassified in Part - Sanitized Copy Approved for Release 2013/01/23 : CIA-RDP81-01043R001600090003-8

Let us express the magnetic moment M_1 in the following manner:

$$M_1 = J_1 v = x H d v,$$

where J_1 = the average plate magnetization,

v = the plate volume

Hd = the average field intensity acting on the plate, producing a magnet.

If the plate thickness is not large then the value Hd in the initial approach can be equal to NJ_0, where N = demagnetization coefficient of the magnet and J_0 = magnetization of the magnet, therefore $M_1 = x NJ_0 v$.

In differentiating this expression becomes:

$$\frac{\partial M_1}{\partial t} = N J_0 v \frac{\partial \lambda}{\partial \tau} + \lambda M_0 \frac{J_0}{\partial \tau}$$

or as $J_0 = \frac{M}{V_0}$ where v_0 = the size of magnet

$$\frac{\partial M_1}{\partial t} = N \frac{V}{V_0} \left[M_0 \frac{\partial x}{\partial t} + \lambda \frac{\partial M}{\partial t} \right]$$

The value $\partial x/\partial t$ represents the variations of calmalloy susceptibility during temperature changes of 1° and has a negative value, because x decreases with a temperature increase. Therefore designating

$$\frac{\partial \lambda}{\partial \tau} = -\beta \quad \lambda = \frac{M_0}{\partial \tau} = -M_0 \mu_0,$$

one has

$$\frac{\partial M_1}{\partial t} = -N M_0 \frac{V}{V_0} (\beta + \lambda \cdot 0).$$

The value $x\mu_0$ is small compared to value β and therefore can be disregarded. In this case substituting the expression for $\partial m / \partial t$ in equation (12.28) one obtains:

$$\alpha + M_0 - \beta N M_0 \frac{V}{V_0} = 0 \qquad (12.29)$$

All the values going into this equation are constant with the exception of v, i. e., plate volume. Therefore, by varying v it is

Declassified in Part - Sanitized Copy Approved for Release 2013/01/23 : CIA-RDP81-01043R001600090003-8

Declassified in Part - Sanitized Copy Approved for Release 2013/01/23 : CIA-RDP81-01043R001600090003-8

always possible to meet the requirements of equation (12.29), i. e., so that the temperature compensation will be accomplished. Under these conditions

$$\nu = \frac{2 + N}{N N_0 \mu_0}$$

It is necessary to observe that the value of the demagnetization coefficient N in the expression (12.29), will remain constant only when the length of the calmalloy plate remains unchanged. Therefore, for a given magnet the volume of the calmalloy plate during temperature compensation has to change by means of varying its thickness.

4. A Unifilar as a Northward and Eastward Component Variometer

In order to record vector components of variations H on axes inclined towards the astronomical meridian (northward component) and parallels (easternward components), it is necessary, in accordance with the conclusions of paragraph 2, to adjust the axis of the unifilar magnet in the direction of the parallels or meridian.

Let us assume that the axis of the magnet is adjusted according to the direction of the astronomical meridian or in opposition to it, in this case, angle $\vartheta = D$, or $\vartheta = 180^\circ - D$, and the equation (12.29) with $\nu_M = 0$ given, will become

$$\vartheta = \frac{M}{I M \times T C} \alpha Y$$

As X = H cos D then

$$\vartheta = \frac{M}{I M H \cos D \times T C} \alpha Y$$

It is seen that the scale value $\frac{M}{I M H \cos D \times T C}$ can take different values depending on the value of declination D and the method of unifilar arrangement.

Several different unifilar arrangements are described. The

Declassified in Part - Sanitized Copy Approved for Release 2013/01/23 : CIA-RDP81-01043R001600090003-8

Declassified in Part - Sanitized Copy Approved for Release 2013/01/23 : CIA-RDP81-01043R001600090003-8

first case assumes that $D < 90^{\circ}$ and the unifilar are set in the direction of the astronomical meridian then

$$\varepsilon_y = \frac{MH \sin \vartheta - C}{I}$$

In this case the scale value of the unifilar depends on C and can assume any minimum value equal to $H \cos \delta$ up to infinity. In this manner as in the case of the variometer set along the magnetic meridian, it is impossible to decrease the scale value of the unifilar to the required value by decreasing the thread torque.

In the second case assume that $D < 90^{\circ}$ and the unifilar is adjusted in an opposition direction to the astronomical meridian.

In this case: $\varepsilon_y = \frac{-MH \sin \vartheta + C}{I}$

i. e., the scale value has any value from zero to infinity in relation to C but with this the torque coefficient C must satisfy the conditions $C > MH \cos \vartheta$ or otherwise the state of equilibrium becomes unstable and the unifilar does not point in an opposite direction to the astronomical meridian.

In the third case, let us assume that $D > 90^{\circ}$ and the unifilar is set in the direction of the astronomical meridian.

This case is analogous to the foregoing with this difference that the magnet with $C < H \cos \vartheta$ will be found in an unstable equilibrium, facing in the direction of the astronomical meridian.

In the fourth case $D > 90^{\circ}$ and the unifilar is set in opposition to the astronomical meridian. This case is completely analogous to the first case but differs from it in that the direction of the magnet is in opposition.

In recording the northward component X it is necessary to set

Declassified in Part - Sanitized Copy Approved for Release 2013/01/23 : CIA-RDP81-01043R001600090003-8

Declassified in Part - Sanitized Copy Approved for Release 2013/01/23 : CIA-RDP81-01043R001600090003-8

the unifilar magnet perpendicular to the astronomical meridian, i. e., make angle $\vartheta = 90^0 - D$ or $\vartheta = 90^0 + D$.

In the first case in accordance with equation (12.6) with $\delta M = 0$ one obtains: $\delta\theta = \frac{\delta X}{MH \sin D + C}$

secondly $\delta\theta = \frac{\delta X}{MH \sin D + C}$

In the first case the minimum value that ε_x can have will be $X \sin \vartheta$, in the second case, when $\vartheta = 90^0 + D$, the scale division can take any value. In a normal field the amount of variation in the whole USSR with the exclusion of the Arctic is not more than 12^0 therefore in any method of adjustment the value ε_y can always be sufficiently small.

5. Vertical Component Variometer Based on Magnetic Balance

One of the instruments used in recording variations of a vertical component of the earth's magnetic field is the magnetic balance which is represented by the magnet N S (Figure 257), freely rotating in a vertical plane around the horizontal axis, similar to a dip needle. The difference between the magnetic balance and the dip needle is that in the former the center of gravity of the magnet is slightly displaced in a horizontal direction from the rotating axis of the magnet and as a result besides the magnetic forces the gravity mg also acts on the magnet which has a counteracting moment and is expressed by the formula:

$$My = m [gl],$$

where m = mass of the magnet,

g = acceleration of the gravity,

l = distance from the center of gravity to the rotating axis.

Designating the angle between l and g by "a," one obtains: $My = mgl \sin a$, from which on the basis of equation (12.10) one obtains:

$$mgl \sin a = MZ \cos \theta - MX \sin \theta \qquad (12.30)$$

Declassified in Part - Sanitized Copy Approved for Release 2013/01/23 : CIA-RDP81-01043R001600090003-8

Declassified in Part - Sanitized Copy Approved for Release 2013/01/23 : CIA-RDP81-01043R001600090003-8

Magnetic balances are used not only for recording measurements of vertical component variations, but also have wide application in magnetometry for relative measurements of vertical components particularly in anomalies. In this case the design is somewhat different from the magnetic balance used for measuring variations; however, in principle they are the same. The theory of balances is used in both cases.

If the angle between the magnetic axis and arm l is designated β (Figure 257) then $a = 90^\circ + \theta - \beta$.

As a result of this the equation (12.30) assumes the form:

$$mgl \cos \beta \cos \theta + mgl \sin \beta \sin \theta = MZ \cos \theta - MX \sin \theta \qquad (12.31)$$

This equation shows that with small values of angle θ the equation practically does not depend on X whereas with angle θ close to 90° it only depends on Z to a small degree. Consequently the variometer readings will be free from variations of element X if the magnet is adjusted to the horizontal position and free from variations of the vertical component when found in a vertical position.

Let us examine the first case when θ is very small. In this case dividing both parts of equation (12.31) by cos θ and differentiating it, considering M, m, l, β and g constant, one obtains:

As variations of δZ and δX are of the same order then the term $Mtg\,\theta\,\delta X$ is small in comparison to $M\,\delta X$ and can be disregarded. Furthermore it is not difficult to see that $l \sin \beta$ is a projection of vector l on the axis perpendicular to the magnetic axis or is the distance of the center of gravity to the magnetic axis. Designating the magnetic axis by zc and solving equation (12.32) in relation to δZ one obtains:

$$\delta Z = \frac{1}{\cos^2 \theta} \left(\frac{mgc}{M} + X \right) d\theta.$$

Declassified in Part - Sanitized Copy Approved for Release 2013/01/23 : CIA-RDP81-01043R001600090003-8

Declassified in Part - Sanitized Copy Approved for Release 2013/01/23 : CIA-RDP81-01043R001600090003-8

Finally adjusting the plane of magnet fluctuations perpendicular to the magnetic meridian one obtains:

$$\delta Z = \frac{mlc}{Mgz} \delta\varphi, \qquad (12.33)$$

as the projection of the magnetic forces on axis x, coinciding with the axis of the magnet becomes equal to zero.

In the second case when the axis of the magnet points in the direction of the verticals, dividing both parts of equation (12.31) by sin θ and differentiating it one obtains:

$$\frac{-mlc\cos\beta}{mz^2\theta}\delta\theta = M\,\mathrm{ctg}\,\theta\,\delta Z - \frac{MZ}{z^2\theta}\delta\theta - H_x\delta X, \qquad (12.34)$$

whereupon as in the foregoing case omitting M ctg θ δ Z and substituting $l\cos\beta = xc$, one obtains:

$$\delta X = \frac{-1}{H_x}\left(\frac{mgxc}{M} - Z\right)\delta\theta(1 \qquad (12.35)$$

If θ = 90°, and the plane of fluctuation is adjusted along the magnetic meridian the component X equal to H cos ζ, will assume the value + H or - H depending on whether ζ = 0° or 180°, and one obtains:

$$\delta H = \pm\left(Z - \frac{Mgxc}{MI}\delta\theta\right) \qquad (12.36)$$

The magnetic balance as a horizontal component variometer has not been widely used except in field measurements of the horizontal component.

The (12.33) equation shows that the amount of variation of the vertical component is proportional to the angle of declination.

The coefficient of proportionality as the scale value of the magnetic balance will be designated as

$$\varepsilon'_z, \text{ i. e., } \varepsilon'_z = \frac{mgzc}{M\cos^2\theta} \qquad (12.37)$$

Consequently the scale value of the magnetic balances is proportional to the mass of the magnet and to the distance of the center

Declassified in Part - Sanitized Copy Approved for Release 2013/01/23 : CIA-RDP81-01043R001600090003-8

Declassified in Part - Sanitized Copy Approved for Release 2013/01/23 : CIA-RDP81-01043R001600090003-8

of gravity of the magnet from its axis going through the axis of rotation and inversely proportional to the magnetic moment.

If the axis of the magnet is proportional, $F_z = \frac{mgc}{M}$ (12.38)

In this case the scale value will be less than the scale value of equation (12.37) not in an horizontal position as $\cos^2\theta$ is always less than one.

In this manner in a horizontal position of the magnetic system the susceptibility of the balances besides stability possesses a maximum value. That is why it is necessary in adjusting the magnetic balances to be sure that the axis system is located closer to the horizontal position.

Let us calculate the permissible amount of declination from the horizontal position in a magnetic system so that the susceptibility will remain constant with 1%.

Let us write the equation (12.37) in the following form:

$$\varepsilon'_z = \varepsilon_z \cos^2\theta.$$

Let us assume that θ has changed from zero to θ'. Then

$$\varepsilon_z - \varepsilon'_z = \varepsilon_z(\cos^2\theta' - 1),$$

whereupon $$\frac{\varepsilon_z - \varepsilon_{z'}}{\varepsilon_z} = \cos^2\theta' - 1$$

According to these conditions this expression must be larger than 0.01, i. e., $\cos^2\theta - 1 \leq 0{,}01$ which corresponds to angle $\theta' = 5^\circ\ 40'$ and is the largest permissible angle when the magnet is set in a horizontal direction taking into account that the declination produced by variations Z does not exceed the extent of the angle.

Formula (12.38) shows that the variations of the scale value of the magnetic balances can be produced by shifting the center of

Declassified in Part - Sanitized Copy Approved for Release 2013/01/23 : CIA-RDP81-01043R001600090003-8

Declassified in Part - Sanitized Copy Approved for Release 2013/01/23 : CIA-RDP81-01043R001600090003-8

gravity perpendicular to the axis of the magnet. The closer the center of gravity is to the axis of the magnet, the higher the susceptibility of the magnetic balances and vice versa. The conditions are actually analogous to an ordinary bar balance.

6. The Influence of the Temperature on the Variometer Readings based on Magnetic Balances

All the foregoing formulas were made with the supposition that the center of gravity and the magnetic moment remain constant. Actually both vary with the change of temperature t, therefore, these changes influence the instrument readings. In order to determine this influence let us write equation (12.31) in the following form:

$$MZ = mgxc + mgzctg\,\theta + M\,X\,tg\,\theta.$$

Considering Z and X constant and M, xc and zc variable, let us differentiate this equation by t then:

$$Z\frac{\delta M}{\delta t} = mg\frac{\delta xc}{\delta t} + mg\frac{\delta zc}{\delta t}tg\theta + \frac{1}{\cos^2\theta}(mgzc + M\,X)\frac{\delta\theta}{\delta t} + Xtg\theta\frac{\delta M}{\delta t}.$$

In a horizontal position of the magnet when $\theta = 0$ and when $X = 0$,

$$\frac{-\delta\theta}{\delta t} = \frac{1}{\delta c}\frac{\delta xc}{\delta t} - \frac{z}{r\,\delta c}\cdot\frac{M}{\delta t} \qquad (12.39)$$

The derivative $\delta\theta/\delta t$ represents the readings of the magnet balance at temperature changes of 1 ^{o} and is called the temperature coefficient of the instrument which will be designated by μ_z. As μ_z is the characteristic, indicating the degree of temperature influence on the instrument reading, let it be expressed by known values.

The derivative $\delta M/\delta t$ is nothing else but the temperature coefficient of the magnet μ, multiplied by the magnetic moment, i. e.,

$$\frac{\delta M}{\delta t} = -\mu M.$$

Declassified in Part - Sanitized Copy Approved for Release 2013/01/23 : CIA-RDP81-01043R001600090003-8

Declassified in Part - Sanitized Copy Approved for Release 2013/01/23 : CIA-RDP81-01043R001600090003-8

The derivative $\delta xc/t$ is nothing but a linear coefficient of expansion "a" multiplied by the length, i. e., $\frac{\delta xc}{\delta t} = \pm xc$, whereupon "a" is understood as the mean coefficient of expansion which can be positive or negative since the system can consist of different materials. If the system is a homogeneous magnet thus "a" will be a linear coefficient of expansion of steel. Consequently, expression (12.39) can be written in the following manner:

$$M_z = \frac{2M\mu}{mgzc} \pm \frac{xc}{zc} a \qquad (12.40)$$

As angle θ according to the hypothesis is equal to zero or is close to it, according to equation (12.31): $xc = \frac{2M}{mg}$. From another standpoint in accordance with equation (12.38)

$$zc = \frac{M}{mg} \varepsilon_z$$

Therefore, substituting these values in the foregoing equation one obtains: $\mu_z = \frac{z}{\varepsilon_z}(u \pm a)$ (12.41)

i. e., the temperature coefficient of the instrument is proportional to the sum of the temperature coefficient of the magnet, the coefficient of expansion and vertical component and inversely proportional to the scale of the instrument.

Ordinarily the magnetic balances are made of several materials, i. e., steel, brass, glass and quartz and, therefore, the theoretical calculation of value μ_z is impossible as the mean coefficient of expansion "a" in this case is unknown.

The temperature coefficient of the magnetic balance depends on the coefficient of expansion of the magnetic system so that the displacement of the center of gravity in an horizontal direction would in addition produce a moment of rotation equal and opposite to the moment produced as a result of the variation of the magnetic moment.

Declassified in Part - Sanitized Copy Approved for Release 2013/01/23 : CIA-RDP81-01043R001600090003-8

Declassified in Part - Sanitized Copy Approved for Release 2013/01/23 : CIA-RDP81-01043R001600090003-8

The condition of temperature compensation is obtained from equation (12.40) which is given in the following form:

$$\frac{\partial z_{xc}}{\partial z} \pm \alpha x_c = 0 \qquad (12.42)$$

This condition is possible only when "a" has a negative value, i. e., when the magnetic system consists of several heterogeneous parts and its common center of gravity during heating is displaced to the side of the axis of rotation.

Temperature compensation of magnetic balance is usually accomplished in the following manner: 2 bars of different materials are fastened symmetrically parallel to the axis of the magnetic system.

The weights can be moved along the threaded bars. The bars has a large coefficient of expansion (zinc or aluminum) pointing to the northern extremity of the needle, the other having a smaller coefficient (made of Invar) pointing to the southern extremity of the needle.

As shown in Figure 258, this system consists of magnets NS and N, S, and 2 rods "a" and "b" with weights "e" and "d".

Let us designate the mass of magnets by m_o, the mass of rods by m_1 and m_2 and mass of the weights by m_3 and m_4. Furthermore, let us designate one of the coordinates of the center of gravity of the magnets by x_o, the coordinates of the center of gravity of the bars by x_1 and x_2 and coordinates of the center of gravity of the weights by x_3 and x_4.

In this case, the coordinate, X_c, of the common center of gravity of the whole system is expressed as $x_c = \sum \frac{m_i x_i}{m}$

where m = mass of the whole magnetic system and the displacement of this center during temperature changes of 1°: $\frac{\partial x_c}{\partial t} = \alpha x_c = \frac{\sum m_i \frac{\partial x_i}{\partial t}}{m}$

Declassified in Part - Sanitized Copy Approved for Release 2013/01/23 : CIA-RDP81-01043R001600090003-8

Declassified in Part - Sanitized Copy Approved for Release 2013/01/23 : CIA-RDP81-01043R001600090003-8

Derivative $\frac{dx_0}{dt} = a_0 x_0$, where a_0 = coefficient of expansion of magnetic materials.

The remaining derivatives if one disregards the displacement of the center of gravity of the weights, produced by the expansion, can be represented in the same form, i. e.,

$$\frac{dx_1}{dt} = a_1 x_1 ; \frac{dx_2}{dt} = a_2 x_2 ; \frac{dx_3}{dt} = a_3 x_3 ; \frac{dx_4}{dt} = a_4 x_4$$

where a_1 and a_2 are coefficients of expansion of the bars "a" and "b" respectively. Furthermore, let us designate the length of each bar by $2l$, and the distance of the centers of gravity of the weights from the axis of rotation by a and b. In this case: $x_1 = l$, $x_2 = l$, $x_3 = a$, $x_4 = b$ and therefore: $a_x c = \frac{m_0 x_0 x_0 + (m_1 l + m_3 a) a_1 - (m_2 l + m_4 b) a_2}{m}$

Substituting value ax_c in equation (12.42) one obtains the condition of compensation:

$$\frac{mZ\mu_{zc}}{\varepsilon_z} = m x_0 x_0 + (m_1 l + m_3 a) a_1 - (m_2 l + m_4 b) a_2$$

or as $M \varepsilon_z = m_z g c$

$$\frac{MZ\mu}{g} + (m_1 l + m_4 b) a_2 = m_0 x_0 a_0 + (m_1 l + m_3 b) a_1$$

Changing the position of the weights, i. e., changing a and b simultaneously by selecting the proper coefficients of expansion, can satisfy the equation, i. e., compensation will be achieved.

Let us assume that terms $m_2 l$ and $m_1 l$ are equal to zero in view of the small mass of the bars compared to the mass of the weights, and that $m_3 = m_4 = m'$ and $a = b$

In this case, $\frac{MZ\mu}{g} + m_0 x_0 a_0 = m' a (a_2 - a_1)$

Equation (12.30) shows that in a balanced system when $\theta = 0$,

$$MZ = m_0 x_0 g$$

Therefore

$$MZ(\mu + a_0) = m' g a (a_2 - a_1)$$

Declassified in Part - Sanitized Copy Approved for Release 2013/01/23 : CIA-RDP81-01043R001600090003-8

Declassified in Part - Sanitized Copy Approved for Release 2013/01/23 : CIA-RDP81-01043R001600090003-8

This formula enables one to compute the distance that the weights must be set from the center of the system for the given values of M, Z, μ, a and $(a_2 - a_1)$.

For example, let us assume that the magnetic moment of the system M = 980 CGSμ, the vertical component Z = 0.5 Oe, the mass of a single weight coefficient of the magnet $\mu = 4.10^{-4}$, $m^1 = 5$ g, temperature coefficient of expansion of one bar pointed to N, equals $a_2 = 20.10^{-6}$, the other $a_1 = 0$. In view of the small value of a_o as compared to $c\mu$, let us assume $A_o = 0$.

Under these conditions: $$a = \frac{980 \cdot (0.5)\, 4 \cdot 10^{-4}}{5 \cdot 980 \cdot 2 \cdot 10^{-5}} \text{ cm} = \text{zcm}.$$

7. Methods of Determining Scale Division of Variometers

In order to convert the variometer readings into units of magnetic field intensity it is necessary to know the value of the scale division in these units.

The general method of obtaining scale values is determined by the very definition of the unit concerned, namely:

$$\varepsilon_H = \frac{\delta H}{n}, \quad \varepsilon_D = \frac{D}{n} \text{ and } \varepsilon_Z = \frac{\delta Z}{n},$$

therefore, measuring the number of divisions n, by which the variometer declines due to known variations δH, δD and δZ, one can determine the values ε_H, εD and εZ.

There are 2 methods of determining scale values of variometers: magnetic and electrical. In the first method variations δH and δD are caused by a permanent magnet, in the second method by the aid of the electrical current flowing through the Helmholtz coils.

The magnetic method consists of the following: the permanent

Declassified in Part - Sanitized Copy Approved for Release 2013/01/23 : CIA-RDP81-01043R001600090003-8

Declassified in Part - Sanitized Copy Approved for Release 2013/01/23 : CIA-RDP81-01043R001600090003-8

magnet is set in the first Gaussian position at a certain distance R from the unifilar which causes the declination of the unifilar to be equal to δ n. The field intensity δH produced by the permanent magnet is expressed by the formula: $\delta H = \frac{2M}{R^3}\beta$, where M = magnetic moment of this magnet and β = a certain constant and therefore,

$$\varepsilon_H = \frac{2M}{\delta n R^3}\beta \qquad (12.43)$$

In this manner in order to determine ε H by this method it is necessary to know the magnetic moment of the magnet M, the constant coefficient β and the distance on which the magnet is located.

In view of the difficulties connected with the determination of these values, the magnetic method is usually not used in its complete form and the formula (12.43) in practice is not used.

The magnetic method serves only to compare the sensitivity of 2 unifilars one of which is a variometer of declination, the scale value of which can be determined on the basis of the direct measurements of the distance from the mirror of the magnet to the scale; and the other is a horizontal component variometer or a vertical component variometer.

The electrical method of determining sensitivity, or scale values, consists of a deviating magnetic field which is produced by Helmholtz coils, through which the electric current flows. The magnetic field in the center of the coils is uniform and the intensity of its H_o is expressed by formula:

$$H_0 = \frac{3,2\pi}{5\sqrt{5}} \cdot \frac{w}{R} I = 0,9\frac{w}{R} I = k\ell,$$

where w = number of windings in one coil and

I = current flowing in the coils expressed in amperes.

R = coil radius in centimeters.

k = constant.

Declassified in Part - Sanitized Copy Approved for Release 2013/01/23 : CIA-RDP81-01043R001600090003-8

Declassified in Part - Sanitized Copy Approved for Release 2013/01/23 : CIA-RDP81-01043R001600090003-8

If one places a variometer magnet in the center of the coils in such a manner that its axis is perpendicular to the axis of the coils, then by the action of the current the magnet declines by several scale divisions δn, which is determined by equation $\delta\eta = \frac{\eta_0}{\varepsilon} = \frac{kI}{\varepsilon}$ from which the scale value of the unifilar ε is expressed as

$$\varepsilon = \frac{I}{\delta n} I \alpha l$$

or

$$\varepsilon = 10^5 \frac{\Delta I}{n} \gamma / \ldots \qquad (12.44)$$

Formula (12.44) is correct for any unifilar adjustment in any magnetic field, i. e., by using it, it is possible to determine the scale value of magnetic balances, the horizontal component unifilar and the declination unifilar.

In the last case in order to express ε in arc divisions (in minutes per mm) it is necessary to divide the right side of the equation (12.44) by H sin 1', i. e., write:

$$\varepsilon_D = \frac{10^5 k I}{\delta n H \sin 1'}$$

For example, let us assume that the coil has a radius of R = 10 cm with one winding each. A unifilar magnet is located in the center of these coils; the unifilar by the action of a current, I = 10 ma, produces a declination, δn = 100 mm. It is necessary to determine the scale value ε_H. Determining the constant k which is equal to 0.09, let us substitute value k, I and n in formula (12.44) and obtain:

$$\varepsilon_H = \frac{10^5 \cdot 0{,}09 \cdot 10^{-2}}{100} = 0{,}9\ \gamma/mm,$$

Accuracy of the scale value is determined by the electrical method depending upon the accuracy of the constant k and current I. By differentiating the equation (12.44) one finds the mean root value of error

$$\frac{\Delta\varepsilon}{\varepsilon} = \sqrt{\left(\frac{\Delta k}{k}\right)^2 + \left(\frac{\Delta I}{I}\right)^2 + \left(\frac{\Delta \delta n}{\delta n}\right)^2}$$

Declassified in Part - Sanitized Copy Approved for Release 2013/01/23 : CIA-RDP81-01043R001600090003-8

Declassified in Part - Sanitized Copy Approved for Release 2013/01/23 : CIA-RDP81-01043R001600090003-8

Considering the relative errors of measurement k, I and n equal, one obtains: $\frac{\Delta \varepsilon}{\varepsilon} = \pm 1.73 \frac{\Delta k}{k}$.

In this manner, in order to determine ε with a relative error of 1% it is necessary that k, I and n be measured with a relative error of 1.73 times less, i. e., approximately with an error of 0.6% which is very insignificant.

8. B. M. Yanovskiy's Vertical Component Variometer

Despite all the merits of the magnetic balance, it has one essential defect and that is the friction between the prism and the cushion, which produces variations in readings.

In the latter part of the nineteenth century a variometer was built by Lamon based on the resulting induction of soft iron, when placed in the earth's magnetic field. The principle of this variometer was similar to the inclinator type instrument. Therefore, the angle of the magnet declination caused by the vertical bar, depended upon the angle of inclination, whereas the fluctuation of the angle depended on the variation of inclination. Therefore, Lamon's variometer was actually a variometer of inclination. This instrument was impractical because its ferromagnetic bars were disproportional to the vertical component; as a consequence, the variations recorded by this instrument were not correct.

In 1936 B. M. Yanovskiy devised a variometer in which the bars, magnetized by the vertical component of the earth's field was made of a ferromagnetic alloy known as permalloy (50% nickel). This alloy is superior to ordinary iron because of its great permeability in weak fields and low coercive force. Whereas in iron the permeability is low and the coercive force reaches 2-3 δ, in permalloy the permability is very high and the coercive force reaches several oersteds.

Declassified in Part - Sanitized Copy Approved for Release 2013/01/23 : CIA-RDP81-01043R001600090003-8

Declassified in Part - Sanitized Copy Approved for Release 2013/01/23 : CIA-RDP81-01043R001600090003-8

Therefore, in accordance with formula (0.76): $J = \frac{\chi}{1 + \chi N}$ the magnetization intensity of the bar J with the ratio of the length to the diameter of the bar equal to 15, in which N = 0.1, will be strictly proportional to the vertical component, since the product xN is equal to a 1,000 and the unit 1 in the denominator can be disregarded.

Another difference in this variometer as compared to Lamon's instrument is that its magnetic system is astatic.

An astatic system consists of 2 magnets, with uniform magnetic moments, located at a certain distance from each other and fixed on one vertical axis in the form of a bar. The axis of the magnets lie horizontally in an opposite direction, as shown in Figure 259.

If this system is placed in a uniform magnetic field of intensity H, the direction of which forms a certain angle θ 1 with one of the magnet axis, then the moment of rotation M_β, exerted by the magnetic field upon the entire system will be:

$$M_\beta = M_1 H \sin \theta_1 + M_2 H \sin \theta_2 = Q,$$

where M_1 and M_2 = magnetic moments of the magnets and θ 2 the angle formed by the axis of the second magnet with direction H.

In an astatic state $M_1 = M_2$, and θ 2 = θ 1 + 180 therefore M = Q, i. e., an astatic magnetic system; located in a uniform magnetic field, will not experience any force. If this system is suspended by a thread and placed in the earth's magnetic field it will remain unsusceptible to the variations of the earth's field.

In order to cause it to react to the variations of the vertical component, a bar NS (Figure 259) made of a soft magnetic material is placed at a certain distance from the magnetic system in a vertical position, one end of which is on the same level with the upper magnet and the second end of which is on the same level with the lower magnet.

Declassified in Part - Sanitized Copy Approved for Release 2013/01/23 : CIA-RDP81-01043R001600090003-8

Declassified in Part - Sanitized Copy Approved for Release 2013/01/23 : CIA-RDP81-01043R001600090003-8

Under the influence of the vertical component the bar becomes magnetized and produces a magnetic field, which reacts in one direction on the upper magnet and in the opposite direction on the lower magnet. If the intensity of the magnetic field is designated by $H_/$, produced by the bar in a horizontal direction in the center of the magnets ns and n's' then the moment of rotation M_δ, reacting on the system is expressed as:

$$M_\delta = MH_/ \sin\theta + MH_/ \sin\theta = 2MH_/ \sin\theta,$$

where θ = the angle between the magnet axis and the direction $H_/$ (the value of the angle will be the same for the upper and lower magnets in view of the fact that the direction $H_/$ in the upper and lower magnets and the direction of the magnetic moments of the upper and lower magnets are in opposition).

Moment M_δ is balanced by the moment of thread torque, therefore, $2MH_/ \sin\theta = C\varphi$, where φ = the angle of thread torque and C = torque coefficient. However, $H_/$ is proportional to the vertical component, i. e., $H_/ = kZ$, therefore,

$$2MkZ\sin\theta = C\varphi$$

Differentiating this expression and substituting the differentials by variations one obtains:

$$2Mk\sin\theta\,\delta Z + 2MkZ\cos\theta\,\delta\theta = C\delta\varphi.$$

Corresponding to that which was shown for an unifilar $\delta\varphi = -\delta\theta$ and, hence,

$$\delta\theta = -\frac{2Mk\sin\theta}{2MkZ\cos\theta + C}\delta Z$$

Ordinarily the axis of the magnets ns and n's' are adjusted approximately perpendicularly to the direction of the field $H_/$. In this case the angle θ can be assumed equal to 90° and written:

$$\delta\theta = -\frac{2Mk}{C}\delta Z$$

or $$\delta Z = \frac{-C}{Mk}\delta\theta,$$

Declassified in Part - Sanitized Copy Approved for Release 2013/01/23 : CIA-RDP81-01043R001600090003-8

Declassified in Part - Sanitized Copy Approved for Release 2013/01/23 : CIA-RDP81-01043R001600090003-8

i. e., variations of the vertical component δZ are proportional to the angle of declination of the astatic system. The coefficient of proportionality with $\delta \theta$ representing the scale value, is determined in the same manner as that used in magnetic balances, i. e., by using the Helmholtz coils.

9. Construction of Variation Instruments

The system of variation instruments or magnetographs, consisting of 3 variometers: D, H, and Z and recording parts, is called a variation station.

Despite the differences in design of various stations, they are all constructed on the same principles, which were described in the foregoing paragraphs and all have some peculiarity depending on the general requirements. The basic requirement of each station is to have clear and precise recordings. In order to obtain such recordings the optical system must focus the reflected source of light in the (refractive) index, converging on the point, so that the thickness of the line of recording is not more than 1/10 of a mm.

The principles of such recordings are the same at all stations and consist of the following: the diverging beam of light from the source of light S passes through the lens L (Figure 260), located in front of the mirror P of the variometer magnet, and by striking it is reflected in a parallel beam, and again by passing through the lens, produces a reflection of the light S' in the main focal plane of the lens FF'. The source of light S and the cylindrical lens L_1L_2 are located in the same focal plane; cylindrical lens L_1L_2 focuses the reflection of the filament thread on the index point which strikes the generatrix of the cylinder drum B.

Declassified in Part - Sanitized Copy Approved for Release 2013/01/23 : CIA-RDP81-01043R001600090003-8

Declassified in Part - Sanitized Copy Approved for Release 2013/01/23 : CIA-RDP81-01043R001600090003-8

In turning the mirror at a certain angle the reflected beam also turns and the light index S" moves along the generatrix of the drum. If the drum rotates along the axis CC' simultaneously with the movement of index S", then the track of the index in the form of a line appears on the tape wound around the drum.

The drum rotates by means of a clock mechanism and usually makes one revolution every 24 hours. The normal diameter of the drum is 16 cm; and the length 20 cm; whereas the length of the band is 50 cm and the width 20 cm. Recording time on the photographic film is carried out automatically by a clock mechanism or by switching a bulb off every hour for 1-2 minutes. The exterior view of the recording equipment is shown in Figure 264.

The instruments are located so that the magnets do not influence one another and so that the diverging beam of light covers the whole variometer. The distance of the recording equipment from the variometers is fixed in accordance with the scale value. As the scale value is inversely proportional to the distance, then if possible, the recorder is installed further from the variometer in order to obtain a smaller value, but ordinarily not more than 3.5 m as a greater distance causes a significant decrease in the illumination of the light beam. The normal distance is 1.753 m during which the scale value of the unifilar D is equal to 1' of the arc per 1 mm.

In order to guide the reflected beam of light to the recording drum and diverge it to the generatrix of the cylinder in a set pattern each variometer has a mechanism which permits the rotation of the reflected beam in any direction. In some variometer systems this mechanism, in the form of micrometer screws, is connected to the mirror of the magnet, in others the mechanism is a prism located outside

Declassified in Part - Sanitized Copy Approved for Release 2013/01/23 : CIA-RDP81-01043R001600090003-8

Declassified in Part - Sanitized Copy Approved for Release 2013/01/23 : CIA-RDP81-01043R001600090003-8

the instrument which can be interchangeably rotated in either direction perpendicularly by means of micrometer screws. The prism is located in a perpendicular line in front of the variometer lens as shown in Figure 261 and therefore the reflected beam during the rotation of the prism moves in the corresponding direction.

Each variometer besides the mirror which is connected to the magnet has a second stationary mirror which produces a straight line on photographic film. This straight line, known as the base line, serves as the bascissa by which the measurement of the amount of variations of this or that element can be carried out. The mirror is located in the interior of the variometer and by means of micrometer screws, located outside, can interchangeably rotate the mirror perpendicularly in either direction, directing the reflected beam on the drum.

As the variometers D and H are basically the same and only differ in the exterior and the construction of their separate parts, the D and H variometers that are used in the B. M Yanovskiy system can be cited as an example.

The variometer D or H (unifilar) represents a cyclindrical tube B (Figure 261) installed on the base A. By means of screws C, the tube can be adjusted in a vertical position.

The upper part of the tube has a "turning knob" D, to which one end of the quartz thread is attached. The other end of the thread has a magnet with a mirror suspended from it.

The "turning knob" can rotate and turn the thread so as to adjust the magnet perpendicular to the magnetic meridian. Besides this, by using screw E, the thread can be raised and lowered with

Declassified in Part - Sanitized Copy Approved for Release 2013/01/23 : CIA-RDP81-01043R001600090003-8

Declassified in Part - Sanitized Copy Approved for Release 2013/01/23 : CIA-RDP81-01043R001600090003-8

the limits of 1 cm adjusting the magnet in a fixed position. The magnet represents a prism or a cylinder having a 1 mm diameter and 25 mm length, made of alnico or magnico. In order to arrest the fluctuations of the magnet it is placed in a cylindrical copper vessel, which is installed in the interior of the tube B.

In front of the magnet mirror there is a circular opening with a 20 mm diameter in which a double convex lens is installed. The prism P with micrometer screws for adjusting light indexes on the drum is installed in front of the lens. A second opening in the tube is located on the opposite side of the lens where a stationary mirror with micrometer screws is placed in order to obtain the base line. The upper part of the tube has a collar F which can be moved along the tube. Two magnets are included in the collar parallel to each other in order to increase the susceptibility of the variometers.

Two coils G are fastened to the circular base which in turn is placed on the base A and can rotate around the vertical axis. These coils serve to determine the scale values of the variometer and to adjust the magnet along the meridian perpendicularly to it.

Temperature compensation in instruments of this system can be accomplished by means of calmalloy.

In design, the B. M. Yanovskiy vertical component variometer is different from H and D variometers because in place of one magnet inside tube B (Figure 252) an astatic system of 2 magnets are suspended and as a consequence the length of tube B is somewhat greater than in variometers H and D.

Besides this, 2 permalloy bars Q and R are fastened to the outside of the tube.

Declassified in Part - Sanitized Copy Approved for Release 2013/01/23 : CIA-RDP81-01043R001600090003-8

Declassified in Part - Sanitized Copy Approved for Release 2013/01/23 : CIA-RDP81-01043R001600090003-8

Bar Q is located parallel and on the same level with the astatic system, bar R is located somewhat higher but with the lower end of the bar on the same level as the upper magnet of this system.

The remaining parts of the equipment (stationary mirror, prism, turning knob, damper device) are similar to the parts found in variometers H and D.

Two rings are used to determine scale value and are located horizontally so that the permalloy bars and the astatic system is found outside this system of rings.

Magnetic balances as a vertical component variometer are arranged similarly to the installation of field magnetic balances in which the recording tube is replaced by a lens and a prism with installed regulating screws for directing the reflected light beam on the drum.

Figure 263 shows the magnetic balances. The recording apparatus is a rectangular box, inside of which there is a drum B (Figure 264) rotating by means of a clock mechanism C. The cylindrical lens L is located in front of the drum, whose length is equal to the length of the drum. The lens is fastened to 2 small legs which in adjusting the lens in focus can be shifted along the bottom of the box perpendicular to the generatrix of the cylinder. The front lid of the box has a slit opening O on the same level with the lens in order to pass the reflected light beam. The length of the drum is 200 mm and the diameter is 150 mm. The speed of drum revolution is either one revolution per 24 hours or one revolution per 2 hours. The variation of speed is carried out by the interchangeable coupling of the clock mechanism and the drum axis which is accomplished by 2 different gears.

Declassified in Part - Sanitized Copy Approved for Release 2013/01/23 : CIA-RDP81-01043R001600090003-8

Declassified in Part - Sanitized Copy Approved for Release 2013/01/23 : CIA-RDP81-01043R001600090003-8

The lighting arrangement consists of a narrow slit, an illuminating bulb or single filament bulb, which is installed alongside the recording apparatus or is located on the front lid of the box somewhat lower than the "zero" aperture.

A general view of the station is shown in Figure 265.

10. B. Ye Bryunelli Magnetograph System

The B. Ye. Bryunelli magnetograph system is used under field conditions. A relatively small network of existing magnetic observatories, particularly in the Arctic, makes it impossible to effect detailed studies of magnetic variations as the radius of observatory operations in medium latitudes does not exceed 400-500 km; in areas close to the Northern Lights, this area becomes even smaller. Therefore, for many years inventors have attempted to develop a variation station which would not need any special housing nor balances, nor adjustment and could operate under any meteorological conditions. This problem was successfully solved in 1947 by B. Ye. Bryunelli.

B. Ye. Bryunelli's station consists of 3 variometers; unifilar H, magnetic balances Z and the recording part installed on a common base with the top covered by a hood. By using an adjustable compass and level the base can be adjusted in a horizontal plane in any azimuth. The first characteristic of this station is that the variometers and recording part are connected to the base restricting the possibility of reciprocal motion and turning. The second characteristic of the station is the small dimensions of the variometers and recording part in comparison to the observatory type instruments. It is sufficient to state that the base on which the variometers are installed has dimensions of 50 x 20 cm with a hood 15 cm in height.

Declassified in Part - Sanitized Copy Approved for Release 2013/01/23 : CIA-RDP81-01043R001600090003-8

Declassified in Part - Sanitized Copy Approved for Release 2013/01/23 : CIA-RDP81-01043R001600090003-8

To reduce station measurements it was necessary to redesign its individual parts. For example the recording part was designed in a new manner so that instead of a rotating drum with a photographic film, a tape conveying mechanism is installed and the recording carried on by a moving film 24 mm in width. The conveying speed of film is from 3 to 18 mm per hour as the complete tape displacement takes place in either 24 hours or 6 full days. Changing film is carried out by a key located outside the station which winds the film from one box to another. It is possible to assemble the equipment and change the tape of the station without the need of a darkroom.

In order to retain the present accuracy of recording on a narrow film it is necessary to diminish the thickness of the recording line by several times in comparison to the line thickness used in present variometers. In the B. Ye. Bryunelli system this is achieved by using achromatic lenses and by improving the quality of the remaining optical parts.

Besides this another characteristic of this system is the special arrangement of the optical system enabling one to increase the number of reflected indices to 3 which shift on film at different speeds, i. e., have different sensitivity. This arrangement enables one to extend the width of the scale 5 times and to register quiet variations as well as intense magnetic storms. A diagram of this system is described by Figure 266. One portion of the light beam I going from the source of light through the optic A and the stationary prism B is reflected at first by the hypotenuse of prism C connected with the magnet then by the arm of the stationary prism D and again by the hypotenuse C consequently producing a rapid (refractive) index "a". The remainder of the light beam from lenses II and III is reflected by the arms of prism C producing indices b and c moving 2 times slower than the first index. The stationary index d is obtained by the reflection from prism D.

Declassified in Part - Sanitized Copy Approved for Release 2013/01/23 : CIA-RDP81-01043R001600090003-8

Declassified in Part - Sanitized Copy Approved for Release 2013/01/23 : CIA-RDP81-01043R001600090003-8

The temperature compensation is achieved by means of calmalloy plates soldered to the magnets.

A general view of the station is shown in Figure 267 where the arrangement of the variometers and recording parts can be seen.

The scale value of the variometers is determined by means of rings fastened to the variometer housing.

11. The LaCour System of Rapid Magnetographs

In 1931 the Danish magnetologist LaCour constructed a magnetograph for checking short period variations such as magnetic pulsations, using a 30 x 39 cm tape capable of recording for a period of 24 hours with a speed of 3 mm per minute. This is achieved by splitting the light beam into many separate beams reflected by the variometer mirror. The divergent light beam from the single filament bulb S (Figure 268) encounters a whole series of equidistant prisms (up to 44) and passing through them is refracted and broken up into 44 separate beams. By turning the prisms the light beam is divided into thirds with each third directed to one of the mirrors of variometers D, H and Z. These beams reflected by the mirror and passing through the objective lens placed in front of the variometer mirror strike the cylindrical lens in front of the drum and produce light indices on the drum equidistant from each other (over 7 mm). In this manner each variometer directs up to 15 light indices to the drum; these indices shift simultaneously by turning the mirror. However of the 15 indices directed to the drum only one strikes since a screen is located in front of the drum behind the cylindrical lens which has an aperture (about 7 mm wide) for each variometer, so that the drum always has a recording of one index regardless of how the mirror is turned, in conjunction with the magnet. A

Declassified in Part - Sanitized Copy Approved for Release 2013/01/23 : CIA-RDP81-01043R001600090003-8

Declassified in Part - Sanitized Copy Approved for Release 2013/01/23 : CIA-RDP81-01043R001600090003-8

diagram of these recordings is shown in Figure 269 where the thick lines designate the tape recording and the thinner lines the movement of indices on the screen.

After a complete revolution the drum automatically shifts along its axis for over 8 mm (a distance slightly more than the width of the opening). As the width of the paper is 300 mm, each variometer is alloted 100 mm and as consequence the drum can make 13 full revolutions in a 24-hour period which increases the tape length by 13 times.

The peculiarity of these variometers is the small dimensions of its magnets: the length of the magnets in H and D variometers do not exceed 6 mm, having a diameter of 1 mm.

The exterior view of the variometers with the recording part and several other components are shown in Figure 270.

Variometers were used in polar station work during the Second International Polar Year, some of which are still in use.

In order to operate a LaCour variometer a special darkened compartment with constant temperatures is required.

12. The A. G. Kalashnikov Station

To intensity the recording of weak variations with amplitudes of several gammas or less, it is necessary to have highly sensitive variometers. In the theory of variation instruments it was demonstrated that the sensitivity of an unifilar can be increased by decreasing the thread diameter and bringing the center of gravity of the magnets in the magnetic balance closer to the axis of rotation. However, these methods have their limitations because with the increase of instrument

Declassified in Part - Sanitized Copy Approved for Release 2013/01/23 : CIA-RDP81-01043R001600090003-8

Declassified in Part - Sanitized Copy Approved for Release 2013/01/23 : CIA-RDP81-01043R001600090003-8

sensitivity the maximum angle is decreased in which the declination of the magnet proportional to the amount of variation and magnet oscillation is stable.

Therefore even during the First International Polar Year (1882-1883) a variometer was installed at a polar station in Iceland based on the inductive action of the variable magnetic field.

A 12 km cable was laid on the surface of the ground in a form of a ring connected to a galvanometer. The current generated during the variations of the vertical component in the cable, was proportional to dx/dt, which was recorded by the galvanometer.

This variometer arrangement was later used at other observatories; however, the recordings of the instruments did not give the value of the variation itself which is measured by amplitude of oscillations, but only the rate of change of variation.

In 1948 A. G. Kalashnikov proposed the idea of measuring circuit currents by means of a fluxmeter whose deflection is proportional to the changes in magnetic flux crossing the given circuit. In order to achieve this it was necessary to change the design of the existing fluxmeters so that the deflections of the fluxmeter are practically independent of the time during which the magnetic flux changes. A. G. Kalashnikov's contribution consists in the fact that he theoretically showed the possibility of designing such a fluxmeter and restored it in practice.

The fluxmeter is a common magnetoelectric measuring instrument (a frame suspended by a thread rotating between the poles of the permanent magnet) with the difference being the small amount of moment of rotation (moment of thread torque) and significant amount of moment

Declassified in Part - Sanitized Copy Approved for Release 2013/01/23 : CIA-RDP81-01043R001600090003-8

Declassified in Part - Sanitized Copy Approved for Release 2013/01/23 : CIA-RDP81-01043R001600090003-8

of electromagnetic drag as compared to the ballistic galvanometer. The theory of this arrangement is as follows: if one writes the equation of frame movement disregarding the moment of thread torque, then it takes the form:

$$K\frac{d^2a}{dt^2} = HS_w I \qquad (12.45)$$

where K = moment of frame inertia,

H = field intensity between the magnet poles,

S = area,

w = the number of windings around the frame,

a = deflection angle of the frame.

Within the frame moving in the magnetic field an emf, $\mathcal{E}_i$ is induced, opposing emf $\mathcal{E}$, therefore, on the basis of Kirchhoff's second law the second equation can be written:

$$\mathcal{E} = \mathcal{E}_i = RI \qquad (12.46)$$

where R = circuit resistance of the fluxmeter.

It is evident that

$$\mathcal{E}_i = HS_w\frac{da}{dt}$$

If besides this, $\mathcal{E}$ is induced by the changes of the magnetic flux ϕ, i. e., $\mathcal{E}_d\frac{\phi}{dt}$, then the equation (12.46) assumes the form:

$$\frac{d\phi}{dt} - HS_w\frac{da}{dt} = RI.$$

Determining the current I and substituting it in equation (12.45) one obtains:

$$K\frac{d^2a}{dt^2} + \frac{(HSw)^2}{R}\cdot\frac{da}{dt} = \frac{HS_w}{R}\cdot\frac{d\phi}{dt}$$

This is an equation showing the movement of the fluxmeter frame in its simpliest form. Designating HSw = q and integrating from a = 0 to the greatest deflection, a = 0, one obtains:

$$\frac{q}{R}\theta = \frac{q}{R}\Delta\phi,$$

because the speed of the frame movement da/dt in the initial and end moment is equal to zero. Hence, $\theta = \frac{1}{q}\Delta\phi$, i. e., the deflection

Declassified in Part - Sanitized Copy Approved for Release 2013/01/23 : CIA-RDP81-01043R001600090003-8

Declassified in Part - Sanitized Copy Approved for Release 2013/01/23 : CIA-RDP81-01043R001600090003-8

of the fluxmeter is proportional to the current change and inversely proportional to value q which is called the constant of the fluxmeter and does not depend on the circuit resistance of the fluxmeter nor on the time it takes to change flux ϕ.

Since neither the moment of rotation of the frame nor the air resistance which drags on the frame are equal to zero, the equation of motion and its solution is more complicated. It shows the dependence of the deflection on both the circuit resistance and the speed of flux changes. A. G. Kalashnikov in his theoretical analysis indicated the range of error caused by these factors and provided a method of fluxmeter calculations for various purposes. Constructed according to his design this fluxmeter for recording variations of the vertical component has a thread torque moment which is almost 10 times less than in present fluxmeters. In addition, the moment of frame inertia is decreased 3 times.

By using this type fluxmeter it is possible to reproduce a recording of variations Z up to 0.01 Γ/mm. To show the comparison Figure 271 indicates variation recordings made with A. G. Kalashnikov's fluxmeter located in the village of Nikolina Gora near Moscow and the magnetic balance located in an observatory in Krasnaya Pakhra also near Moscow.

The curves clearly demonstrate that the fluxmeter recordings give forth greater detail than the ordinary magnetic balances.

The increase in recording sensitivity using fluxmeters is proportional to the area and number of circuit windings with the current in the circuit induced by the action of variations Z. In the tests conducted by A. G. Kalashnikov the circuit diameter was equal to 100 m with the number of windings equal to 36 and the general circuit area $2.83 \cdot 10^9$ cm.

The general view of the station is shown in Figure 272.

Declassified in Part - Sanitized Copy Approved for Release 2013/01/23 : CIA-RDP81-01043R001600090003-8

Declassified in Part - Sanitized Copy Approved for Release 2013/01/23 : CIA-RDP81-01043R001600090003-8

FIGURE CAPTIONS

Figure 1. Ancient Chinese chariot with an indicator pointing to the South.

Figure 2. Floating compasses of Perergrine.

Figure 12. Basic magnetization curve and hysteresis curve.

Figure 17. Correlation between reversible susceptibility and magnetization.

Figure 18. Temperature dependence of hysteresis curves.

Figure 19. Correlation between dJ/dt and magnetization.

Figure 20. Change of coercive force with lapse of time /in the drawing -- horizontal axis/ hours.

Figure 21. Hysteresis curves of different alloys and steels. /in the drawing/

/ B Gauss

magnico
vicalloy
alnico
alni cobalt steel; tungsten steel.

Figure 22. Basic magnetization curves of various soft magnetic materials at H_m = 300 Oe.

/in the drawing/

armco
E4A
KhVP
Kilogauss
M_o - permalloy
Hypernik

Figure 23. Basic magnetization curves at H_m = 7 Oe.

/in the drawing/

E4A
Armco
Armco
Kilogauss
KhVP
Hypernik M_o = permalloy

Figure 25. Isodynes of the vertical component for the 1950 epoch.

Figure 26. Isogons for the 1950 epoch.

Figure 27. Isodynes of the horizontal component for the 1950 epoch.

Figure 28. Isogons in the area of the geographic poles.

Declassified in Part - Sanitized Copy Approved for Release 2013/01/23 : CIA-RDP81-01043R001600090003-8

Declassified in Part - Sanitized Copy Approved for Release 2013/01/23 : CIA-RDP81-01043R001600090003-8

Figure 29. Position of the north magnetic pole.

Figure 30. Magnetic meridians for the 1950 epoch.

Figure 31. Isogons in the area of the Kursk magnetic anomalies.

/in the drawing/ Saltykovo.

Figure 40. Distribution of magnetic masses corresponding to dipoles and quadrupoles on the surface of the terrestrial globe.

/in the drawing/

The lower harmonics are drawn at a scale 10 times greater than that of the upper harmonics.

Figure 42. Isodynes of the vertical component of the residual field for the 1950 epoch.

Figure 43. Isodynes of the north component of the residual field for the 1950 epoch.

Figure 44. Isodynes of the east component of the residual field for the 1950 epoch.

Figure 46. Dependence of the anomaly of gravity and vertical component of the residual field on longitude.

Figure 47. Excess of geoid over spheroid depending on the occurring rock.

/in the drawing/

Europe India Pacific Ocean North America Atlantic Ocean

/////// Basalt Granite.

Figure 48. /in the drawing/ Small towns of the upper Chusov region

Molotov

Okhansk

Kungur

Osa

Krasnoufimsk.

Western Urals

Z Isodynames

1930 Epoch

Declassified in Part - Sanitized Copy Approved for Release 2013/01/23 : CIA-RDP81-01043R001600090003-8

Declassified in Part - Sanitized Copy Approved for Release 2013/01/23 : CIA-RDP81-01043R001600090003-8

Figure 49. Diagram of the trend of Kursk magnetic anomalies.

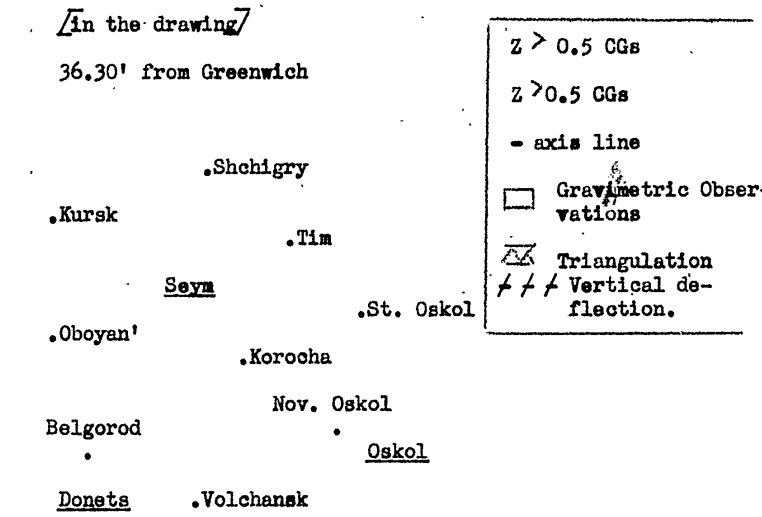

Figure 50a. Isodynes of the vertical component in the region of the Kursk magnetic anomalies, in Oersteds.

/in the drawing/ Shchigry.

Figure 50b. Isodynes of the horizontal component in the region of the Kursk magnetic anomalies, in Oersteds.

Figure 50c. Isogons in the region of the Kursk magnetic anomalies.

Figure 51. Isodynes of the vertical component at the Angara-Ilim anomaly (according to Bersudskiy).

/in the drawing/

Za isolines for components of H_a

positive

negative

Figure 52. Z isodynes within one of the sectors of the Angara-Ilim anomaly.

Figure 53. Isodynes of the vertical component over one of the Pilansberg dikes near Heidelsberg.

/in the drawing/

Northern boundary of Karroo deposit.

Declassified in Part - Sanitized Copy Approved for Release 2013/01/23 : CIA-RDP81-01043R001600090003-8

Declassified in Part - Sanitized Copy Approved for Release 2013/01/23 : CIA-RDP81-01043R001600090003-8

Figure 54. Course of mean annual values of the elements of terrestrial magnetism at the Slutsk Magnetic Observatory.

Figure 55. Course of mean annual values of the elements of terrestrial magnetism at the Sverdlovsk Observatory.

Figure 56. Isopores of the vertical component for the 1942 epoch (in gammas).

Figure 57. Isopores of the north component for the 1942 epoch (in gammas).

Figure 58. Isopores of the east component for the 1942 epoch (in gammas).

Figure 59. Isopores of the vertical component over the territory of the USSR for the 1932-5 epoch (in gammas). (The arrows indicate the magnitude and direction of the horizontal component of the secular variation vector).

Figure 60. Isopores of the north component over the territory of the USSR for the 1932.5 epoch (in gammas).

Figure 61. Isopores of the east component over the territory of the USSR for the 1932.5 epoch (in gammas).

Figure 62. Zones of seismic regions and centers of secular range for the epochs: 1-1885-1922; 2-1912.5; 3-1922.5; 4-1932.5; 5-1942.5. Dots denote epicenters of individual earthquakes.

Figure 63. 1 -- Curve of observed variations of the horizontal component; 2 -- curves corresponding to the first 2 harmonics of the expansion; 3 -- summative curve of 2 harmonics.

Figure 64. Mean annual magnetic activity and its deviations during the year in percent.

/In the drawing/

/Right hand margin/ Magnetic activity

/Bottom/ Months.

Figure 65. Solar and magnetic activity during the period 1830 to 1930.

/In the drawing/

Magnetic activity (u).

Number of sunspots.

Declassified in Part - Sanitized Copy Approved for Release 2013/01/23 : CIA-RDP81-01043R001600090003-8

Declassified in Part - Sanitized Copy Approved for Release 2013/01/23 : CIA-RDP81-01043R001600090003-8

Figure 66. Graph of recurrence of magnetic disturbances.

Figure 67. Diurnal progression of magnetic activity at the Kew observatory and number of days having the characteristic "2" during the period 1913 to 1923.

/in the drawing/

/left margin/ Activity

/right margin/ Number of hours having the characteristic "2".

•_•_• winter

o__ _o_ _o spring

x _ x _ x summer.

Figure 68. Diurnal March of the Elements of Terrestrial Magnetism at the Pavlovsk Magnetic Observatory.

/in the drawing/

Local Mean Time Scale in Gammas

Figure 69,a. Diurnal march of the elements X, Y and Z on quiet days during the period of the summer solstice at various latitudes.

/in the drawing/

Local Mean Time Scale in Gammas

Figure 69,b. Diurnal march of the elements X, Y and Z on quiet days during the periods of the winter solstice at various latitudes.

/in the drawing/

Local Mean Time Scale in Gammas

Figure 69,c. Diurnal march of the elements X, Y and Z on quiet days in the periods of the equinoxes at various latitudes

/in the drawing/

Local Mean Time Scale in Gammas

Figure 70. Diurnal march of variations on stormy days at various latitudes. /in the drawing/

Local Geomagnetic Time Scale in Gammas

Declassified in Part - Sanitized Copy Approved for Release 2013/01/23 : CIA-RDP81-01043R001600090003-8

Declassified in Part - Sanitized Copy Approved for Release 2013/01/23 : CIA-RDP81-01043R001600090003-8

Figure 71. Projection of the Vector of Variations S_q on the horizontal plane.

Figure 72. Projection of the vector of variation S_q on to the vertical planes; (a) on to the plane of the principal meridian; (b) on to the plane of the prime vertical.

Figure 73. System of Electric Currents corresponding to the solar diurnal variations in the equinoctial periods.

Figure 74. System of electric currents corresponding to the mean diurnal variations during the period of the summer solstice.

Figure 75. Diurnal march of northern component at Huancayo observatory. 1. observed curve; 2. calculated in geomagnetic coordinates; 3. calculated in geographic coordinates
abscissa: hours.

Figure 76. System of electrical currents according to calculations of Mac Nish.

Figure 77. System of currents for the summer months, from calculations of N. P. Ben'kova (for functions S_{q1}).

Figure 78. System of currents for the summer months, according to calculations of N. P. Ben'kova (for functions S_q2).

Figure 79. Variation of Magnetic Field strength with height from rocket observations: (a) at 1720 hours; (b) at 1120 hours. 1. theoretical curve; 2. observed curves;

Figure 80. Lunar diurnal variations at Batavia and Greenwich at different phases of the moon.

Figure 81. System of currents corresponding to lunar diurnal variations at equinox (upper figure) and summer solstice (lower figure).

Figure 82. Magnetograms of the horizontal component, from records of various observatories during the magnetic storm of 14 March 1922.

Figure 83. Magnetograms of the horizontal component during the storm of 10 February 1933.

Declassified in Part - Sanitized Copy Approved for Release 2013/01/23 : CIA-RDP81-01043R001600090003-8

Declassified in Part - Sanitized Copy Approved for Release 2013/01/23 : CIA-RDP81-01043R001600090003-8

Figure 84. Aperiodic disturbances of the variation at various observatories.

Figure 85a. System of electric currents corresponding to the variations (view from equatorial plane).

Figure 85b. System of electrical currents corresponding to the variation (view from pole).

Figure 86. System of electric currents corresponding to the aperiodic disturbance of variation: (a) view from equatorial plane; (b) view from pole.

Figure 87. Bay-shaped variations at the western observatory at Kew, England.

Figure 88. (1) observed curve passed through the points; (2) approximation for observed curve by the aid of 6 times of a trigonometric expansion.

Figure 90. Magnetic pulsations at Absiko and Tromso, 12 September 1930.

Figure 91a. Diurnal march of the elements X, Y and Z on quiet days during the period of the summer solstice at high latitudes.

Figure 91b. Diurnal march of the elements X, Y and Z on quiet days during the period of the winter solstice at high latitudes.

Figure 91c. Mean annual diurnal march of the elements X, Y and Z on quiet days in high latitudes.

Figure 92. Diurnal variations on stormy days S_D, in high latitudes (mean values for the year).

Figure 93. Aperiodic disturbed variations in high latitudes.

Figure 94. Diurnal march of the magnetic disturbance at the Tikhaya Bay observatory.

Figure 95. Relation of the morning maximum of disturbance to the universal time (according to Nikol'skiy).

Figure 96. Relation of the diurnal march of magnetic disturbance and the season.

Declassified in Part - Sanitized Copy Approved for Release 2013/01/23 : CIA-RDP81-01043R001600090003-8

Declassified in Part - Sanitized Copy Approved for Release 2013/01/23 : CIA-RDP81-01043R001600090003-8

Figure 97. Relation of the diurnal march of the magnetic disturbance on the total disturbance of the field.

Figure 98. Relation of a maximum of disturbance to the geomagnetic latitude.

Figure 99. Probability of appearance of lower boundary of aurora plotted against height.

Figure 100. Isochasms -- isolines of auroral frequency.

Figure 101. Zone of maximal auroral frequency.

Figure 102. Number of days in the year with sunspots and aurora, observed in Australia from 1940 to 1896.

Figure 103. Scheme of the pulse method of studying the ionosphere.

[in drawing]

Antenna -- radiating and receiving

Pulse modulator

High frequency oscillator

Receiver with amplifier

Cathode oscillograph

Relaxation oscillator

Figure 104. Photogram of height frequency characteristic with reflections from E and F layers.

Figure 105. Density of ionization at various heights, and the paths of rays of various frequencies.

(1) path of waves of medium frequency; (2) path of low frequency waves; (3) path of high frequency waves.

Figure 106. Semi-diurnal fluctuations of the equivalent height of the E layer.

Figure 107. Semi-diurnal fluctuations of equivalent height in the E layer and of critical frequency in the F_2 layer.

(1) fluctuations of the height of the layer; (2) fluctuations of frequency.

Figure 109. The region Q in which electrons may move in the magnetic field of the earth (not blackened).

Declassified in Part - Sanitized Copy Approved for Release 2013/01/23 : CIA-RDP81-01043R001600090003-8

Declassified in Part - Sanitized Copy Approved for Release 2013/01/23 : CIA-RDP81-01043R001600090003-8

Figure 110. Regions Q in which electrons can move in the earth's magnetic field close to the dipole (regions not blackened).

Figure 112. Wire model of trajectories of electrons for various values of γ.

Figure 113. Trajectory of electrons in the equatorial plane when $\gamma < -1$.

Figure 114. Trajectory of electrons when $-1 < \gamma < -0.5$.

Figure 115. Section by the equatorial plane of the cylindrical bean of charged particles and formation of a hollow base around the earth.

Figure 116. Formation of Positive and negative charged particles on the surface of the hollow space around the earth.

Figure 117. Scheme of motion of the positive charged particles (heavy dashed lines) and negative charged particles (fine dashed lines) according to Alfven.

Boundary of Stoermer's forbidden region Q; A auroral zone.

Figure 118. Magnetization curves of a magnetite crystal. (1) magnetization along the axis of easy magnetization; (2) along the axis of medium magnetization; (3) along the axis of difficult magnetization.

Figure 119. Hysteresis and magnetization curves of magnetites: (a) from the Kola peninsula, (b) of Mount Vysokaya (Urals), (c) of Mount Temir-Tau (Urals), (d) of Ural magnetite.

Figure 120. Magnetization curves of a pyrrhotite crystal. (1) magnetization along the OX axis, (2) along the OY axis, (3) along the OZ axis.

Figure 121. Hysteresis and magnetization curves of pyrrhotites: (a) Fe_2O_3 7.5%; (b) $Fe_3O_4 \sim 20\%$.

Declassified in Part - Sanitized Copy Approved for Release 2013/01/23 : CIA-RDP81-01043R001600090003-8

Declassified in Part - Sanitized Copy Approved for Release 2013/01/23 : CIA-RDP81-01043R001600090003-8

Figure 122. Hysteresis curves of pyrrhotite before and after heating to 270° C. The right hand curve is before, and the left after heating.

Figure 123. Hysteresis and magnetization curves of hematite.

Figure 124. Hysteresis and magnetization curves of ilmenites. (a) according to N. I. Spiridovich; (b) according to T. N. Roze.

Figure 125. Hysteresis curve of a diabase specimen according to N. I. Spiridovich.

Figure 126. Hysteresis and magnetization curves of a specimen of gabbronorite, according to N. I. Spiridovich.

Figure 127. Hysteresis and magnetization curves of a specimen of gabbrodiabase, according to N. I. Spiridovich.

Figure 128. Correlation between residual magnetization of magnetite and magnetizing field on heating and subsequent cooling.

Figure 129. Correlation between residual magnetization and magnetizing field during heating and subsequent cooling.
/in the drawing/ J_r of basic curve.

Figure 130. Effect of unilateral compression on residual induction of magnetite, according to M. A. Grabovskiy.
(1) magnetization of non-distorted specimen, (2) magnetization of distorted specimen.
/in the drawing/ B_r Gauss.

Figure 131. Solar-day variations in normal and anomalous field.
(1) Nizhnedevitsk station; (2) station No 1; (3) station No 2.
/in drawing/ 20 gammas 24 hours.

Figure 132. Diagram of ballistic instrument.

Figure 133. Diagram of magnetometric unit in first Gaussian position.

Figure 134. First Gaussian position (a), second Gaussian position (b).

Declassified in Part - Sanitized Copy Approved for Release 2013/01/23 : CIA-RDP81-01043R001600090003-8

Declassified in Part - Sanitized Copy Approved for Release 2013/01/23 : CIA-RDP81-01043R001600090003-8

Figure 137. Diagram of the magnetometer of B. M. Yanovskiy and Ye. T. Chernyshev for determination of the susceptibility of rocks.

Figure 138. ZM NIFI magnetometer.

Figure 139. Wiring diagram of magnetometer coils.

/In drawing/ Helmholtz rings.

Figure 140. Diagram of pole shoes.

Figure 141. Diagram of beam balance instrument for measuring susceptibility.

Figure 142. Correlation between attractive force and distance.

Figure 143. Diagram of torsion balance instrument for measuring susceptibility.

Figure 145. Diagram of a cylinder-method instrument.

/In drawing/ Dimensions in mm.

Figure 146. Diagram of an instrument for the N. I. Spiridovich -- S. Sh. Dolginov method.

Figure 148. Diagram of an instrument for the method of T. N. Roze.

Figure 149. Contact magnetometer.

Figure 150. Diagram of the distribution of observation points and of the method of their tying-in with control points.

/In drawing/ △ control points

o observation points

/V/ woods.

Figure 151. Magnetic field (Z) in the area of Krasnokamen iron ore deposit, according to aeromagnetic survey data.

Figure 152. Geological map of the area of Krasnokamen iron ore deposit.

(1) gabbrodiabases; dioritodiabases; (2) granites; (3) quartz diorites; (4) syenite-porphyrites, diorite-porphyrites; (5) porphyrites. /In drawing/ Dzhab'.

Declassified in Part - Sanitized Copy Approved for Release 2013/01/23 : CIA-RDP81-01043R001600090003-8

Declassified in Part - Sanitized Copy Approved for Release 2013/01/23 : CIA-RDP81-01043R001600090003-8

Figure 154. Z and H curves over sphere magnetized at an angle to the vertical.

Figure 155. Z and H curves over vertically magnetized sphere.

Figure 157. Z and H curves over 2-pole magnet, the axis of which is inclined to the vertical.

Figure 158. Z and H curves over 2-pole magnet, the axis of which is vertical.

Figure 159. Z and H curves over a single-pole magnet.

Figure 160. Z and H curves over 2-axis ellipsoid.
(1) for $q = 1$; (2) for $q = 2$.

Figure 163. Z and H curves over infinite cylinder in the case of oblique magnetization.

Figure 164. Z and H curves over infinite cylinder in the case of straight magnetization.

Figure 165. Z and H curves over infinite elliptical cylinder and thin plate.
/in drawing/ _____ ellipsoid
_ _ _ _ infinitely thin plate
/vertical axis/ intensity of magnetic field
/horizontal axis/ distance along the profile.

Figure 167. Z and H curves over infinitely long plate.
(1) curves for vertical plate; (2) oblique plate with angle of inclination $\varphi = 30^{\circ}$.

Figure 169. Z and H curves over vertical stratum.
(1) width $2a = R$; (2) width $2a = 2R$; (3) 2 plates at a distance R.

Figure 170. Z and H curves over vertical stratum.
(1) width of plate $2a = R$; (2) width $2a = 6R$.

Figure 171. Z and H curves over straight contact.

Declassified in Part - Sanitized Copy Approved for Release 2013/01/23 : CIA-RDP81-01043R001600090003-8

Declassified in Part - Sanitized Copy Approved for Release 2013/01/23 : CIA-RDP81-01043R001600090003-8

Figure 173. Z and H curves over vertically magnetized sloping stratum.

Figure 175. The card of D. S. Mikov.

Figure 178. Z and H curves over fault, as determined by A. G. Kalashnikov.

Figure 179. Z and H curves over fault, as determined by A. G. Kalashnikov.

Figure 182. The card of D. S. Mikov, for determining the shape and depth of occurrence of a rock formation.

Figure 184a. Z_H isolines in the area of the Kursk magnetic anomalies. /In drawing/ Saltykovo.

Figure 184b. H_H isolines in the area of the Kursk magnetic anomalies.

Figures 185a and 185b. /In drawings/ Kilometers.

Figure 186. Z isolines in the area of Western Urals anomalies.

Figure 187a. (1) H and Z observational curves; (2) calculated on the assumption that the occurring rock is a vertically magnetized sphere.

Figure 187b. (1) H and Z observational curves; (2) calculated on the assumption that the occurring rock is a sphere magnetized at an angle of 15° in relation to the vertical.

Figure 188. Diagram of magnetic forces acting on a magnetic compass.

Figure 189. Diagram.

Figure 190. Deflector Magnetometer.

Figure 191. Compass card with needles.

Figure 192. Table 13 — Deviation Table.

Figure 193. Direction finder of the deflector magnetometer.

Figure 194. Sights of the M-1 magnetometer.

Figure 195. Collimator method of reading.

Declassified in Part - Sanitized Copy Approved for Release 2013/01/23 : CIA-RDP81-01043R001600090003-8

Declassified in Part - Sanitized Copy Approved for Release 2013/01/23 : CIA-RDP81-01043R001600090003-8

Figure 196. Mirror method of reading.

Figure 197. Magnetic system of the "combine" instrument.

Figure 200. Needle inclinator.

Figure 201. Magnetic needle of the needle inclinator.

Figure 203. Procedure for magnetizing the needle.

Figure 204. Diagrammatic arrangement of the induction inclinator.

Figure 205. Induction inclinator.

Figure 208. "Combine" magnetic theodolite for measurement of the vertical component.

Figure 209a. First Gaussian position of magnets.

Figure 209b. Second Gaussian position of magnets.

Figure 209c. First Lamontian position of magnets.

Figure 209d. Second Lamontian position of magnets.

Figure 214. Diagram of rotating disks of the synchronous clock.

Figure 215. Diagram of a unit for determination of the period of oscillation of a magnet.

Figure 216. Diagram of Lamont's procedure for determining ν.

Figure 217. Diagram of the magnetometric method for determining ν.

Figure 221. Diagrammatic arrangement of the VNIIM absolute magnetic theodolite.

Figure 222. VNIIM absolute magnetic theodolite.

Figure 223. VNIIM absolute magnetic theodolite.

Figure 224. Housing for oscillation of the magnet.

Figure 225. Wiring diagram of the electric method for determining H.

Figure 226. "Combine" magnetic theodolite.

Figure 228. Quartz magnetometer.

Figure 230. Diagrammatic arrangement of a double compass.

Figure 231. Division scale and pointers of a double compass.

Figure 232. Electric magnetometer of B. Ye. Bryunelli.

Declassified in Part - Sanitized Copy Approved for Release 2013/01/23 : CIA-RDP81-01043R001600090003-8

Declassified in Part - Sanitized Copy Approved for Release 2013/01/23 : CIA-RDP81-01043R001600090003-8

Figure 235. M-1 magnetometer for measuring the vertical component.

Figure 237. Universal balance.

Figure 238. Magnetic system of the balance: (a) for measuring the vertical component; (b) for measuring the horizontal component.

Figure 239. Diagram of the optical system of the magnetic balance and the propagation of rays therein.

Figure 241. Aeromagnetometer of A. A. Logachev.

Figure 242. Electric diagram of the aeromagnetometer.

[K — section of coarse compensation; TK — section of fine compensation; ns — permanent magnets; K — commutator; ∋ M — 1: electric motor of the induction loop; ∋ M-2: electric motor of recorder; PPK-37-500 current — supplying-storage-battery.

/in drawing/

Magnetometer

Recorder

Drum.

Figure 243. Block diagram of a magnetometer with a single sonde.

[— alternating current generator; Ф-I — filter separating oscillations of frequency f; Ф-II — same, of frequency 2f; УС — amplifier; А — ammeter; Д — choke coil; W_1 — primary winding; W_2 — secondary winding.

/in drawing/ W_1 W_2

sonde.

Figure 244. Diagram of a magnetometer with 2 sondes.

Figure 245. Basic magnetization curve of armco iron (1) and tangensoid (2).

Figure 249. Block diagram of aeromagnetometer.

Declassified in Part - Sanitized Copy Approved for Release 2013/01/23 : CIA-RDP81-01043R001600090003-8

Declassified in Part - Sanitized Copy Approved for Release 2013/01/23 : CIA-RDP81-01043R001600090003-8

A -- equipment placed in gondola outside aircraft;
a -- measuring sondes; δ -- orientation sondes; δ --
2-phase reversible servomotors; ∿ -- control phases
of servomotors; ⊃ -- fixed phases of servomotors.
B -- equipment mounted within aircraft cabin:
T -- generator; ⊽ -- direct current battery supply-
ing compensation windings; C -- automatic recording
device; Y_1 -- measuring channel amplifier; Y_2 --
measuring sonde winding feed amplifier; Y_3 -- orienta-
tion sonde winding feel amplifier; Y_4 -- orientation
channel feed amplifier; Y_5 -- fixed phase feed amplifier.

Figure 250. Graph.

Figure 251. Graph

Figure 252. Diagram of unifilar M-magnet; C-suspension thread; P-reflecting mirror; K-twist knob.

Figure 253. Graph

Figure 254. Graph.

Figure 255. Graph.

Figure 256. Graph. ns -- unifilar magnet; n's' -- compensating magnet.

Figure 257. Graph.

Figure 258. Diagram of magnetic system of variometer.

Figure 260. Optical recording system of variational instrument.

Figure 261. Declimation and horizontal component variometer by Yanovskiy.

Figure 262. Vertical component variometer by Yanovskiy.

Figure 263. Magnetic balance.

Figure 264. Recording apparatus.

Figure 265. Variation Station.

Declassified in Part - Sanitized Copy Approved for Release 2013/01/23 : CIA-RDP81-01043R001600090003-8

Declassified in Part - Sanitized Copy Approved for Release 2013/01/23 : CIA-RDP81-01043R001600090003-8

Figure 267. Brunelli magnetic station.
(1) D-variometer; (2) H-variometer; (3) Z-variometer; (4) wire-wound rings to determine sensitivity of magnetic systems; (5) clockwork; (6) photographic film; (7) fastening posts for blackout wood which keeps light from variometers and film during operation of the station.

Figure 268. Optical recording system of La Cour magnetograph.

Figure 269. Recording diagram.

Figure 270. La Cour variometer.

Figure 271. Vertical component variations. Recorded with Kalashnikov fluxmeter and variometer.

Figure 272. Kalashnikov station.

Declassified in Part - Sanitized Copy Approved for Release 2013/01/23 : CIA-RDP81-01043R001600090003-8